

# Progressing the Synthesis, Coordination Chemistry and Biological Evaluation of Phenanthrolines

A thesis submitted to Maynooth University, National University of Ireland  
Maynooth, in fulfilment of the requirements for the degree of

**Doctor of Philosophy**

By

**Pauraic Mc Carron**



Department of Chemistry  
Faculty of Science and Engineering  
Maynooth University  
National University of Ireland Maynooth  
Maynooth  
Co. Kildare  
Ireland

October 2014

**Research Supervisor: Dr. Malachy McCann**

**Head of Department: Dr. John Stephens**

## Table of contents

<b>Table of contents</b> .....	<b>i</b>
<b>DECLARATION OF AUTHORSHIP</b> .....	<b>ix</b>
<b>Acknowledgements</b> .....	<b>x</b>
<b>Abstract</b> .....	<b>xiii</b>
<b>Symbols and Abbreviations</b> .....	<b>xiv</b>
<b>Chapter 1</b> .....	
Aims, structure and general introduction of the thesis.....	<b>1</b>
1.1 Aims of this project.....	<b>2</b>
1.2 Layout/structure of the thesis .....	<b>2</b>
1.3 Introduction .....	<b>3</b>
1.4 References .....	<b>15</b>
<b>Chapter 2</b> .....	
Experimental methods and instrumentation.....	<b>22</b>
2.1 Chemicals.....	<b>23</b>
2.1.2 Chemicals for the preparation of biological preparations – <i>Candida</i> .....	<b>23</b>
<i>Albicans</i> .....	<b>23</b>
2.1.3 Chemicals for the preparation of biological preparations: Bacteria.....	<b>24</b>
2.2 Instrumentation .....	<b>24</b>
2.3 Synthesis of 1, 10-phenanthroline phthalate complexes.....	<b>25</b>
2.3.1 Synthesis of [Mn(ph)]0.5H <sub>2</sub> O (PC 1) <sup>1</sup> .....	<b>25</b>
2.3.2 Synthesis of [Mn(isoph)]2H <sub>2</sub> O (PC 2) <sup>1</sup> .....	<b>26</b>
2.3.3 Synthesis of [Mn(terph)]2.5H <sub>2</sub> O (PC 3) <sup>1</sup> .....	<b>28</b>
2.3.4 Synthesis of [Mn(ph)(phen)]2H <sub>2</sub> O (8) and [Mn(ph)(phen) <sub>2</sub> (H <sub>2</sub> O)]4H <sub>2</sub> O (9) .....	<b>29</b>

2.3.5	Synthesis of $[\text{Mn}_2(\text{isoph})_2(\text{phen})_3]4\text{H}_2\text{O}$ (10) and $\{[\text{Mn}(\text{phen})_2(\text{H}_2\text{O})_2]\}_2(\text{isoph})_2(\text{phen})\cdot 12\text{H}_2\text{O}$ (11) (Crystal structure formulation) <sup>1</sup> .....	30
2.3.6	Synthesis of $[\text{Mn}(\text{terph})(\text{phen})_2]5\text{H}_2\text{O}$ (12) .....	31
2.4	Synthesis of 1, 10-phenanthroline octanedioate (suberate) complexes. ....	32
2.4.1	Synthesis of $[\text{Mn}_2(\eta^1\eta^1\mu_2\text{-oda})(\text{phen})_4(\text{H}_2\text{O})_2][\text{Mn}_2(\eta^1\eta^1\mu_2\text{-oda})(\text{phen})_4(\eta^1\text{-oda})_2]4\text{H}_2\text{O}$ (13) (Crystal structure formulation) <sup>2</sup> .....	32
2.4.2	Synthesis of $[\text{Cu}_2(\text{oda})(\text{phen})_4](\text{ClO}_4)_2\cdot 2.76\text{H}_2\text{O}\cdot \text{EtOH}$ (14) (Crystal structure formulation) <sup>3</sup> .....	33
2.5	Synthesis of 1, 10-phenanthroline 3,6,9-trioxaundecanedioate complexes .....	33
2.5.1	Synthesis of $[\text{Mn}(3,6,9\text{-tdda})]\cdot \text{H}_2\text{O}$ .....	33
2.5.2	Synthesis of $[\text{Cu}(3,6,9\text{-tdda})]\cdot \text{H}_2\text{O}$ (Novel) .....	34
2.5.3	Synthesis of $[\text{Ag}_2(3,6,9\text{-tdda})\cdot 2\text{H}_2\text{O}$ (Novel).....	36
2.5.4	Synthesis of $\{[\text{Mn}(3,6,9\text{-tdda})(\text{phen})_2]\cdot 3\text{H}_2\text{O}\cdot \text{EtOH}\}_n$ (15) (Crystal structure formulation) <sup>4</sup> .....	37
2.5.5	Synthesis of $[\text{Cu}(3,6,9\text{-tdda})(\text{phen})_2]\cdot 3\text{H}_2\text{O}\cdot \text{EtOH}$ (16) (Novel).....	38
2.5.6	Synthesis of $[\text{Ag}_2(3,6,9\text{-tdda})(\text{phen})_4]\cdot \text{EtOH}$ (17) (Novel).....	39
2.6	Synthesis of 1, 10-phenanthroline-5, 6-dione (phendione) (2) <sup>5</sup> .....	40
2.7	Synthesis of 2,9-dimethyl-1,10-phenanthroline-5,6-dione (dmphendio) (4) <sup>6</sup> .....	41
2.8	Synthesis of imidazo[4,5- <i>f</i> ][1,10]phenanthrolines (Im-phens) (Novel Method) .....	43
2.8.1	Microwave synthesis of 4-(1 <i>H</i> -imidazo[4,5- <i>f</i> ][1,10]phenanthrolin-2-yl)phenol (4phip) (18) (Novel method) .....	43
2.8.2	Microwave Synthesis of 2-(naphthalen-1-yl)-1 <i>H</i> -imidazo[4,5- <i>f</i> ][1,10]phenanthroline (nip) (19) (Novel method).....	46
2.8.3	Microwave Synthesis of 2-(anthracen-9-yl)-1 <i>H</i> -imidazo[4,5- <i>f</i> ][1,10]phenanthroline (aip) (20) (Novel method).....	48
2.8.4	Microwave synthesis of 2-(1 <i>H</i> -indol-3-yl)-1 <i>H</i> -imidazo[4,5- <i>f</i> ][1,10]phenanthroline (H <sub>2</sub> IIP) (21) (Novel method).....	50

<b>2.8.5</b> Microwave synthesis of 2-ferroceny-1 <i>H</i> -imidazo[4,5- <i>f</i> ][1,10]-phenanthroline (ferrip) ( <b>22</b> ) (Novel method).....	<b>53</b>
<b>2.8.6</b> Microwave synthesis of 1,4-bis(1 <i>H</i> -imidazo[4,5- <i>f</i> ][1,10]phenanthrolin-2-yl)benzene (bpibH <sub>2</sub> ) ( <b>23</b> ) (Novel method).....	<b>55</b>
<b>2.8.7</b> Microwave synthesis of 2-(4-(trifluoromethyl)phenyl)-1 <i>H</i> -imidazo[4,5- <i>f</i> ][1,10]phenanthroline ( <b>24</b> ) (Novel method).....	<b>57</b>
<b>2.8.8</b> Microwave synthesis of 4-(1 <i>H</i> -imidazo[4,5- <i>f</i> ][1,10]phenanthrolin-2-yl)benzotrile ( <b>25</b> ) (Novel method).....	<b>59</b>
<b>2.8.9</b> Microwave synthesis of 2-(thiophen-3-yl)-1 <i>H</i> -imidazo[4,5- <i>f</i> ][1,10]phenanthroline ( <b>26</b> ) (Novel method).....	<b>61</b>
<b>2.8.10</b> Microwave synthesis of 2-(thiophen-2-yl)-1 <i>H</i> -imidazo[4,5- <i>f</i> ][1,10]phenanthroline ( <b>27</b> ) (Novel method).....	<b>64</b>
<b>2.8.11</b> Microwave synthesis of 2-(6-methylpyridin-2-yl)-1 <i>H</i> -imidazo[4,5- <i>f</i> ][1,10]phenanthroline ( <b>28</b> ) (Novel method).....	<b>66</b>
<b>2.8.12</b> Microwave synthesis of 4-(1 <i>H</i> -imidazo[4,5- <i>f</i> ][1,10]phenanthrolin-2-yl)benzene-1,2-diol ( <b>29</b> ) (Novel method).....	<b>67</b>
<b>2.8.13</b> Microwave synthesis of 4-(1 <i>H</i> -imidazo[4,5- <i>f</i> ][1,10]phenanthrolin-2-yl)benzoic acid ( <b>30</b> ) (Novel method).....	<b>69</b>
<b>2.8.14</b> Synthesis of 2-(4-nitrophenyl)-1 <i>H</i> -imidazo[4,5- <i>f</i> ][1,10]phenanthroline (4nitrip) ( <b>31</b> ) (Novel method).....	<b>72</b>
<b>2.8.15</b> Synthesis of 4-(1 <i>H</i> -imidazo[4,5- <i>f</i> ][1,10]phenanthrolin-2-yl)aniline (anilip) ( <b>32</b> ).....	<b>74</b>
<b>2.8.16</b> Microwave synthesis of 2-(pyridin-3-yl)-1 <i>H</i> -imidazo[4,5- <i>f</i> ][1,10]phenanthroline ( <b>33</b> ) (Novel method).....	<b>76</b>
<b>2.8.17</b> Microwave synthesis of 2-(pyren-1-yl)-1 <i>H</i> -imidazo[4,5- <i>f</i> ][1,10]phenanthroline ( <b>34</b> ) (Novel method).....	<b>79</b>
<b>2.8.18</b> Microwave synthesis of 2-(4-bromophenyl)-1 <i>H</i> -imidazo[4,5- <i>f</i> ][1,10]phenanthroline ( <b>35</b> ) (Novel method).....	<b>81</b>
<b>2.8.19</b> Microwave synthesis of 2-(3-methoxyphenyl)-1 <i>H</i> -imidazo[4,5- <i>f</i> ][1,10]phenanthroline ( <b>36</b> ) (Novel method).....	<b>83</b>



2.8.20	Microwave synthesis of 2-(4-fluorophenyl)-1 <i>H</i> -imidazo[4,5- <i>f</i> ][1,10]phenanthroline ( <b>37</b> ) (Novel method).....	86
2.8.21	Microwave synthesis of 2-( <i>p</i> -tolyl)-1 <i>H</i> -imidazo[4,5- <i>f</i> ][1,10]phenanthroline ( <b>38</b> ) (Novel method).....	88
2.8.22	Microwave synthesis of 2-(3,4-dimethoxyphenyl)-1 <i>H</i> -imidazo[4,5- <i>f</i> ][1,10]phenanthroline ( <b>39</b> ) (Novel method, novel molecule).....	90
2.8.23	Microwave synthesis of 2-(4-(benzyloxy)-3-methoxyphenyl)-1 <i>H</i> -imidazo[4,5- <i>f</i> ][1,10]phenanthroline ( <b>40</b> ) (Novel method, novel molecule) .....	93
2.8.24	Microwave synthesis of 2-([1,1'-biphenyl]-3-yl)-1 <i>H</i> -imidazo[4,5- <i>f</i> ][1,10]phenanthroline (bhipip) ( <b>41</b> ) (Novel method, novel molecule) .....	95
2.8.25	Microwave synthesis of 2-benzhydryl-1 <i>H</i> -imidazo[4,5- <i>f</i> ][1,10]phenanthroline ( <b>42</b> ) (Novel method, novel molecule).....	98
2.8.26	Microwave synthesis of 5-(1 <i>H</i> -imidazo[4,5- <i>f</i> ][1,10]phenanthrolin-2-yl)-2-nitrophenol ( <b>43</b> ) (Novel method, novel molecule).....	99
2.8.27	Microwave synthesis of 2-(9 <i>H</i> -fluoren-3-yl)-1 <i>H</i> -imidazo[4,5- <i>f</i> ][1,10]phenanthroline ( <b>44</b> ) (Novel method, novel molecule).....	101
2.8.28	Microwave synthesis of 2-(3,5-bis(trifluoromethyl)phenyl)-1 <i>H</i> -imidazo[4,5- <i>f</i> ][1,10]phenanthroline ( <b>45</b> ) (Novel method, novel molecule) .....	104
2.8.29	Microwave synthesis of 4-(6,9-dimethyl-1 <i>H</i> -imidazo[4,5- <i>f</i> ][1,10]phenanthrolin-2-yl)phenol ( <b>46</b> ) (Novel method, novel molecule).....	106
2.8.30	Microwave synthesis of 2-ferroceny-(6,9-dimethyl-1 <i>H</i> -imidazo[4,5- <i>f</i> ][1,10]-phenanthroline ( <b>47</b> ) (Novel method, novel molecule).....	108
2.9	Synthesis of imidazo[4,5- <i>f</i> ][1,10]phenanthroline perchlorate complexes .....	111
2.9.1	Synthesis of [Cu(22) <sub>2</sub> ](ClO <sub>4</sub> ) <sub>2</sub> ( <b>54</b> ) (Novel complex) .....	111
2.9.2	Synthesis of [Cu(19) <sub>2</sub> ](ClO <sub>4</sub> ) <sub>2</sub> •7H <sub>2</sub> O ( <b>55</b> ) (Novel complex).....	112
2.9.3	Synthesis of [Cu(20) <sub>2</sub> ](ClO <sub>4</sub> ) <sub>2</sub> •7H <sub>2</sub> O ( <b>56</b> ) (Novel complex).....	113
2.9.4	Synthesis of [Cu(18) <sub>2</sub> ](ClO <sub>4</sub> ) <sub>2</sub> •MeOH•5H <sub>2</sub> O ( <b>57</b> ) (Novel complex) .....	114
2.9.5	Synthesis of [Cu(21) <sub>2</sub> ](ClO <sub>4</sub> ) <sub>2</sub> •2H <sub>2</sub> O ( <b>58</b> ) (Novel complex).....	115
2.9.6	Synthesis of [Cu(21) <sub>2</sub> ](ClO <sub>4</sub> ) <sub>2</sub> •2H <sub>2</sub> O ( <b>59</b> ) (Novel complex).....	116
2.9.7	Synthesis of [Cu(23)](ClO <sub>4</sub> ) <sub>2</sub> •2H <sub>2</sub> O ( <b>60</b> ) (Novel complex, polymer).....	117

<b>2.10</b>	<b>Synthesis of Oxazine (Phenoaxazine) Ligands.....</b>	<b>119</b>
<b>2.10.1</b>	Synthesis of methyl 2-(4-hydroxyphenyl)-2 <i>H</i> -[1,4]oxazino[2,3- <i>f</i> ][1,10]phenanthroline-3-carboxylate, PDTME ( <b>49</b> ).....	<b>119</b>
<b>2.10.2</b>	Microwave synthesis of methyl 2-(4-hydroxyphenyl)-2 <i>H</i> -[1,4]oxazino[2,3- <i>f</i> ][1,10]phenanthroline-3-carboxylate, PDTME ( <b>49</b> ).....	<b>121</b>
<b>2.10.3</b>	Synthesis of ethyl 2-(4-hydroxyphenyl)-2 <i>H</i> -[1,4]oxazino[2,3- <i>f</i> ][1,10]phenanthroline-3-carboxylate, PDTEE ( <b>50</b> ) (Novel molecule).....	<b>122</b>
<b>2.10.4</b>	Synthesis of methyl 2-(3,4-dihydroxyphenyl)-2 <i>H</i> -[1,4]oxazino[2,3- <i>f</i> ][1,10]phenanthroline-3-carboxylate, PDDME ( <b>51</b> ) (Novel molecule).....	<b>124</b>
<b>2.10.5</b>	Microwave synthesis of methyl 2-(3,4-dihydroxyphenyl)-2 <i>H</i> -[1,4]oxazino[2,3- <i>f</i> ][1,10]phenanthroline-3-carboxylate, PDDME ( <b>51</b> ) (Novel molecule).....	<b>126</b>
<b>2.10.6</b>	Synthesis of ethyl 2-(3,4-dihydroxyphenyl)-2 <i>H</i> -[1,4]oxazino[2,3- <i>f</i> ][1,10]phenanthroline-3-carboxylate, PDDEE ( <b>52</b> ) (Novel molecule).....	<b>128</b>
<b>2.10.7</b>	Microwave synthesis of 2-(3,4-dihydroxyphenyl)-2 <i>H</i> -[1,4]oxazino[2,3- <i>f</i> ][1,10]phenanthroline-3-carboxylate, PDDEE ( <b>52</b> ) (Novel molecule).....	<b>130</b>
<b>2.10.8</b>	Synthesis of methyl 2-phenyl-2 <i>H</i> -[1,4]oxazino[2,3- <i>f</i> ][1,10]phenanthroline-3-carboxylate, PDPME ( <b>53</b> ) (Novel molecule).....	<b>132</b>
<b>2.11</b>	<b>Synthesis of Phenoxazine perchlorate complexes.....</b>	<b>133</b>
<b>2.11.1</b>	[Cu(PDDME) <sub>2</sub> ](ClO <sub>4</sub> ) <sub>2</sub> ( <b>92</b> ) (Novel complex).....	<b>133</b>
<b>2.11.2</b>	[Cu(PDDEE) <sub>2</sub> ](ClO <sub>4</sub> ) <sub>2</sub> ( <b>93</b> ) (Novel complex).....	<b>134</b>
<b>2.11.3</b>	[Mn(PDDME) <sub>3</sub> ](ClO <sub>4</sub> ) <sub>2</sub> ( <b>94</b> ) (Novel complex).....	<b>135</b>
<b>2.11.4</b>	[Mn(PDDEE) <sub>3</sub> ](ClO <sub>4</sub> ) <sub>2</sub> ( <b>95</b> ) (Novel complex).....	<b>137</b>
<b>2.12</b>	<b>Amide formation: Folate-NHS ester and 4-(1<i>H</i>-imidazo[4,5-<i>f</i>][1,10]phenanthroline-2-yl)aniline (<b>32</b>) to form Im-phen-fol (<b>45</b>) (Novel molecule).....</b>	<b>138</b>
<b>2.12.1</b>	Synthesis of [Cu(Im-phen-fol) <sub>2</sub> ](ClO <sub>4</sub> ) <sub>2</sub> .2H <sub>2</sub> O ( <b>76</b> ) (Novel complex) ..	<b>140</b>
<b>2.12.2</b>	Synthesis of [Mn(Im-phen-fol) <sub>3</sub> ](ClO <sub>4</sub> ) <sub>2</sub> .2H <sub>2</sub> O ( <b>92</b> ) (Novel complex) ..	<b>141</b>
<b>2.13</b>	<b><i>In vitro</i> Antibacterial Testing.....</b>	<b>142</b>
<b>2.14</b>	<b><i>In vitro</i> Antifungal Testing.....</b>	<b>143</b>

2.15 <i>In vivo</i> <i>Galleria mellonella</i> Experiments.....	144
2.16 <i>In vivo</i> Antifungal Screening .....	145
2.16.1 Prophylactic Treatment .....	146
2.16.2 Treatment of Infection.....	146
2.17 <i>In vitro</i> Anticancer Screening. ....	146
2.18 DNA Interaction Studies. ....	147
2.18.1 DNA cleavage experiments.....	147
2.19 References .....	148
<b>Chapter 3</b> .....	
Antifungal activities of the metal complexes.....	152
3.1 Fungi .....	153
3.2 Fungal infections and etiological species.....	155
3.3 Antifungal phenanthrene derivatives .....	164
3.4 Potentiating the antifungal activity of 1,10-phen carboxylate complexes .....	167
3.5 Complex synthesis, characterisation and proposed structures .....	171
3.6 Antifungal activity and cytoselectivity of selected complexes .....	176
3.7 <i>In vivo</i> systemic toxicity/cytotoxicity studies using <i>Galleria mellonella</i> .....	192
3.8 <i>In vivo</i> antifungal screening using <i>G. mellonella</i> .....	195
3.9 Summary of antifungal activity.....	200
3.10 References .....	200
<b>Chapter 4</b> .....	
Antibacterial activities of the metal complexes .....	209
4.1 Introduction.....	210
4.2 <i>Staphylococcus aureus</i> .....	214
4.3 Methicillin resistant <i>Staphylococcus aureus</i> (MRSA).....	216

4.4 <i>Escherichia coli</i> .....	220
4.5 <i>Pseudomonas aeruginosa</i> (ATCC 27853 and 10145) .....	222
4.6 <i>Mycobacterium tuberculosis</i> .....	224
4.7 Complex synthesis, characterisation and proposed structures .....	226
4.8 Antibacterial activity and cytoselectivity of selected complexes .....	229
4.8.1 <i>S. aureus</i> results .....	232
4.8.2 MRSA results .....	234
4.8.3 <i>E. coli</i> results.....	236
4.8.4 <i>P. aeruginosa</i> (10145) results .....	238
4.8.5 <i>P. aeruginosa</i> (27853) results .....	239
4.8.6 <i>M. tuberculosis</i> (CDC 1551) results.....	241
4.8.7 <i>M. tuberculosis</i> (ATCC 27294) results .....	242
4.9 <i>In vivo</i> systemic toxicity/cytotoxicity studies using <i>Galleria mellonella</i> .....	245
4.10 Summary of antibacterial activity .....	246
4.11 References .....	247
<b>Chapter 5</b> .....	
Cancer, artificial metallonucleases and targeted chemotherapy. ....	261
5.1 An introduction to cancer.....	262
5.2 The cell cycle and tumour growth.....	264
5.3 Metal-based chemotherapeutics and artificial metallonucleases .....	266
5.4 <i>In vitro</i> anticancer screening .....	270
5.5 The derivation and development of 1,10-phenanthroline .....	274
5.6 DNA interaction studies/Nuclease mimetic activity .....	285
5.7 Targeted cytotoxic chemotherapy .....	290
5.7.1 Nutrient targeted chemotherapeutics.....	291

5.7.2 Folic acid mediated targeting .....	297
5.8 <i>In vivo</i> systemic toxicity/cytotoxicity studies using <i>Galleria mellonella</i> .....	302
5.9 Conclusions .....	302
5.10 References .....	303

## DECLARATION OF AUTHORSHIP

I hereby certify that this thesis has not been submitted before, in whole or in part, to this or any other university for any degree and is, except where stated, the original work of the author.

Signed: \_\_\_\_\_ Date: \_\_\_\_\_

Pauraic Mc Carron, B.Sc.

## Acknowledgements

The completion of this work has only been made possible by the guidance, support and help of a large group of people to whom I will be forever grateful.

First and foremost I would like to take this opportunity to sincerely thank my supervisor, Dr. Malachy McCann for all his guidance, patience and encouragement. The completion of this thesis would not have been possible without your untiring enthusiasm for the research, the large amount of time you devote to your students, your always timely and concise advice and for being the true meaning of a mentor. I would also like to thank Dr. Andrew Kellet, Prof. Michael Devereux and Dr. Kevin Kavanagh not only for the use of their labs and equipment but for their expert help and always having the time to discuss the work and for creating a truly collaborative environment.

I would also like to take this opportunity to thank Professor Andre L.S. Santos and his group in the Department of General Microbiology, Federal University of Rio de Janeiro, Brazil, for all of their work on testing my complexes against a myriad of fungi and also for the anti- *Mycobacterium tuberculosis* (27294) testing.

A further thank is due to Dr. Petros Karakousis and his team especially Dr. Ciaran Skerry based in the Centre for Tuberculosis Research, Department of Medicine, Division of Infectious Diseases, Johns Hopkins School of Medicine, Baltimore, USA, for their diligent work and MIC testing of another *M. tuberculosis* strain (CDC1551).

I would like to express my sincere gratitude to Dr. John Stephens, the current head of Department and also to Professor John Lowry, the former head of Department for giving me the opportunity to pursue my Ph.D. Also, I would like to thank Dublin City Council and Monaghan County Council for financial support.

I also must thank all of the staff of the Chemistry Department, particularly to the technicians and the Executive Administrators, for their assistance at all stages of this project. A special mention must go to Noel for always being available to help with software problems or any problem with lab equipment and most importantly for always being there to help despite the hassle and extra work I must have caused.

Thank you to all the postgrads and postdocs, both past and present. You have all provided a friendly work environment and I have thoroughly enjoyed the many conversations, laughs and nights out that we have had together. A special thanks to Dean, Wayne, Orla and Eimear for being true friends. For listening to my rants, for the all the late nights and

weekends in the lab and for just being there to lend a hand or a supportive word at the right time.

To Louise, a very special thank you is most definitely due, just really, really thank you! I know I'm not the easiest person to be around at times, especially during the writing of this thesis but I know it would never have happened without you. I hope you continue to put up with me for a long time to come. Thank you to our boys Jordan and Jamie for driving me mad, making me laugh, giving me perspective and reminding me that there are much more important things in life.

To Richard and Marie, thank you for all your love and support over the years and for listening to my rants and frustrations. I look forward to spending more time with you and your gorgeous girls, my amazing nieces Sarah, Ciara and Aoibheann. To my big sister Michelle, I know I haven't been around very much since you moved back home so hopefully now I'll have more time to spend with you. I'm so happy to have you living in the country again. Thank you for always lending an encouraging word every time one was needed.

To all my friends from home, Danny, Brian (Cozi), Billy, Chris, Dwayne, Mickey, Darrach and my cousin Darragh. Thank you all for being the best friends anyone could wish for. For the constant slags about how I'll not actually be a "Doctor" and for just being yourselves guys, for sharing all of the past and to sharing many of the future adventures of life together, thank you.

Last but by no means least, to my parents, Bridie and Pat, for never losing faith in me, for always being there for me with unending love and support. For giving me the belief and encouragement I have needed to keep going to the end. Everything I am and everything I will be, I owe to you, thank you. I dedicate this thesis to both of you.



*To my parents,*

*Pat and Bridie*

**Abstract**

The work described in this thesis concerns: (i) the synthesis and characterisation of ternary 1,10-phenanthroline/dicarboxylate Ag(I), Cu(II) and Mn(II) complexes and their *in vitro/in vivo* antifungal, antibacterial and antineoplastic capabilities; (ii) the development of a novel, high yielding, rapid and chromatography-free synthetic protocol for the formation of families of existing and new imidazo-phenanthroline ligands that allow for the modular assembly and covalent inclusion of an ensemble of varied functional groups and cellular targeting molecules; (iii) the synthesis of Cu(II) complexes incorporating these imidazo-phenanthroline ligands and their assessment as artificial mellonucleases; (iv) the synthesis of phenanthroline-oxazine (phenoxazine) ligands via an unusual cyclisation reaction with 1,10-phenanthroline-5,6-dione and specific aromatic amino acid esters; (v) the synthesis of a novel imidazo-phenanthroline-folic acid-appended ligand and its corresponding metal complexes with the view to selectively target folate receptor expressing cancer cells and activated macrophages.

A selection of complexes were screened, *in vitro*, for growth inhibition activity against a range of fungal and bacterial pathogens and were found to have broad spectrum activity. The most active complexes were then tested, *in vivo*, for cytotoxicity and antifungal activity using the *Galleria mellonella* insect model. Healthy *G. mellonella* larvae appeared to be unaffected by the complexes at concentrations up to 500  $\mu\text{g}/\text{cm}^3$ . The most active complex,  $[\text{Mn}_2(\eta^1\eta^1\mu^2\text{-oda})(\text{phen})_4(\text{H}_2\text{O})_2][\text{Mn}_2(\eta^1\eta^1\mu^2\text{-oda})(\text{phen})_4(\eta^1\text{-oda})_2].4\text{H}_2\text{O}$  (**13**), increased the survival rate of larvae administered with a lethal dose of *C. albicans* and was much more efficacious than the clinically used antifungal drug, ketoconazole.

Against two different *Mycobacterium tuberculosis* strains, the Mn(II) complexes exhibited potent antimycobacterial activity, with **13** being 3-fold more active than the prescription drug, isoniazid. This Mn(II) complex was also highly cytotoxic towards other bacterial cells. The Cu(II) bis-imidazo-phenanthroline complexes proved to be effective nuclease mimetic agents. In particular, a heteronuclear, ferrocene-appended imidazo-phenanthroline Cu(II) complex, displayed potent DNA scission activity and retained this activity in the presence of a large excess of the powerful metal ion sequesterant, EDTA. Cu(II)-based complexes were generally the most effective anticancer agents (*in vitro*), and  $[\text{Cu}_2(\text{oda})(\text{phen})_4](\text{ClO}_4)_2.2.76\text{H}_2\text{O}. \text{EtOH}$  (**14**) was particularly cytotoxic towards the cancerous A549 alveolar cell line.

## Symbols and Abbreviations

$\nu$	wavenumber ( $\text{cm}^{-1}$ )
$\mu_{\text{eff}}$ (B.M.)	effective magnetic moment (Bohr magneton)
$\Delta_{\nu}$	wavenumber separation in $\text{cm}^{-1}$
$\mu\text{g}$	Micro gram
$\mu\text{l}$	Micro litre
$\mu\text{M}$	Micromolar
1,10-phen	1,10-phenanthroline
3,6,9-tddaH <sub>2</sub>	3,6,9-trioxaundecandioic acid
5FC	Flucytosine
A	adenine
Å	Angstrom ( $10^{-10}$ m)
acacH	acetylacetone
AIDS	acquired immune deficiency syndrome
AMB	amphotericin B
AMR	antimicrobial resistance
ApG	adenine-cisplatin-guanine 1,2-intrastrand adduct
ApXpG	adenine-cisplatin-any base-cisplatin-guanine intrastrand adduct
ATCC	American Type Culture Collection
ATP	adeninetriphosphate
bdoaH <sub>2</sub>	benzene-1,2-dioxyacetic acid
bipy	bipyridine
BLM	bloemycin

bttn	7a,12c-(2,2'-bipyridin-3,3'-diyl)-1,2,7a,12c-tetrahydro-7H,8H-2a,7,8,12b-tetraazacyclopenta(fg)tetracene ethanol (1:1)
C	cytosine
ca.	circa
CAN	Ceric ammonium nitrate
carboplatin	<i>cis</i> -diammine(1,1-cyclobutanedicarboxylato)platinum(II)
CAT	Catalase
CBM	chromoblastomycosis
CDC	Centers for Disease Control and Prevention
CF	cystic fibrosis
CFG	Caspofungin
cisplatin	<i>cis</i> -diamminedichloroplatinum(II)
CV	cyclic voltammetry
DEPT	Distortionless enhancement by polarization transfer
DMF	dimethylformamide
dmphen	2,9-dimethyl-1,10-phenanthroline
dmphendio	2,9-dimethyl-1,10-phenanthroline-5,6-dione
DMSO	Dimethyl sulfoxide
DNA	Deoxyribonucleic acid
dppn	benzo[ <i>i</i> ]dipyrido[3,2- <i>a</i> :2',3'- <i>c</i> ]phenazine
dppz	dipyrido[3,2- <i>a</i> :2',3'- <i>c</i> ]phenazine
dpq	pyrazino[2,3- <i>f</i> ][1,10]phenanthroline
EC <sub>50</sub>	50% effective concentration
EDTA	Ethylenediaminetetraacetic acid

EDTA	ethylenediaminetetraacetic acid
en	ethylenediamine
EtOAc	ethyl acetate
EtOH	ethanol
FDA	Food and Drug Administration
Fol	folate
FR	Folate receptor
fumH <sub>2</sub>	fumaric acid
G	guanine
G <sub>0</sub>	outside cell cycle
G <sub>1</sub>	initial resting phase
G <sub>2</sub>	premitotic or second resting phase
GC	gas phase chromatography
GpG	guanine-cisplatin-guanine 1,2-intrastrand adduct
GpXpG	guanine-cisplatin-any base-cisplatin-guanine intrastrand adduct
GSSG	oxidised glutathione
GSSH	reduced glutathione
h, min, s	hours, minutes and seconds
HisH	histidine
HIV	human immunodeficiency virus infection
HSQC	Heteronuclear Single Quantum Coherence
IC <sub>50</sub>	50% inhibitory concentration
IR	Infrared

IR	infra-red
isophH <sub>2</sub>	isophthalic acid
Itraconazole	ITC
Ketoconazole	KTC
LC/MS	Liquid chromatography mass spectrometry
M	mitosis
M.R.S.A.	<i>Methicillin-resistant Staphylococcus aureus</i>
malH <sub>2</sub>	malonic acid
MeCN	acetonitrile
MEM	Minimal Essential Media
MeOH	methanol
MFC	minimum fungicidal concentration
MFG	Micafungin
MIC	Minimum Inhibitory Concentration
MM	Minimal Growth Media
MS	mass spectrometry
MTT	3-(4,5-dimethylthiazol-2-yl)-2,5-diphenyltetrazolium bromide
NADPH	nicotinamide adenine dinucleotide phosphate
NAG	<i>N</i> -acetylglucosamine
NAM	<i>N</i> -acetylmuramic acid
NaOH	Sodium hydroxide
nda H <sub>2</sub>	nonanedioic acid/azelaic acid
Nedaplatin	Diammine[(hydroxy-κO)acetato(2-)-κO]platinum

NMR	nuclear magnetic resonance
NO	Nitric oxide
norbH <sub>2</sub>	<i>cis</i> -5-norborene- <i>endo</i> -2,3-dicarboxylic acid
°C	Degree Celsius
°C	Degrees Celsius
OD	Optical density
odaH <sub>2</sub>	octanedioic acid/suberic acid
oxaliplatin	[(1 <i>R</i> ,2 <i>R</i> )-cyclohexane-1,2-diamine](ethanedioato- <i>O</i> , <i>O'</i> )platinum(II)
PBS	phosphate buffered saline
PHM	Phaeohyphomycosis
phendiol	1,10-phenanthroline-5,6-diol
phendione	1,10-phenanthroline-5,6-dione
phH <sub>2</sub>	phthalic acid
py	pyridine
R	alkyl, aryl, aromatic substituent
RB	Round bottomed
RNA	Ribonucleic acid
RNS	reactive nitrogen species
ROS	Reactive oxygen species
rpm	revolutions per minute
RPMI	Roswell Park Memorial Institute
RT	Room temperature
S phase	Synthetic phase where DNA replication occurs

salH <sub>2</sub>	salicylic acid
Satraplatin	(OC-6-43)- bis(acetato)amminedichloro(cyclohexylamine)platinum
SDA	Sabouraud Dextrose Agar
SDS	sodium dodecyl sulphate
SI	selectivity index
SOD	Superoxide dismutase
SOD	superoxide dismutase
<i>sym, asym</i>	symmetric and asymmetric, respectively
T	thymine
TB	Tuberculosis
T <sub>D</sub>	tumour doubling time
TE	tris EDTA
terphH <sub>2</sub>	terephthalic acid
Tf	transferrin
TMS	Tetramethylsilane
TSS	Toxic shock syndrome
UV	ultra violet
VRC	Voriconazole
VRSA	Vancomycin resistant <i>Staphylococcus aureus</i>
WHO	World Health Organisation
YEPD	Yeast Extract Peptone Dextrose
ZOI	Zone of inhibition



# **Chapter 1**

## **Aims, structure and general introduction of the thesis**

## 1.1 Aims of this project

One major objective of the work was to expand the range of ternary 1,10-phenanthroline/dicarboxylate metal complexes by synthesising novel analogues and to overcome previous water-solubility issues, inherent with certain metal phenanthroline complexes, via the coordination of hydrophilic dicarboxylates. The *in vitro/in vivo* antimicrobial and antineoplastic capabilities of the phenanthroline ligands and their metal complexes were then to be investigated.

A second major objective was to attempt to develop a more facile method of preparing phenanthroline derivatives, with particular emphasis on incorporating biologically relevant and targeting functional groups onto the backbone of the chelate ligand. The new phenanthrolines would be coordinated to transition metals and their bioactivity probed.

Thirdly, the scope of phenoxazine synthesis and concomitant coordination chemistry would be expanded beyond the first known example which was prepared by reacting 1,10-phenanthroline-5,6-dione with the methyl ester of L-tyrosine. The same synthetic protocol would be employed using related amino acids.

The fourth and final goal was to synthesise an imidazo-phenanthroline-folic acid-appended ligand and its corresponding Cu(II) and Mn(II) complexes. The intention would be to selectively target folate receptor expressing cancer cells and also activated macrophages which act as reservoirs for *Mycobacterium tuberculosis* bacteria.

## 1.2 Layout/structure of the thesis

This thesis has been structured with a brief introduction in Chapter 1 to the history of metal complexes with particular emphasis on those containing nitrogen-substituted phenanthrene-based ligands and their broad-spectrum of applications focusing primarily on their medicinal properties. Each subsequent Chapter contains a very detailed introduction and explanation to the area of interest in that particular chapter. Detailed, relevant background information on the topic in question is given so as to familiarise the reader with the many and varied terms referred to throughout the thesis. A general review of previous relevant work carried out in our laboratory has been outlined to allow the

reader to gain an insight into the background of this research and any previous successes that have directed the current work.

Chapters 3, 4 and 5 are divided into the three main topics of antifungal, antibacterial and anticancer activities of the complexes of interest. Chapter 5 also explores the artificial metallonuclease capabilities that is inherently linked to the anticancer activities of the metal complexes. Finally, the various ligands used in the complexation reactions are highlighted in order to acquaint the reader with the types of metal complexes each one forms. In addition, any previously reported biological activity associated with each ligand or complex is also summarised for comparison were necessary.

### 1.3 Introduction

Metals are ubiquitous in natural and many play a vital role within living organisms, due in part to their redox capabilities and formation of positively charged ions which facilitate solubility in biological fluids.<sup>1</sup> The electron deficient cationic form of metals is of vital importance to their biological role, being strongly attracted to the numerous biological molecules such as proteins and DNA which are often electron rich and/or negatively charged, resulting in metal ions interacting with/binding to these biological molecules.<sup>2</sup> Considering the wide range of interaction capabilities of metals in biology, it is only logical that natural evolution has incorporated metals to such a large extent into essential biological functions such as oxygen transport and electron shuttling.<sup>2-3</sup>

Man has known and utilised various metals for medicinal purposes for almost 5000 years.<sup>2-4</sup> The sterilization of water was achieved by the Egyptians through the use of copper (circa 3000 BC) and gold was applied to limited effect in various remedies almost 3500 years ago in China and Arabia.<sup>5</sup> Around 1500 BC in Egypt iron was used in a variety of medicines and at approximately the same time zinc was found to aid in wound healing.<sup>1</sup> It could be argued though, that the rational design, development and medicinal deployment of inorganic compounds started in the 1900s. At this time the German physician Robert Koch discovered that a gold complex,  $K[Au(CN)_2]$ , was bacteriostatic towards *Mycobacterium tuberculosis* bacteria, the causative agents of tuberculosis.<sup>6</sup> In addition around this time various antimony compounds were being utilised for the treatment of the protozoan disease leishmaniasis.<sup>1</sup> Furthermore in 1929, the French physician Jacques Forestier reported that gold complexes (sodium aurothiopropanol sulfonate) had anti-arthritis activity and represented a possible treatment for rheumatic

arthritis, since that time gold complexes have proven effective treatments for a variety of other rheumatic diseases.<sup>7</sup>

In the early 1900's (1907 - 1910) Dr. Paul Ehrlich devised the concept of high throughput biological screening of numerous compounds in order to elucidate any agents with antimicrobial activity and from this, that a lead compound with selective toxicity towards a pathogen and not the host could be identified.<sup>8</sup> Importantly he theorised that any lead compounds from initial screening could be developed and optimised via rational systematic chemical modification using a structure activity relationship (SAR) model.<sup>1</sup> He referred to these selectively toxic agents or "drugs" as a "magic bullet" and as a consequence formed the basis for nearly all modern pharmaceutical research, hence appropriately he is referred to as the father/founder of chemotherapy.<sup>8</sup> Utilising this method in 1909 he and his colleague Dr. Sahachiro Hata developed the first inorganic compound Arsphenamine (first synthesised in 1907, also known as Salvarsan or Ehrlich 606, Figure 1.1) as a highly effective treatment for syphilis.<sup>8-9</sup>

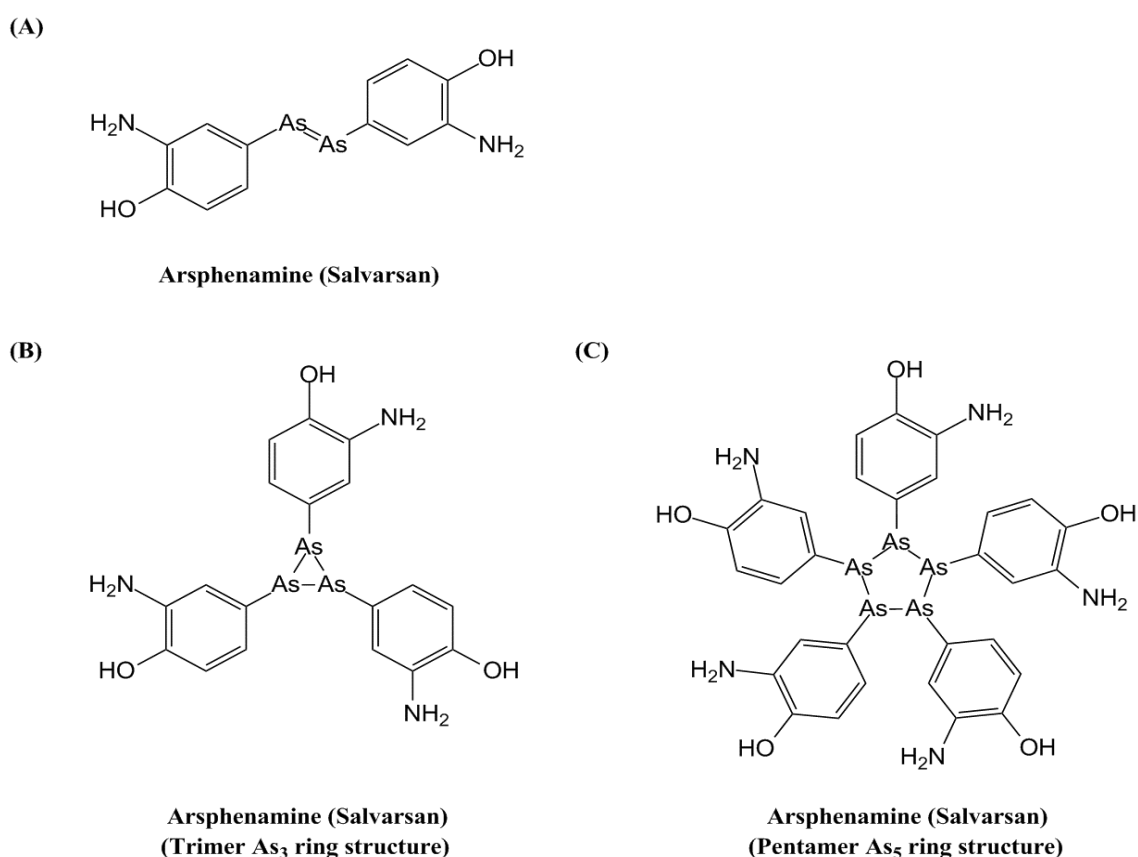


**Fig. 1.1:** (A) Previously accepted structure of Salvarsan. Recent published ESI mass spectral data suggests actual structure is a mixture of trimer (B) and pentamer (C) structures.<sup>10</sup>

This was the first example of a medicinal agent created on the basis of rational theoretical considerations which had a specific therapeutic effect. Ehrlich's ideas have become fundamental concepts of medicinal chemistry, which are often predominately associated with organic molecules but it is interesting to note that the first structure activity relationship was developed from a medicinal inorganic molecule, Salvarsan.

In 1965, the physicist Dr. Barnett Rosenberg *et al* discovered that a soluble platinum complex was generated during the electrolysis of platinum electrodes.<sup>11</sup> This platinum complex was later found to be cis-diamminedichloroplatinum(II) (Cisplatin, Figure 1.2) and Rosenberg further noted that this soluble platinum complex affected the growth of *Escherichia coli* bacteria; although their growth continued resulting in long filaments of bacteria, crucially their cell division had been arrested.<sup>11</sup> That complex cis-diamminedichloroplatinum(II) (Cisplatin) had previously first been synthesised by Michele Peyrone in 1845 (Peyrone's salt) and later its structure was deduced by Alfred Werner in 1893 as part of his work that would earn him a noble prize in 1913.<sup>12</sup> Following this discovery Rosenberg and some new collaborators decided to test cisplatin (*cis*-[PtCl<sub>2</sub>(NH<sub>3</sub>)<sub>2</sub>]) against certain cancer cell types and found that *cis*-[PtCl<sub>2</sub>(NH<sub>3</sub>)<sub>2</sub>] was highly effective at reducing the tumour volume of sarcomas in rats.<sup>13</sup> This ultimately led to cisplatin entering clinical trials as an antineoplastic agent in 1971, eventually being approved for human use and introduced into clinical practise in 1978.<sup>14</sup> It has since been employed in the treatment of various solid neoplastic malignancies including sarcomas and carcinomas such as small cell lung cancer, testicular, ovarian, cervical, endometrial, bladder, head and neck, gastroesophageal and germ cell cancers/tumours.<sup>14-15</sup> It has proven highly effective against testicular cancer in combination with other agents such as bleomycin with cure rates up to 85%.<sup>16</sup>

Cisplatin was the first platinum based solid tumour treatment and it is still extensively utilised, being a major component in first, second and third line treatment regimens for the aforementioned cancer types.<sup>17</sup> Cisplatin forms intrastrand (1,2-GG and 1,3-GTG) and interstrand (1,2-GpC) crosslinks with DNA leading to apoptosis and a cytotoxic effect.<sup>18</sup> Unfortunately it is poorly cell selective and hence the dosage and efficacy of cisplatin are often limited by its side effects on normal cells/tissue; the most prominent of which being nephrotoxicity.<sup>18</sup> Numerous other derivatives of cisplatin have been synthesised over the many years since its discovery in an effort to ameliorate its dose limiting side effects (nephrotoxicity), improve its oral applicability (cisplatin itself is

administered intravenously) and consequently improve its efficacy. In addition to cisplatin, three of these 2<sup>nd</sup> generation platinum based anti-cancer agents (Figure 1.2 Group 1: carboplatin, oxaliplatin and nedaplatin) are currently clinically available for the treatment of various cancers, whilst others are currently undergoing development or in various stages of clinical phase trials (Figure 1.2, Group 2).<sup>19</sup>

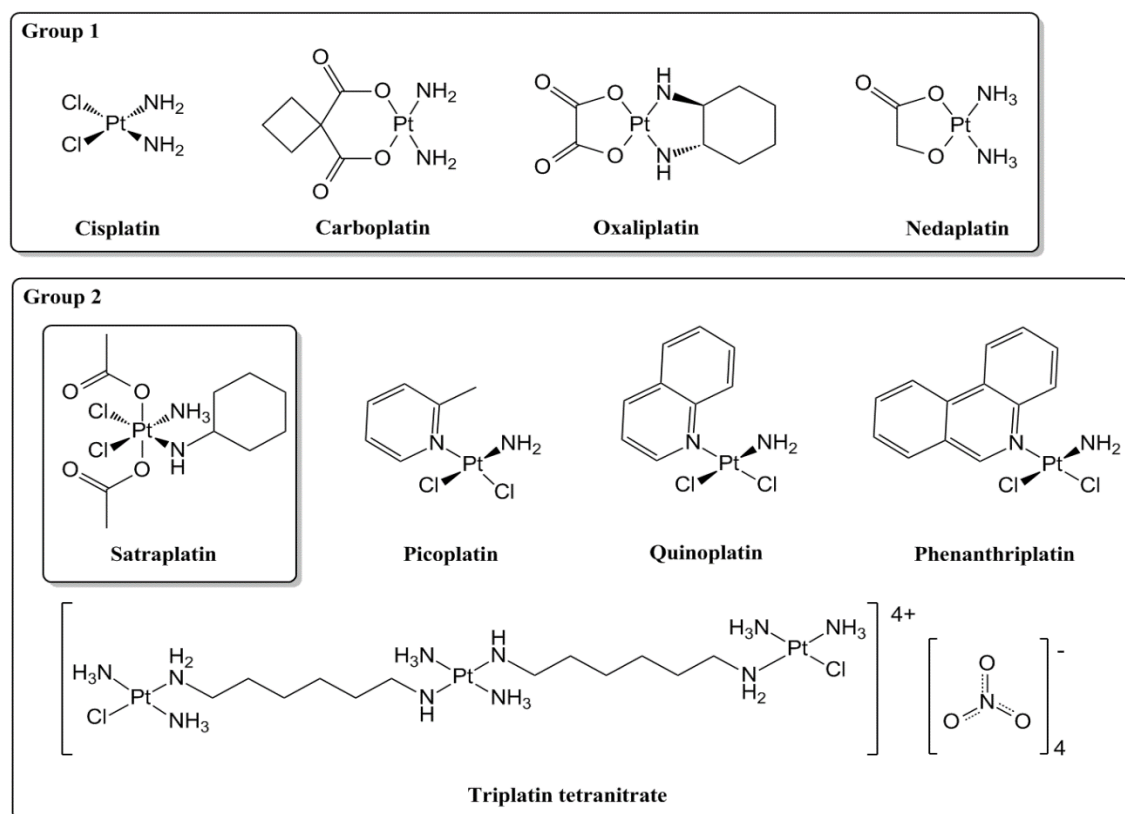


**Fig. 1.2:** Group1 shows the structure of cisplatin and some examples of the 2<sup>nd</sup> generation of approved platinum based anticancer drugs. Group 2 shows the structure of new platinum based agents which are currently undergoing development or in various stages of clinical phase trials. Satraplatin is the only Pt(IV) complex shown.<sup>19-20</sup>

It should also be mentioned that Satraplatin (Figure 1.2, Group 2) is a Pt(IV) based complex unlike that of cisplatin or the other analogues and was designed to be the first orally active platinum-based chemotherapeutic drug, in contrast to cisplatin, carboplatin, oxaliplatin and nedaplatin which are administered intravenously.<sup>19</sup> Satraplatin was designed to be metabolized resulting in the loss of its acetate groups (becoming a Pt(II) complex) and then consequently be structurally similar to cisplatin except for replacement

of one of the amine groups with a cyclohexylamine group.<sup>19</sup> The proposed mode of action of cisplatin (its derivatives function similarly) as mentioned earlier is via DNA intrastrand/interstrand adduct formation and it is known that cisplatin can be deactivated by the action of L-glutathione (Figure 1.3).<sup>20</sup>

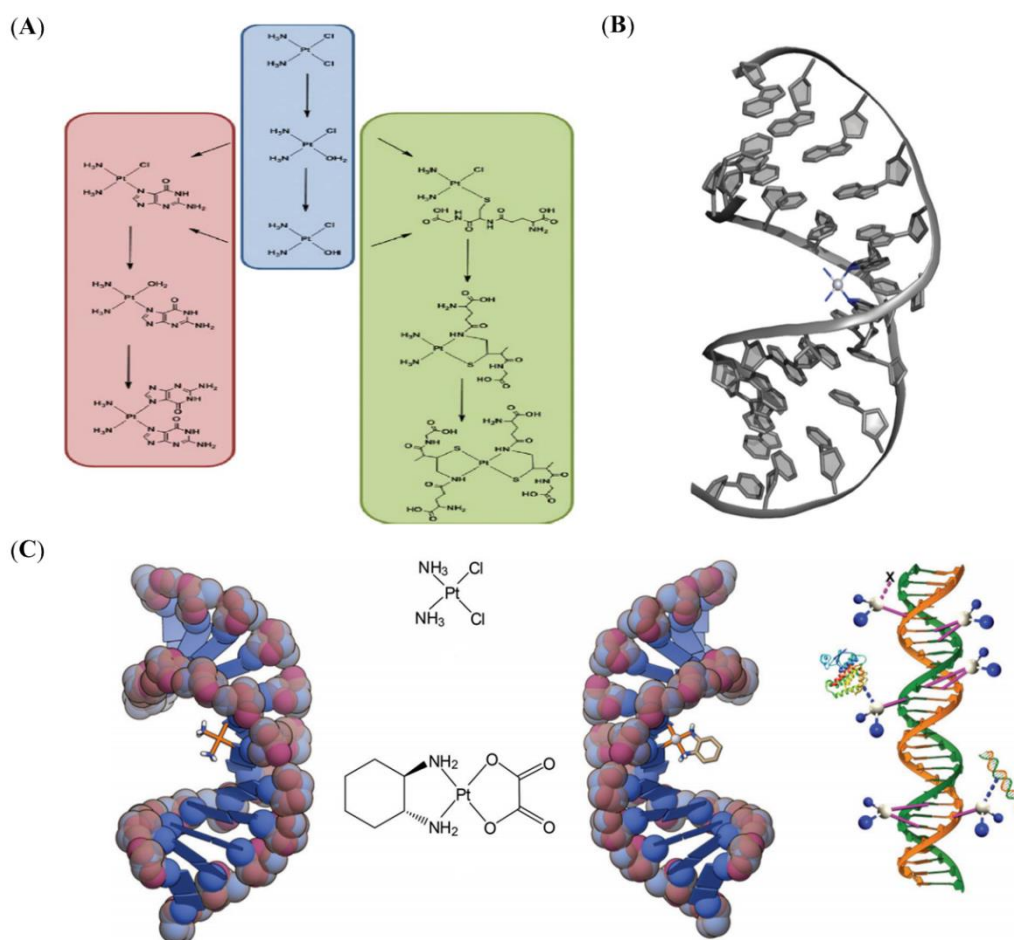


**Fig. 1.3:** (A) Simplified biological processing of cisplatin inside cells showing (blue) drug aquation, (red) DNA binding through the N7 of guanine and (green) deactivation and degradation by the tripeptide L-glutathione. Charges have been omitted for clarity.<sup>20</sup> (B) Crystal structure at 2.6 Å resolution of the intrastrand crosslink between cisplatin and the N7 atoms of adjacent guanines.<sup>21</sup> (C) Examples of 1,2-intrastrand adducts formed between DNA and cisplatin (left) and oxaliplatin (right), and an illustration of the numerous types of possible adduct formations (right).<sup>22</sup>

The clinical success of the platinum(II) drugs is immense, as they are among the most effective anticancer cytotoxins available and are currently utilised in 50% of all treatment regimes for solid tumours. This constitutes the most impressive contribution to the use

of metals in modern cancer chemotherapy but issues still remain. Platinum(II) drugs have severe side-effects, such as dose-limiting toxicity (nephrotoxicity), resistance to apoptosis, poor cancer cell selectivity and high mutagenicity, all of which are impeding factors in the abrogation of human cancer.<sup>23</sup>

The rigid, planar, aromatic and hydrophobic phenanthrene molecule (Figure 1.4) is highly conserved in nature being widely distributed and forming the parent structure or backbone of numerous natural and semi-synthetic alkaloids and opiates, including ascididemin, morphine, codeine and naloxone.<sup>24</sup> There are numerous other heteroaromatic derivatives of phenanthrene, one noteworthy molecule is 1,10-phenanthroline (1,10-phen, (1) Figure 1.4) which in addition to the aforementioned characteristics of planarity and hydrophobicity is also able to efficiently chelate numerous metals resulting in inorganic complexes such as  $[M(\text{phen})(\text{H}_2\text{O})_4]^{n+}$ ,  $[M(\text{phen})_2(\text{H}_2\text{O})_2]^{n+}$  and  $[M(\text{phen})_3]^{n+}$ .<sup>25</sup>

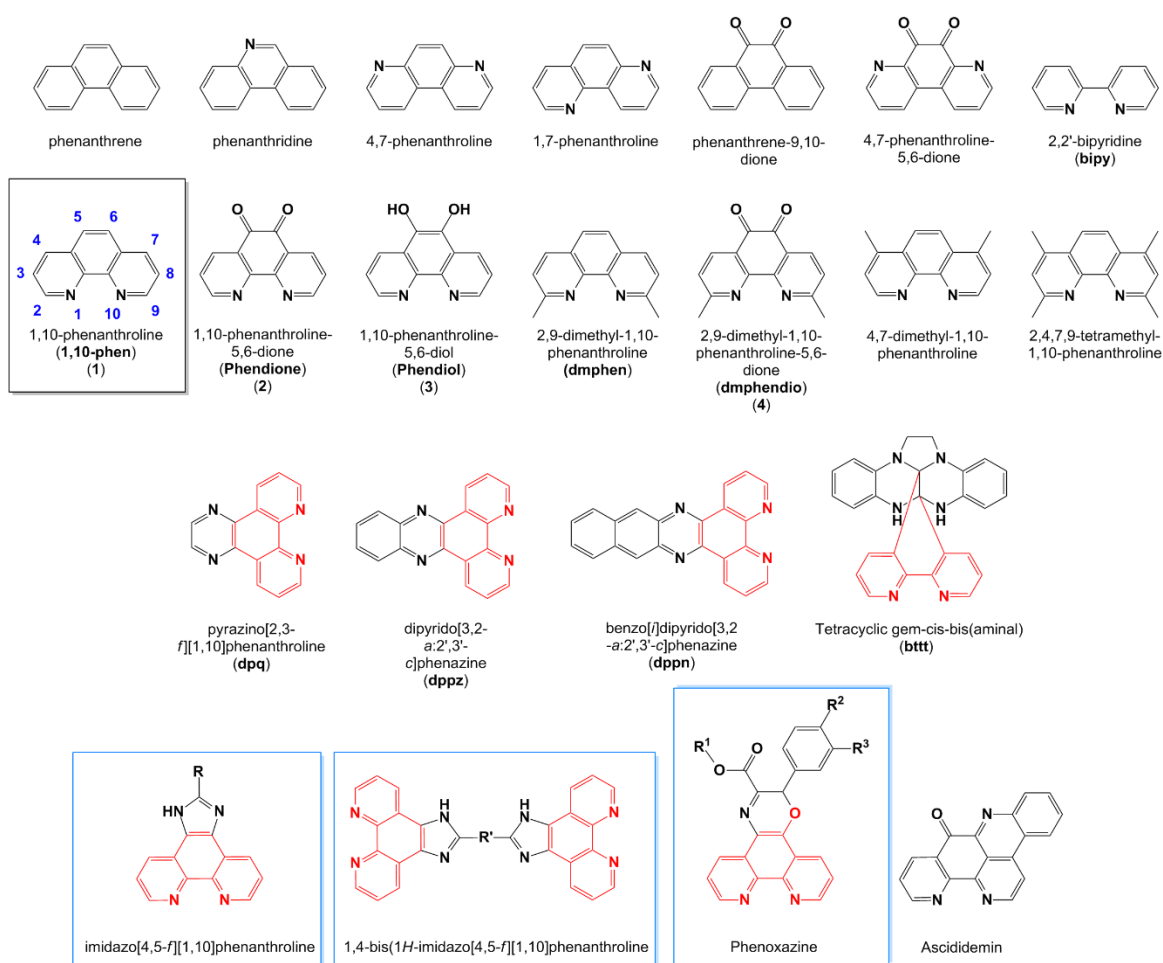


**Fig. 1.4:** Molecular structure of Phenanthrene, its many known and novel derivatives and also the chelating ligand 2,2'-bipyridine. Novel molecules detailed later in this thesis are highlighted in blue.



In addition, the quinone derivatives especially that of 1,10-phenanthroline-5,6-dione (phendione, **(2)** Figure 1.4) are of particular interest, as although they have lost the aromaticity of their central ring, they still retain their rigidity, planarity and lipophilicity/hydrophobicity whilst also having a redox active *O,O'*-quinonoid moiety.<sup>26</sup> Metal complexes of phenanthrene derivatives such as 1,10-phen (**(1)**) and phendione (**(2)**) which contain an *N,N'*-diimine chelation moiety have been extensively reported in the literature and have demonstrated significant potential as broad-spectrum cytotoxic agents towards diseases and infections manifested by cancer, viruses, bacteria and fungi.<sup>24a</sup>

Over 60 years ago, in 1952 Dr. Francis P. Dwyer and his co-workers published what became a landmark study on the biological activity of transition metal polypyridyl complexes, the most active of which were tris-1,10-phenanthroline and bis-1,10-phenanthroline metal complexes (Figure 1.5).<sup>27</sup> These complexes exhibited diverse biological activities, including toxicity in mice, inhibition of the enzyme acetylcholinesterase, antiviral activities (*in vitro/ in vivo* activity against *Herpes simplex*, *Vacinia*, *Polio* and *Adeno* viruses), bacteriostatic/bacteriocidal activity against *Escherichia coli* and *Staphylococcus haemolyticus* and *in vivo* anticancer activity.<sup>27-28</sup>

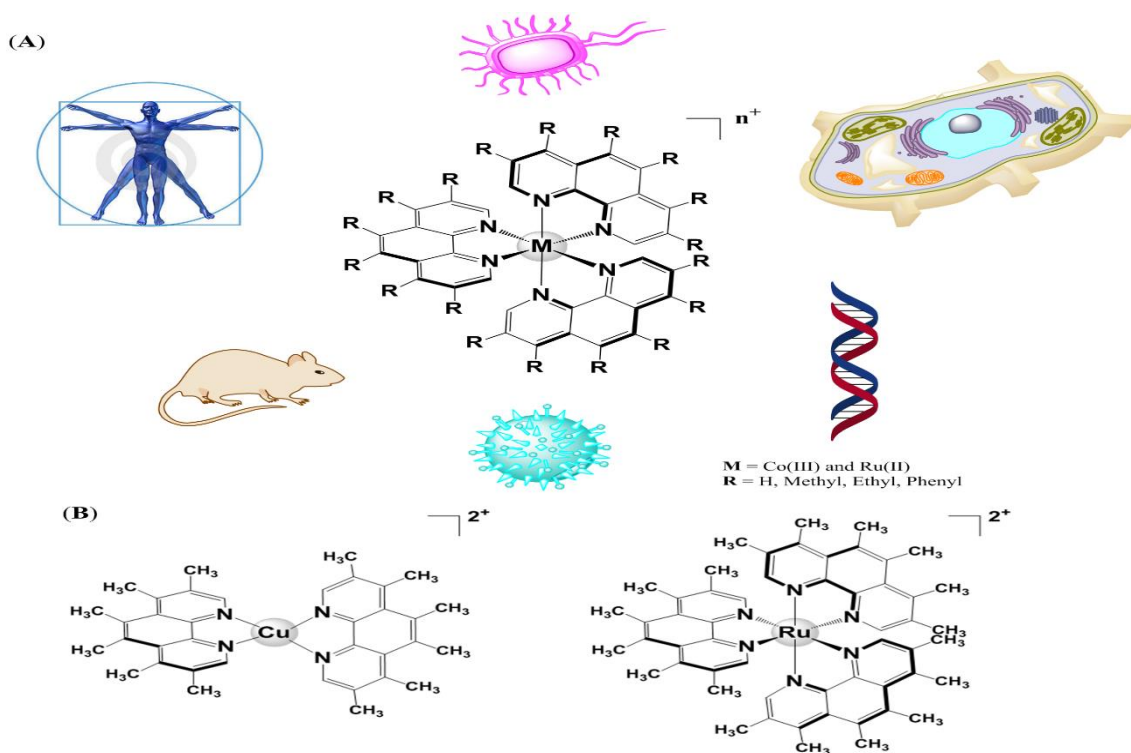


**Fig. 1.5:** (A) Graphical overview of results obtained by Dwyer, Shulman *et al* utilising 1,10-phenanthroline metal complexes. (B) Structure of their most active Cu(II) and Ru(II) 1,10-phen complexes.

Dwyer and his co-workers studied and evaluated these polypyridyl transition metal complexes frequently as chemically, redox, and configurationally stable ruthenium(II) complexes.<sup>27</sup>

Furthermore Dwyer, Shulman and others noted that the choice of ligand determines many pharmacological properties, as the binding of hydrophobic complexes to biomolecular entities is entropically favoured (dehydration processes) and that the higher complexation lipophilicity increases the penetration of complexes through biological membranes.<sup>27</sup> In particular the antibacterial activity of 1,10-phen complexes was found to increase with increasing hydrophobicity of the methyl-, ethyl-, and phenylated derivatives of 1,10-phen such as 3,4,7,8-tetramethyl-1,10-phenanthroline (3,4,7,8-Me<sub>4</sub>phen) (Figure 1.5 (B)).<sup>27, 29</sup> In addition, complexes such as [Cu(3,4,7,8-Me<sub>4</sub>phen)<sub>3</sub>]Cl<sub>2</sub> and [Ru(3,4,7,8-Me<sub>4</sub>phen)<sub>3</sub>]Cl<sub>2</sub> (Figure 1.5 (B)) displayed remarkable *in vivo* anticancer activity against Landshutz ascites tumour cells xenografted into the peritoneal cavity in mice.<sup>30</sup> The potency/efficacy of these complexes (in a similar manner as that observed for their antibacterial and antiviral activities) correlated with increasing hydrophobicity of the ligands and decreasing stability of the metal complex.<sup>27-30</sup> The copper(II) complex [Cu(3,4,7,8-Me<sub>4</sub>phen)<sub>3</sub>]Cl<sub>2</sub> displayed the greatest *in vivo* antitumoural activity, a single 5mg/kg intraperitoneal dose of which was sufficient to halt tumour growth in mice.<sup>27,30</sup> In an effort to elucidate the mode of action of these cytotoxic tris-1,10-phenanthroline metal complexes, Dwyer, Shulman and Mayhew incubated cells with [Ru(3,4,7,8-Me<sub>4</sub>phen)<sub>3</sub>]Cl<sub>2</sub> and observed the localisation of this complex using fluorescence microscopy.<sup>31</sup> The metal complex localised within the mitochondria and also the nucleus, suggesting that respiratory depression (which had been observed previously for virus infected cell lines treated with similar complexes) and reduction of mitochondrial oxidation as possible modes of action.<sup>27,31</sup>

The extraordinary stability of phosphodiester bonds is implicated in the preservation of genetic information with estimated half-lives of 200 x 10<sup>6</sup> and 800 years for DNA and RNA respectively (extrapolated from physiological stability data).<sup>32</sup> Despite the remarkable stability of nucleic acids, they can undergo facile cleavage (within minutes) in the presence of highly specialised protein based enzymes.<sup>32</sup> A nuclease is an enzyme capable of cleaving the phosphodiester bonds between the nucleotide subunits of nucleic

acids (see Chapter 5, section 5.3 for a more detailed discussion).<sup>33</sup> The first artificial nuclease was described by Sigman *et al* in 1979, which was a bis(1,10-phenanthroline) copper(II) complex,  $[\text{Cu}(\text{phen})_2]^{2+}$  (Figure 1.6).<sup>34</sup>

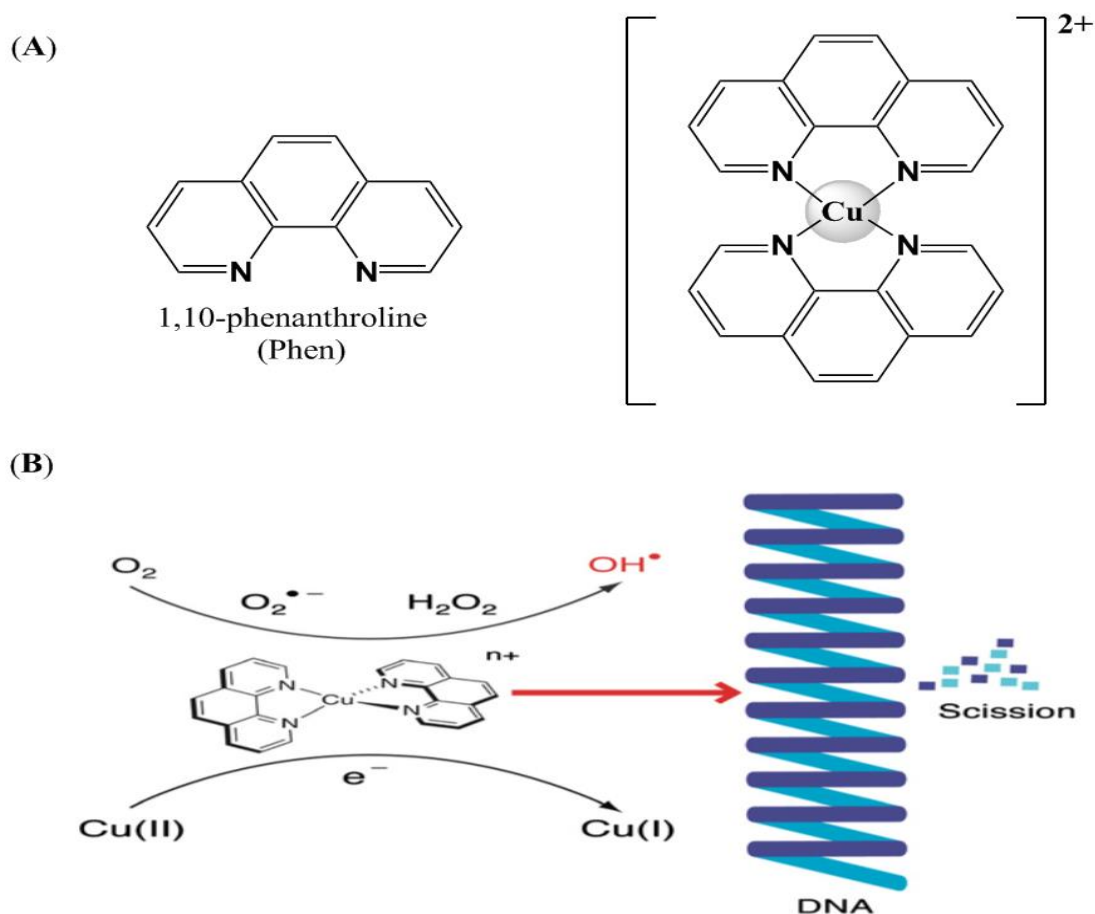


**Fig. 1.6:** (A) Molecular structure of 1,10-phenanthroline (phen) and the first artificial small molecule metallonuclease,  $[\text{Cu}(\text{phen})_2]^{2+}$ . Schematic representation of ROS generation and DNA scission by the first known synthetic artificial metallonuclease,  $[\text{Cu}(\text{phen})_2]^{2+}$ .<sup>34-35</sup>

This complex,  $[\text{Cu}(\text{phen})_2]^{2+}$ , can cleave DNA via a non-covalent binding mode known as intercalation, inserting into the hydrophobic space between the base pairs of DNA (Figure 1.7 (A),  $\pi - \pi$  stacking interactions), then in the presence of oxygen and a reductant generate reactive oxygen species (ROS) which induce chemical scission/cleavage of the DNA phosphodiester backbone (see Chapter 5, section 5.3).<sup>34,36</sup> This complex has several limitations which prevent it being utilised as a possible anticancer agent, such as, poor aqueous solubility, the need for both exogenous reductant

(e.g. L-ascorbic acid) and oxidant (e.g. O<sub>2</sub> or H<sub>2</sub>O<sub>2</sub>) and indiscriminate/ non-sequence specific DNA scission.

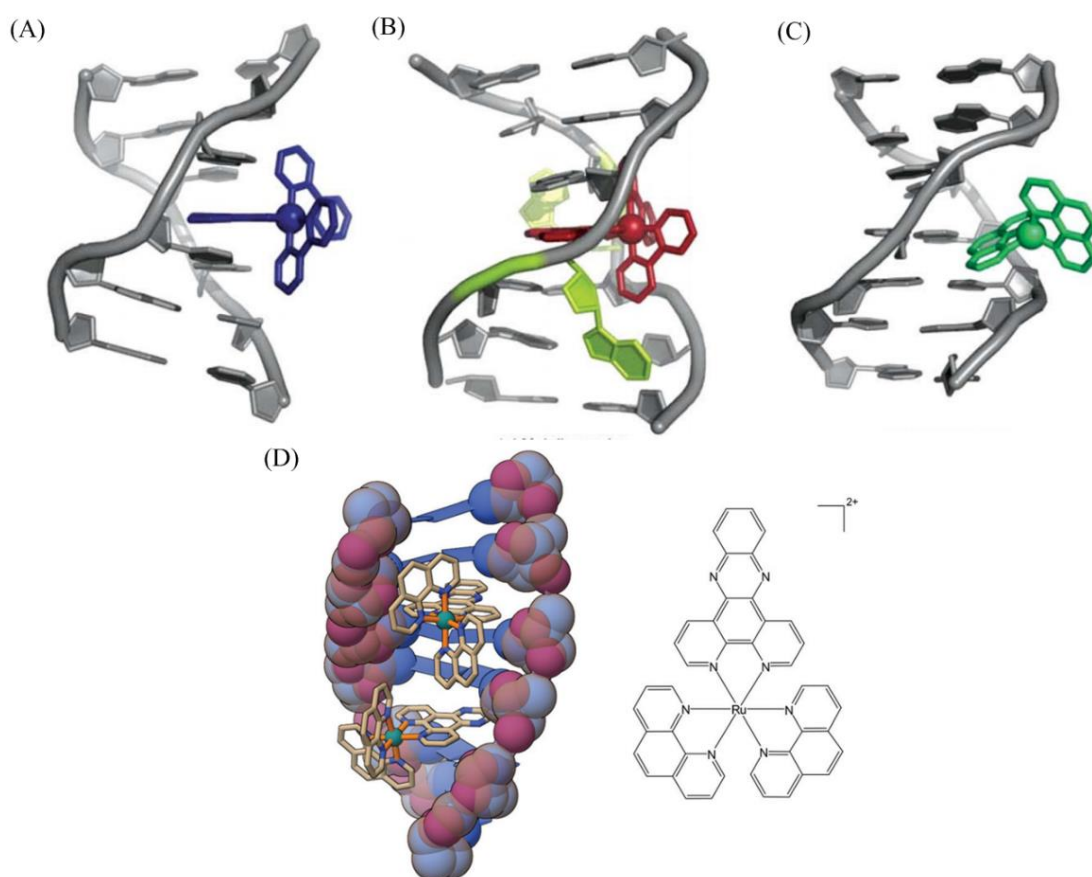


**Fig. 1.7:** The three binding modes of metal complexes with DNA: (A) intercalation, (B) insertion and (C) groove binding. (D) X-ray crystal structure of the complex *rac*-[Ru(phen)<sub>2</sub>(dppz)]<sup>2+</sup> intercalated with the DNA sequence d(ATGCAT)<sub>2</sub>.<sup>22, 37</sup>

Metallonucleases are capable of two types of nucleic acid cleavage, hydrolytic and oxidative cleavage.<sup>38</sup> Metallonucleases with redox-inert metal ions usually cleave nucleic acids hydrolytically whilst those comprised of redox-active metal ions usually cleave oxidatively (e.g. Bleomycin, see Chapter 5, section 5.3).<sup>36a</sup> Depending on the ligand moiety hydrolytic or oxidative (or both) reaction pathways can occur (Cu<sup>II</sup>/Cu<sup>I</sup> redox potential depends on its ligands).<sup>38-39</sup> Cu(II) containing complexes are particularly interesting as they are capable of both DNA hydrolysis as well as oxidation due to Cu(II) Lewis acidity and redox behaviour. The development of new and improved artificial small molecule chemical nucleases is an area of particular interest to molecular biologists and medicinal chemists. The site-selective scission of DNA is one particular goal of novel

artificial metallonucleases, as the cleavage of specific motifs or regions of DNA of viruses, bacteria or fungi might lead to the development of anti-infective agents.<sup>38</sup>

Another desirable attribute of artificial metallonuclease complexes is the cleavage of both DNA strands (double strand scission) as this usually results in irreparable damage to the cell. Improved solubility particularly aqueous solubility is highly desirable, as is a ‘self-activating’ mechanism of cleavage, which is a complex having no requirement for exogenous oxidant or reductant. A ‘self-activating’ complex could therefore be theoretically capable of DNA strand scission in low oxygen or hypoxic environments such as those present within cancerous cells of neoplastic tumours.<sup>40</sup> Many cytotoxic copper(II) complexes have been shown to possess DNA cleavage activity and as such there appears to be a relationship between these two properties.<sup>35, 38, 41</sup> From a medicinal viewpoint metal complexes which are capable of different modes of interaction with DNA such as DNA cleavage, DNA intercalation, DNA insertion and minor/major groove binding (Figure 1.7), in comparison to that of cisplatin could possibly possess a broader spectrum of antitumour activity and perhaps also diminished systemic toxicity and improved cytoselectivity.

Our research group has extensive experience in the synthetic development and use of phenanthrolines, particularly 1,10-phenanthroline, and their various metal complexes as antimicrobial and anticancer agents.<sup>24a, 35, 41-42</sup> We have also developed various 1,10-phenanthroline metal complexes as small molecule enzyme mimetics with particular focus on their nuclease capability as it relates to their cancer cell cytotoxicity.<sup>35, 41-42, 43</sup> One such complex previously synthesised by our research group was a ternary copper(II) 1,10-phen terephthalate complex,  $[\text{Cu}(\text{tereph})(\text{phen})_4]^{2+}$  (Figure 1.8).<sup>44</sup>

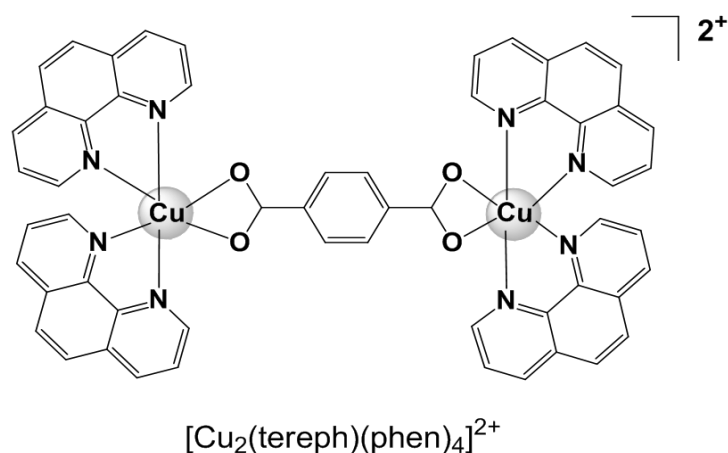


**Fig. 1.8:** Structure of cytotoxic, copper(II) 1,10-phen terephthalate complex,  $[\text{Cu}(\text{tereph})(\text{phen})_4]^{2+}$ .<sup>44</sup>

This complex,  $[\text{Cu}(\text{tereph})(\text{phen})_4]^{2+}$  (Figure 1.8), displayed excellent *in vitro* cytotoxicity towards intrinsically cisplatin-resistant ovarian cancer cells (SK-OV-3), produced intracellular ROS at nano-molar exposure and was a powerful, self-activating, non-sequence-specific, minor-groove oxidizer of duplex DNA.<sup>44</sup> Some of its limitations were poor solubility (organic and aqueous) non-specific DNA scission and it lacked any targeting moiety or cellular recognition functionality.

Building upon our previous successes we wished to synthesis novel analogues of ternary 1,10-phenanthroline/dicarboxylate metal complexes to overcome previous water-solubility issues, the *in vitro/in vivo* antimicrobial and antineoplastic capabilities of which will be discussed later. Secondly to develop a more facile method of preparing 1,10-phenanthroline derivatives namely imidazo[4,5-*f*][1,10]phenanthrolines which can incorporate various biologically relevant and targeting functional groups onto the backbone of the chelate ligand and then to coordinate these novel ligands to transition metals and test their bioactivity. Also to expand the scope of the synthesis of a novel phenoxazine molecule (Figure 1.4) to produce novel derivatives and investigate their concomitant coordination chemistry. Lastly our aim was to synthesise an imidazophenanthroline-folic acid-appended ligand and its corresponding Cu(II) and Mn(II) complexes. We hypothesised that this molecule and its complexes would be capable of selectively targeting the folate receptor expressed by certain cancer cell types and activated macrophages.<sup>45</sup> Macrophages are of interest as they act as reservoirs for *Mycobacterium tuberculosis* bacteria in infected individuals.<sup>46</sup>



## 1.4 References

1. Orvig, C.; Abrams, M. J., Medicinal inorganic chemistry: Introduction. *Chemical Reviews* **1999**, *99* (9), 2201-2203. 10.1021/cr980419w
2. Anastassopoulou, J.; Theophanides, T., The role of metal ions in biological systems and medicine. In *Bioinorganic Chemistry: An Inorganic Perspective of Life*, Kessissoglou, D. P., Ed. Kluwer Academic Publ: Dordrecht, 1995; Vol. 459, pp 209-218.
3. Holm, R. H.; Solomon, E. I., Bioinorganic enzymology - Preface. *Chemical Reviews* **1996**, *96* (7), 2237-2237.
4. Sadler, P. J., Inorganic Chemistry and Drug Design. *Advances in Inorganic Chemistry* **1991**, *36*, 1-48.
5. Nunn, J. F., *Ancient Egyptian Medicine*. University of Oklahoma Press: 2002.
6. Fricker, S. P., Literature highlights .39. Medicinal chemistry and pharmacology of gold compounds. *Transition Metal Chemistry* **1996**, *21* (4), 377-383. 10.1007/bf00139037
7. (a) Kean, W. F.; Lock, C. J. L.; Howardlock, H. E., Chirality in Antirheumatic Drugs. *Lancet* **1991**, *338* (8782-3), 1565-1568. 10.1016/0140-6736(91)92382-c; (b) Sadler, P. J., Gold—Progress in Chemistry, Biochemistry and Technology. H. Schmidbaur (ed.) John Wiley & Sons, Chichester, 1999 908 pages. £250 ISBN 0-471-97369-6. *Applied Organometallic Chemistry* **2000**, *14* (3), 171-171. 10.1002/(sici)1099-0739(200003)14:3<171::aid-aoc921>3.0.co;2-o
8. Williams, K. J., The introduction of 'chemotherapy' using arsphenamine - the first magic bullet. *Journal of the Royal Society of Medicine* **2009**, *102* (8), 343-348. 10.1258/jrsm.2009.09k036
9. (a) Albert, A., *Selective Toxicity: The physico-chemical basis of therapy*. Springer Netherlands: 1985. ; (b) Gibaud, S.; Jaouen, G., Arsenic-Based Drugs: From Fowler's Solution to Modern Anticancer Chemotherapy. In *Medicinal Organometallic Chemistry*, Jaouen, G.; MetzlerNolte, N., Eds. Springer-Verlag Berlin: Berlin, 2010; Vol. 32, pp 1-20. 10.1007/978-3-642-13185-1\_1
10. Lloyd, N. C.; Morgan, H. W.; Nicholson, B. K.; Ronimus, R. S., The composition of Ehrlich's salvarsan: Resolution of a century-old debate. *Angewandte Chemie-International Edition* **2005**, *44* (6), 941-944. 10.1002/aine.200461471

11. Rosenber.B; Vancamp, L.; Krigas, T., Inhibition of cell division in *Escherichia coli* by electrolysis products from a platinum electrode. *Nature* **1965**, 205 (4972), 698-&. 10.1038/205698a0
12. (a) Kauffman, G. B.; Pentimalli, R.; Doldi, S.; Hall, M. D., Michele Peyrone (1813-1883), Discoverer of Cisplatin. *Platinum Metals Review* **2010**, 54 (4), 250-256. 10.1595/147106710x534326; (b) Peyrone, M., Ueber die Einwirkung des Ammoniaks auf Platinchlorür. *Justus Liebigs Annalen der Chemie* **1844**, 51 (1), 1-29. 10.1002/jlac.18440510102
13. Rosenber.B; Vancamp, L.; Trosko, J. E.; Mansour, V. H., Platinum Compounds a new class of potent antitumour agents. *Nature* **1969**, 222 (5191), 385-&. 10.1038/222385a0
14. (a) <http://www.accessdata.fda.gov/scripts/cder/drugsatfda/index.cfm?fuseaction=SearchDrugDetails> Accessed on the 17/06/2014. ; (b) <http://www.cancer.gov/cancertopics/druginfo/cisplatin> Accessed on the 13/05/2014.
15. Hussain, S. A.; Ma, Y. T.; Cullen, M. H., Management of metastatic germ cell tumors. *Expert Review of Anticancer Therapy* **2008**, 8 (5), 771-784. 10.1586/14737140.8.5.771
16. Einhorn, L. H., Treatment of testicular cancer - A new and improved model. *Journal of Clinical Oncology* **1990**, 8 (11), 1777-1781.
17. Oh, W. K.; Tay, M. H.; Huang, J., Is there a role for platinum chemotherapy in the treatment of patients with hormone-refractory prostate cancer? *Cancer* **2007**, 109 (3), 477-486. 10.1002/cncr.22439
18. (a) Enoiu, M.; Jiricny, J.; Scharer, O. D., Repair of cisplatin-induced DNA interstrand crosslinks by a replication-independent pathway involving transcription-coupled repair and translesion synthesis. *Nucleic Acids Research* **2012**, 40 (18), 8953-8964. 10.1093/nar/gks670; (b) Jamieson, E. R.; Lippard, S. J., Structure, recognition, and processing of cisplatin-DNA adducts. *Chemical Reviews* **1999**, 99 (9), 2467-2498. 10.1021/cr980421n
19. Choy, H.; Park, C.; Yao, M., Current status and future prospects for satraplatin, an oral platinum analogue. *Clinical Cancer Research* **2008**, 14 (6), 1633-1638. 10.1158/1078-0432.ccr-07-2176



20. Wheate, N. J.; Walker, S.; Craig, G. E.; Oun, R., The status of platinum anticancer drugs in the clinic and in clinical trials. *Dalton Trans* **2010**, 39 (35), 8113-8127. 10.1039/c0dt00292e
21. Takahara, P. M.; Rosenzweig, A. C.; Frederick, C. A.; Lippard, S. J., Crystal Structure of Double Stranded DNA containing the Major Adduct of the anticancer drug Cisplatin. *Nature* **1995**, 377 (6550), 649-652. 10.1038/377649a0
22. Pages, B. J.; Ang, D. L.; Wright, E. P.; Aldrich-Wright, J. R., Metal complex interactions with DNA. *Dalton Trans* **2015**, 44 (8), 3505-3526. 10.1039/c4dt02700k
23. Kelland, L., The resurgence of platinum-based cancer chemotherapy. *Nat Rev Cancer* **2007**, 7 (8), 573-584. 10.1038/nrc2167
24. (a) McCann, M.; Santos, A. L. S.; da Silva, B. A.; Romanos, M. T. V.; Pyrrho, A. S.; Devereux, M.; Kavanagh, K.; Fichtner, I.; Kellett, A., In vitro and in vivo studies into the biological activities of 1,10-phenanthroline, 1,10-phenanthroline-5,6-dione and its copper(ii) and silver(i) complexes. *Toxicology Research* **2012**, 1 (1), 47. 10.1039/c2tx00010e; (b) Kobayashi, J.; Cheng, J. F.; Nakamura, H.; Ohizumi, Y.; Hirata, Y.; Sasaki, T.; Ohta, T.; Nozoe, S., Ascidiemin, A Novel pentacyclic aromatic alkaloid with potent Antileukemic activity from the Okinawan Tunicate *Didemnum Sp.* *Tetrahedron Letters* **1988**, 29 (10), 1177-1180. 10.1016/s0040-4039(00)86681-2
25. Mingos, D. M. P.; Crabtree, R. H.; Canty, A., *Comprehensive organometallic chemistry III: Compounds of group 10*. Elsevier: 2007.
26. Goss, C. A.; Abruna, H. D., Spectral, electrochemical, and electrocatalytic properties of 1,10-phenanthroline-5,6-dione complexes of transition-metals. *Inorganic Chemistry* **1985**, 24 (25), 4263-4267. 10.1021/ic00219a012
27. Kilah, N. L.; Meggers, E., Sixty Years Young: The Diverse Biological Activities of Metal Polypyridyl Complexes Pioneered by Francis P. Dwyer. *Australian Journal of Chemistry* **2012**, 65 (9), 1325-1332. 10.1071/ch12275
28. White, D. O.; Shulman, A.; Harris, A. W., Actions of Metal Chelates of Substituted 1,10-Phenanthrolines on Viruses and Cells. 2. Inhibition of Viral Multiplication *Australian Journal of Experimental Biology and Medical Science* **1963**, 41 (5), 527-&. 10.1038/icb.1963.43
29. Butler, H. M.; Hurse, A.; Thursky, E.; Shulman, A., Bactericidal Action of selected Phenanthroline Chelates and related compounds. *Australian Journal of*

- Experimental Biology and Medical Science* **1969**, 47, 541-&. 10.1038/icb.1969.148
30. Dwyer, F. P.; Mayhew, E.; Roe, E. M. F.; Shulman, A., Inhibition of Landschutz Ascites Tumour growth by Metal Chelates derived from 3,4,7,8-tetramethyl-1,10-phenanthroline. *British Journal of Cancer* **1965**, 19 (1), 195-&. 10.1038/bjc.1965.24
31. Mayhew, E.; Roe, E. M.; Shulman, A., Microscopical observations on the effects of phenanthroline chelates on Landschutz ascites tumour cells. *Journal. Royal Microscopical Society (Great Britain)* **1965**, 85 (4), 475-483.
32. Zenkova, M. A., *Artificial Nucleases*. Springer Berlin Heidelberg: 2004.
33. Lehninger, A. L.; Nelson, D. L.; Cox, M. M., *Lehninger Principles of Biochemistry*. W. H. Freeman: 2005.
34. Sigman, D. S.; Graham, D. R.; Daurora, V.; Stern, A. M., Oxygen-dependent cleavage of DNA by the 1,10-phenanthroline cuprous complex - inhibition of escherichia-coli DNA-polymerase-I. *Journal of Biological Chemistry* **1979**, 254 (24), 2269-2272.
35. Kellett, A.; Howe, O.; O'Connor, M.; McCann, M.; Creaven, B. S.; McClean, S.; Kia, A. F. A.; Casey, A.; Devereux, M., Radical-induced DNA damage by cytotoxic square-planar copper(II) complexes incorporating o-phthalate and 1,10-phenanthroline or 2,2'-dipyridyl. *Free Radical Biology and Medicine* **2012**, 53 (3), 564-576. 10.1016/j.freeradbiomed.2012.05.034
36. (a) Mancin, F.; Scrimin, P.; Tecilla, P.; Tonellato, U., Artificial metallonucleases. *Chem Commun (Camb)* **2005**, (20), 2540-2548. 10.1039/b418164f; (b) Pitie, M.; Pratviel, G., Activation of DNA Carbon-Hydrogen Bonds by Metal Complexes. *Chemical Reviews* **2010**, 110 (2), 1018-1059. 10.1021/cr900247m; (c) Sigman, D. S., Chemical Nucleases. *Biochemistry* **1990**, 29 (39), 9097-9105. 10.1021/bi00491a001
37. Zeglis, B. M.; Pierre, V. C.; Barton, J. K., Metallo-intercalators and metallo-insertors. *Chem Commun (Camb)* **2007**, (44), 4565-4579. 10.1039/b710949k
38. Wende, C.; Ludtke, C.; Kulak, N., Copper Complexes of N-Donor Ligands as Artificial Nucleases. *European Journal of Inorganic Chemistry* **2014**, (16), 2597-2612. 10.1002/ejic.201400032
39. Marzano, C.; Pellei, M.; Tisato, F.; Santini, C., Copper Complexes as Anticancer Agents. *Anti-Cancer Agents in Medicinal Chemistry* **2009**, 9 (2), 185-211.

40. (a) Blagosklonny, M. V., Antiangiogenic therapy and tumor progression. *Cancer Cell* **2004**, *5* (1), 13-17. 10.1016/s1535-6108(03)00336-2; (b) Ide, T.; Kitajima, Y.; Miyoshi, A.; Ohtsuka, T.; Mitsuno, M.; Ohtaka, K.; Miyazaki, K., The hypoxic environment in tumor-stromal cells accelerates pancreatic cancer progression via the activation of paracrine hepatocyte growth factor/c-Met signaling. *Annals of Surgical Oncology* **2007**, *14* (9), 2600-2607. 10.1245/s10434-007-9435-3; (c) Weber, C. E.; Kuo, P. C., The tumor microenvironment. *Surgical Oncology-Oxford* **2012**, *21* (3), 172-177. 10.1016/j.suronc.2011.09.001
41. (a) Kellett, A.; O'Connor, M.; McCann, M.; Howe, O.; Casey, A.; McCarron, P.; Kavanagh, K.; McNamara, M.; Kennedy, S.; May, D. D.; Skell, P. S.; O'Shea, D.; Devereux, M., Water-soluble bis(1,10-phenanthroline) octanedioate  $\text{Cu}^{2+}$  and  $\text{Mn}^{2+}$  complexes with unprecedented nano and picomolar in vitro cytotoxicity: promising leads for chemotherapeutic drug development. *MedChemComm* **2011**, *2* (7), 579. 10.1039/c0md00266f; (b) Kellett, A.; O'Connor, M.; McCann, M.; McNamara, M.; Lynch, P.; Rosair, G.; McKee, V.; Creaven, B.; Walsh, M.; McClean, S.; Foltyn, A.; O'Shea, D.; Howe, O.; Devereux, M., Bis-phenanthroline copper(II) phthalate complexes are potent in vitro antitumour agents with 'self-activating' metallo-nuclease and DNA binding properties. *Dalton Trans* **2011**, *40* (5), 1024-1027. 10.1039/c0dt01607a
42. (a) Devereux, M.; McCann, M.; Cronin, J. F.; Ferguson, G.; McKee, V., Binuclear and polymeric copper(II) dicarboxylate complexes: syntheses and crystal structures of  $[\text{Cu}_2(\text{pda})(\text{Phen})_4](\text{ClO}_4)_2 \cdot 5\text{H}_2\text{O} \cdot \text{C}_2\text{H}_5\text{OH}$ ,  $[\text{Cu}_2(\text{oda})(\text{Phen})_4](\text{ClO}_4)_2 \cdot 2.67\text{H}_2\text{O} \cdot \text{C}_2\text{H}_5\text{OH}$  and  $\{[\text{Cu}_2(\text{pda})_2(\text{NH}_3)_4(\text{H}_2\text{O})_2] \cdot 4\text{H}_2\text{O}\}_n$  (odaH<sub>2</sub>=octanedioic acid; pdaH<sub>2</sub>=pentanedioic acid; Phen=1,10-phenanthroline). *Polyhedron* **1999**, *18* (16), 2141-2148. 10.1016/s0277-5387(99)00100-x; (b) Devereux, M.; McCann, M.; Leon, V.; Geraghty, M.; McKee, V.; Wikaira, J., Synthesis and fungitoxic activity of manganese(II) complexes of fumaric acid: X-ray crystal structures of  $[\text{Mn}(\text{fum})(\text{bipy})(\text{H}_2\text{O})]$  and  $[\text{Mn}(\text{Phen})_2(\text{H}_2\text{O})_2(\text{fum})] \cdot 4\text{H}_2\text{O}$  (fumH<sub>2</sub> = fumaric acid; bipy=2,2'-bipyridine; phen=1,10-phenanthroline). *Polyhedron* **2000**, *19* (10), 1205-1211. 10.1016/s0277-5387(00)00372-7; (c) Devereux, M.; McCann, M.; Leon, V.; Geraghty, M.; McKee, V.; Wikaira, J., Synthesis and biological activity of manganese (II) complexes of phthalic and isophthalic acid: X-ray crystal

- structures of  $[\text{Mn}(\text{ph})(\text{phen})_2(\text{H}_2\text{O})] \cdot 4\text{H}_2\text{O}$ ,  $[\text{Mn}(\text{phen})_2(\text{H}_2\text{O})_2]_2(\text{Isoph})_2(\text{phen}) \cdot 12\text{H}_2\text{O}$  and  $\{[\text{Mn}(\text{isoph})(\text{bipy})]_4 \cdot 2.75\text{bipy}\}_n$  (phH<sub>2</sub> = phthalic acid; isoph = isophthalic acid; phen = 1,10-phenanthroline; bipy = 2,2-bipyridine). *Metal-Based Drugs* **2000**, *7* (5), 275-288. 10.1155/mbd.2000.275; (d) McCann, M.; Coyle, B.; McKay, S.; McCormack, P.; Kavanagh, K.; Devereux, M.; McKee, V.; Kinsella, P.; O'Connor, R.; Clynes, M., Synthesis and X-ray crystal structure of  $[\text{Ag}(\text{phendio})_2]\text{ClO}_4$  (phendio=1,10-phenanthroline-5,6-dione) and its effects on fungal and mammalian cells. *Biometals* **2004**, *17* (6), 635-645. 10.1007/s10534-004-1229-5; (e) McCann, M.; Geraghty, M.; Devereux, M.; O'Shea, D.; Mason, J.; O'Sullivan, L., Insights into the mode of action of the anti-Candida activity of 1,10-phenanthroline and its metal chelates. *Metal-Based Drugs* **2000**, *7* (4), 185-193. 10.1155/mbd.2000.185; (f) McCann, M.; Kellett, A.; Kavanagh, K.; Devereux, M.; Santos, A. L. S., Deciphering the Antimicrobial Activity of Phenanthroline Chelators. *Current Medicinal Chemistry* **2012**, *19* (17), 2703-2714.
43. (a) McCann, M.; McGinley, J.; Ni, K.; O'Connor, M.; Kavanagh, K.; McKee, V.; Colleran, J.; Devereux, M.; Gathergood, N.; Barron, N.; Prisecaru, A.; Kellett, A., A new phenanthroline-oxazine ligand: synthesis, coordination chemistry and atypical DNA binding interaction. *Chem Commun (Camb)* **2013**, *49* (23), 2341-2343. 10.1039/c3cc38710k; (b) McCann, S.; McCann, M.; Casey, M. T.; Devereux, M.; McKee, V.; McMichael, P.; McCrea, J. G., Manganese(II) complexes of 3,6,9-trioxaundecanedioic acid (3,6,9-tddaH<sub>2</sub>): X-ray crystal structures of  $[\text{Mn}(3,6,9\text{-tdda})(\text{H}_2\text{O})_2] \cdot 2\text{H}_2\text{O}$  and  $\{[\text{Mn}(3,6,9\text{-tdda})(\text{phen})_2 \cdot 3\text{H}_2\text{O}] \cdot \text{EtOH}\}_n$ . *Polyhedron* **1997**, *16* (24), 4247-4252. 10.1016/s0277-5387(97)00233-7
44. Prisecaru, A.; Devereux, M.; Barron, N.; McCann, M.; Colleran, J.; Casey, A.; McKee, V.; Kellett, A., Potent oxidative DNA cleavage by the di-copper cytotoxin:  $[\text{Cu}_2(\mu\text{-terephthalate})(1,10\text{-phen})_4]^{2+}$ . *Chem Commun (Camb)* **2012**, *48* (55), 6906-6908. 10.1039/c2cc31023f
45. (a) Jain, N. K.; Mishra, V.; Mehra, N. K., Targeted drug delivery to macrophages. *Expert Opinion on Drug Delivery* **2013**, *10* (3), 353-367. 10.1517/17425247.2013.751370; (b) Leemans, J. C.; Thepen, T.; Weijer, S.; Florquin, S.; van Rooijen, N.; van de Winkel, J. G.; van der Poll, T., Macrophages play a dual role during pulmonary tuberculosis in mice. *Journal of Infectious*

- Diseases* **2005**, *191* (1), 65-74. 10.1086/426395; (c) Vlahov, I. R.; Leamon, C. P., Engineering folate-drug conjugates to target cancer: from chemistry to clinic. *Bioconjug Chem* **2012**, *23* (7), 1357-1369. 10.1021/bc2005522; (d) Xia, W.; Hilgenbrink, A. R.; Matteson, E. L.; Lockwood, M. B.; Cheng, J. X.; Low, P. S., A functional folate receptor is induced during macrophage activation and can be used to target drugs to activated macrophages. *Blood* **2009**, *113* (2), 438-446. 10.1182/blood-2008-04-150789
46. Podinovskaia, M.; Lee, W.; Caldwell, S.; Russell, D. G., Infection of macrophages with *Mycobacterium tuberculosis* induces global modifications to phagosomal function. *Cellular Microbiology* **2013**, *15* (6), 843-859. 10.1111/cmi.12092

# **Chapter 2**

# **Experimental methods and instrumentation**

## 2.1 Chemicals

The following chemicals were purchased and used as received:

1,10-phenanthroline, KBrO<sub>3</sub>, L-dopa (L-3,4-dihydroxyphenylalanine), L-tyrosine (4-hydroxyphenylalanine), sulfuric Acid (H<sub>2</sub>SO<sub>4</sub>), nitric acid, 1-propanol, cerium (IV) ammonium nitrate (CAN), Ag(ClO<sub>4</sub>), Mn(ClO<sub>4</sub>)<sub>2</sub>.6H<sub>2</sub>O, Cu(ClO<sub>4</sub>)<sub>2</sub>.6H<sub>2</sub>O, 5-nitro-2-furaldehyde, 3-thiophenecarboxaldehyde, 2-thiophenecarboxaldehyde, 3-hydroxy-4-nitrobenzaldehyde, terephthalaldehyde, diphenylacetaldehyde, 4-(trifluoromethyl)benzaldehyde, 4-benzyloxy-3-methoxybenzaldehyde, 4-formylbenzotrile, fluorene-2-carboxaldehyde, 1-pyrenecarboxyaldehyde, Ferrocenecarboxaldehyde, biphenyl-3-carboxyaldehyde, 3,5-bis(trifluoromethyl)benzaldehyde, hydrazine monohydrate, acetyl chloride, ammonium acetate, palladium on carbon (10% and 5% loading), neocuproine hemihydrate, potassium bromide.

### 2.1.2 Chemicals for the preparation of biological preparations – *Candida*

#### *Albicans*

*Candida* ATCC 10231 was obtained from the American Type Culture Collection (ATCC), Manassas, VA, USA.

Yeast Extract Peptone Dextrose (YEPD) media was composed of 2% (w/v) glucose, 2% (w/v) bacteriological peptone and 1% (w/v) yeast extract. To solidify the media to make agar plates 2% (w/v) bacteriological agar was added to the above mixture when required.

Minimal Growth Media (MM) was composed of 2% (w/v) glucose, 0.5% (w/v) ammonium sulphate and 0.17% (w/v) yeast nitrogen base (without amino acids or ammonium sulphate).

Phosphate Buffered Saline (PBS) was obtained from Aldrich and made up according to the manufacturer's instructions (1 tablet in 200 cm<sup>3</sup> deionised water). Deionised water was used to make up all media.

### 2.1.3 Chemicals for the preparation of biological preparations: Bacteria

Chemicals were purchased from commercial sources and were used without further purification. Deionised water was used to make up all media.

The nutrient broth medium containing peptone, yeast extract and nutrient agar was purchased from Scharlau Microbiology and made up using the manufacturer's instructions in sterilised water (13 g in 1 L of deionised water).

*Escherichia coli* (*E.coli*) were supplied as a clinical isolate by the Clinical Microbiology Laboratory, St. James' Hospital, Dublin, Ireland and were originally isolated from a Gastro-intestinal tract infection.

*Staphylococcus aureus* were supplied as a clinical isolate by the Clinical Microbiology Laboratory, St. James' Hospital, Dublin, Ireland and was originally isolated from a Urinary tract infection.

Methicillin resistant *Staphylococcus aureus* (MRSA) was obtained as a clinical isolate from Microbiologics, North St. Cloud Mn, USA and was originally isolated from a wound infection.

*Pseudomonas aeruginosa* 27853 and 10145 were both obtained from the American Type Culture Collection (ATCC) Marassas, VA, USA.

## 2.2 Instrumentation

Melting points were measured on a Stuart melting point apparatus.

Nuclear Magnetic Resonance (NMR) spectra were measured on a Bruker Avance 300 spectrometer using tetramethylsilane as an internal reference for  $^1\text{H}$  shifts. Coupling constants  $J$  are given in Hz. Multiplicity as follows: s (singlet), d (doublet), appd (apparent doublet), t (triplet), appt (apparent triplet), m (multiplet).

Electrospray (ESI) mass spectra were collected on an Agilent Technologies 6410 Time of Flight LC/MS. The interpretation of mass spectra was aided by the program "Agilent Masshunter Workstation" software. Yields refer to isolated amount of compound unless stated otherwise. Solvents were purified according to literature procedures.



Infrared Spectra (IR) were obtained within the region of 4000-400  $\text{cm}^{-1}$  on a Perkin Elmer System 2000 FT-IR spectrometer. The samples were prepared by KBr method.

The CHN elemental analysis was carried out using a FLASH EA 1112 Series Elemental Analyser with Eager 300 operating software.

Magnetic moment measurement was conducted using a Johnson Matthey Magnetic Susceptibility Balance with  $\text{Hg}[\text{Co}(\text{SCN})_4]$  used as a reference standard.

Sterilisation of microbiological equipment and media was carried out in a Dixons ST2228 autoclave at 121 °C and 124 kPa for 20 min. Solutions that were susceptible to decomposition during autoclaving were sterilised by membrane filtration using 0.45  $\mu\text{m}$  Millipore membrane filters. All worktops and benches were sterilised by washing with 70% (v/v) EtOH/water prior to use.

Fungal cell density was measured using a Neubauer hemocytometer under a light microscope at a magnification of x400. Bacterial cell density was recorded at an optical density of 600 nm using an Eppendorf Biophotometer.

Significance of the survival rates of *G. mellonella* larvae was analysed at 24, 48 and 72 h intervals using the log rank (Mantel-Cox) method utilising GraphPad Prism software (version 6). Three categories of significance were used (\* =  $p < 0.05$ , \*\* =  $p < 0.01$  and \*\*\* =  $p < 0.001$ ).

## 2.3 Synthesis of 1, 10-phenanthroline phthalate complexes.

### 2.3.1 Synthesis of $[\text{Mn}(\text{ph})]0.5\text{H}_2\text{O}$ (PC 1)<sup>1</sup>

Please note that throughout the thesis all coordination complex formulations are based on IR, microanalytic and mass spectral data were available. Coordination complex formulas based on X-Ray crystallographic data will be clearly indicated.

The synthesis of this complex is as per previously published<sup>1</sup> with the following modifications:

A solution of 1.25 g (7.52 mmol) phthalic acid ( $\text{pH}_2$ ) in 20  $\text{cm}^3$  EtOH was added to a solution of 2.00 g (8.16 mmol) manganese(II) acetate in 80  $\text{cm}^3$  EtOH in a 250  $\text{cm}^3$  RB flask. The resulting pink mixture was then refluxed for 2 hrs before being allowed to cool

to room temperature, and then cooled further on an ice bath. A white solid precipitated which was then filtered and washed with 80 cm<sup>3</sup> EtOH in two portions and air dried.

Product formula weight (**PC 1**) = 228.06g/mol

Yield: 1.25g (72.89%)

% Calculated: C: 42.13, H: 2.21

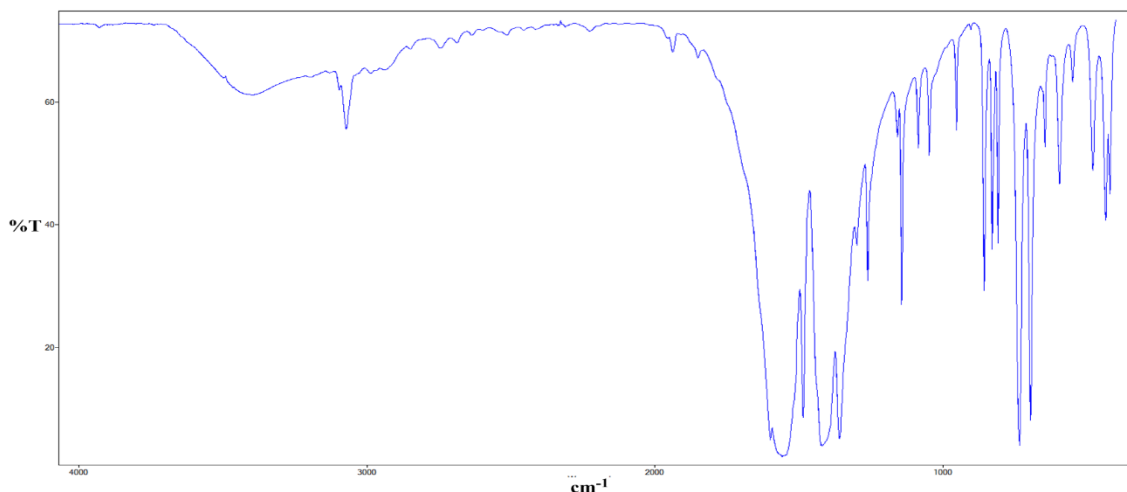
% Found: C: 42.40, H: 1.92

IR (KBr)  $\nu_{\text{max}}$ : 34089, 3073, 1555, 1488, 1420, 1361, 1260, 1146, 1092, 1052, 951, 856, 830, 808, 735, 695, 649, 595 cm<sup>-1</sup>

$\mu_{\text{eff}}$ : 5.91 B.M.

Solubility: Soluble in dist. H<sub>2</sub>O, ether (partially). Insoluble in EtOH, MeOH, acetone and CHCl<sub>3</sub>.

IR (KBr): **[Mn(ph)]0.5H<sub>2</sub>O (PC 1)**



### 2.3.2 Synthesis of [Mn(isoph)]2H<sub>2</sub>O (PC 2)<sup>1</sup>

The synthesis of this complex is as per previously published<sup>1</sup> with the following modifications:

A solution of 1.10 g (6.62 mmol) isophthalic acid (isophH<sub>2</sub>) in 25 cm<sup>3</sup> EtOH was added to a solution of 1.78 g (7.26 mmol) manganese(II) acetate in 75 cm<sup>3</sup> EtOH in a 250 cm<sup>3</sup> round bottomed flask. The resulting pale orange mixture was then refluxed for 2 hrs before being allowed to cool to room temperature, and then cooled further on an ice bath. A white solid precipitated which was then filtered and washed with 80 cm<sup>3</sup> EtOH in two portions and allowed to air dry.

Product formula weight (**PC 2**) = 255.08g/mol

Yield: 1.66g (98.31%)

% Calculated: C: 37.67, H: 3.16

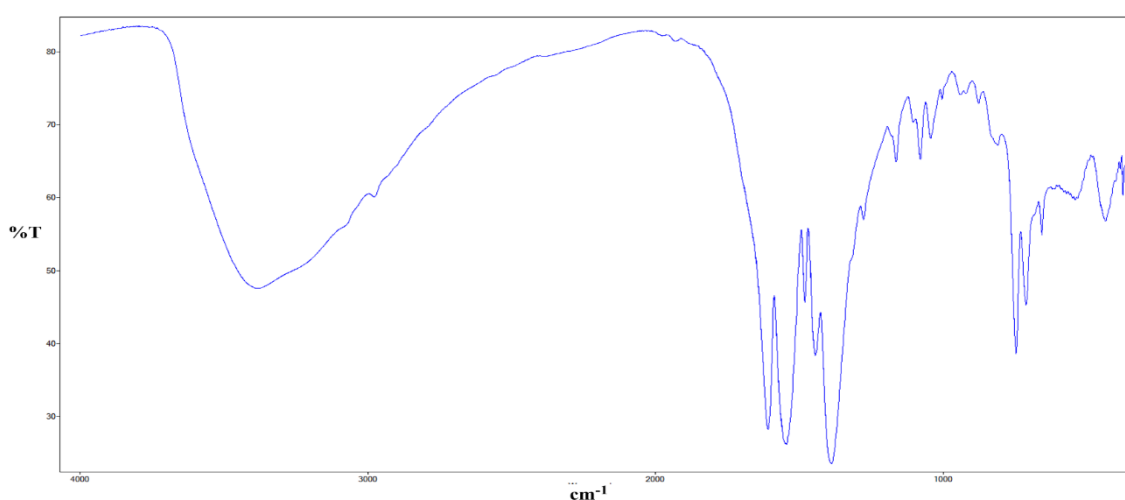
% Found: C: 37.35, H: 2.90

IR (KBr)  $\nu_{\text{max}}$ : 3315, 2281, 1649, 1616, 1548, 1481, 1455, 1381, 1166, 1085, 1005, 944, 816, 808, 736, 696, 541, 447 cm<sup>-1</sup>

$\mu_{\text{eff}}$ : 5.74 B.M.

Solubility: Soluble in H<sub>2</sub>O (hot), MeOH (hot). Insoluble in EtOH, ether, acetone and CHCl<sub>3</sub>.

IR (KBr): **[Mn(isoph)]2H<sub>2</sub>O (PC 2)**



### 2.3.3 Synthesis of $[\text{Mn}(\text{terph})]2.5\text{H}_2\text{O}$ (PC 3)<sup>1</sup>

The synthesis of this complex is as per previously published<sup>1</sup> with the following modifications:

A solution of 0.51 g (3.07 mmol) terephthalic acid ( $\text{terphH}_2$ ) in 25 cm<sup>3</sup> EtOH was added to a solution of 0.83 g (3.39 mmol) manganese(II) acetate in 75 cm<sup>3</sup> EtOH in a 250 cm<sup>3</sup> round bottomed flask. The resulting pale orange mixture was then refluxed for 2 hrs before being allowed to cool to room temperature, and then cooled further on an ice bath. A white solid precipitated which was then filtered and washed with 80 cm<sup>3</sup> EtOH in two portions and allowed to air dry.

Product formula weight (PC 3) = 264.09g/mol

Yield: 0.68g (83.87%)

% Calculated: C: 36.38, H: 3.43

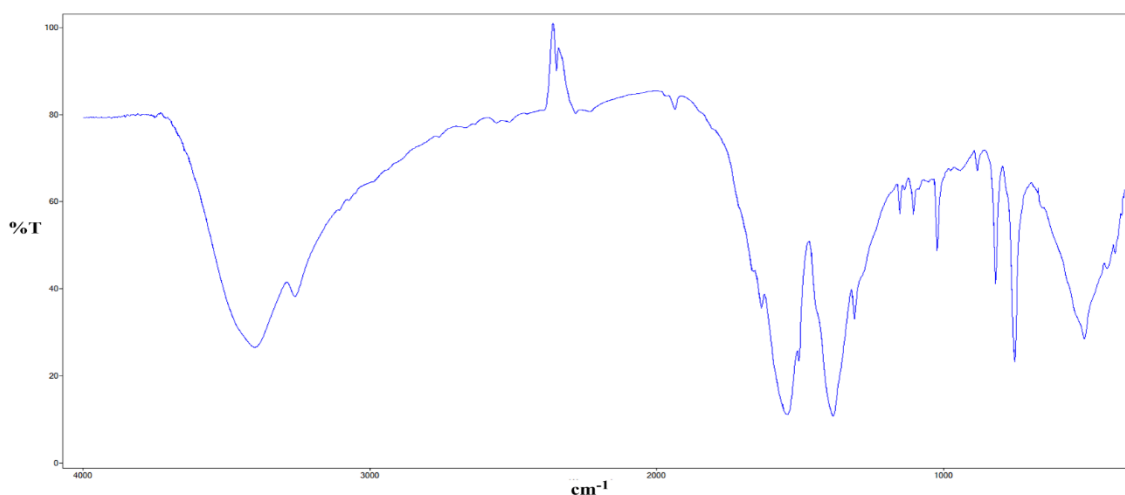
% Found: C: 36.37, H: 3.51

IR (KBr)  $\nu_{\text{max}}$ : 3416, 3255, 1636, 1555, 1495, 1387, 1313, 1152, 1105, 1025, 816, 756, 514 cm<sup>-1</sup>

$\mu_{\text{eff}}$ : 6.17 B.M.

Solubility: Soluble in H<sub>2</sub>O (hot), partially soluble in hot MeOH, EtOH, ether, acetone and CHCl<sub>3</sub>.

IR (KBr):  $[\text{Mn}(\text{terph})]2.5\text{H}_2\text{O}$  (PC 3)



### 2.3.4 Synthesis of [Mn(ph)(phen)]2H<sub>2</sub>O (**8**) and [Mn(ph)(phen)<sub>2</sub>(H<sub>2</sub>O)]4H<sub>2</sub>O (**9**) (Crystal structure formulation)<sup>1</sup>

The synthesis of these complexes is as per previously published<sup>1</sup> with the following modifications:

A solution of 0.50 g (2.19 mmol) [Mn(ph)]0.5H<sub>2</sub>O (**PC 1**) in 25 cm<sup>3</sup> EtOH was added to a solution of 0.81 g (4.50 mmol) 1,10-phenanthroline in 25 cm<sup>3</sup> EtOH in a 250 cm<sup>3</sup> round bottomed flask. The resulting yellow mixture was then refluxed for 2 hrs before being allowed to cool to room temperature, and then cooled further on an ice bath. A yellow solid precipitated which was then filtered and washed with 80 cm<sup>3</sup> EtOH in two portions and allowed to air dry.

Product formula weight (**8**) = 435.29g/mol

Yield ( <b>8</b> ):	0.36g (37.76%)
% Calculated:	C: 55.18, H: 3.70, N: 6.44
% Found:	C: 55.51, H: 3.52, N: 6.48
IR (KBr) $\nu_{\max}$ :	3409, 3073, 1549, 1515, 14078, 1146, 1112, 1085, 857, 769, 729, 696, 649 cm <sup>-1</sup>
$\mu_{\text{eff}}$ :	5.94 B.M.
Solubility:	Soluble in DMSO. Partially soluble in hot H <sub>2</sub> O, MeOH, EtOH, ether, acetone and CHCl <sub>3</sub> .

The yellow filtrate, upon standing for several days, yielded yellow crystals (**9**).

Product formula weight (**9**) = 669.54g/mol

Yield ( <b>9</b> ):	0.39g (26.60%)
% Calculated:	C: 57.40, H: 4.52, N: 8.37

% Found:	C: 59.81, H: 9.04, N: 8.57
IR (KBr) $\nu_{\max}$ :	3415, 3046, 2979, 1608, 1408, 1575, 1508, 1488, 1420, 1380, 1219, 1145, 1098, 861, 847, 790, 778, 762, 728, 722, 693, 652, 637 $\text{cm}^{-1}$
$\mu_{\text{eff}}$ :	5.87 B.M.
Solubility:	Soluble in DMSO. Partially soluble in hot EtOH. Insoluble in $\text{H}_2\text{O}$ , MeOH, ether, acetone and $\text{CHCl}_3$ .

### 2.3.5 Synthesis of $[\text{Mn}_2(\text{isoph})_2(\text{phen})_3]4\text{H}_2\text{O}$ (10) and $\{[\text{Mn}(\text{phen})_2(\text{H}_2\text{O})_2]\}_2(\text{isoph})_2(\text{phen})\cdot 12\text{H}_2\text{O}$ (11) (Crystal structure formulation)<sup>1</sup>

The synthesis of these complexes is as per previously published<sup>1</sup> with the following modifications:

A solution of 0.50 g (1.96 mmol)  $[\text{Mn}(\text{isoph})]2\text{H}_2\text{O}$  (**PC 2**) in 50  $\text{cm}^3$  distilled water was added to a solution of 0.78 g (4.33 mmol) 1,10-phenanthroline in 50  $\text{cm}^3$  distilled water in a 250  $\text{cm}^3$  round bottomed flask and was stirred continuously for 2 hrs at ambient temperature. A yellow solid precipitated which was then filtered and allowed to air dry. Product formula weight (**10**) = 1050.78g/mol

Yield ( <b>10</b> ):	1.12g (54.38%)
% Calculated:	C: 59.44, H: 3.84, N: 8.00
% Found:	C: 58.24, H: 3.14, N: 8.60
IR (KBr) $\nu_{\max}$ :	3550, 3476, 3415, 3053, 1643, 1608, 1575, 1514, 1448, 1428, 1384, 1367, 1219, 1146, 1105, 1078, 857, 756, 728, 642 $\text{cm}^{-1}$
$\mu_{\text{eff}}$ :	5.65 B.M.
Solubility:	Soluble in DMSO, MeOH, acetone and hot ether. Partially soluble in hot EtOH and $\text{CHCl}_3$ . Insoluble in $\text{H}_2\text{O}$ .

The yellow filtrate from the reaction was reduced in volume to approximately 10 cm<sup>3</sup>. Upon standing at room temperature for a week complex **11** deposited as yellow crystals. The crystals were filtered, washed with water and then EtOH and allowed to dry in air. Product formula weight (**11**) = 1627.38g/mol

Yield ( <b>11</b> ):	0.32g (10.03%)
% Calculated:	C: 56.09, H: 4.95, N: 8.61
% Found:	C: 60.84, H: 4.60, N: 9.75
IR (KBr) $\nu_{\max}$ :	3415, 1602, 1562, 1515, 1421, 1367, 863, 843, 749, 729 cm <sup>-1</sup>
$\mu_{\text{eff}}$ :	6.16 B.M.
Solubility:	Soluble in DMSO. Insoluble in H <sub>2</sub> O, MeOH, EtOH, ether, acetone and CHCl <sub>3</sub> .

### 2.3.6 Synthesis of [Mn(terph)(phen)<sub>2</sub>]5H<sub>2</sub>O (**12**)

A solution of 0.50 g (1.89 mmol) [Mn(terph)]2.5H<sub>2</sub>O (**PC 3**) in 50 cm<sup>3</sup> distilled water was added to a solution of 0.76 g (4.22 mmol) 1,10-phenanthroline in 50 cm<sup>3</sup> distilled water in a 250 cm<sup>3</sup> round bottomed flask and was stirred continuously for 2 hrs at ambient temperature. A yellow solid precipitated which was then filtered and allowed to dry in air.

Product formula weight (**12**) = 669.54g/mol

Yield ( <b>12</b> ):	1.15g (90.88%)
% Calculated:	C: 57.40, H: 4.52, N: 8.37
% Found:	C: 57.63, H: 4.20, N: 8.27
IR (KBr) $\nu_{\max}$ :	3422, 1649, 1619, 1562, 1514, 1434, 1405, 1226, 1146, 1100, 1019, 844, 825, 755, 727, 637, 507 cm <sup>-1</sup>

$\mu_{\text{eff}}$ :	6.15 B.M.
Solubility:	Soluble in DMSO, MeOH and acetone. Partially soluble in hot EtOH, ether and $\text{CHCl}_3$ . Insoluble in $\text{H}_2\text{O}$ .

## 2.4 Synthesis of 1, 10-phenanthroline octanedioate (suberate) complexes.

### 2.4.1 Synthesis of $[\text{Mn}_2(\eta^1\eta^1\mu_2\text{-oda})(\text{phen})_4(\text{H}_2\text{O})_2][\text{Mn}_2(\eta^1\eta^1\mu_2\text{-oda})(\text{phen})_4(\eta^1\text{-oda})_2]4\text{H}_2\text{O}$ (**13**) (Crystal structure formulation)<sup>2</sup>

The synthesis of this complex is as per previously published<sup>2</sup> with the following modifications:

0.50 g (2.04 mmol)  $[\text{Mn}(\text{oda})\text{H}_2\text{O}]$  and 1.13 g (6.27 mmol) 1,10-phenanthroline was dissolved in 50  $\text{cm}^3$  of EtOH and refluxed for 45 mins. The resulting solution was then filtered hot.

Product formula weight (**13**) = 2458.23g/mol

Yield ( <b>13</b> ):	1.15g (22.93%)
% Calculated:	C: 64.43, H: 4.90, N: 9.39
% Found:	C: 64.25, H: 5.15, N: 9.47
IR (KBr) $\nu_{\text{max}}$ :	3422, 1649, 1619, 1562, 1514, 1434, 1405, 1226, 1146, 1100, 1019, 844, 825, 755, 727, 637, 507 $\text{cm}^{-1}$
$\mu_{\text{eff}}$ :	5.91 B.M.
Solubility:	Soluble in $\text{H}_2\text{O}$ , MeOH, EtOH, DMF, DMSO, MeCN and acetone.



### 2.4.2 Synthesis of $[\text{Cu}_2(\text{oda})(\text{phen})_4](\text{ClO}_4)_2 \cdot 2.76\text{H}_2\text{O} \cdot \text{EtOH}$ (**14**) (Crystal structure formulation)<sup>3</sup>

The synthesis of this complex is as per previously published<sup>3</sup> with the following modifications:

0.736 g (1 mmol)  $[\text{Cu}(\text{oda})(\text{phen})_2] \cdot 8\text{H}_2\text{O}$  was added to an EtOHic solution of sodium perchlorate (50 cm<sup>3</sup>, 0.4 M) and the resulting mixture was refluxed for 1 hr. The solution was allowed to stand for 10 days resulting in the formation of a green/blue precipitate which was filtered and air dried. The solid was recrystallized from an EtOH: water (1:1) mixture to yield dark blue crystals.

Product formula weight (**14**) = 1309.23g/mol

Yield ( <b>14</b> ):	0.45g (34.37%)
% Calculated:	C: 52.80, H: 4.3, N: 8.5
% Found:	C: 52.60, H: 4.20, N: 8.10
IR (KBr) $\nu_{\text{max}}$ :	3420, 2939, 1560, 1516, 1430, 1406, 1098, 849, 723, 658, 621 cm <sup>-1</sup>
$\mu_{\text{eff}}$ :	1.91 B.M.
Solubility:	Soluble in H <sub>2</sub> O, MeOH, EtOH, DMF, DMSO, MeCN and acetone.

## 2.5 Synthesis of 1, 10-phenanthroline 3,6,9-trioxaundecanedioate complexes

### 2.5.1 Synthesis of $[\text{Mn}(3,6,9\text{-tdda})] \cdot \text{H}_2\text{O}$

The synthesis of this complex is as per previously published<sup>4</sup> with the following modifications:

2.33 g (7.34 mmol) of 3,6,9-trioxaundecanedioic acid ( $\geq 70\%$ ) (3,6,9-tdda) was dissolved in 20 cm<sup>3</sup> of EtOH in a 250 cm<sup>3</sup> round bottomed flask. To this was added a solution of 1.50 g (6.12 mmol) of manganese(II) acetate in 50 cm<sup>3</sup> EtOH and the resulting mixture

refluxed for 1 hr. The reaction mixture was allowed to cool to room temperature before being filtered through a membrane filter to yield a fine white powder, which was washed with two 10cm<sup>3</sup> portions of cold EtOH and then air dried.

Product formula weight = 293.13g/mol

Yield: 1.65g (76.69%)

% Calculated: C: 32.78, H: 4.81

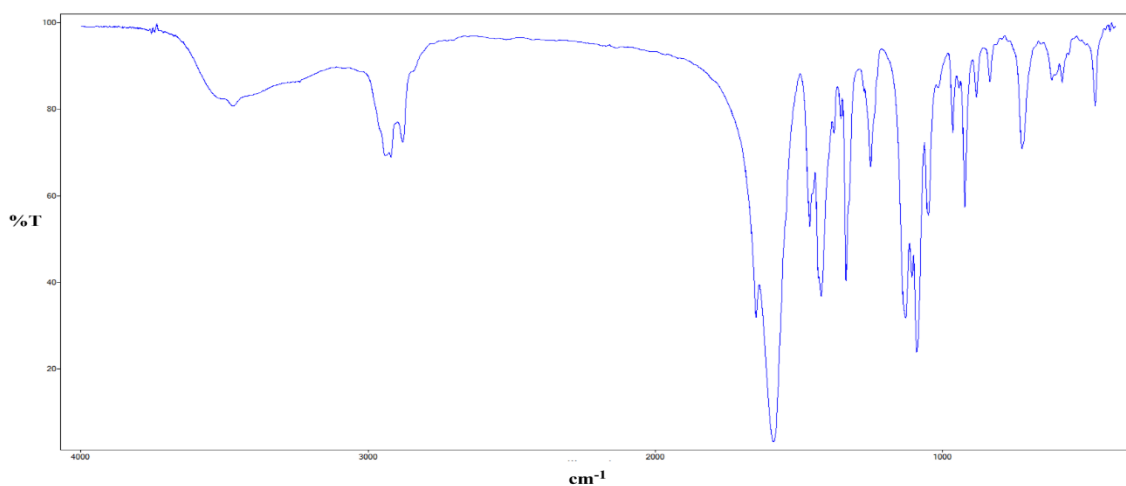
% Found: C: 32.20, H: 4.60

IR (KBr)  $\nu_{\max}$ : 3423, 2925, 1591, 1423, 1330, 1112, 1011, 949, 887, 729, 601 cm<sup>-1</sup>

$\mu_{\text{eff}}$ : 5.41 B.M.

Solubility: Soluble in H<sub>2</sub>O, MeOH, EtOH. Insoluble in CHCl<sub>3</sub>, ethyl acetate and acetone.

IR (KBr): [Mn(3,6,9-tdda)]•H<sub>2</sub>O



### 2.5.2 Synthesis of [Cu(3,6,9-tdda)]•H<sub>2</sub>O (Novel)

1.50 g (7.51 mmol) of copper(II) acetate was dissolved in 50 cm<sup>3</sup> EtOH in a 250 cm<sup>3</sup> round bottomed flask. To this was added a solution of 2.84 g (8.95 mmol) of 3,6,9-tdda

in 25 cm<sup>3</sup> EtOH and the resulting light green mixture refluxed for 1 hr. The reaction mixture was allowed to cool to room temperature before being filtered through a membrane filter to yield a light green powder.

Product formula weight = 301.74g/mol

Yield: 1.88g (82.97%)

% Calculated: C: 31.84, H: 4.68

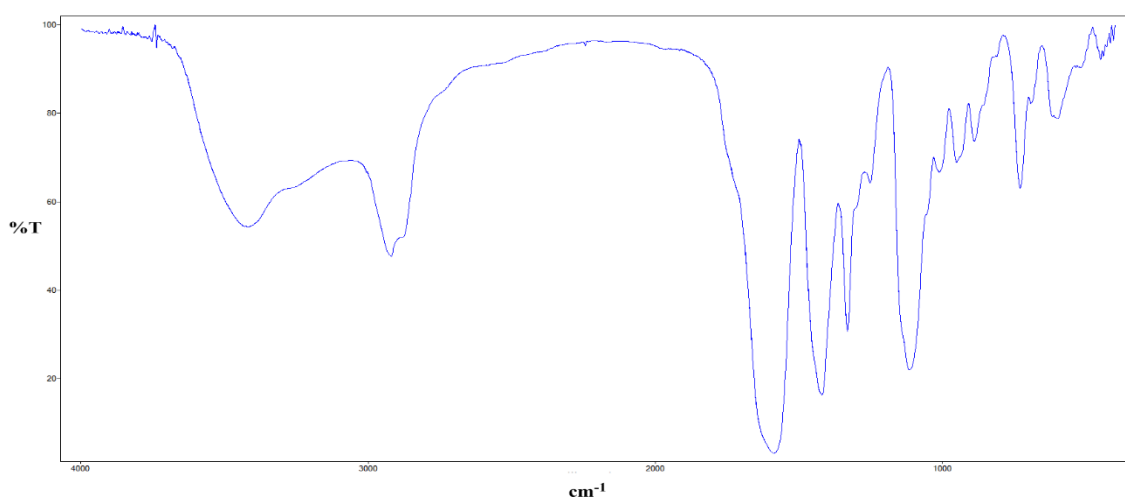
% Found: C: 32.20, H: 4.60

IR (KBr)  $\nu_{\max}$ : 3280, 2930, 1585, 1430, 1330, 1250, 1130, 1090, 1055, 965, 920, 840, 720, 475 cm<sup>-1</sup>

$\mu_{\text{eff}}$ : 1.93 B.M.

Solubility: Soluble in H<sub>2</sub>O, MeOH, EtOH. Insoluble in CHCl<sub>3</sub>, ethyl acetate and acetone.

IR (KBr): [Cu(3,6,9-tdda)]•H<sub>2</sub>O



### 2.5.3 Synthesis of $[\text{Ag}_2(3,6,9\text{-tdda})\cdot 2\text{H}_2\text{O}]$ (Novel)

3.00 g (17.97 mmol) of silver(I) acetate was dissolved in 30 cm<sup>3</sup> EtOH in a 250 cm<sup>3</sup> round bottomed flask. To this was added a solution of 2.85 g (8.98 mmol) of 3,6,9-tdda in 20 cm<sup>3</sup> EtOH and the resulting mixture refluxed for 3 hr. The reaction mixture was allowed to cool to room temperature before being filtered to yield a light orange/brown powder, which was washed with EtOH and air dried.

Product formula weight = 471.94g/mol

Yield: 3.79 g (44.69%)

% Calculated: C: 20.36, H: 2.56

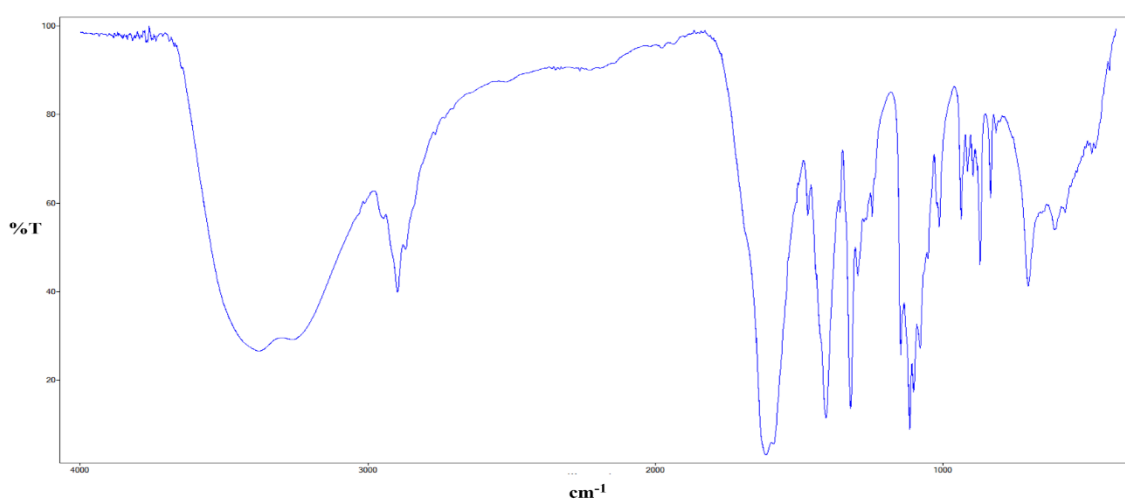
% Found: C: 20.34, H: 2.51

IR (KBr)  $\nu_{\text{max}}$ : 3425, 2896, 1614, 1406, 1116 cm<sup>-1</sup>

<sup>1</sup>H NMR: (D<sub>2</sub>O)  $\delta$  = 3.81 (s, 4H), 3.56 (s, 8H)

Solubility: Soluble in hot H<sub>2</sub>O and hot DMSO.

IR (KBr):  $[\text{Ag}_2(3,6,9\text{-tdda})\cdot 2\text{H}_2\text{O}]$



### 2.5.4 Synthesis of $\{[\text{Mn}(\text{3,6,9-tdda})(\text{phen})_2]\cdot 3\text{H}_2\text{O}\cdot \text{EtOH}\}_n$ (**15**) (Crystal structure formulation)<sup>4</sup>

The synthesis of this complex is as per previously published<sup>4</sup> with the following modifications:

0.65 g (2.22 mmol)  $[\text{Mn}(\text{3,6,9-tdda})]\cdot \text{H}_2\text{O}$  was dissolved in 30 cm<sup>3</sup> EtOH in a 250 cm<sup>3</sup> RB flask. To this was added a solution of 1.50 g (7.57 mmol) of 1,10-phenanthroline in 30 cm<sup>3</sup> EtOH and the resulting yellow mixture was stirred at 30 °C for 2 hrs. The reaction mixture was then filtered and the yellow precipitate washed with cold EtOH and air dried.

Product formula weight (**15**) = 735.64g/mol

Yield: 1.05 g (64.29%)

% Calculated: C: 55.51, H: 5.48, N: 7.47

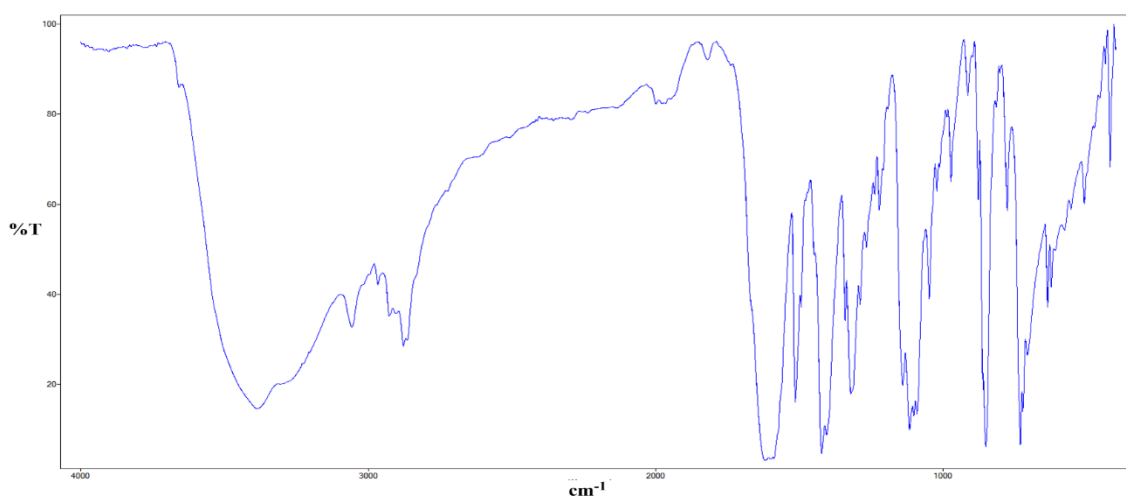
% Found: C: 55.15, H: 5.20, N: 7.40

IR (KBr)  $\nu_{\text{max}}$ : 417, 507, 577, 619, 634, 702, 720, 730, 774, 849, 875, 912, 972, 1020, 1046, 1090, 1101, 1114, 1138, 1218, 1265, 1320, 1340, 1403, 1421, 1513, 1587, 1616, 1818, 1997, 2870, 2918, 2962, 3054, 3384 cm<sup>-1</sup>

$\mu_{\text{eff}}$ : 6.0 B.M.

Solubility: Soluble in H<sub>2</sub>O, MeOH, EtOH. Insoluble in EtOAc and acetone.

IR (KBr):  $\{[\text{Mn}(\text{3,6,9-tdda})(\text{phen})_2\cdot 3\text{H}_2\text{O}\cdot \text{EtOH}\}_n$  (**15**)



### 2.5.5 Synthesis of [Cu(3,6,9-tdda)(phen)<sub>2</sub>] $\cdot$ 3H<sub>2</sub>O $\cdot$ EtOH (16) (Novel)

1.00 g (3.31 mmol) [Cu(3,6,9-tdda)].H<sub>2</sub>O was dissolved in 30 cm<sup>3</sup> EtOH in a 250 cm<sup>3</sup> RB flask. To this was added a solution of 2.39 g (13.26 mmol) of 1,10-phenanthroline in 50 cm<sup>3</sup> EtOH and the resulting dark green mixture was refluxed at 30 °C for 2 hrs. The reaction mixture was then filtered and the green precipitate washed with cold EtOH and air dried.

Product formula weight (**16**) = 744.25g/mol

Yield: 1.63 g (66.09%)

% Calculated: C: 54.87, H: 5.42, N: 7.53

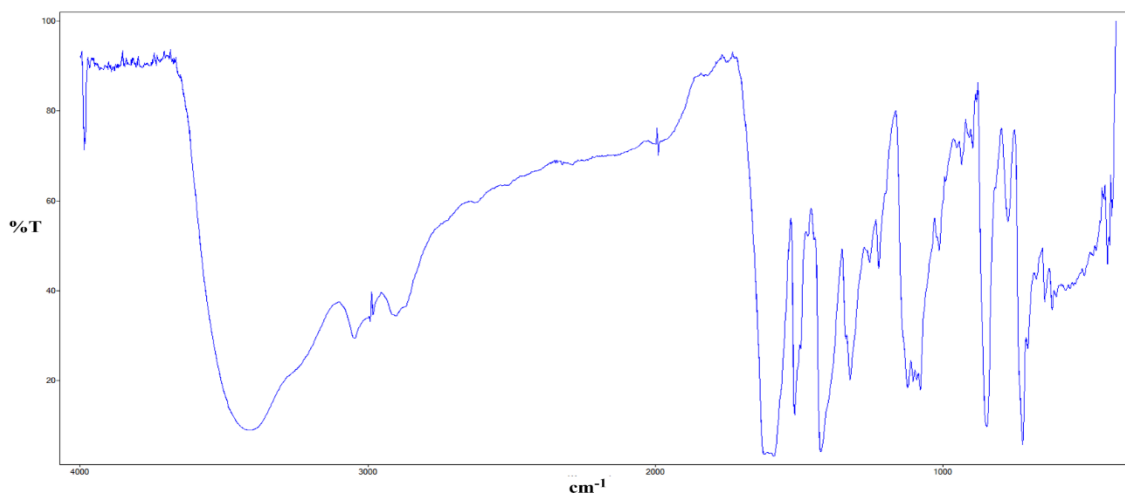
% Found: C: 54.65, H: 5.63, N: 7.39

IR (KBr)  $\nu_{\max}$ : 426, 507, 555, 573, 603, 619, 643, 704, 720, 770, 847, 893, 934, 1011, 1077, 1090, 1101, 1121, 1221, 1252, 1320, 1421, 1513, 1587, 1618, 1752, 1989, 2901, 3041, 3415, 3982 cm<sup>-1</sup>

$\mu_{\text{eff}}$ : 1.92 B.M.

Solubility: Soluble in H<sub>2</sub>O, MeOH, EtOH. Insoluble in ethyl acetate and acetone.

IR (KBr): [Cu(3,6,9-tdda)(phen)<sub>2</sub>] $\cdot$ 3H<sub>2</sub>O $\cdot$ EtOH (16)



### 2.5.6 Synthesis of $[\text{Ag}_2(3,6,9\text{-tdda})(\text{phen})_4]\cdot\text{EtOH}$ (**17**) (Novel)

0.50 g (1.06 mmol)  $[\text{Ag}_2(3,6,9\text{-tdda})]\cdot 2\text{H}_2\text{O}$  was dissolved in 20 cm<sup>3</sup> EtOH in a 250 cm<sup>3</sup> round bottomed flask. To this was added a solution of 0.827 g (4.589 mmol) of 1,10-phenanthroline in 20 cm<sup>3</sup> EtOH and the resulting mixture was refluxed overnight in the absence of light. The solution was allowed to cool to room temperature, and cooled on an ice bath resulting in the formation of a green precipitate which was then filtered (0.832 g, 60.15 %).

Product formula weight (**17**) = 1202.80g/mol

Yield: 0.83 g (65.10%)

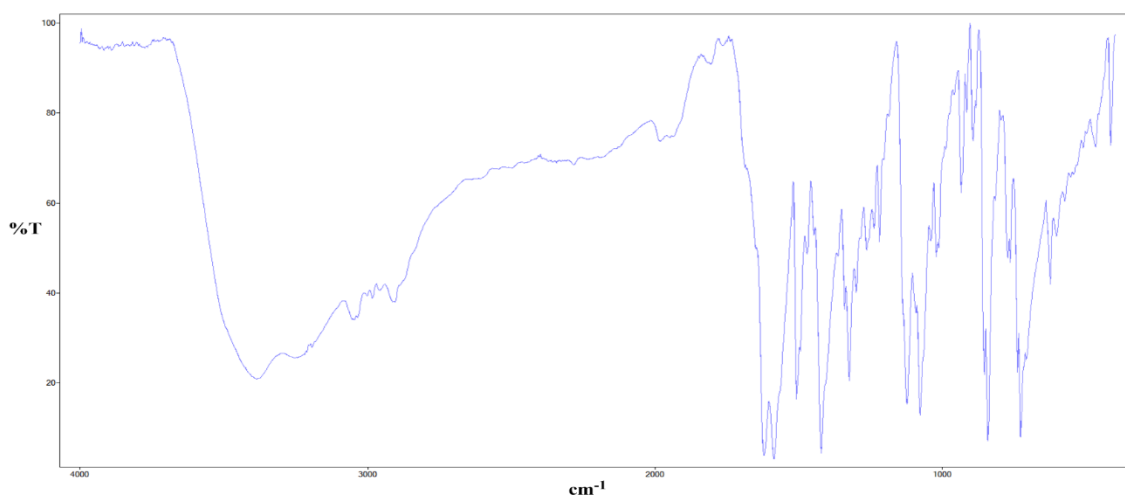
% Calculated: C: 57.92, H: 4.19, N: 9.32

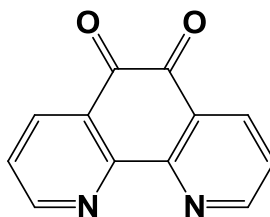
% Found: C: 57.75, H: 5.16, N: 9.02

IR (KBr)  $\nu_{\text{max}}$ : 413, 465, 621, 726, 838, 890, 932, 1018, 1077, 1121, 1215, 1263, 1322, 1421, 1509, 1585, 1618, 1804, 1978, 2905, 3046, 3380 cm<sup>-1</sup>

Solubility: Soluble in H<sub>2</sub>O, MeOH, EtOH. Insoluble in ethyl acetate and acetone.

IR (KBr):  $[\text{Ag}_2(3,6,9\text{-tdda})(\text{phen})_2]\cdot 3\text{H}_2\text{O}\cdot\text{EtOH}$  (**17**)



**2.6 Synthesis of 1, 10-phenanthroline-5, 6-dione (phendione) (2)<sup>5</sup>**

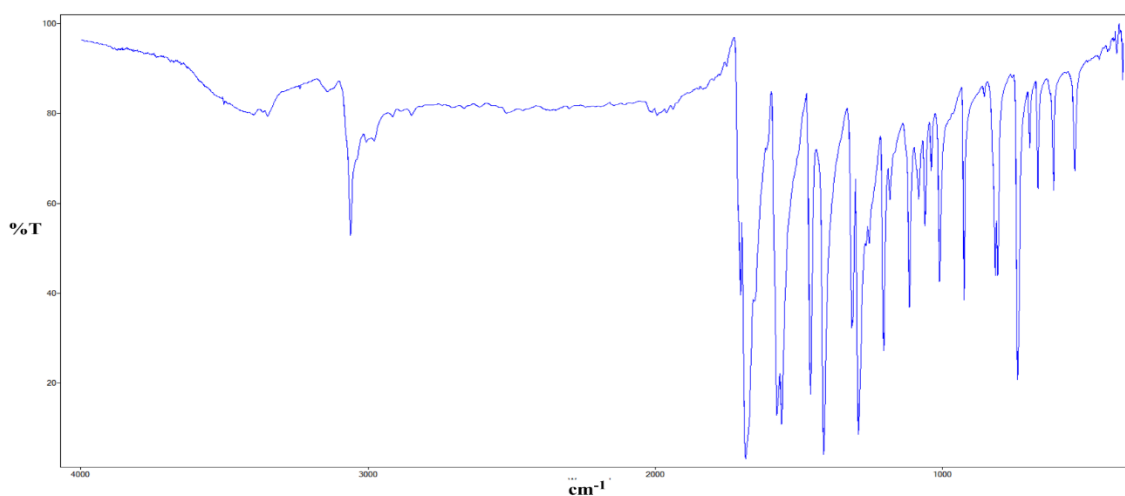
5.00g (0.03 mol) of phenanthroline monohydrate was added to 60 cm<sup>3</sup> of 60 % H<sub>2</sub>SO<sub>4</sub>. When fully dissolved, 6.68 g (0.04 mol) of KBrO<sub>3</sub> was added over a period of 30 mins and the resulting red/brown solution stirred at 30°C for 20 hrs. The resulting mixture was poured over ice and neutralized to pH 7 using a saturated NaOH solution. The resulting solution was then filtered and extracted with dichloromethane and the solvent removed under reduced pressure. The resulting off yellow powder was recrystallized from MeOH to yield a bright yellow powder product.<sup>5</sup>

Product formula weight (2) = 210.19g/mol

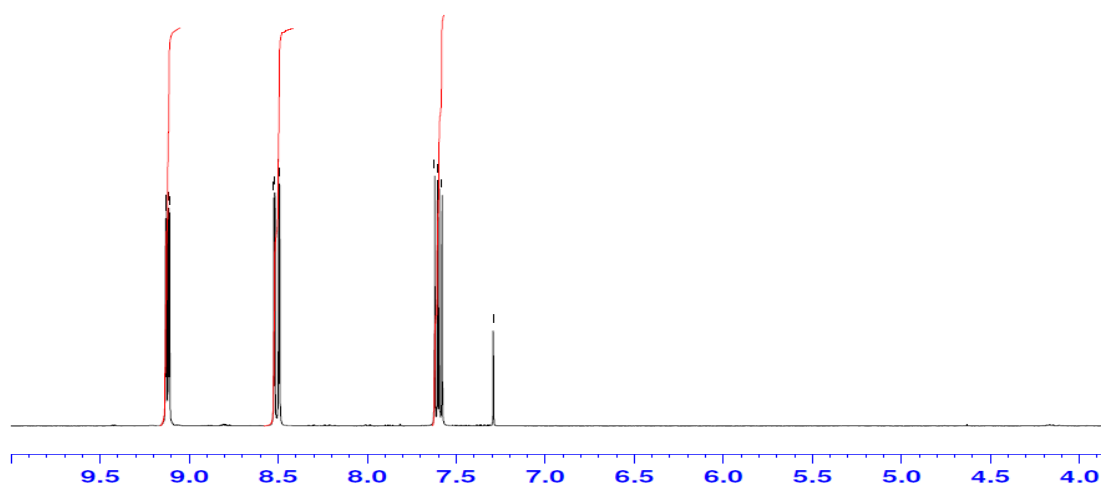
Yield:	4.78g (90.16 %)
IR (KBr) $\nu_{\max}$ :	3413, 3061, 1703, 1685, 1561, 1459, 1414, 1316, 1293, 1205, 1115, 1010, 925, 807, 739 cm <sup>-1</sup>
<sup>1</sup> H NMR:	(CHCl <sub>3</sub> -d <sub>3</sub> ) $\delta$ = 7.58(dd, J <sub>1</sub> = 4.5 Hz, J <sub>2</sub> = 7.8 Hz, 2H), 8.49 (dd, J <sub>1</sub> = 1.8 Hz, J <sub>2</sub> = 7.95 Hz, 2H), 9.11 (dd, J <sub>1</sub> = 1.8 Hz, J <sub>2</sub> = 4.65 Hz, 2H).
LC/TCOF-MS:	Calcd for C <sub>12</sub> H <sub>6</sub> N <sub>2</sub> O <sub>2</sub> [M+H] <sup>+</sup> 211.05017, found 211.0502.
Solubility:	Soluble in MeOH (hot), EtOH (hot), MeCN, DCM, CHCl <sub>3</sub> , DMSO.



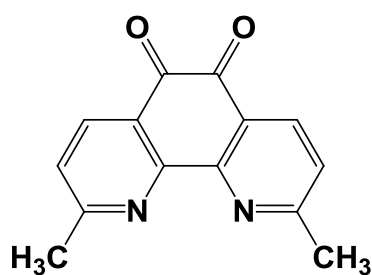
IR (KBr): **Phendione (2)**



<sup>1</sup>H NMR (CHCl<sub>3</sub>-d<sub>3</sub>): **Phendione (2)**



2.7 Synthesis of 2,9-dimethyl-1,10-phenanthroline-5,6-dione (**dmphendio**) (**4**)<sup>6</sup>



2.00 g (9.21 mmol) of neocuprine hemihydrate and 6.80 g (57.14 mmol) of potassium bromide (KBr) were added to a 500 cm<sup>3</sup> round bottom flask and the flask placed on ice

to cool. To this was slowly added 44 cm<sup>3</sup> of conc. sulfuric acid (H<sub>2</sub>SO<sub>4</sub>) to produce a thick orange / red paste which was stirred for 5 mins before the slow addition of 24 cm<sup>3</sup> of 70 % HNO<sub>3</sub>. The resulting red reaction mixture was then heated to 90 °C and reacted for 16 hrs before being poured into 1200 cm<sup>3</sup> of Millipore water to produce a yellow solution which was carefully neutralized by the addition of sodium hydroxide, extracted with DCM and the solvent removed under reduced pressure. The residue was then recrystallized from MeOH to produce 2,9-dimethyl-1,10-phenanthroline-5,6-dione.

Product formula weight (**4**) = 238.07g/mol.

Yield: 1.75 g (79.80 %)

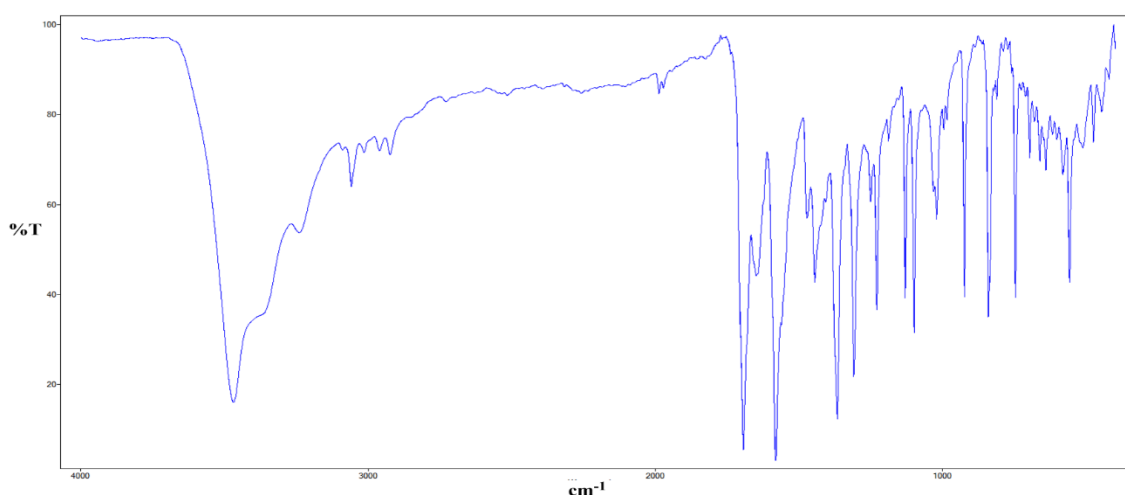
IR (KBr)  $\nu_{\max}$ : 3468, 3058, 1694, 1650, 1582, 1470, 1445, 1368, 1307, 1228, 1132, 1097, 1020, 925, 841, 745, 559 cm<sup>-1</sup>

<sup>1</sup>H NMR: (DMSO-d<sub>6</sub>)  $\delta$  = 2.68 (s, 6H), 7.53 (d, J<sub>1</sub> = 27 Hz, 2H) 8.27 (d, J = 27 Hz, 2H).

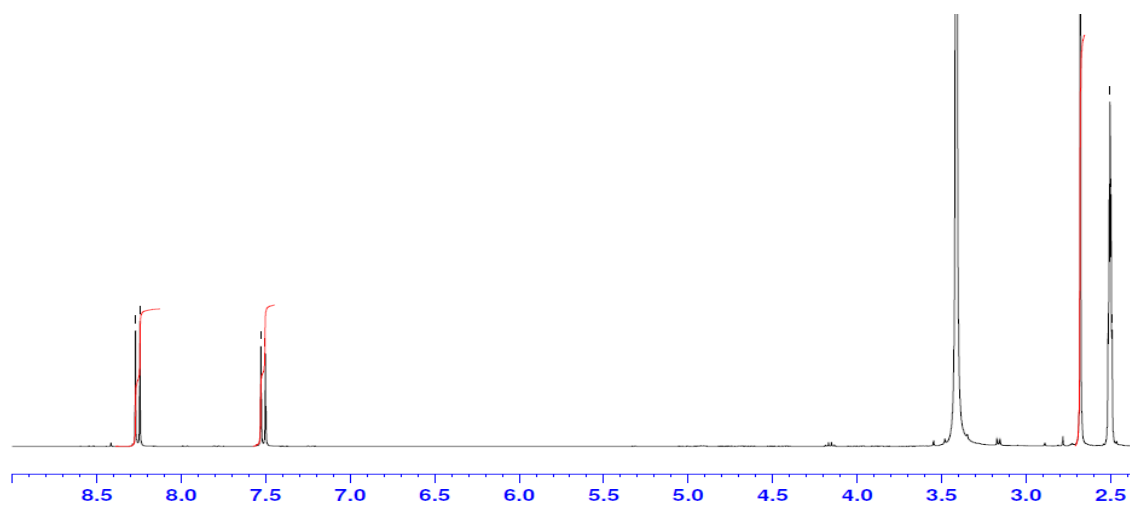
LC/TCOF-MS: Calcd for C<sub>14</sub>H<sub>10</sub>N<sub>2</sub>O<sub>2</sub> [M+H]<sup>+</sup> 239.08147, found 239.0817.

Solubility: Soluble in MeOH (hot), EtOH (hot), MeCN, DCM, CHCl<sub>3</sub>, DMSO.

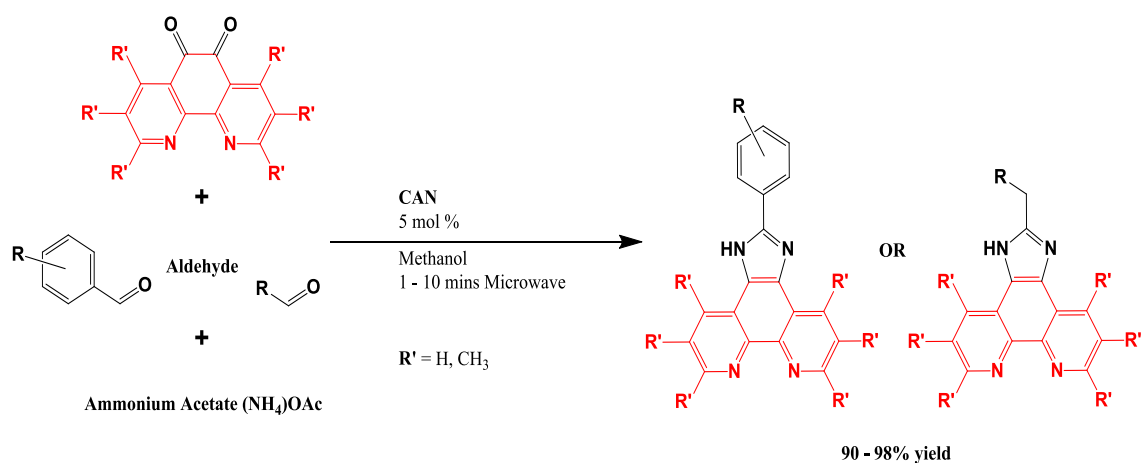
IR (KBr): 2,9-dimethyl-1,10-phenanthroline-5,6-dione (**dmphendio**) (**4**)



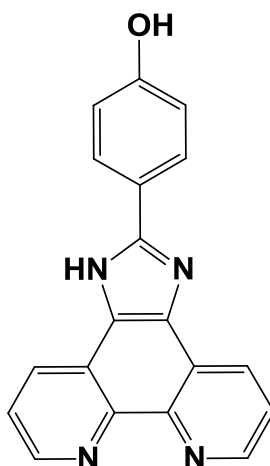
$^1\text{H}$  NMR ( $\text{CHCl}_3\text{-d}_3$ ): 2,9-dimethyl-1,10-phenanthroline-5,6-dione (**dmphendio**) (**4**)



## 2.8 Synthesis of imidazo[4,5-*f*][1,10]phenanthrolines (Im-phens) (Novel Method)



### 2.8.1 Microwave synthesis of 4-(1*H*-imidazo[4,5-*f*][1,10]phenanthrolin-2-yl)phenol (**4hip**) (**18**) (Novel method)

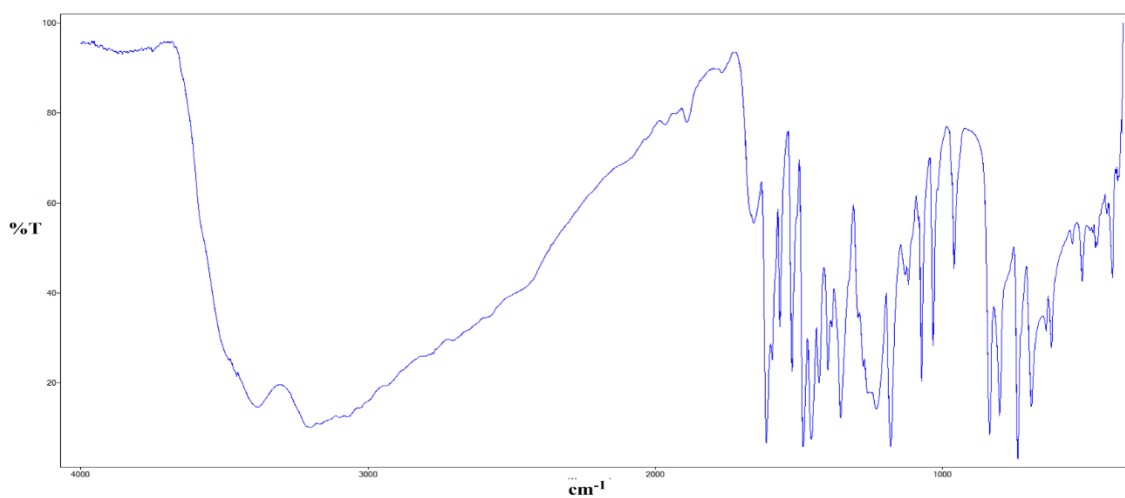


0.40 g (1.90 mmol) of phendione was dissolved in 15 cm<sup>3</sup> of hot dry MeOH, to which 0.052 g (9.52x10<sup>-5</sup> mol) CAN in 2 cm<sup>3</sup> of hot MeOH was added. To the resulting orange reaction mixture was added 1.47 g (0.02 mol) NH<sub>4</sub>OAc in one portion followed by 0.23g (1.90 mmol) of 4-hydroxybenzaldehyde in one portion to produce a dark red solution which was reacted in the microwave at 70 °C (300W, 1 bar) for 5 mins. The resulting solution was then added to 100 cm<sup>3</sup> of deionized water and stirred for 2 mins before being filtered. The resulting yellow powder was washed with more deionized water and then MeOH and dried overnight in an oven at 70 °C.

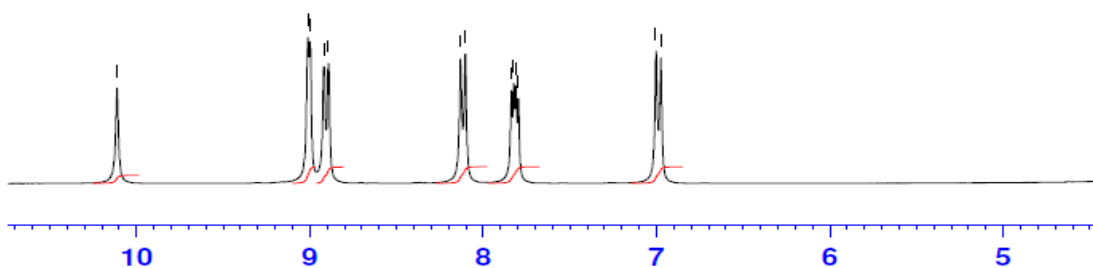
Product formula weight (**18**) = 312.33g/mol.

Yield:	0.546 g (91.86 %)
Mp:	> 250 °C.
% Calculated:	C: 73.07, H: 3.87, N: 17.94
% Found:	C: 73.12, H: 3.93, N: 17.87
IR (KBr) $\nu_{\max}$ :	433, 475, 528, 557, 623, 648, 698, 723, 741, 808, 844, 929, 958, 982, 1052, 1079, 1107, 1178, 1237, 1273, 1366, 1407, 1457, 1483, 1526, 1611, 1774, 1907, 2018, 2168, 2330, 2699, 2890, 2936, 3083, 3299, 3386, 3608, 3750, 3836 cm <sup>-1</sup>
<sup>1</sup> H NMR:	(DMSO-d <sub>6</sub> ) $\delta$ = 6.91-7.01 (m, 2H), 7.76-7.8 (m, 2H), 8.10-8.2 (m, 2H), 8.86-8.89 (m, 2H), 8.97-8.98 (m, 2H), 10.06 (bs, 1H).
<sup>13</sup> C NMR:	(75 MHz DMSO-d <sub>6</sub> ) $\delta$ = 115.77, 120.95, 123.27, 127.99, 129.59, 143.11, 147.55, 151.23, 158.93.
LC/TCOF-MS:	Calcd for C <sub>19</sub> H <sub>12</sub> N <sub>4</sub> O [M+H] <sup>+</sup> 313.1105, found 313.1105.

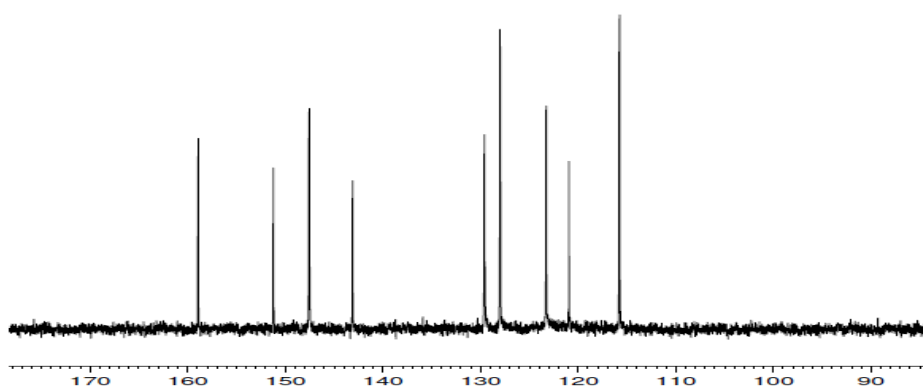
IR (KBr): **4p**hip (**18**)



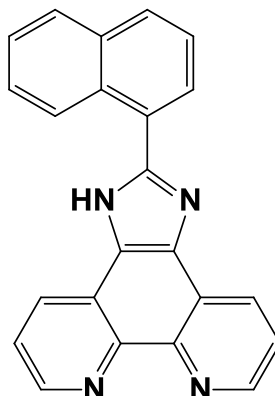
<sup>1</sup>H (DMSO-d<sub>6</sub>) (**18**) **4p**hip



<sup>13</sup>C (DMSO-d<sub>6</sub>) **4p**hip (**18**)



### 2.8.2 Microwave Synthesis of 2-(naphthalen-1-yl)-1*H*-imidazo[4,5-*f*][1,10]phenanthroline (**19**) (Novel method)



0.40 g (1.90 mmol) of phendione was dissolved in 40 cm<sup>3</sup> of hot dry MeOH in a microwave vial. To this was added 0.052 g (9.52x10<sup>-5</sup> mol) of CAN in 2 cm<sup>3</sup> of MeOH and the resulting in a yellow solution. To this was added 1.47 g (0.02 mol) of NH<sub>4</sub>OAc and 0.264 cm<sup>3</sup> (1.94x10<sup>-3</sup> mol) of 1-naphthaldehyde, and the resulting yellow solution was reacted in the microwave at 70 °C (300W, 1 bar) for 10 mins. The reaction mixture was then allowed to cool to room temperature, then added to 100 cm<sup>3</sup> of deionized water and stirred for 2 mins before being filtered and washed with deionized water and MeOH. The resulting orange powder was then dried overnight in an oven at 70 °C.

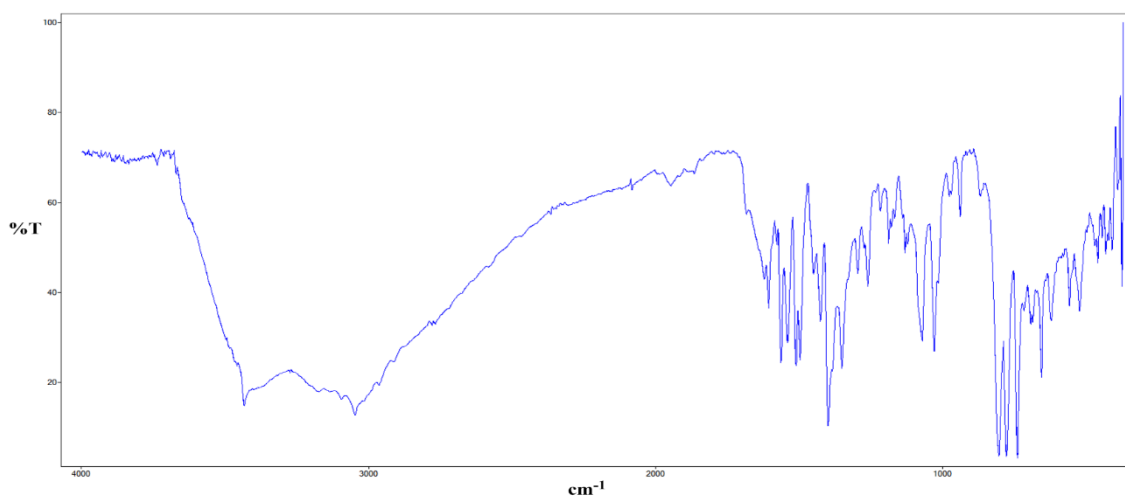
Product formula weight (**19**) = 346.38g/mol.

Yield:	0.655 g (84.54 %)
Mp:	> 250 °C.
% Calculated:	C: 79.75, H: 4.07, N: 16.17
% Found:	C: 79.71, H: 4.10, N: 16.20
IR (KBr) $\nu_{\text{max}}$ :	427, 459, 523, 558, 621, 656, 686, 740, 778, 804, 869, 939, 1029, 1071, 1131, 1188, 1217, 1260, 1296, 1351, 1400, 1426, 1450, 1497, 1511, 1541, 1564, 1578, 1606, 1622, 3047, 3433 cm <sup>-1</sup>
<sup>1</sup> H NMR:	(DMSO-d <sub>6</sub> ): $\delta$ = .61-7.76 (m, 3H), 7.83-7.86 (m, 2H), 8.06-8.14 (m, 3H), 8.95-8.97 (m, 2H), 9.04-9.08 (m, 3H).

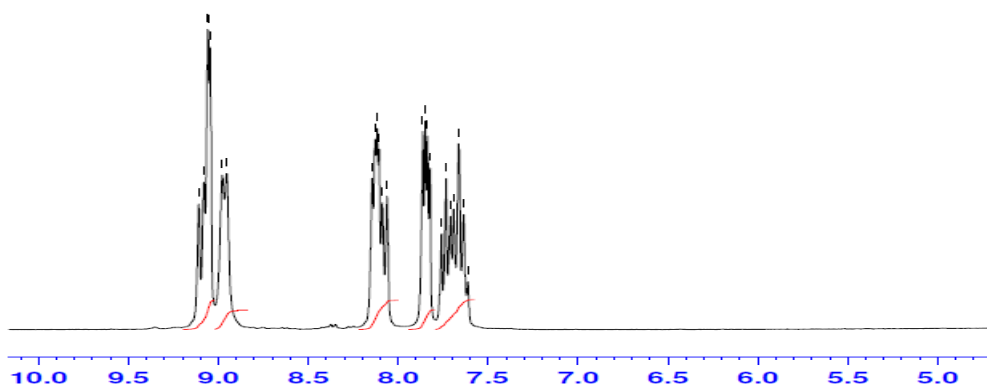
$^{13}\text{C}$  NMR: (75 MHz DMSO-d<sub>6</sub>)  $\delta$  = 123.40, 125.29, 126.13, 126.42, 127.21, 127.33, 127.96, 128.42, 129.78, 130.11, 130.45, 133.58, 135.66, 143.44, 147.87, 150.46

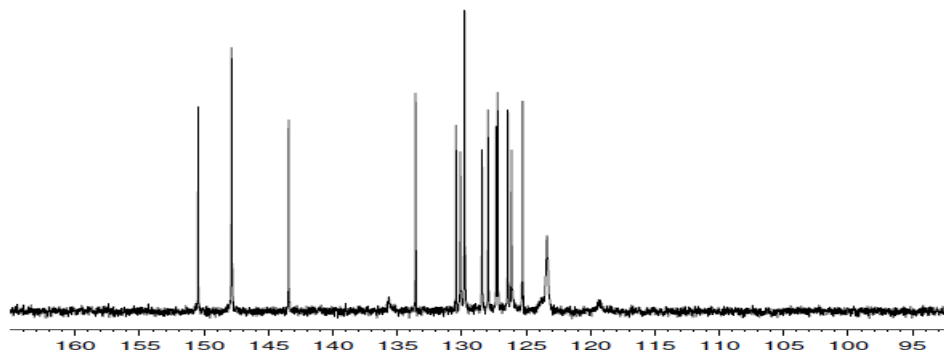
LC/TCOF-MS: Calcd for C<sub>23</sub>H<sub>14</sub>N<sub>4</sub> [M+H]<sup>+</sup> 347.1403, found 347.1403.

IR (KBr): **nip (19)**

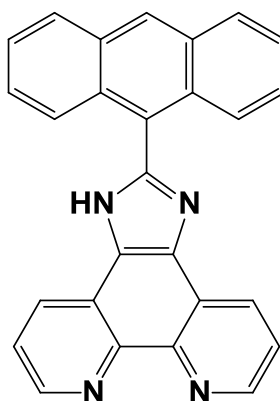


$^1\text{H}$  (DMSO-d<sub>6</sub>) (19) **nip**



<sup>13</sup>C (DMSO-d<sub>6</sub>) (**19**) nip

### 2.8.3 Microwave Synthesis of 2-(anthracen-9-yl)-1*H*-imidazo[4,5-*f*][1,10]phenanthroline (**20**) (Novel method)



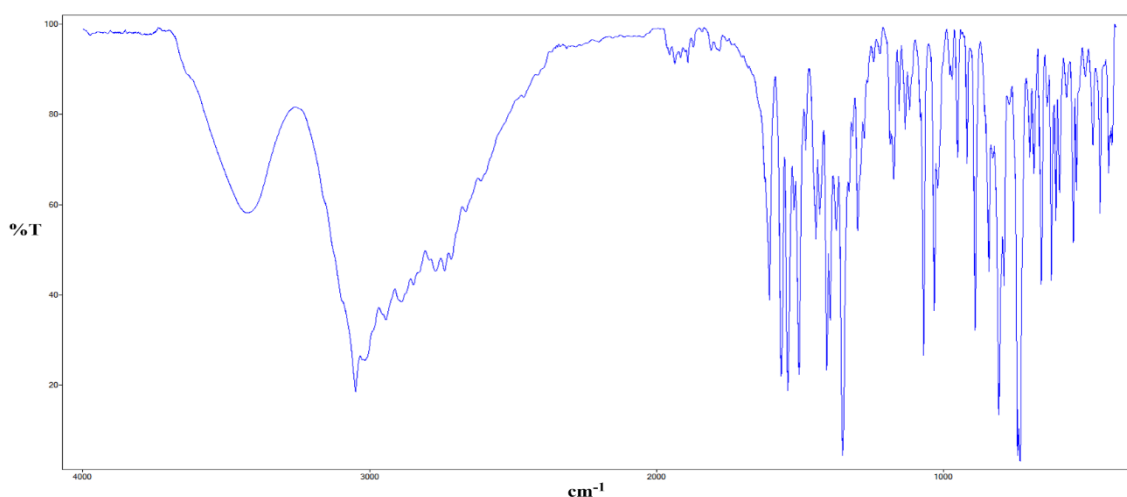
0.40 g (1.90 mmol) of phendione was dissolved in 40 cm<sup>3</sup> of hot dry MeOH in a microwave vial. To this was added 0.052 g (9.52x10<sup>-5</sup> mol) CAN in 2.00 cm<sup>3</sup> of MeOH resulting in a yellow solution. To which 1.47 g (0.02 mol) of NH<sub>4</sub>OAc was added in one portion. To the resulting yellow solution was added 0.392 g (1.90x10<sup>-3</sup> mol) of 9-anthracenecarboxaldehyde in one portion and the resulting orange solution was reacted in the microwave at 70 °C (300W, 1 bar) for 10 mins. The reaction mixture was allowed to cool to room temperature then added to 100 cm<sup>3</sup> of deionized water and stirred for 2 mins before being filtered and washed with deionized water and MeOH. The resulting orange powder was then dried overnight in an oven at 70 °C. (0.605 g, 80.19 %).

Product formula weight (**20**) = 396.44g/mol.

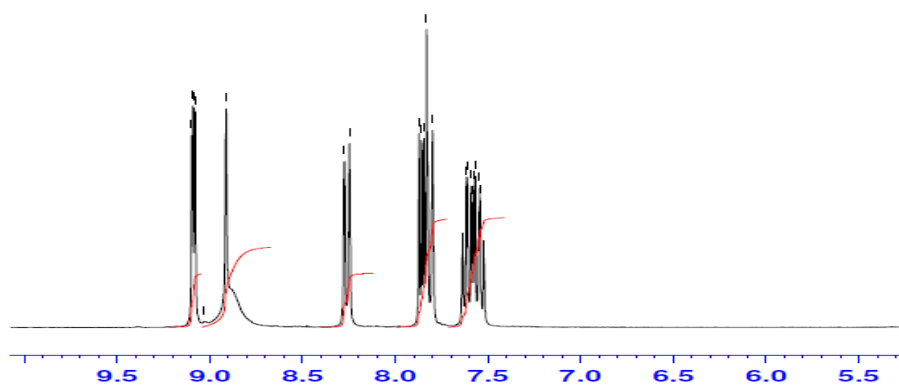


Yield:	0.605 g (80.19 %)
Mp:	> 250 °C.
% Calculated:	C: 81.80, H: 4.07, N: 14.13
% Found:	C: 81.75, H: 4.10, N: 14.15
IR (KBr) $\nu_{\max}$ :	3426, 3049, 1606, 1566, 1543, 1503, 1442, 1407, 1393, 1349, 1298, 1172, 1067, 1030, 951, 918, 890, 841, 806, 731, 657, 622, 545, 456, 426 $\text{cm}^{-1}$
$^1\text{H}$ NMR:	(DMSO- $d_6$ ): $\delta$ = 7.52-7.64 (m, 4H), 7.64-7.87 (m, 4H), 8.24-8.27 (m, 2H), 8.91 (s, 3H), 9.07-9.08 (m, 2H)
$^{13}\text{C}$ NMR:	(75 MHz DMSO- $d_6$ ) $\delta$ = 123.39, 125.36, 125.63, 125.74, 127.08, 128.55, 129.06, 129.66, 130.67, 130.88, 143.59, 147.92, 148.35
LC/TCOF-MS:	Calcd for $\text{C}_{27}\text{H}_{16}\text{N}_4$ $[\text{M}+\text{H}]^+$ 397.14427, found 397.1442

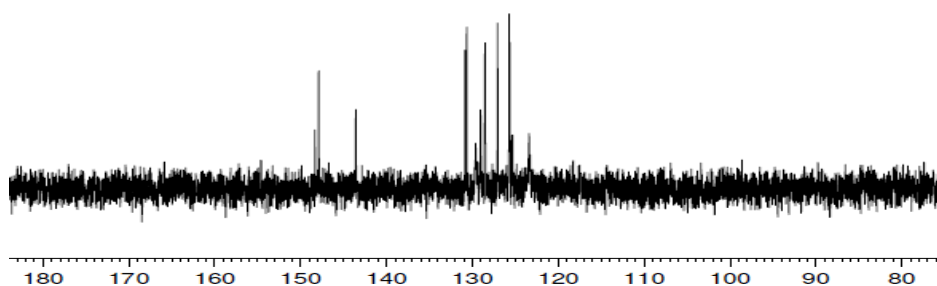
IR (KBr): **aip (20)**



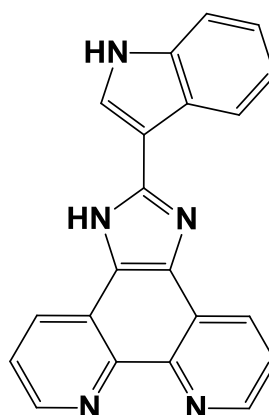
$^1\text{H}$  (DMSO- $d_6$ ) (20) aip



$^{13}\text{C}$  (DMSO- $d_6$ ) (20) aip



#### 2.8.4 Microwave synthesis of 2-(1*H*-indol-3-yl)-1*H*-imidazo[4,5-*f*][1,10]phenanthroline ( $\text{H}_2\text{IIP}$ ) (21) (Novel method)

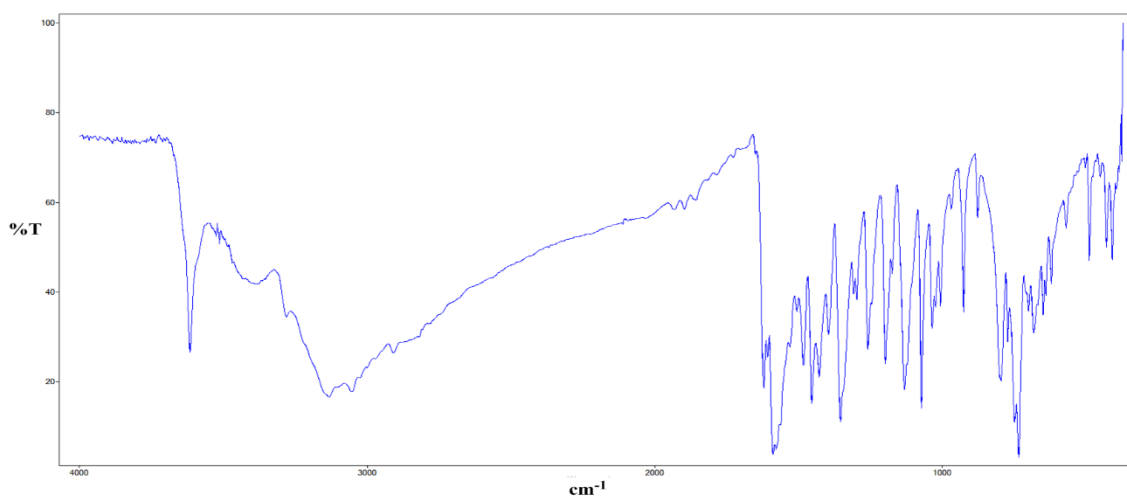


0.40 g (1.90 mmol) of phendione was dissolved in 15 cm<sup>3</sup> of hot dry MeOH, to which 0.052 g (9.52x10<sup>-5</sup> mol) CAN in 2 cm<sup>3</sup> of hot MeOH was added. To the resulting orange reaction mixture was added 1.47 g (0.02 mol) NH<sub>4</sub>OAc in one portion followed by 0.28 g (1.90 mmol) of indole-3-carboxaldehyde in one portion to produce an orange solution which was reacted in the microwave at 75 °C (300W, 1 bar) for 10 mins. The resulting solution was then added to 100 cm<sup>3</sup> of deionized water and stirred for 2 mins before being filtered. The resulting yellow powder was washed with more deionized water and MeOH allowed to air dry followed by drying in an oven at 70 °C overnight. (0.619 g, 97.07 %).

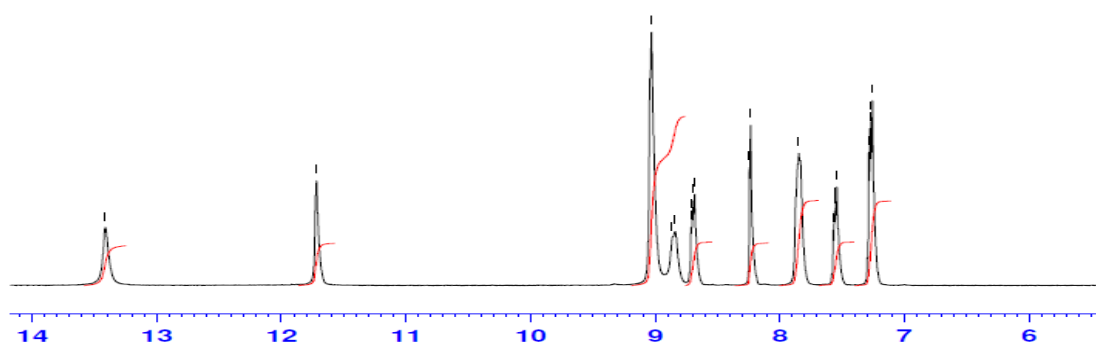
Product formula weight (**21**) = 335.36g/mol.

Yield:	0.619 g (97.07 %)
Mp:	> 250 °C.
% Calculated:	C: 75.21, H: 3.91, N: 20.88
% Found:	C: 75.21, H: 3.87, N: 20.92
IR (KBr) $\nu_{\max}$ :	409, 429, 450, 488, 569, 621, 649, 682, 734, 749, 772, 795, 877, 926, 968, 10006, 1035, 1072, 1131, 1198, 1259, 1297, 1354, 1396, 1428, 1454, 1482, 1505, 1577, 1620, 1727, 1785, 1856, 1929, 2909, 3053, 3133, 3280, 3388, 3513, 3616, 3909 cm <sup>-1</sup>
<sup>1</sup> H NMR:	(DMSO-d <sub>6</sub> ): $\delta$ = 7.25-7.28 (m, 2H), 7.54-7.57 (m, 1H), 7.85-7.86 (m, 2H), 8.23 (s, 1H), 8.68-8.7 (m, 1H), 8.84-9.03 (m, 4H), 11.72 (s, 1H), 13.41 (s, 1H).
<sup>13</sup> C NMR:	(75 MHz DMSO-d <sub>6</sub> ) $\delta$ = 106.58, 111.93, 119.09, 120.28, 121.46, 122.31, 123.01, 123.27, 123.69, 124.82, 125.10, 125.5, 129.18, 129.6, 135.68, 136.46, 143.24, 147.18, 147.39, 148.84.
LC/TCOF-MS:	Calcd for C <sub>21</sub> H <sub>13</sub> N <sub>5</sub> [M+H] <sup>+</sup> 336.12297, found 336.123

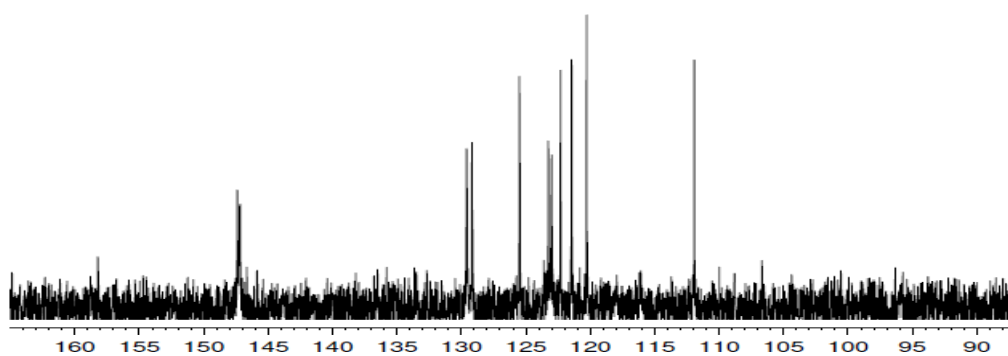
IR (KBr): **H<sub>2</sub>IIP (21)**



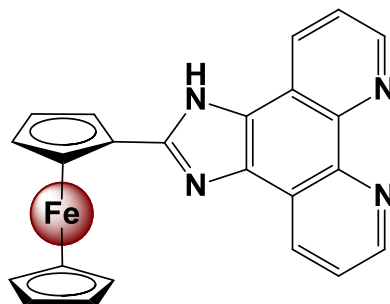
<sup>1</sup>H (DMSO-d<sub>6</sub>) (**21**) **H<sub>2</sub>IIP**



<sup>13</sup>C (DMSO-d<sub>6</sub>) (**21**) **H<sub>2</sub>IIP**



### 2.8.5 Microwave synthesis of 2-ferroceny-1*H*-imidazo[4,5-*f*][1,10]-phenanthroline (ferrip) (**22**) (Novel method)



0.40 g (1.90 mmol) of phendione was dissolved in 15 cm<sup>3</sup> of hot dry MeOH, to which 0.052 g (9.52x10<sup>-5</sup> mol) CAN in 2 cm<sup>3</sup> of hot MeOH was added. To the resulting orange reaction mixture was added 1.47 g (0.02 mol) NH<sub>4</sub>OAc in one portion followed by 0.407 g (1.90 mmol) of ferrocenecarboxaldehyde in one portion. The resulting red mixture was then reacted in the microwave at 75 °C (300W, 1 bar) for 10 mins. The resulting deep red coloured solution was allowed to cool to room temperature and 150 cm<sup>3</sup> of Millipore water was added resulting in a bright orange coloured precipitate which was filtered and washed with millipore water before being dried in an oven at 70 °C overnight (0.70 g, 91 %).

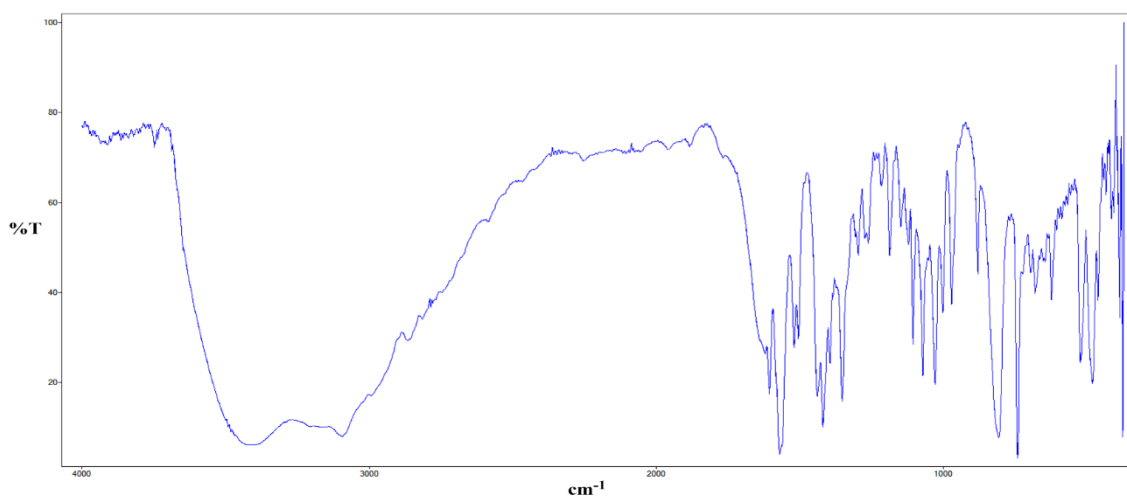
Product formula weight (**22**) = 404.25g/mol.

Yield:	0.70 g (91 %)
Mp:	> 250 °C.
% Calculated:	C: 68.34, H: 3.99, N: 13.86
% Found:	C: 68.39, H: 4.10, N: 13.77
IR (KBr) $\nu_{\max}$ :	415, 433, 481, 523, 624, 681, 697, 742, 807, 880, 971, 1002, 1072, 1106, 1122, 1149, 1187, 1217, 1261, 1297, 1353, 1420, 1439, 1505, 1520, 1570, 1606, 3094, 3417 cm <sup>-1</sup>
<sup>1</sup> H NMR:	(DMSO-d <sub>6</sub> ): $\delta$ = 4.09 (s, 5H), 4.48 (s, 2H), 5.15 (s, 2H), 7.79-7.83 (m, 2H), 8.89-9.01 (m, 4H)

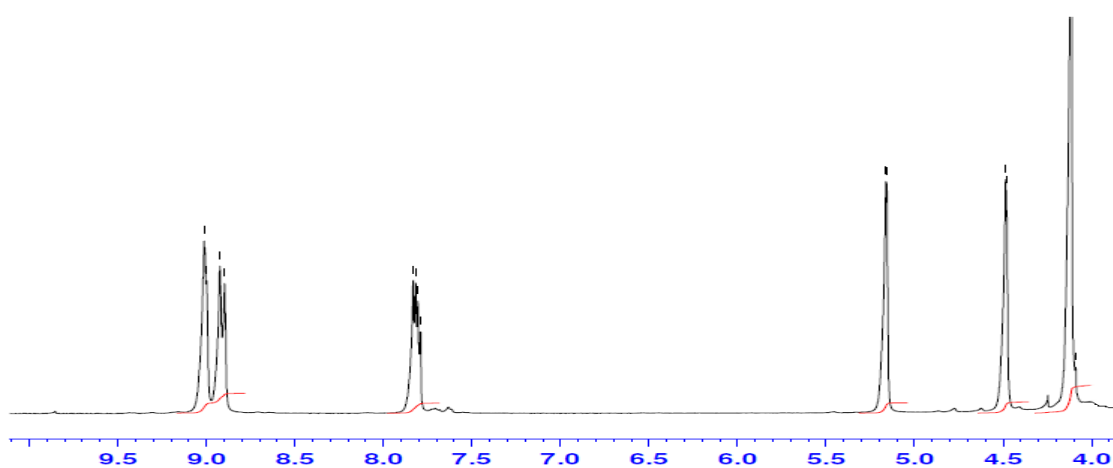
$^{13}\text{C}$  NMR: (75 MHz DMSO- $d_6$ )  $\delta$  = 67.07, 67.30, 69.28, 69.42, 69.73, 74.06, 121.12, 123.22, 123.54, 129.65, 130.34, 132.15, 133.31, 143.07, 147.50, 152.34

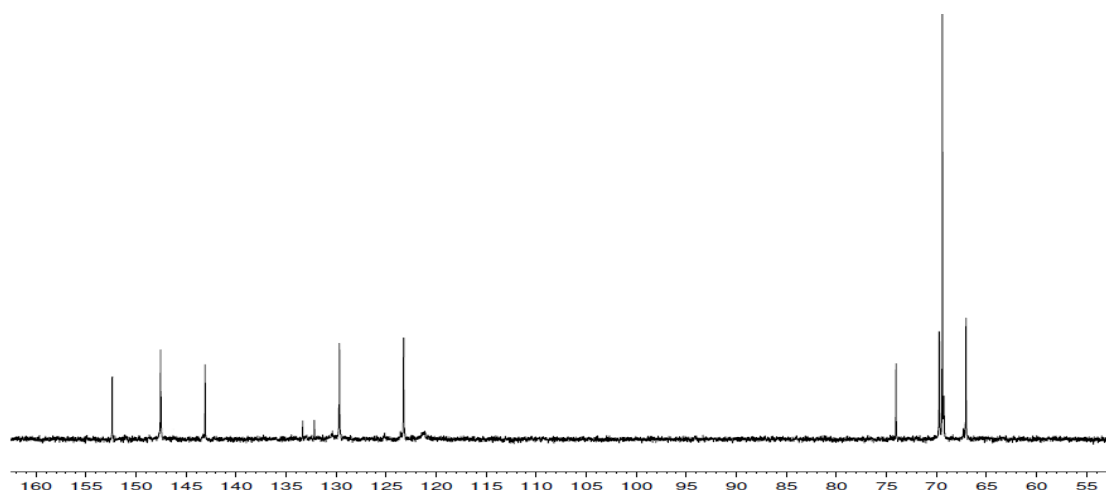
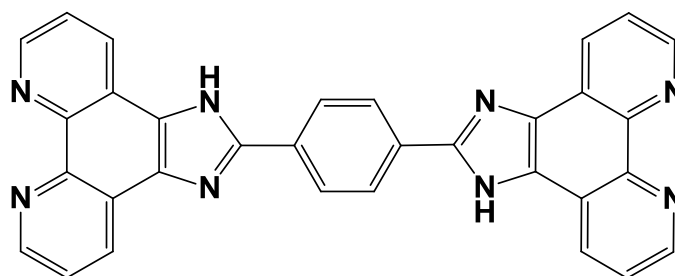
LC/TCOF-MS: Calcd for  $\text{C}_{23}\text{H}_{16}\text{FeN}_4$   $[\text{M}+\text{H}]^+$  405.0797, found 405.0805

IR (KBr): **ferrip (22)**



$^1\text{H}$  (DMSO- $d_6$ ) (22) **ferrip**



$^{13}\text{C}$  (DMSO- $d_6$ ) (**22**) ferrip**2.8.6 Microwave synthesis of 1,4-bis(1*H*-imidazo[4,5-*f*][1,10]phenanthrolin-2-yl)benzene (bpibH<sub>2</sub>) (**23**) (Novel method)**

0.40 g (1.90 mmol) of phendione was dissolved in 15 cm<sup>3</sup> of hot dry MeOH, to which 0.0104 g (1.90x10<sup>-4</sup> mol) CAN in 2 cm<sup>3</sup> of hot MeOH was added. To the resulting orange reaction mixture was added 1.47 g (0.02 mol) NH<sub>4</sub>OAc in one portion followed by 0.128 g (9.52x10<sup>-4</sup> mol) of terephthaldehyde in one portion. The resulting yellow mixture was then reacted in the microwave at 75 °C (300W, 1 bar) for 10 mins. The yellow solution was then allowed to cool to room temperature, filtered and washed with Millipore water and then MeOH to yield a pale yellow solid. The product was then dried in an oven at 70 °C overnight.

Product formula weight (**23**) = 514.54g/mol.

Yield: 0.402 g (82.10 %)

Mp: > 250 °C.

% Calculated: C: 74.70, H: 3.53, N: 15.04

% Found: C: 74.74, H: 3.52, N: 15.01

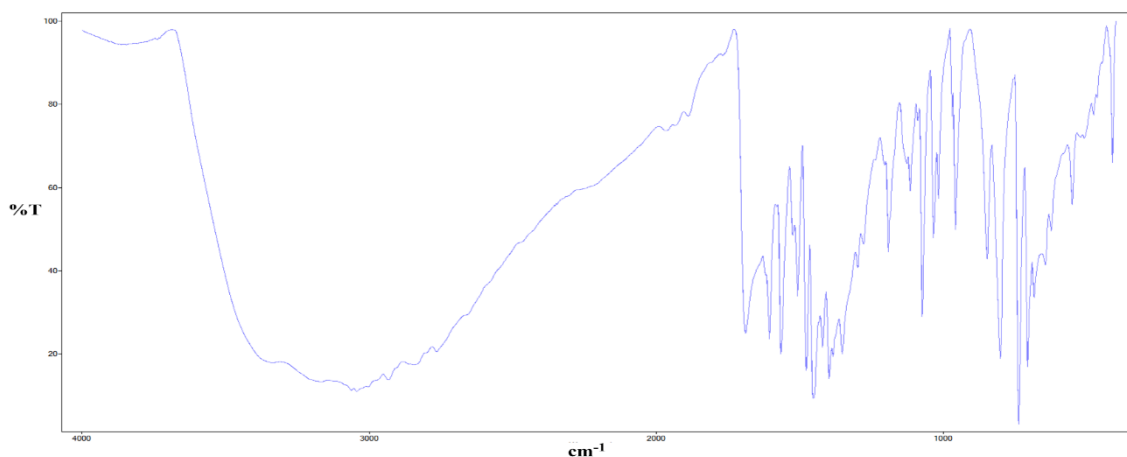
IR (KBr)  $\nu_{\text{max}}$ : 409, 430, 487, 557, 625, 636, 705, 726, 735, 804, 846, 958, 1079, 1192, 1259, 1318, 1360, 1384, 1402, 1452, 1476, 1513, 1565, 1609, 3412, 3855

$^1\text{H}$  NMR: (DMSO- $d_6$ ):  $\delta = 7.81\text{-}7.85$  (m, 4H), 8.42 (s, 4H), 8.91-8.94 (m, 4H), 9.01-9.02 (m, 4H).

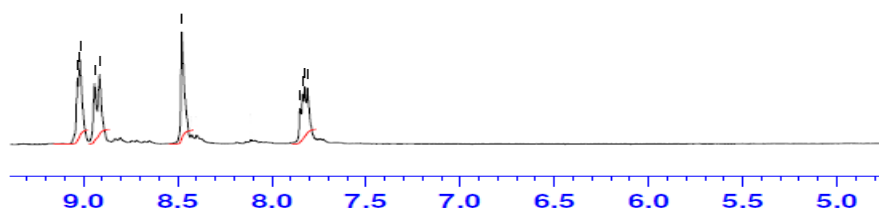
$^{13}\text{C}$  NMR: (75 MHz TFA- $d$ ):  $\delta = 122.2, 128.5, 128.7, 129.7, 132.4, 139.0, 139.4, 150.2, 151.5,$

LC/TCOF-MS: Calcd for  $\text{C}_{25}\text{H}_{16}\text{N}_4$   $[\text{M}+\text{H}]^+$  515.17267, found 515.1727

IR (KBr): **bpibH<sub>2</sub> (23)**

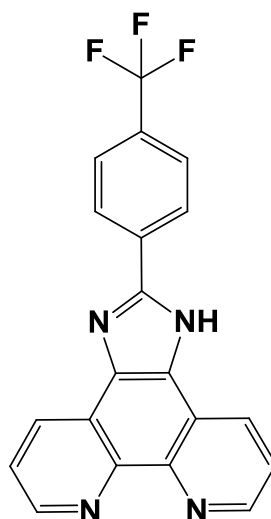


$^1\text{H}$  (DMSO- $d_6$ ) **(23) bpibH<sub>2</sub>**





### 2.8.7 Microwave synthesis of 2-(4-(trifluoromethyl)phenyl)-1*H*-imidazo[4,5-*f*][1,10]phenanthroline (**24**) (Novel method)



0.40 g (1.90 mmol) of phendione was dissolved in 15 cm<sup>3</sup> of hot dry MeOH, to which 0.052 g (9.52x10<sup>-5</sup> mol) CAN in 2 cm<sup>3</sup> of hot MeOH was added. To the resulting orange reaction mixture was added 1.47 g (0.02 mol) NH<sub>4</sub>OAc in one portion followed by 0.26 cm<sup>3</sup> (1.90 mmol) of 4-(trifluoromethyl)benzaldehyde in one portion. The resulting orange mixture was then reacted in the microwave at 75 °C (300W, 1 bar) for 10 mins. The resulting yellow coloured solution was allowed to cool to room temperature then added to 100 cm<sup>3</sup> of Millipore water which resulted in the formation of light yellow precipitate which was filtered and washed with water and acetone before being dried in an oven at 70 °C.

Product formula weight (**24**) = 364.32g/mol.

Yield: 0.605 g (87.25 %)

Mp: > 250 °C.

% Calculated: C: 65.93, H: 3.04, N: 15.38

% Found: C: 65.89, H: 3.02, N: 15.45

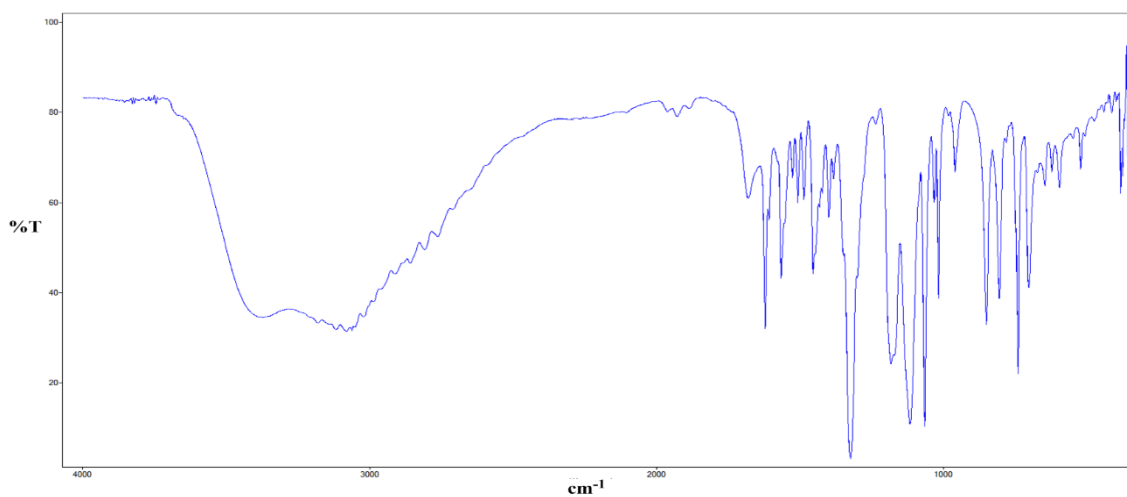
IR (KBr)  $\nu_{\max}$ : 406, 474, 521, 595, 622, 646, 705, 740, 805, 850, 959, 1017, 1032, 1065, 1117, 1169, 1324, 1383, 1398, 1454, 1486, 1507, 1526, 1565, 1621, 1678, 1929, 2215, 2807, 2912, 3180, 3395, 3690, 3871

$^1\text{H}$  NMR: (DMSO-d<sub>6</sub>):  $\delta$  = 7.78-7.82 (m, 2H), 7.92-7.95 (m, 2H), 8.41-8.44 (m, 2H), 8.85-8.89 (m, 2H), 8.99-9.01 (m, 2H).

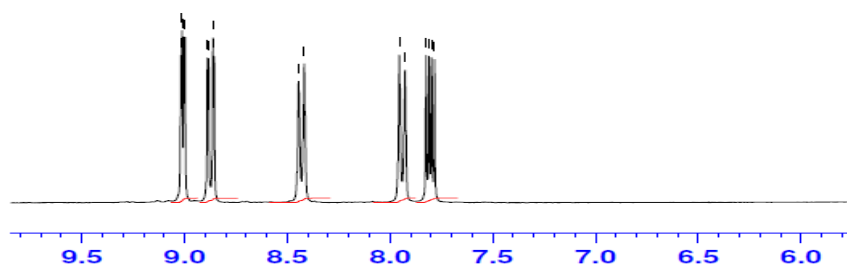
$^{13}\text{C}$  NMR: (75 MHz DMSO-d<sub>6</sub>)  $\delta$  = 121.38, 122.30, 123.37, 125.91, 126.69, 129.09, 129.48, 129.72, 131.33, 133.63, 143.53, 148.02, 149.04, 207.01.

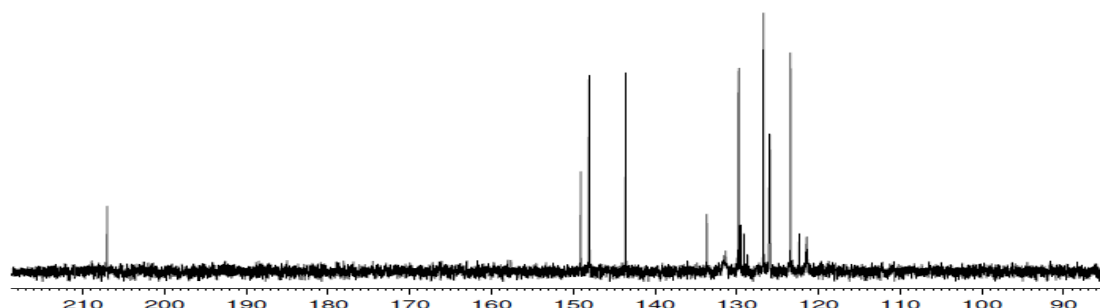
LC/TCOF-MS: Calcd for C<sub>20</sub>H<sub>11</sub>F<sub>3</sub>N<sub>4</sub> [M+H]<sup>+</sup> 365.10047, found 365.1005

IR (KBr): (24)

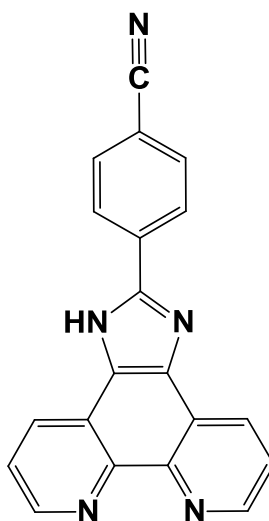


$^1\text{H}$  (DMSO-d<sub>6</sub>) (24)



$^{13}\text{C}$  (DMSO- $d_6$ ) (**24**)

### 2.8.8 Microwave synthesis of 4-(1H-imidazo[4,5-f][1,10]phenanthrolin-2-yl)benzotrile (**25**) (Novel method)

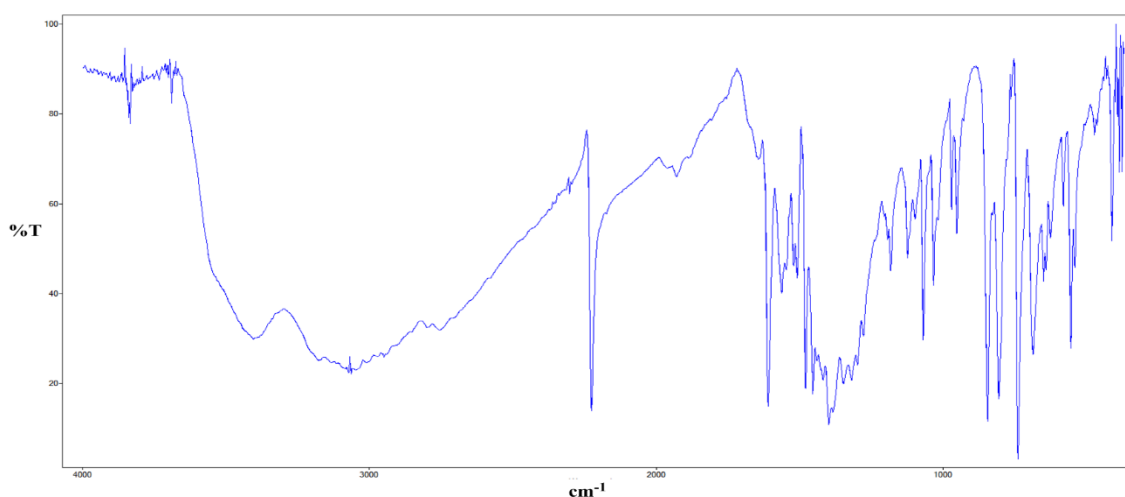


0.30 g (1.43 mmol) of phendione was dissolved in 15 cm<sup>3</sup> of hot dry MeOH, to which 0.039 g (7.14x10<sup>-5</sup> mol) CAN in 2 cm<sup>3</sup> of hot MeOH was added. To the resulting green reaction mixture was added 1.10 g (0.014 mol) NH<sub>4</sub>OAc in one portion followed by 0.187 g (1.43 mmol) of 4-formylbenzotrile in one portion. The resulting mixture was then reacted in the microwave at 75 °C (300W, 1 bar) for 10 mins. The resulting yellow coloured solution was allowed to cool to room temperature before being filtered and the resulting orange/yellow powder was washed with MeOH and 150 cm<sup>3</sup> of Millipore water before being dried in an oven at 70 °C overnight.

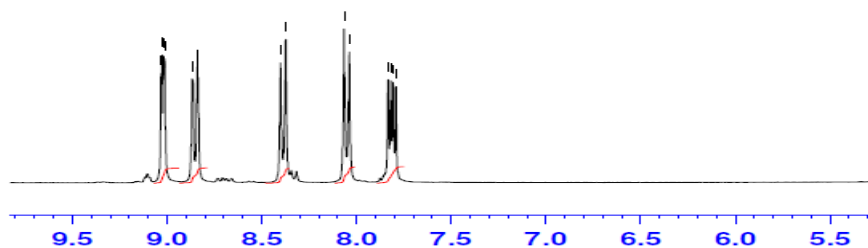
Product formula weight (**25**) = 321.34g/mol.

Yield:	0.395 g (86.20 %)
Mp:	> 250 °C.
% Calculated:	C: 74.76, H: 3.45, N: 21.79
% Found:	C: 74.72, H: 3.48, N: 21.80
IR (KBr) $\nu_{\max}$ :	428, 483, 548, 532, 584, 636, 678, 728, 739, 812, 853, 952, 980, 1016, 1087, 1114, 1145, 1178, 1281, 1318, 1384, 1043, 1424, 1456, 1479, 1516, 1546, 1582, 1610, 2011, 2231, 3073, 3227, 3429
$^1\text{H}$ NMR:	(DMSO-d <sub>6</sub> ): $\delta$ = 7.79-7.83 (m, 2H), 8.03-8.06 (m, 2H), 8.37-8.4 (m, 2H), 8.83-8.86 (m, 2H), 9.01-9.03 (m, 2H).
$^{13}\text{C}$ NMR:	(75 MHz DMSO-d <sub>6</sub> ) $\delta$ = 111.41, 118.68, 123.42, 126.62, 129.72, 133.03, 134.03, 143.78, 148.16, 148.69
LC/TCOF-MS:	Calcd for C <sub>20</sub> H <sub>11</sub> N <sub>5</sub> [M+H] <sup>+</sup> 322.1087, found 322.1098

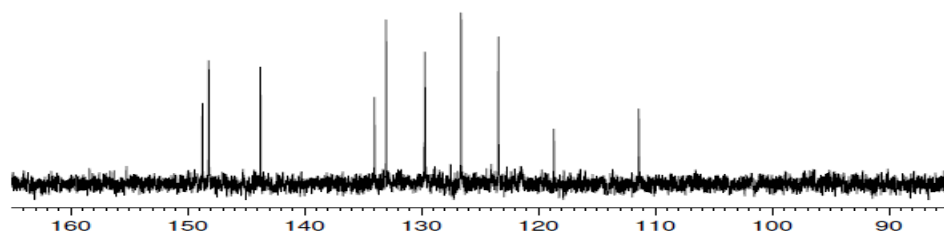
IR (KBr): (25)



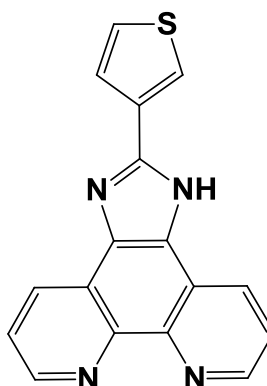
$^1\text{H}$  (DMSO- $d_6$ ) (25)



$^{13}\text{C}$  (DMSO- $d_6$ ) (25)



### 2.8.9 Microwave synthesis of 2-(thiophen-3-yl)-1*H*-imidazo[4,5-*f*][1,10]phenanthroline (26) (Novel method)

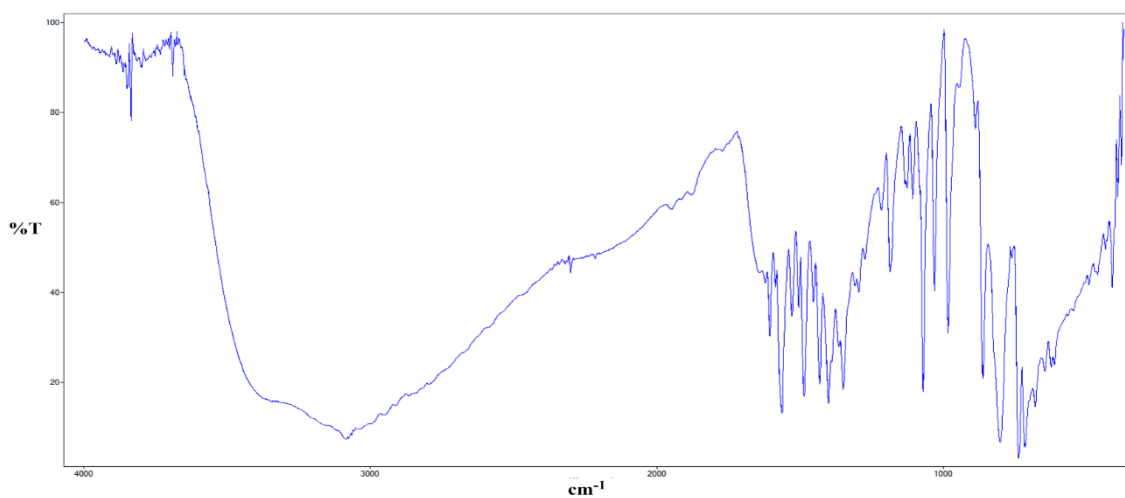


0.30 g (1.43 mmol) of phendione was dissolved in 15 cm<sup>3</sup> of hot dry MeOH, to which 0.039 g (7.14x10<sup>-5</sup> mol) CAN in 2 cm<sup>3</sup> of hot MeOH was added. To the resulting green reaction mixture was added 1.10 g (0.014 mol) NH<sub>4</sub>OAc in one portion followed by 0.125 cm<sup>3</sup> (1.43 mmol) of 3-thiophenecarboxaldehyde in one portion. The resulting orange mixture was then reacted in the microwave at 75 °C (300W, 1 bar) for 10 mins. The resulting yellow coloured solution was allowed to cool to room temperature before being added to 150 cm<sup>3</sup> of Millipore water to produce a dark yellow powder which was filtered, washed with water and MeOH and dried in an oven at 70 °C overnight.

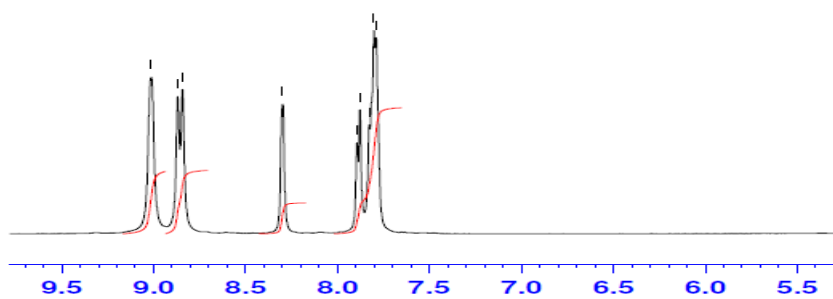
Product formula weight (**26**) = 302.35g/mol.

Yield:	0.381 g (88.21 %)
Mp:	> 250 °C.
% Calculated:	C: 67.53, H: 3.33, N: 18.53
% Found:	C: 67.48, H: 3.30, N: 18.64
IR (KBr) $\nu_{\max}$ :	430, 553, 626, 723, 735, 810, 864, 888, 940, 984, 1080, 1140, 1187, 1271, 1314, 1366, 1387, 1407, 1452, 1485, 1515, 1568, 1609, 2010, 3092, 3413
<sup>1</sup> H NMR:	(DMSO-d <sub>6</sub> ): $\delta$ = 7.77-7.89 (m, 4H), 8.29 (m, 1H), 8.84-9.01 (m, 4H)
<sup>13</sup> C NMR:	(75 MHz DMSO-d <sub>6</sub> ) $\delta$ = 123.23, 124.45, 126.18, 127.76, 129.50, 132.11, 143.43, 147.33, 147.69
LC/TCOF-MS:	Calcd for C <sub>17</sub> H <sub>10</sub> N <sub>4</sub> S [M+H] <sup>+</sup> 303.0696, found 303.0696

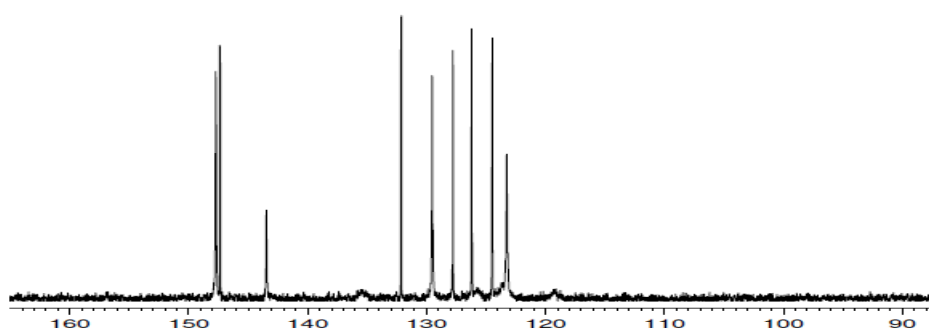
IR (KBr): (26)

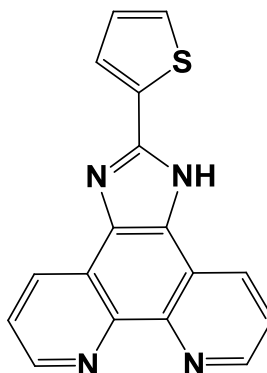


<sup>1</sup>H (DMSO-d<sub>6</sub>) (26)



<sup>13</sup>C (DMSO-d<sub>6</sub>) (26)



**2.8.10 Microwave synthesis of 2-(thiophen-2-yl)-1H-imidazo[4,5-f][1,10]phenanthroline (27) (Novel method)**

0.30 g (1.43 mmol) of phendione was dissolved in 15 cm<sup>3</sup> of hot dry MeOH, to which 0.039 g (7.14x10<sup>-5</sup> mol) CAN in 2 cm<sup>3</sup> of hot MeOH was added. To the resulting green reaction mixture was added 1.10 g (0.014 mol) NH<sub>4</sub>OAc in one portion followed by 0.134 cm<sup>3</sup> (1.43 mmol) of 2-thiophenecarboxaldehyde in one portion. The resulting orange mixture was then reacted in the microwave at 75 °C (300W, 1 bar) for 10 mins. The resulting yellow coloured solution was allowed to cool to room temperature before being filtered to produce a bright pale orange powder. To the filtrate was added 150 cm<sup>3</sup> of Millipore water to produce a bright pale orange powder which was filtered and dried in an oven at 70 °C overnight.

Product formula weight (**27**) = 302.35g/mol.

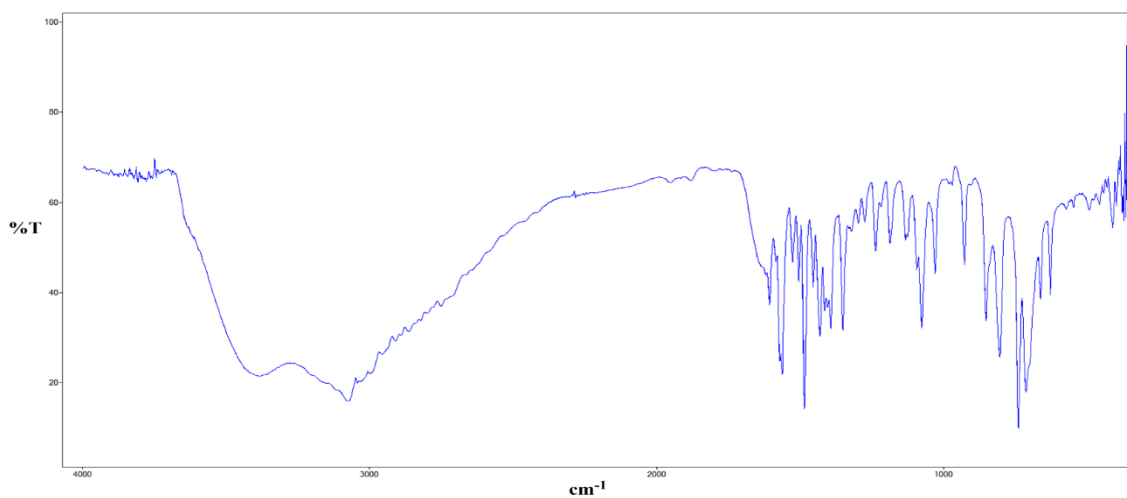
Yield:	0.378 g (87.60 %)
Mp:	> 250 °C.
% Calculated:	C: 67.53, H: 3.33, N: 18.53
% Found:	C: 67.52, H: 3.36, N: 18.49
IR (KBr) $\nu_{\max}$ :	430, 626, 636, 667, 723, 734, 810, 852, 929, 980, 1085, 1116, 1145, 1240, 1277, 1320, 1361, 1405, 1450, 1462, 1484, 1515, 1571, 1609, 2024, 3074, 3421
<sup>1</sup> H NMR:	(DMSO-d <sub>6</sub> ): $\delta$ = 7.29 (s, 1H), 7.75-7.92 (m, 4H), 8.84-9.03 (m, 4H).



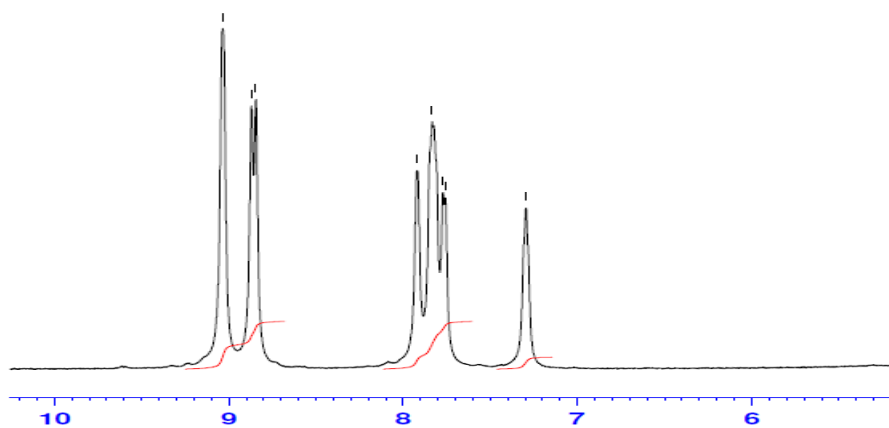
$^{13}\text{C}$  NMR: (75 MHz DMSO-d<sub>6</sub>)  $\delta$  = 123.30, 126.23, 128.32, 129.55,  
133.44, 143.51, 146.36, 147.82

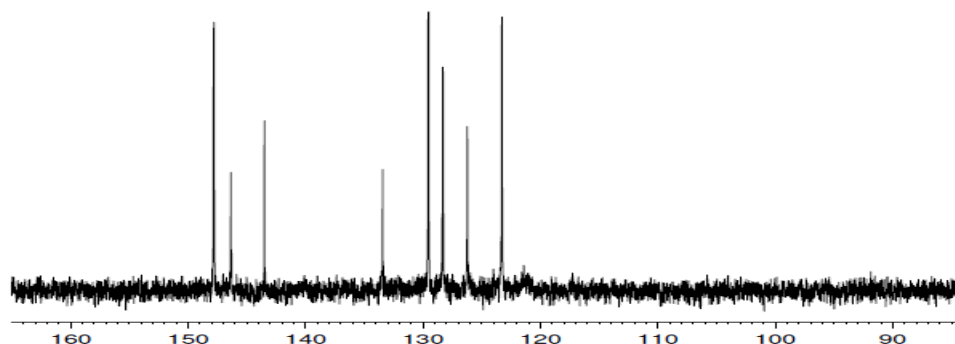
LC/TOF-MS: Calcd for C<sub>17</sub>H<sub>10</sub>N<sub>4</sub>S [M+H]<sup>+</sup> 303.0696, found 303.0696

IR (KBr): (27)

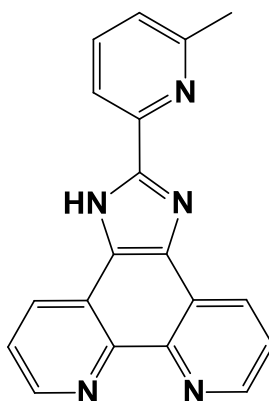


$^1\text{H}$  (DMSO-d<sub>6</sub>) (27)



$^{13}\text{C}$  (DMSO- $d_6$ ) (**27**)

### 2.8.11 Microwave synthesis of 2-(6-methylpyridin-2-yl)-1H-imidazo[4,5-f][1,10]phenanthroline (**28**) (Novel method)

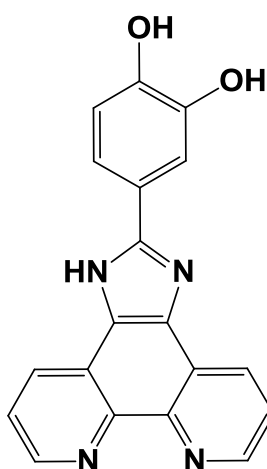


0.30 g (1.43 mmol) of phendione was dissolved in 15 cm<sup>3</sup> of hot dry MeOH, to which 0.039 g (7.14x10<sup>-5</sup> mol) CAN in 2 cm<sup>3</sup> of hot MeOH was added. To the resulting green reaction mixture was added 1.10 g (0.014 mol) NH<sub>4</sub>OAc in one portion followed by 0.173 g (1.43 mmol) of 6-methylpyridine-2-carboxaldehyde in one portion. The resulting mixture was then reacted in the microwave at 75 °C (300W, 1 bar) for 10 mins. The resulting yellow coloured solution was allowed to cool to room temperature before being filtered and the resulting orange/yellow powder was washed with MeOH and 150 cm<sup>3</sup> of Millipore water before being dried in an oven at 70 °C overnight. Known method yields 24.5%<sup>7</sup>, new method yields 93%.

Product formula weight (**28**) = 311.34g/mol.

Yield:	0.414 g (93.00 %)
Mp:	> 250 °C.
% Calculated:	C: 73.30, H: 4.21, N: 22.49
% Found:	C: 72.98, H: 4.38, N: 22.69
IR (KBr) $\nu_{\text{max}}$ :	3060, 3018, 1592, 1565, 1447, 1070, 740
$^1\text{H}$ NMR:	( $\text{CDCl}_3$ -d): $\delta$ = 11.60 (br, s, 1H), 9.17 (d, 2H), 9.05 (d, 1H), 8.52 (d, 1H), 8.49 (d, 1H), 8.30 (d, 1H), 7.80 (dd, 1H), 7.74 (dd, 1H), 7.68 (dd, 1H), 7.24 (d, 1H), 2.66 (s, 3H).
LC/TCOF-MS:	Calcd for $\text{C}_{19}\text{H}_{13}\text{N}_5$ $[\text{M}+\text{H}]^+$ 312.1243, found 312.1243

### 2.8.12 Microwave synthesis of 4-(1H-imidazo[4,5-f][1,10]phenanthrolin-2-yl)benzene-1,2-diol (29) (Novel method)



0.35 g ( $1.67 \times 10^{-3}$  mol) of phendione was dissolved in 15  $\text{cm}^3$  of hot dry MeOH, to which 0.047 g ( $8.33 \times 10^{-5}$  mol) CAN in 2  $\text{cm}^3$  of hot MeOH was added. To the resulting reaction mixture was added 1.284 g (.0167 mol)  $\text{NH}_4\text{OAc}$  in one portion followed by 0.24 g ( $1.67 \times 10^{-3}$  mol) of 3,4-dihydroxybenzaldehyde. The resulting dark brown/orange mixture was then reacted in the microwave at 75 °C (300W, 1 bar) for 10 mins. The resulting solution was allowed to cool to room temperature before being added to 150  $\text{cm}^3$  of Millipore water to yield a green precipitate which was filtered and washed with Millipore water before being dried in an oven at 70 °C overnight.

Product formula weight (**29**) = 328.32g/mol.

Yield: 0.463 g (84.76 %)

Mp: > 250 °C.

% Calculated: C: 69.51, H: 3.68, N: 17.06

% Found: C: 69.48, H: 3.74, N: 17.02

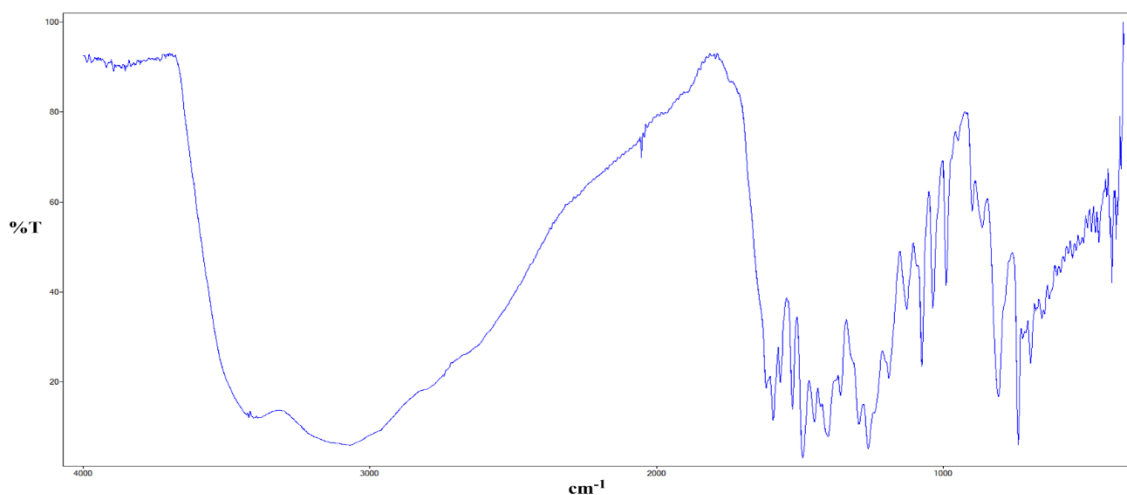
IR (KBr)  $\nu_{\max}$ : 431, 477, 625, 725, 811, 867, 897, 941, 984, 1078, 1275, 1364, 1404, 1454, 1487, 1526, 1610, 3412

$^1\text{H}$  NMR: (DMSO- $d_6$ ):  $\delta$  = 6.93-6.96 (m, 1H), 7.57-7.60 (m, 1H), 7.73-7.74 (m, 1H), 7.81 (s, 2H), 8.88-8.91 (m, 2H), 9.00-9.01 (m, 2H), 9.34 (s, 1H), 9.54 (s, 1H), 13.48 (s, 1H).

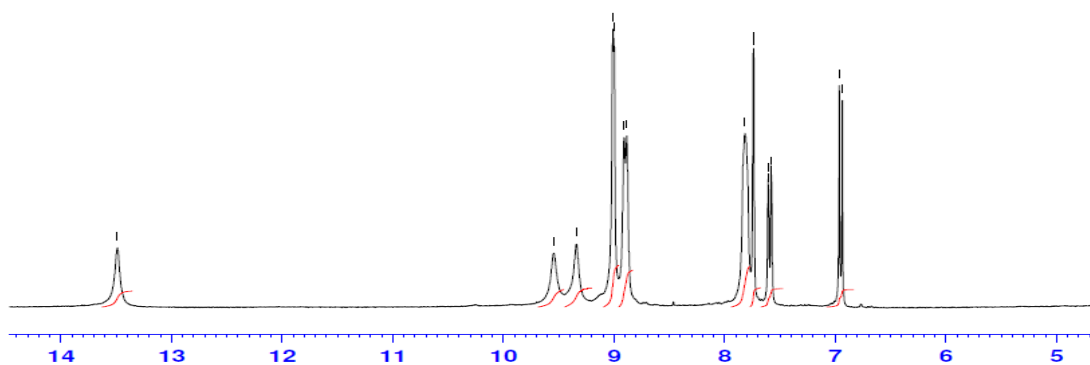
$^{13}\text{C}$  NMR: (75 MHz DMSO- $d_6$ )  $\delta$  = 28.92, 113.94, 115.85, 118.1, 119.27, 121.45, 123.1, 123.63, 125.91, 129.48, 135.57, 143.20, 145.63, 147.30, 147.49, 151.39

LC/TCOF-MS: Calcd for  $\text{C}_{19}\text{H}_{12}\text{N}_4\text{O}_2$   $[\text{M}+\text{H}]^+$  329.1038, found 329.1038

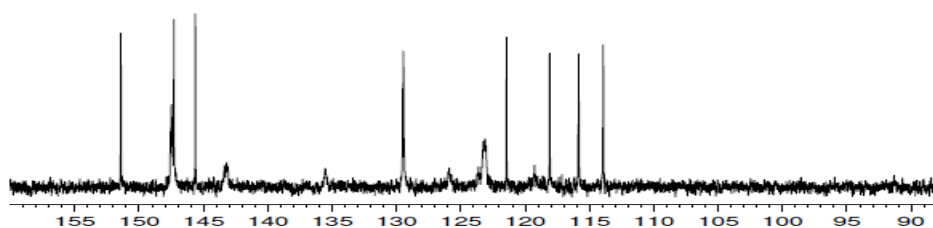
IR (KBr): (**29**)



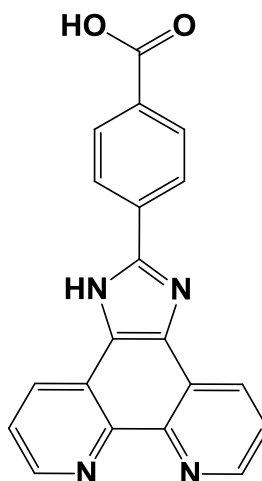
$^1\text{H}$  (DMSO- $d_6$ ) (29)



$^{13}\text{C}$  (DMSO- $d_6$ ) (29)



### 2.8.13 Microwave synthesis of 4-(1*H*-imidazo[4,5-*f*][1,10]phenanthrolin-2-yl)benzoic acid (30) (Novel method)

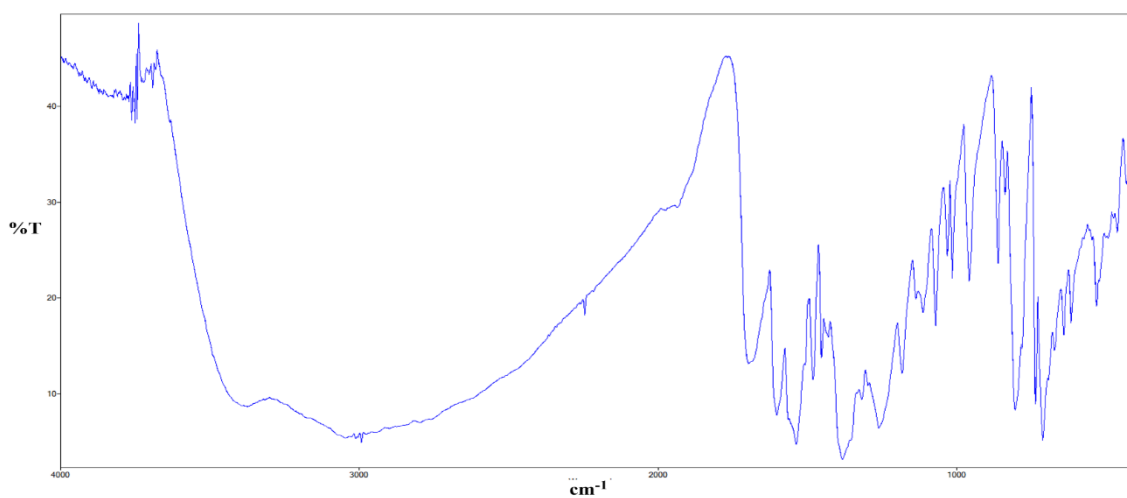


0.40 g ( $1.90 \times 10^{-3}$  mol) of phendione was dissolved in 20 cm<sup>3</sup> of hot dry MeOH, to which 0.052 g ( $9.52 \times 10^{-5}$  mol) CAN in 5 cm<sup>3</sup> of hot MeOH was added. To the resulting reaction mixture was added 1.47 g (0.02 mol) NH<sub>4</sub>OAc in one portion followed by 0.29 g ( $1.90 \times 10^{-3}$  mol) of 4-formylbenzoic acid. The resulting yellow mixture was then reacted in the microwave at 75 °C (300W, 1 bar) for 10 mins before being added to 200 cm<sup>3</sup> of Millipore water and allowed to sit before being filtering to produce a yellow coloured solid that was washed with Millipore water and allowed to dry in air before being dried further in an oven at 70 °C for 3 hrs.

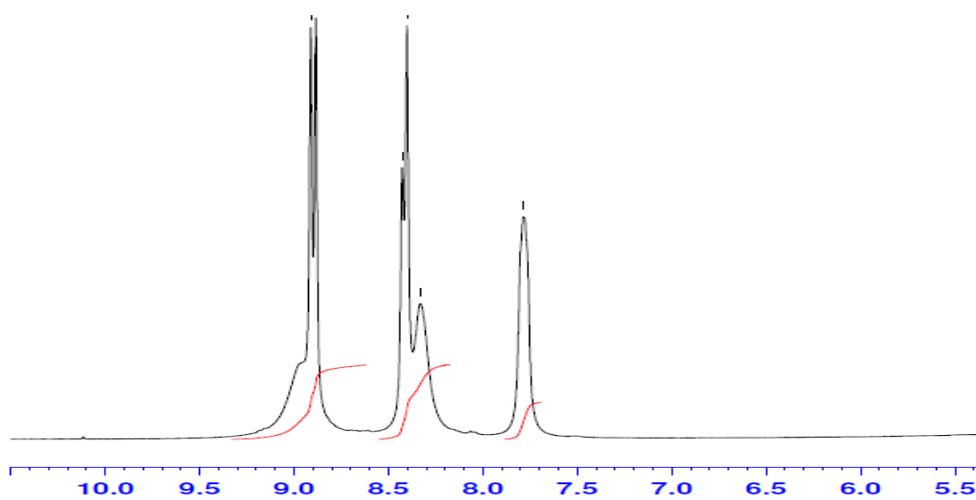
Product formula weight (**30**) = 340.34g/mol.

Yield:	0.535 g (82.6 %)
Mp:	> 250 °C.
% Calculated:	C: 70.58, H: 3.55, N: 16.46
% Found:	C: 70.54, H: 3.60, N: 16.40
IR (KBr) $\nu_{\max}$ :	430, 459, 555, 626, 636, 647, 724, 734, 790, 813, 837, 868, 953, 1011, 1079, 1144, 1387, 1459, 1481, 1550, 1586, 1609, 3409
<sup>1</sup> H NMR:	(DMSO-d <sub>6</sub> ): $\delta$ = 7.78-7.80 (m, 2H), 8.31-8.42 (m, 4H), 8.88-8.91 (m, 4H).
<sup>13</sup> C NMR:	(75 MHz DMSO-d <sub>6</sub> ) $\delta$ = 21.16, 121.54, 123.29, 126.14, 129.68, 130.08, 133.43, 143.50, 147.47, 149.54, 167.52, 172.11.
LC/TCOF-MS:	Calcd for C <sub>19</sub> H <sub>12</sub> N <sub>4</sub> O <sub>2</sub> [M+H] <sup>+</sup> 341.1033, found 341.1047

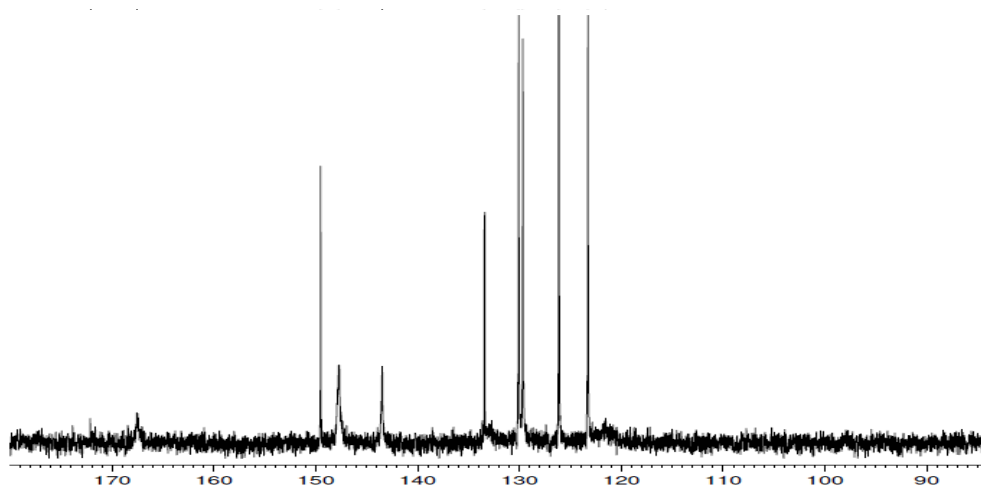
IR (KBr): (30)

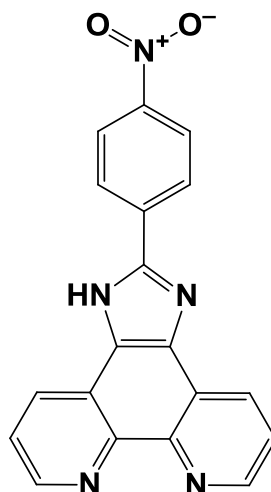


<sup>1</sup>H (DMSO-d<sub>6</sub>) (30)



<sup>13</sup>C (DMSO-d<sub>6</sub>) (30)



**2.8.14 Synthesis of 2-(4-nitrophenyl)-1*H*-imidazo[4,5-*f*][1,10]phenanthroline (4nitrip) (31) (Novel method)**

0.40 g ( $1.90 \times 10^{-3}$  mol) of phendione was dissolved in 50 cm<sup>3</sup> of hot dry MeOH. To this was added 0.052 g ( $9.50 \times 10^{-5}$  mol) CAN in 20 cm<sup>3</sup> of MeOH and 1.47 g (0.02 mol) of NH<sub>4</sub>OAc in one portion. To the resulting yellow solution was added 0.29 g ( $1.90 \times 10^{-3}$  mol) of 4-nitrobenzaldehyde and the resulting yellow solution. The resulting yellow mixture was then reacted in the microwave at 75 °C (300W, 1 bar) for 15 mins before being added to 150 cm<sup>3</sup> of Millipore water and allowed to sit before being filtering to produce a yellow coloured solid that was washed with MeOH and Millipore water and allowed to dry in air before being dried further in an oven at 70 °C for overnight.

Product formula weight (**31**) = 341.32g/mol.

Yield:	0.52 g (80 %)
Mp:	> 250 °C.
% Calculated:	C, 66.86; H, 3.25; N, 20.52
% Found:	C, 66.82; H, 3.31; N, 20.49
IR (KBr) $\nu_{\max}$ :	430, 459, 555, 626, 636, 647, 724, 734, 790, 813, 837, 868, 953, 1011, 1079, 1144, 1387, 1459, 1481, 1550, 1586, 1609, 3409

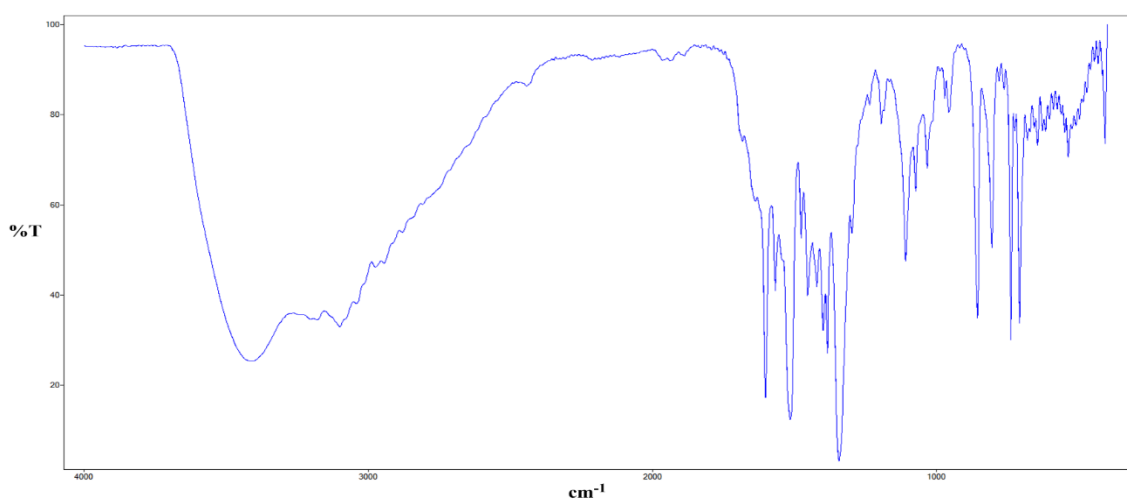


$^1\text{H}$  NMR: (DMSO- $d_6$ ):  $\delta = 7.78\text{-}7.82$  (m, 2H), 8.39-8.47 (m, 4H), 8.84-8.87 (m, 2H), 9.01-9.03 (m, 2H)

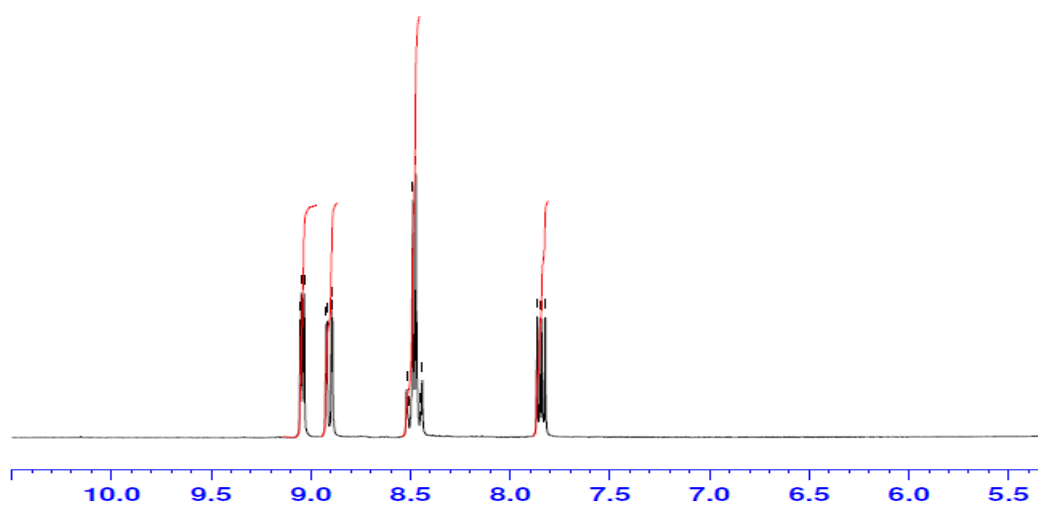
$^{13}\text{C}$  NMR: (75 MHz DMSO- $d_6$ )  $\delta = 28.97, 121.44, 123.34, 124.33, 126.85, 129.69, 135.80, 143.85, 147.35, 148.14, 148.24$

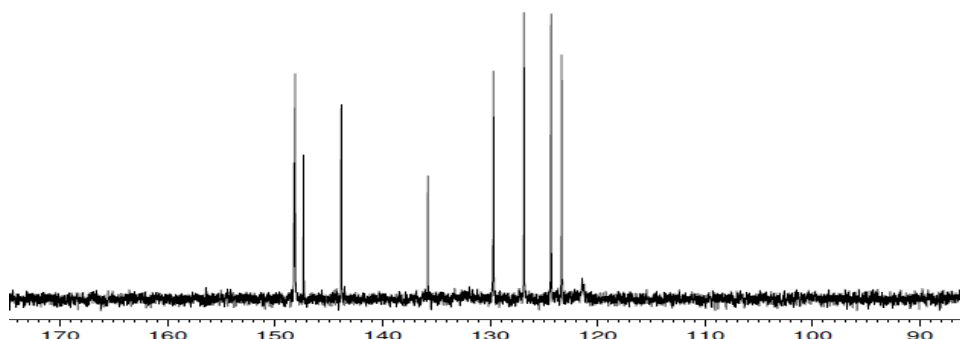
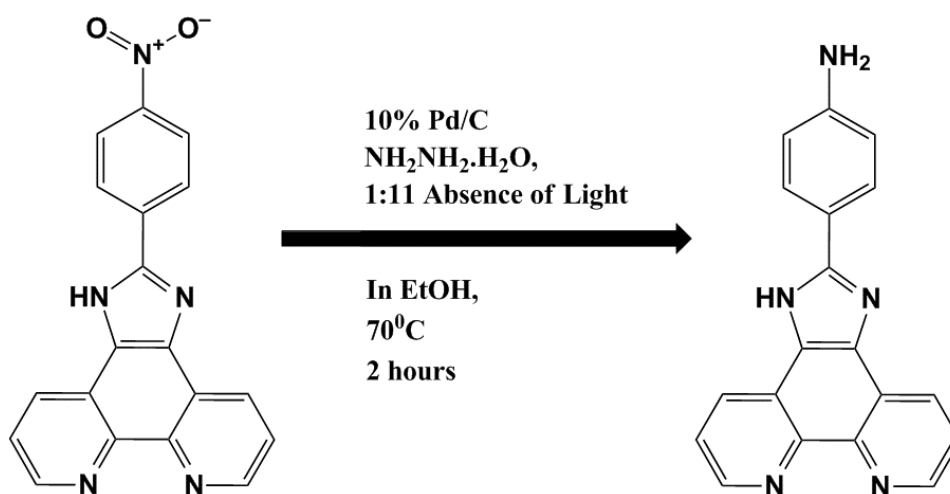
LC/TCOF-MS: Calcd for  $\text{C}_{19}\text{H}_{11}\text{N}_5\text{O}_2$   $[\text{M}+\text{H}]^+$  342.0986, found 342.0996

IR (KBr): **4nitrip (31)**



$^1\text{H}$  (DMSO- $d_6$ ) **4nitrip (31)**



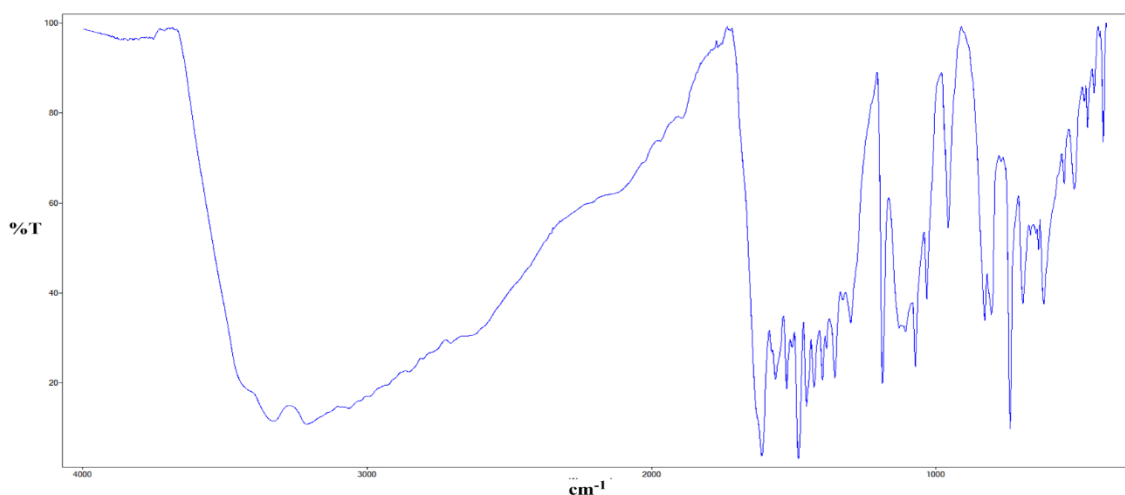
$^{13}\text{C}$  (DMSO- $d_6$ ) 4nitrip (**31**)2.8.15 Synthesis of 4-(1*H*-imidazo[4,5-*f*][1,10]phenanthrolin-2-yl)aniline (**32**)

0.40g (1.172 mmol) of 2-(4-nitrophenyl)-1*H*-imidazo[4,5-*f*][1,10]phenanthroline, 4nitrip (**31**) dissolved in 150 cm<sup>3</sup> EtOH was added to a 250 cm<sup>3</sup> round bottomed flask. To this was added, 0.10g of 10 % Pd/C catalyst and the mixture was refluxed for 1 hr. 626  $\mu\text{L}$  (0.013 mol) hydrazine monohydrate was added in one portion and the resulting mixture was refluxed for 2 hrs.<sup>8</sup> The resulting dark mixture was allowed to cool to room temperature and filtered through a bed of celite to produce a yellow filtrate. The solvent was removed under reduced pressure to yield an orange powder.

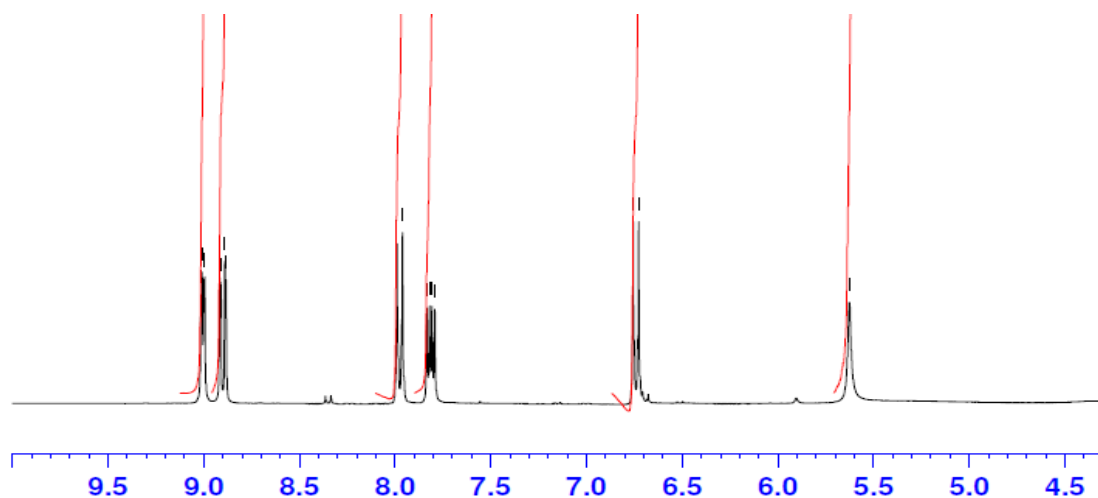
Product formula weight (**32**) = 311.34g/mol.

Yield:	0.24 g (65 %)
Mp:	> 250 °C.
% Calculated:	C, 73.30; H, 4.21; N, 22.49
% Found:	C, 73.10; H, 4.26; N, 22.46
IR (KBr) $\nu_{\max}$ :	411, 443, 466, 477, 513, 548, 620, 638, 694, 738, 804, 827, 956, 1032, 1072, 1106, 1187, 1299, 1355, 1384, 1398, 1428, 1455, 1483, 1524, 1564, 1612, 3212, 3327
$^1\text{H}$ NMR:	(DMSO- $d_6$ ): $\delta$ = 5.32 (s, 2H), 6.72-6.75 (d, 2H), 7.79-7.83 (m, 2H), 7.96-7.99 (m, 2H), 8.88-8.91 (m, 2H), 8.99-9.01 (m, 2H).
$^{13}\text{C}$ NMR:	(75 MHz DMSO- $d_6$ ) $\delta$ = 14.85, 18.50, 24.64, 55.99, 113.60, 117.25, 123.10, 127.55, 129.39, 143.15, 144.16, 147.31, 150.41, 152.06.
LC/TCOF-MS:	Calcd for $\text{C}_{19}\text{H}_{11}\text{N}_5\text{O}_2$ $[\text{M}+\text{H}]^+$ 342.0986, found 342.0996

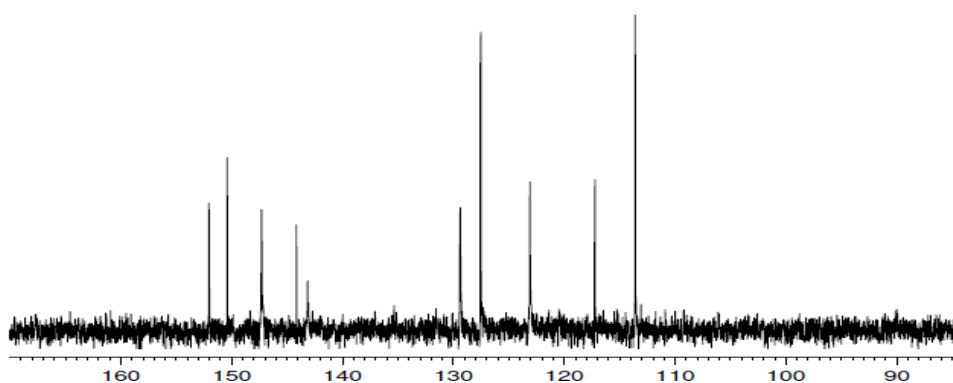
IR (KBr): **anlip (32)**



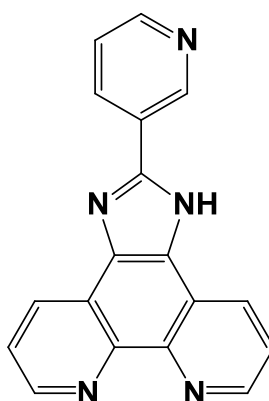
$^1\text{H}$  (DMSO- $d_6$ ) **anilip** (32)



$^{13}\text{C}$  (DMSO- $d_6$ ) **anilip** (32)



**2.8.16 Microwave synthesis of 2-(pyridin-3-yl)-1H-imidazo[4,5-f][1,10]phenanthroline (33) (Novel method)**

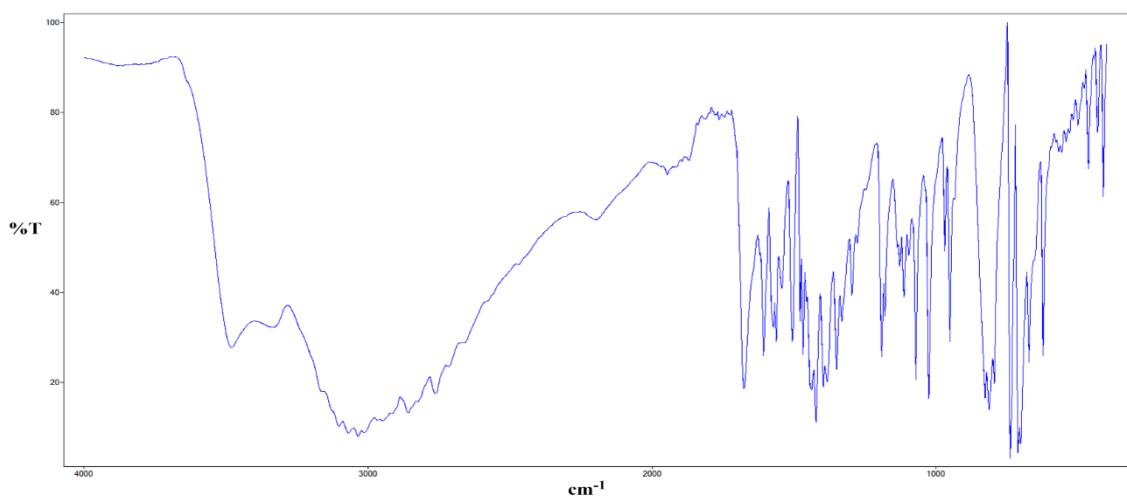


0.20 g ( $9.52 \times 10^{-4}$  mol) of phendione was dissolved in 15 cm<sup>3</sup> of hot dry MeOH, to which 0.026 g ( $4.76 \times 10^{-5}$  mol) CAN in 2 cm<sup>3</sup> of hot MeOH was added. To the resulting reaction mixture was added 0.73 g ( $9.52 \times 10^{-3}$  mol) NH<sub>4</sub>OAc in one portion followed by 91 μL ( $9.52 \times 10^{-4}$  mol) of 2-pyridinecarboxaldehyde. The resulting mixture was then reacted in the microwave at 75 °C (300W, 1 bar) for 10 mins. The resulting solution was allowed to cool to room temperature before being filtered and washed with MeOH and dried further in an oven at 70 °C for overnight.

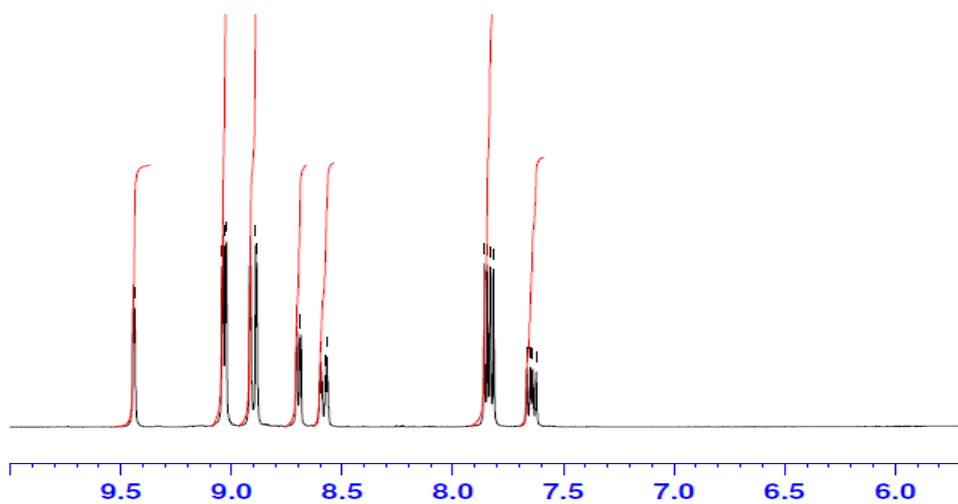
Product formula weight (**33**) = 297.31g/mol.

Yield:	0.255 g (90.11 %)
Mp:	> 250 °C
% Calculated:	C, 72.72; H, 3.73; N, 23.56
% Found:	C, 72.72; H, 3.73; N, 23.56
IR (KBr) $\nu_{\max}$ :	432, 469, 544, 623, 650, 682, 724, 755, 809, 850, 929, 954, 981, 1080, 1187, 1244, 1313, 1363, 1405, 1457, 1483, 1515, 1548, 1604, 1622, 3069, 3415
<sup>1</sup> H NMR:	(DMSO-d <sub>6</sub> ): $\delta$ = 7.62-7.66 (m, 1H), 7.81-7.853 (m, 2H), 8.57-8.59 (m, 1H), 8.68-.8.70 (m, 1H), 8.88-8.91 (m, 2H), 9.012-9.03 (m, 2H), 9.44 (s, 1H)
<sup>13</sup> C NMR:	(75 MHz DMSO-d <sub>6</sub> ) $\delta$ = 123.39, 124.09, 126.09, 129.67, 133.53, 143.56, 147.18, 148.01, 148.17, 150.17
LC/TCOF-MS:	Calcd for C <sub>18</sub> H <sub>11</sub> N <sub>5</sub> [M+H] <sup>+</sup> 298.1083, found 298.1082

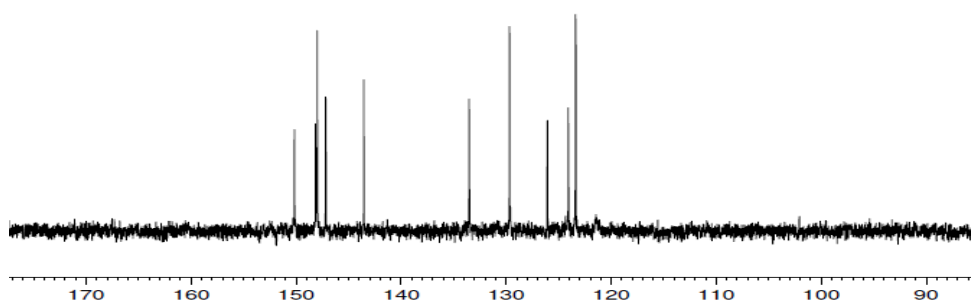
IR (KBr): (33)

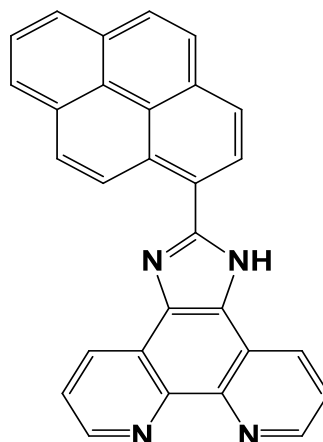


$^1\text{H}$  (DMSO-d6) (33)



$^{13}\text{C}$  (DMSO-d6) (33)



**2.8.17 Microwave synthesis of 2-(pyren-1-yl)-1H-imidazo[4,5-f][1,10]phenanthroline (34) (Novel method)**

0.20 g ( $9.52 \times 10^{-4}$  mol) of phendione was dissolved in 15 cm<sup>3</sup> of hot dry MeOH, to which 0.026 g ( $4.76 \times 10^{-5}$  mol) CAN in 2 cm<sup>3</sup> of hot MeOH was added. To the resulting reaction mixture was added 0.73 g ( $9.52 \times 10^{-3}$  mol) NH<sub>4</sub>OAc in one portion followed by 0.22 g ( $9.52 \times 10^{-4}$  mol) of 1-pyrenecarboxaldehyde. The resulting mixture was then reacted in the microwave at 75 °C (300W, 1 bar) for 10 mins. The yellow reaction mixture was allowed to cool to room temperature to which 300 cm<sup>3</sup> of Millipore water was added and mixed and allowed to sit before being filtering to produce a yellow/brown solid that was washed with Millipore water and allowed to dry in air before being dried further in an oven at 70 °C (0.376 g, 94 %).

Product formula weight (**34**) = 420.46g/mol.

Yield: 0.376 g (94 %)

Mp: > 250 °C.

% Calculated: C, 82.84; H, 3.84; N, 13.32

% Found: C, 82.79; H, 3.88; N, 13.29

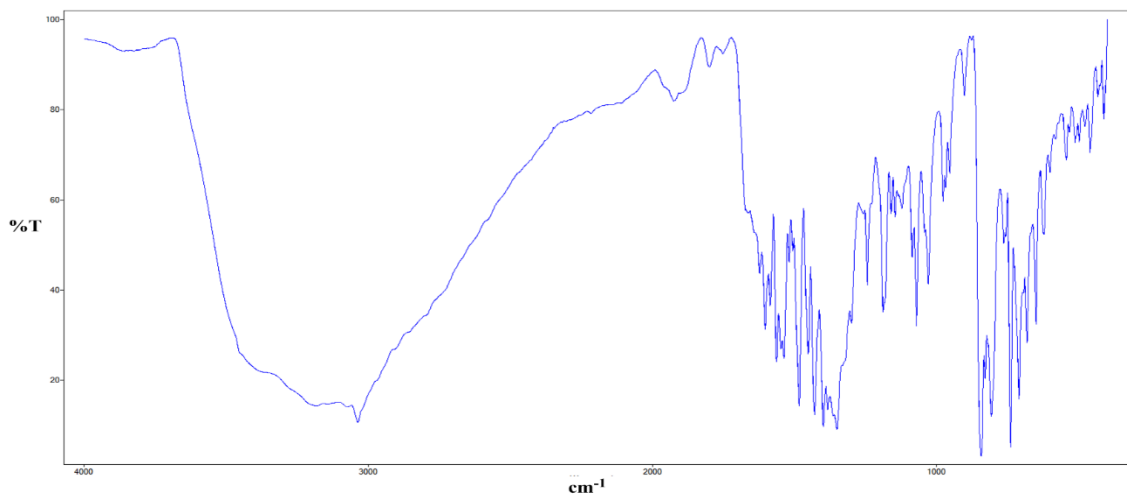
IR (KBr)  $\nu_{\max}$ : 432, 469, 544, 623, 650, 682, 724, 755, 809, 850, 929, 954, 981, 1080, 1187, 1244, 1313, 1363, 1405, 1457, 1483, 1515, 1548, 1604, 1622, 3069, 3415

$^1\text{H}$  NMR: (DMSO-d<sub>6</sub>):  $\delta$  = 7.87-7.91 (m, 2H), 8.13-8.18 (m, 1H), 8.31-8.32 (m, 1H), 8.37-8.41 (m, 3H), 8.52-8.55 (m, 1H), 8.66-8.69 (m, 1H), 9.03-9.09 (m, 4H), 9.51-9.54 (m, 1H).

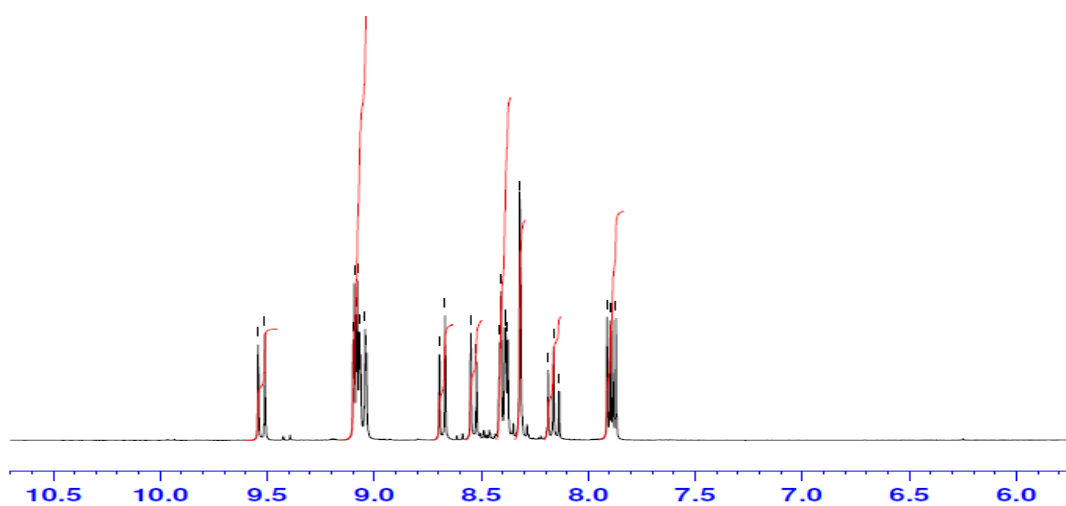
$^{13}\text{C}$  NMR: (75 MHz DMSO-d<sub>6</sub>)  $\delta$  = 123.41, 123.70, 124.35, 124.87, 125.48, 125.60, 125.94, 126.70, 127.31, 127.4, 128.50, 128.56, 128.61, 129.84, 130.31, 130.90, 131.58, 143.61, 147.95, 150.88

LC/TCOF-MS: Calcd for  $\text{C}_{29}\text{H}_{16}\text{N}_4$   $[\text{M}+\text{H}]^+$  421.1453, found 421.1467

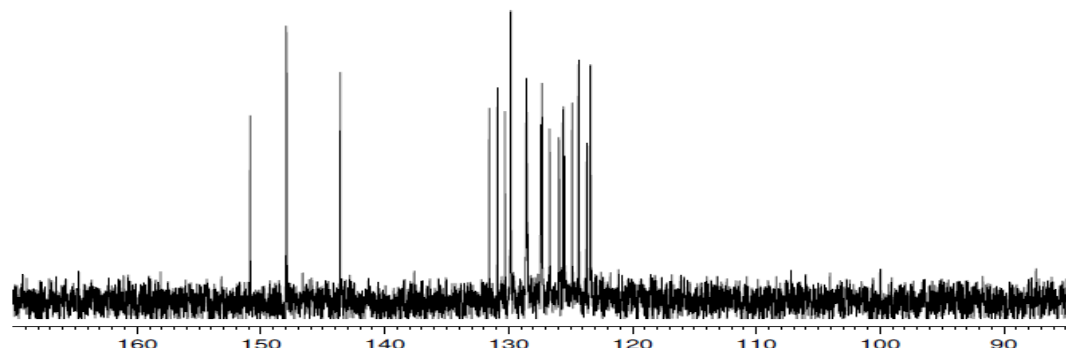
IR (KBr): (34)



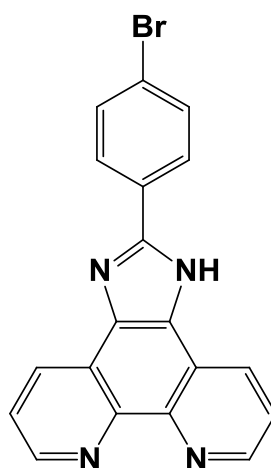
$^1\text{H}$  (DMSO-d<sub>6</sub>) (34)





$^{13}\text{C}$  (DMSO- $d_6$ ) (34)

### 2.8.18 Microwave synthesis of 2-(4-bromophenyl)-1*H*-imidazo[4,5-*f*][1,10]phenanthroline (35) (Novel method)



0.30 g ( $1.43 \times 10^{-3}$  mol) of phendione was dissolved in 15 cm<sup>3</sup> of hot dry MeOH, to which 0.039 g ( $7.15 \times 10^{-5}$  mol) CAN in 2 cm<sup>3</sup> of hot MeOH was added. To the resulting reaction mixture was added 1.10 g (0.014 mol) NH<sub>4</sub>OAc in one portion followed by 0.264 g ( $1.43 \times 10^{-3}$  mol) of 4-bromobenzaldehyde. The resulting mixture was then reacted in the microwave at 75 °C (300W, 1 bar) for 10 mins. The reaction mixture was then added to a 100 cm<sup>3</sup> beaker and allowed to stir in MeOH for 2 hrs. Following this period, 200 cm<sup>3</sup> of Millipore water was added and mixed and allowed to sit before being filtering to produce a cream coloured solid that was washed with Millipore water and allowed to dry in air before being dried further in an oven at 70 °C

Product formula weight (**35**) = 375.22g/mol.

Yield: 0.46 g (85.74 %)

Mp: > 250 °C.

% Calculated: C, 60.82; H, 2.95; N, 14.93

% Found: C, 60.78; H, 3.00; N, 14.92

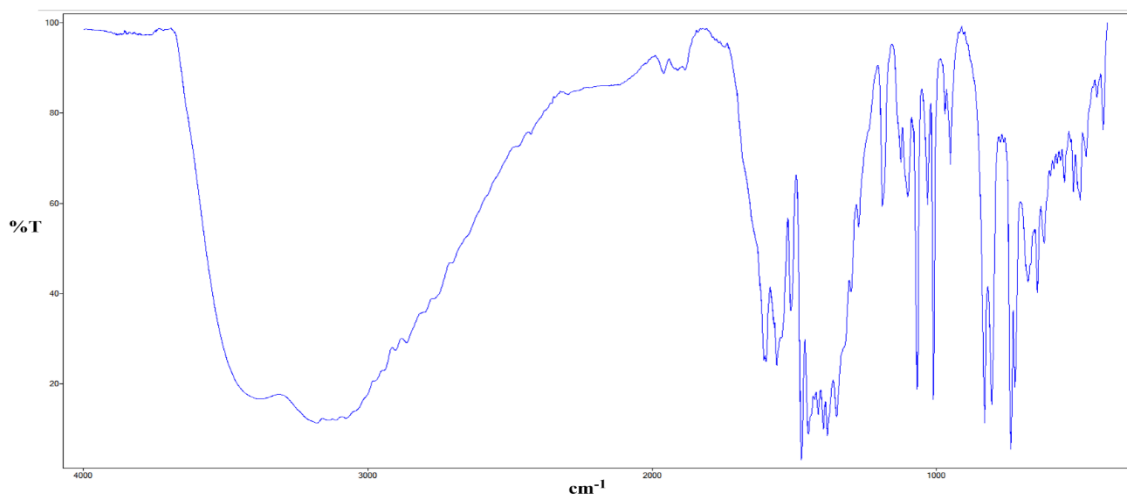
IR (KBr)  $\nu_{\max}$ : 413, 435, 474, 494, 518, 550, 621, 645, 677, 724, 738, 805, 831, 951, 969, 1010, 1031, 1067, 1100, 1125, 1189, 1274, 1300, 1351, 1383, 1397, 1416, 1451, 1474, 1512, 1562, 1599, 1910, 1959, 3179

$^1\text{H}$  NMR: (DMSO- $d_6$ ):  $\delta$  = 7.82-7.85 (m, 4H), 8.21-8.23 (m, 2H), 8.88-8.91 (m, 3H), 9.03 (bs, 1H), 13.83 (bs, 1H)

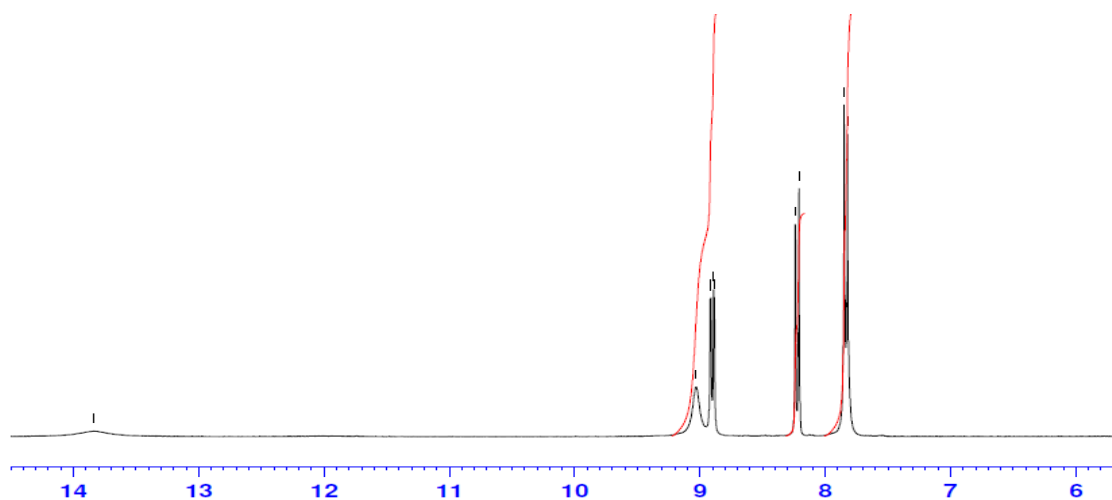
$^{13}\text{C}$  NMR: (75 MHz DMSO- $d_6$ )  $\delta$  = 122.94, 1233.34, 128.07, 129.14, 129.62, 132.04, 147.94, 149.47

LC/TCOF-MS: Calcd for  $\text{C}_{19}\text{H}_{11}\text{BrN}_4$   $[\text{M}+\text{H}]^+$  375.02397, found 375.238

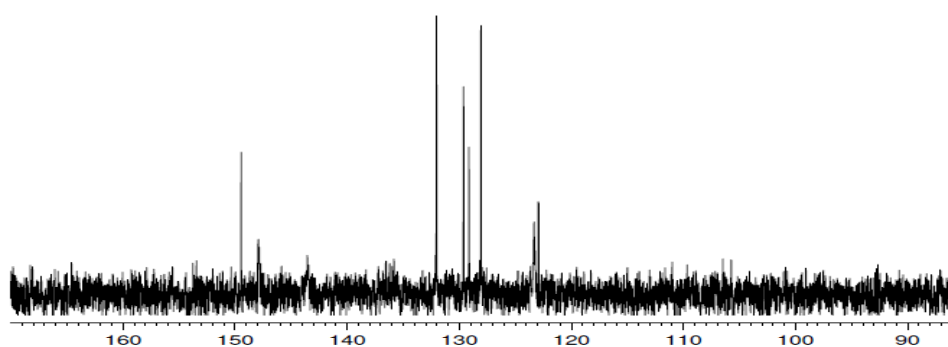
IR (KBr): (**35**)



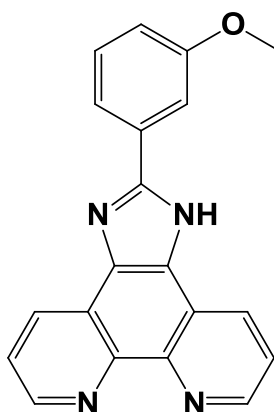
$^1\text{H}$  (DMSO- $d_6$ ) (35)



$^{13}\text{C}$  (DMSO- $d_6$ ) (35)



### 2.8.19 Microwave synthesis of 2-(3-methoxyphenyl)-1*H*-imidazo[4,5-*f*][1,10]phenanthroline (36) (Novel method)

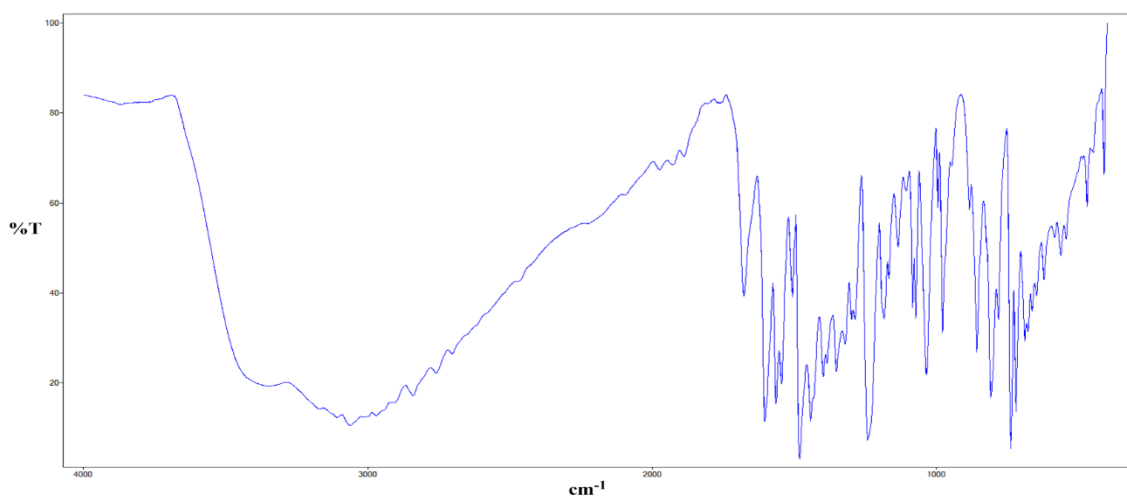


0.30 g ( $1.43 \times 10^{-3}$  mol) of phendione was dissolved in 15 cm<sup>3</sup> of hot dry MeOH, to which 0.039 g ( $7.15 \times 10^{-5}$  mol) CAN in 2 cm<sup>3</sup> of hot MeOH was added. To the resulting reaction mixture was added 1.10 g (0.014 mol) NH<sub>4</sub>OAc in one portion followed by 174 μL ( $1.43 \times 10^{-3}$  mol) of 3-methoxybenzaldehyde. The resulting mixture was then reacted in the microwave at 75 °C (300W, 1 bar) for 10 mins before being added to 200 cm<sup>3</sup> of Millipore water and allowed to sit before being filtering to produce a yellow/cream coloured solid that was washed with Millipore water and allowed to dry in air before being dried further in an oven at 70 °C (0.33 g, 70.72 %).

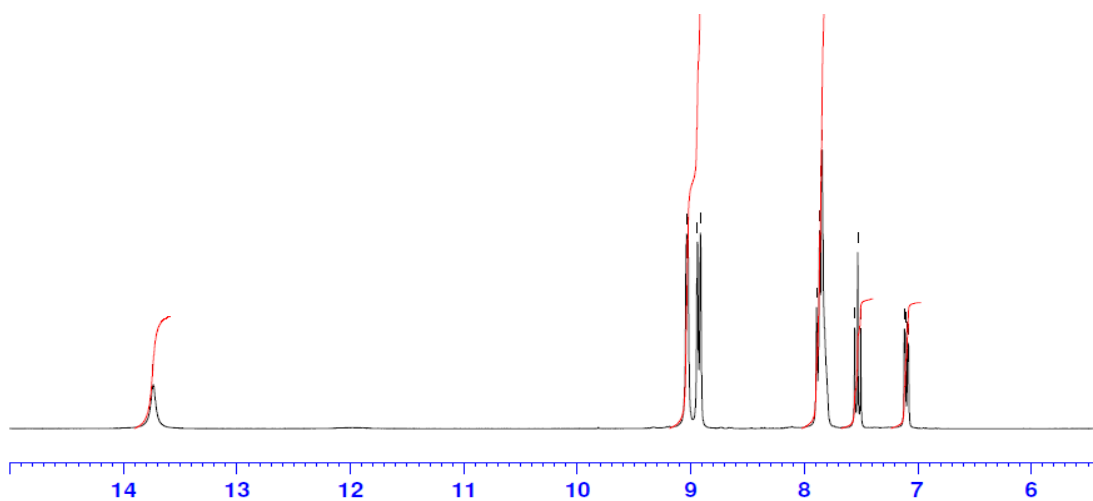
Product formula weight (**36**) = 326.35g/mol.

Yield:	0.33 g (70.72 %)
Mp:	> 250 °C.
% Calculated:	C, 73.61; H, 4.32; N, 17.17
% Found:	C, 73.59; H, 4.36; N, 17.12
IR (KBr) $\nu_{\max}$ :	410, 470, 544, 562, 584, 622, 647, 663, 689, 720, 739, 782, 809, 858, 884, 978, 995, 1035, 1072, 1083, 1106, 1134, 1167, 1184, 1242, 1298, 1321, 1352, 1398, 1442, 1481, 1506, 1545, 1564, 1604, 1677, 2840, 3061
<sup>1</sup> H NMR:	(DMSO-d <sub>6</sub> ): $\delta$ = 3.9 (s, 3H), 7.08-7.11 (m, 1H), 7.50-7.55 (m, 1H), 7.84-7.89 (m, 4H), 8.91-9.03 (m, 4H), 13.73 (bs, 1H).
<sup>13</sup> C NMR:	(75 MHz DMSO-d <sub>6</sub> ) $\delta$ = 55.34, 111.50, 115.24, 118.59, 119.27, 123.15, 123.42, 123.70, 126.35, 129.65, 130.19, 131.22, 135.62, 143.50, 147.83, 150.35, 159.70.
LC/TCOF-MS:	Calcd for C <sub>20</sub> H <sub>14</sub> N <sub>4</sub> O [M+H] <sup>+</sup> 327.1246, found 327.1239

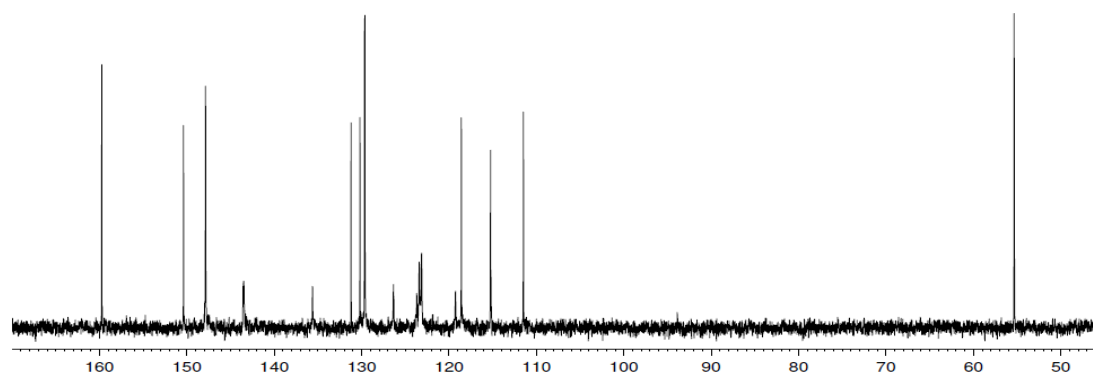
IR (KBr): (36)

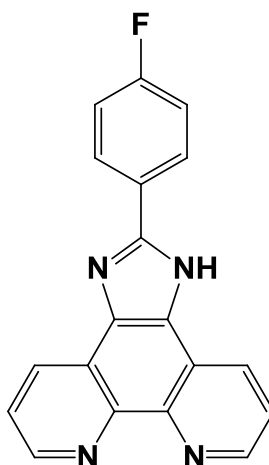


<sup>1</sup>H (DMSO-d6) (36)



<sup>13</sup>C (DMSO-d6) (36)



**2.8.20 Microwave synthesis of 2-(4-fluorophenyl)-1*H*-imidazo[4,5-*f*][1,10]phenanthroline (37) (Novel method)**

0.30 g ( $1.43 \times 10^{-3}$  mol) of phendione was dissolved in 15 cm<sup>3</sup> of hot dry MeOH, to which 0.039 g ( $7.15 \times 10^{-5}$  mol) CAN in 2 cm<sup>3</sup> of hot MeOH was added. To the resulting reaction mixture was added 1.10 g (0.014 mol) NH<sub>4</sub>OAc in one portion followed by 153  $\mu$ L ( $1.43 \times 10^{-3}$  mol) of 4-fluorobenzaldehyde. The resulting mixture was then reacted in the microwave at 75 °C (300W, 1 bar) for 10 mins before being added to 200 cm<sup>3</sup> of Millipore water and allowed to sit before being filtering to produce an orange coloured solid that was washed with Millipore water and allowed to dry in air before being dried further in an oven at 70 °C .

Product formula weight (37) = 314.32g/mol.

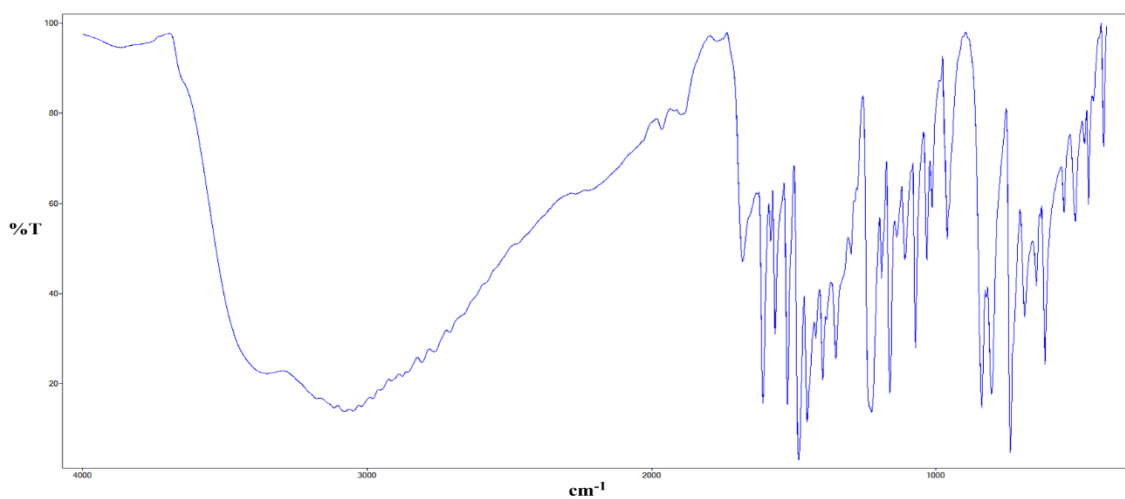
Yield:	0.424 g (94.33 %)
Mp:	> 250 °C.
% Calculated:	C, 72.60; H, 3.53; N, 17.83
% Found:	C, 72.57; H, 3.58; N, 17.79
IR (KBr) $\nu_{\max}$ :	410, 463, 477, 509, 549, 615, 646, 687, 738, 803, 838, 960, 1013, 1032, 1071, 1108, 1137, 1161, 1190, 1225, 1298, 1351, 1397, 1422, 1452, 1482, 1522, 1565, 1580, 1608, 1679, 1963, 3079, 3866

$^1\text{H}$  NMR: (DMSO-d<sub>6</sub>):  $\delta = 7.43\text{-}7.49$  (m, 2H),  $7.80\text{-}7.85$  (m, 2H),  $8.29\text{-}8.34$  (m, 2H),  $8.88\text{-}8.91$  (m, 2H),  $9.02\text{-}9.04$  (m, 2H).

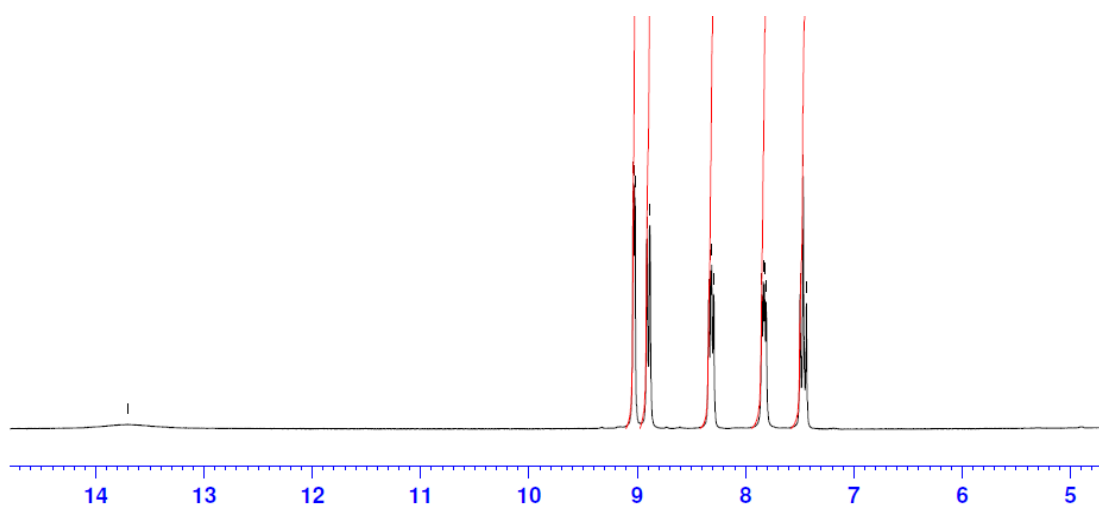
$^{13}\text{C}$  NMR: (75 MHz DMSO-d<sub>6</sub>)  $\delta = 115.92, 116.21, 123.29, 126.58, 126.62, 128.42, 128.54, 129.56, 143.52, 147.83, 149.67, 161.25, 161.83, 164.52$

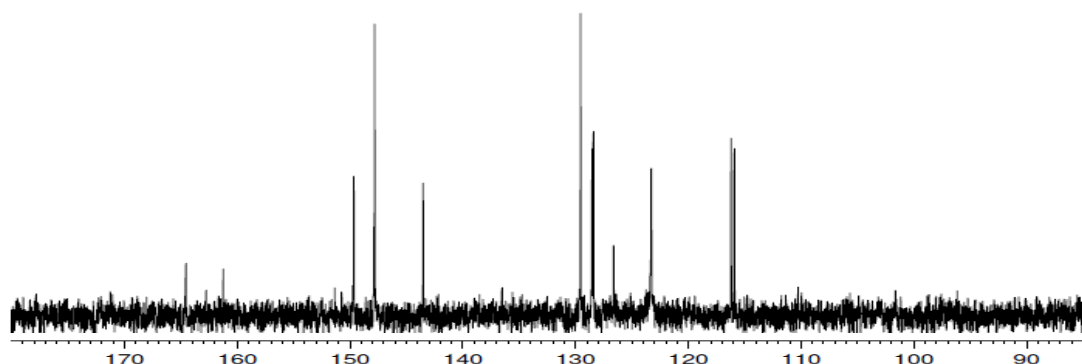
LC/TCOF-MS: Calcd for  $\text{C}_{19}\text{H}_{11}\text{FN}_4$   $[\text{M}+\text{H}]^+$  315.1043, found 315.1059

IR (KBr): (37)

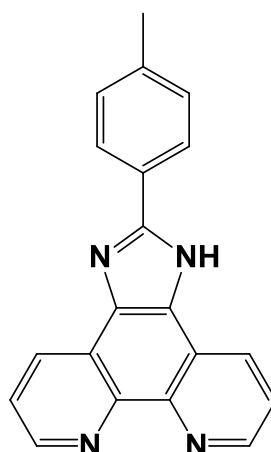


$^1\text{H}$  (DMSO-d<sub>6</sub>) (37)



$^{13}\text{C}$  (DMSO- $d_6$ ) (**37**)

### 2.8.21 Microwave synthesis of 2-(p-tolyl)-1*H*-imidazo[4,5-*f*][1,10]phenanthroline (**38**) (Novel method)



0.30 g ( $1.43 \times 10^{-3}$  mol) of phendione was dissolved in 15 cm<sup>3</sup> of hot dry MeOH, to which 0.039 g ( $7.15 \times 10^{-5}$  mol) CAN in 2 cm<sup>3</sup> of hot MeOH was added. To the resulting reaction mixture was added 1.10 g (0.014 mol) NH<sub>4</sub>OAc in one portion followed by 169  $\mu\text{L}$  ( $1.43 \times 10^{-3}$  mol) of 4-methylbenzaldehyde. The resulting mixture was then reacted in the microwave at 75 °C (300W, 1 bar) for 10 mins before being added to 200 cm<sup>3</sup> of Millipore water and allowed to sit before being filtering to produce a yellow coloured solid that was washed with Millipore water and allowed to dry in air before being dried further in an oven at 70 °C

Product formula weight (**38**) = 310.35g/mol.



Yield: 0.422 g (95.09 %)

Mp: > 250 °C.

% Calculated: C, 77.40; H, 4.55; N, 18.05

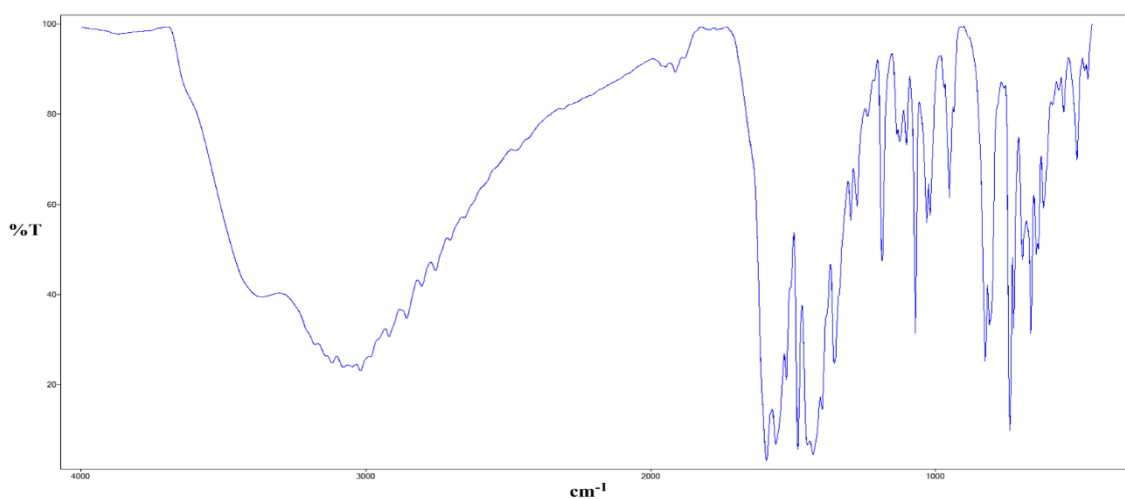
% Found: C, 77.35; H, 4.61; N, 18.01

IR (KBr)  $\nu_{\max}$ : 410, 470, 544, 562, 584, 622, 647, 663, 689, 720, 739, 782, 809, 858, 884, 978, 995, 1035, 1072, 1083, 1106, 1134, 1167, 1184, 1242, 1298, 1321, 1352, 1398, 1442, 1481, 1506, 1545, 1564, 1604, 1677, 2840, 3061

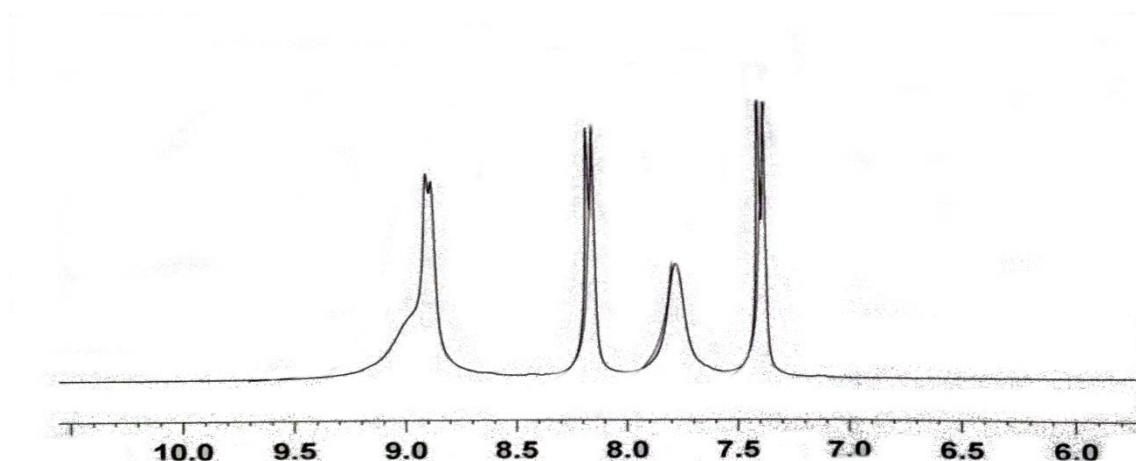
$^1\text{H}$  NMR: (DMSO- $d_6$ ):  $\delta$  = 7.37-7.40 (m, 2H), 7.77 (bs, 2H), 8.15-8.177 (m, 2H), 8.88-8.90 (m, 3H)

$^{13}\text{C}$  NMR: (75 MHz DMSO- $d_6$ )  $\delta$  = 20.94, 121.46, 123.17, 126.14, 127.26, 129.51, 139.26, 143.28, 147.42, 150.76

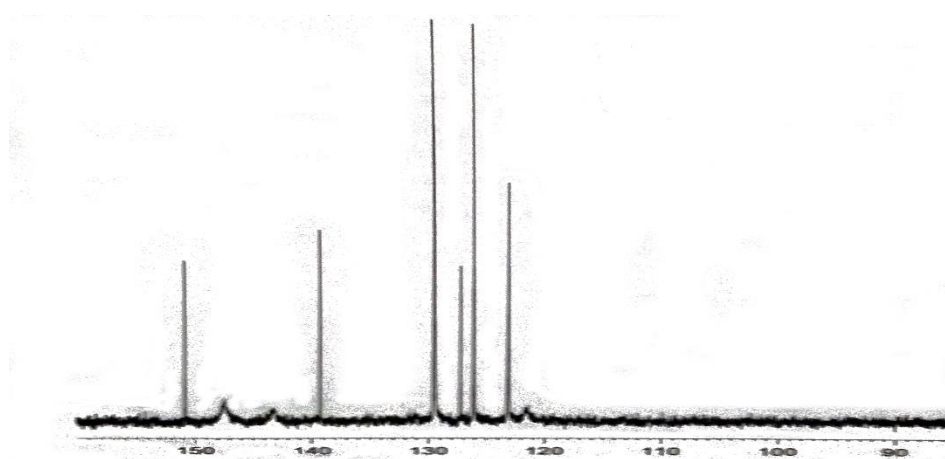
IR (KBr): (38)



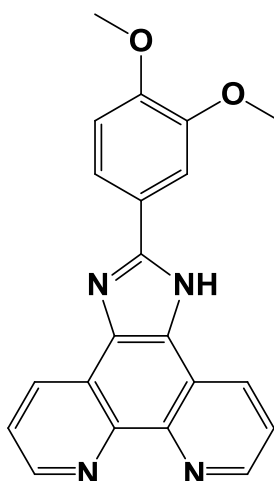
$^1\text{H}$  (DMSO- $d_6$ ) (38)



$^{13}\text{C}$  (DMSO- $d_6$ ) (38)



2.8.22 Microwave synthesis of 2-(3,4-dimethoxyphenyl)-1H-imidazo[4,5-f][1,10]phenanthroline (39) (Novel method, novel molecule)

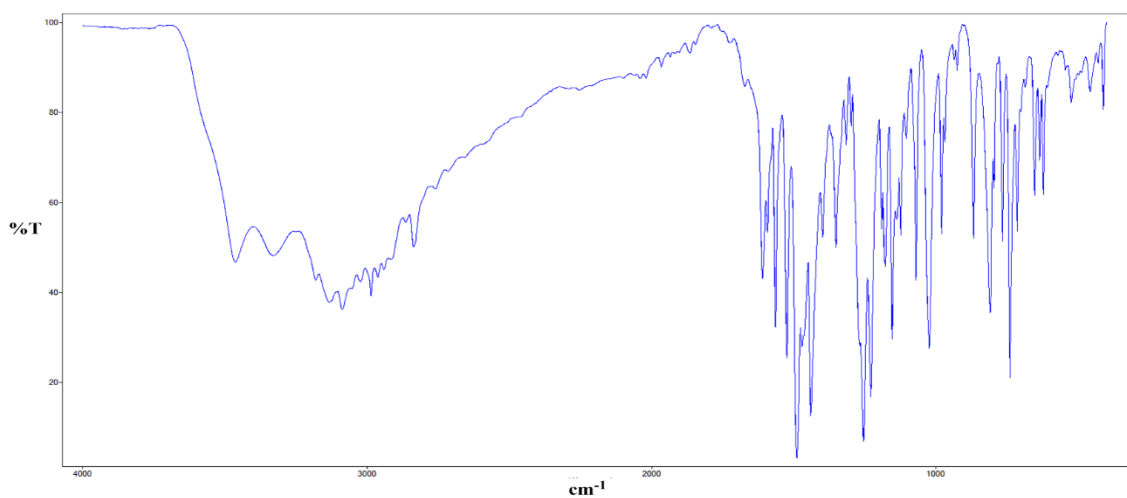


0.40 g ( $1.90 \times 10^{-3}$  mol) of phendione was dissolved in 15 cm<sup>3</sup> of hot dry MeOH, to which 0.052 g ( $9.50 \times 10^{-5}$  mol) CAN in 2 cm<sup>3</sup> of hot MeOH was added. To the resulting orange reaction mixture was added 1.47 g (0.02 mol) NH<sub>4</sub>OAc in one portion followed by 0.32 g (1.90 mmol) of 3,4-dimethoxybenzaldehyde in one portion. The resulting orange mixture was then reacted in the microwave at 75 °C (300W, 1 bar) for 10 mins. The resulting green coloured solution was allowed to cool to room temperature and 150 cm<sup>3</sup> of Millipore water was added. The solution was cooled to 4 °C in a fridge overnight which precipitated an orange powder.

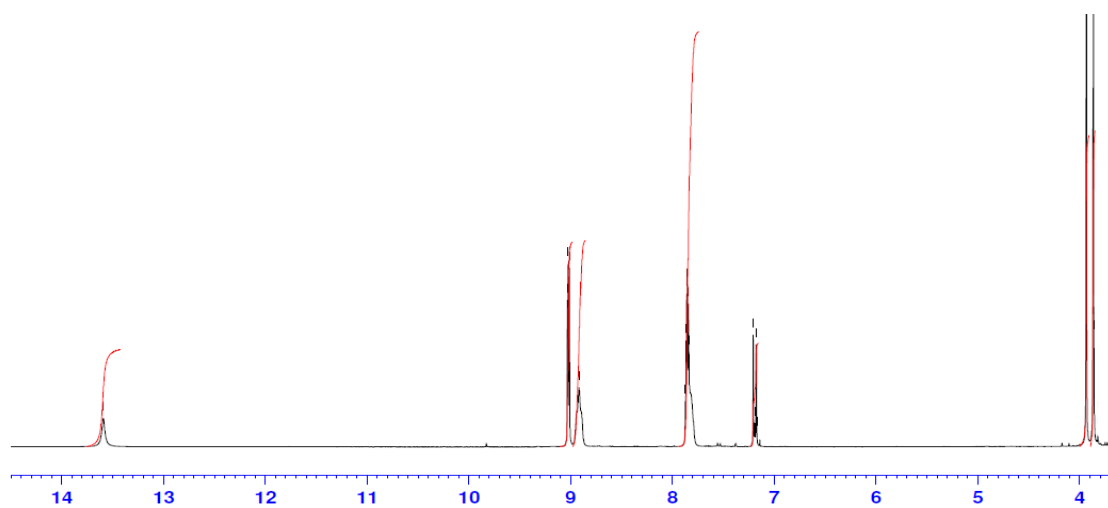
Product formula weight (**39**) = 356.38g/mol.

Yield:	0.584 g (86.26 %)
Mp:	> 250 °C.
% Calculated:	C: 70.77, H: 4.53, N: 15.72
% Found:	C: 70.71, H: 4.55, N: 15.76
IR (KBr) $\nu_{\max}$ :	410, 429, 457, 524, 622, 634, 653, 713, 739, 765, 808, 867, 925, 968, 980, 1022, 1069, 1104, 1123, 1153, 1177, 1229, 1254, 1297, 1315, 1351, 1398, 1440, 1470, 1489, 1524, 1564, 1592, 1609, 2837, 2986, 3087, 3133, 3330, 3464 cm <sup>-1</sup>
<sup>1</sup> H NMR:	(DMSO-d <sub>6</sub> ): $\delta$ = 3.43 (s, 3H), 3.93 (s, 3H), 7.16-7.20 (m, 1H), 7.83-7.87 (m, 4H), 8.91-8.93 (m, 2H), 9.01-9.03 (m, 2H), 13.59 (bs, 1H)
<sup>13</sup> C NMR:	(75 MHz DMSO-d <sub>6</sub> ) $\delta$ = 55.61, 55.68, 109.64, 111.88, 119.19, 122.59, 123.05, 123.32, 123.63, 126.14, 129.48, 129.57, 135.58, 143.28, 143.48, 147.65, 148.97, 150.19, 150.82.
LC/TCOF-MS:	Calcd for C <sub>21</sub> H <sub>16</sub> N <sub>4</sub> O <sub>2</sub> [M+H] <sup>+</sup> 357.1346, found 357.1346

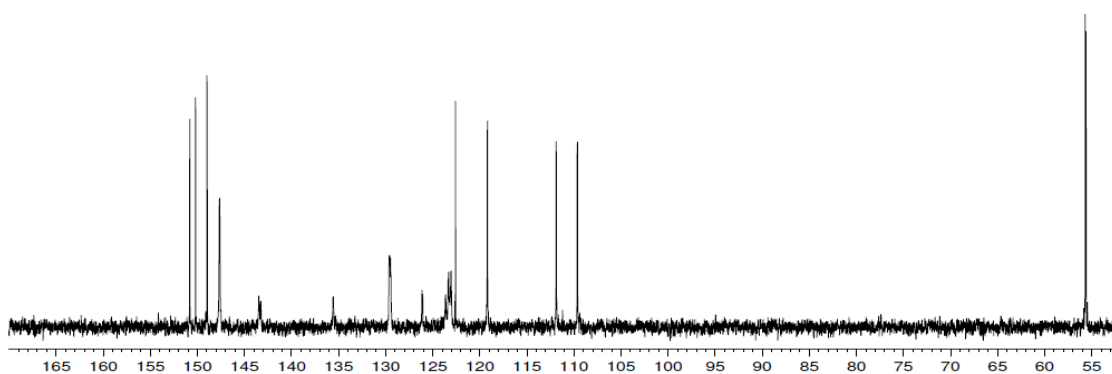
IR (KBr): (39)

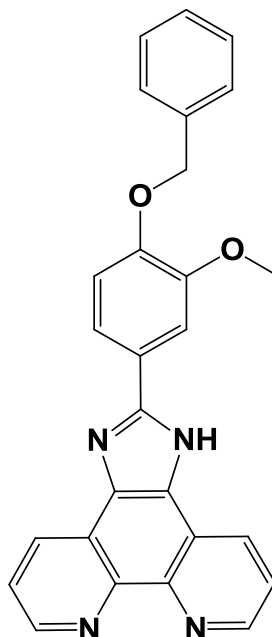


$^1\text{H}$  (DMSO-d<sub>6</sub>) (39)



$^{13}\text{C}$  (DMSO-d<sub>6</sub>) (39)



**2.8.23 Microwave synthesis of 2-(4-(benzyloxy)-3-methoxyphenyl)-1H-imidazo[4,5-f][1,10]phenanthroline (40) (Novel method, novel molecule)**

0.30 g (1.43 mmol) of phendione was dissolved in 15 cm<sup>3</sup> of hot dry MeOH, to which 0.039 g (7.15x10<sup>-5</sup> mol) CAN in 2 cm<sup>3</sup> of hot MeOH was added. To the resulting orange reaction mixture was added 1.10 g (0.014 mol) NH<sub>4</sub>OAc in one portion followed by 0.35 g (1.43 mmol) of 4-benzyloxy-3-methoxybenzaldehyde in one portion. The resulting orange mixture was then reacted in the microwave at 75 °C (300W, 1 bar) for 10 mins. The resulting yellow coloured solution was allowed to cool to room temperature before being filtered. To the filtrate was added 150 cm<sup>3</sup> of Millipore water to produce a bright orange precipitate which was filtered and washed with water before being dried in an oven at 70 °C overnight.

Product formula weight (**40**) = 432.47g/mol.

Yield: 0.504 g (81.50 %)

Mp: > 250 °C.

% Calculated: C, 74.98; H, 4.66; N, 12.95

% Found: C, 74.92; H, 4.70; N, 12.92

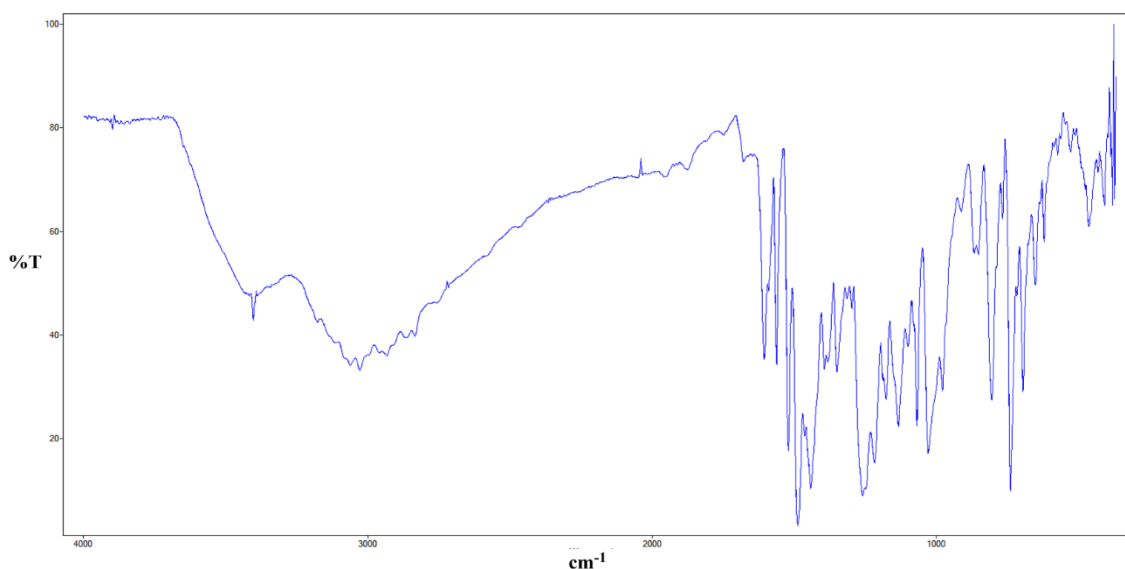
IR (KBr)  $\nu_{\text{max}}$ : 408, 432, 464, 513, 527, 573, 621, 652, 695, 740, 767, 806, 852, 867, 913, 979, 1029, 1068, 1100, 1177, 1218, 1260, 1297, 1314, 1350, 1394, 1442, 1488, 1521, 1532, 1605, 1679, 1748, 1875, 1957, 2033, 2716, 2834, 2933, 3028, 3061, 3177, 3402, 3713, 3858

$^1\text{H}$  NMR: (DMSO- $d_6$ ):  $\delta$  = 3.96 (s, 3H), 5.20 (s, 2H), 7.29-7.52 (m, 6H), 7.82-7.89 (m, 4H), 8.91-8.94 (m, 2H), 9.02-9.04 (m, 2H).

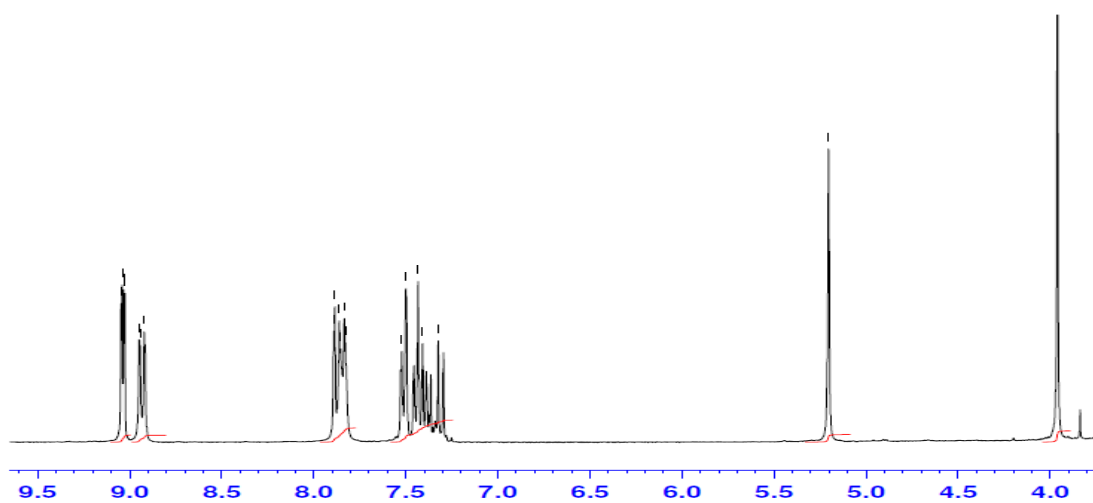
$^{13}\text{C}$  NMR: (75 MHz DMSO- $d_6$ )  $\delta$  = 29.98, 55.77, 69.93, 109.89, 113.51, 119.09, 119.22, 122.93, 123.11, 123.40, 123.64, 126.15, 127.97, 128.44, 129.48, 135.61, 136.77, 143.29, 147.75, 149.19, 149.30, 150.77

LC/TCOF-MS: Calcd for  $\text{C}_{27}\text{H}_{20}\text{N}_4\text{O}_2$   $[\text{M}+\text{H}]^+$  433.1659, found 433.1654

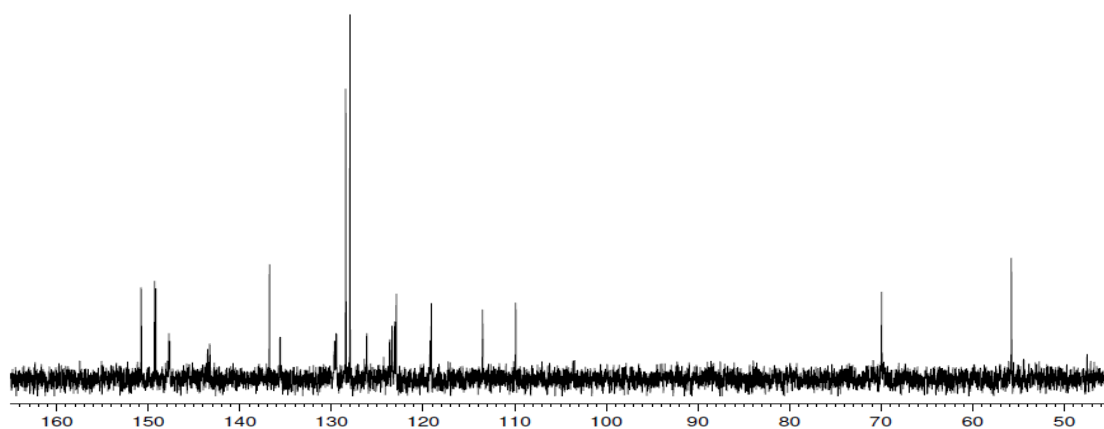
IR (KBr): **(40)**



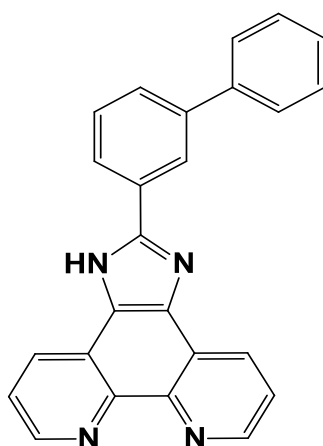
$^1\text{H}$  (DMSO- $d_6$ ) (40)



$^{13}\text{C}$  (DMSO- $d_6$ ) (40)



#### 2.8.24 Microwave synthesis of 2-([1,1'-biphenyl]-3-yl)-1*H*-imidazo[4,5-*f*][1,10]phenanthroline (bhipip) (41) (Novel method, novel molecule)



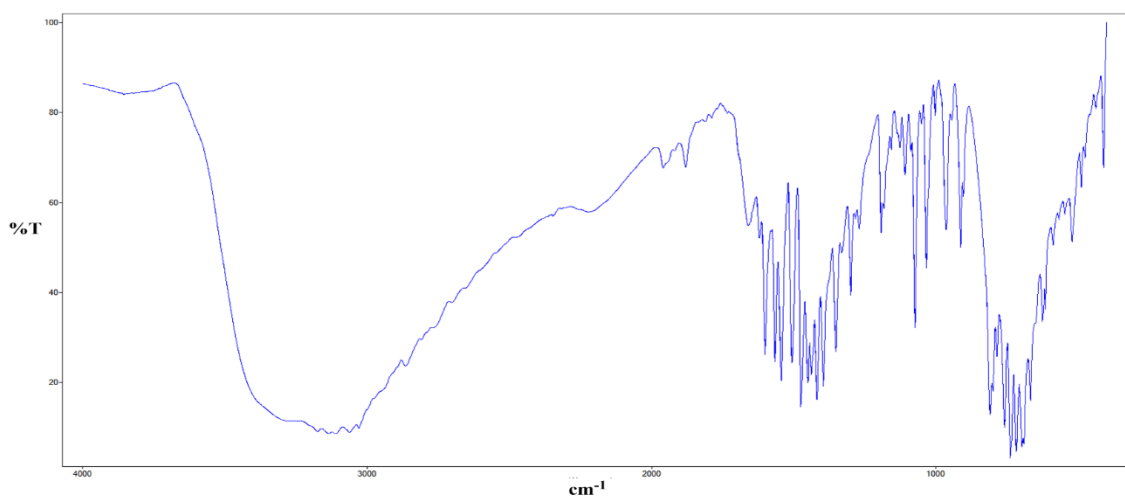
0.40 g (1.90 mmol) of phendione was dissolved in 15 cm<sup>3</sup> of hot dry MeOH, to which 0.052 g (9.52x10<sup>-5</sup> mol) CAN in 2 cm<sup>3</sup> of hot MeOH was added. To the resulting orange reaction mixture was added 1.47 g (0.02 mol) NH<sub>4</sub>OAc in one portion followed by 0.31 cm<sup>3</sup> (1.90 mmol) of biphenyl-3-carboxyaldehyde in one portion. The resulting dark orange mixture was then reacted in the microwave at 75 °C (300W, 1 bar) for 10 mins. The resulting yellow coloured solution was allowed to cool to room temperature and 150 cm<sup>3</sup> of Millipore water was added resulting in a clear yellow coloured precipitate which was filtered and washed with millipore water before being dried in an oven at 70 °C overnight.

Product formula weight (**41**) = 372.42g/mol.

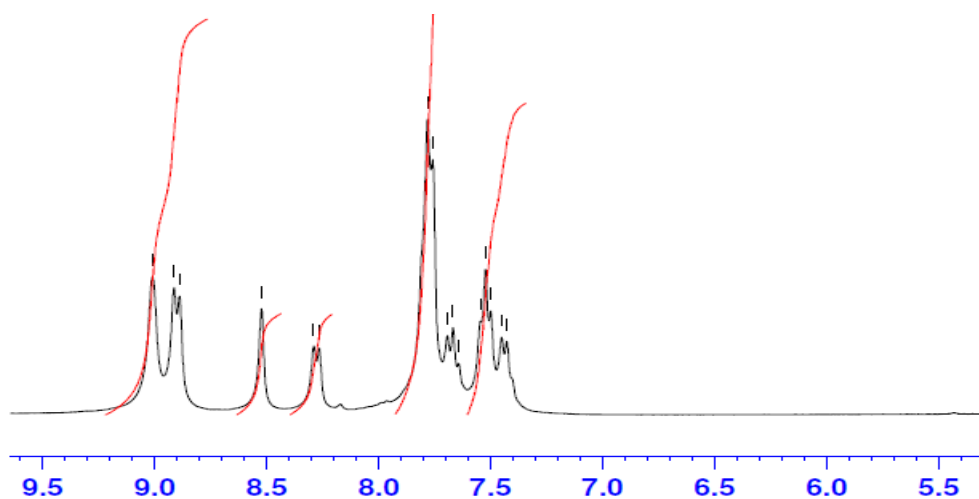
Yield:	0.649 g (91.65 %)
Mp:	> 250 °C.
% Calculated:	C: 80.63, H: 4.33, N: 15.04
% Found:	C: 80.57, H: 4.39, N: 15.04
IR (KBr) $\nu_{\max}$ :	410, 521, 625, 668, 698, 716, 739, 759, 783, 809, 913, 963, 1032, 1072, 1109, 1192, 1269, 1299, 1354, 1396, 1418, 1438, 1454, 1477, 1507, 1546, 1568, 1602, 1659, 3109
<sup>1</sup> H NMR:	(DMSO-d <sub>6</sub> ): $\delta$ = 7.42-7.45 (m, 3H), 7.54-7.78 (m, 6H), 8.26-8.29 (m, 1H), 8.52 (s, 1H), 8.89-9.01 (m, 4H).
<sup>13</sup> C NMR:	(75 MHz DMSO-d <sub>6</sub> ) $\delta$ = 123.23, 124.33, 125.31, 126.84, 127.83, 129.00, 129.63, 130.53, 139.67, 140.95, 143.53, 147.77, 150.35
LC/TCOF-MS:	Calcd for C <sub>25</sub> H <sub>16</sub> N <sub>4</sub> [M+H] <sup>+</sup> 373.14247, found 373.1424



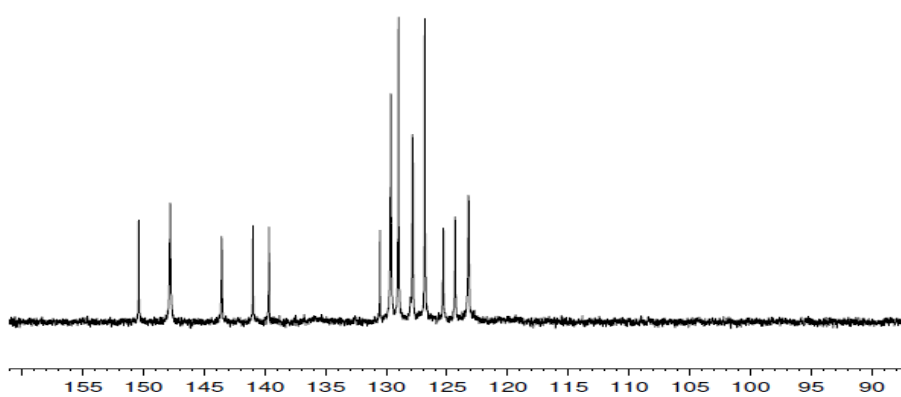
IR (KBr): **bhip** (41)

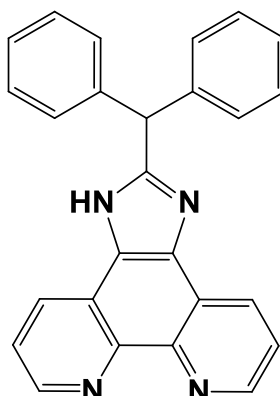


<sup>1</sup>H (DMSO-d6) **bhip** (41)



<sup>13</sup>C (DMSO-d6) **bhip** (41)



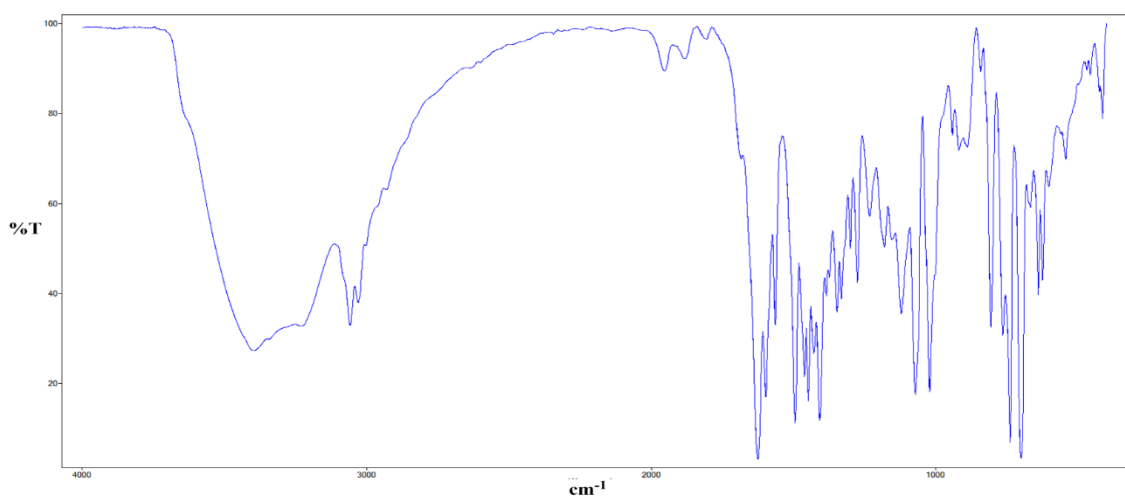
**2.8.25 Microwave synthesis of 2-benzhydryl-1*H*-imidazo[4,5-*f*][1,10]phenanthroline (42) (Novel method, novel molecule)**

0.40 g (1.90 mmol) of phendione was dissolved in 15 cm<sup>3</sup> of hot dry MeOH, to which 0.052 g (9.52x10<sup>-5</sup> mol) CAN in 2 cm<sup>3</sup> of hot MeOH was added. To the resulting orange reaction mixture was added 1.47 g (0.02 mol) NH<sub>4</sub>OAc in one portion followed by 0.34 cm<sup>3</sup> (1.90 mmol) of diphenylacetaldehyde in one portion. The resulting dark orange mixture was then reacted in the microwave at 75 °C (300W, 1 bar) for 10 mins. The resulting yellow coloured solution was allowed to cool to room temperature and 150 cm<sup>3</sup> of Millipore water was added resulting in a yellow coloured precipitate which was filtered and washed with millipore water before being dried in an oven at 70 °C overnight

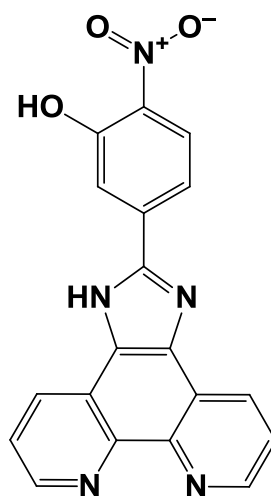
Product formula weight (**42**) = 386.45g/mol.

Yield:	0.584 g (79.54 %)
Mp:	> 250 °C.
% Calculated:	C, 80.81; H, 4.69; N, 14.50
% Found:	C, 80.77; H, 4.74; N, 14.46
IR (KBr) $\nu_{\max}$ :	502, 626, 636, 706, 728, 769, 812, 941, 1087, 1121, 1318, 1375, 1425, 1485, 1620, 2023, 3420
<sup>1</sup> H NMR:	(DMSO-d <sub>6</sub> ): $\delta$ = 6.58-6.60 (m, 2H), 6.89-7.83 (m, 27H), 8.30 (s, 1H), 8.84-9.02 (m, 4H)
LC/TCOF-MS:	Calcd for C <sub>26</sub> H <sub>18</sub> N <sub>4</sub> [M+H] <sup>+</sup> 387.1604, found 387.1619

IR (KBr): (42)



### 2.8.26 Microwave synthesis of 5-(1*H*-imidazo[4,5-*f*][1,10]phenanthrolin-2-yl)-2-nitrophenol (43) (Novel method, novel molecule)

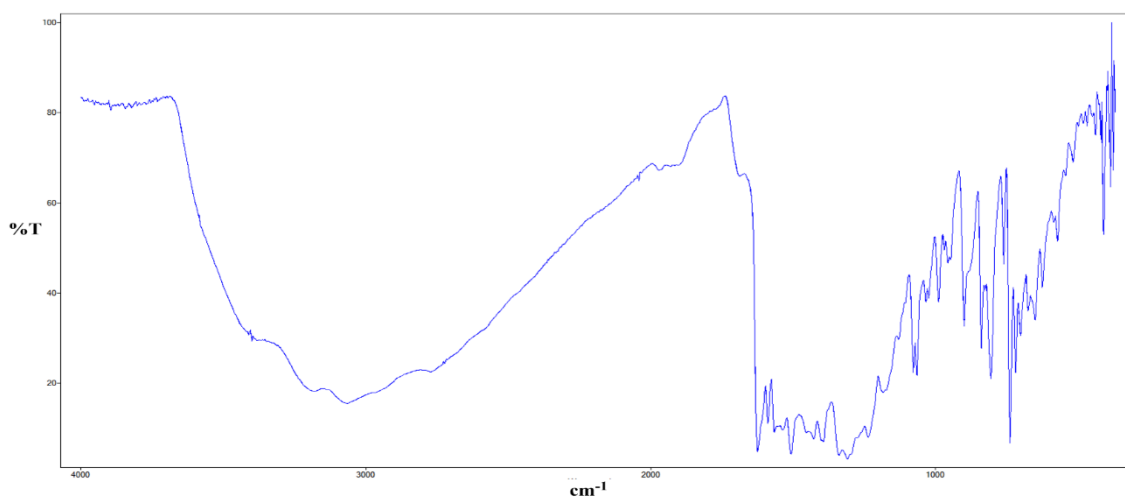


0.40 g (1.90 mmol) of phendione was dissolved in 15 cm<sup>3</sup> of hot dry MeOH, to which 0.052 g (9.52x10<sup>-5</sup> mol) CAN in 2 cm<sup>3</sup> of hot MeOH was added. To the resulting orange reaction mixture was added 1.47 g (0.02 mol) NH<sub>4</sub>OAc in one portion followed by 0.32 g (1.90 mmol) of 3-hydroxy-4-nitrobenzaldehyde in one portion. The resulting orange mixture was then reacted in the microwave at 75 °C (300W, 1 bar) for 10 mins. The resulting orange coloured solution was allowed to cool to room temperature before being filtered and the resulting orange powder was washed with MeOH and 150 cm<sup>3</sup> of Millipore water and then dried in an oven at 70 °C overnight (0.51 g, 75.12 %).

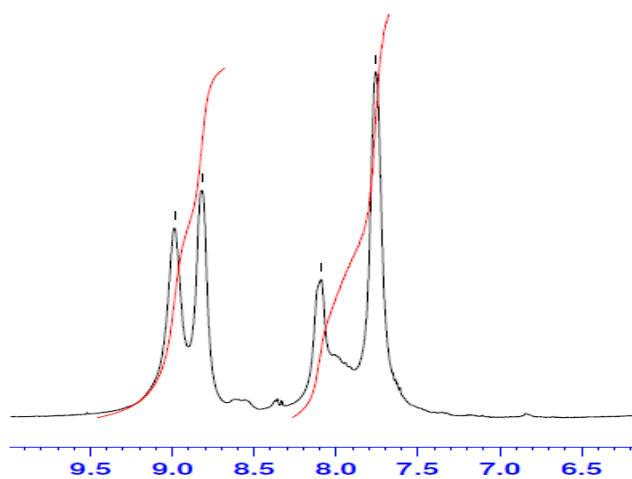
Product formula weight (43) = 357.32g/mol.

Yield:	0.51 g (75.12 %)
Mp:	> 250 °C.
% Calculated:	C, 63.86; H, 3.10; N, 19.60
% Found:	C, 63.81; H, 3.16; N, 19.56
IR (KBr) $\nu_{\max}$ :	427, 480, 551, 597, 623, 691, 727, 736, 760, 815, 841, 876, 900, 929, 993, 1087, 1197, 1259, 1295, 1322, 1361, 1405, 1460, 1511, 1552, 1587, 1611, 1621, 1788, 1996, 2825, 2963, 3086, 3232, 3428, 3540, 3878
$^1\text{H}$ NMR:	(DMSO-d <sub>6</sub> ): $\delta$ = 7.75-8.09 (m, 5H), 8.81-8.98 (m, 4H)
$^{13}\text{C}$ NMR:	(75 MHz DMSO-d <sub>6</sub> ) $\delta$ = 116.02, 121.31, 123.26, 126.28, 129.64, 135.94, 143.53, 147.93, 172.12
LC/TCOF-MS:	Calcd for C <sub>19</sub> H <sub>11</sub> N <sub>5</sub> O <sub>3</sub> [M+H] <sup>+</sup> 358.09177, found 358.0917

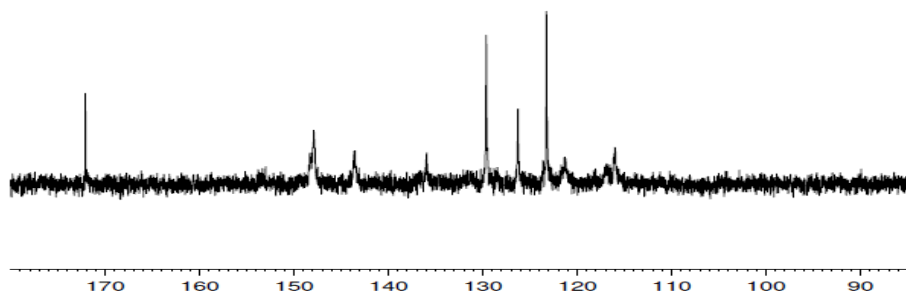
IR (KBr): (43)



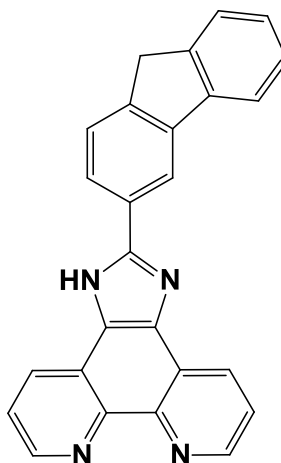
$^1\text{H}$  (DMSO- $d_6$ ) (43)



$^{13}\text{C}$  (DMSO- $d_6$ ) (43)



**2.8.27 Microwave synthesis of 2-(9H-fluoren-3-yl)-1H-imidazo[4,5-f][1,10]phenanthroline (44) (Novel method, novel molecule)**

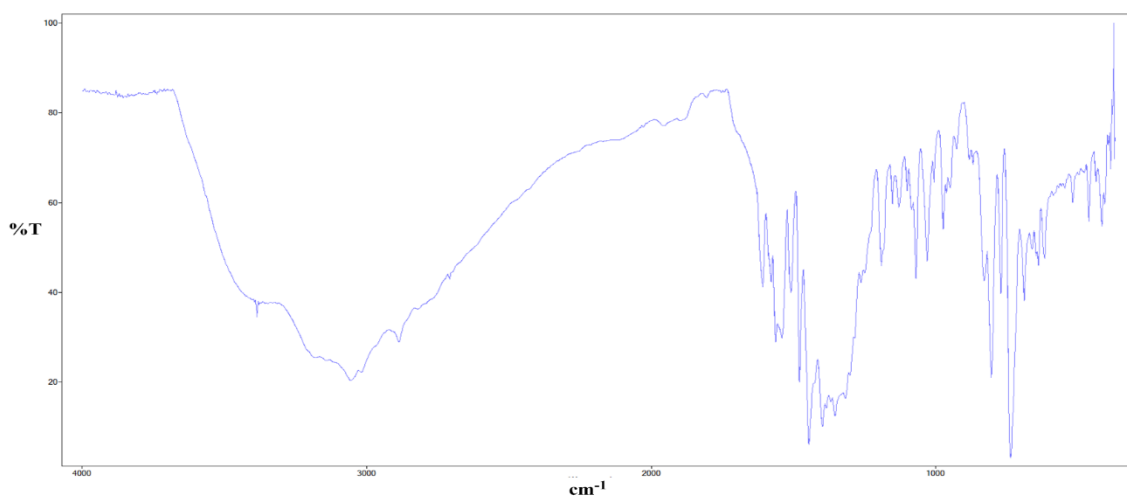


0.40 g (1.90 mmol) of phendione was dissolved in 15 cm<sup>3</sup> of hot dry MeOH, to which 0.052 g (9.52x10<sup>-5</sup> mol) CAN in 2 cm<sup>3</sup> of hot MeOH was added. To the resulting orange reaction mixture was added 1.47 g (0.02 mol) NH<sub>4</sub>OAc in one portion followed by 0.37 g (1.90 mmol) of fluorene-2-carboxaldehyde in one portion. The resulting orange mixture was then reacted in the microwave at 75 °C (300W, 1 bar) for 10 mins. The resulting orange coloured solution was allowed to cool to room temperature before being filtered and the resulting orange powder was washed with MeOH, 150 cm<sup>3</sup> of Millipore water and finally acetone before being dried in an oven at 70 °C overnight.

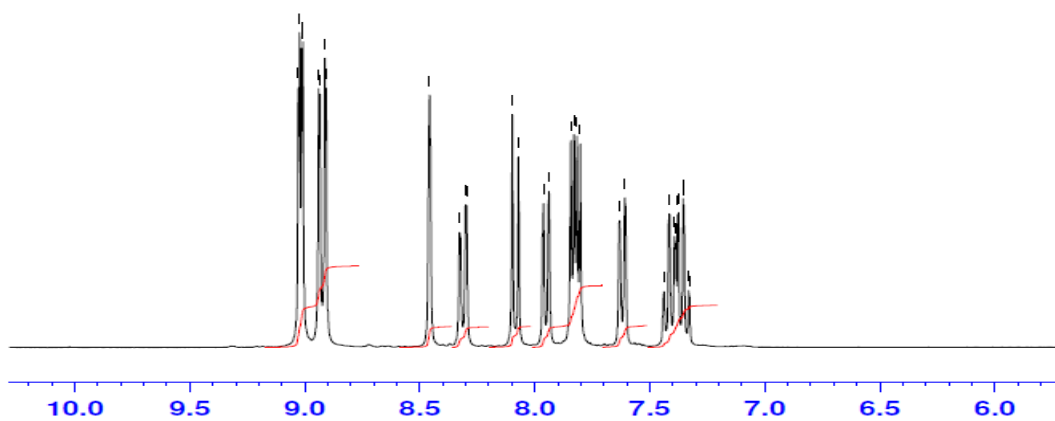
Product formula weight (**44**) = 384.43g/mol.

Yield:	0.658 g (90.09 %)
Mp:	> 250 °C.
% Calculated:	C, 81.23; H, 4.20; N, 14.57
% Found:	C, 81.20; H, 4.24; N, 14.51
IR (KBr) $\nu_{\max}$ :	431, 476, 521, 553, 623, 636, 725, 741, 774, 808, 879, 928, 980, 1087, 1193, 1285, 1309, 1364, 1384, 1403, 1428, 1448, 1478, 1512, 1551, 1585, 1609, 3413
<sup>1</sup> H NMR:	(DMSO-d <sub>6</sub> ): $\delta$ = 4.06 (s, 2H), 7.32-7.43 (m, 2H), 7.60-7.63 (m, 1H), 7.80-7.84 (m, 3H), 7.93-7.96 (m, 1H), 8.07-8.09 (m, 1H), 8.29-8.32 (m, 1H), 8.45 (s, 1H), 8.90-9.02 (m, 4H).
<sup>13</sup> C NMR:	(75 MHz DMSO-d <sub>6</sub> ) $\delta$ = 36.41, 120.40, 122.76, 123.27, 125.11, 125.18, 126.91, 127.29, 128.27, 129.63, 140.41, 142.39, 143.36, 143.57, 143.68, 147.67, 150.91
LC/TCOF-MS:	Calcd for C <sub>26</sub> H <sub>16</sub> N <sub>4</sub> [M+H] <sup>+</sup> 385.1448, found 385.1439

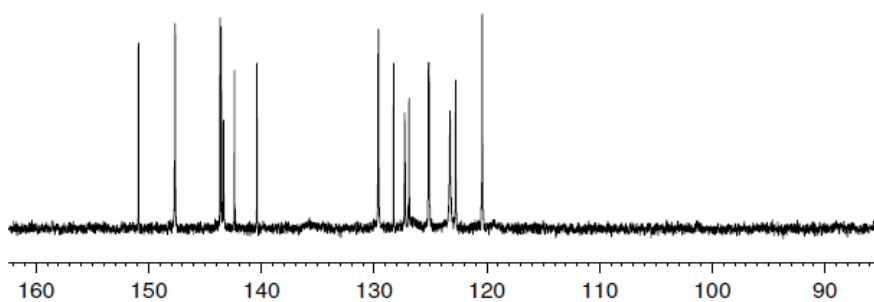
IR (KBr): (44)

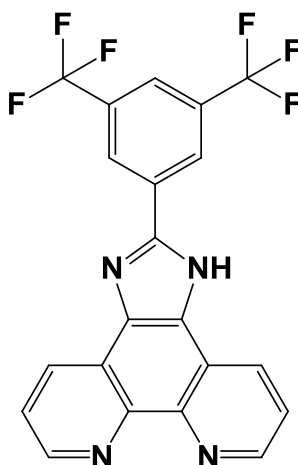


<sup>1</sup>H (DMSO-d<sub>6</sub>) (44)



<sup>13</sup>C (DMSO-d<sub>6</sub>) (44)



**2.8.28 Microwave synthesis of 2-(3,5-bis(trifluoromethyl)phenyl)-1H-imidazo[4,5-f][1,10]phenanthroline (45) (Novel method, novel molecule)**

0.30 g ( $1.43 \times 10^{-3}$  mol) of phendione was dissolved in 15 cm<sup>3</sup> of hot dry MeOH, to which 0.039 g ( $7.15 \times 10^{-5}$  mol) CAN in 2 cm<sup>3</sup> of hot MeOH was added. To the resulting reaction mixture was added 1.10 g (0.014 mol) NH<sub>4</sub>OAc in one portion followed by 236  $\mu$ L ( $1.43 \times 10^{-3}$  mol) of 3,5-bis(trifluoromethyl)benzaldehyde. The resulting mixture was then reacted in the microwave at 75 °C (300W, 1 bar) for 10 mins. The resulting orange coloured solution was allowed to cool to room temperature before being added to 200 cm<sup>3</sup> of Millipore water and allowed to sit before being filtering to produce a cream coloured solid that was washed with Millipore water and allowed to dry in air before being dried further in an oven at 70 °C.

Product formula weight (**45**) = 432.32g/mol.

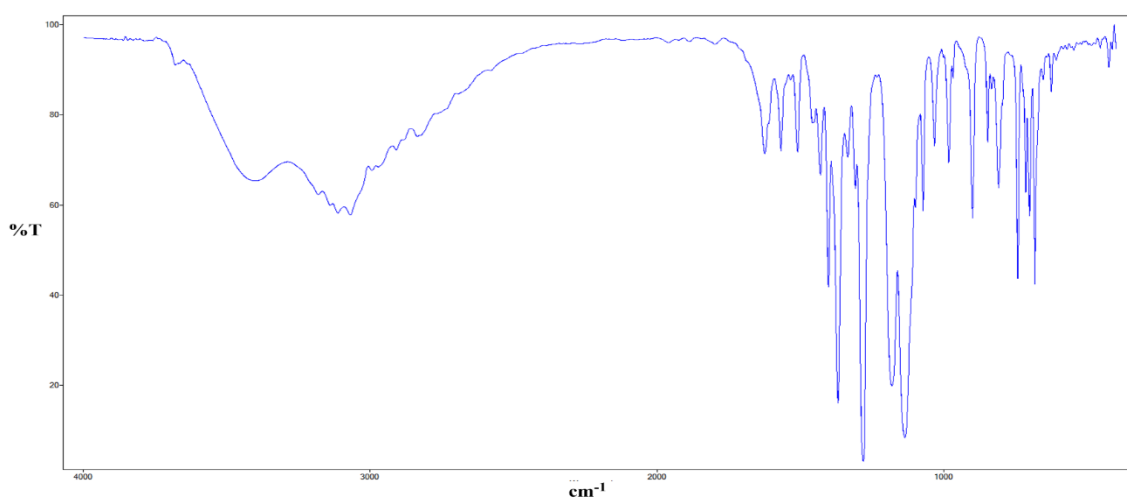
Yield:	0.494 g (79.91 %)
Mp:	> 250 °C.
% Calculated:	C, 58.34; H, 2.33; N, 12.96
% Found:	C, 58.34; H, 2.31; N, 12.94
IR (KBr) $\nu_{\max}$ :	421, 625, 684, 702, 714, 743, 809, 846, 898, 981, 1032, 1070, 1135, 1180, 1281, 1368, 1400, 1430, 1509, 1568, 1625, 3071



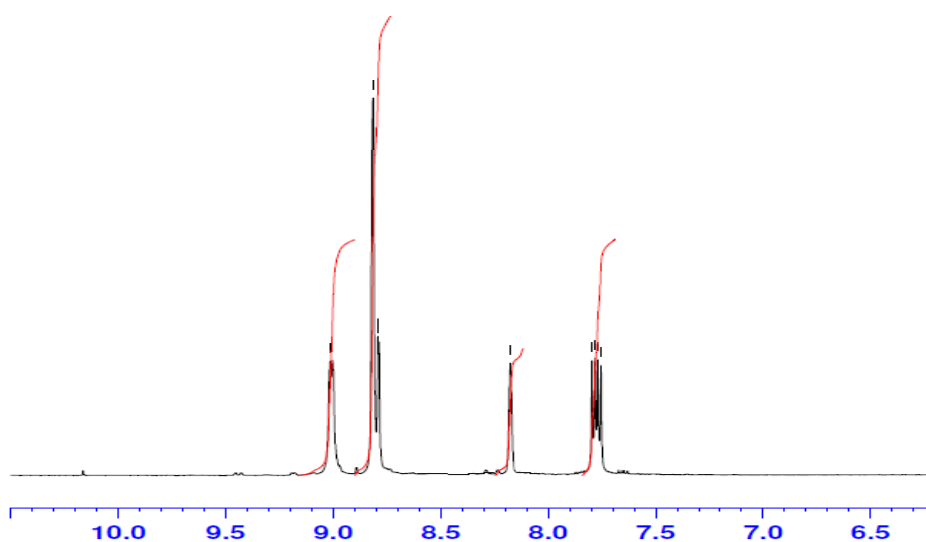
$^1\text{H}$  NMR: (DMSO- $d_6$ ):  $\delta = 7.83\text{-}7.84$  (m, 2H), 8.19 (s, 1H), 8.87 (s, 3H), 9.05-9.06 (m, 2H), 13.99 (bs, 1H)

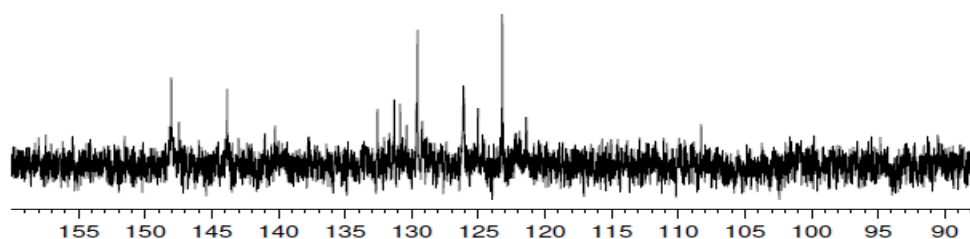
$^{13}\text{C}$  NMR: (75 MHz DMSO- $d_6$ )  $\delta = 123.27, 126.23, 129.60, 131.03, 131.47, 132.51, 144.06, 147.34, 148.23$

IR (KBr): (45)

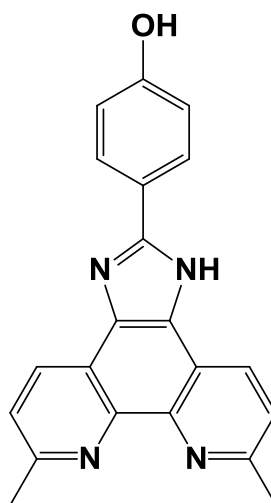


$^1\text{H}$  (DMSO- $d_6$ ) (45)



$^{13}\text{C}$  (DMSO- $d_6$ ) (45)

### 2.8.29 Microwave synthesis of 4-(6,9-dimethyl-1*H*-imidazo[4,5-*f*][1,10]phenanthrolin-2-yl)phenol (46) (Novel method, novel molecule)



0.15 g ( $6.30 \times 10^{-4}$  mol) of 2,9-dimethyl-1,10-phenanthroline-5,6-dione was dissolved in  $15 \text{ cm}^3$  of hot dry MeOH, to which 0.017 g ( $3.15 \times 10^{-5}$  mol) CAN in  $5 \text{ cm}^3$  of hot MeOH was added. To the resulting reaction mixture was added 0.49 g (6.3 mmol)  $\text{NH}_4\text{OAc}$  in one portion followed by 76.94 mg ( $6.30 \times 10^{-4}$  mol) of 4-hydroxybenzaldehyde. The resulting deep orange coloured solution was then reacted in the microwave at  $75 \text{ }^\circ\text{C}$  (300W, 1 bar) for 10 mins. The resulting orange coloured mixture was allowed to cool to room temperature before being added to  $200 \text{ cm}^3$  of Millipore water and allowed to sit before being filtering to produce a dark yellow solid that was washed with Millipore water and allowed to dry in air before being dried further in an oven at  $70 \text{ }^\circ\text{C}$  overnight.

Product formula weight (**46**) = 340.38g/mol.

Yield: 0.045 g (21 %)

Mp: > 250 °C.

% Calculated: C, 74.10; H, 4.74; N, 16.46

% Found: C, 74.15; H, 4.82; N, 16.38

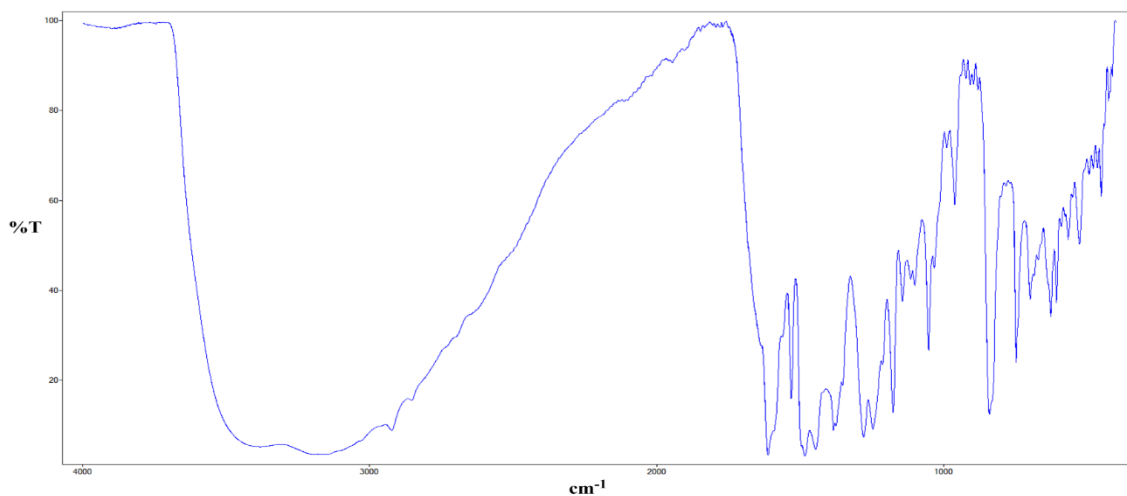
IR (KBr)  $\nu_{\max}$ : 425, 452, 527, 566, 608, 628, 699, 747, 842, 961, 1054, 1100, 1144, 1175, 1246, 1279, 1376, 1383, 1449, 1484, 1528, 1612, 3176

$^1\text{H}$  NMR: (DMSO-d<sub>6</sub>):  $\delta$  = 2.80 (s, 6H), 6.95-6.98 (m, 2H), 7.69-7.72 (m, 2H), 8.08-8.11 (m, 2H), 8.79-8.81 (m, 2H), 10.01 (s, 1H).

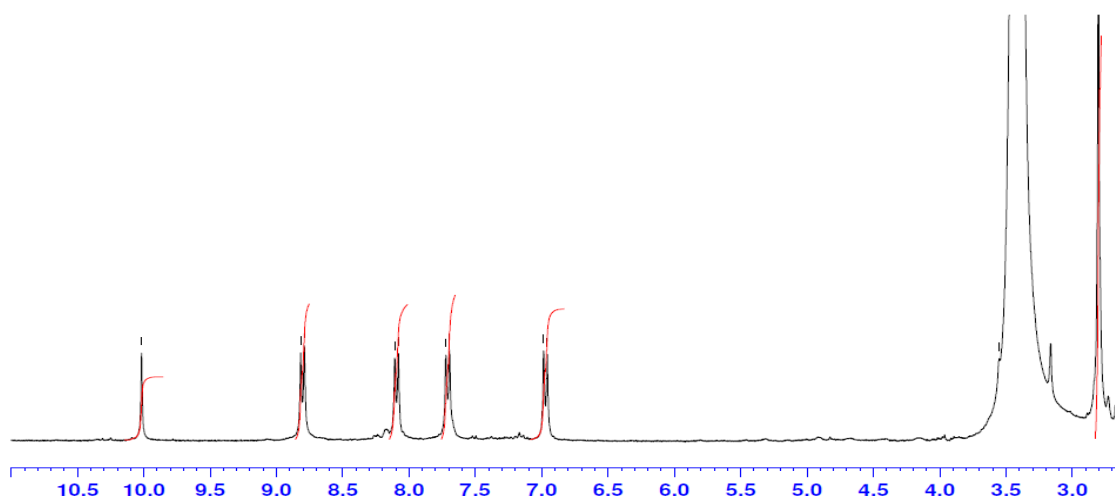
$^{13}\text{C}$  NMR: (75 MHz DMSO-d<sub>6</sub>)  $\delta$  = 24.64, 115.71, 121.15, 123.43, 127.85, 130.20, 141.80, 150.74, 155.67, 158.83

LC/TCOF-MS: Calcd for C<sub>21</sub>H<sub>16</sub>N<sub>4</sub>O [M+H]<sup>+</sup> 341.1397, found 341.1416

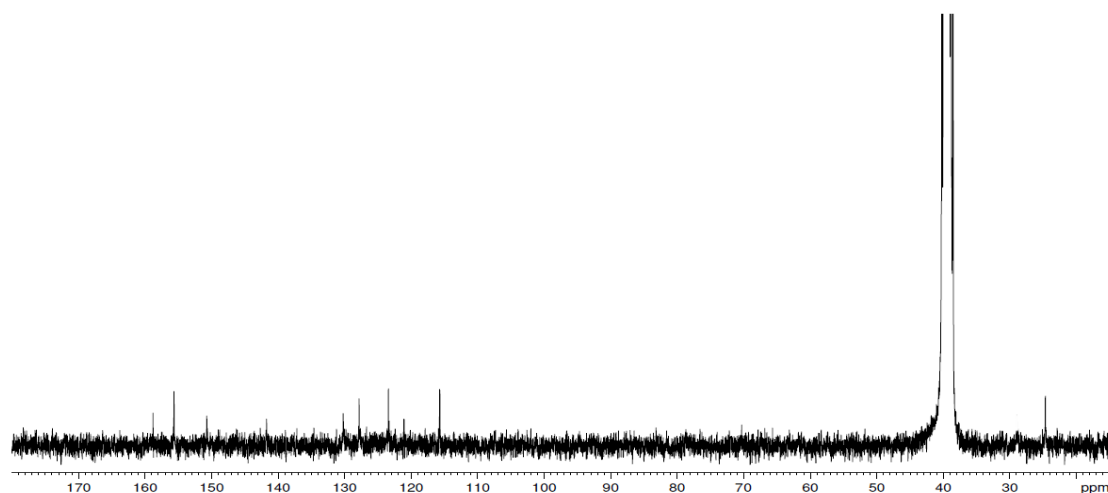
IR (KBr): (**46**)



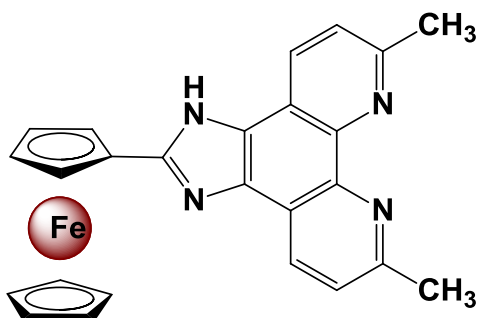
$^1\text{H}$  (DMSO- $d_6$ ) (46)



$^{13}\text{C}$  (DMSO- $d_6$ ) (46)



### 2.8.30 Microwave synthesis of 2-ferroceny-(6,9-dimethyl-1H-imidazo[4,5-f][1,10]-phenanthroline (47) (Novel method, novel molecule)

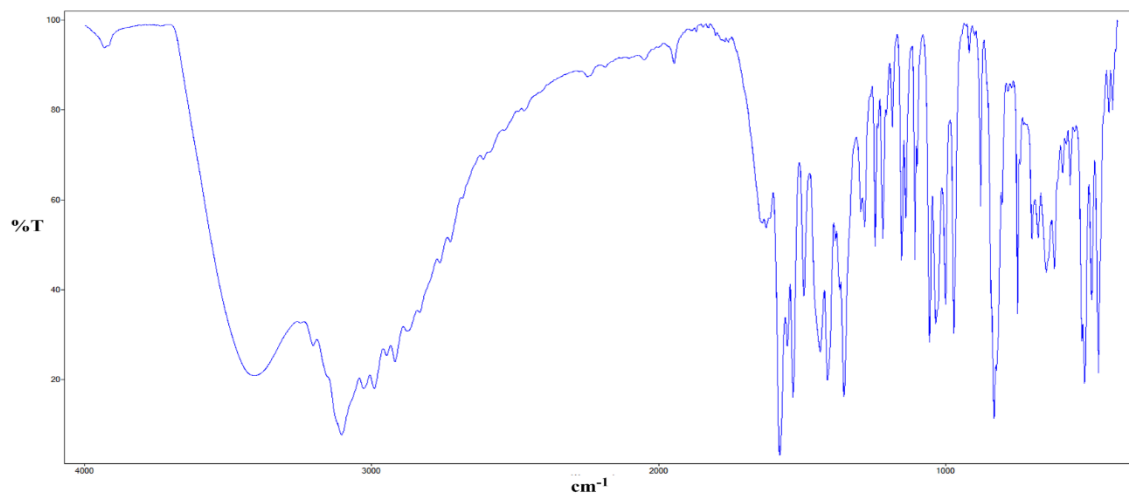


0.15 g ( $6.30 \times 10^{-4}$  mol) of 2,9-dimethyl-1,10-phenanthroline-5,6-dione was dissolved in 15 cm<sup>3</sup> of hot dry MeOH, to which 0.017 g ( $3.15 \times 10^{-5}$  mol) CAN in 5 cm<sup>3</sup> of hot MeOH was added. To the resulting reaction mixture was added 0.49 g (6.30 mmol) NH<sub>4</sub>OAc in one portion followed by 0.14 g ( $6.30 \times 10^{-4}$  mol) of ferrocenecarboxaldehyde. The resulting clear red mixture was then reacted in the microwave at 75 °C (300W, 1 bar) for 10 mins. The resulting solution was allowed to cool to room temperature before being filtered and washed with MeOH, and dried in an oven at 70 °C overnight.

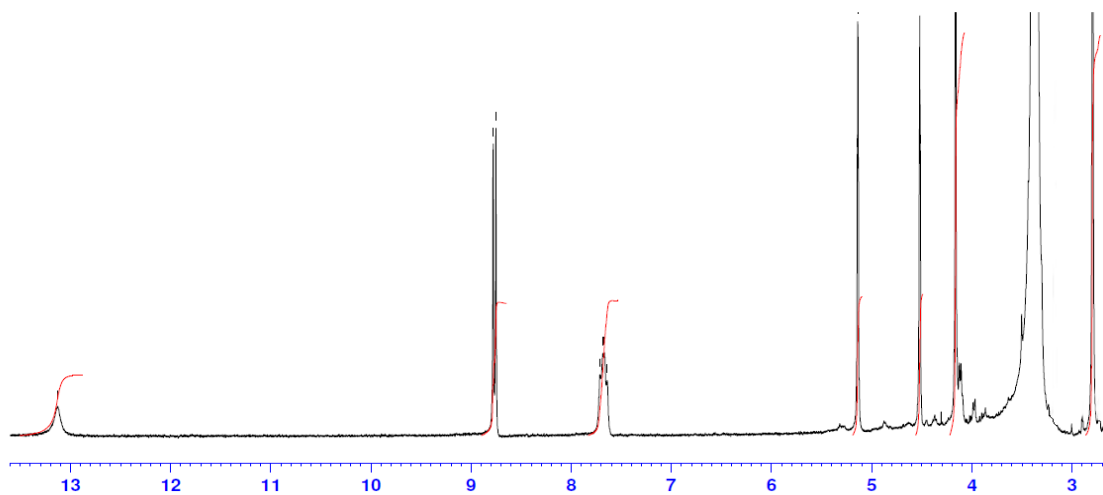
Product formula weight (**47**) = 432.30g/mol.

Yield:	0.22 g (80.79 %)
Mp:	> 250 °C.
% Calculated:	C, 58.34; H, 2.33; N, 12.96
% Found:	C, 58.29; H, 2.41; N, 12.89
IR (KBr) $\nu_{\max}$ :	420, 431, 470, 493, 516, 566, 621, 650, 678, 701, 749, 831, 881, 975, 1000, 1037, 1058, 1108, 1140, 1154, 1188, 1220, 1245, 1284, 1357, 1412, 1437, 1484, 1533, 1554, 1579, 1625, 3107, 3411
<sup>1</sup> H NMR:	(DMSO-d <sub>6</sub> ): $\delta$ = 2.79 (s, 6H), 4.16 (s, 5H), 4.51-4.52 (m, 2H), 5.13-5.14 (m, 2H), 7.64-7.71 (m, 2H), 8.75-8.78 (d, 2H).
LC/TCOF-MS:	Calcd for C <sub>25</sub> H <sub>22</sub> FeN <sub>4</sub> [M+H] <sup>+</sup> 433.1113, found 433.1143

IR (KBr): (47)



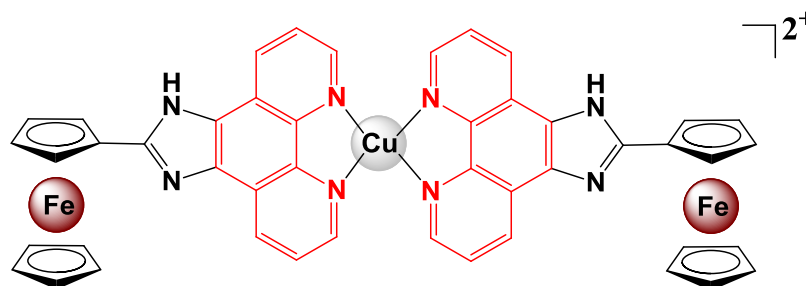
<sup>1</sup>H (DMSO-d<sub>6</sub>) (47)



## 2.9 Synthesis of imidazo[4,5-*f*][1,10]phenanthroline perchlorate complexes

### 2.9.1 Synthesis of [Cu(22)<sub>2</sub>](ClO<sub>4</sub>)<sub>2</sub> (54) (Novel complex)

22 = 2-ferroceny-1*H*-imidazo[4,5-*f*][1,10]-phenanthroline (ferrip)



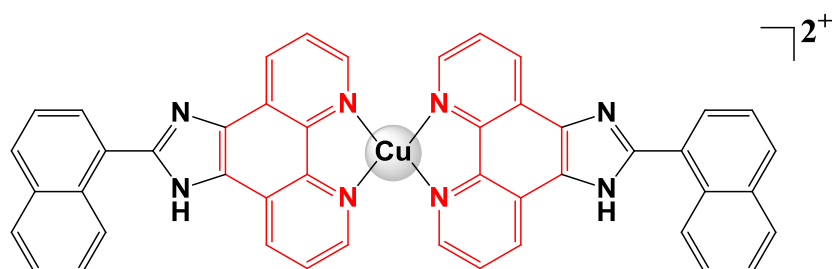
0.10 g ( $2.70 \times 10^{-4}$  mol) [Cu(ClO<sub>4</sub>)<sub>2</sub>·6H<sub>2</sub>O] was dissolved in 20 cm<sup>3</sup> of MeOH at room temperature. To this was added 0.20 g ( $4.95 \times 10^{-4}$  mol) of ferrip (22), 2-ferroceny-1*H*-imidazo[4,5-*f*][1,10]-phenanthroline in one portion to produce an orange mixture which after 1h of refluxing changed to a dark orange/light brown colour, continued refluxing for 4 hrs total. The reaction mixture was allowed to cool to room temperature before being filtered, resulting in a dark orange/light brown powder which was washed with MeOH and air dried.

Complex formula weight (54) = 1070.95g/mol.

Yield:	0.131g (45.30 %)
Mp:	> 250 °C.
% Calculated:	C: 51.59, H: 3.01, N: 10.46
% Found:	C: 51.39, H: 2.72, N: 10.68
IR (KBr) $\nu_{\max}$ :	3431, 3084, 1670, 1568, 1514, 1448, 1439, 1417, 1361, 1310, 1186, 1104, 962, 807, 723, 621, 525, 479, 437 cm <sup>-1</sup>
$\mu_{\text{eff}}$ :	1.95 B.M.

2.9.2 Synthesis of  $[\text{Cu}(\mathbf{19})_2](\text{ClO}_4)_2 \cdot 7\text{H}_2\text{O}$  (**55**) (Novel complex)

**19** = 2-(naphthalen-1-yl)-1*H*-imidazo[4,5-*f*][1,10]phenanthroline (**nip**)

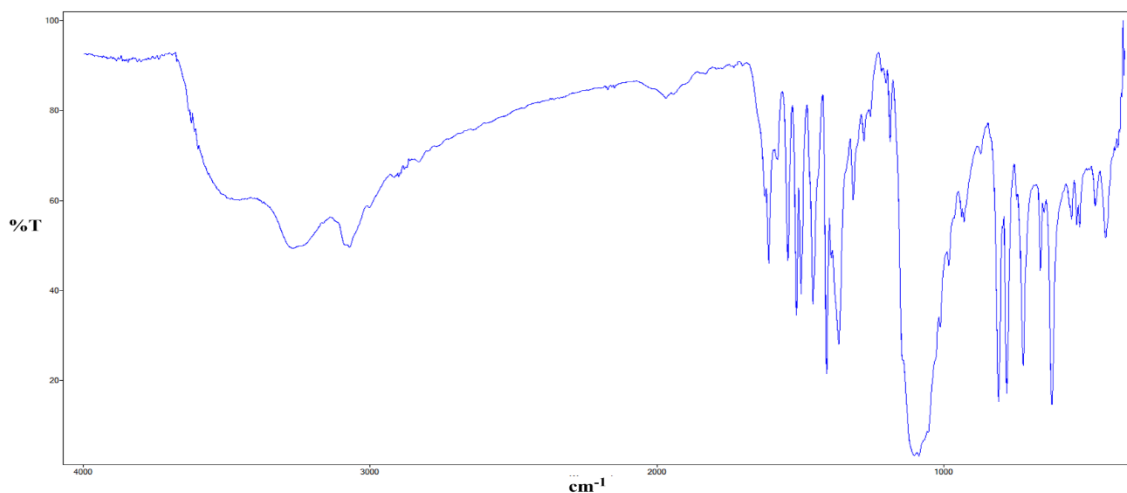


0.13 g ( $3.51 \times 10^{-4}$  mol)  $[\text{Cu}(\text{ClO}_4)_2 \cdot 6\text{H}_2\text{O}]$  was dissolved in 20 cm<sup>3</sup> of MeOH at room temperature. To this was added 0.20 g ( $5.77 \times 10^{-4}$  mol) of nip (**19**), 2-(naphthalen-1-yl)-1*H*-imidazo[4,5-*f*][1,10]phenanthroline in one portion to produce a green solution which was then refluxed for 2 hrs. The reaction mixture was allowed to cool to room temperature before being filtered, washed with MeOH and air dried.

Complex formula weight (**55**) = 1081.32g/mol.

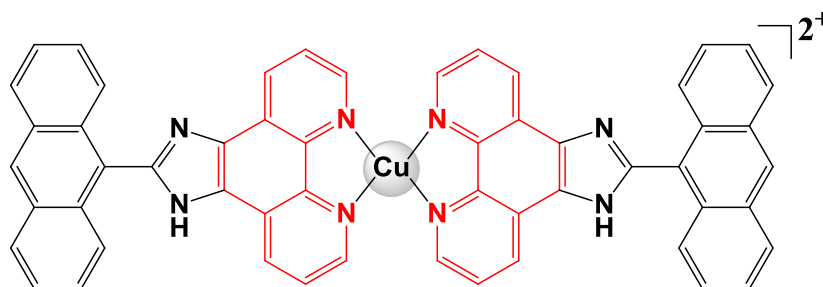
Yield:	0.183g (48.22 %)
Mp:	> 250 °C.
% Calculated:	C: 51.09, H: 3.91, N: 10.36
% Found:	C: 50.91, H: 3.62, N: 10.59
IR (KBr) $\nu_{\text{max}}$ :	435, 472, 526, 536, 554, 622, 662, 722, 780, 809, 1054, 1102, 1187, 1217, 1278, 1315, 1366, 1409, 1456, 1497, 1514, 1543, 1579, 1610, 1624, 3072, 3272
$\mu_{\text{eff}}$ :	1.95 B.M.



IR (KBr): (**55**)

### 2.9.3 Synthesis of $[\text{Cu}(\mathbf{20})_2](\text{ClO}_4)_2 \cdot 7\text{H}_2\text{O}$ (**56**) (Novel complex)

**20** = 2-(anthracen-9-yl)-1*H*-imidazo[4,5-*f*][1,10]phenanthroline (**aip**)



0.15 g ( $4.05 \times 10^{-4}$  mol)  $[\text{Cu}(\text{ClO}_4)_2 \cdot 6\text{H}_2\text{O}]$  was dissolved in 20 cm<sup>3</sup> of MeOH at room temperature. To this was added 0.20 g ( $5.05 \times 10^{-4}$  mol) of aip (**20**), 2-(anthracen-9-yl)-1*H*-imidazo[4,5-*f*][1,10]phenanthroline in one portion to produce a green solution which was then refluxed for 2 hrs. The reaction mixture was allowed to cool to room temperature before being filtered, washed with MeOH and air dried.

Complex formula weight (**56**) = 1181.44g/mol

Yield: 0.187g (39.11%)

Mp: > 250 °C.

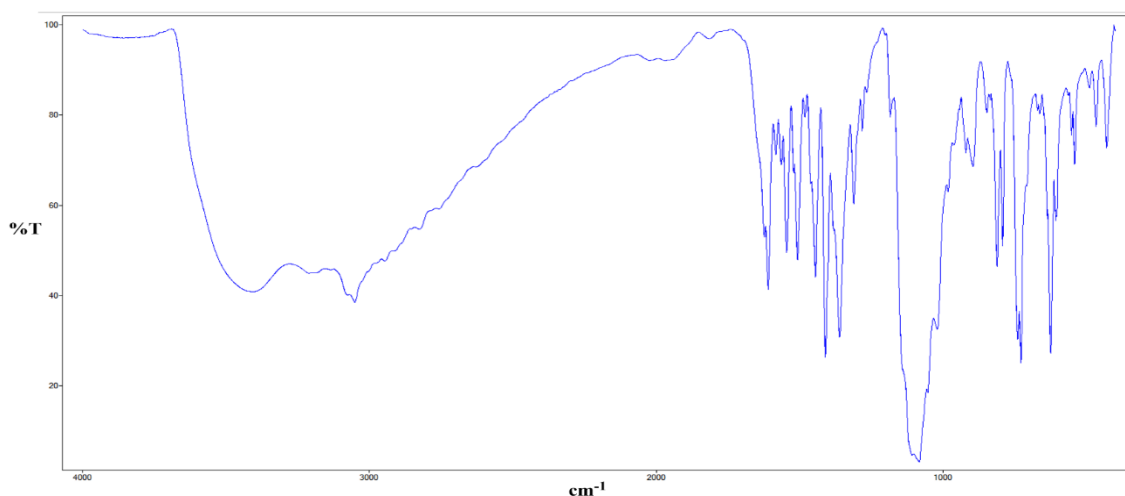
% Calculated: C: 54.90, H: 3.93, N: 9.48

% Found: C: 54.71, H: 3.67, N: 9.69

IR (KBr)  $\nu_{\max}$ : 3054, 1612, 1546, 1510, 1444, 1410, 1362, 1312, 1280, 1185, 1085, 896, 812, 794, 742, 728, 626, 605, 542, 467, 426  $\text{cm}^{-1}$

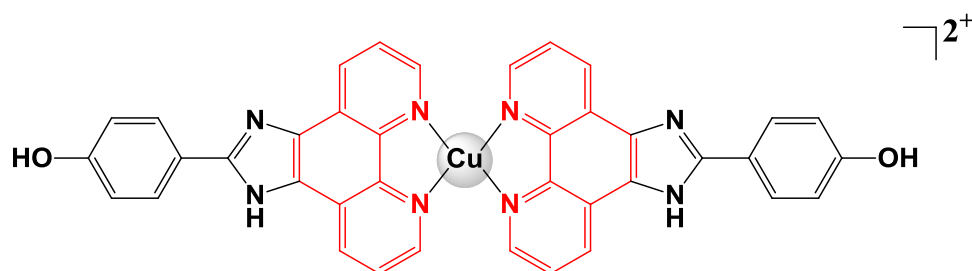
$\mu_{\text{eff}}$ : 1.93 B.M.

IR (KBr): (56)



#### 2.9.4 Synthesis of $[\text{Cu}(\mathbf{18})_2](\text{ClO}_4)_2 \cdot \text{MeOH} \cdot 5\text{H}_2\text{O}$ (**57**) (Novel complex)

**18** = 4-(1*H*-imidazo[4,5-*f*][1,10]phenanthrolin-2-yl)phenol (**18**)



0.14 g ( $3.78 \times 10^{-4}$  mol)  $[\text{Cu}(\text{ClO}_4)_2] \cdot 6\text{H}_2\text{O}$  was dissolved in 30  $\text{cm}^3$  of MeOH at room temperature. To this was added 0.20 g ( $6.40 \times 10^{-4}$  mol) of **18**, 4-(1*H*-imidazo[4,5-*f*][1,10]phenanthrolin-2-yl)phenol in one portion to produce a green solution which was then refluxed for 2 hrs. The reaction mixture was allowed to cool to room temperature before being filtered, washed with MeOH and air dried.

Complex formula weight (**57**) = 1009.22g/mol.

Yield: 0.188g (49.30%)

Mp: > 250 °C.

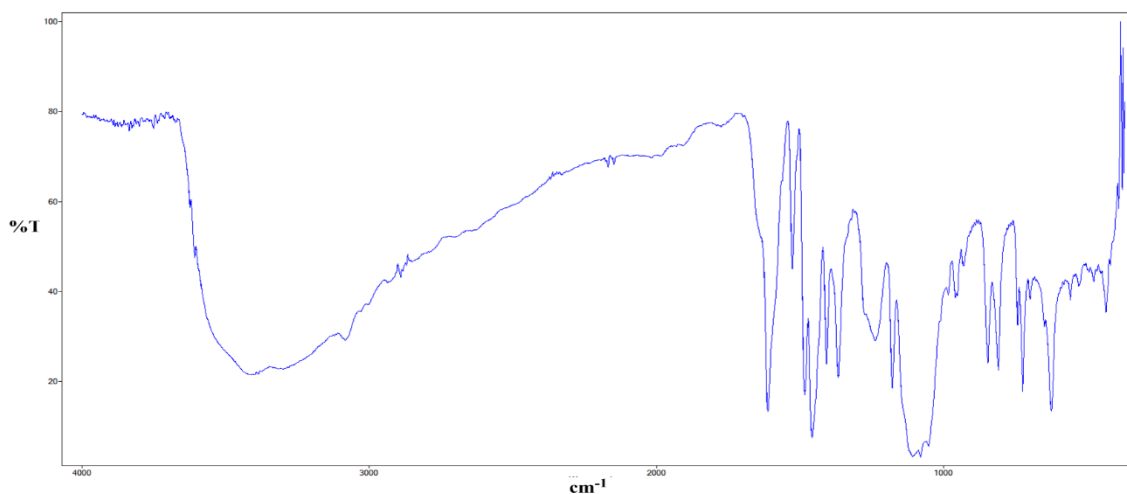
% Calculated: C: 46.41, H: 3.80, N: 11.10

% Found: C: 46.23, H: 3.51, N: 11.33

IR (KBr)  $\nu_{\max}$ : 3386, 3084, 1611, 1526, 1483, 1457, 1407, 1367, 1273, 1237, 1178, 1108, 1079, 1052, 958, 929, 845, 808, 741, 723, 698, 648, 624, 557, 528, 475, 434  $\text{cm}^{-1}$

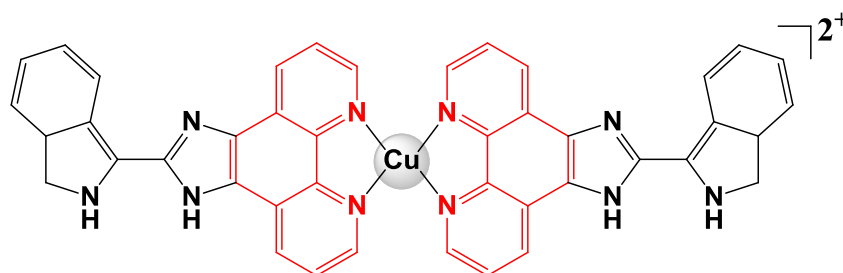
$\mu_{\text{eff}}$ : 1.82 B.M.

IR (KBr): (**57**)



### 2.9.5 Synthesis of $[\text{Cu}(\mathbf{21})_2](\text{ClO}_4)_2 \cdot 2\text{H}_2\text{O}$ (**58**) (Novel complex)

**21** = 2-(1*H*-indol-3-yl)-1*H*-imidazo[4,5-*f*][1,10]phenanthroline (**H<sub>2</sub>IIP**)



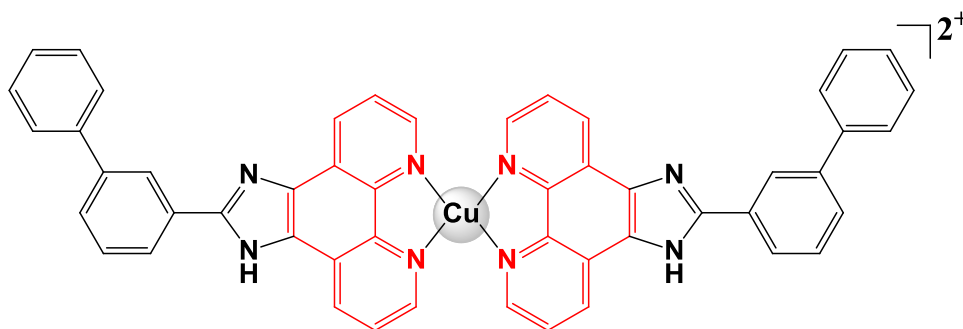
0.13 g ( $3.51 \times 10^{-4}$  mol)  $[\text{Cu}(\text{ClO}_4)_2 \cdot 6\text{H}_2\text{O}]$  was dissolved in  $30 \text{ cm}^3$  of MeOH at room temperature. To this was added 0.20 g ( $5.96 \times 10^{-4}$  mol) of  $\text{H}_2\text{IIP}$  (**21**), 2-(1*H*-indol-3-yl)-1*H*-imidazo[4,5-*f*][1,10]phenanthroline in one portion to produce a yellow solution which was then refluxed for 2 hrs. The resulting brown coloured reaction mixture was allowed to cool to room temperature to produce a dark green precipitate which was filtered, washed with MeOH and air dried.

Complex formula weight (**58**) = 969.20g/mol.

Yield:	0.201g (59.12%)
Mp:	> 250 °C.
% Calculated:	C: 52.05, H: 3.12, N: 14.45
% Found:	C: 51.86, H: 2.86, N: 14.68
IR (KBr) $\nu_{\text{max}}$ :	409, 569, 625, 649, 682, 734, 749, 772, 795, 877, 926, 968, 10006, 1035, 1072, 1131, 1198, 1259, 1297, 1354, 1396, 1428, 1454, 1482, 1505, 1577, 1620, 1727, 1785, 1856, 1929, 2909, 3053, 3133, 3280, 3388, 3513
$\mu_{\text{eff}}$ :	1.98 B.M.

### 2.9.6 Synthesis of $[\text{Cu}(\text{21})_2](\text{ClO}_4)_2 \cdot 2\text{H}_2\text{O}$ (**59**) (Novel complex)

**41** = 2-([1,1'-biphenyl]-3-yl)-1*H*-imidazo[4,5-*f*][1,10]phenanthroline (**biphip**)



0.12 g ( $3.24 \times 10^{-4}$  mol)  $[\text{Cu}(\text{ClO}_4)_2 \cdot 6\text{H}_2\text{O}]$  was dissolved in  $30 \text{ cm}^3$  of MeOH at room temperature. To this was added 0.20 g ( $5.37 \times 10^{-4}$  mol) of biphip (**41**), 2-([1,1'-biphenyl]-

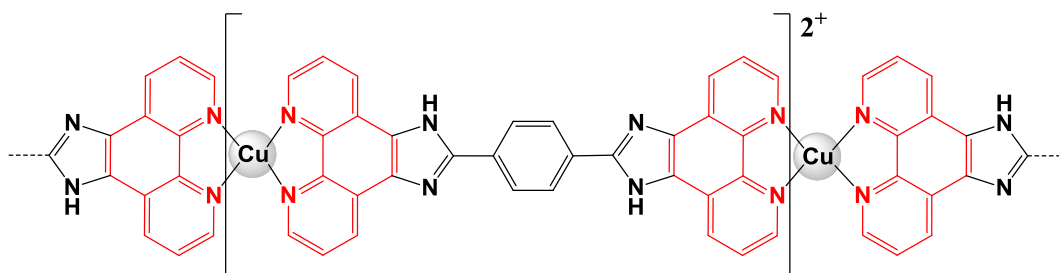
3-yl)-1*H*-imidazo[4,5-*f*][1,10]phenanthroline in one portion to produce a green solution which was then refluxed overnight. The reaction mixture was then allowed to cool to room temperature to produce a dark green precipitate which was filtered, washed with MeOH and air dried.

Complex formula weight (**59**) = 1043.32g/mol.

Yield:	0.159g (47.06%)
Mp:	> 250 °C.
% Calculated:	C: 58.94, H: 3.49, N: 10.78
% Found:	C: 58.76, H: 3.19, N: 10.98
IR (KBr) $\nu_{\max}$ :	410, 521, 625, 698, 718, 741, 761, 785, 811, 915, 965, 1072, 1109, 1192, 1269, 1299, 1354, 1396, 1418, 1438, 1454, 1477, 1507, 1546, 1568, 1602, 1659, 3111
$\mu_{\text{eff}}$ :	1.89 B.M.

### 2.9.7 Synthesis of [Cu(**23**)](ClO<sub>4</sub>)<sub>2</sub>·2H<sub>2</sub>O (**60**) (Novel complex, polymer)

**23** = 1,4-bis(1*H*-imidazo[4,5-*f*][1,10]phenanthrolin-2-yl)benzene (**bpibH<sub>2</sub>**)



0.32 g ( $8.64 \times 10^{-4}$  mol) [Cu(ClO<sub>4</sub>)<sub>2</sub>·6H<sub>2</sub>O] was dissolved in 30 cm<sup>3</sup> of MeOH at room temperature. To this was added 0.20 g ( $3.89 \times 10^{-4}$  mol) of bpibH<sub>2</sub> (**23**), 1,4-bis(1*H*-imidazo[4,5-*f*][1,10]phenanthrolin-2-yl)benzene in one portion to produce a yellow solution which was then refluxed overnight. The reaction mixture was then allowed to cool to room temperature before being filtered, washed with MeOH and air dried.

Complex formula weight (**60**) = 813.02g/mol.

Yield: 0.20g (45%)

Mp: > 250 °C.

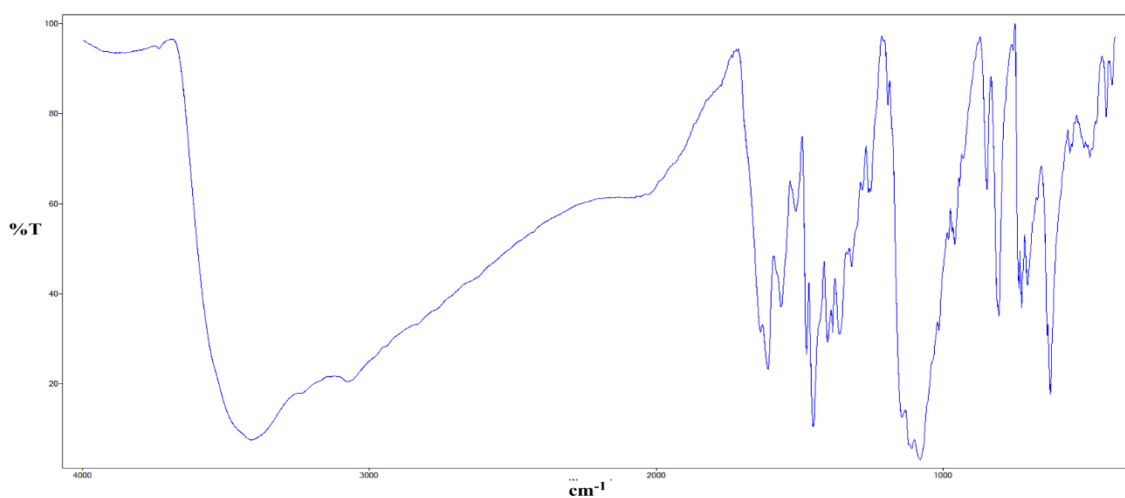
% Calculated: C: 47.27, H: 2.73, N: 13.78

% Found: C: 46.94, H: 2.55, N: 13.59

IR (KBr)  $\nu_{\max}$ : 3412, 1610, 1566, 1513, 1476, 1453, 1403, 1385, 1361, 1319, 1260, 1192, 1080, 959, 846, 805, 735, 726, 705, 637, 625, 558, 488, 431,

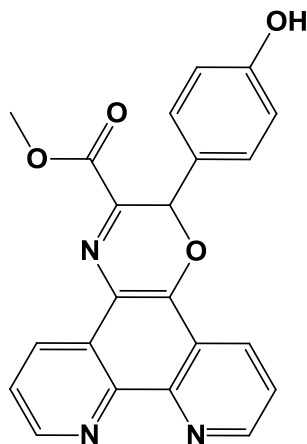
$\mu_{\text{eff}}$ : 2.1 B.M.

IR (KBr): (**60**)



## 2.10 Synthesis of Oxazine (Phenoaxazine) Ligands.

### 2.10.1 Synthesis of methyl 2-(4-hydroxyphenyl)-2H-[1,4]oxazino[2,3-f][1,10]phenanthroline-3-carboxylate, PDTME (49)



0.40 g ( $1.903 \times 10^{-3}$  mol) of phendione was dissolved in 60 cm<sup>3</sup> of refluxing dry MeOH. To this, was added 0.44 g ( $1.90 \times 10^{-3}$  mol) of L-tyrosine methyl ester hydrochloride dissolved in 20 cm<sup>3</sup> of MeOH. The resulting yellow solution was then refluxed for 24 hrs. After which the yellow saturated mixture was filtered hot to yield a yellow powder (Phendiol).

The filtrate orange/yellow was allowed to slowly evaporate at room temperature to yield a precipitate (PDTME) which was filtered and washed with ice-cold MeOH.

Product formula weight (**49**) = 385.37g/mol.

Yield: 0.15g (20.45%)

Mp: > 250 °C.

IR (KBr)  $\nu_{\max}$ : 429, 486, 551, 631, 679, 740, 767, 783, 808, 842, 921, 972, 1020, 1058, 1071, 1111, 1132, 1173, 1259, 1286, 1324, 1345, 1379, 1415, 1433, 1488, 1503, 1515, 1587, 1608, 1712, 1742, 1918, 1965, 2473, 2609, 2685, 2811, 2947, 3069, 3274, 3425, 3880

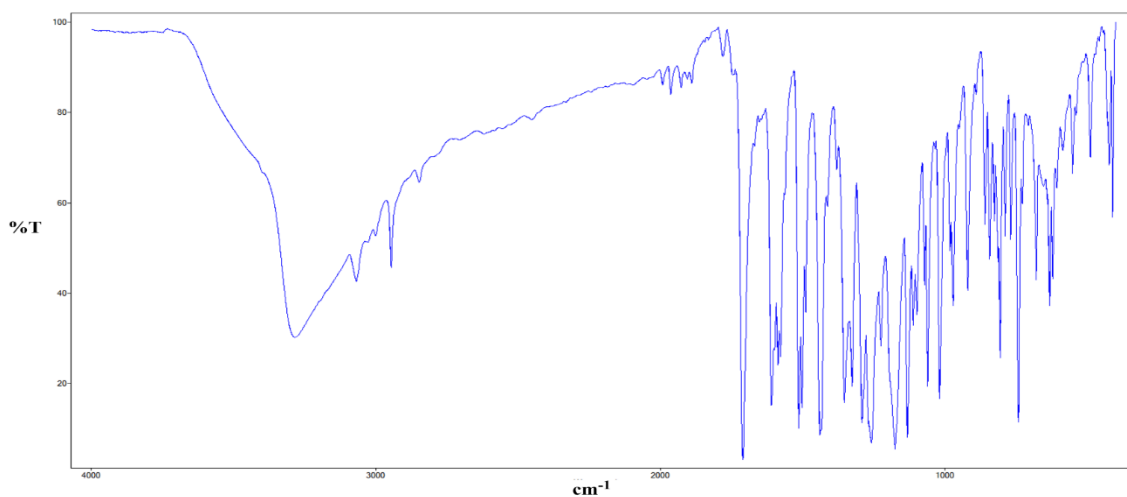
<sup>1</sup>H NMR: (DMSO-d<sub>6</sub>):  $\delta$  = 3.89 (s, 1H), 6.58 (s, 1H), 6.64-6.67 (m, 2H), 7.18-7.21 (m, 2H), 7.77-7.87 (m, 2H), 8.58-8.62 (m,

1H), 8.86-8.90 (m, 1H), 9.02-9.04 (m, 1H), 9.11-9.12 (m, 1H), 9.13 (m, 1H).

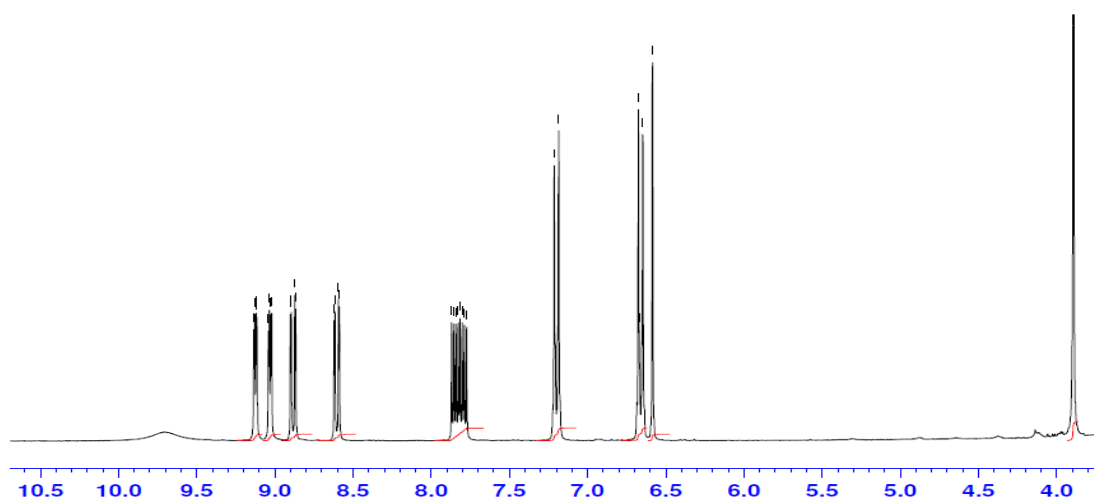
<sup>13</sup>C NMR: (75 MHz DMSO-d<sub>6</sub>) δ = 48.56, 52.92, 71.98, 115.77, 121.19, 121.72, 123.73, 124.10, 124.76, 125.95, 128.94, 129.81, 130.90, 138.39, 142.23, 146.37, 148.61, 149.68, 151.52, 158.72, 162.60.

LC/TCOF-MS: Calcd for C<sub>22</sub>H<sub>15</sub>N<sub>3</sub>O<sub>4</sub> [M+H]<sup>+</sup> 386.1135, found 386.1114

IR (KBr): **PDTME (49)**



<sup>1</sup>H (DMSO-d<sub>6</sub>) **PDTME (49)**





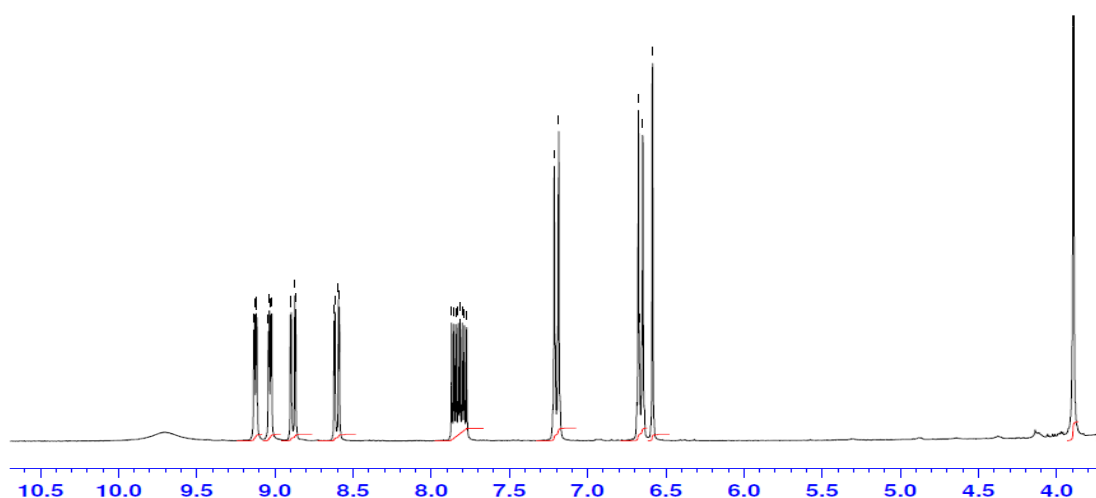
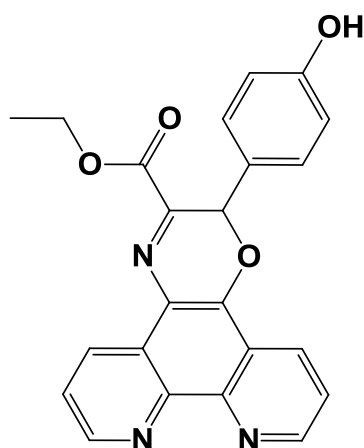
### 2.10.2 Microwave synthesis of methyl 2-(4-hydroxyphenyl)-2*H*-[1,4]oxazino[2,3-*f*][1,10]phenanthroline-3-carboxylate, PDTME (**49**)

0.40 g (1.90 mmol) of phendione was dissolved in 25 cm<sup>3</sup> of refluxing MeOH to produce a yellow coloured solution. To this, was added 0.44 g (1.90 mmol) of L-tyrosine methyl ester hydrochloride and the resulting orange solution was allowed to react for 4 hrs in the microwave at 80 °C (300W, 1 bar) with constant stirring. The resulting brown/sand coloured solution was filtered while hot to yield a sand coloured powder solid which was washed with MeOH (Phendiol).

The orange coloured filtrate was allowed to evaporate slowly at room temperature to yield an orange precipitate (PDTME) which was filtered and washed with ice-cold MeOH.

Product formula weight (**49**) = 385.37g/mol.

Yield:	0.03g (4.09%)
Mp:	> 250 °C.
IR (KBr) $\nu_{\max}$ :	429, 486, 551, 631, 679, 740, 767, 783, 808, 842, 921, 972, 1020, 1058, 1071, 1111, 1132, 1173, 1259, 1286, 1324, 1345, 1379, 1415, 1433, 1488, 1503, 1515, 1587, 1608, 1712, 1742, 1918, 1965, 2473, 2609, 2685, 2811, 2947, 3069, 3274, 3425, 3880
<sup>1</sup> H NMR:	(DMSO- <i>d</i> <sub>6</sub> ): $\delta$ = 3.89 (s, 1H), 6.58 (s, 1H), 6.64-6.67 (m, 2H), 7.18-7.21 (m, 2H), 7.77-7.87 (m, 2H), 8.58-8.62 (m, 1H), 8.86-8.90 (m, 1H), 9.02-9.04 (m, 1H), 9.11-9.12 (m, 1H), 9.13 (m, 1H).
<sup>13</sup> C NMR:	(75 MHz DMSO- <i>d</i> <sub>6</sub> ) $\delta$ = 48.56, 52.92, 71.98, 115.77, 121.19, 121.72, 123.73, 124.10, 124.76, 125.95, 128.94, 129.81, 130.90, 138.39, 142.23, 146.37, 148.61, 149.68, 151.52, 158.72, 162.60.
LC/TCOF-MS:	Calcd for C <sub>22</sub> H <sub>15</sub> N <sub>3</sub> O <sub>4</sub> [M+H] <sup>+</sup> 386.1135, found 386.1114

$^1\text{H}$  (DMSO- $d_6$ ) PDTME (49)**2.10.3 Synthesis of ethyl 2-(4-hydroxyphenyl)-2H-[1,4]oxazino[2,3-f][1,10]phenanthroline-3-carboxylate, PDTEE (50) (Novel molecule)**

0.40 g (1.90 mmol) of phendione was dissolved in 30 cm<sup>3</sup> of refluxing EtOH to produce a yellow coloured solution. To this, was added 0.47 g (1.90 mmol) of L-tyrosine ethyl ester hydrochloride and the resulting orange solution was allowed to react for 4 hrs in the microwave at 80 °C (300W, 1 bar) with constant stirring. The resulting brown/sand coloured solution was filtered while hot to yield a sand coloured powder solid which was washed with EtOH (Phendiol).

The orange coloured filtrate was allowed to evaporate slowly at room temperature to yield an orange/red precipitate (PDTEE) (impure) which was filtered and washed with ice-cold EtOH.

Product formula weight (**50**) = 399.40g/mol.

Yield: 0.09g (12.14%)

Mp: > 250 °C.

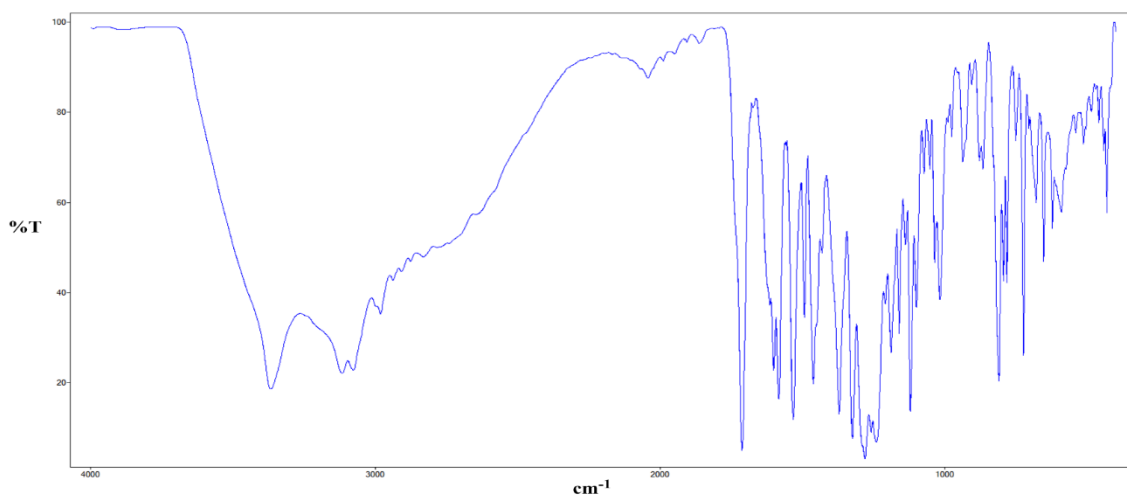
IR (KBr)  $\nu_{\max}$ : 426, 626, 636, 685, 699, 724, 735, 752, 784, 812, 868, 940, 968, 1036, 1115, 1182, 1194, 1250, 1287, 1330, 1375, 1390, 1447, 1472, 1489, 1542, 1585, 1613, 1723, 2021, 3101, 3244, 3481.

$^1\text{H}$  NMR: (DMSO- $d_6$ ):  $\delta$  = 1.30-1.35 (t, 3H), 4.31-4.35 (m, 2H), 6.58 (s, 1H), 6.64-6.67 (m, 2H), 7.16-7.20 (m, 2H), 7.74-7.85 (m, 2H), 8.56-8.60 (m, 1H), 8.84-8.88 (m, 1H), 9.01-9.03 (m, 1H), 9.11-9.12 (m, 1H), 9.12 (m, 1H).

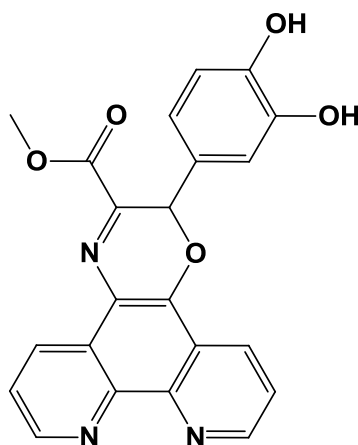
$^{13}\text{C}$  NMR: (75 MHz DMSO- $d_6$ )  $\delta$  = 13.93, 61.40, 71.58, 115.27, 121.09, 121.68, 123.69, 123.95, 124.68, 125.85, 128.91, 129.78, 130.78, 138.34, 142.19, 146.31, 148.58, 149.45, 151.12, 158.52, 162.54.

LC/TCOF-MS: Calcd for  $\text{C}_{23}\text{H}_{17}\text{N}_3\text{O}_4$   $[\text{M}+\text{H}]^+$  400.1293, found 400.1290

IR (KBr): **PDTEE (50)**



#### 2.10.4 Synthesis of methyl 2-(3,4-dihydroxyphenyl)-2H-[1,4]oxazino[2,3-f][1,10]phenanthroline-3-carboxylate, PDDME (51) (Novel molecule)



0.80 g ( $3.81 \times 10^{-3}$  mol) of phendione was dissolved in 100 cm<sup>3</sup> of refluxing dry MeOH. To this was added 0.94 g ( $3.80 \times 10^{-3}$  mol) of L-DOPA methyl ester hydrochloride in one portion. A clear orange solution resulted which was then refluxed for 24 hrs after which was filtered hot to yield a yellow solid which was washed with cold MeOH.

The filtrate was allowed to slowly evaporate at room temperature to yield an orange precipitate which was filtered and washed with ice-cold MeOH (PDDME).

Product formula weight (**51**) = 401.37g/mol.

Yield: 0.38g (24.88%)

Mp: > 250 °C.

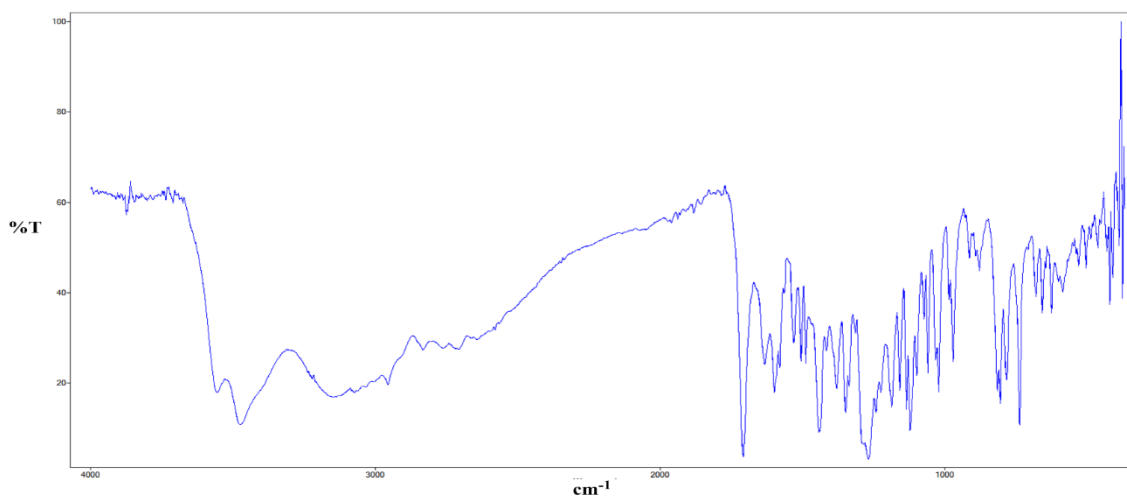
IR (KBr)  $\nu_{\max}$ : 3474, 1708, 1633, 1599, 1580, 1531, 1505, 1489, 1443, 1380, 1348, 1337, 1268, 1242, 1225, 1186, 1158, 1135, 1123, 1099, 1074, 1060, 1032, 986, 971, 914, 879, 816, 806, 783, 737, 680, 658, 626, 586, 421.

<sup>1</sup>H NMR: (DMSO-d<sub>6</sub>):  $\delta$  = 3.89 (s, 3H), 6.51 (s, 1H), 6.62-6.69 (m, 2H), 6.76 (s, 1H), 7.76-7.81 (m, 1H), 7.82-7.86 (m, 1H), 8.56-8.60 (m, 1H), 8.85-8.88 (m, 1H), 9.01-9.03 (m, 1H), 9.10-9.12 (m, 1H)

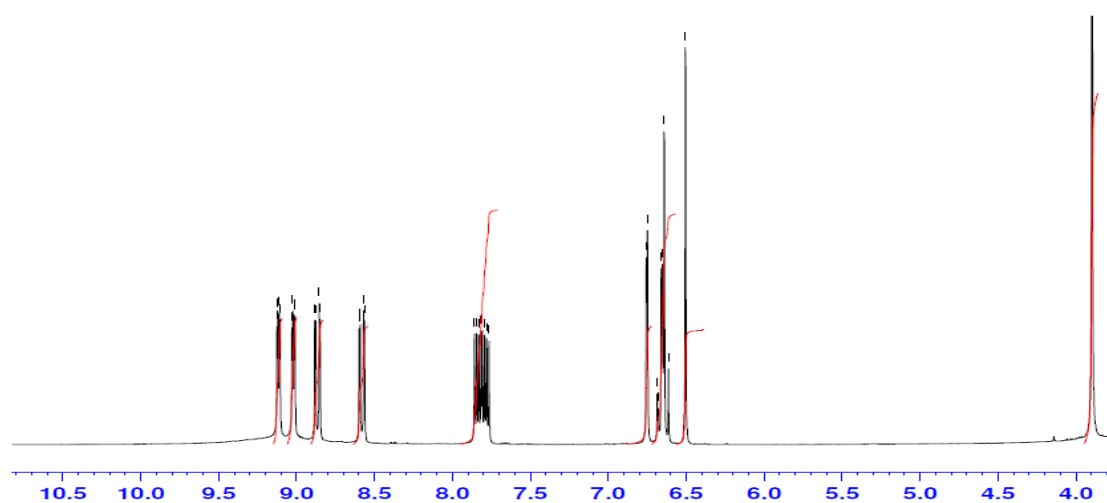
<sup>13</sup>C NMR: (75 MHz DMSO-d<sub>6</sub>) δ = 48.55, 52.98, 72.43, 114.58, 115.87, 118.88, 121.43, 124.45, 124.66, 125.15, 126.37, 131.73, 131.90, 138.99, 139.91, 144.40, 145.51, 147.07, 147.35, 150.13, 151.33, 162.52.

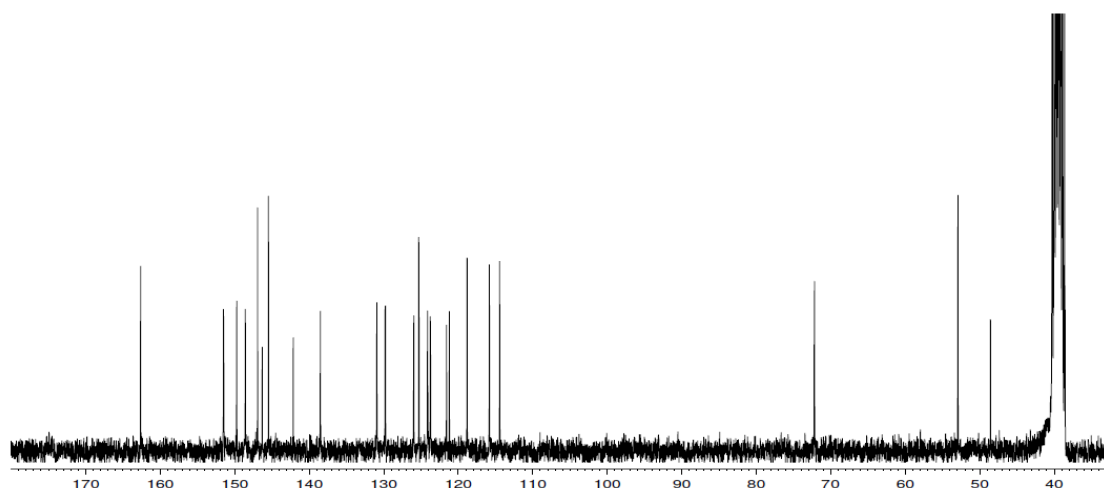
LC/TCOF-MS: Calcd for C<sub>22</sub>H<sub>15</sub>N<sub>3</sub>O<sub>5</sub> [M+H]<sup>+</sup> 402.1084, found 402.1096

IR (KBr): **PDDME (51)**



<sup>1</sup>H (DMSO-d<sub>6</sub>) **PDDME (51)**



$^{13}\text{C}$  (DMSO- $d_6$ ) PDDME (51)**2.10.5 Microwave synthesis of methyl 2-(3,4-dihydroxyphenyl)-2*H*-[1,4]oxazino[2,3-*f*][1,10]phenanthroline-3-carboxylate, PDDME (51) (Novel molecule)**

0.40 g ( $1.90 \times 10^{-3}$  mol) of phendione was dissolved in 25 cm<sup>3</sup> of hot dry MeOH in a microwave reaction vial. To this was added 0.47 g ( $1.90 \times 10^{-3}$  mol) of L-DOPA methyl ester hydrochloride. A clear orange solution resulted which was then reacted for 4 hr in the microwave at 75 °C (300W, 1 bar) with constant stirring. The reaction mixture was filtered whilst hot to yield a yellow solid which was washed with cold MeOH (Phendiol).

The filtrate was allowed to slowly evaporate at room temperature to yield an orange precipitate which was filtered and washed with ice-cold MeOH (PDDME).

Product formula weight (51) = 401.37g/mol.

Yield: 0.07g (9.16%)

Mp: > 250 °C.

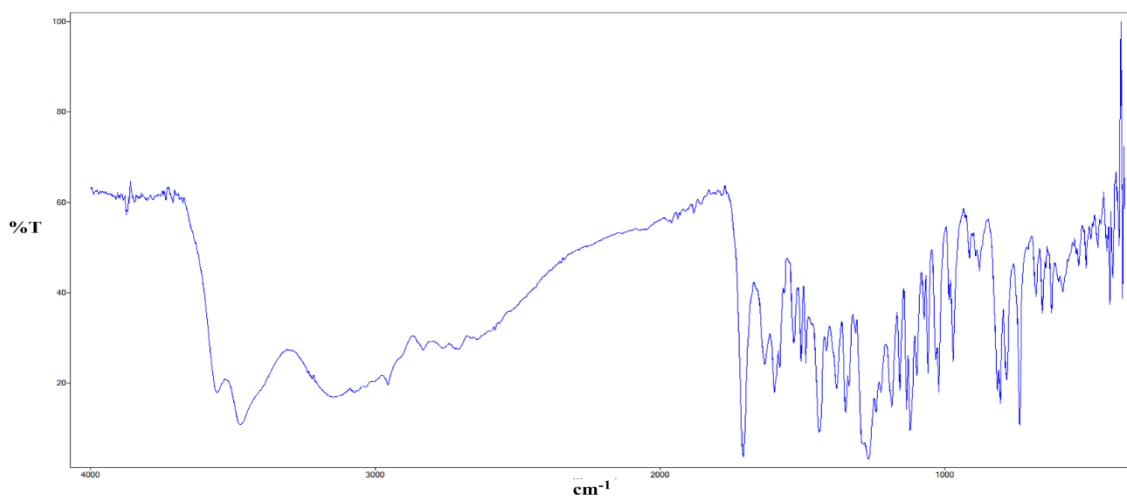
IR (KBr)  $\nu_{\text{max}}$ : 3474, 1708, 1633, 1599, 1580, 1531, 1505, 1489, 1443, 1380, 1348, 1337, 1268, 1242, 1225, 1186, 1158, 1135, 1123, 1099, 1074, 1060, 1032, 986, 971, 914, 879, 816, 806, 783, 737, 680, 658, 626, 586, 421.

$^1\text{H}$  NMR: (DMSO-d<sub>6</sub>):  $\delta$  = 3.89 (s, 3H), 6.51 (s, 1H), 6.62-6.69 (m, 2H), 6.76 (s, 1H), 7.76-7.81 (m, 1H), 7.82-7.86 (m, 1H), 8.56-8.60 (m, 1H), 8.85-8.88 (m, 1H), 9.01-9.03 (m, 1H), 9.10-9.12 (m, 1H)

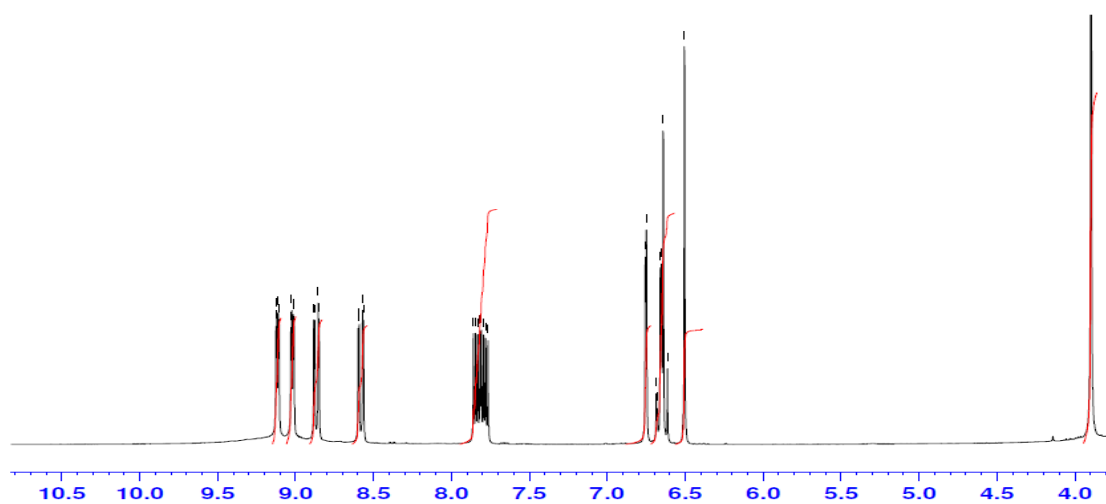
$^{13}\text{C}$  NMR: (75 MHz DMSO-d<sub>6</sub>)  $\delta$  = 48.55, 52.98, 72.43, 114.58, 115.87, 118.88, 121.43, 124.45, 124.66, 125.15, 126.37, 131.73, 131.90, 138.99, 139.91, 144.40, 145.51, 147.07, 147.35, 150.13, 151.33, 162.52.

LC/TCOF-MS: Calcd for C<sub>22</sub>H<sub>15</sub>N<sub>3</sub>O<sub>5</sub> [M+H]<sup>+</sup> 402.1084, found 402.1096

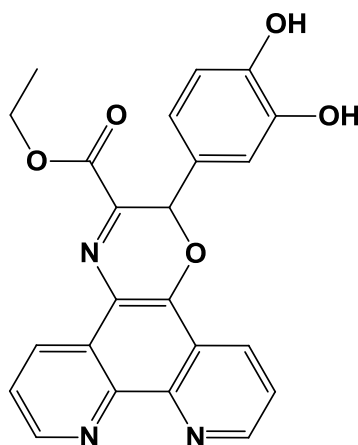
IR (KBr): **PDDME (51)**



$^1\text{H}$  (DMSO-d<sub>6</sub>) **PDDME (51)**



### 2.10.6 Synthesis of ethyl 2-(3,4-dihydroxyphenyl)-2H-[1,4]oxazino[2,3-f][1,10]phenanthroline-3-carboxylate, PDDEE (**52**) (Novel molecule)



0.40 g ( $1.90 \times 10^{-3}$  mol) of phendione was dissolved in 60 cm<sup>3</sup> of refluxing EtOH to produce a yellow coloured solution. To this, was added 0.50 g ( $1.91 \times 10^{-3}$  mol) of L-DOPA ethyl ester hydrochloride and the resulting orange solution was refluxed for 24 hrs. The resulting brown/sand coloured solution was filtered while hot to yield a sand coloured powder solid which was washed with EtOH (Phendiol).

The dark red filtrate was concentrated to approx. 10 cm<sup>3</sup> under reduced pressure and allowed to slowly evaporate at room temperature to yield an orange/yellow powder when filtered (PDDEE).

Product formula weight (**52**) = 415.40g/mol.

Yield: 0.19g (24.03%)

Mp: > 250 °C.

IR (KBr)  $\nu_{\max}$ : 3368, 3117, 3076, 1712, 1601, 1584, 1533, 1493, 1462, 1431, 1372, 1325, 1281, 1259, 1189, 1161, 1139, 1121, 1100, 1036, 1018, 811, 794, 782, 724, 679, 653, 622, 591, 431.

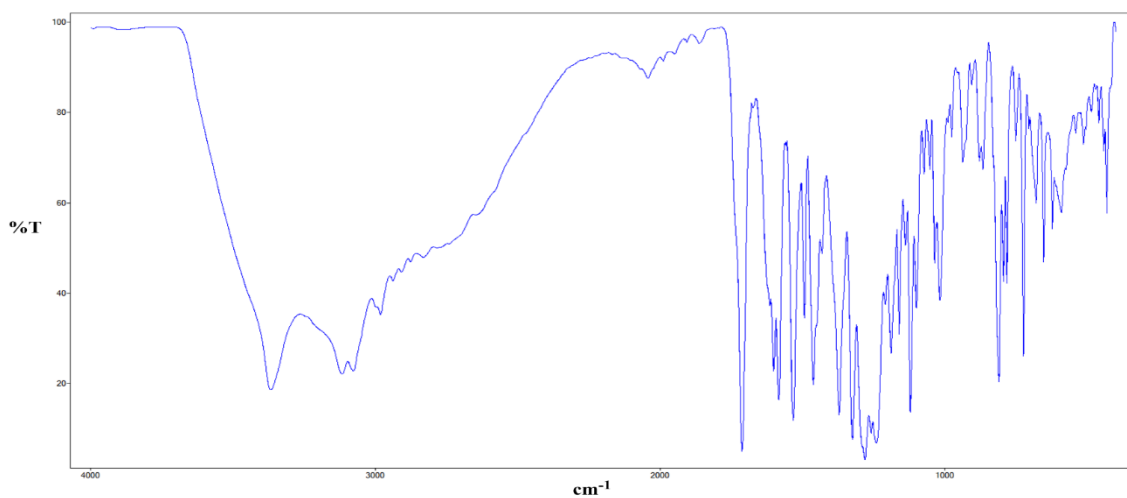
<sup>1</sup>H NMR: (DMSO-d<sub>6</sub>):  $\delta$  = 1.30-1.35 (t, 3H), 4.33-4.39 (m, 2H), 6.60 (s, 1H), 6.63-6.71 (m, 2H), 6.80 (s, 1H), 8.03-8.07 (m, 1H), 8.24-8.26 (m, 1H), 8.80-8.84 (m, 1H), 9.16-9.18 (m, 1H), 9.25-9.31 (m, 2H).



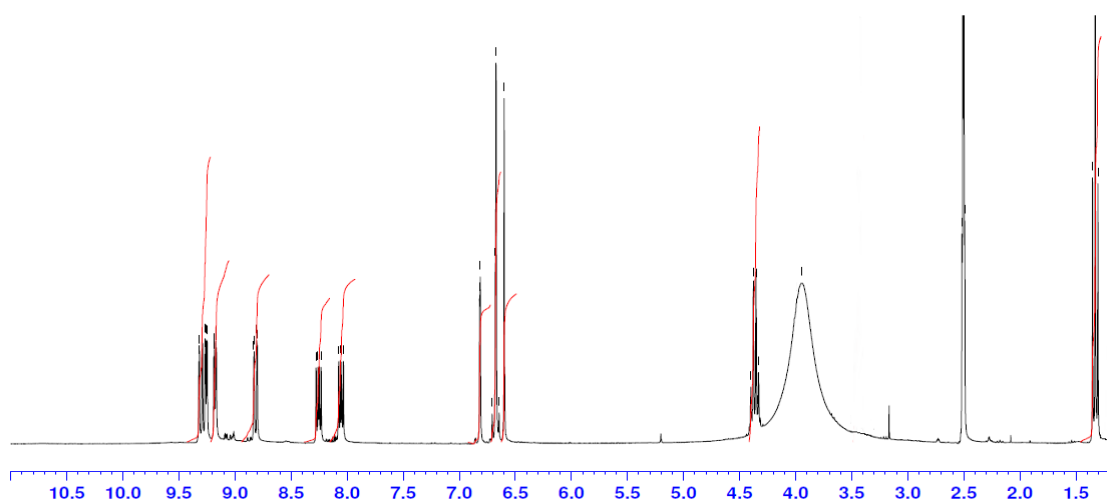
$^{13}\text{C}$  NMR: (75 MHz DMSO-d<sub>6</sub>)  $\delta$  = 13.93, 62.12, 73.00, 114.78, 115.98, 118.94, 121.10, 122.29, 125.02, 125.78, 125.91, 127.22, 133.34, 135.33, 136.21, 139.96, 140.52, 144.85, 145.60, 147.19, 150.98, 151.22, 161.78

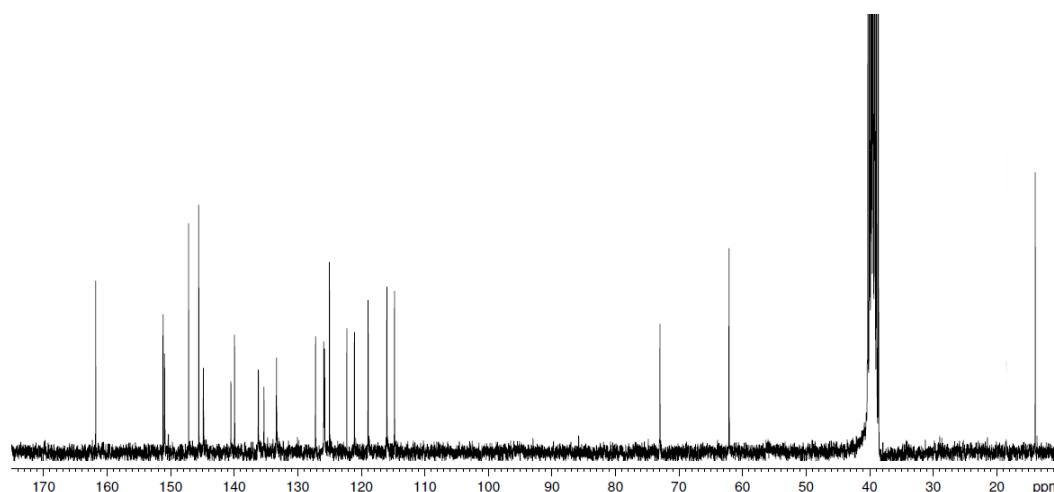
LC/TCOF-MS: Calcd for C<sub>23</sub>H<sub>17</sub>N<sub>3</sub>O<sub>5</sub> [M+H]<sup>+</sup> 416.1241, found 416.1255

IR (KBr): **PDDEE (52)**



$^1\text{H}$  (DMSO-d<sub>6</sub>) **PDDEE (52)**



$^{13}\text{C}$  (DMSO- $d_6$ ) PDDEE (52)**2.10.7 Microwave synthesis of 2-(3,4-dihydroxyphenyl)-2H-[1,4]oxazino[2,3-f][1,10]phenanthroline-3-carboxylate, PDDEE (52) (Novel molecule)**

0.40 g ( $1.90 \times 10^{-3}$  mol) of phendione was dissolved in 60  $\text{cm}^3$  of refluxing EtOH to produce a yellow coloured solution. To this, was added 0.50 g ( $1.91 \times 10^{-3}$  mol) of L-DOPA ethyl ester hydrochloride and the resulting orange solution was allowed to react for 4 hr in the microwave at 90  $^\circ\text{C}$  (300W, 1 bar) with constant stirring. The resulting brown/sand coloured solution was filtered while hot to yield a sand coloured powder solid which was washed with EtOH.

Product formula weight (52) = 415.40g/mol.

Yield: 0.12g (15.18%)

Mp:  $> 250$   $^\circ\text{C}$ .

IR (KBr)  $\nu_{\text{max}}$ : 3368, 3117, 3076, 1712, 1601, 1584, 1533, 1493, 1462, 1431, 1372, 1325, 1281, 1259, 1189, 1161, 1139, 1121, 1100, 1036, 1018, 811, 794, 782, 724, 679, 653, 622, 591, 431.

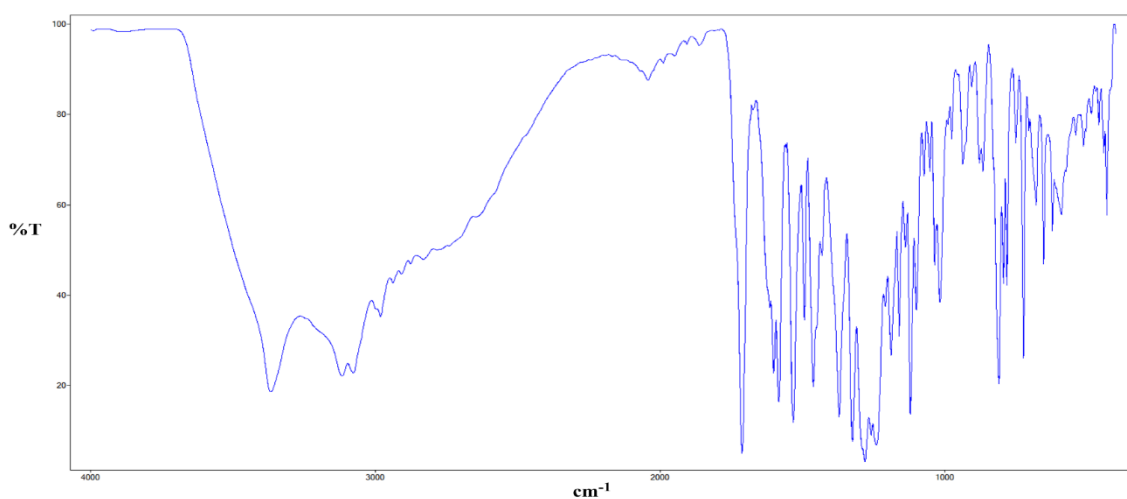
$^1\text{H}$  NMR: (DMSO- $d_6$ ):  $\delta$  = 1.30-1.35 (t, 3H), 4.33-4.39 (m, 2H), 6.60 (s, 1H), 6.63-6.71 (m, 2H), 6.80 (s, 1H), 8.03-8.07 (m, 1H),

8.24-8.26 (m, 1H), 8.80-8.84 (m, 1H), 9.16-9.18 (m, 1H),  
9.25-9.31 (m, 2H).

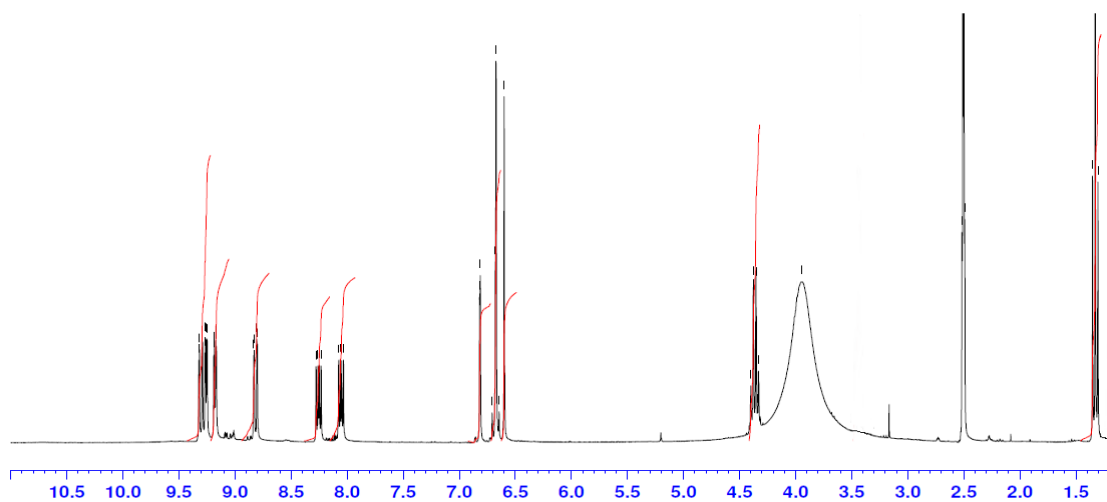
$^{13}\text{C}$  NMR: (75 MHz DMSO-d<sub>6</sub>)  $\delta$  = 13.93, 62.12, 73.00, 114.78,  
115.98, 118.94, 121.10, 122.29, 125.02, 125.78, 125.91,  
127.22, 133.34, 135.33, 136.21, 139.96, 140.52, 144.85,  
145.60, 147.19, 150.98, 151.22, 161.78

LC/TCOF-MS: Calcd for C<sub>23</sub>H<sub>17</sub>N<sub>3</sub>O<sub>5</sub> [M+H]<sup>+</sup> 416.1241, found 416.1255

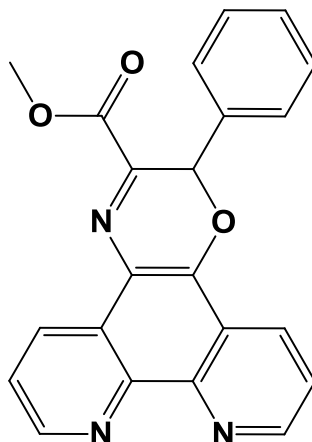
IR (KBr): **PDDEE (52)**



$^1\text{H}$  (DMSO-d<sub>6</sub>) **PDDEE (52)**



### 2.10.8 Synthesis of methyl 2-phenyl-2*H*-[1,4]oxazino[2,3-*f*][1,10]phenanthroline-3-carboxylate, PDPME (**53**) (Novel molecule)



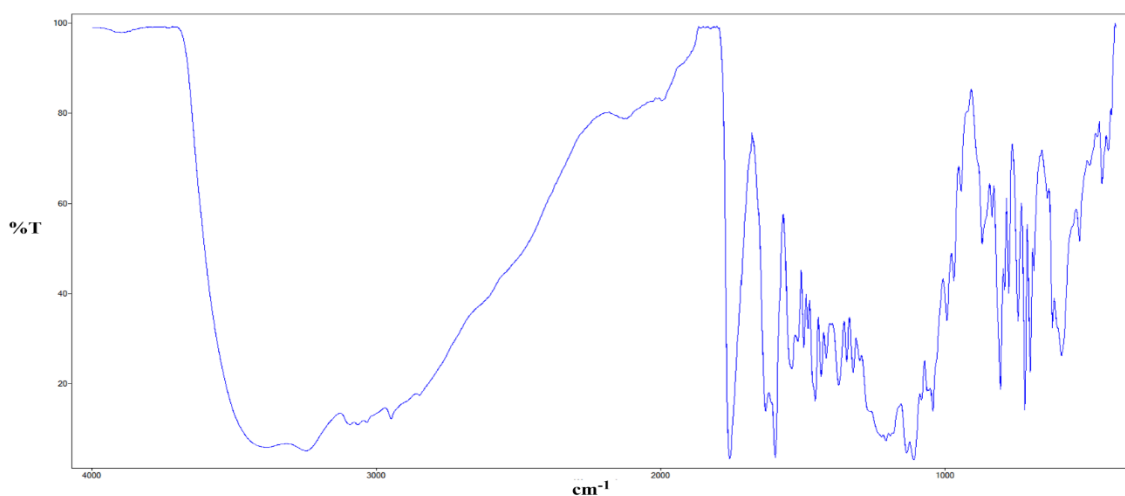
0.40 g ( $1.90 \times 10^{-3}$  mol) of phendione was dissolved in 50 cm<sup>3</sup> of refluxing dry MeOH. To this, was added 0.41 g ( $1.90 \times 10^{-3}$  mol) of L-phenylalanine methyl ester hydrochloride in one portion. The resulting yellow solution was then refluxed for 24 hrs. The resulting orange solution was allowed to cool to room temperature before being filtered to yield a gold coloured powder which was washed with MeOH (Phendiol).

The orange coloured filtrate was reduced in volume to approx. 20 cm<sup>3</sup> under reduced pressure and allowed to slowly evaporate at room temperature to yield an orange precipitate which was filtered and washed with ice-cold MeOH (PDPME).

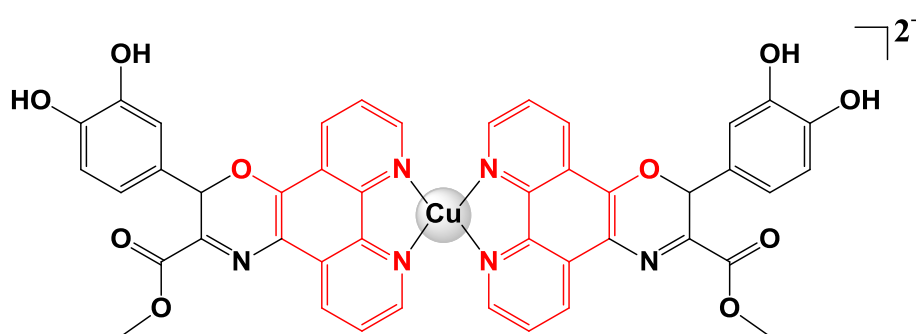
Product formula weight (**53**) = 369.37g/mol.

Yield:	0.084g (11.95%)
Mp:	> 250 °C.
IR (KBr) $\nu_{\max}$ :	448, 529, 593, 723, 806, 993, 1043, 1110, 1136, 1207, 1323, 1347, 1375, 1420, 1437, 1458, 1498, 1541, 1598, 1631, 1757, 3245.
<sup>1</sup> H NMR:	(DMSO- <i>d</i> <sub>6</sub> ): $\delta$ = 3.74 (s, 3H), 5.33 (s, 1H), 7.42-7.57 (m, 5H), 8.02-8.07 (m, 1H), 8.11-8.16 (m, 1H), 8.32 (s, 1H), 8.81-8.84 (m, 1H), 9.0-9.01 (m, 1H), 9.12-9.18 (m, 2H).
LC/TCOF-MS:	Calcd for C <sub>22</sub> H <sub>15</sub> N <sub>3</sub> O <sub>3</sub> [M+H] <sup>+</sup> 370.1186, found 370.121

## IR (KBr): PDPME (53)



## 2.11 Synthesis of Phenoxazine perchlorate complexes.

2.11.1 [Cu(PDDME)<sub>2</sub>](ClO<sub>4</sub>)<sub>2</sub> (92) (Novel complex)

0.11 g ( $2.97 \times 10^{-4}$  mol) of  $[\text{Cu}(\text{ClO}_4)_2] \cdot 6\text{H}_2\text{O}$  was dissolved in  $30 \text{ cm}^3$  of MeOH, to which 0.20 g ( $4.98 \times 10^{-4}$  mol) of PDDME (51) was added in one portion to the light blue solution. The resulting light green reaction mixture was allowed to stir overnight. A dark green coloured precipitate resulted which was filtered and washed with ice-cold MeOH and allowed to air dry.

Complex formula weight (92) = 1065.19g/mol.

Yield: 0.13g (41.11%)

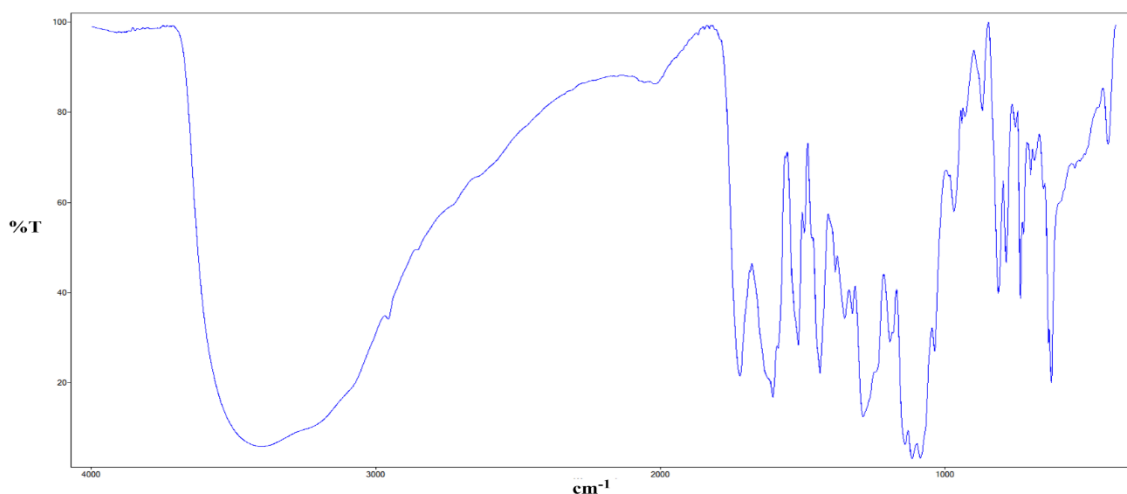
Mp:  $> 250^\circ\text{C}$ .

% Calculated: C, 49.61; H, 2.84; N, 7.89

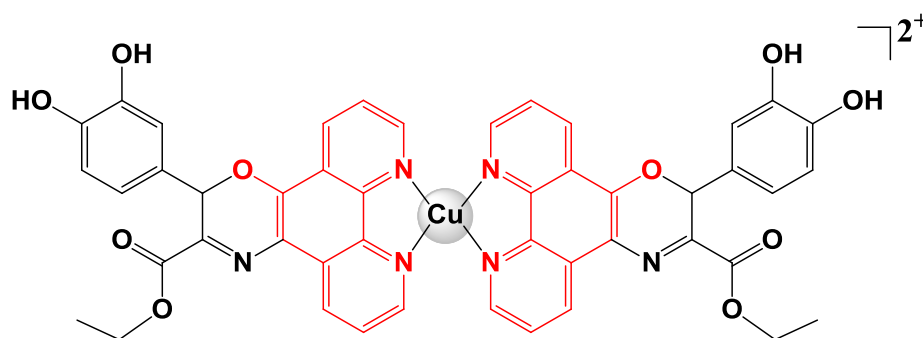
% Found: C, 49.52; H, 2.88; N, 7.78

IR (KBr)  $\nu_{\text{max}}$ : 3401, 1721, 1605, 1515, 1439, 1354, 1325, 1288, 1193, 1140, 1117, 1086, 1036, 968, 870, 813, 785, 735, 626, 425

IR (KBr): [Cu(PDDME)<sub>2</sub>](ClO<sub>4</sub>)<sub>2</sub> (**92**)



### 2.11.2 [Cu(PDDEE)<sub>2</sub>](ClO<sub>4</sub>)<sub>2</sub> (**93**) (Novel complex)



0.05 g ( $1.35 \times 10^{-4}$  mol) of [Cu(ClO<sub>4</sub>)<sub>2</sub>].6H<sub>2</sub>O was dissolved in 30 cm<sup>3</sup> of EtOH, to which 0.10 g ( $2.41 \times 10^{-4}$  mol) of PDDEE (**52**) was added in one portion to the light blue solution. The resulting green reaction mixture was allowed to stir overnight. A green coloured precipitate resulted which was filtered and washed with ice-cold MeOH and allowed to air dry.

Complex formula weight (**93**) = 1093.25g/mol.

Yield: 0.04g (27.12%)

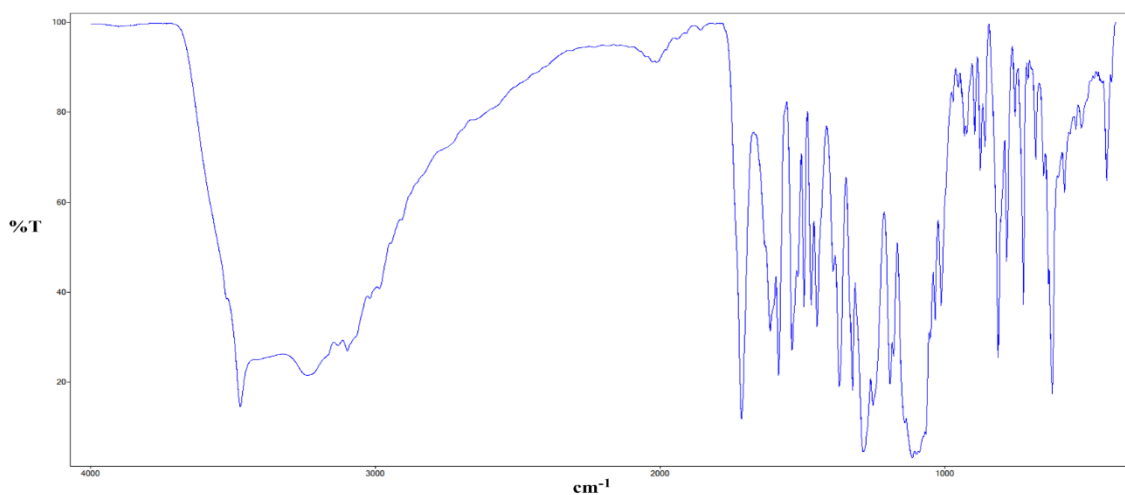
Mp: > 250 °C.

% Calculated: C, 50.54; H, 3.13; N, 7.69

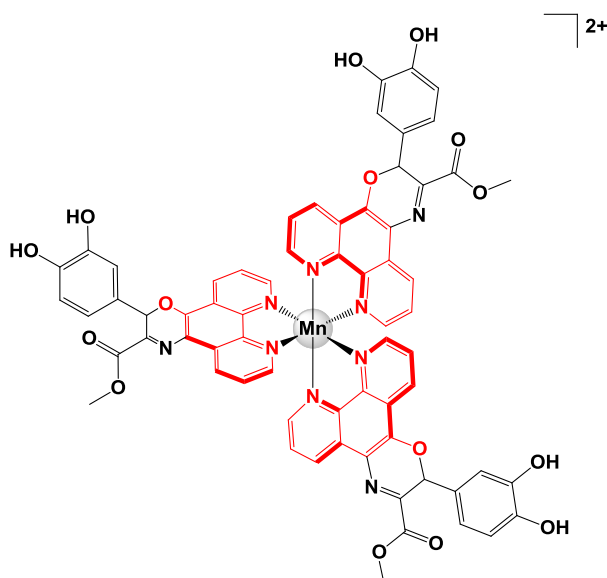
% Found: C, 50.49; H, 3.33; N, 7.58

IR (KBr)  $\nu_{\max}$ : 3475, 3238, 3098, 1714, 1615, 1586, 1537, 1496, 1470, 1451, 1370, 1325, 1285, 1252, 1193, 1114, 1034, 1012, 934, 923, 896, 875, 861, 813, 785, 726, 624, 581, 432

IR (KBr): [Cu(PDDEE)<sub>2</sub>](ClO<sub>4</sub>)<sub>2</sub> (93)



### 2.11.3 [Mn(PDDME)<sub>3</sub>](ClO<sub>4</sub>)<sub>2</sub> (94) (Novel complex)



0.04 g ( $1.11 \times 10^{-4}$  mol) of  $[\text{Mn}(\text{ClO}_4)_2] \cdot 6\text{H}_2\text{O}$  was dissolved in  $30 \text{ cm}^3$  of MeOH, to which 0.10 g ( $2.49 \times 10^{-4}$  mol) of PDDME (**51**) was added in one portion to the light blue solution. The resulting orange reaction mixture was allowed to stir overnight. An orange coloured precipitate resulted which was filtered and washed with cold MeOH and allowed to air dry.

Complex formula weight (**94**) = 1457.96g/mol.

Yield: 0.06g (37.24%)

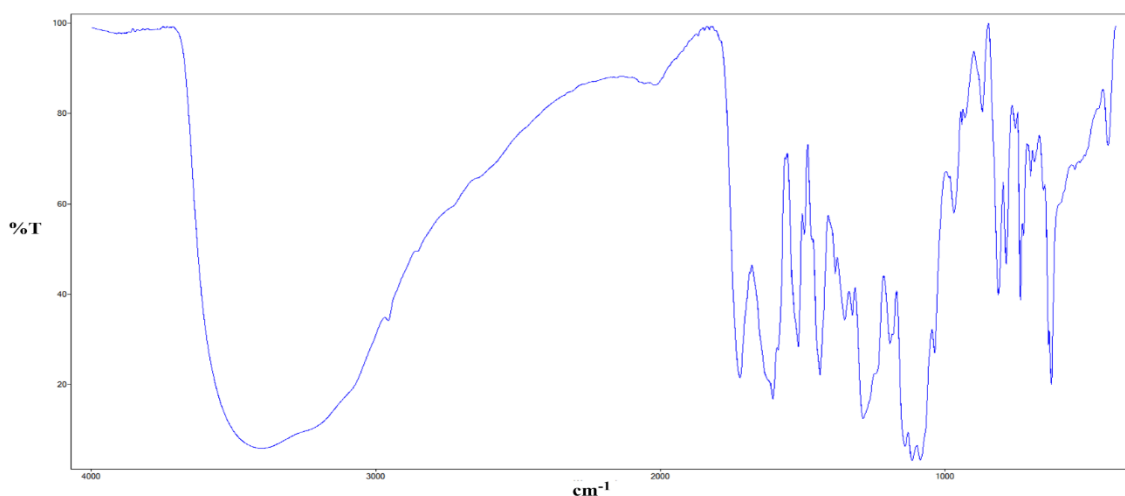
Mp:  $> 250^\circ\text{C}$ .

% Calculated: C, 54.37; H, 3.11; N, 8.65

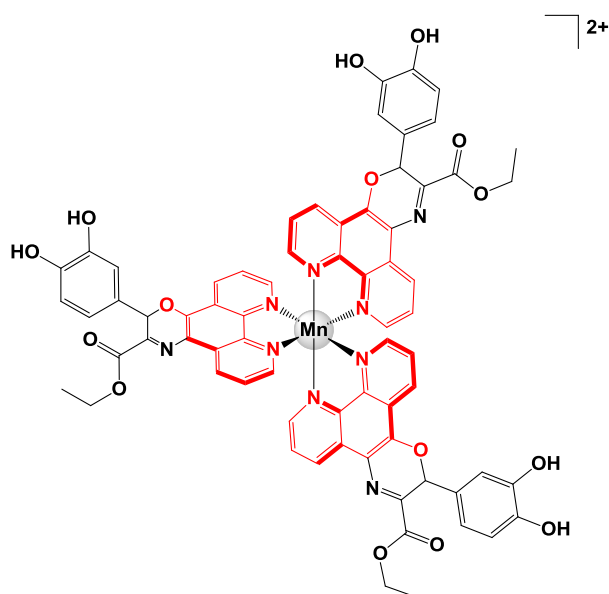
% Found: C, 54.15; H, 3.32; N, 8.55

IR (KBr)  $\nu_{\text{max}}$ : 3401, 1721, 1605, 1515, 1439, 1354, 1325, 1288, 1193, 1140, 1117, 1086, 1036, 968, 870, 813, 785, 735, 626, 425

IR (KBr):  $[\text{Mn}(\text{PDDME})_3](\text{ClO}_4)_2$  (**94**)





2.11.4 [Mn(PDDEE)<sub>3</sub>](ClO<sub>4</sub>)<sub>2</sub> (**95**) (Novel complex)

0.04 g ( $1.11 \times 10^{-4}$  mol) of  $[\text{Mn}(\text{ClO}_4)_2] \cdot 6\text{H}_2\text{O}$  was dissolved in 20 cm<sup>3</sup> of EtOH, to which 0.10 g ( $2.41 \times 10^{-4}$  mol) of PDDEE (**52**) was added in one portion to the light blue solution. The resulting reaction mixture was allowed to stir overnight. A precipitate resulted which was filtered and washed with cold MeOH and allowed to air dry.

Complex formula weight (**95**) = 1500.04g/mol.

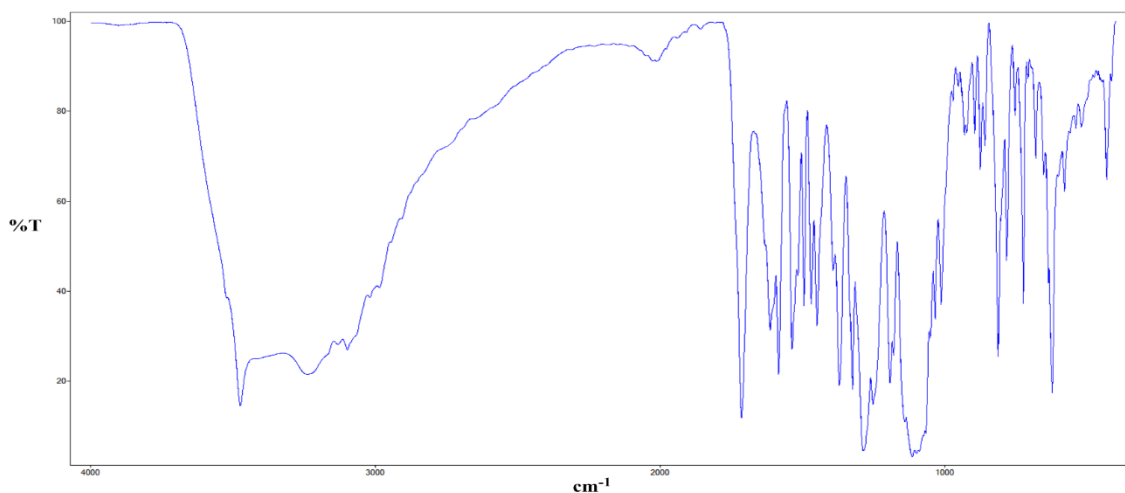
Yield: 0.05g (30.16%)

Mp: > 250 °C.

% Calculated: C, 55.25; H, 3.43; N, 8.40

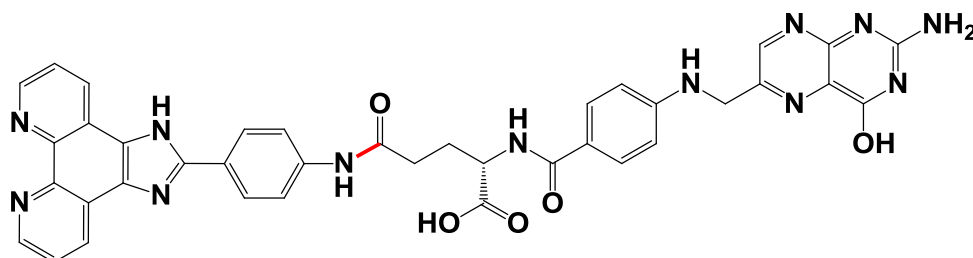
% Found: C, 55.09; H, 3.64; N, 8.28

IR (KBr)  $\nu_{\text{max}}$ : 3475, 3238, 3098, 1714, 1615, 1586, 1537, 1496, 1470, 1451, 1370, 1325, 1285, 1252, 1193, 1114, 1034, 1012, 934, 923, 896, 875, 861, 813, 785, 726, 624, 581, 432

IR (KBr):  $[\text{Mn}(\text{PDDEE})_3](\text{ClO}_4)_2$  (**95**)

### 2.12 Amide formation: Folate-NHS ester and 4-(1*H*-imidazo[4,5-*f*][1,10]phenanthrolin-2-yl)aniline (**32**) to form Im-phen-fol (**45**) (Novel molecule)

(*S*)-5-(((4-(1*H*-imidazo[4,5-*f*][1,10]phenanthrolin-2-yl)phenyl)amino)-2-(4-(((2-amino-4-hydroxypteridin-6-yl)methyl)amino)benzamido)-5-oxopentanoic acid. (**45**)

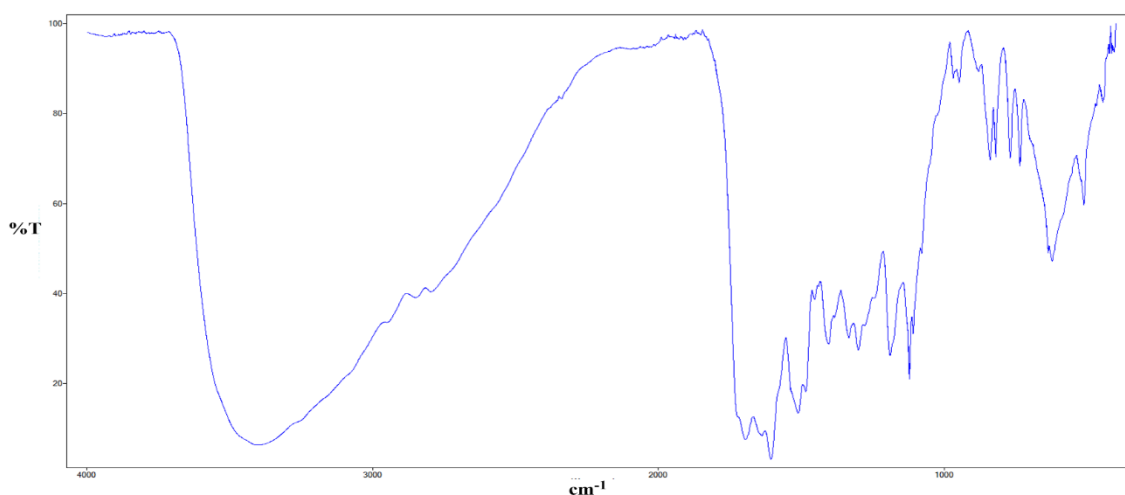


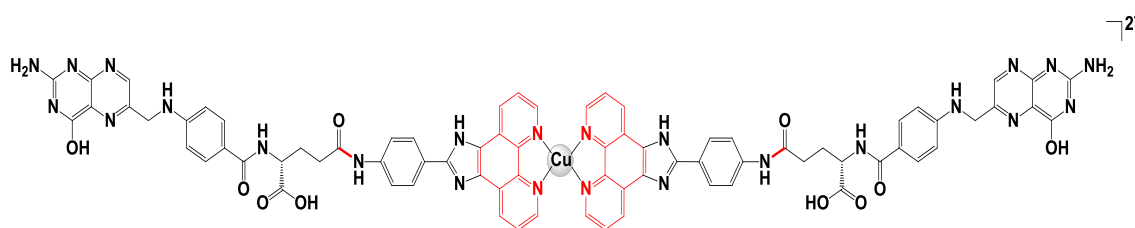
0.17 g ( $3.16 \times 10^{-4}$  mol) of folate-NHS activated ester (PMC275) was dissolved in  $10 \text{ cm}^3$  anhydrous DMSO to which 0.10g ( $3.21 \times 10^{-4}$  mol) of 4-(1*H*-imidazo[4,5-*f*][1,10]phenanthrolin-2-yl)aniline (**32**) dissolved in  $5 \text{ cm}^3$  anhydrous DMSO was added and the orange reaction mixture was allowed to react at room temperature in the dark under nitrogen for 96 hours. The resulting dicyclohexylurea (DCU) was filtered off and the solution dropped into  $100 \text{ cm}^3$  of 30:70 acetone:diethylether, resulting in the immediate formation of a yellow/orange precipitate which was allowed to stir for 1 hour and then retrieved by filtration and subsequently washed with  $50 \text{ cm}^3$  of 30:70 acetone:diethylether and then air dried.

Complex formula weight (**45**) = 734.72g/mol.

Yield:	0.22 g (94.85 %)
% Calculated:	C, 62.12; H, 4.12; N, 22.88
% Found:	C, 62.08; H, 4.16; N, 22.84
IR (KBr) $\nu_{\max}$ :	3361, 1696, 1607, 1512, 1484, 1457, 1408, 1335, 1302, 1190, 1122, 1110, 950, 840, 820, 769, 726, 624, 512, 446, 412.
$^1\text{H}$ NMR:	(DMSO- $d_6$ ): $\delta$ = 1.13-1.19 (m, 2H), 2.35 (m, 2H), 4.32 (m, 1H), 4.48 (s, 2H), 6.6-6.68 (m, 2H), 6.73-6.76 (m, 2H), 6.94 (bs, 2H), 7.61-7.71 (m, 2H), 7.82-7.86 (m, 2H), 7.96-7.99 (m, 2H), 8.14 (s, 1H), 8.64 (s, 1H), 8.91-8.92 (m, 1H), 8.94-9.01 (m, 4H)
$^{13}\text{C}$ NMR:	(75 MHz DMSO- $d_6$ ) $\delta$ = 8.56, 30.37, 45.83, 51.71, 111.17, 113.65, 117.10, 121.20, 123.34, 127.61, 128.95, 129.06, 129.82, 142.54, 147.26, 148.56, 150.46, 150.75, 152.20, 153.76, 161.12, 166.45, 173.73, 176.31
LC/TCOF-MS:	Calcd for $\text{C}_{38}\text{H}_{30}\text{N}_{12}\text{O}_5$ $[\text{M}+\text{Na}]^+$ 757.2365, found 757.2386

IR (KBr): **Im-phen-fol (45)**



2.12.1 Synthesis of  $[\text{Cu}(\text{Im-phen-fol})_2](\text{ClO}_4)_2 \cdot 2\text{H}_2\text{O}$  (**76**) (Novel complex)

0.03 g ( $8.10 \times 10^{-5}$  mol) of  $[\text{Cu}(\text{ClO}_4)_2] \cdot 6\text{H}_2\text{O}$  was dissolved in 30 cm<sup>3</sup> of MeOH, to which 0.10 g ( $1.36 \times 10^{-4}$  mol) of Im-phen-fol (**45**) was added in one portion. The resulting yellow coloured reaction mixture was allowed to stir at room temperature overnight before being filtered to produce a yellow/light brown powder, this powder precipitate was then washed with cold MeOH and air dried.

Complex formula weight (**76**) = 1767.92g/mol.

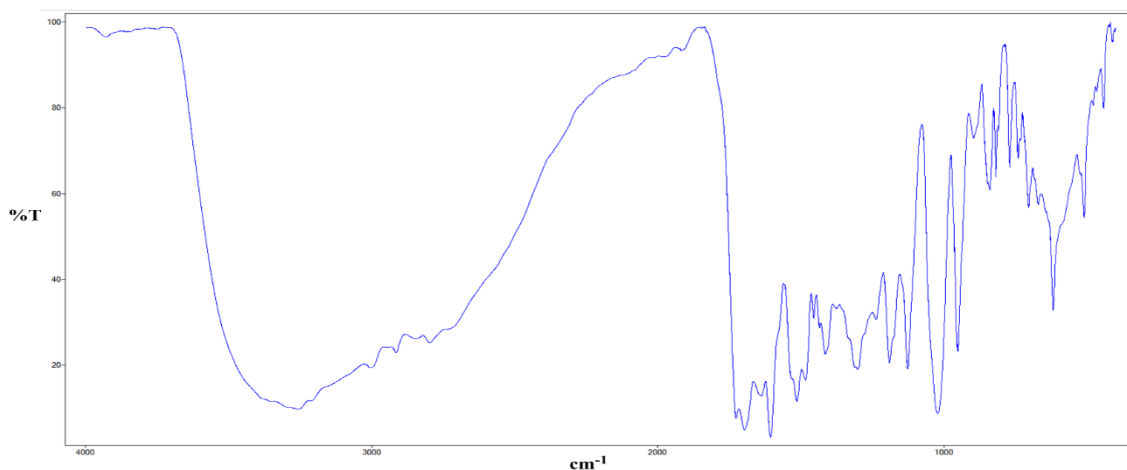
Yield: 0.08 g (55.89 %)

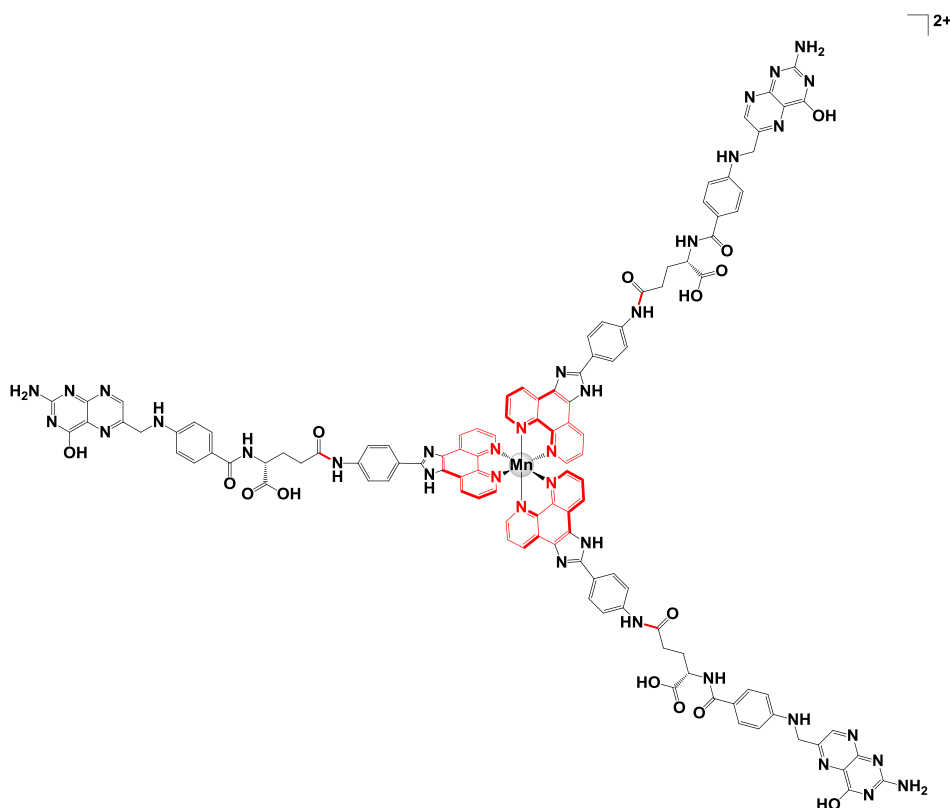
% Calculated: C, 51.63; H, 3.65; N, 19.01

% Found: C, 51.60; H, 3.68; N, 18.94

IR (KBr)  $\nu_{\text{max}}$ : 3254, 1727, 1698, 1607, 1514, 1484, 1455, 1415, 1301, 1191, 1127, 1021, 952, 840, 818, 771, 741, 705, 619, 510, 442.

IR (KBr):  $[\text{Cu}(\text{Im-phen-fol})_2](\text{ClO}_4)_2 \cdot 2\text{H}_2\text{O}$  (**76**)



2.12.2 Synthesis of  $[\text{Mn}(\text{Im-phen-foI})_3](\text{ClO}_4)_2 \cdot 2\text{H}_2\text{O}$  (**92**) (Novel complex)

0.02 g ( $5.53 \times 10^{-5}$  mol) of  $[\text{Mn}(\text{II})(\text{ClO}_4)_2] \cdot 6\text{H}_2\text{O}$  was dissolved in  $30 \text{ cm}^3$  of MeOH, to which 0.10 g ( $1.36 \times 10^{-4}$  mol) of Im-phen-foI (**45**) was added in one portion. The resulting yellow/orange coloured reaction mixture was allowed to stir at room temperature overnight before being filtered to produce an orange powder, this orange powder precipitate was then washed with cold MeOH and air dried.

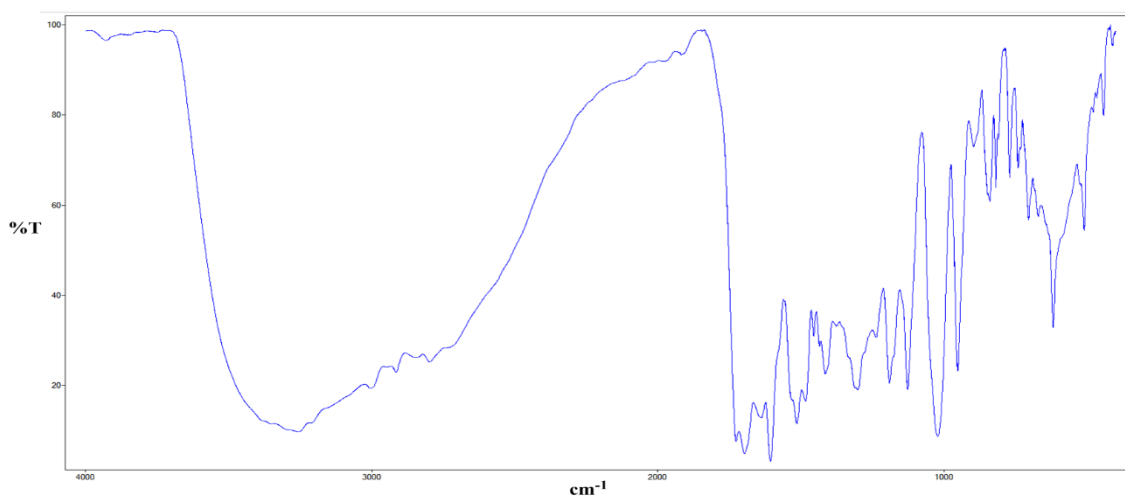
Complex formula weight (**92**) = 2494.04g/mol.

Yield: 0.04 g (29.02 %)

% Calculated: C, 54.90; H, 3.80; N, 20.22

% Found: C, 54.85; H, 3.88; N, 20.19

IR (KBr)  $\nu_{\text{max}}$ : 441, 511, 619, 670, 703, 740, 771, 818, 839, 952, 1022, 1127, 1191, 1240, 1303, 1416, 1456, 1484, 1514, 1606, 1641, 1697, 1728, 3256.

IR (KBr): [Mn(Im-phen-fol)<sub>3</sub>](ClO<sub>4</sub>)<sub>2</sub>·2H<sub>2</sub>O (92)

### 2.13 *In vitro* Antibacterial Testing.

The *in vitro* antibacterial activity of the compounds/complexes were investigated against pathogenic representatives of both Gram-positive bacteria and Gram negative bacteria. All bacteria were grown on nutrient broth agar plates at  $37 \pm 1^\circ\text{C}$  and maintained at  $4 \pm 1^\circ\text{C}$  for short term storage. Cultures were routinely sub-cultured every 4-6 weeks. The five different bacteria were grown overnight to the stationary phase in nutrient broth at  $37 \pm 1^\circ\text{C}$  and 2000 rpm. The cells were diluted to give an OD<sub>600</sub> = 0.05 for the plate and well diffusion assays. For the plate and well assay the bacteria were plated out on the agar plate using the above OD. The plates were incubated for 1 h at  $37 \pm 1^\circ\text{C}$ . For the plate assay the 10 polymer beads were placed on the plates in a circle. The plates were incubated for 1 h at  $37 \pm 1^\circ\text{C}$ , at which point 5 mm diameter holes were cut into the agar gel to create wells which were equally spaced. Test solutions/suspensions of selected compounds/complexes (**1**, **8-17**) and the prescription  $\beta$ -lactam antibiotic, Ampicillin (AMP), were added to the wells (50  $\mu\text{l}$  total volume) at three different concentrations (125, 50 and 5  $\mu\text{g}/\text{cm}^3$ ). The plates were incubated for 24 h at  $37 \pm 1^\circ\text{C}$ , and then the zones of inhibition around the wells were, measured in millimetres. To measure zones of inhibition (ZOI), the vertical and horizontal diameters, of the wells were measured in mm. The vertical and horizontal diameters the zone of inhibition itself were then measured. Then using the formula for the area of a circle,  $A = \pi r^2$  the area of the wells and the total area of inhibition were calculated. The area of the wells were subtracted from the total area of inhibition to give the area of the zone of inhibition.<sup>9</sup> For the negative control, a

petri dish containing only the bacterial culture inoculum was included in each incubation. The known  $\beta$ -lactam antibiotic, Ampicillin (AMP), was utilised as a positive kill control. All assays were performed in triplicate with three repetitions on separate occasions.

The minimum inhibitory concentration ( $MIC_{100}$ ) for all test compounds/complexes (**1**, **2**, **6-17**) and the prescription, antimycobacterial agent, Isoniazid (INH) (positive control), against two different strains of *Mycobacterium tuberculosis* (CDC1551 and ATCC 27294) were determined by the broth microdilution method using 96 well microassay plates. The MIC testing of the *M. tuberculosis* strain (CDC1551) was conducted by Dr. Ciaran Skerry in Dr. Petros Karakousis's Laboratory, Centre for Tuberculosis Research, Department of Medicine, Division of Infectious Diseases, Johns Hopkins School of Medicine, Baltimore, USA. The MIC testing of the second *M. tuberculosis* strain (ATCC 27294) was conducted by Professor Andre L.S. Santos and his group in the Department of General Microbiology, Federal University of Rio de Janeiro, Brazil.

#### **2.14 *In vitro* Antifungal Testing.**

The antifungal susceptibility MIC and MFC values for all test compounds/complexes against the filamentous fungi (*P. verrucosa*, *C. carrionii*, *E. dermatitidis*, *P. boydii*, *P. minutispora*, *S. aurantiacum* and *S. prolificans*) was conducted by Professor Andre L.S. Santos and his group in the Department of General Microbiology, Federal University of Rio de Janeiro, Brazil.

The test complexes or compounds (0.020 g) were dissolved in DMSO (1 cm<sup>3</sup>) and added to water (9 cm<sup>3</sup>) to give a stock solution (concentration 2000 mg/cm<sup>3</sup>). Complexes which displayed low solubility were tested as fine suspensions. A working solution was then prepared for each by taking 0.5 cm<sup>3</sup> of the stock solution (or suspension) and adding it to water (9.5 cm<sup>3</sup>) to give a solution with a concentration of 100  $\mu$ g/cm<sup>3</sup>. The maximum DMSO concentration in any test solution was 0.5% v/v, and at this level the DMSO does not inhibit the growth of the fungal cells.

The antifungal susceptibility MIC and MFC values for all test compounds/complexes against the aforementioned seven filamentous fungi were determined by broth microdilution according to CLSI method M38-A2 with an inoculum of  $2.5 \times 10^3$  CFU/cm<sup>3</sup>. The 96 well microassay plates were incubated at 35°C, and the optical density (OD) value

was determined at 540 nm after 48 hours.<sup>9b</sup> All assays were run in triplicate and on three independent occasions. The MIC<sub>100</sub> and MFC values were then determined and recorded as micrograms per millilitre or cubic centimetre ( $\mu\text{g}/\text{cm}^3$ ) and as micromolar ( $\mu\text{M}$ ) concentration of each test compound/complex.

The MIC results for all test complexes against *C. albicans* (ATTC 10231) were obtained in the Microbiology Laboratory, Department of Chemistry, Maynooth University. The antifungal susceptibility MIC values for all test compounds against the yeast *C. albicans* (ATTC 10231) were determined by broth microdilution according to CLSI method M27-A3.<sup>9a</sup> *C. albicans* was grown to the stationary phase overnight at 37°C on YEPD media. The cells were washed with PBS solution and resuspended in minimal media (MM) at a density of  $5 \times 10^5$  cells/cm<sup>3</sup>. The 96 well microassay round bottomed plates were covered with acetate foil (Sarstedt) to prevent dehydration and incubated at 37°C with continuous shaking for 24 hours. The optical density (OD) value was recorded after 24 hours for each well at 540 nm. All assays were run in triplicate and on three independent occasions. The MIC<sub>100</sub> values were then determined and recorded as micrograms per millilitre or cubic centimetre ( $\mu\text{g}/\text{cm}^3$ ) and as micromolar ( $\mu\text{M}$ ) concentration of each test compound/complex.

### 2.15 *In vivo* Galleria mellonella Experiments.

**Galleria Mellonella toxicity.** *Galleria mellonella* larvae in the 6th developmental stage were used to determine the *in vivo* cytotoxicity of the complexes **1, 2, 6-96** and cisplatin.<sup>10</sup> Thirty healthy larvae between 0.200-0.400 g in weight with no cuticle discolouration were used for each experiment. Fresh solutions of the test complexes were prepared immediately prior to testing under sterile conditions. Each of the tested compounds (0.05 g) were dissolved in DMSO (1 cm<sup>3</sup>) and added to sterile water (9 cm<sup>3</sup>) to give a stock solution (5000  $\mu\text{g}/\text{cm}^3$ ). Each compound was tested across the range; 5000  $\mu\text{g}/\text{cm}^3$  - 200  $\mu\text{g}/\text{cm}^3$ . Test solutions (20  $\mu\text{L}$ ) were administered to the larvae by injection directly into the haemocoel through the last pro-leg. The base of the pro-leg can be opened by applying gentle pressure to the sides of the larvae and this aperture will re-seal after removal of the syringe without leaving a scar. Larvae were placed in sterile Petri dishes and incubated at 30°C for 72 h.



The survival of the larvae was monitored every 24 h. Death was assessed by the lack of movement in response to stimulus together with discolouration of the cuticle. Three controls were employed in all assays. The first consisted of untouched larvae maintained at the same temperature as the test larvae. The second was larvae with the pro-leg pierced with an inoculation needle but no solution injected. The third control was larvae that were inoculated with 20  $\mu\text{L}$  of sterile water.

### 2.16 *In vivo* Antifungal Screening

*G. mellonella* larvae in the 6th developmental stage were used to determine the *in vivo* antimicrobial activity of the test complexes (**13-17**).<sup>11</sup> Ten healthy larvae between 0.200-0.400 g in weight with no cuticle discolouration were used for each experiment. Fresh solutions of complexes were prepared immediately prior to testing. Complexes (0.020 g) were dissolved in DMSO (1 cm<sup>3</sup>) and added to water (9 cm<sup>3</sup>) to give a stock solution (concentration 2000  $\mu\text{g}/\text{cm}^3$ ). The test compounds (**13-17**), along with silver acetate ( $\text{Ag}(\text{CH}_3\text{COO})$ ) and the clinical antifungal agent Ketoconazole (KTC) (used as reference standards), were screened at two concentrations; 100  $\mu\text{g}/\text{cm}^3$  and 50  $\mu\text{g}/\text{cm}^3$ . *C. albicans* was grown to the stationary phase in YEPD media at 37 °C for 24 h. The cell concentration was assessed using a haemocytometer following a dilution of the culture in PBS. The cells were washed three times with PBS and resuspended in sterile PBS following harvesting by centrifugation at 4000 rpm for 10 min to yield a concentration of  $1 \times 10^8$  cell  $\text{cm}^{-3}$ .

Two treatments were employed in the screening of the test solutions. In each case, four controls were employed in all assays along with a reference. The first control consisted of untouched larvae maintained at the same temperature as the test larvae (negative control). The second was larvae with the pro-leg pierced with an inoculation needle but no substance injected into them. The third control was larvae that were inoculated with 20  $\mu\text{l}$  of the same sterile water used to make the test solutions, and the fourth is larvae inoculated with the same sterile PBS solution that was used to wash and make the *C. albicans* suspension. The positive control was larvae inoculated with *C. albicans* but no test solution was administered to them.

### 2.16.1 Prophylactic Treatment

The test solution (20 µl) was administered to the larvae by injection directly into the haemocoel through the last pro-leg.<sup>12</sup> Larvae were then placed in sterile petri dishes and incubated at 30 °C for 1 h, after which time they were inoculated with 20 µl of the *C. albicans* suspension ( $2 \times 10^6$  cells). The larvae were incubated at 30 °C for 72 h and their survival was monitored every 24 h.

### 2.16.2 Treatment of Infection

Larvae were inoculated with 20 µl of the *C. albicans* suspension ( $2 \times 10^6$  cells) by injection directly into the haemocoel through the last pro-leg.<sup>12</sup> Larvae were then placed in sterile petri dishes and incubated at 30 °C for 1 h, after which time the test solution (20 µl) was administered by injection. The larvae were incubated at 30 °C for 72 h and larvae survival was monitored every 24 h.

### 2.17 In vitro Anticancer Screening.

**Cell culture.** For cytotoxicity evaluation HT29 (ATCC, USA), MCF-7 (ATCC, USA), SK-OV-3 (ATCC, USA), DU145 (ATCC, USA), A549 (ATCC, USA) and Vero (ATCC, USA) cell lines were employed; all the cell lines were grown in RPMI 1640 media (Fischer). All media were supplemented with 10% foetal bovine serum (FBS) and 45 IU/ml penicillin and 45 g/ml streptomycin and cells were maintained at 37°C in a 5% CO<sub>2</sub> humidified incubator. Test Sample Preparation. For sterilisation samples were filtered with a 0.2 micron cellulose acetate filter. For cytotoxicological evaluation all samples were prepared fresh on the day of exposure. A stock concentration of test compound was prepared in the exposure media (10% DMEM F-12) necessary for the cell line under test. This sample was vortexed to ensure a uniform dispersion of the compound under test. MTT Assay. This method is based on the reduction of the tetrazolium salt, methylthiazolyldiphenyl-tetrazolium bromide (MTT) into a crystalline blue formazan product by the cellular oxidoreductases of viable cells.<sup>13</sup> The resultant formazan crystal formation is proportional to the number of viable cells. For the cytotoxicity assays cells were seeded in 96-well microplates (Nunc, Denmark) at a density of  $1 \times 10^5$  cells/ml for the 24 h test. This density were found to be optimal to achieve the desired confluence at the end of the exposure period. Six replicate wells were used for each control and test

concentration per microplate. Following the desired time of compound exposure, control medium or test exposures were removed, cells were then rinsed with PBS and 100  $\mu\text{L}$  of fresh medium (without FBS or supplements) was added to each well. 10  $\mu\text{L}$  of MTT (5 mg/mL) prepared in PBS was then added to each well and the plates were incubated for 3 h at 37 °C in a 5% CO<sub>2</sub> humidified incubator. After this incubation period the medium was discarded, the cells were washed with 100  $\mu\text{L}$  of PBS and 100  $\mu\text{L}$  of DMSO was added to each well to extract the dye. The plate was shaken at 240 rpm for 10 min and the absorbance was measured at 570 nm.

**Data Analysis.** At least three independent experiments were conducted in triplicate for each cell line and toxicity endpoint. Test results for each test were expressed as percentage of the unexposed control  $\pm$  standard deviation (SD). Control values were set as 100%. Differences between samples and the control were evaluated using the statistical analysis package SPSS 14.0. Statistically significant differences were set at  $p \leq 0.05$ . One-way analysis of variances (ANOVA) followed by Dunnett's multiple comparison tests were carried out for normally distributed samples with homogeneous variances. The average cytotoxicity data obtained and its associated SD was then fitted to a sigmoidal curve and a four parameter logistic model used to calculate the IC<sub>50</sub> values for each test sample at various time points, which was the concentration of tested compound which caused a 50% cellular lethality in comparison to untreated controls. The IC<sub>50</sub> values are reported  $\pm$  95 % Confidence Intervals ( $\pm$  95% CI).

The IC<sub>50</sub> testing for the A549 and Vero cell lines was conducted by Professor Andre L.S. Santos and his group in the Department of General Microbiology, Federal University of Rio de Janeiro, Brazil. The IC<sub>50</sub> testing for the HT29, SK-OV-3, MCF-7 and DU145 was conducted by Dr. Alan Casey in the inorganic pharmaceutical and biomimetic research centre, Focas Research Institute, Dublin Institute of Technology, Camden Row, Dublin, 8, Ireland.

## **2.18 DNA Interaction Studies.**

### **2.18.1 DNA cleavage experiments.**

**Nuclease Activity:** Reactions were carried out according to the following general procedure; in a total volume of 20  $\mu\text{L}$  using 80 mM HEPES buffer (pH = 7.2) with 20

mM NaCl, 5  $\mu$ M of complex, (test samples were initially prepared in DMF, then diluted in buffer), with 400ng of pBR322 DNA (Roche).<sup>10, 14</sup> Samples were incubated at 37 °C. Quench buffer (4  $\mu$ L; 10mM Tris-HCl (pH 7.6), 0.03% bromophenol blue, 0.03% xylene cyanol, 60% glycerol and 60mM EDTA) was then added and samples were loaded onto agarose gel (1%) containing 2  $\mu$ L of GelRed<sup>TM</sup> (10,000X) solution. Electrophoresis was completed at 80 V for 1.5 h in 1XTAE buffer.

### Experiments were carried out as follows

(A) 30 minute incubation with 1mM added Na-L-ascorbate reductant, lane 1: DNA alone; lane 2: Control 1 Copper(II) acetate, lane 3: Control 2 {Cu(phen)<sub>2</sub>}<sup>2+</sup>, lanes 4-10: 5  $\mu$ M of complexes **54-60**.

(B) 30 minute incubation with 1mM added H<sub>2</sub>O<sub>2</sub> oxidant, lane 1: DNA alone; lane 2: Control 1 Copper(II) acetate, lane 3: Control 2 {Cu(phen)<sub>2</sub>}<sup>2+</sup>, lanes 4-10: 5  $\mu$ M of complexes **54-60**.

(C) 30 minute incubation with 1mM added Na-L-ascorbate reductant and 80  $\mu$ M EDTA, lane 1: DNA alone; lane 2: Control 1 Copper(II) acetate, lane 3: Control 2 {Cu(phen)<sub>2</sub>}<sup>2+</sup>, lanes 4-10: 5  $\mu$ M of complexes **54-60**.

(D) 30 minute incubation with 1mM added H<sub>2</sub>O<sub>2</sub> oxidant and 80  $\mu$ M EDTA, lane 1: DNA alone; lane 2: Control 1 Copper(II) acetate, lane 3: Control 2 {Cu(phen)<sub>2</sub>}<sup>2+</sup>, lanes 4-10: 5  $\mu$ M of complexes **54-60**.

### 2.19 References

1. Devereux, M.; McCann, M.; Leon, V.; Geraghty, M.; McKee, V.; Wikaira, J., Synthesis and biological activity of manganese (II) complexes of phthalic and isophthalic acid: X-ray crystal structures of [Mn(ph)(phen)<sub>2</sub>(H<sub>2</sub>O)]•4H<sub>2</sub>O, [Mn(phen)<sub>2</sub>(H<sub>2</sub>O)<sub>2</sub>](Isoph)<sub>2</sub>(phen)•12H<sub>2</sub>O and {[Mn(isoph)(bipy)]<sub>4</sub>•2.75bipy}<sub>n</sub> (phH<sub>2</sub> = phthalic acid; isoph = isophthalic acid; phen = 1,10-phenanthroline; bipy = 2,2-bipyridine) *Metal-Based Drugs* **2000**, *7* (5), 275-288. 10.1155/mbd.2000.275
2. Casey, M. T.; McCann, M.; Devereux, M.; Curran, M.; Cardin, C.; Convery, M.; Quillet, V.; Harding, C., Synthesis and structure of the Mn<sup>II,III</sup> complex salt

- $[\text{Mn}_2(\eta^1\eta^1\mu_2\text{-oda})(\text{phen})_4(\text{H}_2\text{O})_2][\text{Mn}_2(\eta^1\eta^1\mu_2\text{-oda})(\text{phen})_4(\eta^1\text{-oda})_2]\cdot 4\text{H}_2\text{O}$   
(odaH<sub>2</sub> = octanedioic acid); a Catalyst for H<sub>2</sub>O<sub>2</sub> Disproportionation *Journal of the Chemical Society-Chemical Communications* **1994**, (22), 2643-2645. 10.1039/c39940002643
- Devereux, M.; McCann, M.; Cronin, J. F.; Ferguson, G.; McKee, V., Binuclear and polymeric copper(II) dicarboxylate complexes: syntheses and crystal structures of  $[\text{Cu}_2(\text{pda})(\text{Phen})_4](\text{ClO}_4)_2\cdot 5\text{H}_2\text{O}\cdot \text{C}_2\text{H}_5\text{OH}$ ,  $[\text{Cu}_2(\text{oda})(\text{Phen})_4](\text{ClO}_4)_2\cdot 2.67\text{H}_2\text{O}\cdot \text{C}_2\text{H}_5\text{OH}$  and  $\{[\text{Cu}_2(\text{pda})_2(\text{NH}_3)_4(\text{H}_2\text{O})_2]\cdot 4\text{H}_2\text{O}\}_n$  (odaH<sub>2</sub>=octanedioic acid; pdaH<sub>2</sub>=pentanedioic acid; Phen=1,10-phenanthroline). *Polyhedron* **1999**, 18 (16), 2141-2148. 10.1016/s0277-5387(99)00100-x
  - McCann, S.; McCann, M.; Casey, M. T.; Devereux, M.; McKee, V.; McMichael, P.; McCrea, J. G., Manganese(II) complexes of 3,6,9-trioxaundecanedioic acid (3,6,9-tddaH<sub>2</sub>): X-ray crystal structures of  $[\text{Mn}(3,6,9\text{-tdda})(\text{H}_2\text{O})_2]\cdot 2\text{H}_2\text{O}$  and  $\{[\text{Mn}(3,6,9\text{-tdda})(\text{phen})_2\cdot 3\text{H}_2\text{O}]\cdot \text{EtOH}\}_n$ . *Polyhedron* **1997**, 16 (24), 4247-4252. 10.1016/s0277-5387(97)00233-7
  - Zheng, R. H.; Guo, H. C.; Jiang, H. J.; Xu, K. H.; Liu, B. B.; Sun, W. L.; Shen, Z. Q., A new and convenient synthesis of phendiones oxidated by KBrO<sub>3</sub>/H<sub>2</sub>SO<sub>4</sub> at room temperature. *Chinese Chemical Letters* **2010**, 21 (11), 1270-1272. 10.1016/j.ccllet.2010.05.030
  - (a) Garas, A. M. S.; Vagg, R. S., Synthesis of some novel derivatives of 1,10-phenanthroline. *Journal of Heterocyclic Chemistry* **2000**, 37 (1), 151-158. ; (b) Margiotta, N.; Bertolasi, V.; Capitelli, F.; Maresca, L.; Moliterni, A. G. G.; Vizza, F.; Natile, G., Influence of steric and electronic factors in the stabilization of five-coordinate ethylene complexes of platinum(II): X-ray crystal structure of PtCl<sub>2</sub>(2,9-dimethyl-1,10-phenanthroline-5,6-dione). *Inorganica Chimica Acta* **2004**, 357 (1), 149-158. 10.1016/s0020-1693(03)00382-7
  - (a) Eseola, A. O.; Li, W.; Sun, W. H.; Zhang, M.; Xiao, L. W.; Woods, J. A. O., Luminescent properties of some imidazole and oxazole based heterocycles Synthesis, structure and substituent effects. *Dyes and Pigments* **2011**, 88 (3), 262-273. 10.1016/j.dyepig.2010.07.005; (b) Obi-Egbedi, N. O.; Obot, I. B.; Eseola, A. O., Synthesis, characterization and corrosion inhibition efficiency of 2-(6-methylpyridin-2-yl)-1H-imidazo 4,5-f 1,10 phenanthroline on mild steel in

- sulphuric acid. *Arabian Journal of Chemistry* **2014**, 7 (2), 197-207. 10.1016/j.arabjc.2010.10.025
8. Dewar, M. J. S.; Mole, T., Palladised charcoal as a catalyst for the reduction of aromatic nitro-compounds by Hydrazine Hydrate. *Journal of the Chemical Society* **1956**, (JUL), 2556-2557.
  9. (a) Institute., C. a. L. S., M27-A3 Reference method for broth dilution antifungal susceptibility testing of yeasts: approved standard, third edition. 3rd ed.; Clinical and Laboratory Standards Institute: Clinical and Laboratory Standards Institute, Wayne, PA, USA., 2008; Vol. 28. ; (b) Institute., C. a. L. S., M38-A2 Reference Method for Broth Dilution Antifungal Susceptibility Testing of Filamentous Fungi; Approved Standard, Second Edition. Clinical and Laboratory Standards Institute. 2008.: Clinical and Laboratory Standards Institute, Wayne, PA, USA., 2008; Vol. 28.
  10. Kellett, A.; O'Connor, M.; McCann, M.; Howe, O.; Casey, A.; McCarron, P.; Kavanagh, K.; McNamara, M.; Kennedy, S.; May, D. D.; Skell, P. S.; O'Shea, D.; Devereux, M., Water-soluble bis(1,10-phenanthroline) octanedioate  $\text{Cu}^{2+}$  and  $\text{Mn}^{2+}$  complexes with unprecedented nano and picomolar in vitro cytotoxicity: promising leads for chemotherapeutic drug development. *MedChemComm* **2011**, 2 (7), 579. 10.1039/c0md00266f
  11. (a) Desbois, A. P.; Coote, P. J., Utility of Greater Wax Moth Larva (*Galleria mellonella*) for Evaluating the Toxicity and Efficacy of New Antimicrobial Agents. In *Advances in Applied Microbiology, Vol 78*, Laskin, A. I.; Sariaslani, S.; Gadd, G. M., Eds. Elsevier Academic Press Inc: San Diego, 2012; Vol. 78, pp 25-53. 10.1016/b978-0-12-394805-2.00002-6; (b) Kavanagh, K.; Reeves, E. P., Exploiting the potential of insects for in vivo pathogenicity testing of microbial pathogens. *Fems Microbiology Reviews* **2004**, 28 (1), 101-112. 10.1016/j.femsre.2003.09.002
  12. McCann, M.; Curran, R.; Ben-Shoshan, M.; McKee, V.; Tahir, A. A.; Devereux, M.; Kavanagh, K.; Creaven, B. S.; Kellett, A., Silver(I) complexes of 9-anthracenecarboxylic acid and imidazoles: synthesis, structure and antimicrobial activity. *Dalton Trans* **2012**, 41 (21), 6516-6527. 10.1039/c2dt12166b
  13. (a) Marshall, N. J.; Goodwin, C. J.; Holt, S. J., A critical assessment of the use of microculture tetrazolium assays to measure cell growth and function. *Growth Regul* **1995**, 5 (2), 69-84. ; (b) Scudiero, D. A.; Shoemaker, R. H.; Paull, K. D.;

- Monks, A.; Tierney, S.; Nofziger, T. H.; Currens, M. J.; Seniff, D.; Boyd, M. R., Evaluation of a soluble tetrazolium/formazan assay for cell growth and drug sensitivity in culture using human and other tumor cell lines. *Cancer Res* **1988**, *48* (17), 4827-4833.
14. (a) Kellett, A.; Howe, O.; O'Connor, M.; McCann, M.; Creaven, B. S.; McClean, S.; Kia, A. F. A.; Casey, A.; Devereux, M., Radical-induced DNA damage by cytotoxic square-planar copper(II) complexes incorporating o-phthalate and 1,10-phenanthroline or 2,2'-dipyridyl. *Free Radical Biology and Medicine* **2012**, *53* (3), 564-576. 10.1016/j.freeradbiomed.2012.05.034; (b) Kellett, A.; O'Connor, M.; McCann, M.; McNamara, M.; Lynch, P.; Rosair, G.; McKee, V.; Creaven, B.; Walsh, M.; McClean, S.; Foltyn, A.; O'Shea, D.; Howe, O.; Devereux, M., Bis-phenanthroline copper(II) phthalate complexes are potent in vitro antitumour agents with 'self-activating' metallo-nuclease and DNA binding properties. *Dalton Trans* **2011**, *40* (5), 1024-1027. 10.1039/c0dt01607a; (c) McCann, M.; McGinley, J.; Ni, K.; O'Connor, M.; Kavanagh, K.; McKee, V.; Colleran, J.; Devereux, M.; Gathergood, N.; Barron, N.; Prisecaru, A.; Kellett, A., A new phenanthroline-oxazine ligand: synthesis, coordination chemistry and atypical DNA binding interaction. *Chem Commun (Camb)* **2013**, *49* (23), 2341-2343. 10.1039/c3cc38710k

# **Chapter 3**

## **Antifungal activities of the metal complexes**



### 3.1 Fungi

Mycologists in the past debated for years as to the exact set of characteristics to apply to an organism so that it could be classified as a Fungus. Using modern DNA sequencing techniques, it is now known that all known fungi belong to about 10 phyla and are members of a monophyletic kingdom, i.e. that they all share a common ancestral origin. It was recently (2011) estimated, based on high-throughput sequencing methods, that there may be as many as 5.1 million fungal species, while only approximately 2% (99,000) of these currently have formal classifications.<sup>1</sup>

Fungi are ubiquitous in nature, being found in numerous different types of environments and are the major decomposers in certain ecosystems and essential associates of many organisms.<sup>1-2</sup> They are heterotrophic, essentially aerobic (with limited anaerobic capacity), eukaryotic microorganisms. Fungi possess a cell wall comprised of chitin, plasma membranes containing ergosterol (a sterol unique to fungi and serving the same purpose as cholesterol in animals) and microtubules composed of tubulin (Figure 3.1). They grow as yeasts, molds or a combination of both (dimorphism).<sup>2</sup>

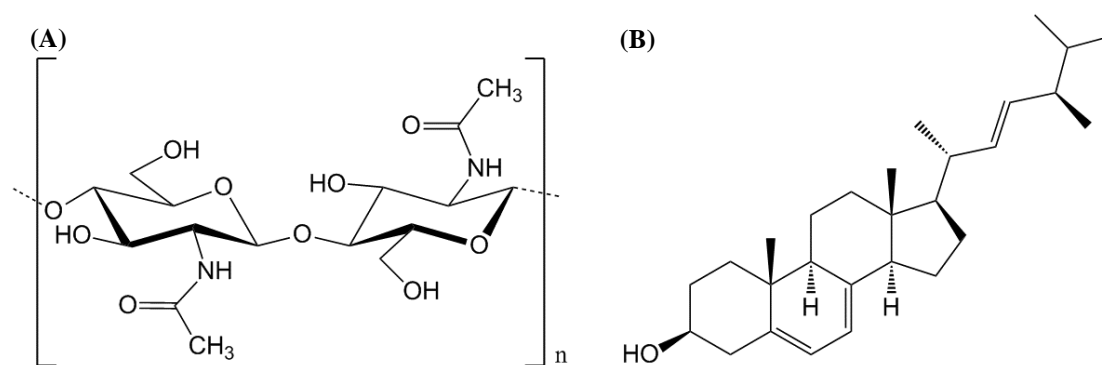


**Fig. 3.1:** (A) Structure of chitin component of fungal cell walls - monomer unit composed of two *N*-acetylglucosamine units that repeat to form long chains with  $\beta$ -1,4 linkage. (B) Ergosterol structure - main component in fungal plasma membranes.<sup>2</sup>

Certain fungi are capable of physiological and morphological conversion from one phenotype to another and this is called dimorphism. This can occur when such fungi change from one environment to another. Various factors within a host control the dimorphism, such as amino acids, temperature, carbohydrates and trace elements (e.g. zinc). Most pathogenic fungi change from a hyphal form into a yeast-like form (or

spherule) in tissue. However, the dimorphism in *Candida albicans* follows the opposite trend, transforming from budding yeast-like structures (blastoconidia) to filamentous structures developing pseudohyphae and hyphae also known as germ tubes (often associated with the formation of a biofilm) (Figure 3.2).<sup>2</sup> These fungal hyphae have the ability to penetrate host cells, the epithelial layer and mucous membranes therefore invading the bloodstream/organs and spreading through the body causing disseminated candidiasis.

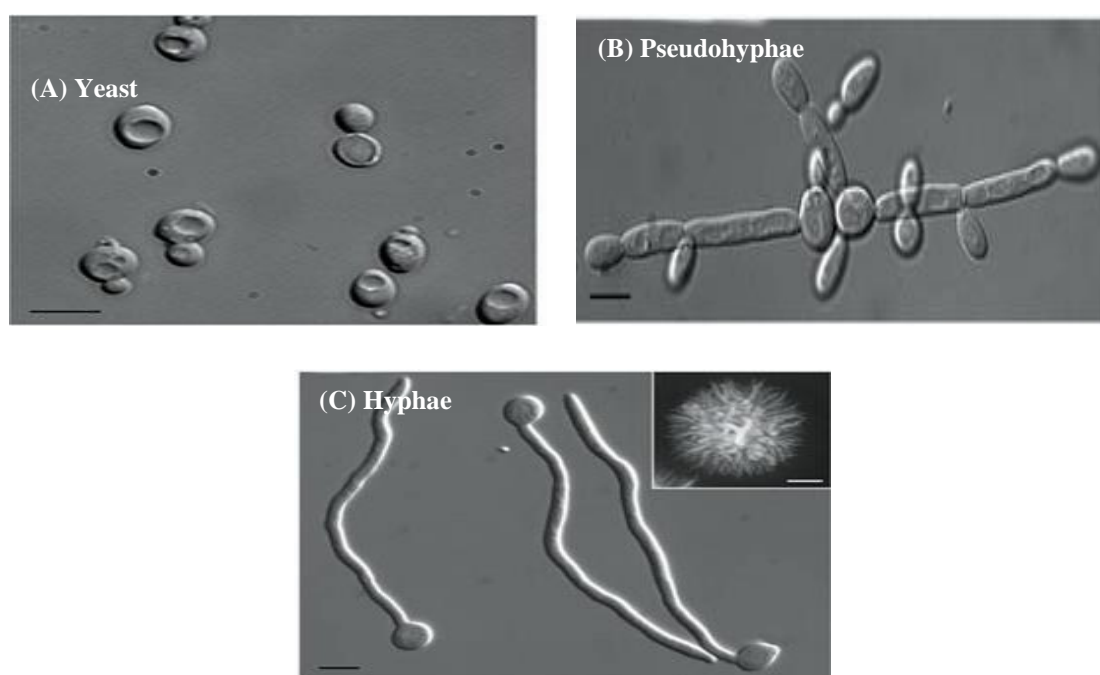


**Fig. 3.2:** *C. albicans* that has been grown for 5 days on Spider medium. (A) Yeast form, (B) pseudohyphal form and (C) true hyphal colony formation. Scale bars in the main panels represent 5  $\mu\text{m}$ , and in the inset on the hyphae panel 1 mm.<sup>3</sup>

Fungi are extremely versatile and adaptable organisms and exist as symbionts with numerous animals, plants and other fungi. In addition to this, many fungi are parasites to plants, animals, humans and other fungi.<sup>4</sup>

Fungi have a complex and fascinating relationship with plants and more importantly, in the context of this chapter, with mankind, possessing the abilities to be saviours, servants and slayers of human beings. Although most known species of fungi have proven either extremely useful or harmless to mankind there are other species that are pathogenic (ca. 300 species) to humans.<sup>4-5</sup> Most fungi in the environment have evolved to be free-living

and although some species are truly pathogenic to healthy immunocompetent humans, usually the infections that fungi cause are opportunistic in nature and therefore specific traits that confer fungal pathogenesis are often difficult to identify.<sup>6</sup>

### 3.2 Fungal infections and etiological species

There are six genus which are referred to as the primary pathogenic and opportunistic fungal pathogens, namely the *Candida*, *Aspergillus*, *Cryptococcus*, *Histoplasma*, *Pneumocystis* and *Stachybotrys* species.<sup>7</sup> These particular fungi can cause a vast array of fungal infections or mycoses and cover a wide spectrum of maladies from superficial infections of the outermost stratum of the skin to systemic infections which involve the brain, heart, lungs, liver, spleen and kidneys. Fungal infections can be broadly separated into four classes based on the site of infection, route of acquisition, and type of virulence; (a) superficial, (b) cutaneous, (c) subcutaneous and (d) systemic infections.<sup>8</sup>

Superficial mycoses are limited to the *stratum corneum* of the epidermis (outermost layer of the skin) and hair and are normally the most benign of the four classes (Figure 3.3).



**Fig. 3.3:** Tinea cruris (superficial mycosis of the skin,) etiologic agents are the anthropophilic dermatophytes.<sup>9</sup>

Superficial mycosis of the skin, tinea cruris (also known as jock itch): the most common etiologic agents for tinea cruris are the anthropophilic dermatophytes, *Trichophyton rubrum* and *Epidermophyton floccosum*.<sup>8</sup>

Tinea corporis (also called ringworm), infects areas of skin not normally covered by hair and results in unbearable itching and produces intricate circular patterns or rings of

infected scaled skin (Figure 3.4).<sup>5</sup> If left untreated, it will cover the entire body. Although distressful and somewhat disfiguring, these infections are rarely life-threatening.

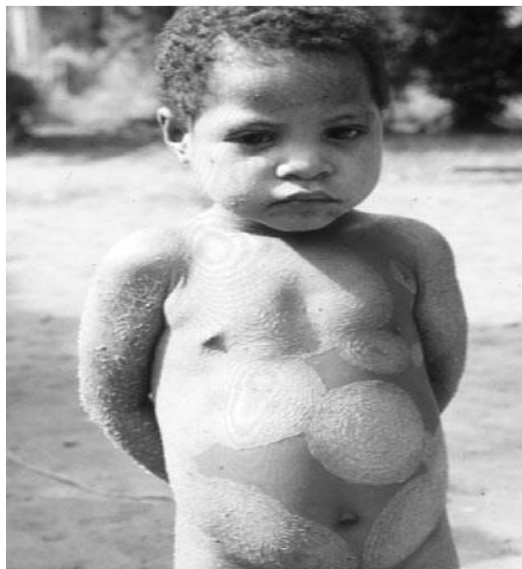


**Fig. 3.4:** Tinea corporis infection (ringworm), these mycoses are caused by various fungi but most commonly the dermatophytes. Photographed in Papua New Guinea by Johannes Mattar.<sup>5</sup>

Mycoses of the nails (tinea unguium or onychomycosis) can prove very difficult to treat, particularly those of the toenails, due to the underlying infection being present in the nail bed, requiring months of treatment and the use of both oral and topical antifungal medications (Figure 3.5). These infections are caused by three types of fungi, namely dermatophytes (*Trichophyton rubrum*), yeasts (*C. albicans*) and molds (*Scopulariopsis brevicaulis*, *Fusarium* and *Aspergillus* spp.).<sup>10</sup>

Subcutaneous mycoses are infections that involve the dermis, subcutaneous tissues, muscle and fascia. There are three general types of subcutaneous mycoses; chromoblastomycosis, mycetoma and sporotrichosis. The main culprits for these infections are molds or dematiaceous fungi. They also can follow after some sort of trauma which implants the causative fungi under the skin or exposes the subcutaneous tissue to infection.<sup>8</sup>

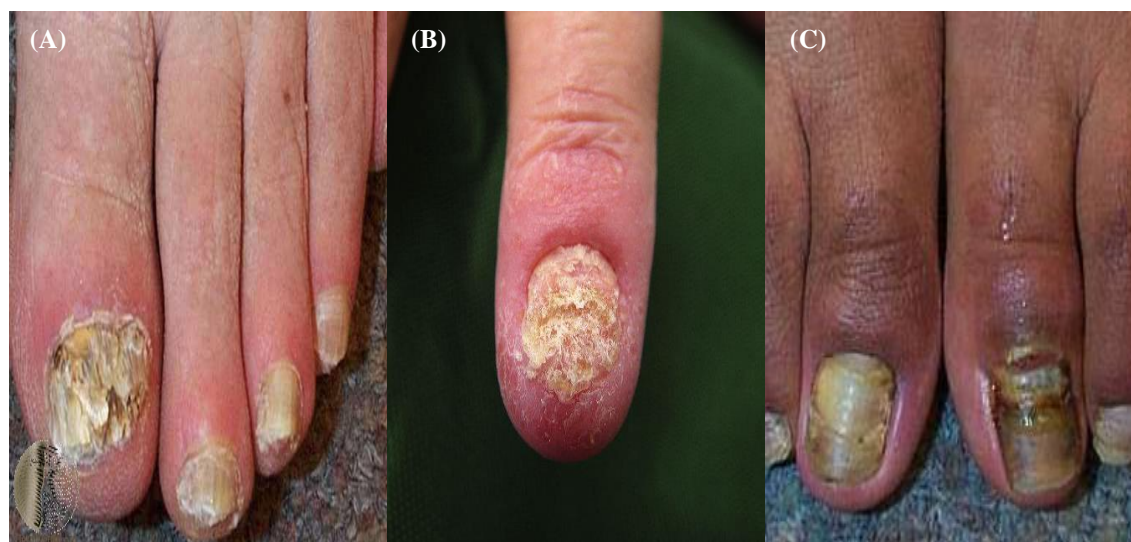


**Fig. 3.5:** Tinea unguium/Onychomycosis - fungal infections of the nail. (A) Onychomycosis caused by the dermatophyte *Trichophyton rubrum*, (B) onychomycosis caused by the yeast *C. albicans* and (C) onychomycosis caused by a mold, *Aspergillus* species.<sup>11</sup>

Chromoblastomycosis (CBM), also called *Verrucous dermatitis*, is a chronic subcutaneous mycosis which induces hyperplasia, and lesions slowly begin to develop around the site of implantation of the fungi (usually the extremities). Characteristic verrucose, crusted, rough, warty nodules form and these may be raised 1-3 cm above the skin surface, and are often said to resemble florets of cauliflower (Figure 3.6).<sup>12</sup>

The etiological fungal agents for this mycosis are most commonly *Fonsecaea* spp., *Phialophora verrucosa*, *Cladophialophora carrionii* and *Rhinocladiella aquaspersa*. Chromoblastomycosis occurs around the world, but is most commonly encountered in rural workers and farm labourers especially in tropical or subtropical climates. Although chromoblastomycosis (CBM) often presents in people who are immunosuppressed it is also often seen in healthy individuals. It is very resistant to treatment; requiring pharmacotherapy (systemic antifungals such as Itraconazole (ITC), Fluconazole (FLC), Ketoconazole (KTC), Voriconazole (VRC) Fluorocytosine (5FC), Terbinafine, Casopofungin (CFG), Micafungin (MFG), Amphotericin B (AMB), see Chapter 1), thermotherapy (cryotherapy, heat therapy) and surgical removal of the lesions by means of wide and deep excision.

Associated complications of this mycosis are secondary bacterial infection, ulceration, development of elephantiasis and myiasis (parasitic infestation by fly larvae/maggots).



In rare incidences, malignant transformations (squamous cell carcinoma) of chromoblastomycosis have been documented. Although rare chromoblastomycosis can spread to other tissues/organs and can potentially spread to the brain becoming life-threatening. This is a particularly significant mycosis due to its disfiguring nature, requirement for long term treatment and the emergence of resistant etiological fungal species.<sup>12</sup>



**Fig. 3.6:** (A) Chromoblastomycosis of the hand, (B) severe chromoblastomycosis of the leg after several years of infection.<sup>13</sup>

Mycetomas are infections which result in chronic inflammation and are caused by two distinct pathogens, either moulds or filamentous bacteria called Actinomycetales belonging to an order of Actinobacteria. Infections of fungal origin are referred to as eumycetomas while those of bacterial origin are termed as actinomycetomas. Eumycetomas affect mainly the extremities especially the feet which is the site of infection in two thirds of cases, also the hands, abdomen, chest, neck and the head.<sup>14</sup> Eumycetomas of the feet are commonly known as Madura foot (Figure 3.7). This mycosis normally presents with suppurative granulomas/tumefaction (swellings which are comprised of macrophages), sinuses and the expulsion of black granules from these sinuses which are fungal colonies (Figure 3.7).

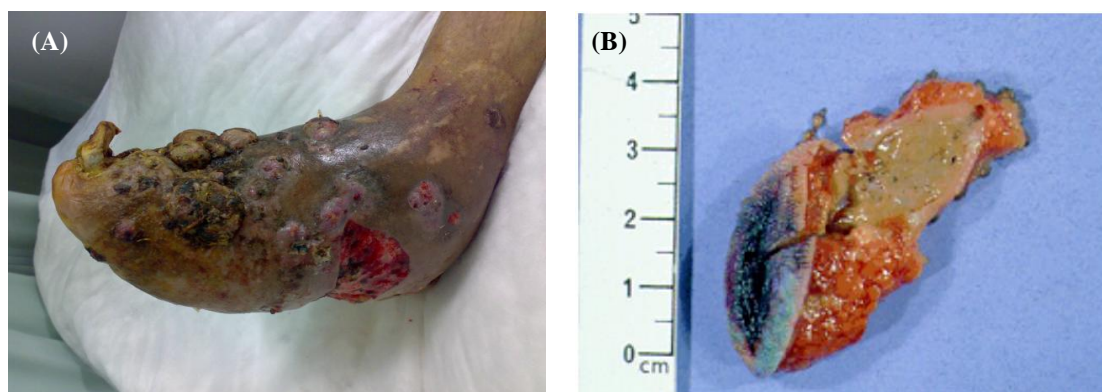


**Fig. 3.7:** (A) *Mycetoma pedis* (eumycetoma of the foot) also known as Madura foot.<sup>15</sup> (B) Excised eumycetoma containing sinus showing black grains.<sup>14b</sup>

The infection is usually caused by the implantation of the etiological fungi into the subcutaneous tissue by a thorn or a piece of wood. The known etiological fungi are *Scedosporium*, *Pseudallescheria*, *Madurella*, *Fusarium*, *Aspergillus* and others. The infection slowly spreads producing nodules on the surface which discharge a viscous serosanguinous fluid containing black, grain-like fungal colonies. It can result in considerable deformity via its ability to invade surrounding tissue, including bone.<sup>14, 16</sup> There are a large number of cases reported but they are limited to the tropics and subtropics, mainly Africa, India and the Central and South Americas. The only treatment, until recently was surgical removal of the infected area (amputation) but the antifungal azole drugs, Itraconazole (ITC) and Ketoconazole (KTC) are known to be effective.<sup>16</sup>

Candidiasis is another sub-type of fungal infection/mycosis and encompasses superficial, cutaneous, subcutaneous and systemic fungal infections. Here, we are referring to Candidiasis of the mucous membranes (oral cavity/mouth, vagina) caused by the *Candida* spp. (most commonly by *C. albicans*), resulting in pain, discomfort and inflammation of the affected areas. Oral candidiasis, commonly known as thrush, can occur in new born infants, the elderly and people with an impaired immune response (Figure 3.8). It is often one of the earliest and sometimes the initial manifestations of human immunodeficiency virus infection / acquired immunodeficiency syndrome (HIV/AIDS).<sup>17</sup>

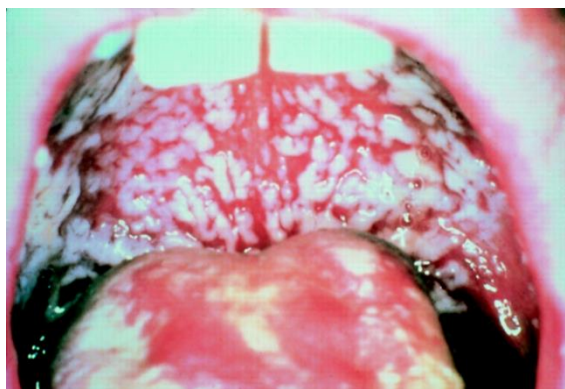


**Fig. 3.8:** Oral candidiasis (thrush) can occur in new born infants, the elderly and people with an impaired immune response.<sup>17-18</sup>

Systemic (deep) mycoses are caused by the primary pathogenic and opportunistic fungal pathogens. The primary pathogenic fungi are comprised of the *Coccidioides immitis*, *Histoplasma capsulatum*, *Blastomyces dermatitidis* and *Paracoccidioides brasiliensis* fungi and are able to establish infection in a normal healthy host. The mode of infection for these primary fungal pathogens is via the respiratory tract of the host. The opportunistic pathogens, which include *Cryptococcus neoformans*, *Candida* spp., *Aspergillus* spp., *Penicillium marneffeii* (the only *Penicillium* species which is a human pathogen), the Zygomycetes, *Trichosporon beigeli* and *Fusarium* spp. generally require an immunosuppressed host in order to establish infection. Both diseases and their therapies can result in immunosuppression, and include cancer and anticancer treatments, organ transplantation and associated antirejection medications, surgery, tuberculosis (TB), those with autoimmune diseases and associated medications i.e. corticosteroids, and those with AIDS. Invasion by the opportunistic fungi, resulting in systemic infections, is usually via the respiratory tract, alimentary tract, or intravascular devices/catheters.<sup>8, 19</sup>

Phaeohyphomycosis (PHM) is group of fungal infections which affects humans and lower animals caused by a number of dematiaceous fungi (brown/black-pigmented due to melanin in their cell walls) resulting in a range of mycoses; superficial, cutaneous, subcutaneous, and systemic/deep tissue infections of various organs, especially the brain. It can be separated from other mycoses involving dematiaceous fungi as the tissue morphology of the causative organism is mycelial, whereas when in mycotic mycetoma



the tissue morphology of the organism is a grain or in chromoblastomycosis it is a sclerotic body. The etiological agents include various dematiaceous hyphomycetes (molds) especially species of *Exophiala*, *Phialophora*, *Wangiella*, *Bipolaris*, *Exserohilum*, *Cladophialophora*, *Phaeoannellomyces*, *Aureobasidium*, *Cladosporium*, *Curvularia* and *Alternaria*.<sup>20</sup>

Phaeohyphomycosis occurs worldwide but, like that of chromoblastomycosis it presents most commonly in areas with tropical or subtropical climates. There has been a recent increase in reported cases of this very dangerous and understudied disease and although widely considered an opportunistic infection, there have been cases reported in healthy individuals.<sup>21</sup> The role which melanin plays in the cell wall of these pathogenic dermataceous fungi is not fully understood but may be a virulence factor for these species. Cases have been reported in otherwise healthy/immunocompetent patients but those primarily at risk are the immunosuppressed. In the case of systemic infections, there are

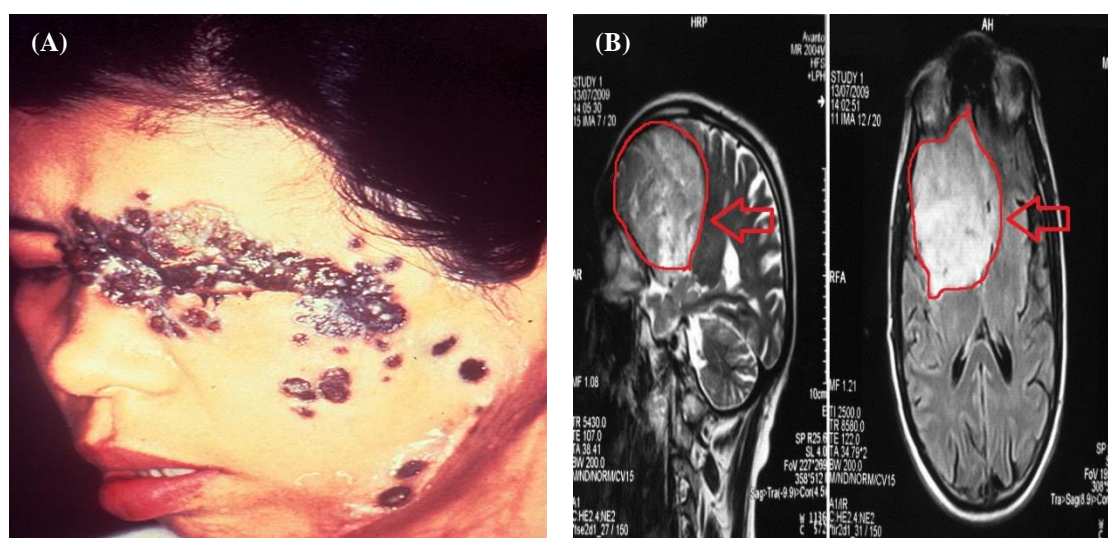


**Fig. 3.9:** (A) Subcutaneous phaeohyphomycosis caused by *Wangiella dermatitidis*, (B) MRI images of a cerebral phaeohyphomycosis in an immunocompetent individual demonstrating a large, space-occupying, fatal lesion, caused by *Thielavia subthermophila*.<sup>20b,22</sup>

numerous clinical signs and effects such as eosinophilia (high white cell count), papules, plaques, granulomatous, and in extreme cases there are deep infections within the eyes, bones, heart (endocarditis, mostly reported on bioprosthetic valves of porcine origin),

central nervous system and brain (Figure 3.9).<sup>22</sup> The most effective therapy is a combination of surgical excision of the fungus and treatment with antifungal drugs. The medicinal capabilities of antifungal treatments (Amphotericin B, 5-Fluorocytosine, Ketoconazole) are limited, necessitating long-term therapy with many drugs not being effective against dematiaceous (black) fungi which have displayed a high resilience. Therefore, systemic phaeohyphomycosis prognosis remains poor, with an overall mortality rate of 79%.<sup>23</sup>

Humans are protected from most mycoses by innate structures that act as physical and chemical barriers to infectious agents and evolved immune responses that grant a high degree of protection and immunity. Our skin protects and guards us from fungal infections of superficial, cutaneous and subcutaneous origin. The mucus membranes that line the body cavities (that are exposed to the external environment) and the internal organs, secrete mucus (a thick sticky liquid) that traps the pathogens and prevents any further disease-causing activity, particularly important for organisms that attack the digestive, respiratory and reproductive systems/tracts. In conjunction with this is the human innate immune response and the adaptive or acquired immune system which protects against systemic infection through the use of specialised signalling proteins, such as cytokines, and immune cells, such as lymphocytes.<sup>24</sup>

However, the frequency in incidences of mycoses, particular those of invasive or opportunistic character, has increased dramatically over the past two decades.<sup>21</sup> This increase has been accompanied by an increase in morbidity and mortality due to invasive fungal infections. *C. albicans*, *Cryptococcus neoformans*, and *Aspergillus fumigatus* are the most well-known causes of opportunistic mycoses. The *Candida* species (Figure 3.10) alone accounts for 28,000 nosocomial bloodstream infections (BSI), with a 40% mortality rate per year in the US.<sup>25</sup> People most at risk to the development of serious/life threatening fungal infections are those who are immunosuppressed. Immunosuppression or impaired immune response can result from a very wide range of factors, such as patients undergoing any type of transplantation (blood, bone or solid-organ), major surgery especially gastrointestinal surgery, patients with any form of neoplastic disease (cancer), those with HIV/AIDS, tuberculosis (TB), the elderly, premature infants and anyone receiving immune modulation/suppression therapy.<sup>21</sup>

As previously stated, not only do these conditions/diseases lead to an increased risk of infection but also in some cases the therapies/medicinal agents used to treat them further exacerbate the infection risk factor. The number of patients who fall into these at risk immunosuppressed/compromised categories are also increasing (first world aging population trends, increasing cancer diagnoses, HIV/AIDS).

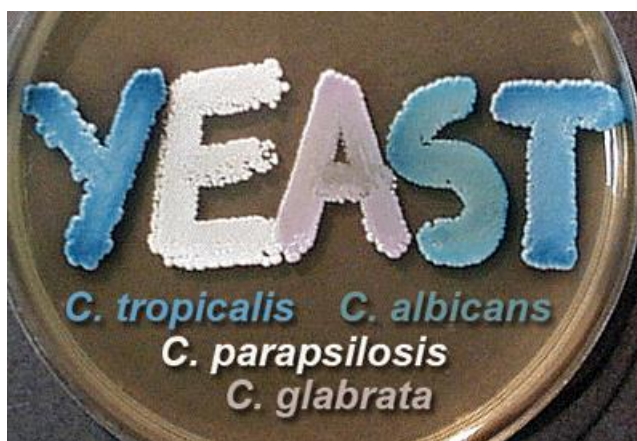


**Fig. 3.10:** Various *Candida* species grown on CHROMagar plate showing chromogenic colour change to identify different species; *C. albicans* (green), *C. tropicalis* (blue), *C. parapsilosis* (white) and *C. glabrata* (pink).<sup>26</sup>

The situation is worsened by the rise of antibacterial resistance, such as Methicillin-resistant *Staphylococcus aureus* (MRSA) and totally drug resistant *Mycobacterium tuberculosis* (TDR-TB) due in part to the over use of broad spectrum antibiotics. This is compounded by intrinsic and acquired resistance to standard (azole, polyene, or echinocandin) antifungal agents and the rise of new/emerging pathogenic fungal species, such as yeast like fungi (*Trichosporon* and *Rhodotorula* species), the Zygomycetes, hyaline molds (*Fusarium* and *Scedosporium* species), other species of *Candida* (e.g. *C. parapsilosis*, *C. tropicalis* and *C. glabrata* Figure 3.10), *Aspergillus* and a wide variety of dermatiaceous fungi.<sup>21</sup>

It is this complex array of factors which has led to the increase in fungal infections in recent years. This has resulted in an intensive search to develop new, efficacious

antifungal agents with unique modes of action which can circumvent intrinsic or acquired resistance and/or preferentially target alternative fungal cellular components or processes.

### 3.3 Antifungal phenanthrene derivatives

Our research group has extensive experience in the use of phenanthrolines, particularly 1,10-phenanthroline, and their metal complexes as antifungal agents against various fungal pathogens.

The use of various phenanthrene and phenanthroline derivatives (Figure 3.11) to inhibit the growth of numerous bacterial and fungal pathogens has been extensively reported over the last seven decades.<sup>27</sup> There is considerable evidence in the literature to support the idea that the metal chelation capability of the nitrogen-substituted derivatives of phenanthrene and their corresponding superior biological efficacy are inherently linked.<sup>27c, 28</sup> One noteworthy derivative, which displayed outstanding bacteriostatic and fungistatic activity against a wide-spectrum of pathogenic bacteria and fungi was the *N,N'*-diimine chelator 1,10-phenanthroline (1,10-phen) (Figure 3.11).<sup>27a, b</sup> 1,10-phen displays superior fungistatic activity over that of 1,7 or 4,7-phenanthroline (Figure 3.11), which is attributed to the chelation capacity of 1,10-phen and which 1,7 or 4,7-phenanthroline do not have. An increase in biological effect was observed for 2,9-dimethyl-1,10-phenanthroline (dmphen, Figure 3.11), wherein hydrogen substituents at the 2- and 9-positions have been replaced with methyl groups.<sup>27a</sup> This increase in antimicrobial effectiveness for dmphen was attributed to the chelation of metal ions akin to that of 1,10-phen and perhaps due to the increased lipophilic nature of the molecule. However further alkylation or chlorination of the 1,10-phenanthroline backbone resulted in a decrease in antifungal activity.<sup>27a</sup>

Therefore, the presence of the *N,N'*-diimine chelation moiety would seem essential in maintaining and improving upon any antimicrobial activity as it provides a classic chelating bidentate site, allowing for the cellular formation of the actual bioactive species, which is considered to be bis-/tris-1,10-phen metal complexes  $[M^{n+}(1,10\text{-phen})_n]^{n+}$ , formed through the sequestering of metal ions from the biological system itself and which

results a in poor survival outcome for microbial pathogens.<sup>29</sup>  $Zn^{2+}$  is an essential trace element for metabolic function and cell homeostasis. It is present in numerous metallo enzymes (e.g. matrix metalloproteinases) and eukaryotic proteins such as zinc finger proteins.<sup>30</sup> It is the ability of 1,10-phen to sequester  $Zn^{2+}$  from the cellular milieu that leads to the death of microbial pathogens, brought about via disruption of homeostasis, enzyme (resulting inactive apoenzymes), protein and metabolic function, that cumulatively and ultimately result in cell death.<sup>29c, 31</sup>

1,10-Phen has been reported to have a fungistatic effect on *C. albicans* (ATCC 10231) with an  $MIC_{100}$  of 1.25-5  $\mu\text{g/ml}$ .<sup>28b</sup> It has also been reported to have potent growth inhibitory activity against clinical isolates of *C. tropicalis*, *C. krusei* and *C. glabrata* at a concentration of 100  $\mu\text{g/ml}$ .<sup>32</sup> Further tests were conducted against three clinical strains of *C. albicans* using a concentration of 20  $\mu\text{g/ml}$  for 1,10-phen and the structurally related 2,2'-bipyridyl (bipy, Figure 3.11). 1,10-Phen demonstrated potent growth inhibition of all fungal strains tested while bipy proved to be essentially inactive.<sup>28b, 31b, 32</sup> This difference in activity may be attributed to the planarity and rigidity of 1,10-phen, especially within its *N,N'*-diimine chelation moiety, leading to entropically favoured metal chelation (complex formation results in large desolvation of metal cations) as opposed to the free rotation about the bonds in the *N,N'*-diimine chelation moiety of bipy. Furthermore, 1,10-phen, compared to bipy, has an extended aromatic ring structure, and it can be hypothesised that this may result in greater hydrophobicity and hence enhanced lipophilicity enabling it to pass through cell membranes and result in cytotoxicity.

Another analogue, namely 1,10-phenanthroline-5,6-dione (phendione, Figure 3.11), has been reported in the literature to possess superior antifungal activity to that of 1,10-phen. Phendione displays an  $MIC_{100}$  value in the range of 0.6-2.5  $\mu\text{g/ml}$  against *C. albicans* (ATCC 10231) in minimal media (MM) at 30 °C, this equates to approximately a 2.5 fold increase in activity when compared to 1,10-phen under the same conditions.<sup>33</sup> Phendione contains the same *N,N'*-diimine chelation moiety as 1,10-phen but also has a diketone functionality/*O,O'*-quinonoid moiety at the 5 and 6 positions which is able to undergo a 2 electron/2 proton reduction leading to the formation of the dihydroxy or diol structural analogue, 1,10-phenanthroline-5,6-diol (phendiol, Figure 3.11). Interestingly, phendiol can undergo oxidation relatively easily and can be oxidised by the action of oxygen from air back to Phendione.<sup>34</sup>

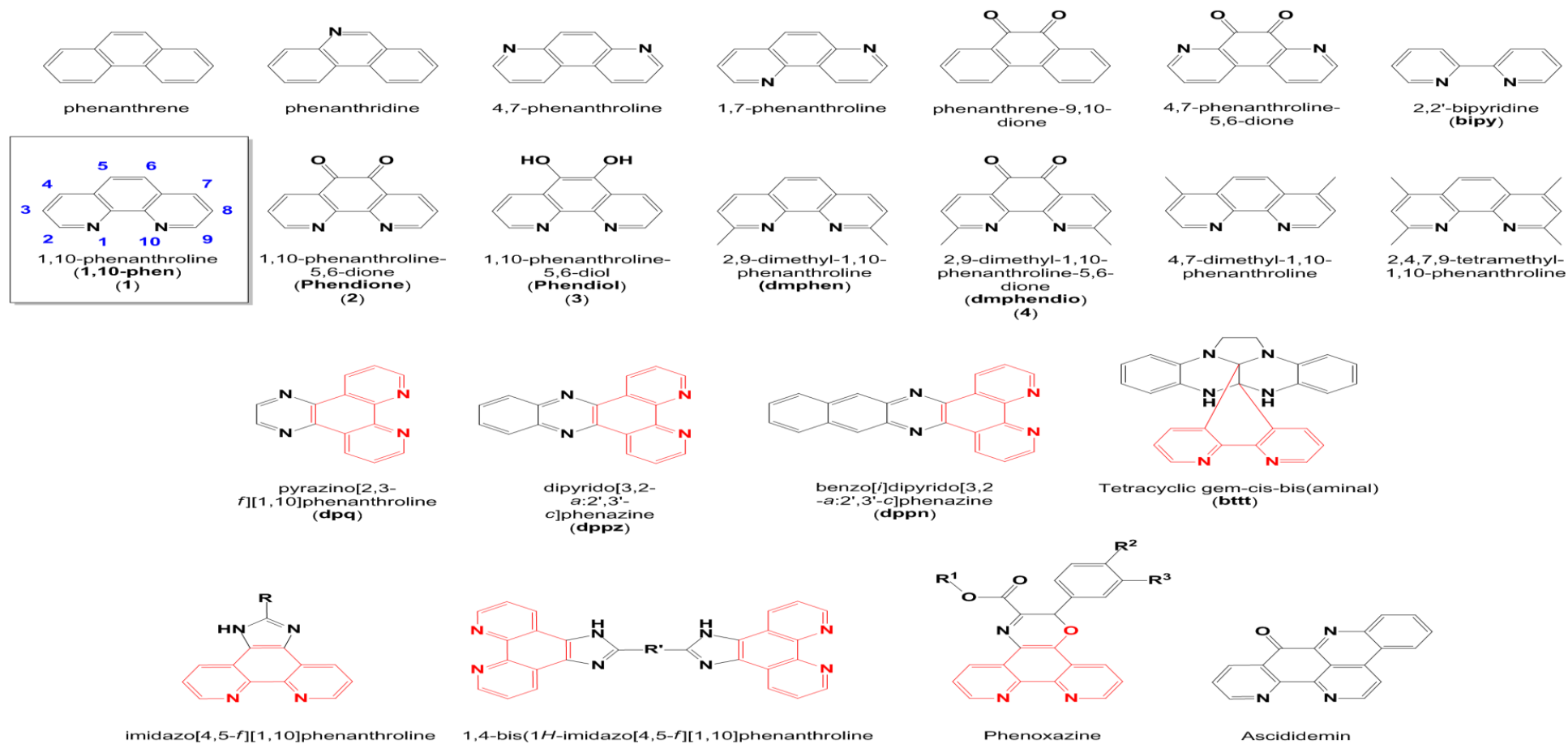


Fig. 3.11: Molecular structure of Phenanthrene, its many known and novel derivatives and also the chelating ligand 2,2'-bipyridine.



The redox capability of the *O,O'*-quinonoid moiety of phendione would seem to explain its superior antifungal activity compared to 1,10-phen. This hypothesis is granted some weight when we consider that the reported anti-*Candida* activity of phendiol is 0.6-1.3 µg/ml; which is an intermediate value between that of phendione and 1,10-phen suggesting that the activity of phendiol may result from possible cellular oxidation back to phendione. Furthermore, the phenanthrene derivative phenanthrene-9,10-dione (Figure 3.11) which contains the same *O,O'*-quinonoid moiety as phendione has only limited activity against *C. albicans* with an MIC<sub>100</sub> = 50-100 µg/ml.<sup>35</sup> This emphasises the importance of the redox functionality of the *O,O'*-quinonoid moiety and the *N,N'*-diimine chelation moiety of phendione (facilitating metal complex formation), and their essential role in phendione's superior antifungal efficacy.

### 3.4 Potentiating the antifungal activity of 1,10-phen carboxylate complexes

Where derivatives of metal-free 1,10-phen have been employed as antifungal agents the true bioactive species is assumed to be the bis-/tris-1,10-phen metal complexes of general formula  $[M^{n+}(1,10\text{-phen})_n]^{n+}$  formed by the sequestration of metal ions from the cellular environment. The chelation of metal ions by 1,10-phen and its derivatives leads to the formation of extremely stable metal complexes. For example the log β stability constant for  $[\text{Cu}(1,10\text{-phen})_2]^{2+} = 21$ . It has been reported by our research group and numerous others that metal complexes (Ag(I), Cu(II), Mn(II) and Co(II)) of 1,10-phen and its derivatives have improved anti-*Candida* activity compared to that of the metal-free 1,10-phen. Our research in recent years has focused on the formation of ternary complexes composed of 1,10-phen/phendione and various aliphatic, bridged cyclic (norbornene-based), ethereal and aromatic dicarboxylic acids coordinated to the metal centre (Figure 3.12). Other ternary complexes were also synthesised whereby these dicarboxylic acids were not coordinated to the metal ion but acted as counter ions to the cationic metal-1,10-phen complexes, to investigate the role of the counter ion in antifungal activity.

In all of the cases reported by our research group, the simple metal salts, the metal-free dicarboxylic acid ligands, the dicarboxylate coordinated metal complexes and metal-free 1,10-phen or phendione were screened for their anti-*Candida* activity.

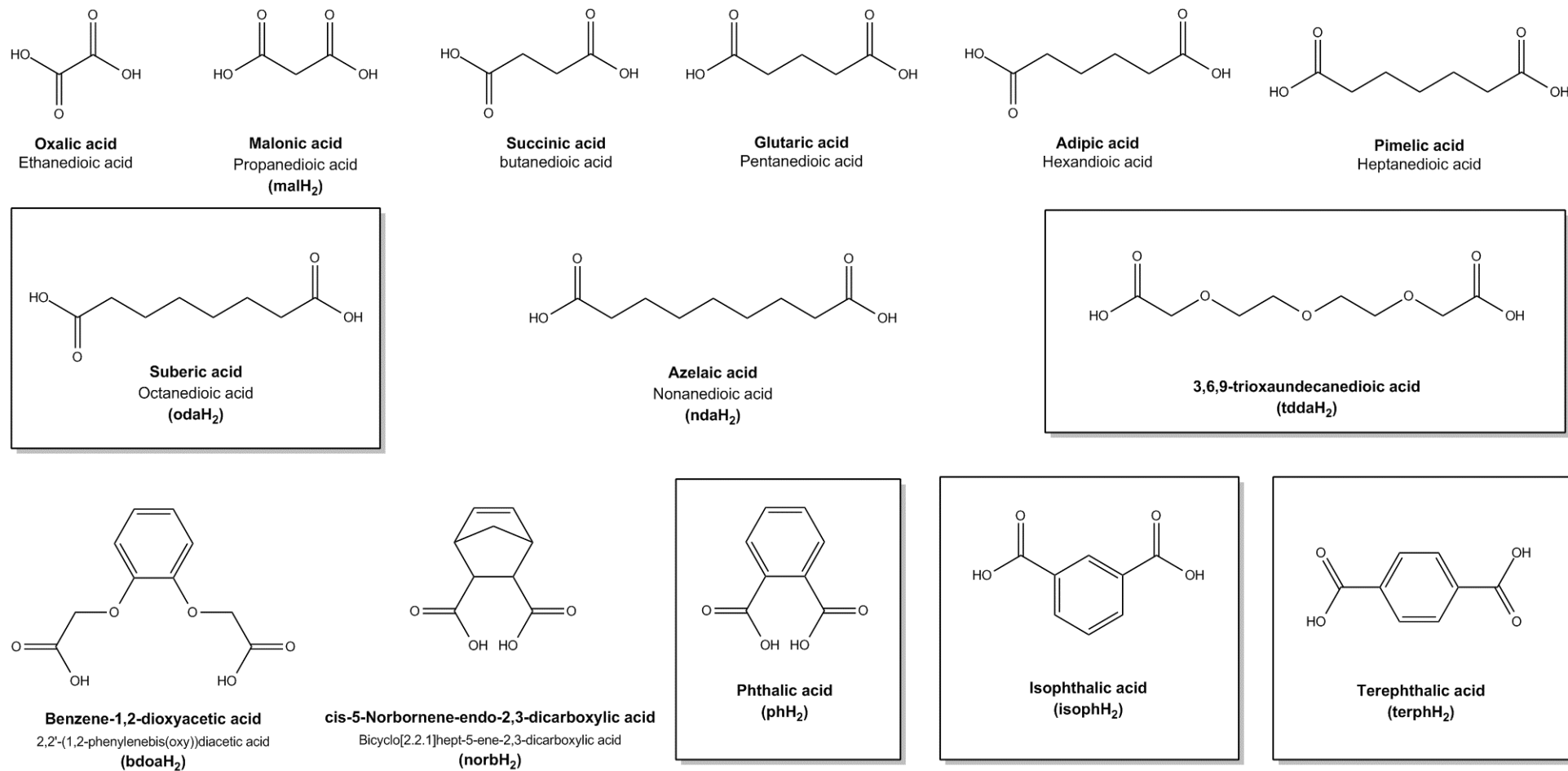


**Fig. 3.12:** Structures of aliphatic, bridged cyclic, ethereal and aromatic dicarboxylic acid ligands utilised by our research group. Highlighted dicarboxylic acids are employed as ligands in the formation of antifungal metal complexes in this chapter.



No significant antifungal activity was observed for the simple metal salts, the metal free dicarboxylic acids or the metal dicarboxylate coordinated complexes (no 1,10-phen present). Exceptions to this trend were the simple metal salts, silver acetate  $\text{Ag}(\text{CH}_3\text{CO}_2)$ , Silver nitrate  $\text{Ag}(\text{NO}_3)$ , silver perchlorate  $\text{Ag}(\text{ClO}_4)$  and the Ag(I) complex  $[\text{Ag}_2(\text{mal})]$ , which all exhibited anti-*Candida* activity (1.25-2.5 and  $>5 \mu\text{g}/\text{cm}^3$ , respectively). It is assumed that the active entity in this case is the  $\text{Ag}^+$  ion, with the acetate, nitrate, perchlorate or malonate anions having no significant biological impact.<sup>28b</sup> As expected, metal-free 1,10-phen and phendione displayed their strong, aforementioned anti-*Candida* activity.

A vast improvement in antifungal activity was observed upon complexation of 1,10-phen, resulting in ternary complexes of the following general formula  $[\text{M}^{n+}(\text{1,10-phen})_n(\text{diacid})_n](\text{diacid})_n$  where  $\text{M} = \text{Co}(\text{II}), \text{Mn}(\text{II}), \text{Cu}(\text{II})$  or  $\text{Ag}(\text{I})$  e.g. =  $[\text{Mn}(\text{1,10-phen})_2(\text{bdoa})] \cdot \text{H}_2\text{O}$ .<sup>32, 36</sup> It should also be noted that in instances where analogous ternary complexes incorporating bipy instead of 1,10-phen were synthesised (e.g.  $[\text{Cu}_2(\text{bipy})_4(\text{bdoa})] \cdot 6\text{H}_2\text{O}$ ) and tested for anti-*Candida* activity, none was observed, again suggesting that the importance of the biologically significant characteristics of 1,10-phen (planarity, rigidity, extended aromatic ring structure and enhanced lipophilicity), which the bipy ligand does not possess.

These anti-*Candida* studies revealed that there are two highly cytotoxic groups of ternary complexes with very different modes of action; those which are Mn(II) and Cu(II) based and those which are Ag(I) based. The mode of action and the level of bioactivity varies markedly between these two groups of complexes indicating the importance of the type of metal ion.<sup>31b</sup> Mn(II) and Cu(II) based ternary complexes contain metals with variable oxidation states and thus are capable of conducting Fenton-type chemistry, resulting in the formation of reactive oxygen/nitrogen species (ROS, RNS) within the cellular environment. ROS is a collective term that includes both oxygen radicals and certain nonradicals that are oxidizing or reducing agents and/or are easily converted into radicals ( $\text{HOCl}, \text{O}_3, \text{ONOO}^-, {}^1\text{O}_2, \text{H}_2\text{O}_2$ ). RNS is also a collective term including nitric oxide and nitrogen dioxide radicals and also includes nonradicals such as  $\text{HNO}_2$  and  $\text{N}_2\text{O}_3$  and  $\text{ONOO}^-$ .

Anti-*Candida* studies on the malonate ternary complexes,  $[\text{Cu}(\text{phen})_2(\text{mal})] \cdot 2\text{H}_2\text{O}$  and  $[\text{Mn}(\text{phen})_2(\text{mal})] \cdot 2\text{H}_2\text{O}$  and  $[\text{Ag}_2(\text{phen})_3(\text{mal})] \cdot 2\text{H}_2\text{O}$  revealed that they were highly

fungistatic ( $MIC_{100}$  1.25 – 5  $\mu\text{g}/\text{cm}^3$ ) and were able to damage mitochondrial function and uncouple cellular respiration.<sup>31b</sup>

Importantly, only the Cu(II) and Mn(II) complexes caused increased oxygen uptake by the *C. albicans* cells. A likely explanation is the formation of highly damaging ROS/RNS by these complexes via Fenton-type chemistry. The Ag(I) complex would most likely be incapable of this redox-mediated ROS/RNS production, as *in vitro* or *in vivo* reduction of the Ag(I) ion would produce Ag(0) and result in precipitation of the metal and therefore destruction of its bioactive complex. Interestingly, all three complexes inhibited cytochrome b and c biosynthesis but only the Ag(I) complex lowers the levels of cytochrome aa<sub>3</sub>. This is noteworthy considering that cytochrome b and c proteins are hemoproteins and contain iron in their active site and that cytochrome aa<sub>3</sub> is different in that it contains copper in its active site, combined with the knowledge that metal-free 1,10-phen has a high affinity for iron, this may begin to explain this observation. In addition the Cu(II) and Ag(I) complexes reduced cellular ergosterol levels whilst the Mn(II) complex [Mn(phen)<sub>2</sub>(mal)].2H<sub>2</sub>O induces an increase in ergosterol concentration. The Ag(I) based ternary complex's mode of antifungal activity is therefore quite different to that of its Cu(II), Mn(II) based counterparts and maybe akin to known effects of nano particulate silver which are expressed through the disruption of the structure of the cell membrane and inhibition of the budding process due to the destruction of the membrane integrity.<sup>37</sup>

In an effort to improve upon the previous encouraging antifungal results for this type of ternary complex, the use of other dicarboxylic acids was investigated (Figure 3.12). We hypothesized that the use of long chain alkyl and long chain ethereal dicarboxylic acids would result in water soluble ternary, metal 1,10-phen carboxylate complexes where the carboxylates would act as inner sphere ligands. In our recent work we synthesised this type of complex via the use of suberic acid and 3,6,9-trioxaundecanedioic acid (Figure 3.12), which did result in highly water soluble Cu(II), Mn(II) and Ag(I) complexes such as [Ag<sub>2</sub>(tdda)(phen)<sub>4</sub>]EtOH (**17**) (Figure 3.13). We wished to exploit the favourable partition coefficients (log P) of suberic acid (log P = 1.03 intermediate hydrophilicity/lipophilicity) and 3,6,9-trioxaundecanedioic acid (log P = -1.69 very hydrophilic) to impart an intermediate lipophilic/hydrophilic nature to the ternary metal complexes which we hoped, may result in improved biological effectiveness. The idea

was to produce complexes that were lipophilic enough to cross the lipid membranes of fungal cells but also hydrophilic enough to ensure efficient transport throughout the organism.

### 3.5 Complex synthesis, characterisation and proposed structures

All relevant chemicals were purchased from commercial sources and used as received without further purification. 1,10-Phenanthroline-5,6-dione (phendione (**2**)), [Cu(phendione)<sub>3</sub>](ClO<sub>4</sub>)<sub>2</sub>·4H<sub>2</sub>O (**6**), [Ag(phendione)<sub>2</sub>]ClO<sub>4</sub> (**7**) and complexes **8-14** (Figure **3.14**) were prepared in accordance with the literature methods with some slight modifications.<sup>33, 38</sup> The phthalic acid (phH<sub>2</sub>), octanedioic acid (odaH<sub>2</sub>) and 3,6,9-trioxaundecanedioic acid (tddaH<sub>2</sub>) complexes were synthesised by heating a solution containing the metal acetate salt and an excess of the dicarboxylic acid for the required time (3 hours) which resulted in the formation of the metal dicarboxylate precursor complexes (e.g. [Mn(ph)]0.5H<sub>2</sub>O) (Scheme **3.1**). The metal carboxylate complexes were then added to a solution of 1,10-phen and heated which resulted in the formation of the ternary metal 1,10-phen carboxylate complexes (Scheme **3.1**). All of the Ag(I) complexes were synthesised in the absence of light and the products were stored in the dark.

All ligands and complexes were characterised by Infrared (IR) spectroscopy (spectra were recorded in the region 4,000–370 cm<sup>-1</sup>) using anhydrous potassium bromide to form solid KBr discs on a Perkin Elmer System 2000 FT spectrometer. Elemental analysis (CHN) was carried out for all ligands and complexes using a FLASH EA 1112 Series Elemental Analyser with Eager 300 operating software. Mass spectrometry data was acquired for all complexes and ligands using an Agilent Technologies 6210 Time of Flight LC/MS mass spectrometer. Solid state magnetic susceptibility measures were obtained for all Cu(II) and Mn(II) complexes using a Johnson Matthey Magnetic Susceptibility Balance. The IR spectra of complexes **8-15**, were compared to their known spectra and all were found to contain the characteristic 1,10-phen stretches at *ca.* 844 and 729 cm<sup>-1</sup> (**8**), *ca.* 849 and 733 cm<sup>-1</sup> (**9**), *ca.* 842 and 724 cm<sup>-1</sup> (**10**), *ca.* 842 and 727 cm<sup>-1</sup> (**11**), *ca.* 847 and 729 cm<sup>-1</sup> (**12**), *ca.* 850 and 730 cm<sup>-1</sup> (**13**), *ca.* 845 and 730 cm<sup>-1</sup> (**14**), *ca.* 852 and 730 cm<sup>-1</sup> (**15**), the band at *ca.* 735 cm<sup>-1</sup> can be assigned to the out of plane motion of hydrogen atoms on the heterocyclic rings and the band at *ca.* 850 cm<sup>-1</sup> to the two adjacent hydrogens on the centre aromatic ring. As expected, upon coordination these bands are shifted to lower

frequency compared to the metal-free 1,10-phen (*ca.* 858 and 742  $\text{cm}^{-1}$ ) (see Ch. 2 / Appendix). The CHN, mass spectral and magnetic moment data acquired for these complexes match the expected values and are in line with all data previously published.

The IR spectrum of complex, **15**, contains the characteristic 1,10-phen stretches at *ca.* 852 and 731  $\text{cm}^{-1}$  which can be assigned to the two hydrogens on the centre aromatic ring and the two sets of three hydrogens on the heterocyclic rings, respectively. The  $\nu_{(\text{OCO})_{\text{asym}}}$  and  $\nu_{(\text{OCO})_{\text{sym}}}$  vibrations for the carboxylate function of the tdda ligand in **15** occur at 1620 and 1405  $\text{cm}^{-1}$ , respectively, giving a  $\Delta_{(\text{OCO})}$  value of 215  $\text{cm}^{-1}$  (see Ch. 2 / Appendix). This value indicates a monodentate coordination mode. Although a crystal structure for **15**, has yet to be obtained, the monodentate coordination mode of the tdda ligand in **15** suggested by its IR spectrum, would compare favourable to its Mn(II)-based analogue, **14**, the crystal structure of which had the tdda ligand in monodentate coordination mode. In addition, the mass spectrum and elemental analysis data are in accordance with the proposed formulation of **15**,  $[\text{Cu}(3,6,9\text{-tdda})(\text{phen})_2]3\text{H}_2\text{O}\cdot\text{EtOH}$ .

The IR spectrum of complex, **17**, contains the characteristic 1,10-phen stretches at *ca.* 855 and 738  $\text{cm}^{-1}$  which can be assigned to the two hydrogens on the centre aromatic ring and the two sets of three hydrogens on the heterocyclic rings, respectively. The  $\nu_{(\text{OCO})_{\text{asym}}}$  and  $\nu_{(\text{OCO})_{\text{sym}}}$  vibrations for the carboxylate function of the tdda ligand in **17** occur at 1622 and 1422  $\text{cm}^{-1}$ , respectively, giving a  $\Delta_{(\text{OCO})}$  value of 200  $\text{cm}^{-1}$ . This value of separation between the bands is difficult to assign with any certainty but would suggest either free (uncoordinated) carboxylate or possibly a monodentate coordination mode. A crystal structure of **17** has proven difficult to obtain as it forms unusual long (2 mm) crystalline fibres, which give limited x-ray crystallographic data. The preliminary crystal data is able to confirm the presence of Ag(I) bis-1,10-phenanthroline units  $\{[\text{Ag}(\text{phen})_2]\}_c$  linked in some fashion to one another by the tdda ligand. This would suggest that the tdda is acting as either a monodentate bridging ligand ( $\eta^1 \eta^1 \mu^2\text{-tdda}$ ) linking two of the  $[\text{Ag}(\text{phen})_2]$  units together or as an uncoordinated counter ion (Figure 3.13).

The favoured coordination geometry of  $[\text{Ag}(\text{phen})_2]$  as a d10 ion would most likely be tetrahedral in order to limit the ligand electron-electron repulsion with the 10 d electrons of the Ag(I). Most often however, with Ag(I) and 1,10-phen, a pseudo square planar geometry is assumed due to steric limitations of the 1,10-phen ligands and in this case the tdda dicarboxylate would act as non-coordinated counter ion.

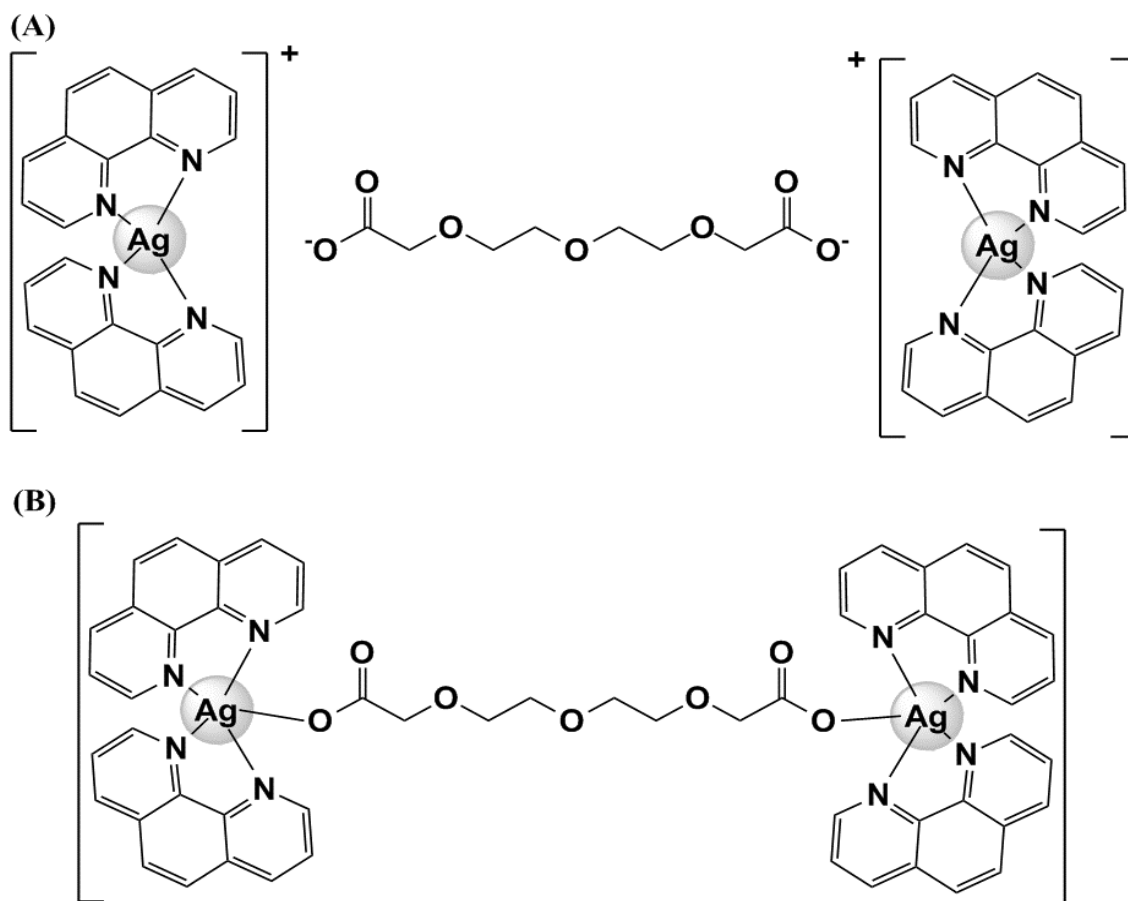
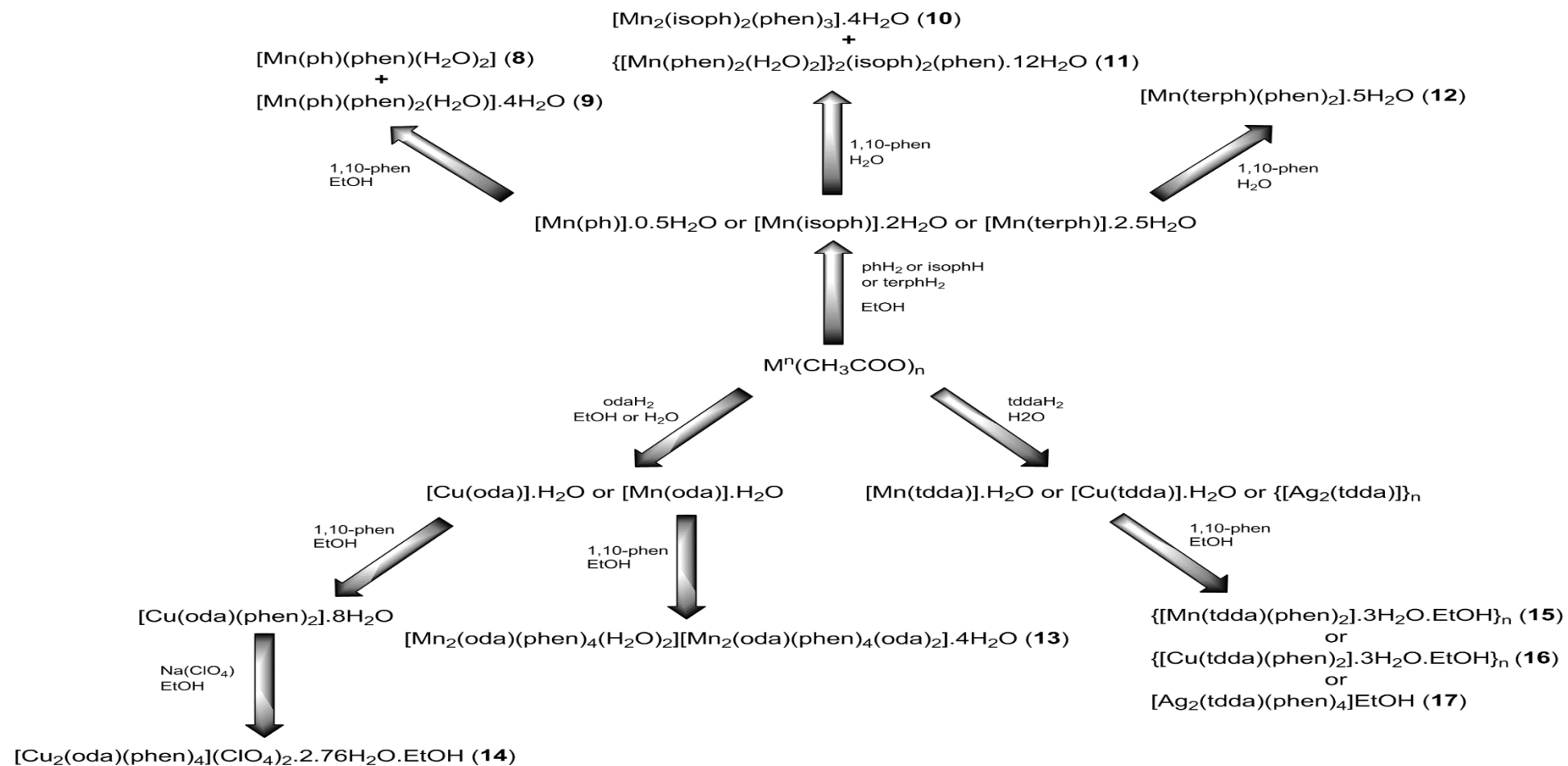


**Fig. 3.13:** Proposed structures of complex **17**. (A) Pseudo square planar geometry of  $[\text{Ag}(\text{phen})_2]^+$  with the dicarboxylate (tdda), acting solely as a counter ion (non-coordinated). (B) Square pyramidal or trigonal bipyramidal coordination geometry with tdda ligand acting as a monodentate bridging ligand eg.  $(\eta^1 \eta^1 \mu^2\text{-tdda})$ .

Hence, given the incomplete x-ray crystallographic data, the hypothesis is that the structure of **17** would be that given in part (A) Figure 3.13. The mass spectrum and elemental analysis data are in accordance with the proposed formulation of **17**,  $[\text{Ag}_2(3,6,9\text{-tdda})(\text{phen})_4]\text{EtOH}$ .



**Scheme 3.1:** Synthetic routes to complexes. Complexes in group 1–3 and complex **15** in group 4 have previously been published. In Group 4 complexes **16** and **17** are novel.

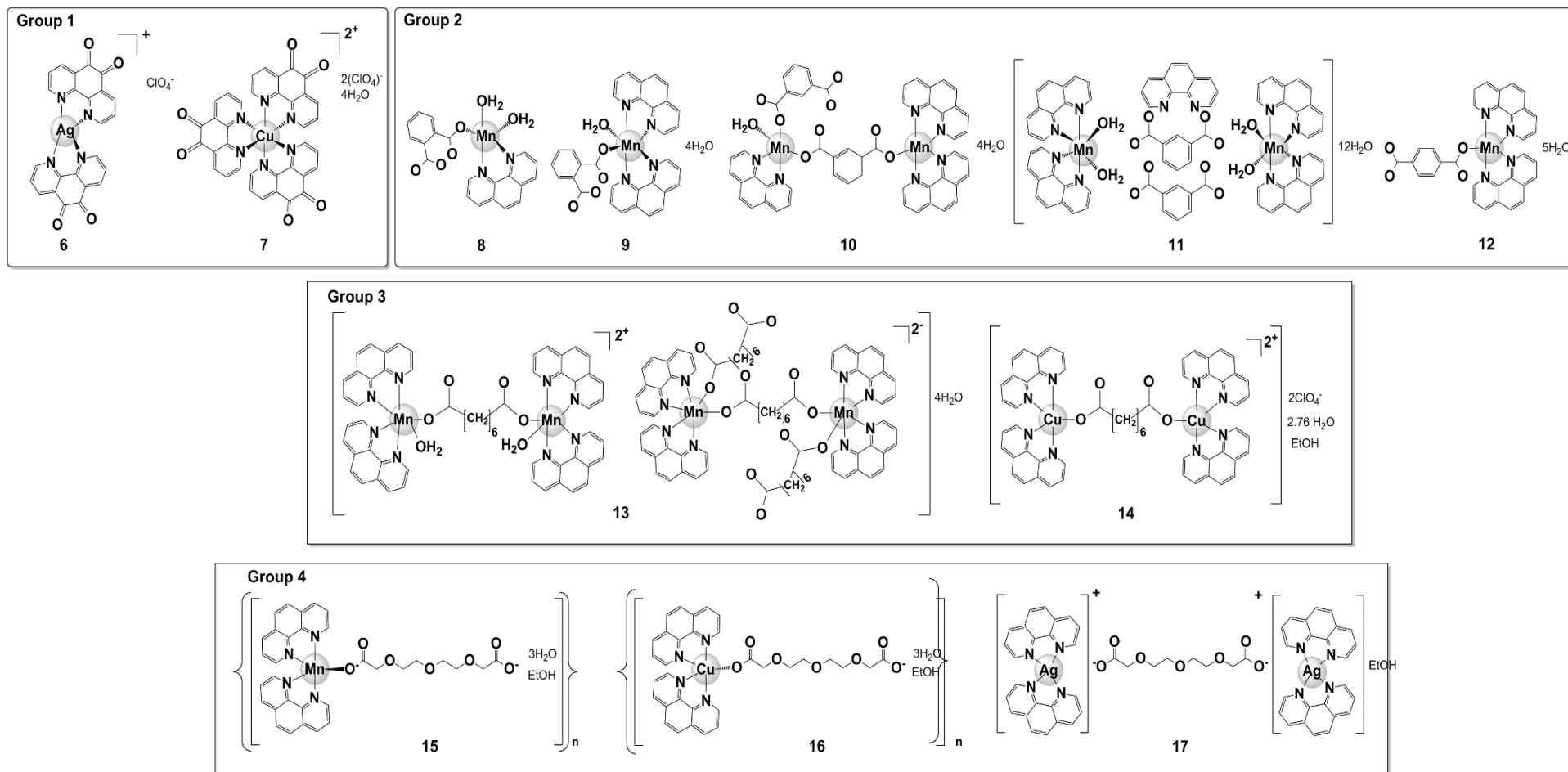


**Fig. 3.14:** Structure of four groups of metal complexes used for antifungal testing. Group 1 is comprised of Ag(I) and Cu(II) phenanthroline perchlorate complexes.<sup>33,51(b)</sup> Group 2 Mn(II) 1,10-phen phthalate, isophthalate and terephthalate complexes.<sup>38(b)</sup> Group 3 Cu(II) and Mn(II) 1,10-phen octanedioate complexes<sup>38(c-d)</sup> and Group 4 is comprised of Mn(II), Cu(II) and Ag(I) 1,10-phen 3,6,9-trioxaundecanedioates.<sup>38(e)</sup> Complexes in group 1–3 and complex **15** in group 4 have previously been published. Complexes **16** and **17** in group 4 are novel.



### 3.6 Antifungal activity and cytoselectivity of selected complexes

The Mn(II), Cu(II) and Ag(I) complexes, **6-17**, their simple metal salts, the metal-free ligands and selected, clinical antimicrobial agents (Amphotericin B (AMB), Ketoconazole (KTC), Fluconazole (FLC), Voriconazole VRC, Itraconazole (ITC), Caspofungin (CFG), Micafungin (MFG) and Flucytosine (5FC)) were screened *in vitro* for their ability to inhibit the growth of pathogenic fungal cells.<sup>39</sup> The minimum inhibitory concentration (MIC<sub>100</sub>), is defined as the lowest concentration of an antimicrobial agent that causes a specified reduction/inhibition in the visible growth of a microorganism in an agar or broth dilution susceptibility test after overnight incubation. Related to the MIC is the minimum fungicidal concentration (MFC), it is defined as the minimum concentration of an antifungal agent that results in no observable fungal growth. A fungicidal effect is considered when the MFC value is equal to, or up to, four times the MIC value. The activities (MIC<sub>100</sub> and MFC values) are reported for eight species of fungi which are causative agents for human mycoses such as Chromoblastomycosis (*Phialophora verrucosa*, *Cladophialophora carrionii*), Phaeophomycosis (*Exophiala dermatitidis*), Eumycetoma (*Pseudallescheria boydii*, *Pseudallescheria minutispora*, *Seudosporium aurantiacum*, *Seudosporium proliticans*) and Candidiasis (*Candida albicans*) (Tables **1-8**). The values are given as  $\mu\text{g}/\text{cm}^3$  and  $\mu\text{M}$  concentrations of the complexes.

The half maximal inhibitory concentration (IC<sub>50</sub>) represents the concentration of an agent/"drug" that is required for 50% inhibition of a biological/biochemical process or function *in vitro*. In this case, the IC<sub>50</sub> values obtained for all complexes are the half maximal dose which induced cytotoxicity or cell death to a normal mammalian cell line (Vero cells). The IC<sub>50</sub> values for all test complexes were obtained using Vero cells which are isolated kidney epithelial cells extracted from an African green monkey. These IC<sub>50</sub> values were required in order to ascertain the level of cytotoxicity of the complexes towards normal mammalian epithelial cells and to devise a selectivity index/parameter to deduce if the complexes were cytoselective for fungal cells over mammalian cells. The selectivity index (SI) is a measure of the cytotoxicity of an agent for its intended target (e.g. fungal pathogen cells) over that of the hosts normal cells (represented by the Vero cells). The selectivity index can be calculated for a particular test agent/"drug" by dividing its MIC value obtained for a particular pathogen (e.g. *C.albicans*) by the IC<sub>50</sub> value obtained for a normal mammalian or human cell line (e.g. Vero cells) (**Figure 3.15**).



$$\text{Selectivity Index (SI)} = \frac{\text{IC}_{50}}{\text{MIC}}$$

**Fig 3.15:** Selectivity index equation.

The MIC, MFC testing for seven for the fungal species represented in Tables 1-7 was conducted by Professor Andre L.S. Santos and his group in the Department of General Microbiology, Federal University of Rio de Janeiro, Brazil. The IC<sub>50</sub> testing utilising the Vero cells was also conducted by the same group.<sup>40</sup> The MIC results for all test complexes against *C. albicans* (ATTC 10231) (Table 3.8) were obtained in the Microbiology Laboratory, Department of Chemistry, Maynooth University.

The test complexes or compounds (0.020 g) were dissolved in DMSO (1 cm<sup>3</sup>) and added to water (9 cm<sup>3</sup>) to give a stock solution (concentration 2000 mg/cm<sup>3</sup>). Complexes which displayed low solubility were tested as fine suspensions. A working solution was then prepared for each by taking 0.5 cm<sup>3</sup> of the stock solution (or suspension) and adding it to water (9.5 cm<sup>3</sup>) to give a solution with a concentration of 100 µg/cm<sup>3</sup>. The maximum DMSO concentration in any test solution was 0.5% v/v, and at this level the DMSO does not inhibit the growth of the fungal cells.

The antifungal susceptibility MIC and MFC values for all test compounds/complexes against the filamentous fungi (*P. verrucosa*, *C. carrionii*, *E. dermatitidis*, *P. boydii*, *P. minutispora*, *S. aurantiacum* and *S. prolificans*) were determined by broth microdilution according to CLSI method M38-A2 with an inoculum of 2.5x10<sup>3</sup> CFU/cm<sup>3</sup>. The 96 well microassay plates were incubated at 35°C, and the optical density (OD) value was determined at 540 nm after 48 hours.<sup>41</sup> All assays were run in triplicate and on three independent occasions. The MIC<sub>100</sub> and MFC values were then determined and recorded as micrograms per millilitre or cubic centimetre (µg/cm<sup>3</sup>) and as micromolar (µM) concentration of each test compound/complex.

The antifungal susceptibility MIC values for all test compounds against the yeast *C.albicans* (ATTC 10231) were determined by broth microdilution according to CLSI method M27-A3.<sup>42</sup> *C. albicans* was grown to the stationary phase overnight at 37°C on YEPD media. The cells were washed with PBS solution and resuspended in minimal media (MM) at a density of 5 × 10<sup>5</sup> cells/cm<sup>3</sup>. The 96 well microassay round bottomed plates were covered with acetate foil (Sarstedt) to prevent dehydration and incubated at 37°C.with continuous shaking for 24 hours. The optical density (OD) value was recorded

after 24 hours for each well at 540 nm. All assays were run in triplicate and on three independent occasions. The MIC<sub>100</sub> values were then determined and recorded as micrograms per millilitre or cubic centimetre ( $\mu\text{g}/\text{cm}^3$ ) and as micromolar ( $\mu\text{M}$ ) concentration of each test compound/complex.

The test complexes/compounds are arranged into six groups or families of compounds which will be referred to as such based on their similarities. The first group is comprised of 1,10-phen (**1**) and phendione (**2**). The second family is contains Ag(I) and Cu(II) bis-phendione perchlorate complexes (**6** and **7**). The third family is comprised of Mn(II) 1,10-phen phthalate, isophthalate and terephthalate complexes (**8-12**). The fourth family are Mn(II) and Cu(II) 1,10-phen octanedioate complexes (**13-14**). The fifth family contains Mn(II), Cu(II) and Ag(I) 1,10-phen trioxaundecanedioate complexes (**15-17**) and finally the sixth group contains a selection of known antifungal agents.

The growth inhibitory effects of the test compounds/complexes against the fungi *P. verrucosa* (a causative agent of human Chromoblastomycosis) and the Vero mammalian cell line are shown in Table **3.1**. It should be noted that although we currently have no IC<sub>50</sub> values against Vero cells for the seven clinical antifungal agents utilised in this study, it has been extensively documented in the literature that Amphotercin B and the azole antifungals cause severe side effects associated with their usage; (such as nephrotoxicity, hepatotoxicity including complete liver failure and congestive heart failure) which can result in dose-limiting concerns and lead to incomplete infection eradication and/or fatal outcomes due to infection reoccurrence or vital organ damage.<sup>43</sup>

The most active fungistatic agent against *P. verrucosa* was the dinuclear Ag(I) complex, **17** [Ag<sub>2</sub>(tdda)(phen)<sub>4</sub>]EtOH, MIC<sub>100</sub> = 0.37  $\mu\text{M}$ . This complex was also the only agent tested to display a significant fungicidal effect, MFC = (0.75  $\mu\text{M}$ ). Furthermore, the IC<sub>50</sub> value obtained for this complex (25.02  $\mu\text{M}$ ) indicates that it is tolerated to a moderate degree by normal African green monkey kidney epithelial cells (Vero cells) and this resulted in a high selectivity index of 120. This is a very significant result, showing that complex **17** possesses a high degree of cytoselectivity for *P. verrucosa* fungal cells over that of normal, mammalian epithelial cells. Interestingly, its mononuclear Cu(II) (**16**) and Mn(II) (**15**) analogues displayed only moderate fungistatic activity (MIC<sub>100</sub> values 12.5 and 6.25  $\mu\text{M}$  respectively) and were not fungicidal.

**Table 3.1:** *In vitro* fungistatic (MIC<sub>100</sub>), fungicidal (MFC and selectivity index (SI) values for 1,10-phen, phendione, selected metal complexes and known clinically employed antifungal agents against the dermaticeous fungi *Phialophora verrucosa*, an etiological agent of human Chromoblastomycosis. IC<sub>50</sub> values obtained using Vero cells, which are kidney epithelial cells harvested from a green African monkey. MIC, MFC and IC<sub>50</sub> compound concentration values are supplied in µg/cm<sup>3</sup> and micromolar (µM) in brackets.

<i>Phialophora verrucosa</i> (Causes Chromoblastomycosis)					
Compound		MIC <sub>100</sub>	MFC	IC <sub>50</sub>	Selectivity Index
		µg/cm <sup>3</sup> (µM)	µg/cm <sup>3</sup> (µM)	µg/cm <sup>3</sup> (µM) VERO cells	(SI) (IC <sub>50</sub> /MIC)
1	1,10-phenanthroline (1,10-phen)	0.8 (4.44)	6.2 (34.4)	>10 (55.49)	13
2	1,10-phenanthroline-5,6-dione (phendione)	2.5 (11.89)	20 (95.15)	6.6 (31.40)	3
6	[Ag(phendione) <sub>2</sub> ](ClO <sub>4</sub> )	5.00 (7.97)	>20.00 (31.86)	6.5 (10.36)	1
7	[Cu(phendione) <sub>3</sub> ](ClO <sub>4</sub> ) <sub>2</sub> ·4H <sub>2</sub> O	5.00 (5.18)	10 (10.36)	6.6 (6.84)	1
8	[Mn(ph)(phen)(H <sub>2</sub> O) <sub>2</sub> ]	2.72 (6.25)	>50	15.6 (35.84)	6
9	[Mn(ph)(phen) <sub>2</sub> (H <sub>2</sub> O)] <sub>2</sub> ·4H <sub>2</sub> O	2.18 (3.25)	>50	11.7 (17.47)	5
10	[Mn <sub>2</sub> (isoph) <sub>2</sub> (phen) <sub>3</sub> ] <sub>2</sub> ·4H <sub>2</sub> O	6.57 (6.25)	>50	125 (118.95)	19
11	{[Mn(phen) <sub>2</sub> (H <sub>2</sub> O) <sub>2</sub> ]} <sub>2</sub> (isoph) <sub>2</sub> (phen)·12H <sub>2</sub> O	10.17 (6.25)	>50	46.9 (28.82)	5
12	[Mn(tereph)(phen) <sub>2</sub> ] <sub>2</sub> ·5H <sub>2</sub> O	16.74 (25)	>50	46.9 (70.05)	3
13	[Mn <sub>2</sub> (η <sub>1</sub> η <sub>1</sub> μ <sub>2</sub> -oda)(phen) <sub>4</sub> (H <sub>2</sub> O) <sub>2</sub> ][Mn <sub>2</sub> (η <sub>1</sub> η <sub>1</sub> μ <sub>2</sub> -oda)(phen) <sub>4</sub> (η <sub>1</sub> -oda) <sub>2</sub> ] <sub>2</sub> ·4H <sub>2</sub> O	15.36 (6.25)	>50	375 (152.55)	24
14	[Cu <sub>2</sub> (oda)(phen) <sub>4</sub> ](ClO <sub>4</sub> ) <sub>2</sub> ·2.76H <sub>2</sub> O·EtOH	8.18 (6.25)	>50	11.7 (8.94)	1
15	{[Mn(3,6,9-tdda)(phen) <sub>2</sub> ] <sub>2</sub> ·3H <sub>2</sub> O·EtOH} <sub>n</sub>	4.60 (6.25)	>50	62.5 (84.96)	14
16	{[Cu(3,6,9-tdda)(phen) <sub>2</sub> ] <sub>2</sub> ·3H <sub>2</sub> O·EtOH} <sub>n</sub>	9.30 (12.5)	>50	5.85 (7.86)	1
17	[Ag <sub>2</sub> (3,6,9-tdda)(phen) <sub>4</sub> ] <sub>2</sub> ·EtOH	0.25 (0.37)	0.90 (0.75)	30.1 (25.02)	120
AMB	Amphotericin B	4 (4.33)	n.t	n.t	
FLC	Fluconazole	64 (208.97)	n.t	n.t	
VRC	Voriconazole	1 (2.86)	n.t	n.t	
ITC	Itraconazole	3.12 (4.42)	n.t	n.t	
CFG	Caspofungin	16 (14.63)	n.t	n.t	
5FC	Flucytosine	64 (495.77)	n.t	n.t	

Fungicidal compounds highlighted in yellow. All of the metal-free dicarboxylic acid ligands, the simple metal acetate salts and the metal carboxylate complexes displayed no significant antifungal activity (MIC<sub>100</sub> > 20µg/cm<sup>3</sup>). n.t. = not tested.

As each of the complexes **15-17** contain 1,10-phen and the 3,6,9-trioxaundecanedioate (tdda) dicarboxylate ligand, it can be surmised that there must be a certain degree of metal ion specificity to the mode of antifungal activity displayed by complex **17**. Metal-free 1,10-phen also displayed high fungastatic activity but was not fungicidal. When we compare the micromolar (µM) activity of **17** (which contains four 1,10-phen ligands per molecule) to that of metal-free 1,10-phen in micromolar it can be seen that complex **17** is 12 fold more active and remains 3 fold more active than metal-free 1,10-phen when adjusted for the four fold ratio of 1,10-phen content of complex **17**.

The dinuclear structure of Ag(I) complex **17** must also be considered, as the only other Ag(I)-based complex, **6**, also displayed some fungistatic activity ( $MIC_{100} = 7.97 \mu M$ ) but was ca. 22 fold less active than **17**. In addition, **6** did not prove to be fungicidal. Complex **6** is a mononuclear Ag(I) species and does not contain the dicarboxylate tdda ligand and, as such, is insoluble in water. These properties of **6** may explain its moderate fungistatic activity in comparison to the dinuclear, water soluble complex, **17**. Also, the selectivity index for **6** is very low (1.30), and may be due to the fact that it contains coordinated phendione instead of 1,10-phen. This is significant, as metal-free 1,10-phen had a ca. fivefold better selectivity index than metal-free phendione (12.50 and 2.64 respectively).

Four different classes (polyene, azole, echinocandin and fluorinated pyrimidine analogue) of clinical antifungal agents were also tested. Only the polyene, AMB, and the azoles VRC and ITC showed any significant fungistatic activity ( $MIC_{100} = 4.33, 2.86, 4.42 \mu M$ , respectively) and all were much less effective than complex **17**. Based upon these results, complex **17** would appear to be a promising lead antifungal agent against *P. verrucosa*.

Growth inhibitory data for the test compounds/complexes and clinically used drugs against *C. carrionii* (a causative agent of human Chromoblastomycosis) and Vero cells are shown in Table 3.2. The prescription antifungal agent, ITC, proved to be the most active fungistatic agent ( $MIC_{100} = 0.09 \mu M$ ), followed by another azole antifungal, VOR ( $MIC_{100} = 0.72 \mu M$ ). The dinuclear Ag(I) complex, **17** [ $Ag_2(tdda)(phen)_4$ ]EtOH, was the next most active agent ( $MIC_{100} = 1.25 \mu M$ ). Complex **17** also exhibited a notable fungicidal effect ( $MFC = 2.5 \mu M$ ). The low to medium cytotoxicity of **17** towards Vero cells ( $SI = 20$ ) suggests that this complex may not differentiate to a high enough extent between fungal and mammalian cells. Furthermore, the Mn(II) (**15**) and Cu(II) (**16**) analogues of complex **17** also exhibited low fungistatic MIC's, with the Mn(II) complex **15** also proving fungicidal ( $MFC = 12.5 \mu M$ ) and also having a slightly better selectivity index ( $SI = 27$ ) compared to **17**. The Ag(I), Mn(II) and Cu(II) 1,10-phen tdda complexes (**15**, **16** and **17**) all display good fungistatic/fungicidal activity against *C. carrionii* cells, suggesting that the mode of antifungal activity for these compounds is not highly metal ion specific.

Metal-free 1,10-phen (**1**) and phendione (**2**) displayed similar fungistatic values ( $MIC_{100} = 15.6, 12.5 \mu M$ ), had very low selectivity indexes. In addition, phendione (**2**) was ca. 2-

fold more fungicidal than 1,10-phen. Complexes **6**, **7**, **11-14**, 1,10-phen (**1**) and phendione (**2**) exhibited MIC<sub>100</sub> values in the range of 3.12.-12.5 μM and all proved to be fungicidal (MFC range 6.25-50 μM).

The Mn(II) 1,10-phen octanedioate complex, **13**, had a reasonably high selectivity index (SI = 49) due to its extremely high IC<sub>50</sub> value (152.55 μM), showing that it is very well tolerated by Vero cells and also exhibited relatively good fungistatic and fungicidal activity.

**Table 3.2:** *In vitro* fungistatic (MIC<sub>100</sub>), fungicidal (MFC and selectivity index (SI) values for 1,10-phen, phendione, selected metal complexes and known clinically employed antifungal agents against the dermaticeous fungi *Cladophialophora carrionii*, an etiological agent of human Chromoblastomycosis. IC<sub>50</sub> values obtained using Vero cells, which are kidney epithelial cells harvested from a green African monkey. MIC, MFC and IC<sub>50</sub> compound concentration values are supplied in μg/cm<sup>3</sup> and micromolar (μM) in brackets

<i>Cladophialophora carrionii</i> (Causes Chromoblastomycosis)					
Compound		MIC <sub>100</sub>	MFC	IC <sub>50</sub>	Selectivity Index
		μg/cm <sup>3</sup> (μM)	μg/cm <sup>3</sup> (μM)	μg/cm <sup>3</sup> (μM) VERO cells	(SI) (IC <sub>50</sub> /MIC)
<b>1</b>	1,10-phenanthroline (1,10-phen)	2.81 (15.6)	10.81 (60)	>10 (55.49)	4
<b>2</b>	1,10-phenanthroline-5,6-dione (phendione)	2.63 (12.5)	5.25 (25)	6.6 (31.40)	3
<b>6</b>	[Ag(phendione) <sub>2</sub> ](ClO <sub>4</sub> )	7.85 (12.5)	15.69 (25)	6.5 (10.36)	1
<b>7</b>	[Cu(phendione) <sub>3</sub> ](ClO <sub>4</sub> ) <sub>2</sub> ·4H <sub>2</sub> O	12.06 (12.5)	12.06 (12.5)	6.6 (6.84)	1
<b>8</b>	[Mn(ph)(phen)(H <sub>2</sub> O) <sub>2</sub> ]	5.44 (12.5)	43.53 (100)	15.6 (35.84)	3
<b>9</b>	[Mn(ph)(phen) <sub>2</sub> (H <sub>2</sub> O)]4H <sub>2</sub> O	2.14 (3.2)	16.74 (25)	11.7 (17.47)	5
<b>10</b>	[Mn <sub>2</sub> (isoph) <sub>2</sub> (phen) <sub>3</sub> ]4H <sub>2</sub> O	6.57 (6.25)	105.08 (100)	125 (118.95)	19
<b>11</b>	{[Mn(phen) <sub>2</sub> (H <sub>2</sub> O) <sub>2</sub> ] <sub>2</sub> (isoph) <sub>2</sub> (phen).12H <sub>2</sub> O	5.08 (3.12)	20.34 (12.5)	46.9 (28.82)	9
<b>12</b>	[Mn(tereph)(phen) <sub>2</sub> ]5H <sub>2</sub> O	8.37 (12.5)	33.48 (50)	46.9 (70.05)	6
<b>13</b>	[Mn <sub>2</sub> (η <sub>1</sub> ,η <sub>1</sub> ,μ <sub>2</sub> -oda)(phen) <sub>4</sub> (H <sub>2</sub> O) <sub>2</sub> ][Mn <sub>2</sub> (η <sub>1</sub> ,η <sub>1</sub> ,μ <sub>2</sub> -oda)(phen) <sub>4</sub> (η <sub>1</sub> -oda) <sub>2</sub> ]4H <sub>2</sub> O	7.67 (3.12)	15.36 (6.25)	375 (152.55)	49
<b>14</b>	[Cu <sub>2</sub> (oda)(phen) <sub>4</sub> ](ClO <sub>4</sub> ) <sub>2</sub> ·2.76H <sub>2</sub> O·EtOH	16.37 (12.5)	32.73 (25)	11.7 (8.94)	1
<b>15</b>	{[Mn(3,6,9-tdda)(phen) <sub>2</sub> ]3H <sub>2</sub> O·EtOH} <sub>n</sub>	2.30 (3.12)	9.20 (12.5)	62.5 (84.96)	27
<b>16</b>	{[Cu(3,6,9-tdda)(phen) <sub>2</sub> ]3H <sub>2</sub> O·EtOH} <sub>n</sub>	4.65 (6.25)	37.21 (50)	5.85 (7.86)	1
<b>17</b>	[Ag <sub>2</sub> (3,6,9-tdda)(phen) <sub>4</sub> ]EtOH	1.50 (1.25)	3.01 (2.5)	30.1 (25.02)	20
<b>AMB</b>	Amphotericin B	8.00 (8.66)	n.t.	n.t.	
<b>FLC</b>	Fluconazole	64 (208.97)	n.t.	n.t.	
<b>VRC</b>	Voriconazole	0.25 (0.72)	n.t.	n.t.	
<b>ITC</b>	Itraconazole	0.063 (0.09)	n.t.	n.t.	
<b>CFG</b>	Caspofungin	2 (1.83)	n.t.	n.t.	
<b>5FC</b>	Flucytosine	8 (61.97)	n.t.	n.t.	

Fungicidal compounds highlighted in yellow. n.t. = not tested.

Although ITC is by far the most active compound against *C. carrionii* complexes **13**, **15** and **17** still represent promising antifungal agents considering that all three exhibit

fungistatic and fungicidal activity. Furthermore, the Mn(II) complex, **13**, is not particularly cytotoxic to Vero cells giving it a reasonably high selectivity index (SI = 49) for *C. carrionii* cells.

Growth inhibitory data for the test compounds/complexes and five clinically used drugs against *E. dermatitidis* (an etiological agent of human Phaeohyphomycosis) and Vero cells are shown in Table 3.3.

**Table 3.3:** *In vitro* fungistatic (MIC<sub>100</sub>), fungicidal (MFC and selectivity index (SI) values for 1,10-phen, phendione, selected metal complexes and known clinically employed antifungal agents against the dermaticeous fungi *Exophiala dermatitidis*, an etiological agent of human Phaeohyphomycosis. IC<sub>50</sub> values obtained using Vero cells, which are kidney epithelial cells harvested from a green African monkey. MIC, MFC and IC<sub>50</sub> compound concentration values are supplied in µg/cm<sup>3</sup> and micromolar (µM) in brackets.

		<i>Exophiala dermatitidis</i> (Causes Phaeohyphomycosis)			
Compound		MIC <sub>100</sub>	MFC	IC <sub>50</sub>	Selectivity Index
		µg/cm <sup>3</sup> (µM)	µg/cm <sup>3</sup> (µM)	µg/cm <sup>3</sup> (µM) VERO cells	(SI) (IC <sub>50</sub> /MIC)
1	1,10-phenanthroline (1,10-phen)	3.12 (17.31)	>200 (1110)	>10 (55.49)	3
2	1,10-phenanthroline-5,6-dione (phendione)	2.50 (11.89)	20 (95.15)	6.6 (31.40)	3
6	[Ag(phendione) <sub>2</sub> ](ClO <sub>4</sub> )	5.00 (7.97)	>20.00 (32)	6.5 (10.36)	1
7	[Cu(phendione) <sub>3</sub> ](ClO <sub>4</sub> ) <sub>2</sub> ·4H <sub>2</sub> O	5.00 (5.18)	>20.00 (21)	6.6 (6.84)	1
8	[Mn(ph)(phen)(H <sub>2</sub> O) <sub>2</sub> ]	2.72 (6.25)	>43.53 (100)	15.6 (35.84)	6
9	[Mn(ph)(phen) <sub>2</sub> (H <sub>2</sub> O)]4H <sub>2</sub> O	2.09 (3.12)	>66.96 (100)	11.7 (17.47)	6
10	[Mn <sub>2</sub> (isoph) <sub>2</sub> (phen) <sub>3</sub> ]4H <sub>2</sub> O	6.57 (6.25)	>105.08 (100)	125 (118.95)	19
11	{[Mn(phen) <sub>2</sub> (H <sub>2</sub> O) <sub>2</sub> ] <sub>2</sub> (isoph) <sub>2</sub> (phen).12H <sub>2</sub> O	10.17 (6.25)	>162.74 (100)	46.9 (28.82)	5
12	[Mn(tereph)(phen) <sub>2</sub> ]5H <sub>2</sub> O	16.74 (25)	>66.96 (100)	46.9 (70.05)	3
13	[Mn <sub>2</sub> (η <sub>1</sub> η <sub>1</sub> μ <sub>2</sub> -oda)(phen) <sub>4</sub> (H <sub>2</sub> O) <sub>2</sub> ][Mn <sub>2</sub> (η <sub>1</sub> η <sub>1</sub> μ <sub>2</sub> -oda)(phen) <sub>4</sub> (η <sub>1</sub> -oda) <sub>2</sub> ]4H <sub>2</sub> O	15.36 (6.25)	>245.82 (100)	375 (152.55)	24
14	[Cu <sub>2</sub> (oda)(phen) <sub>4</sub> ](ClO <sub>4</sub> ) <sub>2</sub> ·2.76H <sub>2</sub> O·EtOH	8.18 (6.25)	>130.92 (100)	11.7 (8.94)	1
15	{[Mn(3,6,9-tda)(phen) <sub>2</sub> ]3H <sub>2</sub> O·EtOH} <sub>n</sub>	4.60 (6.25)	>73.56 (100)	62.5 (84.96)	14
16	{[Cu(3,6,9-tda)(phen) <sub>2</sub> ]3H <sub>2</sub> O·EtOH} <sub>n</sub>	9.30 (12.5)	>74.43 (100)	5.85 (7.86)	1
17	[Ag <sub>2</sub> (3,6,9-tda)(phen) <sub>4</sub> ]EtOH	0.18 (0.15)	0.75 (0.62)	30.1 (25.02)	167
AMB	Amphotericin B	0.5 (0.54)		n.t	
FLC	Fluconazole	16 (52.24)		n.t	
VRC	Voriconazole	0.5 (1.43)		n.t	
ITC	Itraconazole	0.25 (0.35)		n.t	
CFG	Caspofungin	16 (14.63)		n.t	

Fungicidal compounds highlighted in yellow. n.t. = not tested.

Again the most active fungistatic agent was the Ag(I) complex, **17**, ( $MIC_{100} = 0.15 \mu M$ ) and was the only test complex that was also fungicidal ( $MFC = 0.62 \mu M$ ), and this was coupled with a high selectivity index ( $SI = 167$ ). The next most active fungistatic agent was the known antifungal azole, Itraconazole (ITC) ( $MIC = 0.35 \mu M$ ). This was followed by the most widely used antifungal agent, Amphotericin B (AMB) ( $MIC = 0.54 \mu M$ ). Voriconazole (VRC) also exhibited good fungistatic activity ( $MIC = 1.43 \mu M$ ).

Immunocompromised patients have a diminished capacity to cope with “drug” induced organ toxicity and hence an *in vitro* high selectivity index like that displayed by complex **17** is encouraging for possible further development as a lead antifungal agent. The Mn(II) 1,10-phen phthalate complex **9** also exhibited a low  $MIC_{100}$  value of  $3.12 \mu M$  but as its  $IC_{50}$  against Vero cells is also quite low ( $17.47 \mu M$ ), this resulted in a low selectivity index for the complex.

Growth inhibitory data for the test compounds/complexes and five clinically used drugs against *P. boydii* (a causative agent of human Eumycetoma) and Vero cells are shown in Table 3.4. *P. boydii* is the sexual reproductive form (telemorph), and the asexual form of this fungus is named *Scedosporium apiospermum*. Both fungi are emerging causes of opportunistic granulomatous fungal infections in humans (termed Eumycetoma). As previously stated, these fungi have in the past proven to be pharmacologically refractory and the most effective treatment was surgical removal of the infected area and even amputation of entire limbs has been necessary. However, recently certain members of the azole class of antifungals have proven to be effective in treating these mycoses.<sup>16, 44</sup>

Interestingly the metal-free phendione (**2**) and 1,10-phen (**1**) proved to be more active than their metal complexes, and were also vastly superior to the known antifungal agents (Table 3.4). This suggests that the metal sequestering, chelation capability of phendione (**2**) and 1,10-phen (**1**) may be the cause of their greater antifungal activity against *P. boydii* cells. The higher activity of phendione (**2**) compared to 1,10-phen (**1**), may be a consequence of the redox activity of the diketone moiety in **2**.<sup>34a</sup>



**Table 3.4:** *In vitro* fungistatic (MIC<sub>100</sub>) activity and selectivity index (SI) values for 1,10-phen, phendione, selected metal complexes and known clinically employed antifungal agents against *Pseudallescheria boydii*, an etiological agent of human Eumycetoma. IC<sub>50</sub> values obtained using Vero cells, which are kidney epithelial cells harvested from a green African monkey. MIC and IC<sub>50</sub> compound concentration values are supplied in µg/cm<sup>3</sup> and micromolar (µM) in brackets

		<i>Pseudallescheria boydii</i> (Causes Eumycetoma)		
Compound		MIC <sub>100</sub>	IC <sub>50</sub>	Selectivity Index (SI) (IC <sub>50</sub> /MIC)
		µg/cm <sup>3</sup> (µM)	µg/cm <sup>3</sup> (µM) VERO cells	
1	1,10-phenanthroline (1,10-phen)	0.125 (0.69)	>10 (55.49)	80
2	1,10-phenanthroline-5,6-dione (phendione)	0.0313 (0.15)	6.6 (31.40)	211
6	[Ag(phendione) <sub>2</sub> ](ClO <sub>4</sub> ) <sub>2</sub>	0.5 (0.8)	6.5 (10.36)	3
7	[Cu(phendione) <sub>3</sub> ](ClO <sub>4</sub> ) <sub>2</sub> ·4H <sub>2</sub> O	2 (2.07)	6.6 (6.84)	3
8	[Mn(ph)(phen)(H <sub>2</sub> O) <sub>2</sub> ]	1 (2.3)	15.6 (35.84)	16
9	[Mn(ph)(phen) <sub>2</sub> (H <sub>2</sub> O)]·4H <sub>2</sub> O	2 (2.99)	11.7 (17.47)	6
10	[Mn <sub>2</sub> (isoph) <sub>2</sub> (phen) <sub>3</sub> ] <sub>2</sub> ·4H <sub>2</sub> O	1 (0.95)	125 (118.95)	125
11	{[Mn(phen) <sub>2</sub> (H <sub>2</sub> O) <sub>2</sub> ]} <sub>2</sub> (isoph) <sub>2</sub> (phen)·12H <sub>2</sub> O	1 (0.61)	46.9 (28.82)	47
12	[Mn(tereph)(phen) <sub>2</sub> ] <sub>2</sub> ·5H <sub>2</sub> O	2 (2.99)	46.9 (70.05)	23
13	[Mn <sub>2</sub> (η <sub>1</sub> ,η <sub>1</sub> ,μ <sub>2</sub> -oda)(phen) <sub>4</sub> (H <sub>2</sub> O) <sub>2</sub> ][Mn <sub>2</sub> (η <sub>1</sub> ,η <sub>1</sub> ,μ <sub>2</sub> -oda)(phen) <sub>4</sub> (η <sub>1</sub> -oda) <sub>2</sub> ] <sub>2</sub> ·4H <sub>2</sub> O	2 (0.81)	375 (152.55)	188
14	[Cu <sub>2</sub> (oda)(phen) <sub>4</sub> ](ClO <sub>4</sub> ) <sub>2</sub> ·2.76H <sub>2</sub> O·EtOH	2 (1.53)	11.7 (8.94)	6
15	{[Mn(3,6,9-tdda)(phen) <sub>2</sub> ] <sub>3</sub> ·3H <sub>2</sub> O·EtOH} <sub>n</sub>	2 (2.72)	62.5 (84.96)	31
16	{[Cu(3,6,9-tdda)(phen) <sub>2</sub> ] <sub>3</sub> ·3H <sub>2</sub> O·EtOH} <sub>n</sub>	16 (21.5)	5.85 (7.86)	0
17	[Ag <sub>2</sub> (3,6,9-tdda)(phen) <sub>4</sub> ] <sub>2</sub> ·EtOH	1 (0.83)	30.1 (25.02)	30
AMB	Amphotericin B	>16 (17.33)	n.t.	
FLC	Fluconazole	32 (104.48)	n.t.	
VRC	Voriconazole	1 (2.86)	n.t.	
ITC	Itraconazole	8 (11.34)	n.t.	
MFG	Micafungin	>32 (25.19)	n.t.	

n.t. = not tested.

Of the metal complexes **6**, **11**, **13** and **17** were quite active, with **6** and **13** being almost equal in activity (based on their molarity) closely followed by **17** but they complex had very different selectivity indexes. For example, **6** had a very low SI (3) whilst **13** was high (188). Complex **17** had a low to mid-range SI (30). Both **6** and **17** are Ag(I)-based complexes and exhibited very similar MIC<sub>100</sub> values, suggesting that the Ag(I) ion is mostly responsible for the antifungal effect. It is also noteworthy that complex **13** proved to be very active given that our groups previous studies on this complex have proven that it is an avid producer of redox generated intracellular reactive oxygen species (ROS) and unlike the Ag(I)-based complexes (**6** and **17**) is Mn(II)-based.<sup>31a</sup>



Our collaborators in Professor Andre L.S. Santos's laboratory in Brazil also conducted a study using the *P. boydii* asexual form, *S. apiospermum*.<sup>45</sup> They found that 1,10-phen (**1**) was able to completely inhibit metallopeptidases secreted by *S. apiospermum*, most likely via metal ion sequestration from the active site of these metallopeptidases. The metallopeptidases secreted by *S. apiospermum* are directly linked to the destruction of key host mammalian cell proteins and therefore to the proliferation of the fungus. If metal-free phendione (**2**) is acting as a metallopeptidase inhibitor via its metal chelation moiety (*N,N'*-diimine) whilst also inducing redox-generated oxidative stress via its diketone moiety and perhaps further redox-generated oxidative damage via the formation of an in cellulo/*in vitro* metal complex, this synergistic/dual action could, in part, explain its superior activity.

It is also clear that the Mn(II)-based complexes (**8-13** and **15**) are all relatively active. In addition Cu(II)-based octanedioate and trioxaundecanedioate complexes **14** and **16** were much less active than their Mn(II)-based analogues. Hence, it would seem that there is some metal ion specificity to their antifungal activity. This specificity may be due in part, to the type of free radicals or ROS/RNS (superoxide  $O_2^{\bullet-}$ , hydroxyl radical  $OH^{\bullet}$ , nitric oxide  $\bullet NO$ ) that each complex produces and the associated differing biological damaging capacities of those radicals. The hydroxyl radical ( $OH^{\bullet}$ ), for example, is much more reactive than both superoxide ( $O_2^{\bullet-}$ ) or nitric oxide ( $\bullet NO$ ) which can react directly with only a few molecules in the human body, whereas the  $OH^{\bullet}$  can react with almost anything, including DNA purine base pairs (forming further DNA base radicals/mutations and DNA scission) and hydrocarbons (including the fatty acid side-chains of membrane lipids) to abstract  $H^{\bullet}$  and leave behind another radical.<sup>46</sup> The resulting free radical chain reaction can cause a multitude of damaging biological consequences including DNA strand scission and lipid membrane peroxidation.<sup>47</sup>

Previously our group has studied the Mn(II)-based complex **13** and the Cu(II)-based complex **14** which are analogues of one another and discovered that both complexes produce intracellular ROS.<sup>31a</sup> Complex **13** is much more active in this regard than **14**, with **13** producing exceptionally high levels of ROS. In addition, mechanistic experiments showed that **13** has exceptional superoxide dismutase (SOD) and catalase (CAT) mimic activity. **13** can convert superoxide to hydrogen peroxide and oxygen (SOD like action) and then also convert hydrogen peroxide to water and oxygen (CAT like action). In contrast the Cu(II)-based complex **14**, is only capable of SOD mimic

activity but to a lesser extent than **13**. It is possible then to surmise that the Mn(II)-based complexes (**8**, **13** and **15**) are capable of producing higher levels of ROS than their Cu(II) analogues which may explain their superior antifungal properties. In addition, these results would suggest that the type of ROS being produced by Mn(II)-based complexes is different to that of Cu(II)-based complexes, perhaps the Mn(II)-based complexes produce higher quantities of the more reactive and damaging hydroxyl radical (OH•). Efforts are currently underway in our laboratory to establish direct experimental evidence to ascertain the identity and quantity of each reactive species being produced by these complexes.

**Table 3.5:** *In vitro* fungistatic (MIC<sub>100</sub>) activity and selectivity index (SI) values for 1,10-phen, phendione, selected metal complexes and known clinically employed antifungal agents against *Pseudallescheria minutispora*, an etiological agent of human Eumycetoma. IC<sub>50</sub> values obtained using Vero cells, which are kidney epithelial cells harvested from a green African monkey. MIC and IC<sub>50</sub> compound concentration values are supplied in µg/cm<sup>3</sup> and micromolar (µM) in brackets

		<i>Pseudallescheria minutispora</i> (Causes Eumycetoma)		
Compound		MIC <sub>100</sub> µg/cm <sup>3</sup> (µM)	IC <sub>50</sub> µg/cm <sup>3</sup> (µM) VERO cells	Selectivity Index (SI) (IC <sub>50</sub> /MIC)
<b>1</b>	1,10-phenanthroline (1,10-phen)	0.031 (0.17)	>10 (55.49)	323
<b>2</b>	1,10-phenanthroline-5,6-dione (phendione)	0.063 (0.297)	6.6 (31.40)	105
<b>6</b>	[Ag(phendione) <sub>2</sub> ](ClO <sub>4</sub> )	1 (1.59)	6.5 (10.36)	7
<b>7</b>	[Cu(phendione) <sub>3</sub> ](ClO <sub>4</sub> ) <sub>2</sub> ·4H <sub>2</sub> O	1 (1.04)	6.6 (6.84)	7
<b>8</b>	[Mn(ph)(phen)(H <sub>2</sub> O) <sub>2</sub> ]	2 (4.59)	15.6 (35.84)	8
<b>9</b>	[Mn(ph)(phen) <sub>2</sub> (H <sub>2</sub> O)] <sub>2</sub> ·4H <sub>2</sub> O	4 (5.97)	11.7 (17.47)	3
<b>10</b>	[Mn <sub>2</sub> (isoph) <sub>2</sub> (phen) <sub>3</sub> ] <sub>2</sub> ·4H <sub>2</sub> O	2 (1.90)	125 (118.95)	63
<b>11</b>	{[Mn(phen) <sub>2</sub> (H <sub>2</sub> O) <sub>2</sub> ] <sub>2</sub> (isoph) <sub>2</sub> (phen)} <sub>2</sub> ·12H <sub>2</sub> O	2 (1.23)	46.9 (28.82)	23
<b>12</b>	[Mn(tereph)(phen) <sub>2</sub> ] <sub>2</sub> ·5H <sub>2</sub> O	2 (2.99)	46.9 (70.05)	23
<b>13</b>	[Mn <sub>2</sub> (η <sub>1</sub> η <sub>1</sub> μ <sub>2</sub> -oda)(phen) <sub>4</sub> (H <sub>2</sub> O) <sub>2</sub> ][Mn <sub>2</sub> (η <sub>1</sub> η <sub>1</sub> μ <sub>2</sub> -oda)(phen) <sub>4</sub> (η <sub>1</sub> -oda) <sub>2</sub> ] <sub>2</sub> ·4H <sub>2</sub> O	0.063 (0.03)	375 (152.55)	5952
<b>14</b>	[Cu <sub>2</sub> (oda)(phen) <sub>4</sub> ](ClO <sub>4</sub> ) <sub>2</sub> ·2.76H <sub>2</sub> O·EtOH	0.125 (0.10)	11.7 (8.94)	94
<b>15</b>	{[Mn(3,6,9-tdda)(phen) <sub>2</sub> ] <sub>2</sub> ·3H <sub>2</sub> O·EtOH} <sub>n</sub>	1 (1.36)	62.5 (84.96)	63
<b>16</b>	{[Cu(3,6,9-tdda)(phen) <sub>2</sub> ] <sub>2</sub> ·3H <sub>2</sub> O·EtOH} <sub>n</sub>	1 (1.34)	5.85 (7.86)	6
<b>17</b>	[Ag <sub>2</sub> (3,6,9-tdda)(phen) <sub>4</sub> ] <sub>2</sub> ·EtOH	0.125 (0.10)	30.1 (25.02)	241
<b>AMB</b>	Amphotericin B	>16 (17.33)	n.t.	
<b>FLC</b>	Fluconazole	0.031 (0.102)	n.t.	
<b>VRC</b>	Voriconazole	>16 (45.80)	n.t.	
<b>ITC</b>	Itraconazole	0.031 (0.044)	n.t.	
<b>MFG</b>	Micafungin	>32 (25.19)	n.t.	

n.t. = not tested.

Table 3.5 shows the fungistatic ( $MIC_{100}$ ) and  $IC_{50}$  results obtained for the test agents against *P. minutispora* (an etiological agent of human Eumycetoma) and the Vero mammalian cell line. Whilst none of the test complexes were fungicidal a varying degree of fungistatic activity was observed. By far the most active fungistatic agent was the Mn(II) complex, **13**, with an extremely low  $MIC_{100}$  value ( $0.03 \mu M$ ). In addition, this complex also had an extremely high SI (ca. 6000), making it very highly cytoselective for *P. minutispora* fungal cells over mammalian Vero cells. Complex **13** was 1.5 fold more active than the azole, ITC. Complexes **17** and **14** were also quite active and both had an  $MIC_{100}$  value of  $0.10 \mu M$ . However, the latter two complexes had vastly different SI's, with **17** being twice as cytoselective for *P. minutispora* cells.

It should be noted that **13**, **14** and **17** are water-soluble complexes a property conferred by their dicarboxylate ligands (oda and tdda) and it may be significant that all three complexes are also dinuclear. The Mn(II) and Cu(II) octanedioate complexes **13** and **14** respectively, are known potent producers of ROS,<sup>31a</sup> and this may be a mediating factor for their fungistatic effect. Complex **17** is a dinuclear Ag(I) 1,10-phen trioxaundecanedioate complex and would be unlikely to be redox active, therefore a reasonable assumption would be that its fungistatic capability is due to the Ag(I) ion's and that its superior fungistatic activity to the only other Ag(I) complex **6** is due to its improved aqueous solubility and dinuclearity. The polyene, Amphotercin B (AMB), and the echinocandin, Micafungin (MFG), were essentially inactive at the concentrations used.

In Table 3.6 are displayed the *in vitro* fungistatic ( $MIC_{100}$ ) and  $IC_{50}$  results against *S. aurantiacum* and the simian kidney epithelial Vero cell line. None of the test compounds/complexes were fungicidal. The know antifungal, Voriconazole (VRC), proved to be the most active fungistatic agent ( $MIC_{100} = 0.36 \mu M$ ). The next most active was the Ag(I) complex **17**, ( $MIC_{100} = 0.42 \mu M$ ). This complex also demonstrated a reasonable level of cytoselectivity, signified by its mid-range SI (60). Complex **17** was vastly more active than complex **6** which was the only other Ag(I) complex tested. The high activity of **17** may be due to its water-solubility and dinuclear structure. Once again, the Mn(II) complex, **13**, had a very low  $MIC_{100}$  value ( $0.81 \mu M$ ) and consequently maintained its high cytoselectivity (SI = 188).

The next most active agent was complex **15** with an MIC<sub>100</sub> of 1.36 μM, although this Mn(II) 1,10-phen trioxaundecanedioate complex, **15**, was also quite active it was ca. 3 fold less active than its Ag(I) analogue **17**. Furthermore, the Cu(II) 1,10-phen trioxaundecanedioate analogue, **15**, was even less active, suggesting that there is some metal ion specificity. This proposed Ag(I)-specific antifungal effect is granted additional weight considering that all three complexes **15**, **16** and **17** are water soluble to the same degree and contain the same ligands (1,10-phen and tdda). Whilst 1,10-phen (**1**) also demonstrated significant activity, phendione (**2**) showed only limited inhibitory effects.

**Table 3.6:** *In vitro* fungistatic (MIC<sub>100</sub>) activity and selectivity index (SI) values for 1,10-phen, phendione, selected metal complexes and known clinically employed antifungal agents against *Scedosporium aurantiacum*, an etiological agent of human Eumycetoma. IC<sub>50</sub> values obtained using Vero cells, which are kidney epithelial cells harvested from a green African monkey. MIC and IC<sub>50</sub> compound concentration values are supplied in μg/cm<sup>3</sup> and micromolar (μM) in brackets

		<i>Scedosporium aurantiacum</i> (Causes Eumycetoma)		
Compound		MIC <sub>100</sub>	IC <sub>50</sub>	Selectivity Index
		μg/cm <sup>3</sup> (μM)	μg/cm <sup>3</sup> (μM) VERO cells	(SI) (IC <sub>50</sub> /MIC)
<b>1</b>	1,10-phenanthroline (1,10-phen)	0.5 (2.78)	>10 (55.49)	20
<b>2</b>	1,10-phenanthroline-5,6-dione (phendione)	2 (9.52)	6.6 (31.40)	3
<b>6</b>	[Ag(phendione) <sub>2</sub> ](ClO <sub>4</sub> )	4 (6.37)	6.5 (10.36)	2
<b>7</b>	[Cu(phendione) <sub>3</sub> ](ClO <sub>4</sub> ) <sub>2</sub> ·4H <sub>2</sub> O	4 (4.14)	6.6 (6.84)	2
<b>8</b>	[Mn(ph)(phen)(H <sub>2</sub> O) <sub>2</sub> ]	4 (9.19)	15.6 (35.84)	4
<b>9</b>	[Mn(ph)(phen) <sub>2</sub> (H <sub>2</sub> O)] <sub>2</sub> ·4H <sub>2</sub> O	8 (11.95)	11.7 (17.47)	1
<b>10</b>	[Mn <sub>2</sub> (isoph) <sub>2</sub> (phen) <sub>3</sub> ] <sub>2</sub> ·4H <sub>2</sub> O	4 (3.81)	125 (118.95)	31
<b>11</b>	{[Mn(phen) <sub>2</sub> (H <sub>2</sub> O) <sub>2</sub> ] <sub>2</sub> (isoph) <sub>2</sub> (phen)} <sub>2</sub> ·12H <sub>2</sub> O	4 (2.46)	46.9 (28.82)	12
<b>12</b>	[Mn(tereph)(phen) <sub>2</sub> ] <sub>2</sub> ·5H <sub>2</sub> O	2 (2.99)	46.9 (70.05)	23
<b>13</b>	[Mn <sub>2</sub> (η <sub>1</sub> η <sub>1</sub> μ <sub>2</sub> -oda)(phen) <sub>4</sub> (H <sub>2</sub> O) <sub>2</sub> ][Mn <sub>2</sub> (η <sub>1</sub> η <sub>1</sub> μ <sub>2</sub> -oda)(phen) <sub>4</sub> (η <sub>1</sub> -oda) <sub>2</sub> ] <sub>2</sub> ·4H <sub>2</sub> O	2 (0.81)	375 (152.55)	188
<b>14</b>	[Cu <sub>2</sub> (oda)(phen) <sub>4</sub> ](ClO <sub>4</sub> ) <sub>2</sub> ·2.76H <sub>2</sub> O·EtOH	4 (3.06)	11.7 (8.94)	3
<b>15</b>	{[Mn(3,6,9-tdda)(phen) <sub>2</sub> ] <sub>3</sub> ·3H <sub>2</sub> O·EtOH} <sub>n</sub>	1 (1.36)	62.5 (84.96)	63
<b>16</b>	{[Cu(3,6,9-tdda)(phen) <sub>2</sub> ] <sub>3</sub> ·3H <sub>2</sub> O·EtOH} <sub>n</sub>	2 (2.69)	5.85 (7.86)	3
<b>17</b>	[Ag <sub>2</sub> (3,6,9-tdda)(phen) <sub>4</sub> ] <sub>2</sub> ·EtOH	0.5 (0.42)	30.1 (25.02)	60
<b>AMB</b>	Amphotericin B	>16 (17.33)	n.t.	
<b>FLC</b>	Fluconazole	16 (52.24)	n.t.	
<b>VRC</b>	Voriconazole	0.125 (0.36)	n.t.	
<b>ITC</b>	Itraconazole	4 (5.67)	n.t.	
<b>MFG</b>	Micafungin	>32 (25.19)	n.t.	

n.t. = not tested.

The Mn(II) 1,10-phen phthalate complexes **8-12** all exhibited reasonable fungistatic activity, the best of which was complex **11** ( $\text{MIC}_{100} = 2.46 \mu\text{M}$ ). This family of complexes (**8-12**) were also poorly cytoselective with the most active of member complex **11**, displaying a low SI (12). Finally none of the other known antifungal agents tested demonstrated any significant fungistatic activity against *S. aurantiacum*, with AMB, FLC and MFG all having  $\text{MIC}_{100}$  values  $> 17 \mu\text{M}$ .

The fungistatic ( $\text{MIC}_{100}$ ) and  $\text{IC}_{50}$  results against *S. proliticans* and the Vero cell line are shown in Table 3.7. Again, none of the test complexes/compounds had a fungicidal effect. In addition, none of clinical antifungal agents were particularly effective, the being Micafungin, MFG ( $\text{MIC}_{100} = 6.30 \mu\text{M}$ ). Again, the Mn(II) complex, **13**, was the most active fungistatic agent ( $\text{MIC}_{100} = 0.81 \mu\text{M}$ ). This complex was ca. two fold more active than the Mn(II) terephthalate, **12**, and ca. 8 fold more active Micafungin, MFG. In addition, **13** was highly cytoselective ( $\text{SI} = 188$ ). In comparison, complex **14**, which is the Cu(II) analogue of **13**, exhibited only moderate fungistatic activity ( $\text{MIC}_{100} = 3.06 \mu\text{M}$ ) and poor cytoselectivity ( $\text{SI} = 3$ ).

Complex **12** was the next most active fungistatic agent tested with a low  $\text{MIC}_{100} = 1.49 \mu\text{M}$  and a good degree of cytoselectivity ( $\text{SI} = 47$ ). Although the Cu(II) phendione complex, **7**, was quite fungistatic ( $\text{MIC}_{100} = 2.07 \mu\text{M}$ ) it was, however, poorly selective ( $\text{SI} = 3$ ). Furthermore, its Ag(I) analogue, **6**, exhibited even less fungistatic activity ( $\text{MIC}_{100} = 3.179 \mu\text{M}$ ) and was also poorly cytoselectivity ( $\text{SI} = 3$ ).

The most active of the trioxaundecanedioate family of complexes was the Cu(II) complex, **16**, ( $\text{MIC}_{100} = 2.69 \mu\text{M}$ ). However, this complex displayed very poor cytoselectivity ( $\text{SI} = 3$ ). Its Mn(II) analogue, **15** displayed comparable fungistatic activity ( $\text{MIC}_{100} = 2.72 \mu\text{M}$ ) but was much more cytoselective ( $\text{SI} = 31$ ). The final member of the trioxaundecanedioate family of complexes, the dinuclear Ag(I) complex, **17**, was less active than **15** and **16** and also had a low SI value (8).

1-10-Phen (**1**) was also quite fungistatic ( $\text{MIC}_{100} = 2.78 \mu\text{M}$ ) and moderately cytoselective ( $\text{SI} = 20$ ). In comparison to phendione (**2**), 1,10-phen (**1**) was ca. 4 fold more fungistatic and ca. 6 fold more cytoselective.

**Table 3.7:** *In vitro* fungistatic (MIC<sub>100</sub>) activity and selectivity index (SI) values for 1,10-phen, phendione, selected metal complexes and known clinically employed antifungal agents against *Scedosporium prolificans*, an etiological agent of human Eumycetoma. IC<sub>50</sub> values obtained using Vero cells, which are kidney epithelial cells harvested from a green African monkey. MIC and IC<sub>50</sub> compound concentration values are supplied in µg/cm<sup>3</sup> and micromolar (µM) in brackets

		<i>Scedosporium prolificans</i> (Causes Eumycetoma)		
Compound		MIC <sub>100</sub>	IC <sub>50</sub>	Selectivity Index (SI) (IC <sub>50</sub> /MIC)
		µg/cm <sup>3</sup> (µM)	µg/cm <sup>3</sup> (µM) VERO cells	
1	1,10-phenanthroline (1,10-phen)	0.5 (2.78)	>10 (55.49)	20
2	1,10-phenanthroline-5,6-dione (phendione)	2 (9.52)	6.6 (31.40)	3
6	[Ag(phendione) <sub>2</sub> ](ClO <sub>4</sub> ) <sub>2</sub>	2 (3.19)	6.5 (10.36)	3
7	[Cu(phendione) <sub>3</sub> ](ClO <sub>4</sub> ) <sub>2</sub> ·4H <sub>2</sub> O	2 (2.07)	6.6 (6.84)	3
8	[Mn(ph)(phen)(H <sub>2</sub> O) <sub>2</sub> ]	8 (18.38)	15.6 (35.84)	2
9	[Mn(ph)(phen) <sub>2</sub> (H <sub>2</sub> O)]·4H <sub>2</sub> O	8 (11.95)	11.7 (17.47)	1
10	[Mn <sub>2</sub> (isoph) <sub>2</sub> (phen) <sub>3</sub> ] <sub>2</sub> ·4H <sub>2</sub> O	4 (3.81)	125 (118.95)	31
11	{[Mn(phen) <sub>2</sub> (H <sub>2</sub> O) <sub>2</sub> ]} <sub>2</sub> (isoph) <sub>2</sub> (phen)·12H <sub>2</sub> O	4 (2.46)	46.9 (28.82)	12
12	[Mn(tereph)(phen) <sub>2</sub> ] <sub>2</sub> ·5H <sub>2</sub> O	1 (1.49)	46.9 (70.05)	47
13	[Mn <sub>2</sub> (η <sub>1</sub> ,η <sub>1</sub> ,μ <sub>2</sub> -oda)(phen) <sub>4</sub> (H <sub>2</sub> O) <sub>2</sub> ][Mn <sub>2</sub> (η <sub>1</sub> ,η <sub>1</sub> ,μ <sub>2</sub> -oda)(phen) <sub>4</sub> (η <sub>1</sub> -oda) <sub>2</sub> ] <sub>2</sub> ·4H <sub>2</sub> O	2 (0.81)	375 (152.55)	188
14	[Cu <sub>2</sub> (oda)(phen) <sub>4</sub> ](ClO <sub>4</sub> ) <sub>2</sub> ·2.76H <sub>2</sub> O·EtOH	4 (3.06)	11.7 (8.94)	3
15	{[Mn(3,6,9-tdda)(phen) <sub>2</sub> ] <sub>3</sub> ·3H <sub>2</sub> O·EtOH} <sub>n</sub>	2 (2.72)	62.5 (84.96)	31
16	{[Cu(3,6,9-tdda)(phen) <sub>2</sub> ] <sub>3</sub> ·3H <sub>2</sub> O·EtOH} <sub>n</sub>	2 (2.69)	5.85 (7.86)	3
17	[Ag <sub>2</sub> (3,6,9-tdda)(phen) <sub>4</sub> ] <sub>2</sub> ·EtOH	4 (3.33)	30.1 (25.02)	8
AMB	Amphotericin B	>16 (17.33)	n.t.	
FLC	Fluconazole	>64 (208.97)	n.t.	
VRC	Voriconazole	8 (22.90)	n.t.	
ITC	Itraconazole	>16 (22.67)	n.t.	
MFG	Micafungin	>8 (6.30)	n.t.	

n.t. = not tested.

It would appear that the overall trend of all the tested complexes in Table 3.7, is that there is some metal ion specificity, favouring the Mn(II)-based complexes.

Table 3.8 displays the fungistatic (MIC<sub>100</sub>) and IC<sub>50</sub> results against *C. albicans* (ATTC 10231) and the Vero cell line obtained for 1,10-phen (**1**), phendione (**2**), complexes **6-17** and three clinical antimicrobial agents. The most active fungistatic agent was the dinuclear Ag(I) 1,10-phen trioxaundecanedioate complex, **17**, (MIC<sub>100</sub> = 0.21 µM), and the complex also had a moderate to high cytoselectivity index (SI = 40). Its Mn(II) and Cu(II) analogues, **15** and **16**, were also quite active but were ca. 8 and 11 fold less active than **17**.

**Table 3.8:** *In vitro* fungistatic ( $MIC_{100}$ ) activity and selectivity index (SI) values for 1,10-phen, phendione, selected metal complexes and known clinically employed antifungal agents against the yeast *Candida albicans* (ATCC 10231), an etiological agent of human candidiasis.  $IC_{50}$  values obtained using Vero cells, which are kidney epithelial cells harvested from a green African monkey.  $MIC$  and  $IC_{50}$  compound concentration values are supplied in  $\mu\text{g}/\text{cm}^3$  and micromolar ( $\mu\text{M}$ ) in brackets

		<i>Candida albicans</i> (ATCC 10231)		
Compound		$MIC_{100}$	$IC_{50}$	Selectivity Index (SI) ( $IC_{50}/MIC$ )
		$\mu\text{g}/\text{cm}^3$ ( $\mu\text{M}$ )	$\mu\text{g}/\text{cm}^3$ ( $\mu\text{M}$ ) VERO cells	
1	1,10-phenanthroline (1,10-phen)	2.5 (13.87)	>10 (55.49)	4
2	1,10-phenanthroline-5,6-dione (phendione)	1.25 (5.95)	6.6 (31.40)	5
6	$[\text{Ag}(\text{phendione})_2]\text{ClO}_4$	0.3 (0.48)	6.5 (10.36)	5
7	$[\text{Cu}(\text{phendione})_3](\text{ClO}_4)_2 \cdot 4\text{H}_2\text{O}$	1.25 (1.30)	6.6 (6.84)	4
8	$[\text{Mn}(\text{ph})(\text{phen})(\text{H}_2\text{O})_2]$	7.5 (17.23)	15.6 (35.84)	1
9	$[\text{Mn}(\text{ph})(\text{phen})_2(\text{H}_2\text{O})]4\text{H}_2\text{O}$	6.25 (9.33)	11.7 (17.47)	1
10	$[\text{Mn}_2(\text{isoph})_2(\text{phen})_3]4\text{H}_2\text{O}$	8 (7.61)	125 (118.95)	10
11	$\{[\text{Mn}(\text{phen})_2(\text{H}_2\text{O})_2]_2(\text{isoph})_2(\text{phen})\} \cdot 12\text{H}_2\text{O}$	5.5 (3.38)	46.9 (28.82)	4
12	$[\text{Mn}(\text{tereph})(\text{phen})_2]5\text{H}_2\text{O}$	6.5 (9.71)	46.9 (70.05)	7
13	$[\text{Mn}_2(\eta_1\eta_1\mu_2\text{-oda})(\text{phen})_4(\text{H}_2\text{O})_2][\text{Mn}_2(\eta_1\eta_1\mu_2\text{-oda})(\text{phen})_4(\eta_1\text{-oda})_2]4\text{H}_2\text{O}$	2 (0.81)	375 (152.55)	188
14	$[\text{Cu}_2(\text{oda})(\text{phen})_4](\text{ClO}_4)_2 \cdot 2.76\text{H}_2\text{O} \cdot \text{EtOH}$	2 (1.53)	11.7 (8.94)	6
15	$\{[\text{Mn}(3,6,9\text{-tdda})(\text{phen})_2]3\text{H}_2\text{O} \cdot \text{EtOH}\}_n$	1.25 (1.70)	62.5 (84.96)	36
16	$\{[\text{Cu}(3,6,9\text{-tdda})(\text{phen})_2]3\text{H}_2\text{O} \cdot \text{EtOH}\}_n$	1.75 (2.35)	5.85 (7.86)	3
17	$[\text{Ag}_2(3,6,9\text{-tdda})(\text{phen})_4]\text{EtOH}$	0.25 (0.21)	30.1 (25.02)	40
AMB	Amphotericin B	0.25 (0.27)	n.t.	
KTC	Ketoconazole	2.5 (4.7)	n.t.	
CFG	Caspofungin	0.25 (0.23)	n.t.	

n.t. = not tested.

The Mn(II) complex, **15**, displayed a median SI (36) and the Cu(II) complex, **16**, demonstrated a low SI (3). The water-solubility and dinuclearity of the Ag(I)-based **17** may be a factor as the fourth most active complex, **6**, was also a Ag(I)-based complex. Although complex **6** is poorly soluble in water it displayed a similarly low  $MIC_{100}$  value (0.48  $\mu\text{M}$ ) but in contrast to **17**, it exhibited poor cytoselctivity (SI = 5). **17** was ca. 2 fold more fungistatic than complex **6**, this suggests that it is the dinuclear structure of **17** that resulted in its superior efficacy as it is almost exactly twofold more active than **6**. Thus, the aqueous solubility of **17** may also play a part in its enhanced fungistatic activity over that of **6**.



The next most active fungistatic agents were the known antifungals, CFG and AMB, and these were followed by the Mn(II) 1,10-phen octanedioate, **13**, ( $MIC_{100} = 0.81 \mu M$ ). This complex also proved to be the most for *C.albicans* (SI = 188). The Cu(II) 1,10-phen octanedioate analogue **14** was almost twofold less fungistatic than **13** and was much less cytoselective (SI = 6). Likewise the Cu(II) bis-phendione complex, **7**, also demonstrated good fungistatic activity but was poorly cytoselective (SI = 4). The metal-free ligands, **1** and **2**, although moderately fungistatic, had poor cytoselectivities.

It would seem from these results that this particular strain of *C.albicans* is susceptible to the antifungal action of Ag(I) ions and also possibly to ROS/RNS generated by certain Mn(II) and Cu(II) complexes.

### 3.7 *In vivo* systemic toxicity/cytotoxicity studies using *Galleria mellonella*

The innate defences of insects are akin to that of vertebrate mammals, which are comprised of active and passive barriers as well as humoral and cellular responses within the haemolymph, which is considered as analogous to the blood of mammals.<sup>48</sup> It is this high degree of structural and functional homology between the innate immune systems of insects and mammals that afford certain insect models to be utilised to evaluate the *in vivo* therapeutic potential of novel antimicrobial compounds, the results of which are highly comparable to those obtained using mammalian models.<sup>49</sup> Furthermore, in vertebrates the innate immune response is the main line of defence against many microbial pathogens and since there is a strong correlation between mammalian and insect responses to microbial infection, certain insect models, such as *G. mellonella*, have been employed effectively for *in vivo* studies of the pathogenicity of some bacteria and fungi.<sup>48</sup><sup>50</sup> In addition, particular cellular responses within the haemolymph of *G.mellonella* to infection with *C.albicans* are comparable to those in mice, with the results between the insect and murine models strongly correlating to each other.<sup>49a</sup> *G.mellonella* larvae possess an immune system which is analogous to the human innate immune system and hence are a convenient, inexpensive and less ethically sensitive *in vivo* screening model to ascertain the systemic toxicity profile of novel antifungals, the results of which are comparable to murine models.<sup>51</sup>

Table **3.9** contains mortality data for *G. mellonella* larvae (expressed as a %) over a range of injected concentrations of 15 selected test compounds/complexes.



**Table 3.9:** Percentage mortality of *Galleria mellonella* larvae 72 hours post injection with various dosages of test compounds/complexes and the known cytotoxic agent cis-diammineplatinum(II) dichloride (Cisplatin).


Compound		Administred amount/% mortality µg per larvae (mg/kg)					
		100 (333.3)	40 (133.3)	20 (67.67)	10 (33.33)	4 (13.33)	2 (6.67)
<b>1</b>	% Mortality	100%	80%	80%	0%	0%	0%
	µmol	0.5549	0.2220	0.1110	0.0555	0.0222	0.0111
<b>2</b>	% Mortality	90%	80%	80%	0%	0%	0%
	µmol	0.4758	0.1903	0.0952	0.0476	0.0190	0.0095
<b>6</b>	% Mortality	90%	80%	80%	0%	0%	0%
	µmol	0.1593	0.0637	0.0319	0.0159	0.0064	0.0032
<b>7</b>	% Mortality	90%	80%	80%	0%	0%	0%
	µmol	0.1036	0.0414	0.0207	0.0104	0.0041	0.0021
<b>8</b>	% Mortality	90%	90%	80%	0%	0%	0%
	µmol	0.2297	0.0919	0.0459	0.0230	0.0092	0.0046
<b>9</b>	% Mortality	90%	90%	80%	0%	0%	0%
	µmol	0.1494	0.0597	0.0299	0.0149	0.0060	0.0030
<b>10</b>	% Mortality	90%	80%	60%	0%	0%	0%
	µmol	0.0952	0.0381	0.0190	0.0095	0.0038	0.0019
<b>11</b>	% Mortality	90%	90%	80%	0%	0%	0%
	µmol	0.0614	0.0246	0.0123	0.0061	0.0025	0.0012
<b>12</b>	% Mortality	90%	90%	80%	0%	0%	0%
	µmol	0.1494	0.0597	0.0299	0.0149	0.0060	0.0030
<b>13</b>	% Mortality	90%	90%	40%	0%	0%	0%
	µmol	0.0407	0.0163	0.0081	0.0041	0.0016	0.0008
<b>14</b>	% Mortality	90%	90%	50%	0%	0%	0%
	µmol	0.0764	0.0306	0.0153	0.0076	0.0031	0.0015
<b>15</b>	% Mortality	90%	80%	50%	0%	0%	0%
	µmol	0.1359	0.0544	0.0272	0.0136	0.0054	0.0027
<b>16</b>	% Mortality	90%	90%	80%	0%	0%	0%
	µmol	0.1344	0.0537	0.0269	0.0134	0.0054	0.0027
<b>17</b>	% Mortality	90%	90%	70%	0%	0%	0%
	µmol	0.0831	0.0333	0.0166	0.0083	0.0033	0.0017
<b>Cisplatin</b>	% Mortality	100%	100%	100%	60%	0%	0%
	µmol	0.3333	0.1333	0.0667	0.0333	0.0133	0.0067

At the highest administered concentration (100 µg per larvae), 10% of the larvae treated with test agents **6-17** survived, whilst all of the larvae injected at this concentration with **1,10-phen (1)** and cisplatin died. The second administered concentration (40 µg per larvae) resulted in an increased survival rate to 20% of the test population of larvae for **1, 2, 6, 7, 10** and **15**, whilst complexes **8, 9, 11-14** and **16** maintained their lower 10% survival percentage, whilst cisplatin was the only agent to kill all larvae at this concentration. At a concentration of 20 µg per larvae, 20% of larvae treated with **1, 2, 6-9, 11, 12** and **16** survived. Complex **10** rendered a survival rate of 40%, **13** displayed 60% survival, **14** and **15** demonstrated 50% survival and **17** exhibited a survival value of 30%. Again, all of the larvae subjected to cisplatin perished. At a dosage of 10 µg per larvae all larvae treated with **1-17** were still alive after 72 hours, and this is compared to

a 40% survival for those treated with cisplatin. All of the larvae survived at the final two concentrations (4 and 2  $\mu\text{g}$  per larvae) for each compound tested.

It is clear that cisplatin is considerably more toxic to *G.mellonella* larvae than any of the other test compounds/complexes. Of particular note is that at a dosage of 10  $\mu\text{g}$  per larvae (33.3 mg/kg) cisplatin causes a low survival value (40%) whilst all of the other compounds are essentially non-toxic to the larvae at this dosage (100% survival rate). In terms of *G.mellonella* tolerance to each test agent, when expressed as  $\mu\text{mol}$  per larvae, the following order emerges: **13 > 15 > 14 > 10 > 17 > 1 ≈ 2 > 8 > 9 = 12 > 16 > 7 > 11** >> cisplatin. Furthermore, the *in vivo* tolerance order/trend results using the *G. mellonella* insect model for complexes **1, 2, 6-17** correlate closely with the *in vitro* IC<sub>50</sub> tolerance order results obtained using the Vero cell line, when the comparison is expressed in  $\mu\text{moles}$  (Table 3.10). The general order of tolerance in Table 3.10 between *in vitro* and *in vivo* toxicity results are comparable, bearing in mind the difference in complexity of the *in vitro* and *in vivo* models. The least toxic/most tolerated complex is **13** and the general trend for all tested complexes is similar between the two sets of results.

**Table 3.10:** Tabulated *in vivo* tolerance results (using the *G. mellonella* insect model) with the *in vitro* IC<sub>50</sub> results (Vero cell line) obtained for complexes **1, 2, 6-17** and cisplatin. Complexes are listed from most tolerated to least tolerated.

	<i>In vitro</i> Vero cells (IC <sub>50</sub> ) Order in $\mu\text{mol}$	<i>In vivo</i> <i>G.mellonella</i> Order in $\mu\text{mol}$	
<b>1st</b>	13	13	
<b>2nd</b>	10	15	
<b>3rd</b>	15	14	
<b>4th</b>	12	10	
<b>5th</b>	1	17	
<b>6th</b>	8	1	
<b>7th</b>	2	2	
<b>8th</b>	11	8	
<b>9th</b>	17	6	
<b>10th</b>	9	9	
<b>11th</b>	6	12	
<b>12th</b>	14	16	
<b>13th</b>	16	7	
<b>14th</b>	7	11	
<b>15th</b>		cisplatin	

### 3.8 *In vivo* antifungal screening using *G. mellonella*

*In vivo* antifungal screening was conducted using the *G. mellonella* insect model and the opportunistic fungal pathogen, *C. albicans* (ATTC 10231). A small sub-group of complexes were chosen which had previously demonstrated good fungistatic activity against *C. albicans* (low MIC<sub>100</sub> values) and excellent aqueous solubility. Test solutions were made by dissolving the sample in DMSO and diluting with distilled water to yield the required concentration. The maximum DMSO concentration in any test solution was 0.5% v/v, and at this level the DMSO does not inhibit the growth of the microbial cells. All test solutions were administered by direct injection into the haemocoel through the last pro-leg of each *G. mellonella* larvae (Figure 3.16). The survival of all larvae was monitored every 24 hours for up to 72 hours, and death was assessed by the lack of movement in response to stimulus in conjunction with discolouration of the cuticle.

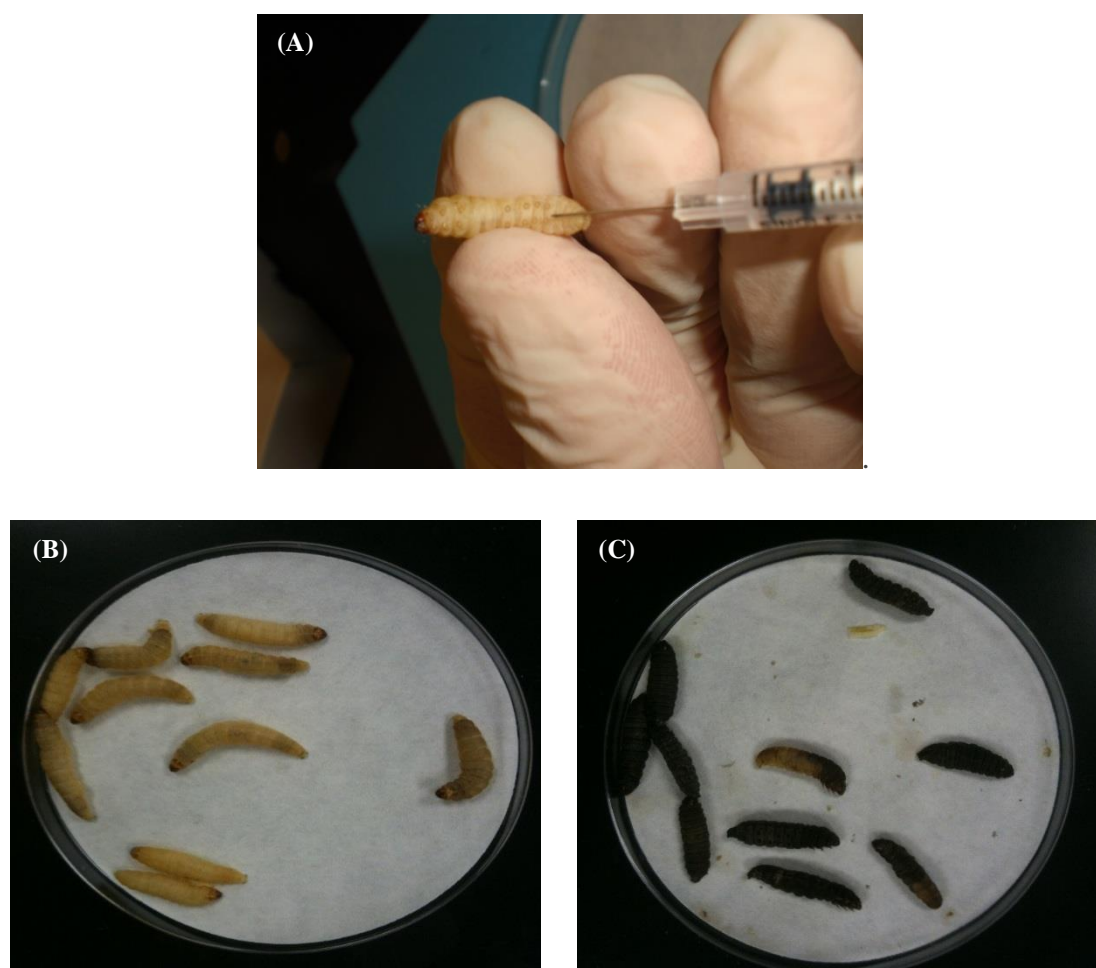


**Fig. 3.16:** (A) Injection of test solutions into the haemocoel of *G. mellonella* through the last pro-leg. *G. mellonella* larvae after 72 hours of incubation at 30 °C: (B) healthy control specimens and (C) specimens treated with a lethal dose of *C. albicans*.

The anti-*Candida in vivo* screening was conducted utilising two different protocols, prophylactic treatment and post infection treatment (i.e. larvae were pre-infected). A lethal dose per larvae had been pre-determined to be  $2 \times 10^6$  *C. albicans* cells administered in an aliquot of 20  $\mu\text{L}$  of phosphate buffered saline (PBS) solution.

The test compounds (**13-17**), along with silver acetate ( $\text{Ag}(\text{CH}_3\text{COO})$ ) and the clinical antifungal agent Ketoconazole (KTC) (used as reference standards), were screened at two concentrations;  $100 \mu\text{g}/\text{cm}^3$  and  $50 \mu\text{g}/\text{cm}^3$ . The prophylactic protocol entailed that each test solution (20  $\mu\text{L}$ ) was injected 1 hour prior to infection of the larvae with a lethal dose of *C. albicans* cells. The post infection protocol consisted of each test solution (20  $\mu\text{L}$ ) being administered 1 hour after each larvae had been infected with a lethal dose of *C. albicans* cells. The survival of all larvae were accessed at 24, 48 and 72 hour intervals (Figures **3.18** and **3.19**).

Complexes **17**, **13** and **14**, when administered prophylactically at a concentration of  $100 \mu\text{g}/\text{cm}^3$ , dramatically increased the *G. mellonella* larvae survival rate (90, 87 and 87 %, respectively) after infection with a lethal dose of *C. albicans* cells (Figure **3.18**). However, the administered dosage of  $100 \mu\text{g}/\text{cm}^3$  translates to  $83.139 \mu\text{M}$  for **17**,  $76.381 \mu\text{M}$  for **14** and  $40.68 \mu\text{M}$  for **13**, demonstrating that in terms of micromolar concentration, **13** was almost twice as effective as **17** and **14**. This protection was superior to that given by  $\text{Ag}(\text{CH}_3\text{COO})$  (80%) and KTC (73%), whilst the least protective agent, complex **16**, afforded a survival rate of 60%.

When the prophylactic experiment was repeated at the lower dosage of  $50 \mu\text{g}/\text{cm}^3$  of the test agent, the % survival of the larvae decreased in all cases. At this lower dosage complex **17** and  $\text{Ag}(\text{CH}_3\text{COO})$  demonstrated equal protective activity (63% survival rate) (Figure **3.18**). Complexes **13**, **15** and KTC exhibited equal activity (53% survival) which was closely followed by **16** (50% survival) and then **14** (47% survival). Once again, micromolar concentrations must be considered and although **17** demonstrated 10% better protection than **13**, the molar quantity of **13** was ca. half that of **17**. Furthermore, the molarity of  $\text{Ag}(\text{CH}_3\text{COO})$  at  $50 \mu\text{g}/\text{cm}^3$  is  $299.563 \mu\text{M}$ , as compared to **17** and **13** ( $41.57$  and  $20.34 \mu\text{M}$ , respectively).

The larvae that were pre-infected with a lethal dose of *C. albicans* and then 1 hour later treated with  $100 \mu\text{g}/\text{cm}^3$  of the test solutions responded best to complex **17** (80% survival rate) (Figure **3.19**). Complex **13**,  $\text{Ag}(\text{CH}_3\text{COO})$  and KTC at  $100 \mu\text{g}/\text{cm}^3$  demonstrated

equal protection (77% survival). Complexes **15** and **16** were almost equally active (63 and 60% survival) followed by **14** (57% survival). At the lower 50  $\mu\text{g}/\text{cm}^3$  dosage, all of the test compounds displayed a reduced survival rate. Complex **17** and  $\text{Ag}(\text{CH}_3\text{COO})$  afforded the best prognosis and exhibited equal activity (63% survival rate). This was then followed by **15** (50%), **13** (43%), **16** (40%). Finally **14** and KTC demonstrated equal activity (37% survival rate).

The results for the *in vivo* prophylactic and post infection treatment experiments are comparable to the activity trend observed from the *in vitro*  $\text{MIC}_{100}$  fungistatic activity experiments with *C. albicans*. The most active complexes were the Ag(I)-based **17**, followed by the Mn(II)-based complexes **13** and **15**, and lastly the Cu(II)-based **16** and **14**. It would appear that there is metal ion specificity to the activity trend, favouring the dinuclear Ag(I) highly water-soluble complex, **17**, followed by the Mn(II)-based and then the Cu(II)-based complexes. Furthermore, prophylactic protection was the more efficacious method, resulting in an increased survival rate of *G. mellonella* larvae infected with a lethal dose of *C. albicans*. There are two possible explanations for this. Firstly, this may be a direct consequence of the efficacy of the test compound, a true *in vivo* antifungal effect (direct anti-effect). Secondly, either in conjunction with or separately, the presence of an administered foreign substance results in an increased immune response by the innate immune system of the insect. This results in the production of an increased number of haemocytes, antimicrobial peptides and proteins (indirect anti-effect) that work in combination with the antifungal properties of the compounds to arrest and kill *C. albicans* and hence, prevent larval death.<sup>36b</sup>

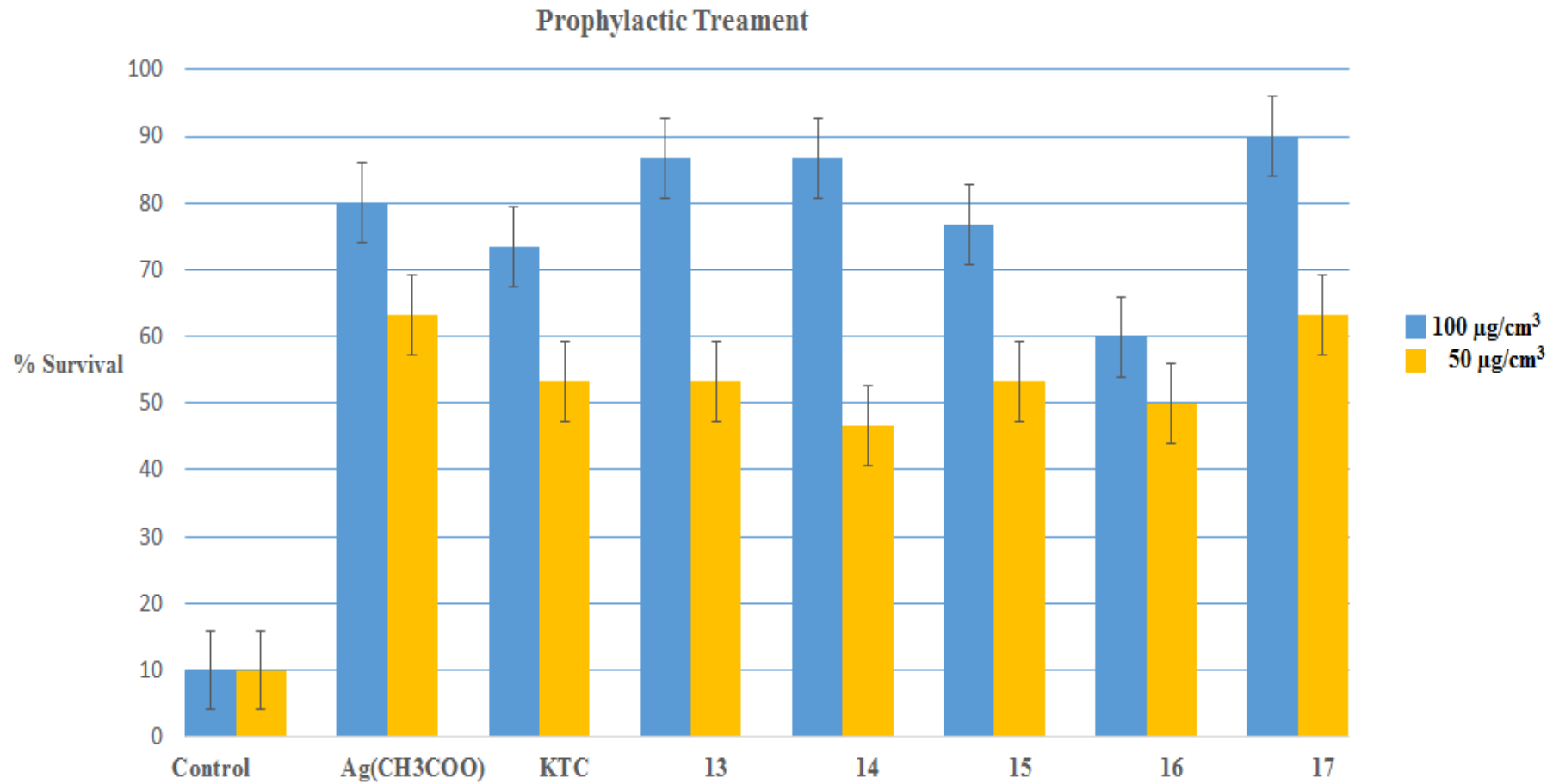


**Fig. 3.18:** Percentage survival accessed after 72 hours of *G. mellonella* larvae prophylactically inoculated with test agents (Ag(CH<sub>3</sub>COO), KTC, **13-17**), at two different concentrations (100 or 50 µg/cm<sup>3</sup>) one hour prior to infection with a lethal dose of *C. albicans* (2 x 10<sup>6</sup> fungal cells).

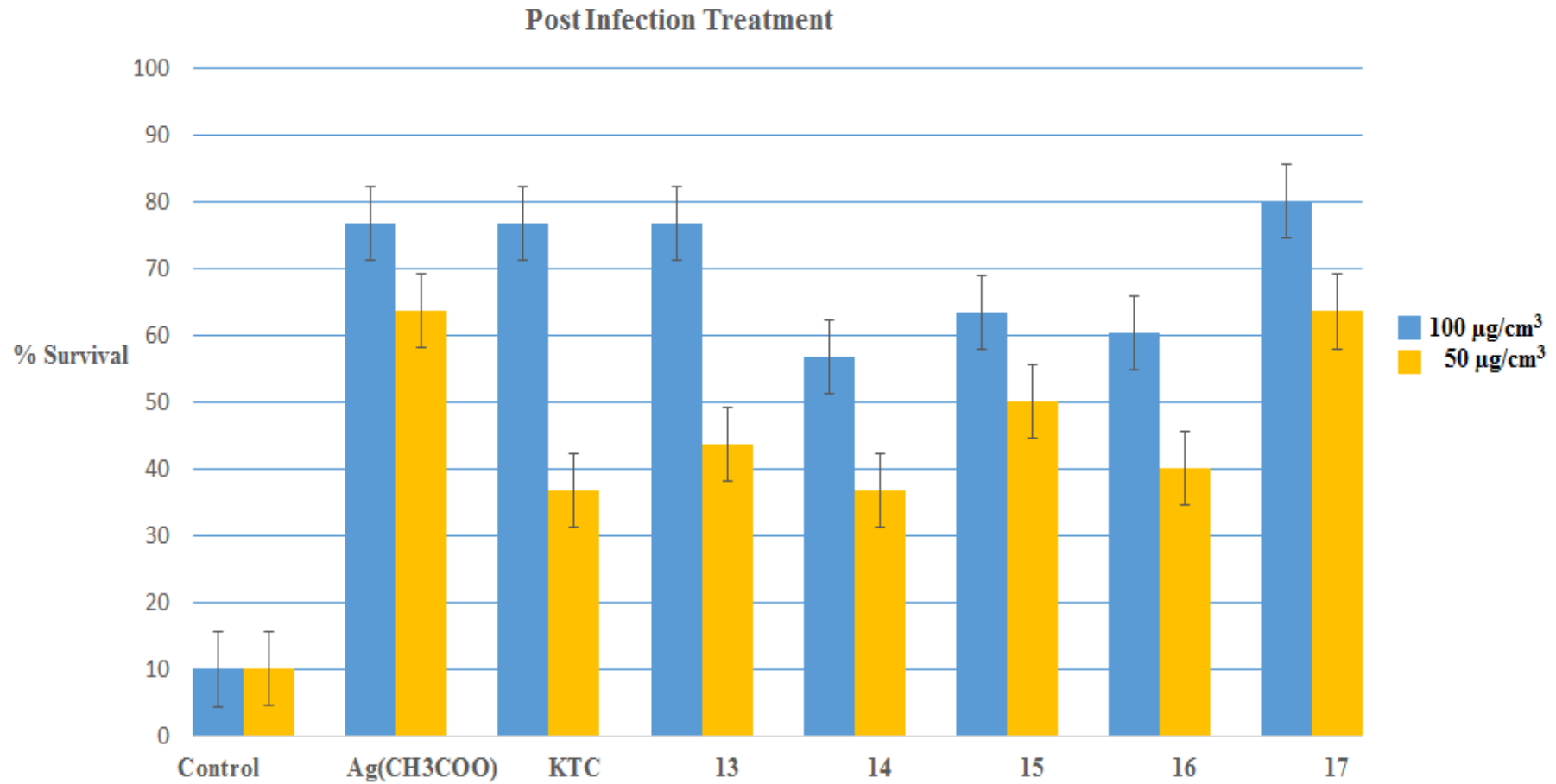


**Fig. 3.19:** Percentage survival accessed after 72 hours of *G. mellonella* larvae inoculated with test agents (Ag(CH<sub>3</sub>COO), KTC, 13-17), at two different concentrations (100 or 50  $\mu\text{g}/\text{cm}^3$ ) one hour after infection with a lethal dose of *C. albicans* ( $2 \times 10^6$  fungal cells).

### 3.9 Summary of antifungal activity

The diverse nature of the eight different fungi tested make it difficult to directly compare the activity profile of the test complexes **1**, **2**, **6-17**. However, some activity trends were apparent. Consistently, the most active complexes *in vitro* were **17** and **13** and these were also the most promising candidates in the *in vivo* anti-Candida screening using *G. mellonella* larvae. The Ag(I)-based complex, **17**, proved to be the most active complex against five of the fungal species (*P. verrucosa*, *C. carrionii*, *E. dermatitidis*, *S. aurantiacum* and *C. albicans*). This may be due to an innate susceptibility of these fungi to the known antifungal action of Ag(I) ions.<sup>52</sup> Complex **17** also demonstrated a fungicidal effect towards three of the aforementioned fungi (*P. verrucosa*, *C. carrionii* and *E. dermatitidis*) and displayed greater fungistatic activity towards *P. verrucosa*, *C. carrionii* and *C. albicans* than the known clinically administered antifungal agents. Furthermore, the *in vivo* anti-Candida activity of **17** was also superior to the known antifungal drug, Ketoconazole.

The Mn(II)-based complex, **13**, was the most efficacious fungistatic complex against *P. boydii*, *P. minutispora* and *S. proliticans*, and also proved to be the second/third most active complex against a further five fungi. In addition, **13** demonstrated an *in vitro* fungicidal effect against *C. carrionii*, and its *in vivo* anti-Candida activity was only marginally less than that of **17**. The combination of the *in vitro* fungistatic/fungicidal and *in vivo* activity shown by **17** and **13**, in conjunction with their very low toxicity profile both *in vitro* and *in vivo*, implies that these complexes are exciting prospects as lead antifungal agents for the possible treatment of Candidiasis, Chromoblastomycosis, Phaeohyphomycosis and Eumycetoma infections.

### 3.10 References

1. Blackwell, M., The fungi: 1, 2, 3 ... 5.1 million species? *American Journal of Botany* **2011**, 98 (3), 426-438. 10.3732/ajb.1000298
2. Murray, P. R.; Rosenthal, K. S.; Pfaller, M. A., *Medical Microbiology*. Mosby/Elsevier: 2009.
3. Sudbery, P. E., Growth of *Candida albicans* hyphae. *Nature Reviews Microbiology* **2011**, 9 (10), 737-748. 10.1038/nrmicro2636



4. Moore, D., *Slayers, Saviors, Servants, and Sex: An Exposé of Kingdom Fungi*. Springer New York: 2001.
5. Money, N. P., *Mr. Bloomfield's Orchard: The Mysterious World of Mushrooms, Molds, and Mycologists*. OUP USA: 2004.
6. Moran, G. P.; Coleman, D. C.; Sullivan, D. J., Comparative Genomics and the Evolution of Pathogenicity in Human Pathogenic Fungi. *Eukaryotic Cell* **2011**, *10* (1), 34-42. 10.1128/ec.00242-10
7. San-Blas, G.; Calderone, R. A., *Pathogenic Fungi: Insights in Molecular Biology*. Caister Academic Press: 2008.
8. Baron, S., *Medical Microbiology*. University of Texas Medical Branch at Galveston: 1996.
9. 

<http://www.globalskinatlas.com/imagdetail.cfm?topLevelID=790&imageID=1966&did=6> Accessed on the 14/07/2014.
10. Grover, C.; Khurana, A., Onychomycosis: newer insights in pathogenesis and diagnosis. *Indian J Dermatol Venereol Leprol* **2012**, *78* (3), 263-270. 10.4103/0378-6323.95440
11. <http://www.dermnetnz.org/fungal/onychomycosis.html> Accessed on the 14/07/2014.
12. Esterre, P.; Queiroz-Telles, F., Management of chromoblastomycosis: novel perspectives. *Current Opinion in Infectious Diseases* **2006**, *19* (2), 148-152. 10.1097/01.qco.0000216625.28692.67
13. (a) <http://www.mold.ph/fonsecaea.htm> Accessed on the 14/07/2014. ; (b) Brown, M.; Pasvol, G., Chromoblastomycosis. *New England Journal of Medicine* **2005**, *352* (20), E19-E19. 10.1056/NEJMicm040848
14. (a) Davidson, S.; Macleod, J., *Davidson's principles and practice of medicine: a textbook for students and doctors*. Churchill Livingstone: 1974. ; (b) <http://www.mycology.adelaide.edu.au/Mycoses/Subcutaneous/Mycetoma/> Accessed on the 20/07/2014.
15. 

<http://faculty.ksu.edu.sa/bismar/Pictures%20Library/Forms/DispForm.aspx?ID=64> Accessed on the 20/07/2014.

16. [http://itg.content-eu/Generated/pubx/173/medical\\_mycology/subcutaneous\\_mycoses.htm](http://itg.content-eu/Generated/pubx/173/medical_mycology/subcutaneous_mycoses.htm)  
Accessed on the 20/07/2014.
17. Williams, D.; Lewis, M., Pathogenesis and treatment of oral candidosis. *Journal of Oral Microbiology* **2011**, *3* (0). 10.3402/jom.v3i0.5771
18. [http://www.exodontia.info/Oral\\_Candidiasis.html](http://www.exodontia.info/Oral_Candidiasis.html) Accessed on the 14/07/2014.
19. Ashley, E. S. D.; Lewis, R.; Lewis, J. S.; Martin, C.; Andes, D., Pharmacology of systemic antifungal agents. *Clinical Infectious Diseases* **2006**, *43*, S28-S39. 10.1086/504492
20. (a) Ajello, L.; Georg, L. K.; Steigbig.Rt; Wang, C. J. K., Case of phaeohyphomycosis caused by a new species of Phialophora. *Mycologia* **1974**, *66* (3), 490-498. 10.2307/3758492; (b) <http://www.mycology.adelaide.edu.au/Mycoses/Oppportunistic/Phaeohyphomycosis/> Accessed on the 14/07/2014.
21. Pfaller, M. A.; Pappas, P. G.; Wingard, J. R., Invasive fungal pathogens: Current epidemiological trends. *Clinical Infectious Diseases* **2006**, *43*, S3-S14. 10.1086/504490
22. Badali, H.; Chander, J.; Gupta, A.; Rani, H.; Punia, R. S.; De Hoog, G. S.; Meis, J. F., Fatal Cerebral Phaeohyphomycosis in an Immunocompetent Individual Due to *Thielavia subthermophila*. *Journal of Clinical Microbiology* **2011**, *49* (6), 2336-2341. 10.1128/jcm.02648-10
23. Revankar, S. G.; Patterson, J. E.; Sutton, D. A.; Pullen, R.; Rinaldi, M. G., Disseminated phaeohyphomycosis: Review of an emerging mycosis. *Clinical Infectious Diseases* **2002**, *34* (4), 467-476. 10.1086/338636
24. Janeway, C., *Immunobiology: The Immune System In Health And Disease*. Garland Science Taylor & Francis Group: 2005.
25. Pfaller, M. A.; Diekema, D. J., Epidemiology of invasive candidiasis: a persistent public health problem. *Clinical Microbiology Reviews* **2007**, *20* (1), 133-+. 10.1128/cmr.00029-06
26. [http://www.mycology.adelaide.edu.au/Fungal\\_Descriptions/Yeasts/Candida/](http://www.mycology.adelaide.edu.au/Fungal_Descriptions/Yeasts/Candida/)  
Accessed on the 29/07/2014.
27. (a) Blank, F., In vitro fungistatic action of phenanthrolines against pathogenic fungi. *Nature* **1951**, *168* (4273), 516-517. 10.1038/168516a0; (b) Dwyer, F. P.; Reid, I. K.; Shulman, A.; Laycock, G. M.; Dixon, S., Biological actions of 1,10-

- phenanthroline and 2,2'-bipyridine hydrochlorides quaternary salts and metal chelates and related compounds.1. Bacteriostatic action on selected gram-positive gram-negative and acid-fast bacteria. *Australian Journal of Experimental Biology and Medical Science* **1969**, *47*, 203-&. 10.1038/icb.1969.21; (c) Husseini, R. H.; Stretton, R. J., Anti Bacterial Activity Of Some Phenanthroline and Phenanthrene Compounds. *Microbios Letters* **1981**, *16* (62), 85-94. ; (d) Roy, S.; Hagen, K. D.; Maheswari, P. U.; Lutz, M.; Spek, A. L.; Reedijk, J.; van Wezel, G. P., Phenanthroline derivatives with improved selectivity as DNA-targeting anticancer or antimicrobial drugs. *Chemmedchem* **2008**, *3* (9), 1427-1434. 10.1002/cmdc.200800097
28. (a) Igdaloff, D.; Santi, D. V.; Eckert, T. S.; Bruice, T. C., Effects of 1,7-phenanthroline dione and 1,10-phenanthroline dione on tissue-culture cells. *Biochemical Pharmacology* **1983**, *32* (1), 172-174. 10.1016/0006-2952(83)90674-3; (b) McCann, M.; Geraghty, M.; Devereux, M.; O'Shea, D.; Mason, J.; O'Sullivan, L., Insights into the mode of action of the anti-Candida activity of 1,10-phenanthroline and its metal chelates. *Metal-Based Drugs* **2000**, *7* (4), 185-193. 10.1155/mbd.2000.185
29. (a) Husseini, R.; Stretton, R. J., Studies on the anti-bacterial activity of phanquone - chelating properties in relation to mode of action against Escherichia coli and Staphylococcus aureus. *Microbios* **1980**, *29* (116), 109-125. ; (b) Brul, S.; Stratford, M.; van der Vaart, J. M.; Dielbandhoesing, S. K.; Steels, H.; Klis, F. M.; Verrips, C. T., The antifungal action of 1,10-o-phenanthroline and EDTA is mediated through zinc chelation and involves cell wall construction. *Food Technology and Biotechnology* **1997**, *35* (4), 267-274. ; (c) McCann, M.; Kellett, A.; Kavanagh, K.; Devereux, M.; Santos, A. L. S., Deciphering the Antimicrobial Activity of Phenanthroline Chelators. *Current Medicinal Chemistry* **2012**, *19* (17), 2703-2714.
30. (a) Klimova, N.; Yeung, R.; Kachurina, N.; Turcotte, B., Phenotypic Analysis of a Family of Transcriptional Regulators, the Zinc Cluster Proteins, in the Human Fungal Pathogen *Candida glabrata*. *G3-Genes Genomes Genetics* **2014**, *4* (5), 931-940. 10.1534/g3.113.010199; (b) Kisselev, L. L.; Favorova, O. O.; Nurbekov, M. K.; Dmitriyenko, S. G.; Engelhardt, W. A., Bovine tryptophanyl-transfer RNA-synthetase - a zinc metalloenzyme. *European Journal of Biochemistry* **1981**, *120* (3), 511-517. 10.1111/j.1432-1033.1981.tb05729.x; (c)

- Felber, J. P.; Coombs, T. L.; Vallee, B. L., Mechanism of inhibition of carboxypeptidase a by 1,10-phenanthroline. *Biochemistry* **1962**, *1* (2), 231-&. 10.1021/bi00908a006; (d) Klug, A., The Discovery of Zinc Fingers and Their Applications in Gene Regulation and Genome Manipulation. In *Annual Review of Biochemistry, Vol 79*, Kornberg, R. D.; Raetz, C. R. H.; Rothman, J. E.; Thorner, J. W., Eds. Annual Reviews: Palo Alto, 2010; Vol. 79, pp 213-231. 10.1146/annurev-biochem-010909-095056
31. (a) Kellett, A.; O'Connor, M.; McCann, M.; Howe, O.; Casey, A.; McCarron, P.; Kavanagh, K.; McNamara, M.; Kennedy, S.; May, D. D.; Skell, P. S.; O'Shea, D.; Devereux, M., Water-soluble bis(1,10-phenanthroline) octanedioate  $\text{Cu}^{2+}$  and  $\text{Mn}^{2+}$  complexes with unprecedented nano and picomolar in vitro cytotoxicity: promising leads for chemotherapeutic drug development. *MedChemComm* **2011**, *2* (7), 579-584. 10.1039/c0md00266f; (b) Coyle, B.; Kavanagh, K.; McCann, M.; Devereux, M.; Geraghty, M., Mode of anti-fungal activity of 1,10-phenanthroline and its Cu(II), Mn(II) and Ag(I) complexes. *Biometals* **2003**, *16* (2), 321-329. 10.1023/a:1020695923788
32. Geraghty, M.; Cronin, J. F.; Devereux, M.; McCann, M., Synthesis and antimicrobial activity of copper(II) and manganese(II) alpha,omega-dicarboxylate complexes. *Biometals* **2000**, *13* (1), 1-8. 10.1023/a:1009271221684
33. McCann, M.; Coyle, B.; McKay, S.; McCormack, P.; Kavanagh, K.; Devereux, M.; McKee, V.; Kinsella, P.; O'Connor, R.; Clynes, M., Synthesis and X-ray crystal structure of  $[\text{Ag}(\text{phendio})_2]\text{ClO}_4$  (phendio=1,10-phenanthroline-5,6-dione) and its effects on fungal and mammalian cells. *Biometals* **2004**, *17* (6), 635-645. 10.1007/s10534-004-1229-5
34. (a) Gillard, R. D.; Hill, R. E. E., Optically-active coordination-compounds .34. Modification of reaction pathways in 1,10-phenanthroline and its derivatives by metal-ions. *Journal of the Chemical Society-Dalton Transactions* **1974**, (11), 1217-1236. 10.1039/dt9740001217; (b) Goss, C. A.; Abruna, H. D., Spectral, electrochemical, and electrocatalytic properties of 1,10-phenanthroline-5,6-dione complexes of transition-metals. *Inorganic Chemistry* **1985**, *24* (25), 4263-4267. 10.1021/ic00219a012; (c) Kano, K.; Uno, B., Surface-redox reaction-mechanism of quinones adsorbed on basal-plane-pyrolytic graphite-electrodes. *Analytical Chemistry* **1993**, *65* (8), 1088-1093. 10.1021/ac00056a024; (d) Rezvani, A. R.; Saravani, H.; Hadadzadeh, H., Synthesis, Crystal Structure, Electrochemical and

- Fluorescence Studies of a Novel Zn(II)-Fluorophore, 1,10-Phenanthroline-5,6-dione (Phen-dione). *Journal of the Iranian Chemical Society* **2010**, 7 (4), 825-833.
35. Coyle, B., Synthesis, Characterization and Testing of Metal-Based Anti-Fungal and Anti-Cancer Drugs. National University of Ireland, Maynooth: National University of Ireland, Maynooth, 2003.
36. (a) Geraghty, M.; McCann, M.; Devereux, M.; Cronin, F.; Curran, M.; McKee, V., Synthesis and anti-Candida activity of cobalt(II) complexes of benzene-1,2-dioxyacetic acid (bdoaH<sub>2</sub>). X-ray crystal structures of [Co(bdoa)(H<sub>2</sub>O)<sub>3</sub>] $\cdot$ 3.5H<sub>2</sub>O and {[CO(phen)<sub>3</sub>(bdoa)]<sub>2</sub> $\cdot$ 24H<sub>2</sub>O (phen = 1,10-phenanthroline). *Metal-Based Drugs* **1999**, 6 (1), 41-48. 10.1155/mbd.1999.41; (b) Rowan, R.; Moran, C.; McCann, M.; Kavanagh, K., Use of *Galleria mellonella* larvae to evaluate the in vivo anti-fungal activity of [Ag<sub>2</sub>(mal)(phen)<sub>3</sub>]. *Biometals* **2009**, 22 (3), 461-467. 10.1007/s10534-008-9182-3
37. Kim, K. J.; Sung, W. S.; Suh, B. K.; Moon, S. K.; Choi, J. S.; Kim, J.; Lee, D. G., Antifungal activity and mode of action of silver nano-particles on *Candida albicans*. *Biometals* **2009**, 22 (2), 235-242. 10.1007/s10534-008-9159-2
38. (a) Zheng, R. H.; Guo, H. C.; Jiang, H. J.; Xu, K. H.; Liu, B. B.; Sun, W. L.; Shen, Z. Q., A new and convenient synthesis of phendiones oxidated by KBrO<sub>3</sub>/H<sub>2</sub>SO<sub>4</sub> at room temperature. *Chinese Chemical Letters* **2010**, 21 (11), 1270-1272. 10.1016/j.ccllet.2010.05.030; (b) Devereux, M.; McCann, M.; Leon, V.; Geraghty, M.; McKee, V.; Wikaira, J., Synthesis and biological activity of manganese (II) complexes of phthalic and isophthalic acid: X-ray crystal structures of [Mn(ph)(phen)<sub>2</sub>(H<sub>2</sub>O)] $\cdot$ 4H<sub>2</sub>O, [Mn(phen)<sub>2</sub>(H<sub>2</sub>O)<sub>2</sub>]<sub>2</sub>(Isoph)<sub>2</sub>(phen) $\cdot$ 12H<sub>2</sub>O and {[Mn(isoph)(bipy)]<sub>4</sub> $\cdot$ 2.75bipy}<sub>n</sub> (phH<sub>2</sub> = phthalic acid; isoph = isophthalic acid; phen = 1,10-phenanthroline; bipy = 2,2-bipyridine). *Metal-Based Drugs* **2000**, 7 (5), 275-288. 10.1155/mbd.2000.275; (c) Casey, M. T.; McCann, M.; Devereux, M.; Curran, M.; Cardin, C.; Convery, M.; Quillet, V.; Harding, C., Synthesis and structure of the Mn<sup>II,II</sup> complex salt [Mn<sub>2</sub>( $\eta^1\eta^1\mu_2$ -oda)(phen)<sub>4</sub>(H<sub>2</sub>O)<sub>2</sub>][Mn<sub>2</sub>( $\eta^1\eta^1\mu_2$ -oda)(phen)<sub>4</sub>( $\eta^1$ -oda)<sub>2</sub>] $\cdot$ 4H<sub>2</sub>O (odaH<sub>2</sub> = octanedioic acid); a Catalyst for H<sub>2</sub>O<sub>2</sub> Disproportionation *Journal of the Chemical Society-Chemical Communications* **1994**, (22), 2643-2645. 10.1039/c39940002643; (d) Devereux, M.; McCann, M.; Cronin, J. F.; Ferguson, G.; McKee, V., Binuclear and polymeric copper(II) dicarboxylate complexes:

- syntheses and crystal structures of  $[\text{Cu}_2(\text{pda})(\text{Phen})_4](\text{ClO}_4)_2 \cdot 5\text{H}_2\text{O} \cdot \text{C}_2\text{H}_5\text{OH}$ ,  $[\text{Cu}_2(\text{oda})(\text{Phen})_4](\text{ClO}_4)_2 \cdot 2.67\text{H}_2\text{O} \cdot \text{C}_2\text{H}_5\text{OH}$  and  $\{[\text{Cu}_2(\text{pda})_2(\text{NH}_3)_4(\text{H}_2\text{O})_2] \cdot 4\text{H}_2\text{O}\}_n$  (odaH<sub>2</sub>=octanedioic acid; pdaH<sub>2</sub>=pentanedioic acid; Phen=1,10-phenanthroline). *Polyhedron* **1999**, *18* (16), 2141-2148. 10.1016/s0277-5387(99)00100-x; (e) McCann, S.; McCann, M.; Casey, M. T.; Devereux, M.; McKee, V.; McMichael, P.; McCrea, J. G., Manganese(II) complexes of 3,6,9-trioxaundecanedioic acid (3,6,9-tddaH<sub>2</sub>): X-ray crystal structures of  $[\text{Mn}(3,6,9\text{-tdda})(\text{H}_2\text{O})_2] \cdot 2\text{H}_2\text{O}$  and  $\{[\text{Mn}(3,6,9\text{-tdda})(\text{phen})_2] \cdot 3\text{H}_2\text{O}\} \cdot \text{EtOH}\}_n$ . *Polyhedron* **1997**, *16* (24), 4247-4252. 10.1016/s0277-5387(97)00233-7
39. Pfaller, M. A.; Sheehan, D. J.; Rex, J. H., Determination of fungicidal activities against yeasts and molds: Lessons learned from bactericidal testing and the need for standardization. *Clinical Microbiology Reviews* **2004**, *17* (2), 268-+. 10.1128/cmr.17.2.268-280.2004
40. Santos, A. L. S., Unpublished antimicrobial studies. Department of General Microbiology, Federal University of Rio de Janeiro, Brazil., 2014.
41. Institute., C. a. L. S., M38-A2 Reference Method for Broth Dilution Antifungal Susceptibility Testing of Filamentous Fungi; Approved Standard, Second Edition. Clinical and Laboratory Standards Institute. 2008.: Clinical and Laboratory Standards Institute, Wayne, PA, USA., 2008; Vol. 28.
42. Institute., C. a. L. S., M27-A3 Reference method for broth dilution antifungal susceptibility testing of yeasts: approved standard, third edition. 3rd ed.; Clinical and Laboratory Standards Institute: Clinical and Laboratory Standards Institute, Wayne, PA, USA., 2008; Vol. 28.
43. (a) FDA, The safety of Sporanox capsules and Lamisil tablets for the treatment of Onychomycosis. <http://web.archive.org/web/20090528160344/http://www.fda.gov/cder/drug/adv/sory/sporanox-lamisil/advisory.htm>, 2001. ; (b) Baginski, M.; Czub, J., Amphotericin B and Its New Derivatives - Mode of Action. *Current Drug Metabolism* **2009**, *10* (5), 459-469.
44. Guarro, J.; Kantarcioglu, A. S.; Horre, R.; Rodriguez-Tudela, J. L.; Estrella, M. C.; Berenguer, J.; De Hoog, G. S., *Scedosporium apiospermum*: changing clinical spectrum of a therapy-refractory opportunist. *Medical Mycology* **2006**, *44* (4), 295-327. 10.1080/13693780600752507



45. Silva, B. A.; Souza-Goncalves, A. L.; Pinto, M. R.; Barreto-Bergter, E.; Santos, A. L. S., Metallopeptidase inhibitors arrest vital biological processes in the fungal pathogen *Scedosporium apiospermum*. *Mycoses* **2011**, *54* (2), 105-112. 10.1111/j.1439-0507.2009.01767.x
46. Cooke, M. S.; Evans, M. D.; Dizdaroglu, M.; Lunec, J., Oxidative DNA damage: mechanisms, mutation, and disease. *Faseb Journal* **2003**, *17* (10), 1195-1214. 10.1096/fj.02-0752rev
47. (a) Halliwell, B., Free Radicals and Other Reactive Species in Disease. In *eLS*, John Wiley & Sons, Ltd: 2001. 10.1038/npg.els.0003913; (b) Trumbore, C. N.; Ehrlich, R. S.; Myers, Y. N., Changes in DNA conformation induced by gamma irradiation in the presence of copper. *Radiation Research* **2001**, *155* (3), 453-465. 10.1667/0033-7587(2001)155[0453:cidcib]2.0.co;2
48. Kavanagh, K.; Reeves, E. P., Exploiting the potential of insects for in vivo pathogenicity testing of microbial pathogens. *Fems Microbiology Reviews* **2004**, *28* (1), 101-112. 10.1016/j.femsre.2003.09.002
49. (a) Brennan, M.; Thomas, D. Y.; Whiteway, M.; Kavanagh, K., Correlation between virulence of *Candida albicans* mutants in mice and *Galleria mellonella* larvae. *Fems Immunology and Medical Microbiology* **2002**, *34* (2), 153-157. 10.1016/s0928-8244(02)00374-7; (b) Hamamoto, H.; Tonoike, A.; Narushima, K.; Horie, R.; Sekimizu, K., Silkworm as a model animal to evaluate drug candidate toxicity and metabolism. *Comparative Biochemistry and Physiology C-Toxicology & Pharmacology* **2009**, *149* (3), 334-339. 10.1016/j.cbpc.2008.08.008
50. (a) Bergin, D.; Murphy, L.; Keenan, J.; Clynes, M.; Kavanagh, K., Pre-exposure to yeast protects larvae of *Galleria mellonella* from a subsequent lethal infection by *Candida albicans* and is mediated by the increased expression of antimicrobial peptides. *Microbes and Infection* **2006**, *8* (8), 2105-2112. 10.1016/j.micinf.2006.03.005; (b) Renwick, J.; Daly, P.; Reeves, E. P.; Kavanagh, K., Susceptibility of larvae of *Galleria mellonella* to infection by *Aspergillus fumigatus* is dependent upon stage of conidial germination. *Mycopathologia* **2006**, *161* (6), 377-384. 10.1007/s11046-006-0021-1
51. (a) Desbois, A. P.; Coote, P. J., Utility of Greater Wax Moth Larva (*Galleria mellonella*) for Evaluating the Toxicity and Efficacy of New Antimicrobial Agents. In *Advances in Applied Microbiology, Vol 78*, Laskin, A. I.; Sariaslani, S.; Gadd, G. M., Eds. Elsevier Academic Press Inc: San Diego, 2012; Vol. 78, pp

- 25-53. 10.1016/b978-0-12-394805-2.00002-6; (b) McCann, M.; Santos, A. L. S.; da Silva, B. A.; Romanos, M. T. V.; Pyrrho, A. S.; Devereux, M.; Kavanagh, K.; Fichtner, I.; Kellett, A., In vitro and in vivo studies into the biological activities of 1,10-phenanthroline, 1,10-phenanthroline-5,6-dione and its copper(II) and silver(I) complexes. *Toxicology Research* **2012**, *1* (1), 47-54. 10.1039/c2tx00010e
52. Wright, J. B.; Lam, K.; Hansen, D.; Burrell, R. E., Efficacy of topical silver against fungal burn wound pathogens. *American Journal of Infection Control* **1999**, *27* (4), 344-350. 10.1016/s0196-6553(99)70055-6



**Chapter 4**

**Antibacterial  
activities of the  
metal complexes**

## 4.1 Introduction

Bacteria are among the most abundant forms of life, with an estimated  $4.6 \times 10^{30}$  bacterial cells on Earth which forms a biomass that far exceeds that of plants and animals combined.<sup>1</sup> They are thought to be one of the earliest forms of life on Earth and have adapted over the millennia to almost every environment imaginable. Bacteria are known to inhabit soil, water, acidic hot springs, radioactive waste and have even been found in such extreme locations as in sediments at the Challenger Deep in the Mariana Trench, which at almost 11,000 m depth represents the deepest oceanic site on Earth.<sup>2</sup> Bacteria are termed as prokaryotes and as such are relatively simple unicellular organisms which lack a membrane-bound nucleus.<sup>3</sup> Prokaryotes have a nucleoid (nuclear body) rather than an enveloped nucleus and lack membrane-bound cytoplasmic organelles. The plasma membrane in prokaryotes performs many of the functions carried out by membranous organelles in eukaryotes.<sup>4</sup> The bacterial genome is contained within a chromosomal double stranded circular DNA molecular, although other small loops of double stranded circular DNA, called plasmids, may also be present and these are physically separate from the chromosomal bacterial DNA and can replicate independently.<sup>5</sup>

All prokaryotes possess a cell wall which maintains the shape of the cell, protects the organism from the environment and can prevent the cell from lysing due to osmotic pressure if it comes in contact with a hypotonic medium.<sup>6</sup> Bacterial cells are quite small being typically 0.5 to 5.0 micrometres in length (although larger and smaller species do exist) which makes them approximately one tenth the size of eukaryotic cells. Bacteria exist in a wide variety of morphologies (shapes and sizes), the three most common of which are round (cocci), rod shaped (bacilli) and spiral (spirilla).<sup>3</sup> Many bacterial species exist as single individual cells, while others are known to group together or associate in characteristic patterns forming pairs (diploids), chains, clusters, branched filaments, bacterial mats or biofilms and even complex star shaped groups are known.<sup>7</sup> A biofilm is an assemblage of surface-associated microbial cells that is enclosed in an extracellular polymeric substance matrix. Biofilms range in thickness (micrometres to centimetres) and can be multicellular communities which contain multiple different bacterial species and various other organisms.<sup>8</sup> Biofilms are of particular importance in a medical setting as they are often present during chronic bacterial infections and they can also form on implanted medical devices such as catheters. Importantly, biofilm formation provides a

means of protection for bacteria, making bacteria within biofilms much more resilient to treatment than that of the isolated bacterial cells.<sup>9</sup>

There are two main classes into which bacteria can be divided, based on the differences in the structure of the bacterial cell walls. The first class is termed as Gram positive and these bacteria have a cell wall which is composed of a thick layer of peptidoglycan (20 to 80 nanometers thick). Peptidoglycan is a biopolymer comprised of a carbohydrate scaffold which is cross-linked with oligopeptides, and this gives the cell wall significant structural strength and rigidity (Figure 4.1).<sup>6</sup> Gram positive bacterial cell walls can contain up to forty layers of peptidoglycan, which in turn makes these cells structurally very strong. It is this thick layer of peptidoglycan in the cell wall of Gram positive bacteria that takes up and retains the crystal violet stain used in the Gram staining method of bacterial differentiation and identification.

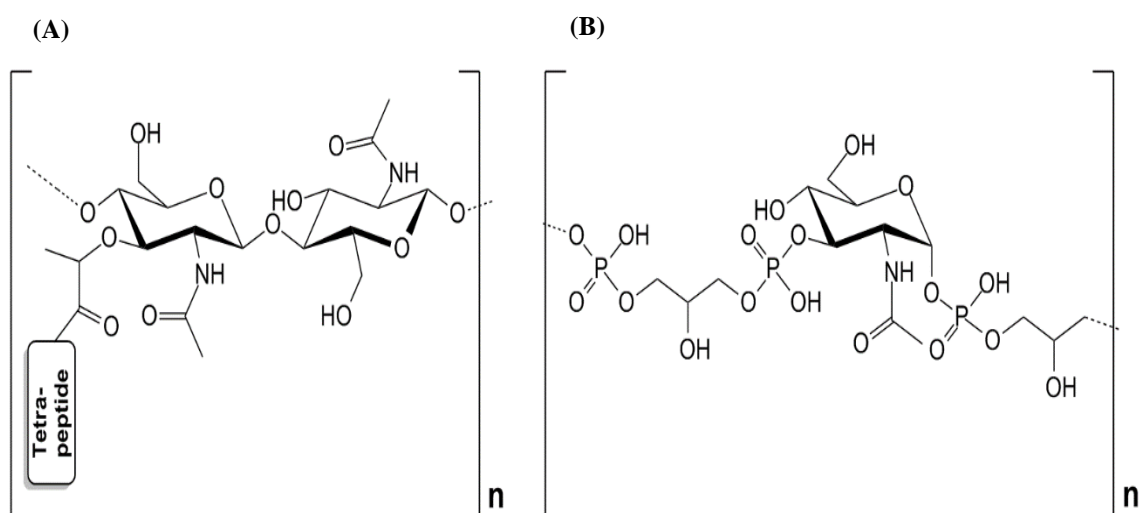
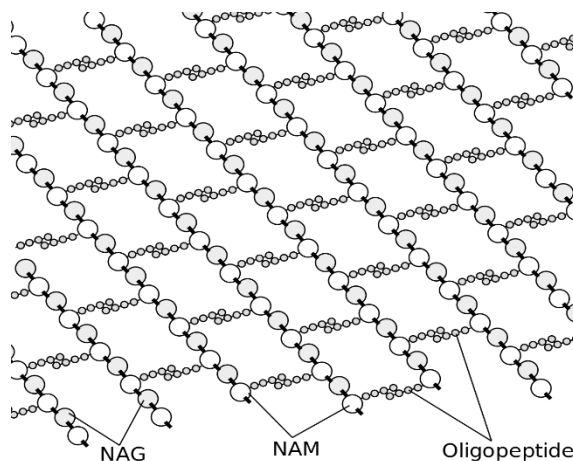


Fig. 4.1: (A) Peptidoglycan structure and (B) teichoic acid structure.<sup>10</sup>

The peptidoglycan layers form a crystal lattice comprised of two alternating amino acid carbohydrates (*N*-acetylglucosamine (NAG) and *N*-acetylmuramic acid (NAM)) connected by a  $\beta$ -(1,4)-glycosidic bond (Figure 4.2).<sup>10</sup> These peptidoglycan layers are highly hydrophobic and therefore repel hydrophilic molecules preventing their entrance to the cell. Conversely lipophilic/hydrophobic molecules can diffuse across/through this peptidoglycan layer with relative ease. The cell wall of Gram positive bacterial cells also contains other components such as teichuronic and teichoic acid which are dispersed throughout and transverse peptidoglycan layer (Figure 4.1 (B) and 4.3).<sup>11</sup> It is these

biopolymers (peptidoglycan, teichoic and teichuronic acid) that can act as antigens during infection of a host by a Gram positive bacterium. Teichoic acid may also act as a receptor for other molecules and has been implicated as a possible receptor for bacteriophages.<sup>12</sup>



**Fig. 4.2:** General structure of a Gram-positive bacterial cell wall, composed of peptidoglycan.

The second class of bacteria are termed Gram negative bacteria. Both Gram-positive and Gram-negative bacteria are enclosed in a cell membrane which can contain various different membrane proteins, dispersed throughout the membrane. Beyond this membrane lies the periplasmic space which contains enzymes of various functions and beyond this is the cell wall. Gram negative bacteria have only one or two layers of peptidoglycan (7 or 8 nanometers thick) in their cell walls which in turn makes them structurally weaker than Gram positive cells. Gram negative bacterial cells have an outer membrane beyond the peptidoglycan layer, this membrane contains porins (channels) and other membrane proteins which facilitate the transit of hydrophilic species through the otherwise hydrophobic cell wall (Figure 4.3). This outer membrane is coated with lipopolysaccharides, which are hydrophilic in nature and prevent lipophilic/hydrophobic molecules from entering or gaining access to the cell wall. This outermost lipopolysaccharide surface of the cell wall of Gram negative bacteria does not absorb or retain the crystal violet stain used in the Gram staining method and therefore are termed Gram negative. The lipopolysaccharides can act as antigens and upon destruction of the cell wall, are released into the surrounding environment, acting as endotoxins. It is the presence of this outermost, lipopolysaccharide coating which generally results in Gram negative bacteria being more virulent/toxic to human hosts and also more resistant to the immune response and the action of known antibacterial treatments, over that of Gram positive species.

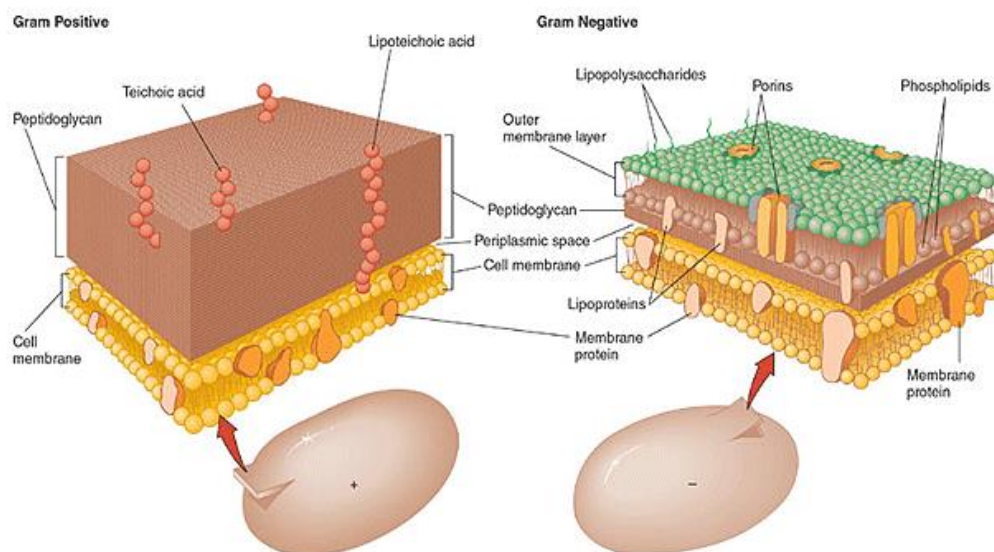


**Fig. 4.3:** A schematic diagram of the cell walls of Gram positive and Gram negative bacteria.<sup>10</sup>

In addition, many of the current prescription antibiotics are lipophilic and therefore will be repelled by the hydrophilic lipopolysaccharide coating of Gram negative cell walls. In contrast, the lipophilic nature of the peptidoglycan cell wall of Gram positive bacteria will allow unhindered, passive diffusion of these predominantly lipophilic drug molecules. Furthermore, the penicillin or  $\beta$ -lactam class of antibiotics exert their bactericidal effect by binding to and inhibiting bacterial enzymes that form the bonds between oligopeptide crosslinks in peptidoglycan hence preventing the formation of a fully functional bacterial cell wall. Thus, they are much more effective against Gram-positive bacteria.<sup>4</sup>

The World Health Organisation (WHO) recently released (April 2014) a global report on the ever increasing rise of multi-drug resistant bacteria, parasites, viruses and fungi.<sup>13</sup> In this report antimicrobial resistance (AMR) is assessed as being one of the greatest threats to human health, “A post-antibiotic era in which common infections and minor injuries can kill, far from being an apocalyptic fantasy, is instead a very real possibility for the 21st Century”.<sup>13</sup> Therefore the emergence of totally, extensively and multidrug resistant bacterial strains with few, or no treatment options, will have a detrimental effect on the general populace and consequently on all public health services.<sup>14</sup> Hence, there is an urgent and as of yet, an unmet necessity, to develop novel, efficacious and cost effective

antimicrobial agents possessing unique modes of action in order to circumvent intrinsic and acquired bacterial resistance.

Our aim was to produce a series of new, metal-based (Mn(II), Cu(II) and Ag(I)) 1,10-phen/dicarboxylate antimicrobial compounds for the treatment of a range of bacterial infections of community acquired and nosocomial origin. Four groups/families of complexes were synthesized and their *in vitro* antibacterial activity and *in vivo* systemic toxicity was evaluated against four different species (seven strains) of pathogenic bacteria. The bacteria were as follows: (a) Gram-positive bacteria, *Staphylococcus aureus* (clinical isolate), and methicillin-resistant *Staphylococcus aureus* (MRSA), (b) Gram negative bacteria, *Pseudomonas aeruginosa* (ATCC 27853), *Pseudomonas aeruginosa* (ATCC 10145), *Escherichia coli* (clinical isolate) and (c) *Mycobacterium tuberculosis* (CDC1551) and *Mycobacterium tuberculosis* (ATCC 27294) which are classified as acid-fast Gram positive bacteria due to an unusual waxy coating of mycolic acids on their cell surface.<sup>15</sup> This coating of mycolic acids (composed of a long  $\beta$ -hydroxy chain with a shorter  $\alpha$ -alkyl side chain) makes the *Mycobacterium tuberculosis* cells impervious to Gram staining and requires another type of cell staining identification termed Ziehl-Neelsen staining, or acid-fast staining.<sup>15</sup> Although difficult to classify, they fit the Gram-positive category as acid-fast Gram-positive bacteria due to their lack of an outer cell membrane. Two types of biological assays were conducted on the bacteria, an agar plate well diffusion zone of growth inhibition assay and a 96-well microplate broth dilution susceptibility assay, with the latter being used to determine a minimum inhibitory concentration (MIC) value for each test compound.

#### 4.2 *Staphylococcus aureus*

*Staphylococcus aureus* (*S. aureus*) is a Gram positive coccal bacterium and is frequently found on the skin, forming part of the normal skin flora, in the anterior nares of the nasal passages and the human respiratory tract. It is estimated that, in any population, 30-50% of healthy people are carriers of *S. aureus*, with 20% of these individuals being described as persistent carriers.<sup>16</sup> This bacterium derives its name from the appearance of its colonies, which grow in clusters of golden/yellow spheres and resemble a bunch of grapes. Hence, the name *Staphylococcus* from the Greek word *staphyle* which translates as “a bunch of grapes” (Figure 4.4 (A)).<sup>17</sup>

*S. aureus* is a versatile pathogen, being able to survive on nutrient-limited, dry environmental surfaces for hours to weeks, or even months.<sup>18</sup> Furthermore, *S. aureus* has numerous routes by which infection can take place, such as, by direct contact with wounds or any surface which is carrying the bacteria, airborne carriage and any contact with indwelling medical devices such as catheters.<sup>19</sup> It is these attributes of *S. aureus* that contribute to its highly infectious nature in a hospital environment.

There are many different strains of *Staphylococci* bacteria that can infect humans, but *S. aureus* is still the most common strain of pathogenic *Staphylococci* bacteria. *S. aureus* is a highly significant pathogen particularly in a hospital setting and has been identified as one of the main pathogens associated directly (or commensally) with ca. 40% of all reported infections of the skin and soft tissue.<sup>20</sup> In addition, *S. aureus* infection can result in more serious and life threatening conditions such as Staphylococcal scalded skin syndrome (SSS), bacteraemia, pneumonia, meningitis, osteomyelitis (bone/bone marrow infection), endocarditis (infection of the inner layer of the heart), toxic shock syndrome (TSS) and it is also a significant cause of blood infections (sepsis) in people requiring haemodialysis (Figure 4.4).<sup>21</sup>

Another common community acquired illness caused by *S. aureus* is food poisoning, which can occur after ingesting food contaminated with the exotoxins (enterotoxin type E) produced/secreted by *S. aureus* surface colonisation.<sup>22</sup> *S. aureus* has a number of mechanisms to evade or resist attack by the immune system of a host and therefore these infections can be difficult to treat and overcome.<sup>23</sup> *S. aureus* is currently one of the most common causes of nosocomial infections and is often implicated in postsurgical wound infections.<sup>18</sup>

In addition to the serious implications for public health there is also the considerable negative economic impact of treating the myriad of infections caused by *S. aureus*. One 15 year study conducted in New York hospitals determined that the direct cost of treating a patient with a *S. aureus* infection ranged between \$29,000 and \$35,000.<sup>24</sup> In the USA each year, an estimated 500,000 patients contract a staphylococcal infection. In the UK, 20,000 cases of *S. aureus* infection occur annually and in Ireland, 1,412 cases were reported in 2006.<sup>25</sup> These figures reveal the enormity of the public health treat and fiscal burden that the treatment of *S. aureus* infections currently pose.





**Fig. 4.4:** (A) Electron micrograph of *S. aureus* cells, (B) young child with Staphylococcal scalded skin syndrome (SSS) and (C) a leg ulcer caused by *S. aureus* infection.<sup>26</sup>

### 4.3 Methicillin resistant *Staphylococcus aureus* (MRSA)

MRSA, is defined as any strain of *S. aureus* that has developed resistance to  $\beta$ -lactam antibiotics and, like *S. aureus*, it is a facultative anaerobic, Gram-positive, coccial bacterium.<sup>27</sup> It is catalase and nitrate reduction positive, meaning that it can secrete enzymes with the capability to decompose hydrogen peroxide and various nitrogen oxides to produce water, oxygen and nitrogen.

$\beta$ -Lactam antibiotics target and efficiently inhibit the bacterial transpeptidase enzymes (localized to the outer leaflet of the bacterial cytoplasmic membrane) which catalyse the peptide bond formation of the oligopeptide crosslinks in the peptidoglycan forming the bacterial cell wall. The  $\beta$ -lactam moiety is stereochemically similar to the D-alanine–D-alanine substrate and hence forms a lethal, covalent, penicilloyl-enzyme complex that blocks the transpeptidation reaction. The  $\beta$ -lactam amide bond is broken and a new



covalent bond is formed with the catalytic serine residue in the transpeptidase enzyme active site. This is an irreversible reaction and inactivates the enzyme. This reduces cell wall integrity from weakly cross-linked peptidoglycan, which makes the growing bacteria highly susceptible to cell lysis and death.<sup>27a</sup>

When penicillin was first used to treat bacterial infections in the early 1940s, penicillin-resistant strains of *S. aureus* were unknown, but by the 1950s they were becoming common in hospitals.<sup>28</sup> In 1959, methicillin was introduced to treat these penicillin-resistant strains, but within a few years, methicillin-resistant *S. aureus* strains were encountered. There are now numerous different strains of MRSA that are simultaneously resistant to various different classes of antibiotics. Some strains are even resistant to vancomycin (glycopeptide antibiotic class) termed VRSA, which is a cause for serious concern as vancomycin is often considered the antibiotic of last resort.<sup>29</sup>

Unlike *S. aureus*, MRSA contains an additional gene termed the *mecA* gene, which encodes a protein (penicillin binding protein/transpeptidase enzyme, PBP2A) which has a low affinity for the  $\beta$ -lactam moiety and hence all  $\beta$ -lactam antibiotics such as the penicillins and the Cephalosporin class of  $\beta$ -lactam antibiotics (Figure 4.5).<sup>30</sup>

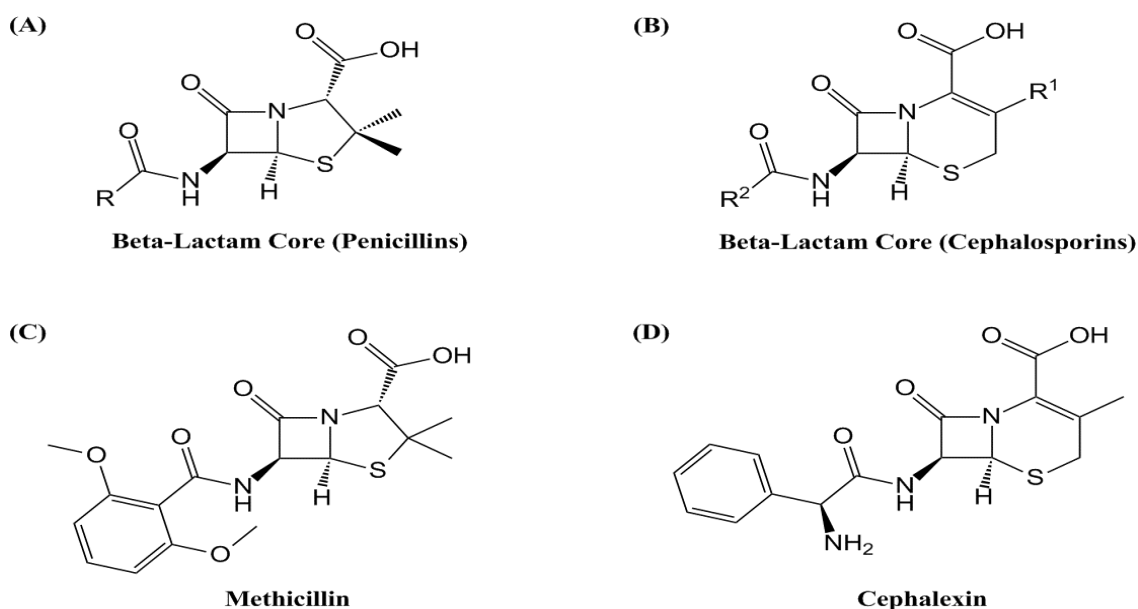


**Fig. 4.5:** (A)  $\beta$ -Lactam moiety common to all penicillin antibiotics, (B)  $\beta$ -lactam moiety of the cephalosporin antibiotics, (C) Methicillin and (D) Cephalexin. (C) and (D) are ineffective against MRSA.

Recent evidence (2012) indicates that MRSA and other highly antibiotic resistant strains of *S. aureus* obtain their antibiotic resistance from exchanging plasmids via horizontal gene transfer (the transfer of genes between organisms in a manner other than traditional reproduction) from other bacteria.<sup>31</sup> Therefore, MRSA with the *mecA* gene can effectively utilise its transpeptidase enzymes in the presence of  $\beta$ -lactam antibiotics, preventing them from inhibiting peptidoglycan cell wall synthesis. Methicillin is no longer used for antimicrobial susceptibility testing having been superseded by the more stable oxacillin, and its role in therapy has been largely replaced by other derivatives of oxacillin such as flucloxacillin and dicloxacillin, although these are all still ineffective against MRSA. (Figure 4.6).<sup>32</sup>

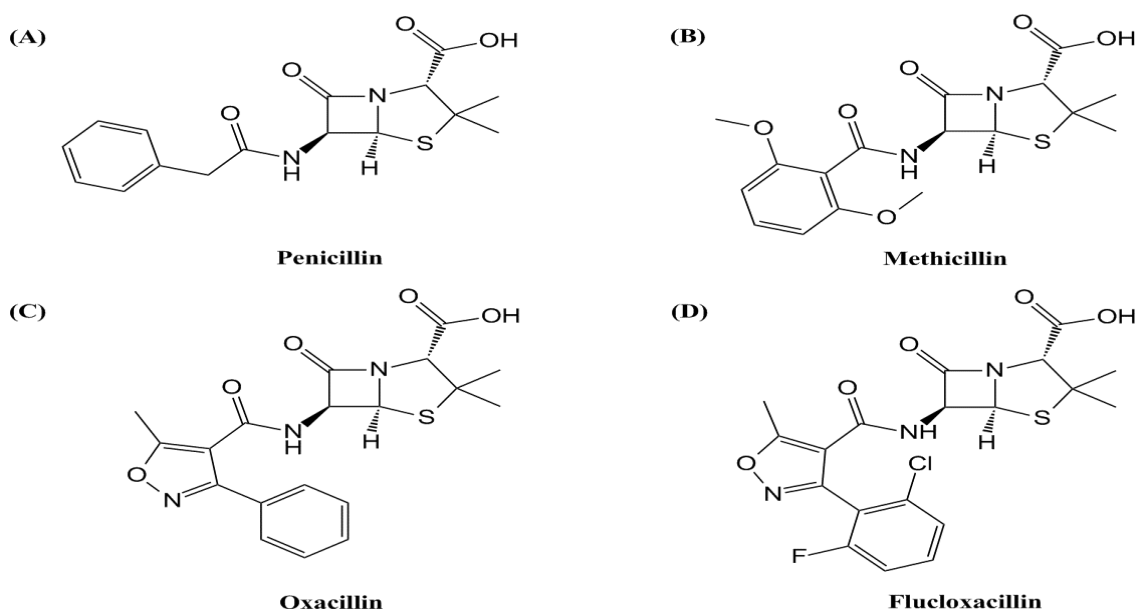


**Fig. 4.6:** (A) The first  $\beta$ -lactam antibiotic penicillin, (B) methicillin, (C) oxacillin and (D) current clinically employed acid-stable orally administered  $\beta$ -lactam antibiotic, flucloxacillin.

The develop of this resistance gene (*mecA*) makes MRSA infections much more difficult to treat than that of normal strains of *S. aureus*, as MRSA is highly resistant to treatment with standard first line prescription antibiotics. MRSA like *S. aureus*, has numerous different transmission routes and can be spread by touch alone, making it especially dangerous when it occurs in hospitals or nursing homes where people may have open wounds, weakened immune systems or be undergoing invasive/surgical procedures and hence, are at greater risk of this nosocomial infection than the general public.<sup>33</sup> MRSA

infections, like *S. aureus* infections, in general initially present as a red rash which can progress into abscesses that require surgical treatment (Figure 4.7 B).

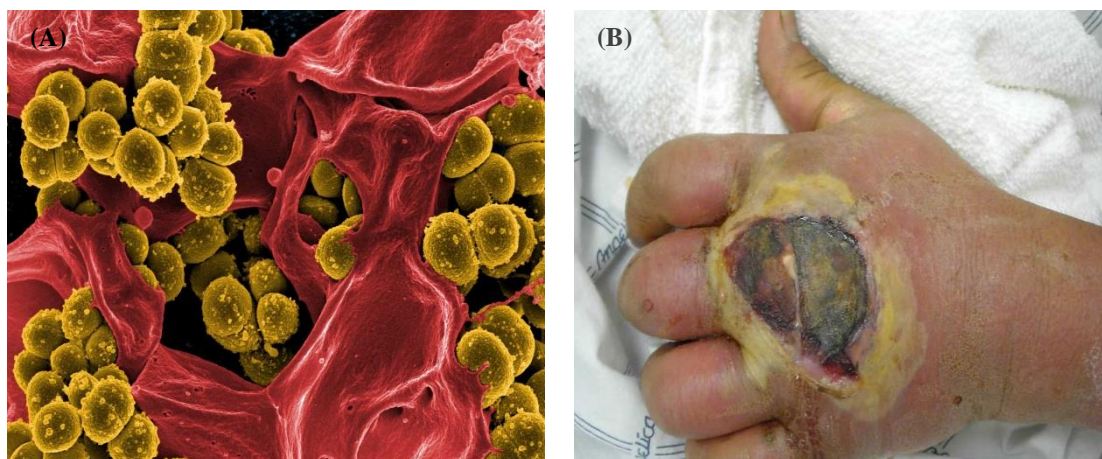


**Fig. 4.7:** (A) Scanning electron micrograph of methicillin-resistant *S. aureus* (MRSA) and a dead human neutrophil. (B) Photograph of methicillin-resistant *S. aureus* infection of the hand.<sup>34</sup>

In addition to causing skin infection the bacteria can also cause invasive disease by infecting other parts of the body including the bones, bloodstream and lungs, and is most often the cause surgical site infection.<sup>35</sup> Although MRSA began as a hospital-acquired infection (HA-MRSA) it is now also a community acquired infection (CA-MRSA), with both types showing a huge increase in incidence over the last few years.<sup>35-36</sup>

Although HA-MRSA and CA-MRSA have distinct clinical differences, both are transmitted in the same fashion, most frequently through direct skin to skin contact. Like HA-MRSA, CA-MRSA transmission is associated with crowding, frequent skin-to-skin contact, compromised skin (cuts or abrasions), contaminated items and surfaces and a lack of cleanliness. Therefore, areas where these factors are common include schools, university dormitories, military barracks, households, correctional facilities and childcare centres.

The number of cases of MRSA infection reported in Ireland is also very high according to a recent study (2014) by The Health Protection Surveillance Centre (HPSC) on invasive isolates of *S. aureus* as part of the European Antimicrobial Resistance Surveillance

Network (EARS-Net) placing Ireland 9<sup>th</sup> highest of 28 countries regarding the number of MRSA cases reported.<sup>37</sup> In addition, Ireland ranks 4<sup>th</sup> in Europe for MRSA bloodstream infection (BSI) rates at 33.1%, with only Portugal, Greece and Italy reporting higher numbers in 2009. The cost associated with treating MRSA infections in Ireland has been estimated as €23 million per annum and there is also a high incidence of frequent after-care which adds to this figure.<sup>38</sup> This cost for treating MRSA infection represents 10% of the total cost of additional expenditure as a result of all health-care associated infections (HCAI) which is estimated at €233.75 million annually. Furthermore, it has been estimated that patients who acquire an infection in hospital stayed in hospital 2.5 times longer than other patients and most significantly, they are 7.1 times more likely than uninfected patients to die in hospital.<sup>38</sup> This has led to unprecedented global concern and intense research focus to develop new classes of compounds to treat/combat MRSA and other health-care/community associated infections with acquired and intrinsic resistance to the known antimicrobial agents.

#### 4.4 *Escherichia coli*

*Escherichia coli* (*E. coli*) are Gram-negative, facultative anaerobic, bacilli (rod-shaped) bacteria that exist either singly or in pairs (Figure 4.8).<sup>39</sup> They form part of the normal flora of the gastrointestinal tract and as such are commonly found in the lower intestine of warm-blooded organisms, including humans.<sup>39a</sup>

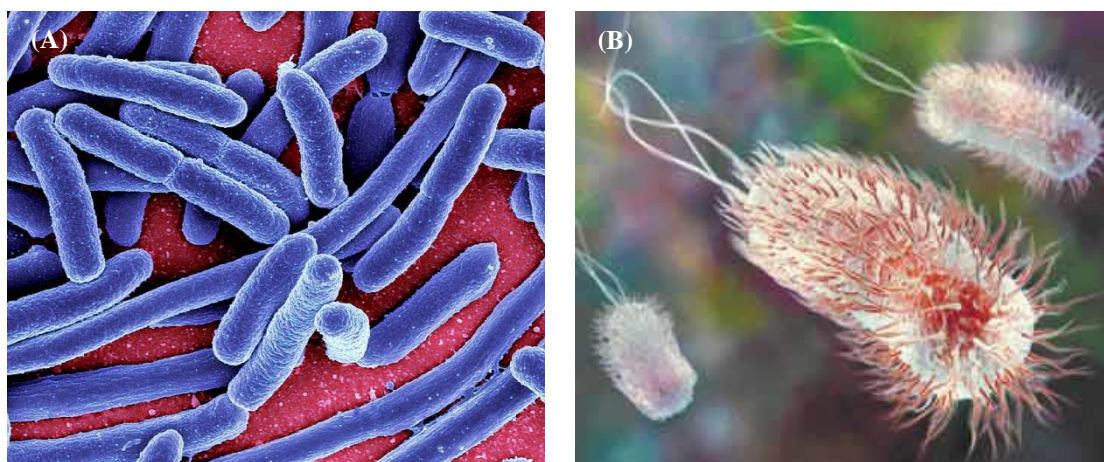


**Fig. 4.8:** (A) Scanning electron micrograph of *E. coli* cells and (B) *E. coli* cells with flagella.<sup>40</sup>

*E. coli* cells are typically about 2.0  $\mu\text{m}$  long and 0.5  $\mu\text{m}$  in diameter and, depending on the environmental conditions. They can form thin hair-like structures, called flagella, which allow the bacteria to move and to attach to human cells.<sup>41</sup> *E. coli* is one of the most diverse bacterial species, it encompasses a huge population of bacteria; as such there are numerous different strains of *E. coli*, the majority of which are harmless to their hosts and can even be beneficial by producing vitamin K<sub>2</sub> and by preventing colonisation of the gastrointestinal tract by other harmful, pathogenic, bacterial species.<sup>42</sup>

The non-pathogenic *E. coli* strains can cause disease if they move outside of their normal environment of the intestines, and this can result in colonisation/infection of the urinary tract, bladder and kidneys, leading to organ damage and other complications.<sup>43</sup> Certain strains of *E. coli* are a major cause of foodborne illness associated with food poisoning, while other more virulent strains can cause gastroenteritis, cholecystitis (inflammation of the gallbladder) and mastitis. Less commonly encountered strains can cause hemolytic-uremic syndrome (HUS), bacteraemia, peritonitis, septicaemia, neonatal meningitis and Gram-negative pneumonia, which without urgent medical treatment can have a high incidence of mortality.<sup>44</sup>

Enterovirulent strains of *E. coli* (highly pathogenic strains) which can infect the intestines after consuming contaminated food can produce toxins, termed verotoxin or shiga-like toxin (Figure 4.9).<sup>45</sup> These strains can result in hemolytic-uremic syndrome (HUS) which can manifest acute renal failure, anemia (low red cell count) and thrombocytopenia (low platelet count).

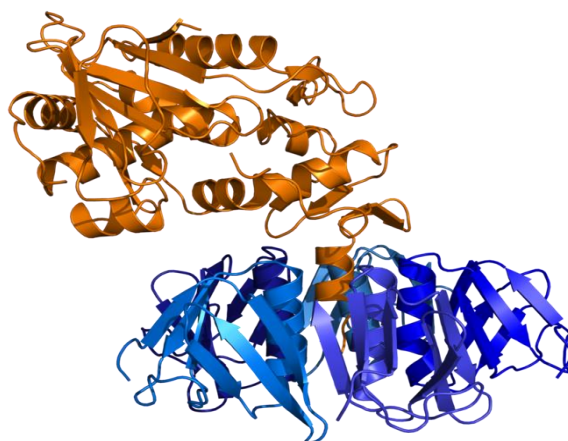


**Fig. 4.9:** Ribbon-structure of shiga toxin type 2 ( Stx2) from *E. coli* O157:H7.<sup>46</sup>



In addition, the verocytotoxin (shiga-like toxin) can directly damage vascular and endothelial cells.<sup>45</sup> The overall mortality rate from HUS is 5-15%, with young children and the elderly having a worse prognosis.<sup>47</sup> Patients with HUS can suffer irreversible brain damage and as many as 25% die during the acute phase of infection. Furthermore, up to one third can have abnormal kidney function many years later and have other lifelong complications, such as high blood pressure, seizures, blindness, paralysis, and adverse effects of surgical intention to remove part of their colon.<sup>47-48</sup> Antibiotic treatment is ineffective for HUS as they can increase the release of shiga-like toxins, which results in the aforementioned lifelong complications from damage caused by the verotoxin producing *E. coli* infection.<sup>49</sup>

#### 4.5 *Pseudomonas aeruginosa* (ATCC 27853 and 10145)

*Pseudomonas aeruginosa* (*P. aeruginosa*) belongs to the family *Pseudomonadaceae* and is a Gram-negative, rod-shaped (bacilli) bacterium whose cell size ranges from 0.5 to 0.8  $\mu\text{m}$  by 1.5 to 3.0  $\mu\text{m}$  (Figure 4.10).<sup>50</sup> It requires oxygen to survive and therefore is defined as an obligate aerobic bacterium, using aerobic respiration to achieve its optimal metabolism. However, it can also respire anaerobically on nitrate or other alternative electron acceptors and can catabolize a wide range of organic molecules. *P. aeruginosa* has been documented surviving in hypoxic conditions with very low oxygen levels.<sup>51</sup> In general, almost all strains are able to move via a single polar flagellum.

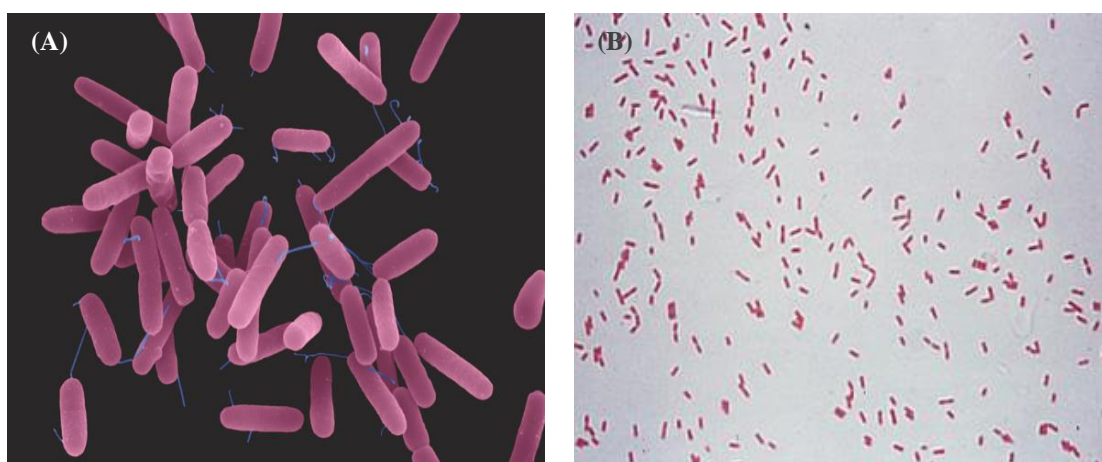


**Fig. 4.10:** (A) Scanning electron micrograph of *P. aeruginosa* bacteria. (B) Gram stain of *P. aeruginosa* cells.<sup>51-52</sup>

*P. aeruginosa* are citritase, catalase and cytochrome c oxidase/ indophenol oxidase positive, possessing these enzymes with the capability to decompose hydrogen peroxide and various nitrogen oxides to produce water, oxygen and nitrogen.<sup>53</sup> Typically, *Pseudomonas* bacteria are found attached to a surface having formed a biofilm but, alternatively, they can also be found in a mobile planktonic form.<sup>6, 54</sup> *P. aeruginosa* is a highly adaptable bacterium, it is a ubiquitous organism present in many diverse environmental settings and has colonized various environmental niches, being commonly found in soil and water.<sup>50a</sup> There are a number of strains that can survive and grow in harsh conditions (high temperatures of 42 °C) and with little nutrition. In addition, other strains have been documented with resistance to heavy metals and a number of antibiotics.<sup>55</sup> This ability of *P. aeruginosa* to survive on minimal nutrition and to tolerate a variety of physical conditions has allowed this organism to persist in both community and hospital settings.<sup>55a</sup>

*P. aeruginosa*, similar to *E. coli* and *S. aureus*, are classified as an opportunistic pathogen in that they rarely cause serious infection or disease in a healthy individual.<sup>54a, 56</sup> Due to its opportunistic nature, if a barrier to infection, such as the skin is broken from a minor injury, by mechanical ventilation, tracheostomy, catheters, or surgery, *P. aeruginosa* infection can occur and people with impaired immunity have higher risks for colonization by this organism. Furthermore, disruption in the normal microbial flora as a result of antimicrobial therapy has also been shown to increase colonization by *P. aeruginosa*.<sup>55a</sup> As such, *P. aeruginosa* is also a versatile leading opportunistic pathogen and is associated with a broad spectrum of infections in humans and typically infects the urinary tract, burns, the blood/circulatory system and the pulmonary tract.<sup>50a, 57</sup> As previously stated *P. aeruginosa* is widely distributed in nature but, despite this, serious infections with *P. aeruginosa* are predominantly hospital acquired.<sup>55a</sup>

In immunocompromised/immune deficient people and individuals with cystic fibrosis or chronic pulmonary disease, *P. aeruginosa* can cause severe, systemic and potentially fatal infections.<sup>50a, 56, 57b, 58</sup> *P. aeruginosa* is the dominant pathogen causing chronic respiratory infections in cystic fibrosis (CF) patients. This results in progressive lung damage and is the major cause of morbidity and mortality in CF patients.<sup>59</sup> *P. aeruginosa* can form biofilm-like microcolonies embedded in the lung mucus of patients with CF. It is *P. aeruginosa*'s ability to adapt to hypoxic (low oxygen level) or anaerobic environments that facilitates its survival, as thick layers of lung mucus and alginate secreted by the

bacterium surround the bacterial cells and limit the diffusion of oxygen. It is this biofilm formation that protects *P. aeruginosa* in hostile environments, like the CF lung, from the immune response of the host and leads to its high antibiotic tolerance.<sup>54b</sup>

Test compounds/complexes **1**, **2** and **6-17** (Table **4.1**) were evaluated against two different strains of *P. aeruginosa*. *P. aeruginosa* (ATCC 27853) is a biofilm-forming strain and is considered to be highly virulent due to its ability to secrete large quantities of two fluorescent siderophores. The major siderophore is known as pyoverdine and the minor siderophore termed pyochelin. Pyoverdine is an Fe(III) binding molecule and is known to be important for bacterial virulence and biofilm development.<sup>60</sup> Pyochelin, although not as important for bacterial virulence, is able to bind Cu(II) and Zn(II) ions in addition to Fe(III) (unlike pyoverdine).<sup>60a</sup> The second strain, *P. aeruginosa* (ATCC 10145), is a mobile planktonic form of the bacterium and only produces limited quantities of siderophores, especially pyoverdine, therefore, reducing its virulence and biofilm-forming ability.

#### 4.6 *Mycobacterium tuberculosis*

*Mycobacterium tuberculosis* (*M. tuberculosis*) is a Gram-positive, pathogenic bacterium first discovered in 1882 by Robert Koch, and is responsible for the highly contagious and potentially fatal disease, Tuberculosis (TB) (Figure **4.11**).<sup>15</sup>

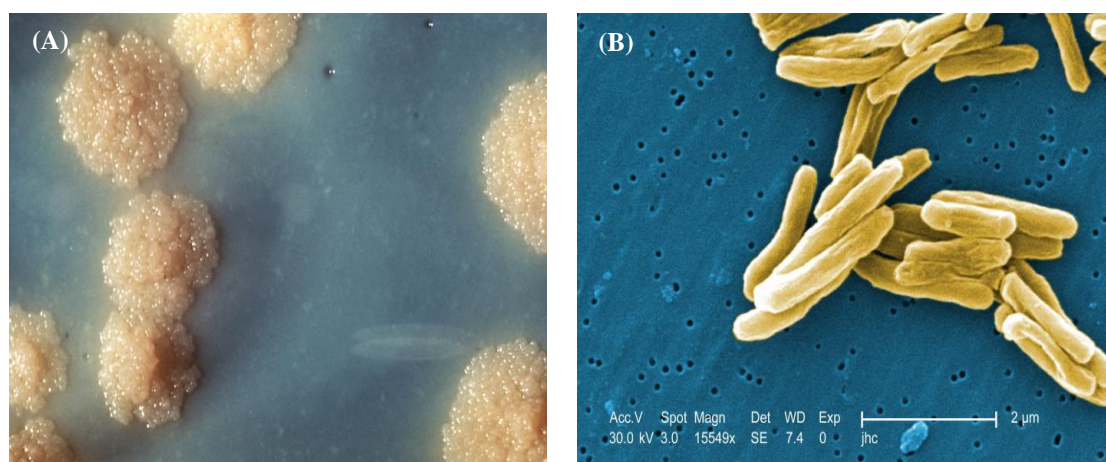


**Fig. 4.11:** (A) *M. tuberculosis* culture. (B) Scanning electron micrograph of *M. tuberculosis* bacteria.<sup>61</sup>



*M. tuberculosis* has an unusual, waxy coating composed mainly of mycolic acid on its cell surface, which makes the cells impervious to Gram staining, thus, acid-fast staining is used instead.<sup>15</sup> *M. tuberculosis* is a very aerobic organism and requires high levels of oxygen to survive, therefore, infection is restricted to the lungs and it is primarily a pathogen of the mammalian respiratory system. *M. tuberculosis* can reside for a long period of time in the alveolar macrophages of the lungs, with the macrophages acting as reservoirs for this organism.<sup>62</sup> The bacterium is easily spread from person to person via bacteria laden droplets expelled from the infectious individual during sneezing or coughing. After a person is exposed to *M. tuberculosis*, the bacterium can lie dormant in the infected person's lungs for years. While only ca. 5-10% of infected people will go on to develop active tuberculosis at some point in their lifetime, those with the disease in its active state are highly contagious and in this active state the disease is life-threatening.

The WHO has estimated that, globally, almost one third of the population is infected with TB (latent TB), 9.4 million are ill (2009) and nearly 1.5 million people die from TB each year.<sup>63</sup> HIV sufferers are known to be 20-40 times more likely to develop active TB than that of otherwise healthy individuals. This is due to latent TB being activated when the immune system is comprised.<sup>64</sup> The treatment of TB in HIV-infected individuals can often be more expensive, produce additional side effects and require less pleasant regimes due to some of the current anti-tubercular drugs being incompatible with common anti-retro viral treatments used to control HIV.<sup>63</sup>

The rise of treatment-resistant strains of TB, particularly multidrug-resistant strains (MDR-TB) where the strain is resistant to two or more front line drugs and extensively drug-resistant strains (XDR-TB) where the strain is resistant to the two most important second line drug classes, is cause for great concern.<sup>14b</sup> In 2012, about 450,000 people developed MDR-TB, while XDR-TB and totally drug-resistant (TDR) strains are also on the increase.<sup>65</sup> These strains are proving extremely difficult to treat. The long and expensive treatment regime, combined with poor drug management and incomplete treatment of the MDR and XDR strains, has led to the emergence of totally drug-resistant (TDR) tuberculosis. There is clearly a need for new compounds with unique, novel mechanisms of action to treat these highly resistant strains of *M. tuberculosis* and more effectively combat this worrisome trend.

#### 4.7 Complex synthesis, characterisation and proposed structures

1,10-Phenanthroline-5,6-dione (phendione (**2**)), and complexes **8-14** (Figure **4.12**) were prepared in accordance with the literature methods with some slight modifications.<sup>66</sup> The proposed structures of all test complexes, **6-17** are shown in Figure **4.12**. The complexes are divided into 5 groups/families based on their ligand similarities (Figure **4.12**). The first group is comprised of 1,10-phen (**1**) and 1,10-phenanthroline-5,6-dione (phendione, **2**). The second group is comprised of Ag(I) and Cu(II) phendione perchlorate complexes. The third group is comprised of Mn(II) 1,10-phen phthalate, isophthalate and terephthalate complexes (**8-12**). The fourth group are Mn(II) and Cu(II) 1,10-phen octanedioate complexes (**13-14**). The fifth group contains Mn(II), Cu(II) and Ag(I) 1,10-phen trioxaundecanedioate complexes (**15-17**).

All ligands and complexes were characterised using standard spectroscopic techniques, please refer to sections **2.3 – 2.6** of experimental chapter 2 and section **3.5**, chapter 3 page 171 for a more detailed description of their synthesis and characterisation.

The IR spectra of complexes **8-15**, were compared to their known spectra and all were found to contain the characteristic 1,10-phen stretches.<sup>67</sup> As expected, upon coordination these bands are shifted to lower frequency compared to the metal-free 1,10-phen (*ca.* 858 and 742 cm<sup>-1</sup>). The %CHN, mass spectral and magnetic moment data acquired for these complexes match the expected values and are in line with all data previously published.<sup>66c</sup>

The IR spectrum of complex **15** contains the characteristic 1,10-phen stretches and stretches for the carboxylate function of the tdda ligand, indicating that the tdda ligand is in a monodentate coordination mode.<sup>68</sup> Furthermore the IR data for **15** compares favourably to its Mn(II)-based analogue, **14**, the X-ray crystal structure of which shows the tdda ligand in a monodentate coordination mode. In addition, the mass spectral and elemental analysis data are in accordance with the proposed formulation of **15**, [Cu(3,6,9-tdda)(phen)<sub>2</sub>].3H<sub>2</sub>O·EtOH.

The IR spectrum of **17** contains characteristic 1,10-phen stretching bands (*ca.* 855 and 738 cm<sup>-1</sup>) with the  $\nu_{(\text{OCO})_{\text{asym}}}$  and  $\nu_{(\text{OCO})_{\text{sym}}}$  vibrations for the tdda carboxylate groups at 1622 and 1422 cm<sup>-1</sup>, respectively, giving a  $\Delta_{(\text{OCO})}$  value of 200 cm<sup>-1</sup>. This  $\Delta_{(\text{OCO})}$  value leaves it difficult to assign the coordination with any certainty but would suggest either free (uncoordinated) carboxylate or possibly a monodentate coordination mode.<sup>68</sup>

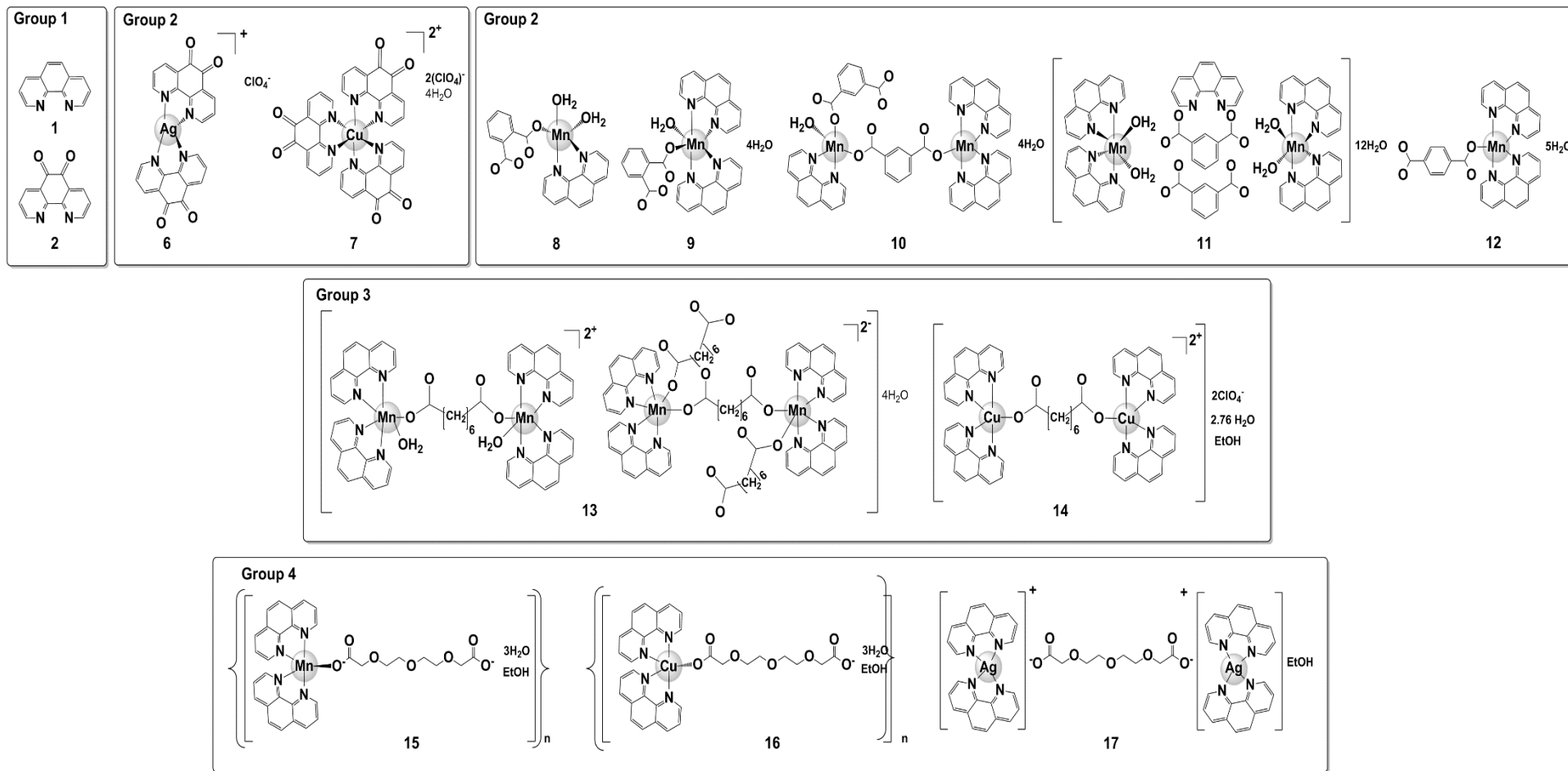


**Fig. 4.12:** Structure and group assignments of metal complexes used for antibacterial testing. Complexes in groups 2–3 and complex **15** in group 4 have previously been published. Complexes **16** and **17** in group 4 are novel.

A full crystal structure of **17** has proven difficult to obtain as it forms long (2 mm) thin crystalline fibres and there appears to be disorder in the tdda portion of the complex. The limited crystallographic data was able to confirm the presence of  $\{[Ag(phen)_2]\}$  units linked in some fashion to one another through the tdda ligand. This would suggest that the tdda is acting as either a monodentate bridging ligand ( $\eta^1 \eta^1 \mu^2$ -tdda) linking two of the  $[Ag(phen)_2]$  units together, or as an uncoordinated counter ion (Figure 4.13). The favoured coordination geometry of the d10 Ag(I) ion centre in  $[Ag(phen)_2]$  would most likely be tetrahedral in order to limit the ligand-ligand (electron-electron) repulsion with the 10 d electrons of the Ag(I).<sup>69</sup>

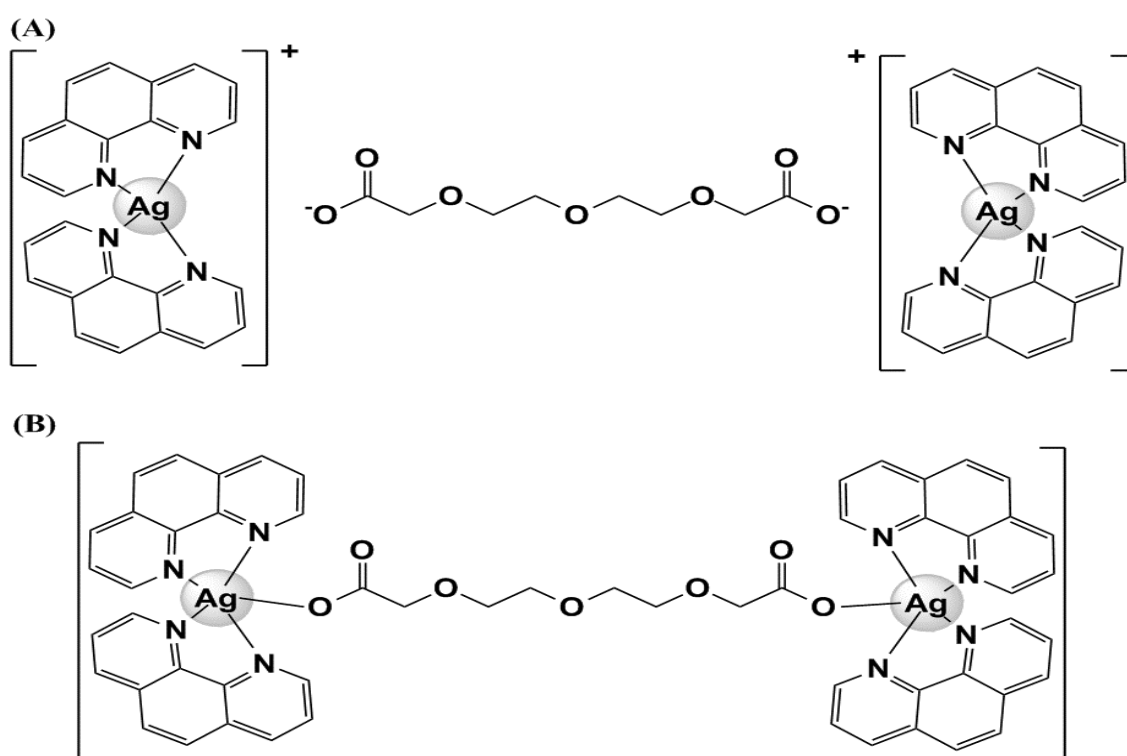


**Fig. 4.13:** Proposed structures for complex **17**. (A) Pseudo square planar geometry of  $[Ag(phen)_2]$  with the dicarboxylate (tdda), acting solely as a counter ion (non-coordinated). (B) Square pyramidal or trigonal bipyramidal coordination geometry with tdda ligand acting as a monodentate bridging ligand eg. ( $\eta^1 \eta^1 \mu^2$ -tdda).

Mass spectral and elemental analysis data are in accordance with the proposed formulation of **17**,  $[Ag_2(3,6,9\text{-tdda})(phen)_4].EtOH$ .

#### 4.8 Antibacterial activity and cytoselectivity of selected complexes

The Mn(II), Cu(II) and Ag(I) complexes, **8-17** (Figure 4.12, Table 4.1), their simple metal salts, the metal-free ligands, the prescription  $\beta$ -lactam antibiotic, Ampicillin (AMP), and antitubercular/antimycobacterial agent, Isoniazid (INH), were screened, *in vitro*, for their ability to inhibit the growth of pathogenic bacterial cells. Two different assays were performed in order to ascertain the antibacterial efficacy of the test compounds/complexes.

**Table 4.1:** List of all test compounds/complexes utilized for antibacterial assays.

Compound	Molecular Mass (g/mol)
<b>1</b> 1,10-phenanthroline (1,10-phen)	180.21
<b>2</b> 1,10-phenanthroline-5,6-dione (Phendione)	210.19
<b>6</b> [Ag(phendione) <sub>2</sub> ]ClO <sub>4</sub>	627.70
<b>7</b> [Cu(phendione) <sub>3</sub> ](ClO <sub>4</sub> ) <sub>2</sub> .4H <sub>2</sub> O	965.02
<b>8</b> [Mn(ph)(phen)(H <sub>2</sub> O) <sub>2</sub> ]	435.30
<b>9</b> [Mn(ph)(phen) <sub>2</sub> (H <sub>2</sub> O)].4H <sub>2</sub> O	669.56
<b>10</b> [Mn <sub>2</sub> (isoph) <sub>2</sub> (phen) <sub>3</sub> ].4H <sub>2</sub> O	1050.82
<b>11</b> {[Mn(phen) <sub>2</sub> (H <sub>2</sub> O) <sub>2</sub> ] <sub>2</sub> (isoph) <sub>2</sub> (phen)}.12H <sub>2</sub> O	1627.42
<b>12</b> [Mn(tereph)(phen) <sub>2</sub> ].5H <sub>2</sub> O	669.56
<b>13</b> [Mn <sub>2</sub> ( $\eta_1\eta_1\mu_2$ -oda)(phen) <sub>4</sub> (H <sub>2</sub> O) <sub>2</sub> ][Mn <sub>2</sub> ( $\eta_1\eta_1\mu_2$ -oda)(phen) <sub>4</sub> ( $\eta_1$ -oda) <sub>2</sub> ].4H <sub>2</sub> O	2458.23
<b>14</b> [Cu <sub>2</sub> (oda)(phen) <sub>4</sub> ](ClO <sub>4</sub> ) <sub>2</sub> .2.76H <sub>2</sub> O.EtOH	1309.23
<b>15</b> {[Mn(3,6,9-tdda)(phen) <sub>2</sub> ].3H <sub>2</sub> O.EtOH} <sub>n</sub>	735.64
<b>16</b> {[Cu(3,6,9-tdda)(phen) <sub>2</sub> ].3H <sub>2</sub> O.EtOH} <sub>n</sub>	744.25
<b>17</b> [Ag <sub>2</sub> (3,6,9-tdda)(phen) <sub>4</sub> ].EtOH	1202.80
<b>AMP</b> Ampicillin	349.41
<b>INH</b> Isoniazid (isonicotinohydrazide)	137.14

The first was an agar well diffusion assay which is closely related to the Kirby-Bauer disc diffusion antibiotic sensitivity test. This assay was utilised for three species of bacteria (five different strains); Gram-positive bacteria tested were *S. aureus* and MRSA; Gram-negative bacterial species were *E. coli* and two strains of *P. aeruginosa* (ATCC 27853, 10145). The five different bacteria were grown overnight to the stationary phase in nutrient broth at  $37 \pm 1^\circ\text{C}$  and with shaking at 2000 rpm. The cells were diluted to give an OD<sub>600</sub> = 0.05 and then the bacteria were plated out on agar. The plates were incubated for 1 h at  $37 \pm 1^\circ\text{C}$ , at which point 5 mm diameter holes were cut into the agar gel to

create wells which were equally spaced. Test solutions/suspensions of selected compounds/complexes (**1, 8-17**) and the prescription  $\beta$ -lactam antibiotic, Ampicillin (AMP), were added to the wells (50  $\mu$ l total volume) at three different concentrations (125, 50 and 5  $\mu$ g/cm<sup>3</sup>). Data are only displayed for the 5  $\mu$ g/cm<sup>3</sup> concentration. The plates were incubated for 24 h at  $37 \pm 1^\circ\text{C}$ , and then the zones of inhibition around the wells were, measured in millimetres and graphed as total area of zone of inhibition (average area) versus concentration of test complex/compound in micromolar ( $\mu$ M) (Figures **4.16-4.20**). For the negative control, a petri dish containing only the bacterial culture inoculum was included in each incubation. The known  $\beta$ -lactam antibiotic, Ampicillin (AMP), was utilised as a positive kill control. All assays were performed in triplicate with three repetitions on separate occasions. It should be noted that agar well diffusion assays are known to have a high degree of correlation with minimum inhibitory (MIC) values.<sup>70</sup> The zone of inhibition results for all test compounds/complexes at 125, 50 and 5  $\mu$ g/cm<sup>3</sup> against the five aforementioned strains of bacteria were obtained in the Medical Mycology Laboratory, Department of Biology, Maynooth University.

The minimum inhibitory concentration (MIC<sub>100</sub>) for all test compounds/complexes (**1, 2, 6-17**) and the prescription, antimycobacterial agent, Isoniazid (INH) (positive control), against two different strains of *Mycobacterium tuberculosis* (CDC1551 and ATCC 27294) were determined by the broth microdilution method using 96 well microassay plates. The minimum inhibitory concentration (MIC<sub>100</sub>) is defined as the lowest concentration of an antimicrobial agent that causes a specified (in this case 100%) reduction/inhibition in the visible growth of a microorganism in an agar or broth dilution susceptibility test after overnight incubation. The MIC testing of the *M. tuberculosis* strain (CDC1551) (Table **4.3**) was conducted by Dr. Ciaran Skerry in Dr. Petros Karakousis's Laboratory, Centre for Tuberculosis Research, Department of Medicine, Division of Infectious Diseases, Johns Hopkins School of Medicine, Baltimore, USA. The MIC testing of the second *M. tuberculosis* strain (ATCC 27294) (Table **4.4**) was conducted by Professor Andre L.S. Santos and his group in the Department of General Microbiology, Federal University of Rio de Janeiro, Brazil.

The half maximal inhibitory concentration (IC<sub>50</sub>) represents the concentration of an agent that is required for 50% inhibition of a biological/biochemical process or function *in vitro*. In this case, the IC<sub>50</sub> values obtained for all compounds/complexes are the half maximal dose which induced cytotoxicity or cell death to a normal mammalian cell line (Vero

cells). The IC<sub>50</sub> values for all test complexes were obtained using Vero cells which are isolated kidney epithelial cells extracted from an African green monkey. These IC<sub>50</sub> values were required in order to ascertain the level of cytotoxicity of the complexes towards normal mammalian epithelial cells and to devise a selectivity index/parameter to deduce if the complexes were cytoselective for bacterial cells over mammalian cells. The selectivity index (SI) is a measure of the cytotoxicity of an agent for its intended target (e.g. *M. tuberculosis* pathogenic bacterial cells) over that of the host's normal cells (represented by the Vero cells). The IC<sub>50</sub> testing was conducted by Professor Andre L.S. Santos and his group in the Department of General Microbiology, Federal University of Rio de Janeiro, Brazil.

For the zone of inhibition/well diffusion assays the test complexes/compounds are arranged into four groups of compounds/complexes which will be referred to as such based upon their ligand similarities (Table 4.2).

**Table 4.2:** List of selected test compounds/complexes utilized for the zone of inhibition/well diffusion antibacterial assays.

Compound	Molecular Mass (g/mol)
1 1,10-phenanthroline (1,10-phen)	Group 1 180.21
8 [Mn(ph)(phen)(H <sub>2</sub> O) <sub>2</sub> ]	435.30
9 [Mn(ph)(phen) <sub>2</sub> (H <sub>2</sub> O)].4H <sub>2</sub> O	669.56
10 [Mn <sub>2</sub> (isoph) <sub>2</sub> (phen) <sub>3</sub> ].4H <sub>2</sub> O	Group 3 1050.82
11 {[Mn(phen) <sub>2</sub> (H <sub>2</sub> O) <sub>2</sub> ] <sub>2</sub> (isoph) <sub>2</sub> (phen)}.12H <sub>2</sub> O	1627.42
12 [Mn(tereph)(phen) <sub>2</sub> ].5H <sub>2</sub> O	669.56
13 [Mn <sub>2</sub> (η <sub>1</sub> η <sub>1</sub> μ <sub>2</sub> -oda)(phen) <sub>4</sub> (H <sub>2</sub> O) <sub>2</sub> ][Mn <sub>2</sub> (η <sub>1</sub> η <sub>1</sub> μ <sub>2</sub> -oda)(phen) <sub>4</sub> (η <sub>1</sub> -oda) <sub>2</sub> ].4H <sub>2</sub> O	Group 4 2458.23
14 [Cu <sub>2</sub> (oda)(phen) <sub>4</sub> ](ClO <sub>4</sub> ) <sub>2</sub> .2.76H <sub>2</sub> O.EtOH	1309.23
15 {[Mn(3,6,9-tdda)(phen) <sub>2</sub> ].3H <sub>2</sub> O.EtOH} <sub>n</sub>	735.64
16 {[Cu(3,6,9-tdda)(phen) <sub>2</sub> ].3H <sub>2</sub> O.EtOH} <sub>n</sub>	Group 5 744.25
17 [Ag <sub>2</sub> (3,6,9-tdda)(phen) <sub>4</sub> ].EtOH	1202.80
AMP Ampicillin	349.41



The second group of complexes shown in Table 4.1 were not tested, therefore, only groups 1, 3-5 were utilized for these zone of inhibition/well diffusion assays. The first group is comprised of 1,10-phen (**1**). The third group is comprised of Mn(II) 1,10-phen phthalate, isophthalate and terephthalate complexes (**8-12**). The fourth group are Mn(II) and Cu(II) 1,10-phen octanedioate complexes (**13-14**). The fifth family/group contains Mn(II), Cu(II) and Ag(I) 1,10-phen trioxaundecanedioate complexes (**15-17**) and finally the positive control, the prescription  $\beta$ -lactam antibiotic, Ampicillin (AMP).

#### 4.8.1 *S. aureus* results

The growth inhibitory effects of the test compounds/complexes against the Gram-positive *S. aureus* are shown in Figure 4.14. The dinuclear Mn(II) 1,10-phen/octanedioate complex, **13**, proved to be the most active bacteriostatic agent ( $2.03 \mu\text{M} = 18.9 \text{ mm}^2$ ) taking into account the total zone of inhibition and the micromolar concentration.

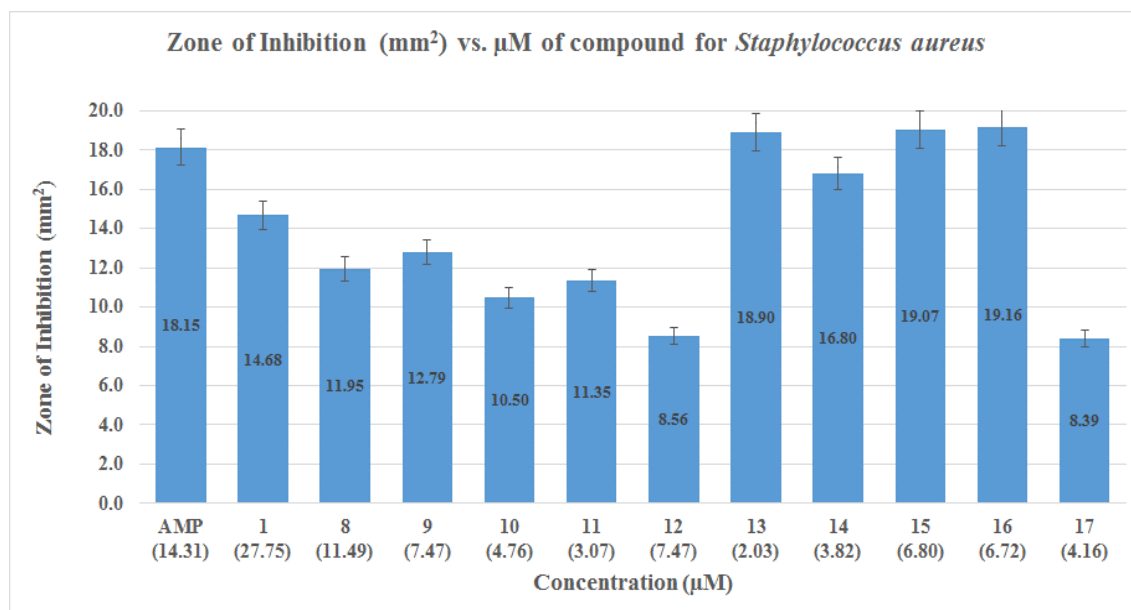


**Fig. 4.14:** Total area of zone of inhibition ( $\text{mm}^2$ ) versus molarity ( $\mu\text{M}$ ) of test complex/compound ( $5 \mu\text{g}/\text{cm}^3$ ) against *S. aureus*.

The Cu(II) 1,10-phen/octanedioate complex, **14**, was the next most active, displaying a large zone of inhibition with a low micromolar concentration ( $3.82 \mu\text{M} = 16.8 \text{ mm}^2$ ). The Mn(II) 1,10-phen/isophthalate complex, **11**, was the next most active, although its total area of inhibition was less than the other test agents its ratio of inhibitory effect ( $\text{mm}^2$ ) to



micromolar concentration was higher ( $3.07 \mu\text{M} = 11.4 \text{ mm}^2$ ). Following this was the Cu(II) and Mn(II) 1,10-phen trioxaundecanedioate complexes, **16** and **15** ( $6.72 \mu\text{M} = 19.2 \text{ mm}^2$  and  $6.8 \mu\text{M} = 19.1 \text{ mm}^2$ , respectively).

The dinuclear Ag(I) 1,10-phen/trioxaundecanedioate complex, **17**, whilst active, was much less so than its Mn(II) and Cu(II) analogues, **15** and **16**. Interestingly, in terms of molarity complexes **9-17** were all more active than the known  $\beta$ -lactam antibiotic, Ampicillin (AMP).

It is noteworthy that the most active complexes, **13** and **14**, are water-soluble, a property conferred by their dicarboxylate ligands (oda). While facilitating dissolution of the complexes in a mainly aqueous medium, it might be anticipated that it would prevent diffusion across the hydrophobic peptidoglycan cell wall of *S. aureus*. It might be that the complexes dissociate one or more of their dicarboxylate ligands or undergo ligand exchange when approaching the bacterial cell wall, creating a much more lipophilic metal complex ( $[\text{M}(\text{phen})_2]^{2+}$  or  $[\text{M}(\text{phen})]^{2+}$ ), which could more easily diffuse across the cell membrane of Gram-positive bacteria like *S. aureus*. It should also be noted that the peptidoglycan in bacterial cell walls can have a negative charge, thus possibly further preventing access of the cationic metal complexes to the cell via an intact cell wall.

The Mn(II) and Cu(II) octanedioate complexes, **13** and **14**, are known potent producers of reactive oxygen species (ROS) and therefore, initial diffusion into the bacterial cell may not be necessary to induce an inhibitory effect. A very recent paper on mammalian innate immunity proteins, called Peptidoglycan Recognition Proteins (PGRPs), demonstrated that these immune proteins express their bactericidal effect through synergistic induction of ROS, depletion of thiols and increasing intracellular concentration of metals (Cu(II), Zn(II)), which are all required, but individually not sufficient, for bacterial killing.<sup>71</sup> The production of ROS, either extra- or intra-cellularly, by **13** and **14** would result in cell membrane damage/oxidation, protein damage/inactivation and thiol depletion (due to oxidative stress). In addition, oxidative and thiol stress not only directly damages cells, but also releases Fe, Zn and Cu ions from proteins, increasing the intracellular concentration of these ions, which can then undergo Fenton-type chemistry and cause further ROS generation.<sup>71</sup> This, coupled with possible intercalation of the complexes with the non-membrane bound bacterial DNA, would

cause deformation of the DNA and/or nuclease-like scission via ROS generation, resulting in synergistic and cascade effects that would lead to bacterial cell death.

#### 4.8.2 MRSA results

The growth inhibitory effects of the test compounds/complexes against Gram-positive MRSA are shown in Figure 4.15. There is striking change in the activity of the  $\beta$ -lactam antibiotic, Ampicillin (AMP), against MRSA, with the prescription drug being completely inactive at the lower test concentration of  $5 \mu\text{g}/\text{cm}^3$  ( $14.31 \mu\text{M}$ ). This result is to be expected given the resistant nature of MRSA (*mecA* gene) to the bactericidal activity of  $\beta$ -lactam antibiotics and correlates closely with documented observations.<sup>72</sup>

The Mn(II)-based complex, **13**, once again displayed the best bacteriostatic activity ( $2.03 \mu\text{M} = 25.9 \text{ mm}^2$ ), followed by its Cu(II)-based relative **14** ( $3.82 \mu\text{M} = 25.9 \text{ mm}^2$ ). The activity profiles of the test materials against MRSA mirrored the results obtained against *S. aureus* (Figure 4.14).

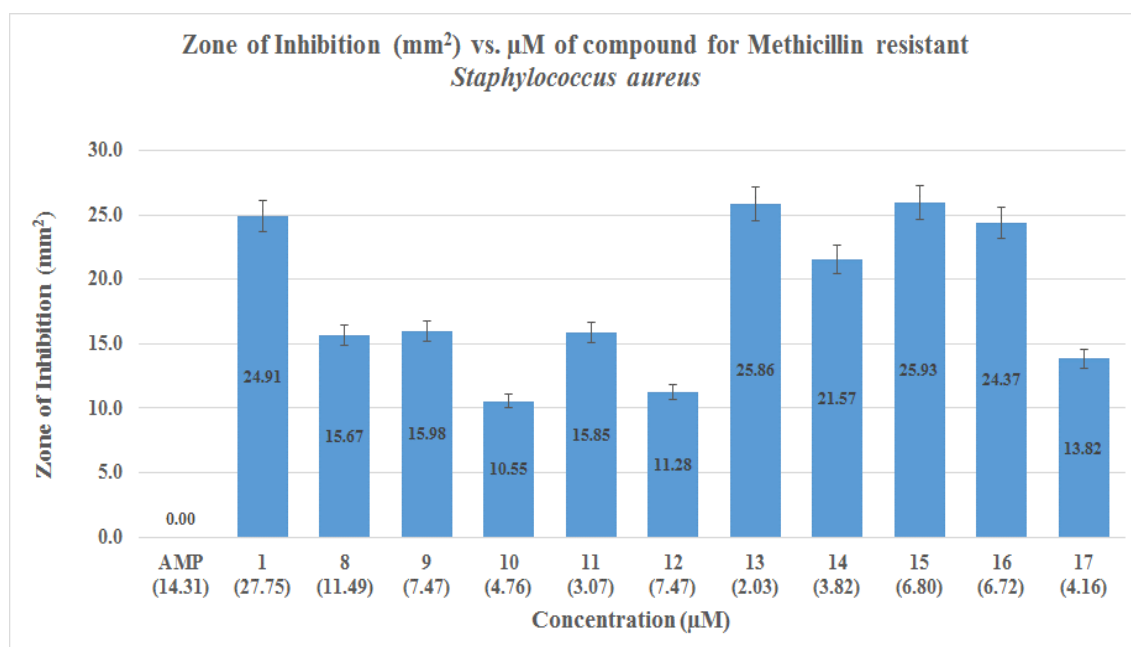


**Fig. 4.15:** Total area of zone of inhibition ( $\text{mm}^2$ ) versus micromolarity ( $\mu\text{M}$ ) of test complex/compound ( $5 \mu\text{g}/\text{cm}^3$ ) against pathogenic, Gram-positive MRSA.

The dinuclear Ag(I)-based 1,10-phen trioxaundecanedioate complex, **17**, also displayed reasonable good growth inhibition ( $4.16 \mu\text{M} = 13.8 \text{ mm}^2$ ). In a somewhat unexpected fashion, the top five most active complexes, **13**, **14**, **11**, **15** – **17**, all displayed superior bacteriostatic activity against MRSA compared to its non- $\beta$ -lactam antibiotic resistant variant, *S. aureus*. It would seem that the production of Penicillin binding protein/transpeptidase enzyme, PBP2A, via its *mecA* gene, by MRSA is inducing a change in the cell that makes it more vulnerable to the antibacterial effects of the test complexes. A similar, multimodal antibacterial mechanism of action as discussed in relation to *S. aureus* is the likely explanation for the bacteriostatic activity expressed by **13**, **14**, **11**, **15**, **16**, i.e. ROS production leading to cell membrane/protein damage, thiol depletion, DNA intercalation/scission, cumulatively resulting in bacterial cell death.

In addition, the activity profile of the test complexes is the same for both *S. aureus* and MRSA, with the most potent bacteriostatic complexes being Mn(II)-based in each group tested (Group 3 = complex **11**, Group 4 = **13** and Group 5 = **15**). Hence, it would seem that there is some metal ion specificity to their antibacterial activity. This specificity, may be due in part, to the type and quantity of free radicals or ROS/RNS (superoxide  $\text{O}_2^{\bullet-}$ , hydroxyl radical  $\text{OH}^{\bullet}$ , nitric oxide  $\bullet\text{NO}$ ) that the Mn(II) complexes produce and the associated differing biological damaging capacities of those radicals, in comparison to the radicals generated by their Cu(II)-based analogues. The hydroxyl radical ( $\text{OH}^{\bullet}$ ), for example, is much more reactive than both superoxide ( $\text{O}_2^{\bullet-}$ ) or nitric oxide ( $\bullet\text{NO}$ ), be able to react with almost anything, including DNA purine base pairs and hydrocarbons to abstract  $\text{H}^{\bullet}$  and leave behind another radical.<sup>73</sup>

The resulting free radical chain reaction can cause a multitude of damaging biological consequences including DNA strand scission and lipid membrane peroxidation.<sup>74</sup> It is reasonable to surmise that perhaps the Mn(II)-based complexes produce higher quantities of the more reactive and damaging hydroxyl radical which may explain their superior antibacterial activity.

The Ag(I)-based complex, **17**, may be expressing a different mode/modes of bacteriostatic action, as it would be unlikely to be able to produce ROS via redox cycling due to a lack of readily accessible variable oxidation states. As Ag(I)(d10) is kinetically labile, it may be that, in the biological environment, there is a degree of dissociation of the  $[\text{Ag}(\text{phen})_2]^+$  moiety and that the “free” Ag(I) ions and the “free” 1,10-phen ligands have separate but synergistic effects. Uncoordinated 1,10-phen and Ag(I) ions are both

known to exhibit growth inhibitory effects against bacteria. Dissociation may be promoted by a favourable soft-soft (HSAB theory) interaction of the Ag(I) ions with the thiol groups of bacterial enzymes and proteins and would be entropically favoured. This would result in a steady stream of Ag(I) ions akin to the way that silver sulfadiazine gradually dissociates releasing the majority of its Ag(I) ions into solution over an extended period of time and resulting in a bacteriostatic/bactericidal effect.<sup>75</sup> However, the thick, hydrophobic and negatively charged peptidoglycan layers of Gram-positive bacteria such as *S. aureus* and MRSA, would likely trap most of the Ag(I) ions preventing their diffusion into the cell.

The Ag(I) ions may be able to access the cytoplasm through transmembrane proteins that normally function to transport other ions. The transmembrane protein, CopB-ATPase, from *Enterococcus hirae*, has been shown to be able to transport Ag(I) ions into the bacterial cytoplasm, although its normal function is as a Cu(II) ion transporter.<sup>76</sup>

Although the mechanisms underlying the antibacterial actions of Ag(I) ions are still not fully understood, Ag(I) ions can bond to proteins by binding to sulfur-containing residues in enzymes, inactivating them and causing the release of K<sup>+</sup> ions from the bacteria.<sup>75, 77</sup> Also, Ag(I) ions have been documented to damage the cell envelope and to intercalate with the bases in DNA rather than with the phosphate groups. This disrupts base pair hydrogen bonding in the double helix and denatures the DNA. Furthermore, if **17** is able to dissociate in this fashion then the metal-free 1,10-phen would be free to diffuse across the cell membrane and sequester metal ions from the cytoplasm inactivating proteins/enzymes and possibly forming new *in vitro* ROS-generating complexes.<sup>78</sup>

### 4.8.3 *E. coli* results

The growth inhibitory effects of the test compounds/complexes against Gram-negative *E. coli* are shown in Figure 4.16.

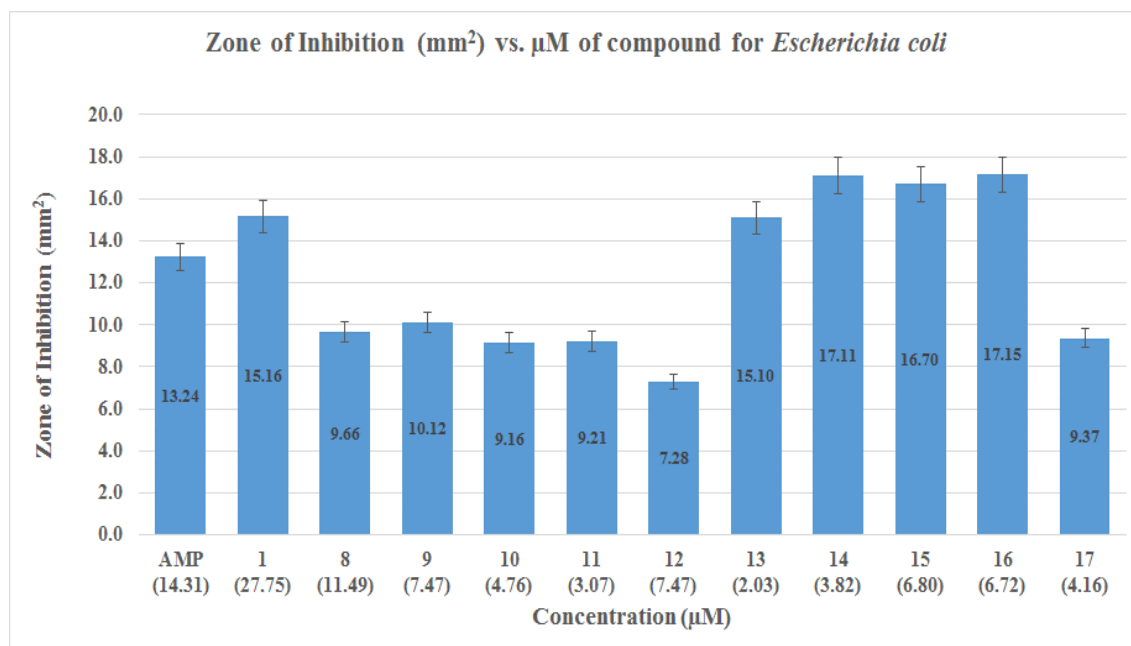


**Fig. 4.16:** Total area of zone of inhibition (mm<sup>2</sup>) versus micromolarity (µM) of test complex/compound in 5 µg/cm<sup>3</sup> against the pathogenic Gram-negative bacteria *Escherichia coli*.

The Mn(II) complex, **13**, demonstrated potent growth inhibition (2.03 µM = 15.1 mm<sup>2</sup>), **13** was almost 2 fold more active than the next most active complex, its Cu(II)-base analogue **14** (3.82 µM = 17.1 mm<sup>2</sup>).

Once again, a similar activity trend was observed as with the Gram positive species, although all active complexes were bacteriostatic to a lesser extent against the Gram-negative bacteria *E. coli* than both of the two Gram-positive strains, *S. aureus* and MRSA. The additional exterior membrane of Gram-negative bacteria is composed of lipopolysaccharide in its outer leaflet and phospholipids in the inner leaflet. These are hydrophilic, and repel lipophilic molecules/drugs, such as β-lactam antibiotics and therefore provide protection/resistance to the bacteria from several antibiotics, dyes and detergents that would normally damage either the inner membrane or the cell wall (peptidoglycan). The porins (hydrophilic channels) in Gram-negative bacteria, like *E. coli*, facilitate the transit of hydrophilic species through the otherwise hydrophobic cell wall (peptidoglycan layer) into the cytoplasm, which may partly explain the superior activity of the water-soluble complexes **13**, **14**, **15-17** over that of the other less water-soluble test complexes.

#### 4.8.4 *P. aeruginosa* (10145) results

Figure 4.17 displays the growth inhibitory effects of the test compounds/complexes against planktonic, Gram-negative *P. aeruginosa* (10145). The dinuclear Mn(II) 1,10-phen/octanedioate complex, **13**, was the most active bacteriostatic agent once again ( $2.03 \mu\text{M} = 8.8 \text{ mm}^2$ ). In contrast to previous activity trends, the Ag(I)-based complex, **17**, was the second most active complex ( $4.16 \mu\text{M} = 12.9 \text{ mm}^2$ ).

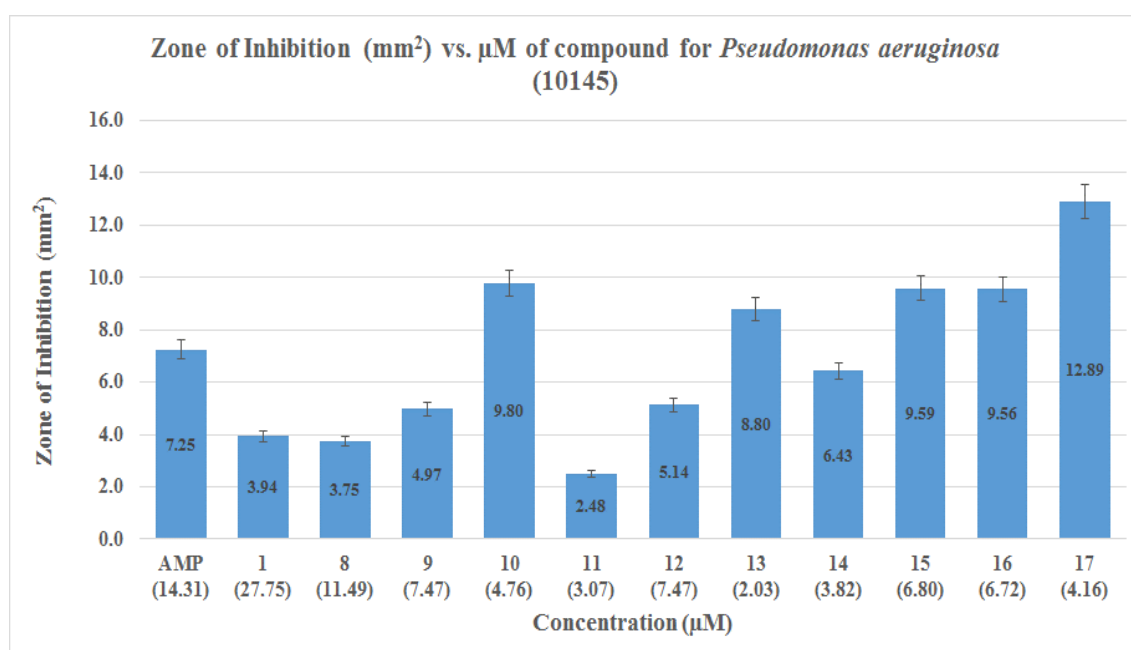


**Fig. 4.17:** Total area of zone of inhibition ( $\text{mm}^2$ ) versus micromolarity ( $\mu\text{M}$ ) of test complex/compound in  $5 \mu\text{g}/\text{cm}^3$  against the pathogenic Gram-negative bacteria *Pseudomonas aeruginosa* (10145).

The third most active complex was the Mn(II)-based complex **10** ( $4.76 \mu\text{M} = 9.8 \text{ mm}^2$ ). The Cu(II) 1,10-phen/octanedioate complex, **14**, was also quite active displaying a median sized zone of inhibition ( $3.82 \mu\text{M} = 6.4 \text{ mm}^2$ ). The Cu(II) and Mn(II) 1,10-phen trioxaundecanedioate complexes, **16** and **15** were almost equally bacteriostatic against *P. aeruginosa* (10145) cells ( $6.72 \mu\text{M} = 9.6 \text{ mm}^2$  and  $6.8 \mu\text{M} = 9.6 \text{ mm}^2$  respectively). The level of activity expressed by all of the bacteriostatic complexes against *P. aeruginosa* (10145) cells was lower than that observed for Gram-negative *E. coli*.

This trend would seem to suggest that *P. aeruginosa* cells possess greater resistance to the bacteriostatic activity of these complexes. *P. aeruginosa* contains Protein F (OprF) which functions as a porin, allowing certain molecules and ions into the cell, and it also

offers structural support to maintain the bacterial cell shape. OprF provides the *P. aeruginosa* outer membrane with an exclusion limit of 500 Da, lowering the permeability of the outer membrane in order to decrease the intake of harmful substances into the cell and give *P. aeruginosa* cells a high resistance to antibiotics.<sup>79</sup>

In addition, *P. aeruginosa* cells under oxidative-stress conditions have the capability to synthesize Fe- or Mn-containing superoxide dismutase (SOD) enzymes that can catalyse the dismutation of the toxic superoxide ( $O_2^{\bullet-}$ ) radical into  $O_2$  and  $H_2O_2$ . The cells also have catalase enzymes to detoxify the  $H_2O_2$  to  $O_2$  and  $H_2O$ .<sup>80</sup> The catalase and SOD capabilities of planktonic strains has been documented in the literature to be lower than that of biofilm forming strains.<sup>81</sup> Therefore, in theory, *P. aeruginosa* would be able to nullify, to a certain degree, the damaging effects of ROS generation by the test complexes, either extra or intracellularly, via these enzymatic and cell wall associated capabilities. This may partly explain the decreased activity profile for the test complexes against *P. aeruginosa* (10145) in comparison to the other bacteria tested.

#### 4.8.5 *P. aeruginosa* (27853) results

Displayed in Figure 4.18 are the growth inhibitory effects of the test compounds/complexes against virulent, biofilm-forming Gram-negative *P. aeruginosa* (27853). As has been the case with every bacterium tested thus far, the Mn(II) complex **13** demonstrated the highest level of growth inhibition ( $2.03 \mu\text{M} = 8.6 \text{ mm}^2$ ), with the Mn(II) 1,10-phen/isophthalate complex, **11**, being the second most active ( $3.07 \mu\text{M} = 10.6 \text{ mm}^2$ ). Once again, as was the case with the planktonic strain of *P. aeruginosa* (10145), the Ag(I) complex, **17**, displayed a relatively high growth inhibitory affect against the biofilm-forming strain, *P. aeruginosa* (27853) ( $4.16 \mu\text{M} = 12.5 \text{ mm}^2$ ). This was followed by the Mn(II) 1,10-phen/isophthalate complex, **10** ( $4.76 \mu\text{M} = 10.9 \text{ mm}^2$ ).

In a reverse of the trend observed for the 10145 strain of *P. aeruginosa*, the Mn(II)-based complex, **15**, was 2 fold more active than its Cu(II) analogue, **16** ( $6.8 \mu\text{M} = 12.6 \text{ mm}^2$  and  $6.72 \mu\text{M} = 5.45 \text{ mm}^2$ , respectively).

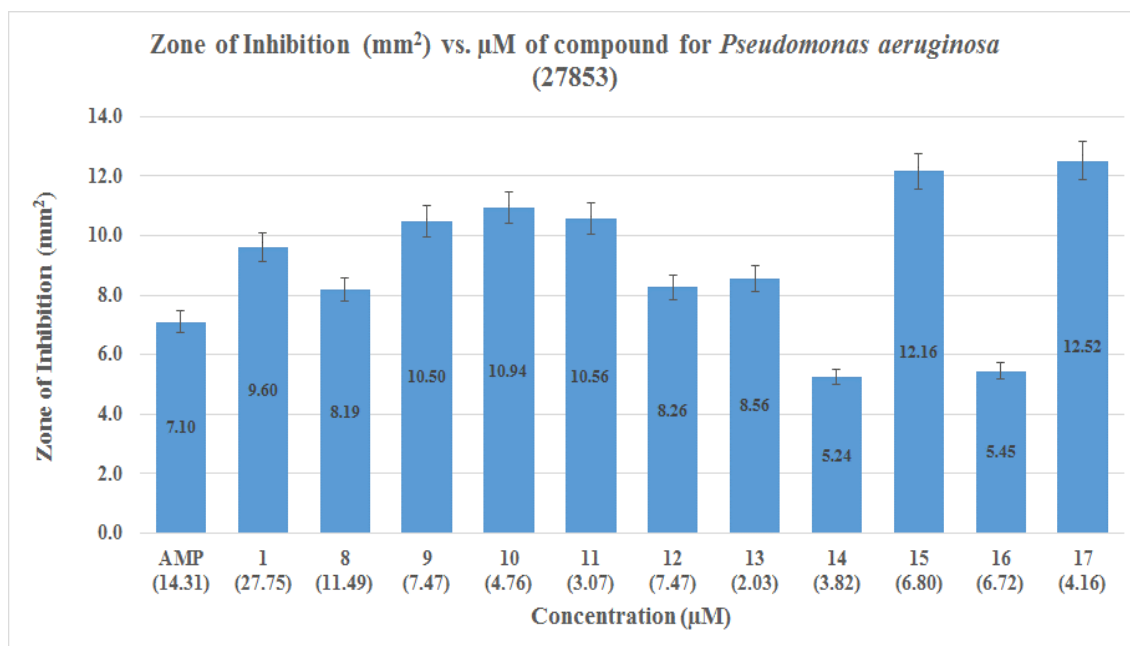


**Fig. 4.18:** Total area of zone of inhibition (mm<sup>2</sup>) versus micromolarity (µM) of test complex/compound in 5 µg/cm<sup>3</sup> against the pathogenic Gram-negative bacteria *Pseudomonas aeruginosa* (27853).

In addition to the increased levels of superoxide dismutase and catalase expressed by biofilm-forming strains such as *P. aeruginosa* (27853), the *P. aeruginosa* cells within a biofilm can sense their population via quorum sensing and can communicate with one another via the secretion of low molecular weight pheromones.<sup>82</sup> This quorum sensing communication gives them the ability to resist many offences, such as anti-*Pseudomonas* antibiotics. This is achieved by the bacteria sensing the destruction of the outer layer of the biofilm and consequently, the inner layers will grow stronger to protect the biofilms integrity. *P. aeruginosa* also has other intrinsic resistance mechanisms such as efflux pumps, to shuttle harmful molecules/ions out of the cytoplasm. The cells also have the ability to produce and secrete β-lactamases enzymes which break the amide bond in β-lactam rings of antibiotics and hence, inactivate their bactericidal effect.

Furthermore, the increased biosynthesis and secretion of metal ion sequestering siderophores, pyoverdine (Pvd) and pyochelin (Pch), by *P. aeruginosa* (27853) cells could also explain the decreased bacteriostatic activity trend observed by all test complexes. It is plausible that the high binding constants of these siderophores for certain metal ions, enables them to remove the metal ions from the test complexes and hence inactivate their ROS-generation capability or perhaps preferentially transport certain complexes (eg. Mn(II)-based complexes) into the cell. A recent study on *P. aeruginosa*



cells demonstrated that the binding affinity of Pch is the highest for Fe(III) ions, but it is still able to bind many other metal ions, with Pch having a very similar affinity for Mn(II) ions and Fe(III) ions.<sup>83</sup> Interestingly, Pch showed the lowest affinity for Ag(I) and Cu(II) ions. Metal ions transported in this manner is an energy-dependent process and therefore the water-soluble test complexes would still be able to diffuse through hydrophilic porins.

In conclusion the use of efflux pumps and increased expression of siderophores by *P. aeruginosa* (27853), combined with its superior enzymatic detoxifying capabilities, may explain the lower bacteriostatic profile displayed by the test complexes in comparison to the planktonic 10145 strain and other Gram-negative and Gram-positive bacteria.

#### 4.8.6 *M. tuberculosis* (CDC 1551) results

Growth inhibitory data for the test compounds/complexes and prescription antimycobacterial agent, Isoniazid (INH), against *Mycobacterium tuberculosis* (CDC 1551) and Vero cells are shown in Table 4.3. The most active bacteriostatic agent against *M. tuberculosis* (CDC 1551) was the Mn(II) 1,10-phen/isophthalate complex, **11**, which displayed potent activity ( $MIC_{100} = 0.12 \mu M$ ) and was ca. 4-fold more active than the prescription antimycobacterial agent, Isoniazid (INH). Complex **11** also demonstrated a median-to-high level of cytoselectivity ( $SI > 240$ ). The next most active species was another Mn(II)-based complex, **13**, which had a similarly impressive growth inhibitory value ( $MIC_{100} = 0.15 \mu M$ ) and was also ca. 3-fold better than INH. Furthermore, **13** had the highest selectivity value of any complex/compound tested ( $SI = 1017$ ), making it extremely cytoslective.

The Mn(II) 1,10-phen/isophthalate complex, **10**, was also highly bacteriostatic ( $MIC_{100} = 0.18 \mu M$ ) and was even more cytoselective ( $SI > 661$ ) than the most active complex, **11**, but not as cytoslective as **13**. Complex **8** displayed equal bacteriostatic activity as that of INH ( $MIC_{100} = 0.44 \mu M$ ) coupled with a very high selectivity parameter ( $SI = 782$ ). Mn(II)-based complexes **9** and **12** also demonstrated equal bacteriostatic activity to one another ( $MIC_{100} = 0.57 \mu M$ ), with **12** being 4-fold more cytoselective than **9** ( $SI = 31$  and  $123$  respectively).

**Table 4.3:** *In vitro* bacteriostatic (MIC<sub>100</sub>) and selectivity index (SI) values for 1,10-phen, selected metal complexes and the prescription antimycobacterial agent, Isoniazid (INH), against *Mycobacterium tuberculosis* (CDC 1551). IC<sub>50</sub> values were obtained for mammalian Vero cells. MIC<sub>100</sub> and IC<sub>50</sub> values are given in µg/cm<sup>3</sup> and micromolar (µM) in brackets.

		<b><i>Mycobacterium tuberculosis</i> (CDC 1551)</b>		
Compound		MIC <sub>100</sub>	IC <sub>50</sub>	Selectivity Index
		µg/cm <sup>3</sup> (µM)	µg/cm <sup>3</sup> (µM) VERO cells	(SI) (IC <sub>50</sub> /MIC)
1	1,10-phenanthroline (1,10-phen)	3 (16.65)	>10 (55.49)	3
6	[Ag(phendione) <sub>2</sub> ]ClO <sub>4</sub>	0.75 (1.19)	6.5 (10.36)	9
7	[Cu(phendione) <sub>3</sub> ](ClO <sub>4</sub> ) <sub>2</sub> ·4H <sub>2</sub> O	1.50 (1.55)	6.6 (6.84)	4
8	[Mn(ph)(phen)(H <sub>2</sub> O) <sub>2</sub> ]	<0.19 (0.44)	15.6 (35.84)	>82
9	[Mn(ph)(phen) <sub>2</sub> (H <sub>2</sub> O)]4H <sub>2</sub> O	0.38 (0.57)	11.7 (17.47)	31
10	[Mn <sub>2</sub> (isoph) <sub>2</sub> (phen) <sub>3</sub> ]4H <sub>2</sub> O	<0.19 (0.18)	125 (118.95)	>661
11	{[Mn(phen) <sub>2</sub> (H <sub>2</sub> O) <sub>2</sub> ] <sub>2</sub> (isoph) <sub>2</sub> (phen)}·12H <sub>2</sub> O	<0.19 (0.12)	46.9 (28.82)	>240
12	[Mn(tereph)(phen) <sub>2</sub> ]5H <sub>2</sub> O	0.38 (0.57)	46.9 (70.05)	123
13	[Mn <sub>2</sub> (η <sub>1</sub> ,η <sub>1</sub> ,μ <sub>2</sub> -oda)(phen) <sub>4</sub> (H <sub>2</sub> O) <sub>2</sub> ][Mn <sub>2</sub> (η <sub>1</sub> ,η <sub>1</sub> ,μ <sub>2</sub> -oda)(phen) <sub>4</sub> (η <sub>1</sub> -oda) <sub>2</sub> ]4H <sub>2</sub> O	0.38 (0.15)	375 (152.55)	1017
14	[Cu <sub>2</sub> (oda)(phen) <sub>4</sub> ](ClO <sub>4</sub> ) <sub>2</sub> ·2.76H <sub>2</sub> O·EtOH	1.50 (1.15)	11.7 (8.94)	8
15	{[Mn(3,6,9-tdda)(phen) <sub>2</sub> ]3H <sub>2</sub> O·EtOH} <sub>n</sub>	0.75 (1.02)	62.5 (84.96)	83
16	{[Cu(3,6,9-tdda)(phen) <sub>2</sub> ]3H <sub>2</sub> O·EtOH} <sub>n</sub>	0.75 (1.01)	5.85 (7.86)	8
17	[Ag <sub>2</sub> (3,6,9-tdda)(phen) <sub>4</sub> ]EtOH	1.50 (1.25)	30.1 (25.02)	20
INH	Isoniazid	0.06 (0.44)	n.t.	

n.t. = not tested

Thus, there appears to be a high degree of metal ion specificity associated with this *M. tuberculosis* (CDC 1551) strain, as other than INH, only the Mn(II)-based complexes demonstrated potent bacteriostatic activity.

#### 4.8.7 *M. tuberculosis* (ATCC 27294) results

Similar screening protocols were conducted against the second *M. tuberculosis* strain (ATCC 27294) and Vero cells (Table 4.4). The most active bacteriostatic agent for this strain was the known prescription drug, Isoniazid (INH) (MIC<sub>100</sub> = 0.44 µM).

**Table 4.4:** *In vitro* bacteriostatic (MIC<sub>100</sub>) and selectivity index (SI) values for 1,10-phen, selected metal complexes and the prescription antimycobacterial agent, Isoniazid (INH), against *Mycobacterium tuberculosis* (ATCC 27294). IC<sub>50</sub> values were obtained for mammalian Vero cells. MIC<sub>100</sub> and IC<sub>50</sub> values are given in µg/cm<sup>3</sup> and micromolar (µM) in brackets.

		<i>Mycobacterium tuberculosis</i> (ATCC 27294)		
Compound		MIC <sub>100</sub>	IC <sub>50</sub>	Selectivity Index
		µg/cm <sup>3</sup> (µM)	µg/cm <sup>3</sup> (µM) VERO cells	(SI) (IC <sub>50</sub> /MIC)
1	1,10-phenanthroline (1,10-phen)	11.16 (61.93)	>10 (55.49)	1
2	1,10-phenanthroline-5,6-dione (phendione)	2.64 (12.56)	6.6 (55.49)	4
6	[Ag(phendione) <sub>2</sub> ](ClO <sub>4</sub> )	23.26 (37.06)	6.5 (10.36)	0.28
7	[Cu(phendione) <sub>3</sub> ](ClO <sub>4</sub> ) <sub>2</sub> ·4H <sub>2</sub> O	6.14 (6.36)	6.6 (6.84)	1
8	[Mn(ph)(phen)(H <sub>2</sub> O) <sub>2</sub> ]	0.57 (1.31)	15.6 (35.84)	27
9	[Mn(ph)(phen) <sub>2</sub> (H <sub>2</sub> O)]4H <sub>2</sub> O	1.42 (2.12)	11.7 (17.47)	8
10	[Mn <sub>2</sub> (isoph) <sub>2</sub> (phen) <sub>3</sub> ]4H <sub>2</sub> O	1.56 (1.48)	125 (118.95)	80
11	{[Mn(phen) <sub>2</sub> (H <sub>2</sub> O) <sub>2</sub> ] <sub>2</sub> (isoph) <sub>2</sub> (phen)}·12H <sub>2</sub> O	3.01 (1.85)	46.9 (28.82)	16
12	[Mn(tereph)(phen) <sub>2</sub> ]5H <sub>2</sub> O	3.41 (5.09)	46.9 (70.05)	14
13	[Mn <sub>2</sub> (η <sub>1</sub> ,η <sub>1</sub> ,μ <sub>2</sub> -oda)(phen) <sub>4</sub> (H <sub>2</sub> O) <sub>2</sub> ][Mn <sub>2</sub> (η <sub>1</sub> ,η <sub>1</sub> ,μ <sub>2</sub> -oda)(phen) <sub>4</sub> (η <sub>1</sub> -oda) <sub>2</sub> ]4H <sub>2</sub> O	1.15 (0.47)	375 (152.55)	325
14	[Cu <sub>2</sub> (oda)(phen) <sub>4</sub> ](ClO <sub>4</sub> ) <sub>2</sub> ·2.76H <sub>2</sub> O·EtOH	16.60 (12.68)	11.7 (8.94)	0.71
15	{[Mn(3,6,9-tdda)(phen) <sub>2</sub> ]3H <sub>2</sub> O·EtOH} <sub>n</sub>	0.56 (0.76)	62.5 (84.96)	112
16	{[Cu(3,6,9-tdda)(phen) <sub>2</sub> ]3H <sub>2</sub> O·EtOH} <sub>n</sub>	10.03 (13.48)	5.85 (7.86)	0.58
17	[Ag <sub>2</sub> (3,6,9-tdda)(phen) <sub>4</sub> ]EtOH	8.28 (6.88)	30.1 (25.02)	4
INH	Isoniazid	0.06 (0.44)	n.t.	

n.t. = not tested

The second most active agent was **13** (MIC<sub>100</sub> = 0.47 µM) and this complex was only very marginally less active than INH and displayed a very high selectivity index (SI = 325). The Mn(II) 1,10-phen/trioxundecanedioate complex, **15**, also proved to be an avid mycobacterial growth inhibitory agent (MIC<sub>100</sub> = 0.76 µM) and was highly tolerated by Vero cells (SI = 112). The Mn(II) 1,10-phen/phthalate and isophthalate complexes, **8**, **10** and **11** were also quite active (MIC<sub>100</sub> = 1.31, 1.48 and 1.85 µM respectively), with complex **10** showing the highest degree of cytoselectivity (SI = 80).

There is a very clear bacteriostatic activity correlation for the test complexes against the two different strains of *M. tuberculosis* examined (Tables 4.3-4.4). The most active complexes in both cases were Mn(II)-based, with the Mn(II) 1,10-phen/octanedioate complex, **13**, being by far the most impressive agent, equally in terms of MIC<sub>100</sub> and cytoselectivity. Intense research effort is currently underway around the globe in an effort

to understand the pathogen-host interaction of *M. tuberculosis* and its virulence mechanisms in order to identify any vulnerabilities, or dependencies of the bacterium that may become new exploitable therapeutic targets.

Recent research has shown that *Mycobacterium tuberculosis* may be highly susceptible to reactive oxygen species (ROS) and reactive nitrogen species (NOS).<sup>84</sup> *M. tuberculosis* can reside for a long period of time in the alveolar macrophages of the lungs, with the macrophages acting as reservoirs for this organism.<sup>62</sup> In order to avoid being destroyed after being phagocytosed by the macrophages, *M. tuberculosis* cells release a host of proteins/enzymes such as kinases, phosphatases, metalloproteinases, and pore forming proteins that block or modulate the immune response. One particularly interesting protein secreted by *M. tuberculosis* cells is called the enhanced intracellular survival (Eis) protein and is known to prevent natural killer (NK) cell-dependent reactive oxygen species (ROS) generation via its aminoglycosylamino-transferase activity.<sup>85</sup> Eis protein dually dampens tumor necrosis factor- $\alpha$  (TNF $\alpha$ ) and interleukin-10/gamma interferon (IFN- $\gamma$ ) production. TNF and IFN- $\gamma$  induce mitochondrial ROS and NOS increasing macrophage microbicidal activity. Hence, Eis protein inhibits the generation of ROS in the cell and thereby prevents the onset of macrophage activation and autophagy.<sup>86</sup>

The type of reactive oxygen or reactive nitrogen species is of utmost importance, as previously *M. tuberculosis* cells were thought to be quite resistant to oxidative and nitrosative stress. It has been demonstrated that *M. tuberculosis* cells exposed to nitric oxide ( $\bullet$ NO) resulted in a bacteriostatic effect, while H<sub>2</sub>O<sub>2</sub> exposure was not bacteriostatic at concentrations below 50 mM while at or above this concentration H<sub>2</sub>O<sub>2</sub> was bactericidal.<sup>84e</sup> Therefore, it would seem that *M. tuberculosis* cells are not equally or universally susceptible to ROS or NOS and this may explain the superior growth inhibitory effects exhibited by the Mn(II)-based test complexes. Complex **13** is an avid generator of intracellular ROS and the Mn(II) specific antimycobacterial activity observed (Tables **4.3-4.4**), may be due to the type and quantity of free radicals or ROS/RNS (superoxide O<sub>2</sub> $\bullet^-$ , hydroxyl radical OH $\bullet$ , nitric oxide  $\bullet$ NO) that the Mn(II) complexes produce. For example, perhaps **13**, is generating higher levels of O<sub>2</sub> $\bullet^-$ ,  $\bullet$ NO and H<sub>2</sub>O<sub>2</sub> than its Cu(II)-based analogue **14**. In addition the production of hydroxyl radicals, by **13** and the known increased biological damaging capacity of hydroxyl radicals, may also account for the superior antimycobacterial activity of **13** and perhaps all of the Mn(II) based complexes tested. If this is the mode of action of these Mn(II)

complexes then they would theoretically be able to overcome any strain with acquired resistance to the prescription antimycobacterial agent, Isoniazid (INH). INH is a prodrug and must be activated by a bacterial catalase-peroxidase enzyme (KatG) in *M. tuberculosis*. KatG then couples the isonicotinic acyl moiety of the activated INH with NADH to form isonicotinic acyl-NADH complex which binds the enoyl-acyl carrier protein reductase (InhA) blocking fatty acid synthesis.<sup>87</sup> Fatty acid synthesis is required for the production of mycolic acid which is a key component of the mycobacterial cell wall. Most of the known INH resistance is associated with KatG structural gene alterations resulting in KatG mutant enzymes with reduced ability to form activated INH compounds. Both KatG and Mn complexes are able to oxidize isoniazid and form the active isonicotinoyl–NAD adduct. Therefore co-administration of a Mn(II)-based complex like **11** or **13**, with INH, could hypothetically act as an alternative oxidant mimicking the activity of KatG and thus providing a non-enzymatic isoniazid activation method, whilst also synergically expressing its ROS mediated bacteriostatic/bactericidal effect on the *M. tuberculosis* cells.

#### 4.9 *In vivo* systemic toxicity/cytotoxicity studies using *Galleria mellonella*

As discussed in earlier in chapter 3 the innate defences of insects are akin to that of vertebrate mammals. *G.mellonella* larvae possess an immune system which is analogous to the human innate immune system and hence are a convenient, inexpensive and less ethically sensitive *in vivo* screening model for ascertaining the systemic toxicity profile of novel antibacterials, the results of which are comparable to murine models. Table 3.9 Chapter 3, contains the mortality data for *G. mellonella* larvae (expressed as a %) of 15 selected test compounds/complexes over a range of test concentrations.

From the data displayed in Table 3.9 it is evident that cisplatin is considerably more toxic to *G.mellonella* larvae than any of the other test compounds/complexes. Of particular note, is that at a dosage of 10 µg per larvae (33.3 mg/kg) cisplatin causes a low survival value (40%) whilst all of the other compounds are essentially non-toxic to the larvae at this dosage (100% survival rate). In terms of *G.mellonella* tolerance to each test agent, when expressed as µmol per larvae, the following order emerges: **13** > **15** > **14** > **10** > **17** > **1** ≈ **2** > **8** > **9** = **12** > **16** > **7** > **11** >> cisplatin. Furthermore, the *in vivo* tolerance order/trend results using the *G. mellonella* insect model for complexes **1**, **2**, **6-17** correlate

closely with the *in vitro* IC<sub>50</sub> tolerance order of results obtained using the Vero cell line, when the comparison is expressed in  $\mu\text{moles}$  (Table 3.9). Taking into consideration the differences in complexity between the *in vitro* and *in vivo* models, the results are comparable between the two, with the general order of tolerance being highly similar. The least toxic/most tolerated complex is **13** and the general trend for all tested complexes is similar between the two sets of results (Table 3.10, Chapter 3).

#### 4.10 Summary of antibacterial activity

The dinuclear Mn(II) 1,10-phen/octanedioic complex **13**, demonstrated potent broad spectrum bacteriostatic activity against all seven strains of bacteria tested. **13** was extremely and equally active against Gram-positive *S. aureus*, MRSA and Gram-negative *E. coli* but exhibited a slightly reduced activity profile against the two strains of *P. aeruginosa* (10145 and 27853). This was coupled with exceptionally low MIC values against two strains of *M. tuberculosis* (CDC 1551 and ATCC 27294). In addition, **13** was highly tolerated *in vitro* and *in vivo*, being essentially non-toxic to *G. mellonella* larvae up to a concentration of  $500 \mu\text{g}/\text{cm}^3$  ( $203.4 \mu\text{M}$ ), coupled with an exceedingly high cytoselective index for mycobacterial cells (SI = 1017 ) over mammalian cells. It should also be noted that in all cases across all bacterial species tested that the complexes were more active than their metal-free ligand 1,10-phen, **1**.

The Ag(I)-based complex, **17**, also displayed broad spectrum growth inhibitory activity against Gram-positive *S. aureus*, MRSA and Gram-negative *E. coli* and *P. aeruginosa* (10145, and 27853), but had limited activity against both strains of *M. tuberculosis*. In an unexpected result only the Mn(II)-based complexes presented high growth inhibition activity against the two test strains of *M. tuberculosis*. Based on these results it is plausible to surmise that there are different modes of action at play for the Mn(II), Cu(II)-based complexes and that of the Ag(I)-based complexes. In particular it would appear that a ROS/NOS mediated mechanism of cell membrane damage/oxidation, protein damage/inactivation, thiol depletion, intercalation/scission of bacterial DNA, by Mn(II)/Cu(II) complexes, may be responsible for the observed bacteriostatic (possibly bactericidal) activity. The Mn(II) specific antimycobacterial activity observed may result from the superior ROS generation ability of these complexes and in particular to the possibly exclusive capability of these Mn(II) complexes to generate the far more reactive

and biologically damaging hydroxyl radical, over that of their Cu(II) analogues. The Ag(I) complexes lesser broad spectrum bacteriostatic activity may be a result of complex dissociation into free Ag(I) ions and metal-free 1,10-phen and the synergistic antibacterial activities of these individual entities.

In conclusion, Mn(II)-based complex **13** and Ag(I) based complex, **17**, represent highly promising lead broad spectrum antibacterial agents. In addition, **13** and other Mn(II) complexes are extremely active antimycobacterial agents, with high cytoselectivity *in vitro*/low systemic toxicity *in vivo* and potentially possess unique modes of action which could circumvent intrinsic and acquired resistance to the treatment of Tuberculosis.

#### 4.11 References

1. Whitman, W. B.; Coleman, D. C.; Wiebe, W. J., Prokaryotes: The unseen majority. *Proceedings of the National Academy of Sciences of the United States of America* **1998**, *95* (12), 6578-6583. 10.1073/pnas.95.12.6578
2. (a) Fredrickson, J. K.; Zachara, J. M.; Balkwill, D. L.; Kennedy, D.; Li, S. M. W.; Kostandarithes, H. M.; Daly, M. J.; Romine, M. F.; Brockman, F. J., Geomicrobiology of high-level nuclear waste-contaminated vadose sediments at the Hanford Site, Washington State. *Applied and Environmental Microbiology* **2004**, *70* (7), 4230-4241. 10.1128/aem.70.7.4230-4241.2004; (b) Glud, R. N.; Wenzhofer, F.; Middelboe, M.; Oguri, K.; Turnewitsch, R.; Canfield, D. E.; Kitazato, H., High rates of microbial carbon turnover in sediments in the deepest oceanic trench on Earth. *Nature Geoscience* **2013**, *6* (4), 284-288. 10.1038/ngeo1773
3. Black, J. G., *Microbiology: Principles and Explorations*. John Wiley & Sons: 2008.
4. Baron, S., *Medical Microbiology*. University of Texas Medical Branch at Galveston: 1996.
5. Thomas, C. M.; Summers, D., Bacterial Plasmids. In *eLS*, John Wiley & Sons, Ltd: 2001. 10.1002/9780470015902.a0000468.pub2
6. Reece, J. B., *Campbell Biology*. Benjamin Cummings / Pearson: 2011.
7. (a) Douwes, K. E.; Schmalzbauer, E.; Linde, H. J.; Reisberger, E. M.; Fleischer, K.; Lehn, N.; Landthaler, M.; Vogt, T., Branched filaments no fungus, ovoid



- bodies no bacteria: Two unusual cases of mycetoma. *Journal of the American Academy of Dermatology* **2003**, *49* (2), S170-S173. 10.1067/mjd.2003.302; (b) Wanger, G.; Onstott, T. C.; Southam, G., Stars of the terrestrial deep subsurface: A novel 'star-shaped' bacterial morphotype from a South African platinum mine. *Geobiology* **2008**, *6* (3), 325-330. 10.1111/j.1472-4669.2008.00163.x
8. (a) Branda, S. S.; Vik, A.; Friedman, L.; Kolter, R., Biofilms: the matrix revisited. *Trends in Microbiology* **2005**, *13* (1), 20-26. 10.1016/j.tim.2004.11.006; (b) Donlan, R. M., Biofilms: Microbial life on surfaces. *Emerging Infectious Diseases* **2002**, *8* (9), 881-890.
9. Donlan, R. M.; Costerton, J. W., Biofilms: Survival mechanisms of clinically relevant microorganisms. *Clinical Microbiology Reviews* **2002**, *15* (2), 167-+. 10.1128/cmr.15.2.167-193.2002
10. Prescott, L. M.; Harley, J. P.; Klein, D. A., *Microbiology*. McGraw-Hill Higher Education: 2005.
11. Ward, J. B., Teichoic and teichuronic acids - biosynthesis, assembly, and location. *Microbiological Reviews* **1981**, *45* (2), 211-243.
12. Raisanen, L.; Draing, C.; Pfitzenmaier, M.; Schubert, K.; Jaakonsaari, T.; von Aulock, S.; Hartung, T.; Alatosava, T., Molecular interaction between lipoteichoic acids and *Lactobacillus delbrueckii* phages depends on D-alanyl and alpha-glucose substitution of poly(glycerophosphate) backbones. *Journal of Bacteriology* **2007**, *189* (11), 4135-4140. 10.1128/jb.00078-07
13. Antimicrobial resistance: global report on surveillance. <http://www.who.int/drugresistance/documents/surveillancereport/en/>. 2014.
14. (a) Drew, R. H., Emerging options for treatment of invasive, multidrug-resistant *Staphylococcus aureus* infections. *Pharmacotherapy* **2007**, *27* (2), 227-249. 10.1592/phco.27.2.227; (b) Velayati, A. A.; Masjedi, M. R.; Farnia, P.; Tabarsi, P.; Ghanavi, J.; ZiaZarifi, A. H.; Hoffner, S. E., Emergence of New Forms of Totally Drug-Resistant Tuberculosis Bacilli Super Extensively Drug-Resistant Tuberculosis or Totally Drug-Resistant Strains in Iran. *Chest* **2009**, *136* (2), 420-425. 10.1378/chest.08-2427
15. Ryan, K.; Ray, C. G.; Ahmad, N.; Drew, W. L.; Plorde, J., *Sherris Medical Microbiology, Sixth Edition*. McGraw-Hill Education: 2014.



16. Kluytmans, J.; vanBelkum, A.; Verbrugh, H., Nasal carriage of *Staphylococcus aureus*: Epidemiology, underlying mechanisms, and associated risks. *Clinical Microbiology Reviews* **1997**, *10* (3), 505-&.
17. Ruimy, R.; Armand-Lefevre, L.; Andremont, A., Short time to positivity in blood culture with clustered gram-positive cocci on direct smear examination is highly predictive of *Staphylococcus aureus*. *American Journal of Infection Control* **2005**, *33* (5), 304-306. 10.1016/j.ajic.2005.03.004
18. Cimolai, N., MRSA and the environment: implications for comprehensive control measures. *European Journal of Clinical Microbiology & Infectious Diseases* **2008**, *27* (7), 481-493. 10.1007/s10096-008-0471-0
19. Clements, M. O.; Watson, S. P.; Foster, S. J., Characterization of the major superoxide dismutase of *Staphylococcus aureus* and its role in starvation survival, stress resistance, and pathogenicity. *Journal of Bacteriology* **1999**, *181* (13), 3898-3903.
20. Kirby, J. T.; Mutnick, A. H.; Jones, R. N.; Biedenbach, D. J.; Pfaller, M. A.; Grp, S. P., Geographic variations in garenoxacin (BMS284756) activity tested against pathogens associated with skin and soft tissue infections: report from the SENTRY Antimicrobial Surveillance Program (2000). *Diagnostic Microbiology and Infectious Disease* **2002**, *43* (4), 303-309. 10.1016/s0732-8893(02)00415-7
21. (a) Hanakawa, Y.; Schechter, N. M.; Lin, C. Y.; Garza, L.; Li, H.; Yamaguchi, T.; Fudaba, Y.; Nishifuji, K.; Sugai, M.; Amagai, M.; Stanley, J. R., Molecular mechanisms of blister formation in bullous impetigo and staphylococcal scalded skin syndrome. *Journal of Clinical Investigation* **2002**, *110* (1), 53-60. 10.1172/jci200215766; (b) Plano, L. R. W., *Staphylococcus aureus* exfoliative toxins: How they cause disease. *Journal of Investigative Dermatology* **2004**, *122* (5), 1070-1077. ; (c) Fitzgerald, S. F.; O'Gorman, J.; Morris-Downes, M. M.; Crowley, R. K.; Donlon, S.; Bajwa, R.; Smyth, E. G.; Fitzpatrick, F.; Conlon, P. J.; Humphreys, H., A 12-year review of *Staphylococcus aureus* bloodstream infections in haemodialysis patients: more work to be done. *The Journal of hospital infection* **2011**, *79* (3), 218-221. 10.1016/j.jhin.2011.06.015
22. Ostyn, A.; De Buyser, M. L.; Guillier, F.; Groult, J.; Felix, B.; Salah, S.; Delmas, G.; Hennekinne, J. A., First evidence of a food poisoning outbreak due to staphylococcal enterotoxin type E, France, 2009. *Eurosurveillance* **2010**, *15* (13), 10-13.

23. Haupt, K.; Reuter, M.; van den Elsen, J.; Burman, J.; Halbich, S.; Richter, J.; Skerka, C.; Zipfel, P. F., The Staphylococcus aureus Protein Sbi Acts as a Complement Inhibitor and Forms a Tripartite Complex with Host Complement Factor H and C3b. *Plos Pathogens* **2008**, *4* (12). 10.1371/journal.ppat.1000250
24. Rubin, R. J.; Harrington, C. A.; Poon, A.; Dietrich, K.; Greene, J. A.; Moiduddin, A., The economic impact of Staphylococcus aureus infection in New York City hospitals. *Emerging Infectious Diseases* **1999**, *5* (1), 9-17.
25. (a) <http://www.cdc.gov/abcs/reports-findings/survreports/mrsa11.pdf> Accessed on the 20/09/2014. ; (b) Garcia-Lara, J.; Masalha, M.; Foster, S. J., Staphylococcus aureus: the search for novel targets. *Drug Discovery Today* **2005**, *10* (9), 643-651. 10.1016/s1359-6446(05)03432-x; (c) <http://www.hpsc.ie/A-Z/MicrobiologyAntimicrobialResistance/EuropeanAntimicrobialResistanceSurveillanceSystemEARSS/ReferenceandEducationalResourceMaterial/SaureusMRSALatestSaureusMRSAdat/File,3990,en.pdf> Accessed on the 20/09/2014.
26. (a) <http://textbookofbacteriology.net/staph.html> Accessed on the 20/09/2014. ; (b) <http://www.woundsinternational.com/case-reports/a-new-treatment-for-the-management-of-a-chronic-venous-leg-ulcer> Accessed on the 20/09/2014. ; (c) <http://www.dermnetnz.org/common/image.php?path=/bacterial/img/s/ssss2.jpg> Accessed on the 20/09/2014.
27. (a) Wilke, M. S.; Lovering, A. L.; Strynadka, N. C. J., beta-lactam antibiotic resistance: a current structural perspective. *Current Opinion in Microbiology* **2005**, *8* (5), 525-533. 10.1016/j.mib.2005.08.016; (b) Kotra, L. P.; Mobashery, S., beta-Lactam antibiotics, beta-lactamases and bacterial resistance. *Bulletin De L Institut Pasteur* **1998**, *96* (3), 139-150. 10.1016/s0020-2452(98)80009-2
28. Enright, M. C.; Robinson, D. A.; Randle, G.; Feil, E. J.; Grundmann, H.; Spratt, B. G., The evolutionary history of methicillin-resistant Staphylococcus aureus (MRSA). *Proceedings of the National Academy of Sciences of the United States of America* **2002**, *99* (11), 7687-7692. 10.1073/pnas.122108599
29. Howden, B. P.; Davies, J. K.; Johnson, P. D. R.; Stinear, T. P.; Grayson, M. L., Reduced Vancomycin Susceptibility in Staphylococcus aureus, Including Vancomycin-Intermediate and Heterogeneous Vancomycin-Intermediate Strains: Resistance Mechanisms, Laboratory Detection, and Clinical Implications. *Clinical Microbiology Reviews* **2010**, *23* (1), 99-+. 10.1128/cmr.00042-09

30. (a) Ender, M.; McCallum, N.; Berger-Bachi, B., Impact of *mecA* promoter mutations on *mecA* expression and beta-lactam resistance levels. *International Journal of Medical Microbiology* **2008**, *298* (7-8), 607-617. 10.1016/j.ijmm.2008.01.015; (b) Ubukata, K.; Nonoguchi, R.; Matsubishi, M.; Konno, M., Expression and inducibility in staphylococcus-aureus of the *mecA* gene, which encodes a methicillin-resistant *s. aureus* specific penicillin-binding protein. *Journal of Bacteriology* **1989**, *171* (5), 2882-2885.
31. Kriegeskorte, A.; Peters, G., Horizontal gene transfer boosts MRSA spreading. *Nature Medicine* **2012**, *18* (5), 662-663. 10.1038/nm.2765
32. Newsom, S. W. B., MRSA - past, present, future. *Journal of the Royal Society of Medicine* **2004**, *97* (11), 509-510. 10.1258/jrsm.97.11.509
33. Chiappetta, D. A.; Degrossi, J.; Teves, S.; D'Aquino, M.; Bregni, C.; Sosnik, A., Triclosan-loaded poloxamine micelles for enhanced topical antibacterial activity against biofilm. *European Journal of Pharmaceutics and Biopharmaceutics* **2008**, *69* (2), 535-545. 10.1016/j.ejpb.2007.11.021
34. (a) <http://www.cdc.gov/mrsa/community/photos/photo-mrsa-7.html> Accessed on the 20/09/2014. ; (b) [http://commons.wikimedia.org/wiki/File:Scanning\\_electron\\_micrograph\\_of\\_Methicillin-resistant\\_Staphylococcus\\_aureus\\_%28MRSA%29\\_and\\_a\\_dead\\_Human\\_neutrophil\\_-\\_NIAID.jpg](http://commons.wikimedia.org/wiki/File:Scanning_electron_micrograph_of_Methicillin-resistant_Staphylococcus_aureus_%28MRSA%29_and_a_dead_Human_neutrophil_-_NIAID.jpg) Accessed on the 10/10/2014.
35. Moore, C. L.; Hingwe, A.; Donabedian, S. M.; Perri, M. B.; Davis, S. L.; Haque, N. Z.; Reyes, K.; Vager, D.; Zervos, M. J., Comparative evaluation of epidemiology and outcomes of methicillin-resistant *Staphylococcus aureus* (MRSA) USA300 infections causing community- and healthcare-associated infections. *International Journal of Antimicrobial Agents* **2009**, *34* (2), 148-155. 10.1016/j.ijantimicag.2009.03.004
36. (a) Maree, C. L.; Daum, R. S.; Boyle-Vavra, S.; Matayoshi, K.; Miller, L. G., Community-associated methicillin-resistant *Staphylococcus aureus* isolates causing healthcare-associated infections. *Emerging Infectious Diseases* **2007**, *13* (2), 236-242. ; (b) Schramm, G. E.; Johnson, J. A.; Doherty, J. A.; Micek, S. T.; Kollef, M. H., Increasing incidence of sterile-site infections due to non-multidrug-resistant, oxacillin-resistant *Staphylococcus aureus* among hospitalized patients.

- Infection Control and Hospital Epidemiology* **2007**, 28 (1), 95-97.  
10.1086/509856
37. <http://www.hpsc.ie/A-Z/MicrobiologyAntimicrobialResistance/EuropeanAntimicrobialResistanceSurveillanceSystemEARSS/ReferenceandEducationalResourceMaterial/SaureusMRSALatestSaureusMRSAdata/> Accessed on the 20/09/2014.
38. [http://www.pfizer.ie/in\\_the\\_news.cfm?action=showArticle&articleID=62](http://www.pfizer.ie/in_the_news.cfm?action=showArticle&articleID=62)  
Accessed on the 20/09/2014.
39. (a) Singleton, P., *Bacteria in biology, biotechnology, and medicine*. John Wiley: 1999. ; (b) Koch, A. L., Orientation of the peptidoglycan chains in the sacculus of *Escherichia coli*. *Research in Microbiology* **1998**, 149 (10), 689-701.  
10.1016/s0923-2508(99)80016-3
40. [http://en.wikipedia.org/wiki/File:EscherichiaColi\\_NIAID.jpg](http://en.wikipedia.org/wiki/File:EscherichiaColi_NIAID.jpg) Accessed on the 02/09/2014.
41. Byrd, W.; de Lorimier, A.; Zheng, Z. R.; Cassels, F. J., Microencapsulated subunit vaccine approach to enterotoxigenic *Escherichia coli* and other mucosal pathogens. *Advanced Drug Delivery Reviews* **2005**, 57 (9), 1362-1380.  
10.1016/j.addr.2005.01.014
42. (a) Hudault, S.; Guignot, J.; Servin, A. L., *Escherichia coli* strains colonising the gastrointestinal tract protect germfree mice against *Salmonella typhimurium* infection. *Gut* **2001**, 49 (1), 47-55. 10.1136/gut.49.1.47; (b) Lukjancenko, O.; Wassenaar, T. M.; Ussery, D. W., Comparison of 61 Sequenced *Escherichia coli* Genomes. *Microbial Ecology* **2010**, 60 (4), 708-720. 10.1007/s00248-010-9717-3
43. (a) Rastogi, S. K.; Rutledge, V. J.; Gibson, C.; Newcombe, D. A.; Branen, J. R.; Branen, A. L., Ag colloids and Ag clusters over EDAPTMS-coated silica nanoparticles: synthesis, characterization, and antibacterial activity against *Escherichia coli*. *Nanomedicine-Nanotechnology Biology and Medicine* **2011**, 7 (3), 305-314. 10.1016/j.nano.2010.11.003; (b) Vosti, K. L., A prospective, longitudinal study of the behavior of serologically classified isolates of *Escherichia coli* in women with recurrent urinary tract infections. *Journal of Infection* **2007**, 55 (1), 8-18. 10.1016/j.jinf.2007.01.006
44. (a) Bonacorsi, S.; Bingen, E., Molecular epidemiology of *Escherichia coli* causing neonatal meningitis. *International Journal of Medical Microbiology* **2005**, 295 (6-

- 7), 373-381. 10.1016/j.ijmm.2005.07.011; (b) Chung, H. C.; Lai, C. H.; Lin, J. N.; Huang, C. K.; Liang, S. H.; Chen, W. F.; Shih, Y. C.; Lin, H. H.; Wang, J. L., Bacteremia Caused by Extended-Spectrum-beta-Lactamase-Producing Escherichia coli Sequence Type ST131 and Non-ST131 Clones: Comparison of Demographic Data, Clinical Features, and Mortality. *Antimicrobial Agents and Chemotherapy* **2012**, *56* (2), 618-622. 10.1128/aac.05753-11; (c) Colling, J.; Allaouchiche, B.; Floccard, B.; Pilleul, F.; Monneuse, O.; Tissot, E., Pneumatocele formation in adult Escherichia coli pneumonia revealed by pneumothorax. *The Journal of infection* **2005**, *51* (3), e109-111. 10.1016/j.jinf.2004.10.009; (d) Sawada, S.; Harada, K.; Isse, K.; Sato, Y.; Sasaki, M.; Kaizaki, Y.; Nakanuma, Y., Involvement of Escherichia coli in pathogenesis of xanthogranulomatous cholecystitis with scavenger receptor class A and CXCL16-CXCR6 interaction. *Pathology International* **2007**, *57* (10), 652-663. 10.1111/j.1440-1827.2007.02154.x
45. Karch, H.; Tarr, P. I.; Blelaszewska, M., Enterohaemorrhagic Escherichia coli in human medicine. *International Journal of Medical Microbiology* **2005**, *295* (6-7), 405-418. 10.1016/j.ijmm.2005.06.009
46. <http://www.rcsb.org/pdb/explore/explore.do?structureId=1R4Q> Accessed on the 26/09/2014.
47. Buchholz, U.; Bernard, H.; Werber, D.; Bohmer, M. M.; Remschmidt, C.; Wilking, H.; Delere, Y.; an der Heiden, M.; Adlhoch, C.; Dreesman, J.; Ehlers, J.; Ethelberg, S.; Faber, M.; Frank, C.; Fricke, G.; Greiner, M.; Hohle, M.; Ivarsson, S.; Jark, U.; Kirchner, M.; Koch, J.; Krause, G.; Lubner, P.; Rosner, B.; Stark, K.; Kuhne, M., German Outbreak of Escherichia coli O104:H4 Associated with Sprouts. *New England Journal of Medicine* **2011**, *365* (19), 1763-1770. 10.1056/NEJMoal106482
48. <http://emedicine.medscape.com/article/201181-overview#a0199> Accessed on the 25/09/2014.
49. Panos, G. Z.; Betsi, G. I.; Falagas, M. E., Systematic review: are antibiotics detrimental or beneficial for the treatment of patients with Escherichia coli O157 : H7 infection? *Alimentary Pharmacology & Therapeutics* **2006**, *24* (5), 731-742. 10.1111/j.1365-2036.2006.03036.x
50. (a) Hoiby, N., Isolation and treatment of cystic-fibrosis patients with lung infections caused by Pseudomonas-(burkholderia)-cepacia and multiresistant

- Pseudomonas-aeruginosa*. *Netherlands Journal of Medicine* **1995**, 46 (6), 280-287. 10.1016/0300-2977(95)00020-n; (b) Schultz, M. J.; Speelman, P.; Zaat, S. A. J.; Hack, C. E.; van Deventer, S. J. H.; van der Poll, T., The effect of *Pseudomonas* exotoxin A on cytokine production in whole blood exposed to *Pseudomonas aeruginosa*. *Fems Immunology and Medical Microbiology* **2000**, 29 (3), 227-232. 10.1111/j.1574-695X.2000.tb01527.x; (c) Vukomanovic, D. V.; Zoutman, D. E.; Marks, G. S.; Brien, J. F.; vanLoon, G. W.; Nakatsu, K., Analysis of pyocyanin from *Pseudomonas aeruginosa* by adsorptive stripping voltammetry. *Journal of Pharmacological and Toxicological Methods* **1996**, 36 (2), 97-102. 10.1016/s1056-8719(96)00104-9
51. <http://textbookofbacteriology.net/pseudomonas.html> Accessed on the 28/09/2014.
52. Potera, C., Common Bacterium Induces Histamine Production in Neutrophils. *Environmental Health Perspectives* **2012**, 120 (5), A190-A190.
53. Isenberg, H. D., *Essential Procedures for Clinical Microbiology*. ASM Press: 1998.
54. (a) Iversen, B. G.; Brantsaeter, A. B.; Aavitsland, P., Nationwide study of invasive *Pseudomonas aeruginosa* infection in Norway: Importance of underlying disease. *Journal of Infection* **2008**, 57 (2), 139-146. 10.1016/j.jinf.2008.05.010; (b) Schreiber, K.; Boes, N.; Eschbach, M.; Jaensch, L.; Wehland, J.; Bjarnsholt, T.; Givskov, M.; Hentzer, M.; Schobert, M., Anaerobic survival of *Pseudomonas aeruginosa* by pyruvate fermentation requires an Usp-type stress protein. *Journal of Bacteriology* **2006**, 188 (2), 659-668. 10.1128/jb.188.2.659-668.2006
55. (a) Lister, P. D.; Wolter, D. J.; Hanson, N. D., Antibacterial-Resistant *Pseudomonas aeruginosa*: Clinical Impact and Complex Regulation of Chromosomally Encoded Resistance Mechanisms. *Clinical Microbiology Reviews* **2009**, 22 (4), 582-+. 10.1128/cmr.00040-09; (b) Roy, U.; Nair, D., Biodiversity of organotin resistant *Pseudomonas* from west coast of India. *Ecotoxicology* **2007**, 16 (2), 253-261. 10.1007/s10646-006-0125-x
56. Song, Z.; Kong, K. F.; Wu, H.; Maricic, N.; Ramalingam, B.; Priestap, H.; Schneper, L.; Quirke, J. M. E.; Hoiby, N.; Mathee, K., *Panax ginseng* has anti-infective activity against opportunistic pathogen *Pseudomonas aeruginosa* by inhibiting quorum sensing, a bacterial communication process critical for



- establishing infection. *Phytomedicine* **2010**, *17* (13), 1040-1046. 10.1016/j.phymed.2010.03.015
57. (a) Bitsori, M.; Maraki, S.; Koukouraki, S.; Galanakis, E., Pseudomonas Aeruginosa Urinary Tract Infection in Children: Risk Factors and Outcomes. *Journal of Urology* **2012**, *187* (1), 260-264. 10.1016/j.juro.2011.09.035; (b) Kerr, K. G.; Snelling, A. M., Pseudomonas aeruginosa: a formidable and ever-present adversary. *Journal of Hospital Infection* **2009**, *73* (4), 338-344. 10.1016/j.jhin.2009.04.020; (c) Kobayashi, M.; Tsuda, Y.; Yoshida, T.; Takeuchi, D.; Utsunomiya, T.; Takahashi, H.; Suzuki, F., Bacterial sepsis and chemokines. *Current Drug Targets* **2006**, *7* (1), 119-134. 10.2174/138945006775270169; (d) Zavascki, A. P.; Barth, A. L.; Goldani, L. Z., Nosocomial bloodstream infections due to metallo-beta-lactamase-producing Pseudomonas aeruginosa. *Journal of Antimicrobial Chemotherapy* **2008**, *61* (5), 1183-1185. 10.1093/jac/dkn082
58. Marin, A.; Monso, E.; Garcia-Nunez, M.; Sauleda, J.; Noguera, A.; Pons, J.; Agusti, A.; Morera, J., Variability and effects of bronchial colonisation In patients with moderate COPD. *European Respiratory Journal* **2010**, *35* (2), 295-302. 10.1183/09031936.00126808
59. Vijgenboom, E.; Busch, J. E.; Canters, G. W., In vivo studies disprove an obligatory role of azurin in denitrification in Pseudomonas aeruginosa and show that azu expression is under control of RpoS and ANR. *Microbiology-Sgm* **1997**, *143*, 2853-2863.
60. (a) Brandel, J.; Humbert, N.; Elhabiri, M.; Schalk, I. J.; Mislin, G. L. A.; Albrecht-Gary, A. M., Pyochelin, a siderophore of Pseudomonas aeruginosa: Physicochemical characterization of the iron(III), copper(II) and zinc(II) complexes. *Dalton Trans* **2012**, *41* (9), 2820-2834. 10.1039/c1dt11804h; (b) Meyer, J. M.; Neely, A.; Stintzi, A.; Georges, C.; Holder, I. A., Pyoverdine is essential for virulence of Pseudomonas aeruginosa. *Infection and Immunity* **1996**, *64* (2), 518-523. ; (c) Peek, M. E.; Bhatnagar, A.; McCarty, N. A.; Zughair, S. M., Pyoverdine, the Major Siderophore in Pseudomonas aeruginosa, Evades NGAL Recognition. *Interdiscip Perspect Infect Dis* **2012**, *2012*, 843509. 10.1155/2012/843509
61. (a) [http://en.wikipedia.org/wiki/File:TB\\_Culture.jpg](http://en.wikipedia.org/wiki/File:TB_Culture.jpg) Accessed on the 05/10/2014. ; (b) <http://textbookofbacteriology.net/tuberculosis.html> Accessed on the 20/07/2014.

62. Jain, N. K.; Mishra, V.; Mehra, N. K., Targeted drug delivery to macrophages. *Expert Opinion on Drug Delivery* **2013**, *10* (3), 353-367. 10.1517/17425247.2013.751370
63. <http://www.who.int/mediacentre/factsheets/fs104/en/> Accessed on the 05/10/2014.
64. [http://www.who.int/tb/publications/2009/tbfactsheet\\_2009update\\_one\\_page.pdf](http://www.who.int/tb/publications/2009/tbfactsheet_2009update_one_page.pdf) Accessed on the 05/10/2014.
65. [http://www.who.int/tb/challenges/mdr/mdr\\_tb\\_factsheet.pdf?ua=1](http://www.who.int/tb/challenges/mdr/mdr_tb_factsheet.pdf?ua=1) Accessed on the 25/09/2014.
66. (a) McCann, M.; Coyle, B.; McKay, S.; McCormack, P.; Kavanagh, K.; Devereux, M.; McKee, V.; Kinsella, P.; O'Connor, R.; Clynes, M., Synthesis and X-ray crystal structure of [Ag(phendio)<sub>2</sub>]ClO<sub>4</sub> (phendio=1,10-phenanthroline-5,6-dione) and its effects on fungal and mammalian cells. *Biometals* **2004**, *17* (6), 635-645. 10.1007/s10534-004-1229-5; (b) Zheng, R. H.; Guo, H. C.; Jiang, H. J.; Xu, K. H.; Liu, B. B.; Sun, W. L.; Shen, Z. Q., A new and convenient synthesis of phendiones oxidated by KBrO<sub>3</sub>/H<sub>2</sub>SO<sub>4</sub> at room temperature. *Chinese Chemical Letters* **2010**, *21* (11), 1270-1272. 10.1016/j.ccllet.2010.05.030; (c) Devereux, M.; McCann, M.; Leon, V.; Geraghty, M.; McKee, V.; Wikaira, J., Synthesis and biological activity of manganese (II) complexes of phthalic and isophthalic acid: X-ray crystal structures of [Mn(ph)(phen)<sub>2</sub>(H<sub>2</sub>O)]•4H<sub>2</sub>O, [Mn(phen)<sub>2</sub>(H<sub>2</sub>O)<sub>2</sub>]<sub>2</sub>(Isoph)<sub>2</sub>(phen)•12H<sub>2</sub>O and {[Mn(isoph)(bipy)]<sub>4</sub>•2.75bipy}<sub>n</sub> (phH<sub>2</sub> = phthalic acid; isoph = isophthalic acid; phen = 1,10-phenanthroline; bipy = 2,2-bipyridine). *Metal-Based Drugs* **2000**, *7* (5), 275-288. 10.1155/mbd.2000.275; (d) Casey, M. T.; McCann, M.; Devereux, M.; Curran, M.; Cardin, C.; Convery, M.; Quillet, V.; Harding, C., Synthesis and structure of the Mn<sup>II,III</sup> complex salt [Mn<sub>2</sub>(η<sup>1</sup>η<sup>1</sup>μ<sub>2</sub>-oda)(phen)<sub>4</sub>(H<sub>2</sub>O)<sub>2</sub>][Mn<sub>2</sub>(η<sup>1</sup>η<sup>1</sup>μ<sub>2</sub>-oda)(phen)<sub>4</sub>(η<sup>1</sup>-oda)<sub>2</sub>]•4H<sub>2</sub>O (odaH<sub>2</sub> = octanedioic acid); a Catalyst for H<sub>2</sub>O<sub>2</sub> Disproportionation *Journal of the Chemical Society-Chemical Communications* **1994**, (22), 2643-2645. 10.1039/c39940002643; (e) Devereux, M.; McCann, M.; Cronin, J. F.; Ferguson, G.; McKee, V., Binuclear and polymeric copper(II) dicarboxylate complexes: syntheses and crystal structures of [Cu<sub>2</sub>(pda)(Phen)<sub>4</sub>](ClO<sub>4</sub>)<sub>2</sub>•5H<sub>2</sub>O•C<sub>2</sub>H<sub>5</sub>OH, [Cu<sub>2</sub>(oda)(Phen)<sub>4</sub>](ClO<sub>4</sub>)<sub>2</sub>•2.67H<sub>2</sub>O•C<sub>2</sub>H<sub>5</sub>OH and {[Cu<sub>2</sub>(pda)<sub>2</sub>(NH<sub>3</sub>)<sub>4</sub>(H<sub>2</sub>O)<sub>2</sub>]•4H<sub>2</sub>O}<sub>n</sub> (odaH<sub>2</sub>=octanedioic acid; pdaH<sub>2</sub>=pentanedioic acid; Phen=1,10-



- phenanthroline). *Polyhedron* **1999**, *18* (16), 2141-2148. 10.1016/s0277-5387(99)00100-x; (f) McCann, S.; McCann, M.; Casey, M. T.; Devereux, M.; McKee, V.; McMichael, P.; McCrea, J. G., Manganese(II) complexes of 3,6,9-trioxaundecanedioic acid (3,6,9-tddaH<sub>2</sub>): X-ray crystal structures of [Mn(3,6,9-tdda)(H<sub>2</sub>O)<sub>2</sub>]•2H<sub>2</sub>O and {[Mn(3,6,9-tdda)(phen)<sub>2</sub>•3H<sub>2</sub>O]•EtOH}<sub>n</sub>. *Polyhedron* **1997**, *16* (24), 4247-4252. 10.1016/s0277-5387(97)00233-7
67. Schilt, A. A.; Taylor, R. C., Infra-red spectra of 1-10-phenanthroline metal complexes in the rock salt region below 2000 cm<sup>-1</sup>. *Journal of Inorganic & Nuclear Chemistry* **1959**, *9* (3-4), 211-221. 10.1016/0022-1902(59)80224-4
68. Mehrotra, R. C.; Bohra, R., *Metal carboxylates*. Academic Press: 1983.
69. (a) Carvajal, M. A.; Novoa, J. J.; Alvarez, S., Choice of coordination number in d(10) complexes of group 11 metals. *Journal of the American Chemical Society* **2004**, *126* (5), 1465-1477. 10.1021/ja038416a; (b) Fox, B. S.; Beyer, M. K.; Bondybey, V. E., Coordination chemistry of silver cations. *J Am Chem Soc* **2002**, *124* (45), 13613-13623.
70. Dimitriu, G.; Poiata, A.; Tuchilus, C.; Buiuc, D., Correlation between linezolid zone diameter and minimum inhibitory concentration values determined by regression analysis. *Rev Med Chir Soc Med Nat Iasi* **2006**, *110* (4), 1016-1019.
71. Kashyap, D. R.; Rompca, A.; Gaballa, A.; Helmann, J. D.; Chan, J.; Chang, C. J.; Hozo, I.; Gupta, D.; Dziarski, R., Peptidoglycan Recognition Proteins Kill Bacteria by Inducing Oxidative, Thiol, and Metal Stress. *Plos Pathogens* **2014**, *10* (7). 10.1371/journal.ppat.1004280
72. Palmer, S. M.; Rybak, M. J., An evaluation of the bactericidal activity of ampicillin/sulbactam, piperacillin/tazobactam, imipenem or nafcillin alone and in combination with vancomycin against methicillin-resistant *Staphylococcus aureus* (MRSA) in time-kill curves with infected fibrin clots. *Journal of Antimicrobial Chemotherapy* **1997**, *39* (4), 515-518. 10.1093/jac/39.4.515
73. Cooke, M. S.; Evans, M. D.; Dizdaroglu, M.; Lunec, J., Oxidative DNA damage: mechanisms, mutation, and disease. *Faseb Journal* **2003**, *17* (10), 1195-1214. 10.1096/fj.02-0752rev
74. (a) Halliwell, B., Free Radicals and Other Reactive Species in Disease. In *eLS*, John Wiley & Sons, Ltd: 2001. 10.1038/npg.els.0003913; (b) Trumbore, C. N.; Ehrlich, R. S.; Myers, Y. N., Changes in DNA conformation induced by gamma

- irradiation in the presence of copper. *Radiation Research* **2001**, 155 (3), 453-465. 10.1667/0033-7587(2001)155[0453:cidcib]2.0.co;2
75. Fox, C. L.; Modak, S. M., Mechanism of silver sulfadiazine action on burn wound infections. *Antimicrobial Agents and Chemotherapy* **1974**, 5 (6), 582-588.
76. Solioz, M.; Odermatt, A., Copper and silver transport by Copb-atpase in membrane-vesicles of *Enterococcus hirae*. *Journal of Biological Chemistry* **1995**, 270 (16), 9217-9221.
77. (a) Feng, Q. L.; Wu, J.; Chen, G. Q.; Cui, F. Z.; Kim, T. N.; Kim, J. O., A mechanistic study of the antibacterial effect of silver ions on *Escherichia coli* and *Staphylococcus aureus*. *Journal of Biomedical Materials Research* **2000**, 52 (4), 662-668. 10.1002/1097-4636(20001215)52:4<662::aid-jbm10>3.0.co;2-3; (b) Kawahara, K.; Tsuruda, K.; Morishita, M.; Uchida, M., Antibacterial effect of silver-zeolite on oral bacteria under anaerobic conditions. *Dental Materials* **2000**, 16 (6), 452-455. 10.1016/s0109-5641(00)00050-6; (c) Klueh, U.; Wagner, V.; Kelly, S.; Johnson, A.; Bryers, J. D., Efficacy of silver-coated fabric to prevent bacterial colonization and subsequent device-based biofilm formation. *Journal of Biomedical Materials Research* **2000**, 53 (6), 621-631. 10.1002/1097-4636(2000)53:6<621::aid-jbm2>3.0.co;2-q; (d) Silvestry-Rodriguez, N.; Sicairos-Ruelas, E. E.; Gerba, C. P.; Bright, K. R., Silver as a disinfectant. In *Reviews of Environmental Contamination and Toxicology, Vol 191*, Ware, G. W., Ed. Springer: New York, 2007; Vol. 191, pp 23-45. 10.1007/978-0-387-69163-3\_2
78. (a) Alvarez, V. M.; von der Weid, I.; Seldin, L.; Santos, A. L. S., Influence of growth conditions on the production of extracellular proteolytic enzymes in *Paenibacillus peoriae* NRRL BD-62 and *Paenibacillus polymyxa* SCE2. *Letters in Applied Microbiology* **2006**, 43 (6), 625-630. 10.1111/j.1472-765X.2006.02015.x; (b) Hussein, R.; Stretton, R. J., Studies on the anti-bacterial activity of phanquone - chelating properties in relation to mode of action against *Escherichia coli* and *Staphylococcus aureus*. *Microbios* **1980**, 29 (116), 109-125. ; (c) Hussein, R. H.; Stretton, R. J., Anti Bacterial Activity Of Some Phenanthroline and Phenanthrene Compounds. *Microbios Letters* **1981**, 16 (62), 85-94.

79. Baumberg, S., Genetics and biochemistry of pseudomonas: Edited by P. H. Clarke and M. H. Richmond. Pp. 366. John Wiley and Sons, 1975. £14.00. *Biochemical Education* **1975**, 3 (3), 46-46. 10.1016/0307-4412(75)90048-5
80. Alexander, M.; Bloom, B. R.; Hopwood, D. A.; Hull, R.; Iglewski, B. H.; Laskin, A. I.; Oliver, S. G.; Schaechter, M.; Summers, W. C.; Lederberg, J., *Encyclopedia of Microbiology, Four-Volume Set*. Elsevier Science: 2000.
81. Hassett, D. J.; Ma, J. F.; Elkins, J. G.; McDermott, T. R.; Ochsner, U. A.; West, S. E.; Huang, C. T.; Fredericks, J.; Burnett, S.; Stewart, P. S.; McFeters, G.; Passador, L.; Iglewski, B. H., Quorum sensing in *Pseudomonas aeruginosa* controls expression of catalase and superoxide dismutase genes and mediates biofilm susceptibility to hydrogen peroxide. *Mol Microbiol* **1999**, 34 (5), 1082-1093.
82. (a) Hassett, D. J.; Korfhagen, T. R.; Irvin, R. T.; Schurr, M. J.; Sauer, K.; Lau, G. W.; Sutton, M. D.; Yu, H.; Hoiby, N., *Pseudomonas aeruginosa* biofilm infections in cystic fibrosis: insights into pathogenic processes and treatment strategies. *Expert Opin Ther Targets* **2010**, 14 (2), 117-130. 10.1517/14728220903454988; (b) Kirisits, M. J.; Parsek, M. R., Does *Pseudomonas aeruginosa* use intercellular signalling to build biofilm communities? *Cellular Microbiology* **2006**, 8 (12), 1841-1849. 10.1111/j.1462-5822.2006.00817.x; (c) Nalca, Y.; Jansch, L.; Bredenbruch, F.; Geffers, R.; Buer, J.; Hussler, S., Quorum-sensing antagonistic activities of azithromycin in *Pseudomonas aeruginosa* PAO1: a global approach. *Antimicrobial Agents and Chemotherapy* **2006**, 50 (5), 1680-1688. 10.1128/aac.50.5.1680-1688.2006; (d) Wiley, J.; Ltd, S.; Wiley; Clavier, *Encyclopedia of Life Sciences*. Wiley: 2005.
83. Braud, A.; Hannauer, M.; Mislin, G. L. A.; Schalk, I. J., The *Pseudomonas aeruginosa* Pyochelin-Iron Uptake Pathway and Its Metal Specificity. *Journal of Bacteriology* **2009**, 191 (11), 3517-3525. 10.1128/jb.00010-09
84. (a) Cirillo, S. L. G.; Subbian, S.; Chen, B.; Weisbrod, T. R.; Jacobs, W. R.; Cirillo, J. D., Protection of *Mycobacterium tuberculosis* from Reactive Oxygen Species Conferred by the mel2 Locus Impacts Persistence and Dissemination. *Infection and Immunity* **2009**, 77 (6), 2557-2567. 10.1128/iai.01481-08; (b) Mestre, O.; Hurtado-Ortiz, R.; Dos Vultos, T.; Namouchi, A.; Cimino, M.; Pimentel, M.; Neyrolles, O.; Gicquel, B., High Throughput Phenotypic Selection of *Mycobacterium tuberculosis* Mutants with Impaired Resistance to Reactive

- Oxygen Species Identifies Genes Important for Intracellular Growth. *Plos One* **2013**, 8 (1). 10.1371/journal.pone.0053486; (c) Roca, F. J.; Ramakrishnan, L., TNF Dually Mediates Resistance and Susceptibility to Mycobacteria via Mitochondrial Reactive Oxygen Species. *Cell* **2013**, 153 (3), 521-534. 10.1016/j.cell.2013.03.022; (d) Vilcheze, C.; Hartman, T.; Weinrick, B.; Jacobs, W. R., Mycobacterium tuberculosis is extraordinarily sensitive to killing by a vitamin C-induced Fenton reaction. *Nature Communications* **2013**, 4. 10.1038/ncomms2898; (e) Voskuil, M. I.; Bartek, I. L.; Visconti, K.; Schoolnik, G. K., The response of Mycobacterium tuberculosis to reactive oxygen and nitrogen species. *Frontiers in Microbiology* **2011**, 2. 10.3389/fmicb.2011.00105
85. Kim, K. H.; An, D. R.; Song, J.; Yoon, J. Y.; Kim, H. S.; Yoon, H. J.; Im, H. N.; Kim, J.; Kim, D. J.; Lee, S. J.; Lee, H. M.; Kim, H. J.; Jo, E. K.; Lee, J. Y.; Suh, S. W., Mycobacterium tuberculosis Eis protein initiates suppression of host immune responses by acetylation of DUSP16/MKP-7. *Proceedings of the National Academy of Sciences of the United States of America* **2012**, 109 (20), 7729-7734. 10.1073/pnas.1120251109
86. Shin, D. M.; Jeon, B. Y.; Lee, H. M.; Jin, H. S.; Yuk, J. M.; Song, C. H.; Lee, S. H.; Lee, Z. W.; Cho, S. N.; Kim, J. M.; Friedman, R. L.; Jo, E. K., Mycobacterium tuberculosis Eis Regulates Autophagy, Inflammation, and Cell Death through Redox-dependent Signaling. *Plos Pathogens* **2010**, 6 (12). 10.1371/journal.ppat.1001230
87. Oliveira, C. G.; da, S. M. P. I.; Souza, P. C.; Pavan, F. R.; Leite, C. Q.; Viana, R. B.; Batista, A. A.; Nascimento, O. R.; Deflon, V. M., Manganese(II) complexes with thiosemicarbazones as potential anti-Mycobacterium tuberculosis agents. *J Inorg Biochem* **2014**, 132, 21-29. 10.1016/j.jinorgbio.2013.10.011

## **Chapter 5**

**Cancer, artificial  
metallonucleases  
and targeted  
chemotherapy.**

## 5.1 An introduction to cancer

Cancer (malignant neoplasm/tumour) can be defined as a group of diseases which involves the creation of abnormal cells from normal cells, that undergo uncontrolled cell division/growth, spread beyond their usual boundaries and have the potential to invade other tissues/organs or adjoining parts of the organism.<sup>1</sup> Plants, animals (in addition to humans) and in fact any multicellular organism, are all subject to cell growth abnormalities and hence are susceptible to cancer.<sup>2</sup> Cancer is capable of occurring in almost any tissue/organ of the human body, and tissues that contain rapidly dividing cells are particularly prone, such as the skin, digestive organs, lungs and breast. Cancer is often thought of as a modern disease, one which may be a result of modern sedentary/unhealthy lifestyles, increased environmental pollution and the enhanced longevity afforded by industrialisation and modern medical care. Although the prevalence of cancer would appear to be much higher in the present age, evidence has been found in the human fossil record which indicates that ancient humans were also afflicted with cancer.

The Edwin Smyth Papyrus, a copy of a part of an ancient Egyptian medical textbook on trauma surgery, which dates back to *ca.* 3000 B.C. is widely believed to contain the earliest known reference to cancer. It describes 8 cases of tumours or ulcers of the breast that were removed by cauterization with a tool called the fire drill. The writing says about the disease, “There is no treatment.”<sup>3</sup> A recent paper which presents the complete skeleton of a young adult male from ancient Nubia, dating back to *ca.* 1200 B.C., is the oldest complete skeleton of a human displaying metastatic carcinoma/cancer.<sup>4</sup> However, as we now know, a large proportion of cancers develop late in life, hence, the number of people affected in the human fossil record is low, due to low life expectancies in ancient times.<sup>5</sup>

Cancer was also known to and documented by, the ancient Greeks. In fact, it was the Greek physician, Hippocrates (460-370 BC, considered the father of medicine), that used the terms *carcinoma* and *carcinoma* to describe non-ulcer-forming and ulcer-forming tumours.<sup>3b</sup> These words in Greek refer to a crab, because of the finger-like spreading projections from a cancer called to mind the shape of a crab. Celsus (28-50 BC), a Roman physician, later translated the Greek term into *cancer*, the Latin word for crab. It wasn't until the 17<sup>th</sup> century that the first descriptions of operations for the treatment of cancer were documented. The first reports of distinctive tumours in scientific literature included

scrotal cancer in chimney sweeps in 1775 and nasal cancer in snuff users in 1761.<sup>3b</sup> By the middle of the 19<sup>th</sup> century, people's life expectancy had dramatically improved due to advances in medicine and improvements in public health care and, as a result, the proportion of older people in the population increased and so too did the reported incidences of cancer.<sup>6</sup>

The WHO classifies neoplasms into four main groups: benign neoplasms, *in situ* neoplasms, malignant neoplasms and neoplasms of uncertain or unknown behaviour.<sup>7</sup> In modern medicine, the term tumour (Latin for swelling), means a neoplasm that has formed a lump.<sup>3a</sup> A malignant neoplasm or visible tumour is the culmination of a series of cell transformations that can take place over months and even years, often then metastasising (spreading from the tissue of origin to other sites).<sup>8</sup> The invasion of local or neighbouring tissue and the possible formation and subsequent growth of secondary tumours on distant organs/tissues are the defining characteristics of a malignant neoplasm and hence separates it from the other three main groups. A crucial problem in the treatment of cancer is metastasis. Primary tumours can invade and destroy surrounding normal tissues and small numbers of cancerous cells can travel via the lymphatic or circulatory systems to other sites forming secondary tumours called metastases. The occurrence of metastasis is associated with a staggering 90% of cancer deaths.<sup>9</sup> The first line of treatment, which is often highly successful, is surgical removal of the visible primary tumour(s) combined with irradiation. However, if the cancer metastasises to other sites this often defeats this method of therapy.<sup>10</sup> It is in this domain, or in the event that the tumour(s) are inoperable or too numerous, where chemotherapeutics play a vital role in augmenting and supplementing the efforts of clinicians, surgeons and radiotherapists in combating localized and metastatic malignant disease.

Cancer is a leading cause of death worldwide and in particular in developed nations. Over the past decade, only ischaemic heart disease, stroke, lower respiratory infections and chronic obstructive lung disease have resulted in the death of more people in developed nations.<sup>11</sup> In a recent edition of the *World Cancer Report* (2014) from the IARC, the current worldwide burden of cancer is an estimated 14 million new cases per year, a figure expected to rise to 22 million annually within the next two decades.<sup>12</sup> Cancer deaths in the same period are predicted to rise from the current 8.2 million to 13 million per year. Currently, the most common cancers diagnosed are those of the lung (1.8 million cases, 13.0% of the total), breast (1.7 million, 11.9%) and large bowel (1.4 million, 9.7%), with

the most deaths attributed to cancers of the lung (1.6 million, 19.4% of the total), liver (0.8 million, 9.1%) and stomach (0.7 million, 8.8%). Clearly from these shocking statistics better strategies and treatments are required to deal with the now commonplace clinical occurrence of patients presenting with disseminated metastatic disease. One of the primary aims of this project was to build upon our groups previous successes and to develop new, metal-based chemotherapeutic compounds for the treatment of specific cancers.

## 5.2 The cell cycle and tumour growth

Mitosis is the process of cell division used by the majority of cells in the human body, with the exception of reproductive cells which utilise the meiosis process of cellular division.<sup>13</sup> Mitosis (M phase) involves division of the cell nucleus, whereby the chromosomal DNA must initially be precisely duplicated and then during mitosis correctly segregated into two identical daughter nuclei. This represents the most important step in cellular reproduction.<sup>14</sup> It is during this event that the entire genetic blueprint encoding the complete characteristics and functions of the cell must be accurately reproduced. This stage is referred to as the mitotic phase (M phase) and is a relatively short period of the cell cycle. This mitotic process occurs in four stages, namely prophase, metaphase, anaphase and telophase, combined with a resting/preparative period which occurs between cell cycles that is, as termed, interphase (Figure 5.1).

Interphase is a much longer process and takes up roughly 90% of a cell's lifespan. During interphase, the cell prepares itself for the mitotic process of cellular division.<sup>14</sup> There is an obvious gap which exists during interphase, both before and after DNA synthesis, with DNA synthesis itself occurring over a relatively short period of the cell cycle. The three phases of interphase are G<sub>1</sub> (first gap), S (DNA synthesis) and G<sub>2</sub> (second gap). All of the phases of the cell cycle are highly regulated (via proteins) and follow one another in strict order. DNA is replicated during S phase, and then the replicated DNA strands are accurately partitioned to the two daughter cells during M phase. There is a fourth stage in interphase which the cell can enter, called G<sub>0</sub>. Cells will continue to proliferate until they become too crowded, at which point they can exit the cell cycle and enter into G<sub>0</sub> (Figure 5.2). This contact or cell density-dependant inhibition feedback mechanism, is extremely important for the normal function/proliferation of all cells, tissues and organs.



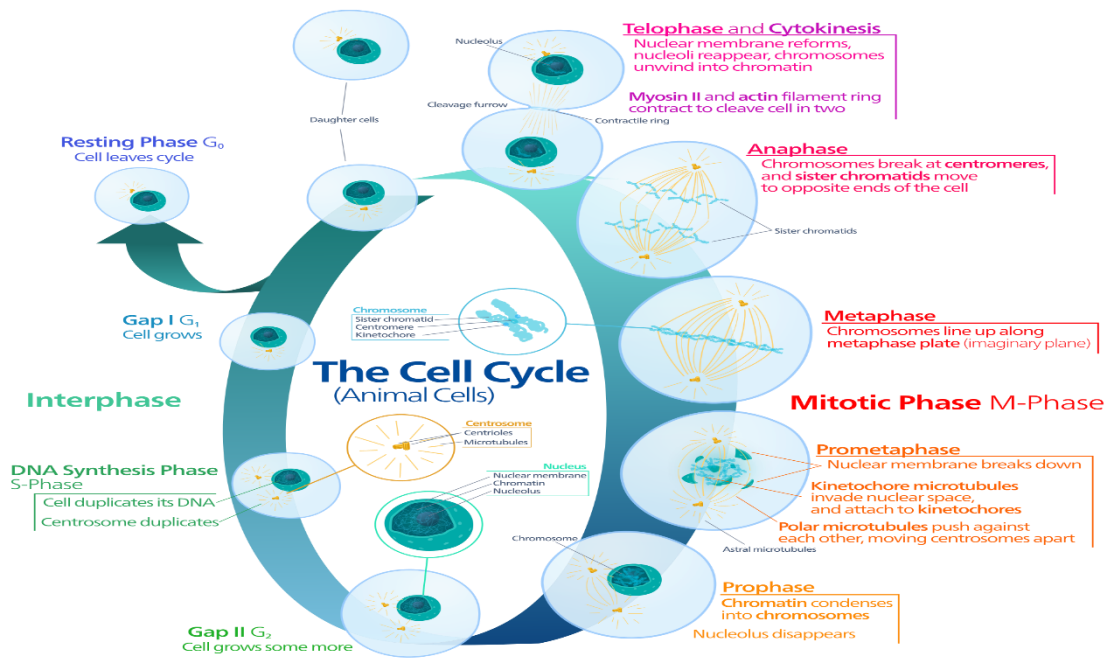


Fig. 5.1: The details of the four stages of the mitotic process or M phase of the animal cell cycle.<sup>13</sup>

Cancer can arise from a change or transformation of a single cell and this change may be initiated by external agents (such as carcinogens) or via inherited genetic factors. The prolific/unrestrained growth of cells which is characteristic of cancer is attributed to the

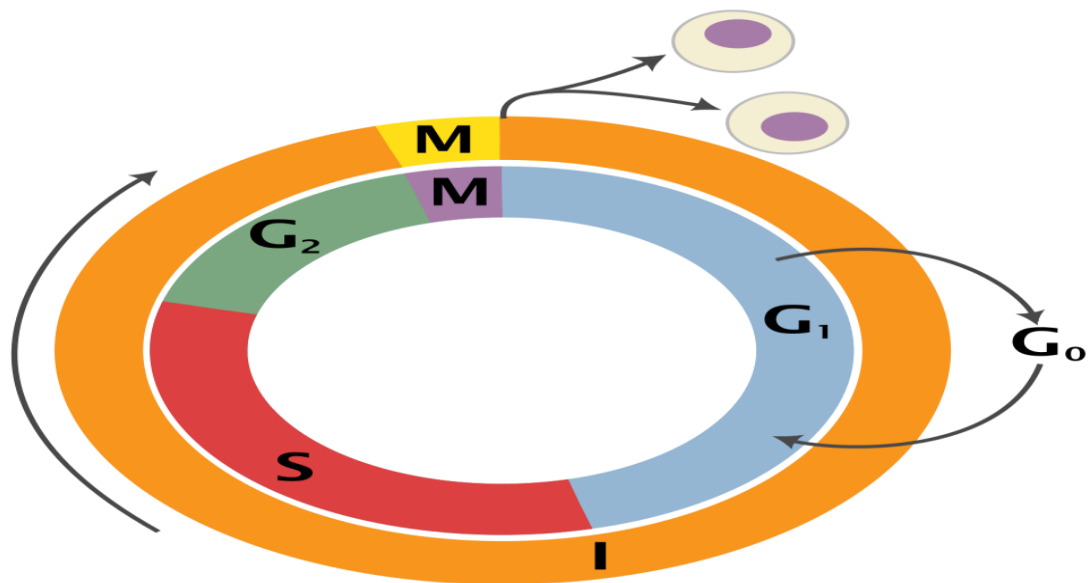


Fig. 5.2: Schematic representation of the entire animal cell cycle, with relative ratios of time periods spend in each phase.<sup>15</sup>

loss of the specific control mechanisms (enzymes/proteins) that tightly regulate mitosis in normal cells. Cyclins and cyclin-dependent kinases (CDKs) are the two key classes of regulatory molecules.<sup>16</sup> Cells monitor and regulate the progress of the cell cycle by using cell cycle checkpoints, and these checkpoints are designed to safeguard against damaged or incomplete DNA being passed on to daughter cells. When damage beyond the capacity of the cell to repair is detected, specific genes are activated, producing proteins (p16, p21, p27, p53 and p53) which can prevent the progression of the cell cycle via programmed cell death (apoptosis).<sup>17</sup> These genes/proteins are hence paramount in the prevention of tumour formation and, as such, are known as tumour suppressors.

The formation of a tumour by uncontrolled cell grow/proliferation can be brought about via mutations in the genes responsible for these cell cycle inhibitors (p53, p21).<sup>18</sup> In tumour cells, the duration of the cell cycle can be equal to or longer than that of a normal cell cycle, but, importantly, the proportion of cells that are in active cell division (versus quiescent cells in G<sub>0</sub> phase) in tumours is much higher than that in normal tissue. This results in a huge net increase in the cell number as the number of cells that die by apoptosis either decreases or remains constant, and the proportion of senescent cells remains the same.<sup>19</sup> When cells are in the active cell cycle, their DNA is relatively exposed during cell division and, hence, are susceptible to damage by radiation or chemotherapeutics (ROS mediated DNA scission, DNA intercalation). The level of sensitivity of the DNA to damage correlates with the level of thiol compounds such as glutathione, glutaredoxin and thioredoxin present in the cell. These thiol-containing molecules help protect the DNA and tend to be at their highest levels in the S phase and at their lowest near mitosis.<sup>20</sup>

### 5.3 Metal-based chemotherapeutics and artificial metallonucleases

The field of medicinal inorganic chemistry has become a clinically relevant component of the pharmaceutical sector. This sector has given rise to metallo-drugs as breakthrough therapies for the treatment of cancer using cisplatin (*cis*-diamminedichloroplatinum(II)) [Platinol®], carboplatin [Paraplatin®], nedaplatin [Aqupla®], arsenic trioxide [Trisenox®] and both iron and copper bleomycin [Blenoxane®]. The majority of these clinical agents function through interacting with nucleotide targets and prevent DNA synthesis/replication, which ultimately leads to tumour cell death. The nature of both the metal centre and coordinated ligand(s) is highly significant as both influence drug-DNA

interactions.<sup>21</sup> While the platinum(II) drugs are among the most effective cytotoxins available, and are currently utilised in 50% of treatment regimes for solid tumours, issues including; severe side-effects, dose-limiting toxicity, resistance to apoptosis, cancer cell selectivity and mutagenicity are impeding factors in the abrogation of human cancer.<sup>22</sup>

A nuclease is an enzyme capable of cleaving the phosphodiester bonds between the nucleotide subunits of nucleic acids, and they can be divided into endo and exonucleases. Endonucleases cleave polynucleotides in the middle of the chain and can cut DNA either non-sequence specifically or be highly sequence specific. Exonucleases cleave nucleotides one at a time from the end of a polynucleotide chain.<sup>23</sup>

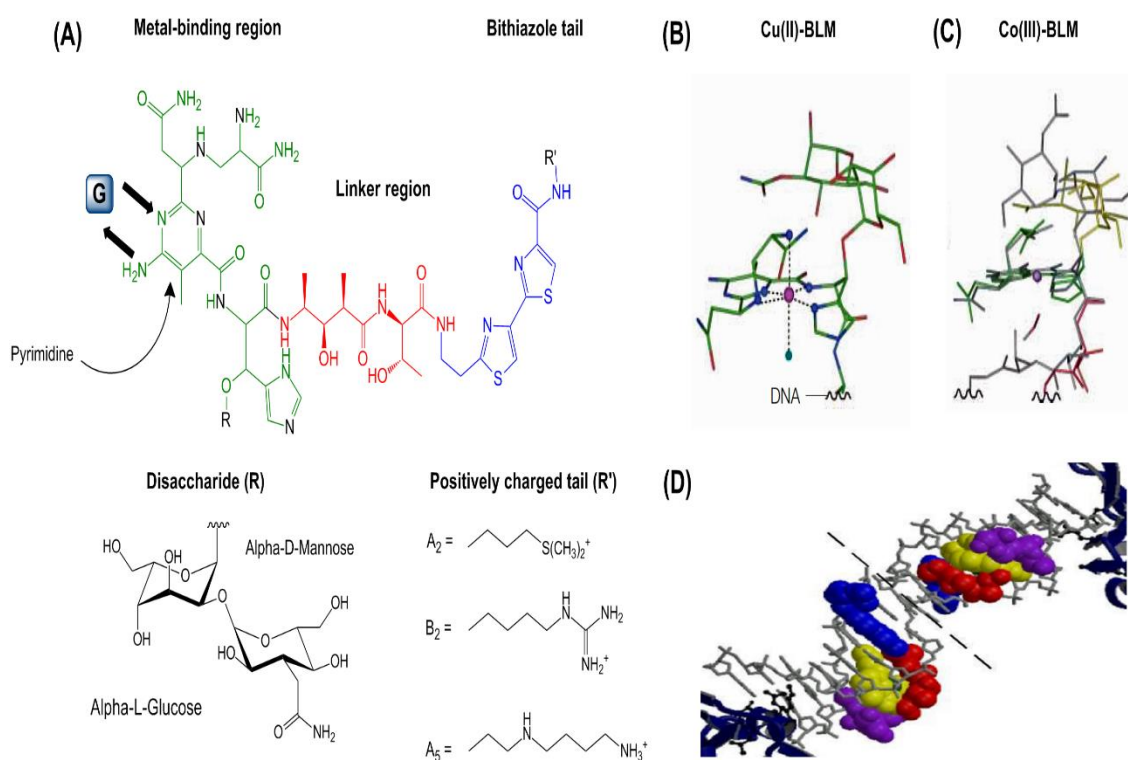


**Fig. 5.3:** (A) Structure of bleomycins, metal-binding domain in green, linker in red and bithiazole tail in blue, G is guanine. (B) X-ray crystal structure of Cu(II)-BLM bound to DNA (bithiazole tail omitted for clarity). (C) X-ray crystal structure of Co(III)-BLM bound to DNA. (D) The crystal structure of the DNA-Co-BLM complex intercalated into the minor groove, (DNA is shown in a gray stick model, bithiazole tail in blue, linker in red, metal-binding domain in yellow with Co in green, disaccharide in purple).<sup>24</sup>

Artificial metallonucleases are small molecule, nuclease mimetic, metal-containing complexes that induce chemical DNA scission, and agents of this nature have found

clinical application. Cleaving reagents function using one of two distinct mechanisms; (i) oxidative scission of deoxyribose residues through redox chemistry, and (ii) hydrolysis of the phosphodiester sugar backbone.<sup>25</sup> A known example is the natural glycopeptide, (antimitotic antibiotic) chemotherapeutic drug, bleomycin (BLM) (Figure 5.3).

The bleomycin (BLM) family of compounds was first isolated in the late 1960s from the bacteria, *Streptomyces verticillus*, and are a widely-studied family of glycopeptide antibiotics that have been successfully utilised in the treatment of some forms of cancer.<sup>24a</sup> The structure of BLM contains three domains, a metal chelator section comprised of a pyrimidine moiety and five nitrogen atoms for octahedral metal coordination, a DNA binding domain consisting of a peptide linker region bearing a disaccharide side-chain and a bithiazole unit with an appended, positively charged tail (Figure 5.3).<sup>26</sup> BLM is a prodrug, becoming activated after it forms complexes with transition metals (Cu(II), Fe(II)). These *in situ* generated cytotoxic complexes have been shown, *in vitro* and in the presence of oxygen, to generate reactive oxygen species (ROS) (e.g. Fe<sup>2+</sup>-BLM and Cu<sup>2+</sup>-BLM).<sup>24a</sup> Metallobleomycins bind non-covalently with DNA via the minor groove, though neither affinity nor specificity is particularly high.<sup>24a, 26</sup> Complexes of this type are known to bind tightly to nuclear duplex DNA via intercalation and, subsequently, induce chemical single strand (ss) and double strand (ds) scission/cleavage by removing the 4'-hydrogen atom from C4' of the deoxyribose moiety of the pyrimidine 3' to a guanine by a high valent Fe-oxo species, producing a radical which results in ds scission in the presence of O<sub>2</sub> and ss cleavage in the presence of H<sub>2</sub>O<sub>2</sub>.<sup>24a</sup>

BLM is often clinically combined with the anthracycline topoisomerase inhibitor doxorubicin, to treat lymphomas, squamous-cell carcinomas and germ-cell tumours.<sup>24a</sup> The intercalative action of doxorubicin inhibits topoisomerase II $\alpha$ , an enzyme involved in the regulation of DNA supercoiling and which is known to be crucial for cellular replication.<sup>27</sup> This co-administration is thought to result in a synergistic effect by BLM degrading duplex DNA via ROS generation, coupled with doxorubicin acting as a topoisomerase poison inhibiting the relegation of duplex DNA. This is a particularly attractive chemotherapeutic strategy and one which could possibly be accomplished by a single 1,10-phenanthroline metal complex, which is capable of inhibiting topoisomerase via DNA intercalation of the phenanthroline moiety and DNA scission/cleavage mediated by ROS generation via the metal centre. The first reported synthetic chemical nuclease or artificial metallonuclease possessing DNA cleavage properties was [Cu(phen)<sub>2</sub>]<sup>2+</sup>.<sup>25, 28</sup>

The redox action of the complex was dependent on the presence of both exogenous reductant (e.g. L-ascorbic acid) and oxidant (e.g.  $O_2$  or  $H_2O_2$ ), which resulted in a cascade of redox reactions (i–v) that ultimately lead to the formation of hydroxo (iv and v) and metal-oxo (iv) radical species, which are thought to be the active agents for initiating DNA scission and hence cytotoxicity (Figure 5.4).<sup>25, 28</sup>

- (i)  $[Cu(1,10\text{-phen})_2]^{2+} + \text{red} \rightarrow [Cu(1,10\text{-phen})_2]^+ + \text{red}\cdot$
- (ii)  $[Cu(1,10\text{-phen})_2]^+ + O_2 \rightarrow [Cu(1,10\text{-phen})_2]^{2+} + O_2\cdot^-$
- (iii)  $2 O_2\cdot^- + 2H^+ \rightarrow H_2O_2 + O_2$
- (iv)  $[Cu(1,10\text{-phen})_2]^+ + O_2 + H^+ + e^- \rightarrow [\cdot O-Cu(1,10\text{-phen})_2]^{2+} + \cdot OH$
- (v)  $[Cu(1,10\text{-phen})_2]^+ + H_2O_2 \rightarrow [^{\cdot}O-Cu(1,10\text{-phen})_2]^{2+} + \cdot OH + H^+$

The vulnerability of some tumour cells to oxidative stress/damage, due their higher levels of ROS and a depleted ability to modulate cellular redox status through the glutathione, glutaredoxin and thioredoxin systems, means that reactive oxygen and reactive nitrogen species (ROS/RNS-producing compounds) can induce cellular senescence and apoptosis and can, therefore, function as anti-tumourigenic species.<sup>29</sup>

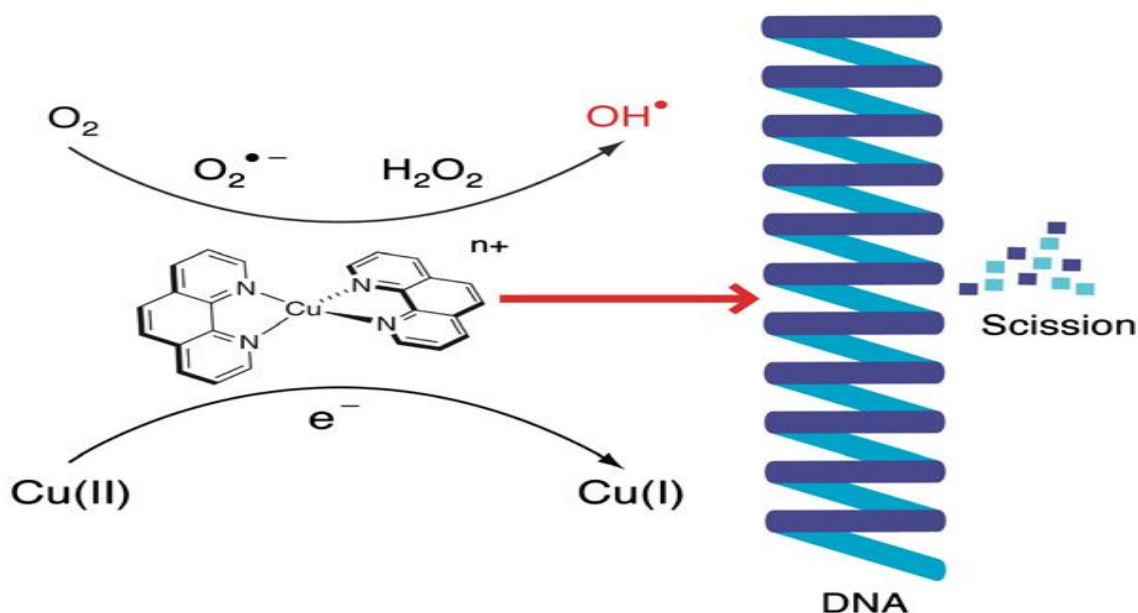


**Fig. 5.4:** Schematic representation of ROS generation and DNA scission by the first known synthetic artificial metallonuclease,  $[Cu(1,10\text{-phen})_2]^{2+}$ .<sup>21b</sup>

#### 5.4 *In vitro* anticancer screening

To date, we have established an anticancer/antimicrobial synergism for a number of our existing  $\text{Ag}^+$ ,  $\text{Cu}^{2+}$  and  $\text{Mn}^{2+}$  ternary 1,10-phen dicarboxylate complexes which is viewed as a desirable attribute for a potential drug candidate.<sup>21b, c, 30</sup> Some of our previously reported Cu(II) and Mn(II) bis-1,10-phen complexes incorporating coordinated dicarboxylate groups (e.g. octanedioate, **13** and **14**) displayed avid DNA binding and cleaving capability along with powerful *in vitro* chemotherapeutic activity via the redox-generation of ROS.<sup>21b, c, 30b, 30f, g</sup> Results arising from the present work are given below.

The selected metal complexes **8-17** (Table **5.1**) for *in vitro* anticancer screening were synthesised as follows, all chemicals were purchased from commercial sources and used as received. 1,10-Phenanthroline-5,6-dione (phendione (**2**)), and complexes **8-14** (Table **5.1**) were prepared in accordance with the literature methods, with some slight modifications.<sup>30a, 31</sup> Precursor dicarboxylate complexes containing phthalic acid ( $\text{phH}_2$ ), octanedioic acid ( $\text{odaH}_2$ ) and 3,6,9-trioxaundecanedioic acid ( $\text{tddaH}_2$ ) were synthesised by heating a solution containing the metal acetate salt and an excess of the dicarboxylic acid (e.g.  $[\text{Mn}(\text{ph})]\cdot 0.5\text{H}_2\text{O}$ ) (See Scheme **3.1**, page 175). The metal carboxylate complexes were then added to a solution of 1,10-phen to give the ternary metal 1,10-phen carboxylate complexes (See Scheme **3.1**, page 175). All of the Ag(I) complexes were synthesised in the absence of light and the products were stored in the dark.

The cytotoxicity ( $\text{IC}_{50}$  values) of a selection of Mn(II), Cu(II) and Ag(I) complexes, **8-17** (Groups 1-4 in Table **5.1**), the metal-free ligands, **1** and **2**, and the clinical antitumour agent, cisplatin (CDDP), were measured *in vitro* against the five human-derived cancer cell lines, MCF-7, SK-OV-3, DU145, HT29 and A549 along with the non-cancerous simian kidney epithelial Vero cell line.  $\text{IC}_{50}$  values were determined (after 24 h and repeated in triplicate) using the standard colorimetric MTT (3-(4,5-dimethylthiazol-2-yl)-2,5-diphenyltetrazolium bromide) assay for assessing cell viability (Table **5.2**).

The five human-derived cancer cell lines were: (i) MCF-7 which are metastatic adenocarcinoma (epithelial) breast cells, (ii) SK-OV-3 which are intrinsically cisplatin-resistant, adenocarcinoma (epithelial) ovarian cells, (iii) DU145 which are prostate cancer cells with moderate metastatic potential, (iv) HT29 which are primary tumour colorectal adenocarcinoma cells and (v) A549 which are adenocarcinomic alveolar basal epithelial cells.<sup>32</sup>

**Table 5.1:** Selected complexes for cytotoxicity screening.

Compound		Molecular Mass (g/mol)
1	1,10-phenanthroline (1,10-phen)	Group 1 180.21
2	1,10-phenanthroline-5,6-dione (phendione)	
8	[Mn(ph)(phen)(H <sub>2</sub> O) <sub>2</sub> ]	435.30
9	[Mn(ph)(phen) <sub>2</sub> (H <sub>2</sub> O)].4H <sub>2</sub> O	669.56
10	[Mn <sub>2</sub> (isoph) <sub>2</sub> (phen) <sub>3</sub> ].4H <sub>2</sub> O	Group 2 1050.82
11	{[Mn(phen) <sub>2</sub> (H <sub>2</sub> O) <sub>2</sub> ] <sub>2</sub> (isoph) <sub>2</sub> (phen).12H <sub>2</sub> O	
12	[Mn(tereph)(phen) <sub>2</sub> ].5H <sub>2</sub> O	669.56
13	[Mn <sub>2</sub> (η <sub>1</sub> η <sub>1</sub> μ <sub>2</sub> -oda)(phen) <sub>4</sub> (H <sub>2</sub> O) <sub>2</sub> ][Mn <sub>2</sub> (η <sub>1</sub> η <sub>1</sub> μ <sub>2</sub> -oda)(phen) <sub>4</sub> (η <sub>1</sub> -oda) <sub>2</sub> ].4H <sub>2</sub> O	Group 3 2458.23
14	[Cu <sub>2</sub> (oda)(phen) <sub>4</sub> ](ClO <sub>4</sub> ) <sub>2</sub> .2.76H <sub>2</sub> O.EtOH	
15	{[Mn(3,6,9-tdda)(phen) <sub>2</sub> ].3H <sub>2</sub> O.EtOH} <sub>n</sub>	735.64
16	{[Cu(3,6,9-tdda)(phen) <sub>2</sub> ].3H <sub>2</sub> O.EtOH} <sub>n</sub>	Group 4 744.25
17	[Ag <sub>2</sub> (3,6,9-tdda)(phen) <sub>4</sub> ].EtOH	
CDDP	Cisplatin	300.01

In addition to the intrinsically cisplatin-resistant ovarian cell line, SK-OV-3, the colorectal adenocarcinoma (HT29) and prostate epithelial (DU145) carcinomas are also inherently resistant to cisplatin and they also possess mutant versions of the *p53* gene, while the MCF-7 cell line contains a normal and fully characterised wild-type *p53* gene.<sup>33</sup>

The cancer cell lines chosen represent the most commonly diagnosed cancer types in Ireland (lung, female breast, prostate and colorectal cancer) and are also the most lethal having the lowest associated survival rates.<sup>34</sup>



**Table 5.2:** IC<sub>50</sub> values for compounds/complexes **1**, **2**, **8-17** and cisplatin (CDDP), against the five human-derived cancer cell lines, MCF-7, SK-OV-3, DU145, HT29 and A549 along with the non-cancerous, simian kidney epithelial Vero cell line. Experiments were conducted independently in triplicate and readings taken after an exposure period of 24 h.

	Antitumour activity IC <sub>50</sub> (μM) after 24 h					
	MCF-7	SK-OV-3	DU145	HT29	A549	Vero
<b>1</b>	337.70	286.00	272.50	376.80	>355.41	> 55.49
<b>2</b>	n.t.	n.t.	n.t.	n.t.	9.66	31.40
<b>8</b>	>100	>100	>100	>100	>500	35.84
<b>9</b>	>100	>100	>100	>100	387.33	17.47
<b>10</b>	18.50	>100	85.00	>100	243.50	118.95
<b>11</b>	86.70	52.40	40.00	49.70	154.70	28.82
<b>12</b>	>100	>100	>100	>100	376.28	70.05
<b>13</b>	n.t.	n.t.	n.t.	108.00	>512	152.55
<b>14</b>	n.t.	n.t.	n.t.	9.61	0.75	8.94
<b>15</b>	n.t.	n.t.	n.t.	n.t.	355.70	84.96
<b>16</b>	n.t.	n.t.	n.t.	n.t.	1.43	7.86
<b>17</b>	n.t.	n.t.	n.t.	n.t.	1.84	25.02
<b>CDDP</b>	90.80	>500	>500	166.00	16.11	15.38

It should be noted that the cell viability results for the test compounds/complexes specified in Table 5.2 were obtained after a 24 h exposure time and would need to be taken in the future after 72 and 96 h exposure to the test agents. This is of particular importance as the IC<sub>50</sub> values obtained for the clinical antitumour drug, cisplatin, are unusually high at 24 hours (HT29 = 166 μM) and can be explained by the slow ligand exchange that cisplatin undergoes *in vivo*, whereby, following administration, one of the chloride ligands is slowly exchanged/displaced by H<sub>2</sub>O resulting in a cationic complex [PtCl(H<sub>2</sub>O)(NH<sub>3</sub>)<sub>2</sub>]<sup>+</sup>.<sup>35</sup> Upon entrance into the cell nucleus [PtCl(H<sub>2</sub>O)(NH<sub>3</sub>)<sub>2</sub>]<sup>+</sup> becomes attracted to the anionic DNA and the aqua ligand is displaced forming a new platinum bond to a guanine in a DNA strand [Pt(guanine-DNA)(NH<sub>3</sub>)<sub>2</sub>]<sup>+</sup>. Crosslinking of the DNA can then occur via displacement of the second chloride by another guanine in an adjacent DNA strand forming the final cytotoxic complex [PtCl(guanine-DNA)<sub>2</sub>(NH<sub>3</sub>)<sub>2</sub>]<sup>2+</sup>, (cisplatin IC<sub>50</sub> values after 72 h exposure are 6.75, 11.6 and 15.9 μM for A549, MCF-7 and HT29 cells respectively).<sup>36</sup> In addition, complexes **13** and **14** were previously found to display nano and picomolar cytotoxicity after 96 hours (0.092 and <0.001 μM)<sup>21c</sup>



against the same HT29 cell line specified in Table 5.2. Therefore, it would seem likely that the true level of cytotoxicity of these current complexes may only be fully expressed over a longer time period (e.g. 96 h). Given this, there are still some observable trends in activity in Table 5.2.

The Mn(II) 1,10-phen/isophthalate complex, **11**, displayed median, broad spectrum cytotoxicity against all of the cell lines tested, being most active against the prostate cell line DU145 ( $IC_{50} = 40 \mu\text{M}$ ). Although **11** displayed superior activity to cisplatin in all but the alveolar cell line, A549, its  $IC_{50}$  value against non-cancerous Vero cells was low ( $IC_{50} = 28.82$ ), indicating a low level of tolerance and hence a low selectivity for cancerous cells over that of normal cells. The Cu(II)-based complex, **14**, exhibited excellent activity against the adenocarcinomic alveolar A549 cells ( $IC_{50} = 0.75 \mu\text{M}$ ), combined with a median level of tolerance against Vero cells ( $IC_{50} = 8.94 \mu\text{M}$ ), indicating a high level of cytoselectivity for cancerous cells. Similarly, the only other Cu(II)-based complex, **15**, also displayed good activity against the A549 cells and also had a median level of tolerance against Vero cells ( $IC_{50} = 7.86 \mu\text{M}$ ), thus giving a high degree of cytoselectivity. The Ag(I)-based complex, **17**, also exhibited good activity against A549 cells combined with a high level of tolerance against the Vero cells ( $IC_{50} = 25.02 \mu\text{M}$ ), signifying a preferential activity profile against cancerous cells over normal cells.

A clear pattern is evident from the results presented in Table 5.2, the Cu(II) and Ag(I)-based complexes perform better than the Mn(II)-based complexes. This trend may reflect an accurate metal ion specificity correlation or it may be due to the shorter time interval (24 h) utilised in this particular assay. The Mn(II)-based complexes may require a longer time period before they express their true  $IC_{50}$  values, and the previously published  $IC_{50}$  values for complex **13** against the colorectal cell line, HT29, would seem to suggest this ( $IC_{50} = 108 \mu\text{M}$  at 24 h and  $IC_{50} = 0.092 \mu\text{M}$  at 96 h).

These results suggest that these complexes are promising antineoplastic agents especially given the short exposure time utilised to determine their  $IC_{50}$  values (24 h). In addition, complexes **12-17** are extremely water soluble and as was previously discussed in chapter 4, these complexes (**1, 2, 8-17**) are highly tolerated *in vivo* by *Galleria mellonella* larvae with cisplatin being considerably more toxic to the larvae.

## 5.5 The derivation and development of 1,10-phenanthroline

An emerging field in chemotherapeutics and nucleic acid research is the design of small molecules that are capable of targeting specific sequences of DNA with high affinity. Metal complexes with structurally rigid ligands of varying structure and size are remarkably good mimics of proteins that recognise specific sequences and grooves (major or minor groove) within the helical structure of DNA.<sup>37</sup> Complexes of this nature would act as enhanced DNA probes, novel chemotherapeutics and highly sensitive diagnostic agents.<sup>38</sup>

We had previously been concerned with the development and refinement of ternary complexes of 1,10-phen and various dicarboxylate ligands (phthalates, octanedioates and trixaundecanedioates) and succeeded in synthesising Ag(I), Cu(II) and Mn(II) complexes with better solubility profiles combined with superior nuclease mimetic (via ROS generation), antimicrobial and anticancer activities.<sup>21b, c, 30a, b, 30d, 30f, g</sup> In an effort to improve upon these highly encouraging results, we decided to investigate the derivation of the 1,10-phen backbone in order to include a variety of structural and functional group entities/moieties of varying electronic and steric nature which may have possible biological applications. Of particular interest, was the possible enhancement in DNA intercalative, ROS/RNS generation and subsequent DNA cleavage/scission capabilities of phenanthrene-based complexes which could ultimately act as DNA probes and cytotoxic antitumour agents (Figure 5.5).

The literature contains numerous examples of metallo-intercalators containing bidentate phenanthrene ligands which possess unique structural chemotypes, which have shown encouraging biological potential.<sup>26, 39</sup> Recently, it was reported that the inclusion of phenanthridine as a coordinated ligand into cisplatin which resulted in the new cationic complex, cis-[Pt(NH<sub>3</sub>)<sub>2</sub>(phenanthridine)Cl]<sup>+</sup> (phenanthriplatin), which exhibited superior *in vitro* cellular uptake and an enhanced range of activity, compared to that of cisplatin, against a panel of 60 cancerous cell lines (Figure 5.6).<sup>36, 40</sup>

In addition, the extension of the 1,10-phen backbone, via imine/Schiff base formation using 1,10-phenanthroline-5,6-dione and various diamines, results in the formation of dipyridophenazine ligands (DPQ, DPPZ, DPPN) which possess extended planar aromatic ring systems that facilitate efficient intercalation with helical DNA (Figure 5.6).

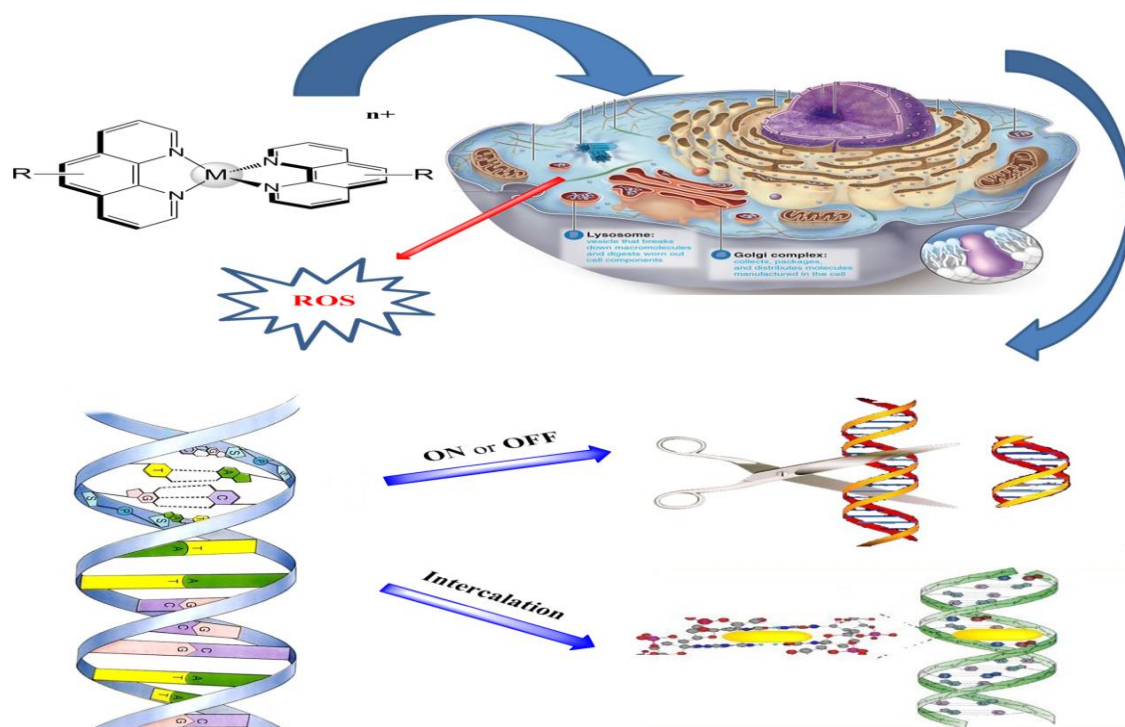


**Fig. 5.5:** Schematic representation of our proposed novel phenanthroline-based complexes, with the dual capability to intercalate into DNA and, depending on the synthetically variable ligand functional groups, to also generate ROS species which are capable of inducing DNA strand scission.

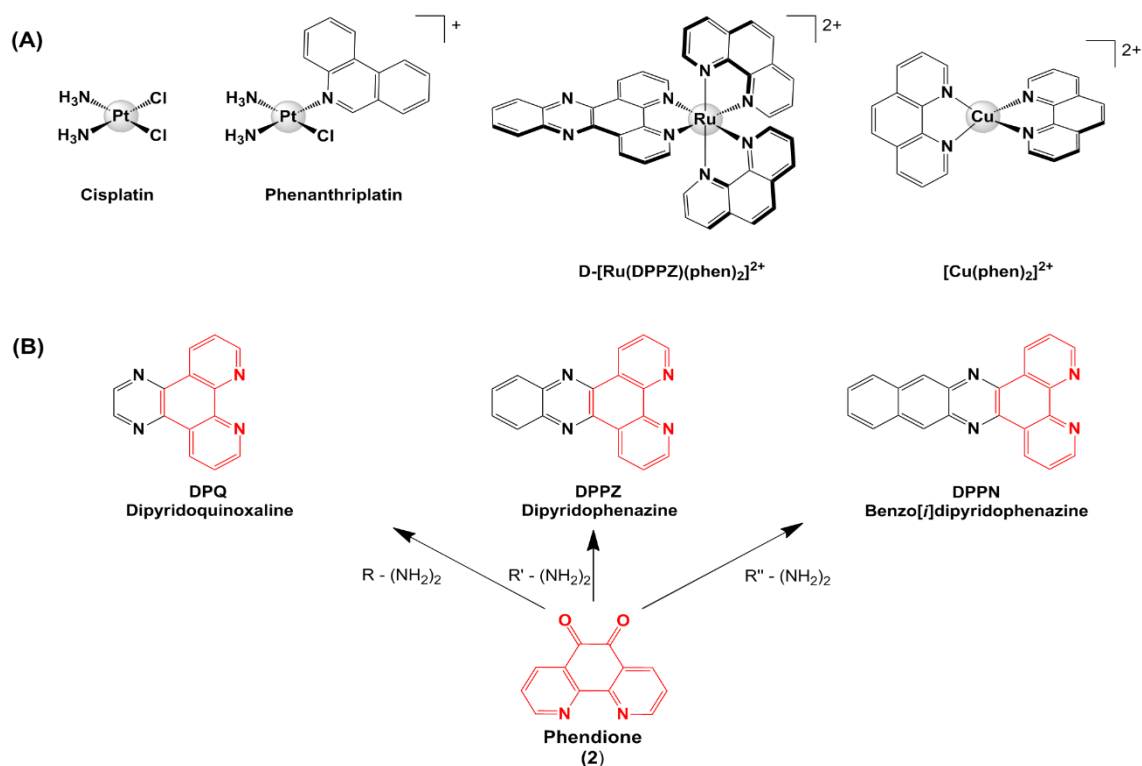


**Fig. 5.6:** (A) Molecular structures of the cytotoxic Pt(II) complexes cisplatin and phenanthriplatin, the Ru(II) DNA light switch, complex  $\Delta$ -[Ru(DPPZ)(phen)<sub>2</sub>]<sup>2+</sup>, and the Cu(II) chemical nuclease, [Cu(phen)<sub>2</sub>]<sup>2+</sup>. (B) Reaction schematic for the formation of phenazine ligands, DPQ, DPPZ and DPPN starting with phendione (2) and the appropriate diamine.

One extensively studied example of this type of metal complex incorporating a dipyridophenazine ligand is the Ru(II) species,  $\Delta$ -[Ru(DPPZ)(phen)<sub>2</sub>]<sup>2+</sup>, which, due to its cationic nature, specific symmetry, extended planar aromatic system and hydrophobicity displays excellent DNA recognition properties.<sup>41</sup> This complex can act as a “light switch” due to photoluminescent enhancement upon intercalation into the hydrophobic environment between nucleotides which act to protect it from the luminescent quenching properties of the mainly aqueous cellular environment.<sup>41</sup> Furthermore, as previously discussed, the Cu(II) bis-1,10-phen complex, [Cu(phen)<sub>2</sub>]<sup>2+</sup>, is an effective chemical nuclease that can induce DNA cleavage via ROS generation, and whose limitations are the need for exogenous reductant and oxidant and minor groove localised non-nucleotide sequence specific DNA oxidation.

We were particularly interested in synthesising 1,10-phen derivatives which allow for the modular assembly and covalent inclusion of an ensemble of varied functional groups, bioisosteres and specific cellular targeting/recognition molecules. To this end, we hoped to design new ligands that, besides containing the expansively aromatic “dppz” type of structure, would also contain other bioactive subunits/moieties that, when coordinated to specific transition metals (Cu(II) and Mn(II)), would intercalate and cleave duplex DNA. The purine bases in DNA have a five-membered imidazole ring component and there are numerous imidazole derivatives that are known to have an extensive spectrum of interesting biological activities. Hence, we focused our attention on synthesising and studying polypyridyl ligands such as imidazole-modified 1,10-phen (imidazophenanthrolines).<sup>42</sup> In particular, the imidazo[4,5-*f*][1,10]-phenanthroline core appeared to be very promising given that the 2-phenylimidazo[4,5-*f*][1,10]-phenanthroline (PIP) ligand, its substituted derivatives and their Ru(II) complexes have proven to be excellent DNA probes and possible anticancer agents due to their cytotoxic effects on primary tumours.<sup>43</sup>

In 1882, Radziszewski and Japp reported the first synthesis of the imidazoles, using 1, 2-dicarbonyl compounds, various aldehydes and ammonia.<sup>44</sup> The conventional literature synthetic procedure for the production of imidazo[4,5-*f*][1,10]-phenanthroline and various its derivatives are closely related to the Radziszewski reaction. This involves the reaction of 1,10-phenanthroline-5,6-dione with an aromatic aldehyde, in a 1:1.5 mole ratio, in the presence of a large excess of ammonium acetate in anhydrous acetic acid under an inert atmosphere. The mixture is refluxed for 4 to 24 hours after which the

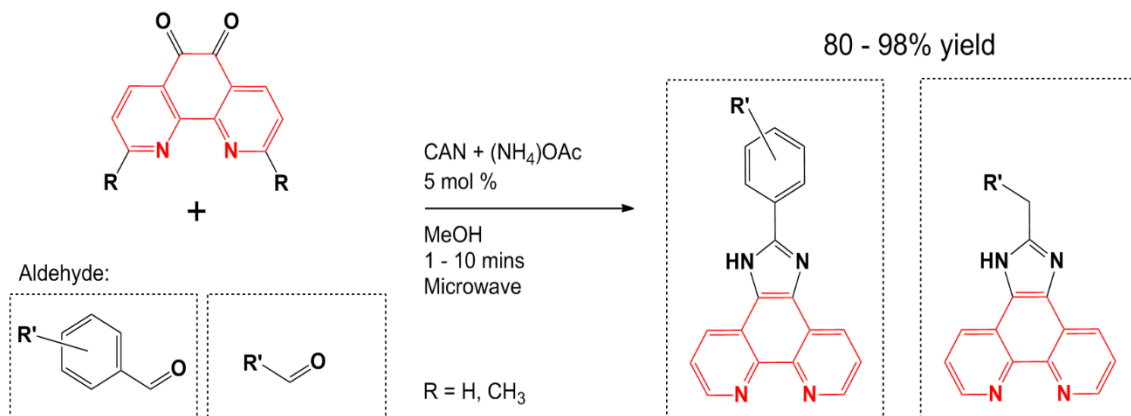
product is precipitated by the dropwise addition of concentrated aqueous ammonia to the cooled reaction mixture. An extensive workup of the products is required and necessitates chromatographic purification. Products are recovered in moderate to low yields depending on the nature of the functional groups present on the chosen aldehyde.

In an effort to improve upon the above synthetic protocol we encountered a report in the literature of the use of cerium(IV) ammonium nitrate (CAN) to catalyse the one-pot synthesis of 2, 4, 5-triaryl imidazoles from the 1, 2-diketone benzoin or the  $\alpha$ -hydroxyketone, benzyl and aromatic aldehydes (1:1 mole ratio), which resulted in improved yields and purer products.<sup>45</sup> We hypothesised that, given the electronic and structural similarities between benzoin and phendione/2,9-dimethyl-1,10-phenanthroline-5,6-dione (dmphendio, **4**), each of which contains aromatic 1,2-diketone moieties, that a similar reaction would occur and result in the formation of imidazo[4,5-*f*][1,10]-phenanthroline or imidazo-phenanthroline (Im-phen) derivatives. This proved to be correct. Methanol was employed as the optimum solvent in which was dissolved the CAN catalyst (5 mol%) the dione, a small excess of ammonium acetate and lastly the aldehyde. Thus, a highly efficient reaction, giving pure products in high yields, without the need for column chromatographic purification, was developed.

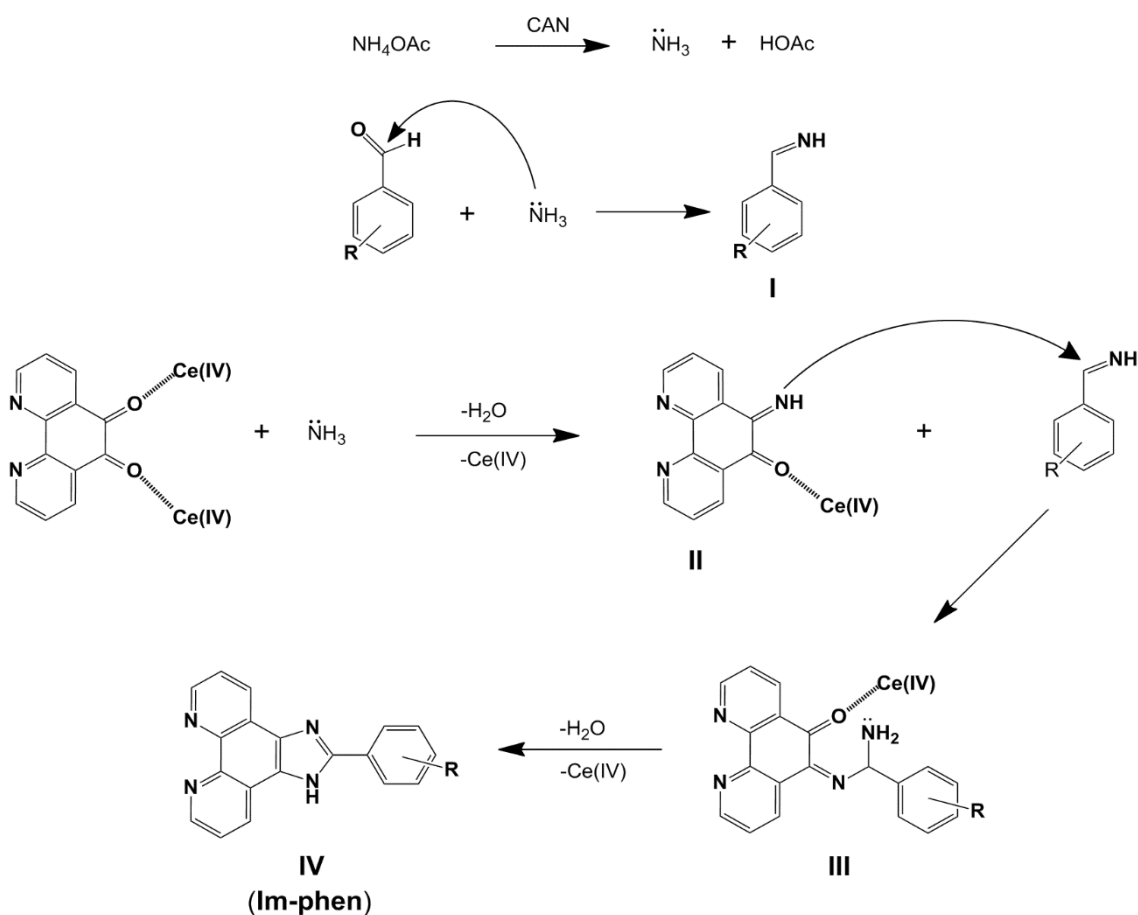
It is well known the microwave heating can result in drastically reduced reaction times and improved product yields in organic reactions.<sup>46</sup> Unlike oil-bath thermal heating, microwave irradiation results in inverted temperature gradients. Microwave heating raises the temperature of the whole volume simultaneously (bulk heating), whereas with oil-bath heating the reaction mixture in contact with the vessel wall is heated first.<sup>46</sup> In an attempt to further refine the above mentioned reaction protocol microwave heating was utilised. This resulted in high to almost quantitative product yields and for the production of imidazo-phenanthrolines in very short reaction times (1-10 minutes) (Scheme 5.1).

CAN is a known strong oxidant in organic synthesis. In addition, the Ce(III) and Ce(IV) cations have large ionic radii (115/128.3 pm and 101/111 pm, respectively). We postulate that CAN enhances/promotes the heterocyclization reaction by virtue of its inherent Lewis acidity, which allows it to bind through a lone pair of electrons on the carbonyl oxygen. This increases the electrophilic nature of the carbon of the carbonyl moieties of phendione. The one electron redox cycling of CAN between its Ce(IV) and Ce(IV) states

promotes the splitting of the ammonium acetate providing the ammonia required for the initial condensation (Scheme 5.2).

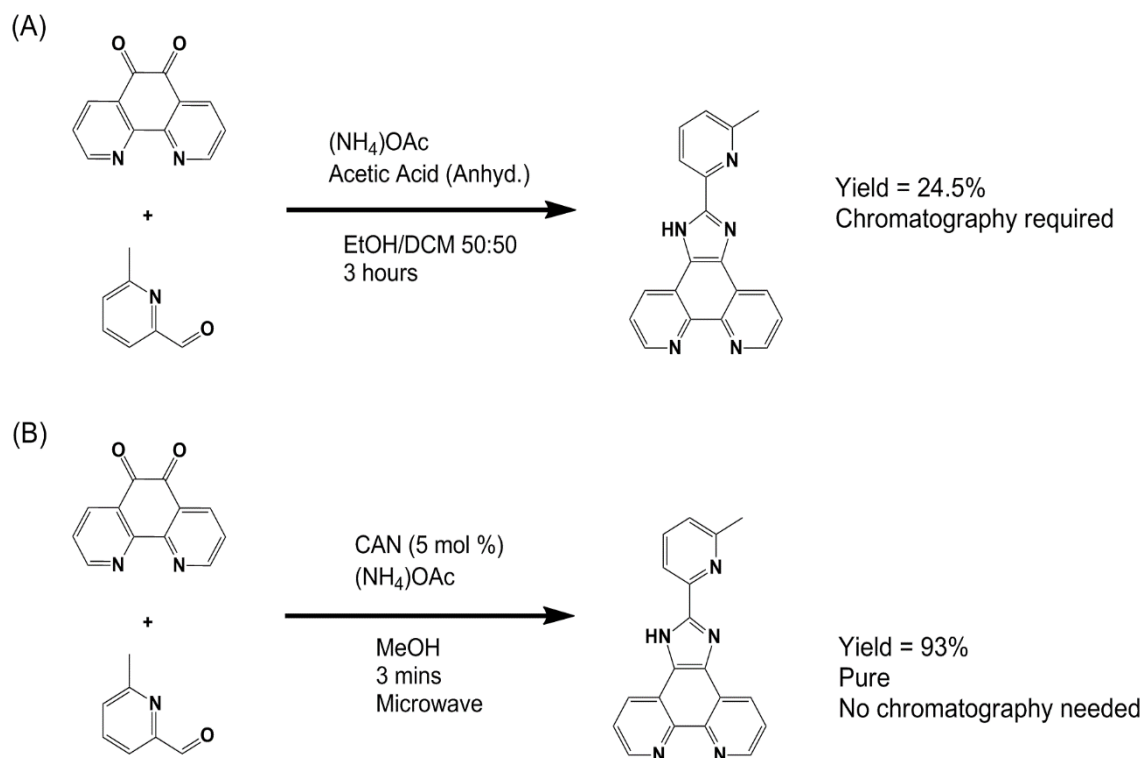


**Scheme 5.1:** Novel, high yielding, rapid and chromatography-free synthetic method for the production of imidazo-phenanthrolines (Im-phens).



**Scheme 5.2:** Postulated general reaction scheme for the CAN catalyzed/promoted formation of various imidazo[4,5-f][1,10]-phenanthroline (Im-phen) derivatives.

Using the aforementioned synthetic protocol (Scheme 5.1), a small library of 20 known and 10 novel Im-phens were prepared (Figure 5.7).



**Scheme 5.3:** (A) Our novel, microwave-mediated, CAN catalysed synthetic protocol for a C-2 pyridyl Im-Phen derivative and (B) the reported synthetic protocol to the same Im-Phen derivative.<sup>47</sup>

Taking the known C-2 pyridyl derivative shown in Scheme 5.3 as a specific example, the advantages of our novel synthetic method over that reported in the literature are apparent. The previously reported method required oil-bath heating for 3 h, the use of chlorinated solvents, time-consuming chromatographic purification and resulted in product recovery of < 30% yield.<sup>47</sup> In contrast, our new synthetic protocol, employing 5 mol% CAN catalyst, MeOH as the solvent and microwave-activation, for just 3 minutes, afforded the same Im-phen compound in 93% yield and with no requirement for purification by column chromatography.

A library of 21 known and 9 novel imidazo[4,5-*f*][1,10]-phenanthroline (Im-phen) derivatives were synthesised utilising this novel method (Figure 5.7). The known Im-phen derivatives were synthesised with improved yields, vastly diminished reaction time and with no requirement for purification by column chromatography.



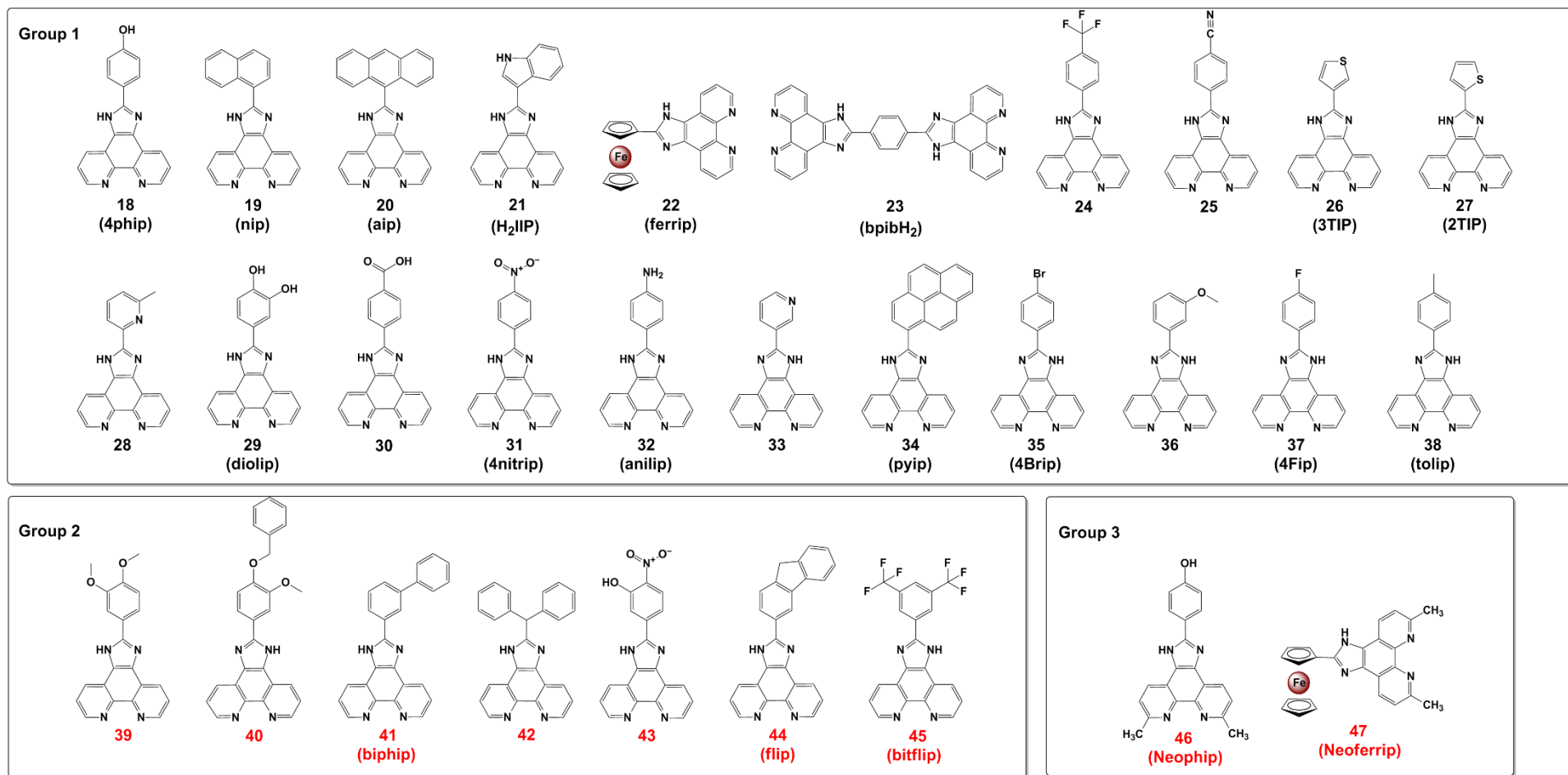


**Figure 5.7:** Molecular structures of Im-phen derivatives synthesized using the novel, microwave assisted, CAN catalyzed method. Group 1 contains known Im-phen derivatives, 18-38. Group 2 contains novel Im-phen derivatives. Group 3 consists of further novel Im-dmphen derivatives synthesized from 2,9-dimethyl-1,10-phenanthroline-5,6-dione.



A group of ligands were selected from this library (Figure 5.7) and used to make the corresponding Cu(II) and Mn(II) perchlorate complexes. The general formulae of these complexes were  $[\text{Cu}(\text{Im-phen})_2](\text{ClO}_4)_2$  and  $[\text{Mn}(\text{Im-phen})_3](\text{ClO}_4)_2$ . For Im-phen = bitflip, the structure of the free ligand, together with the proposed structures of the Cu(II) and Mn(II) bitflip complexes, are given in Figure 5.8.

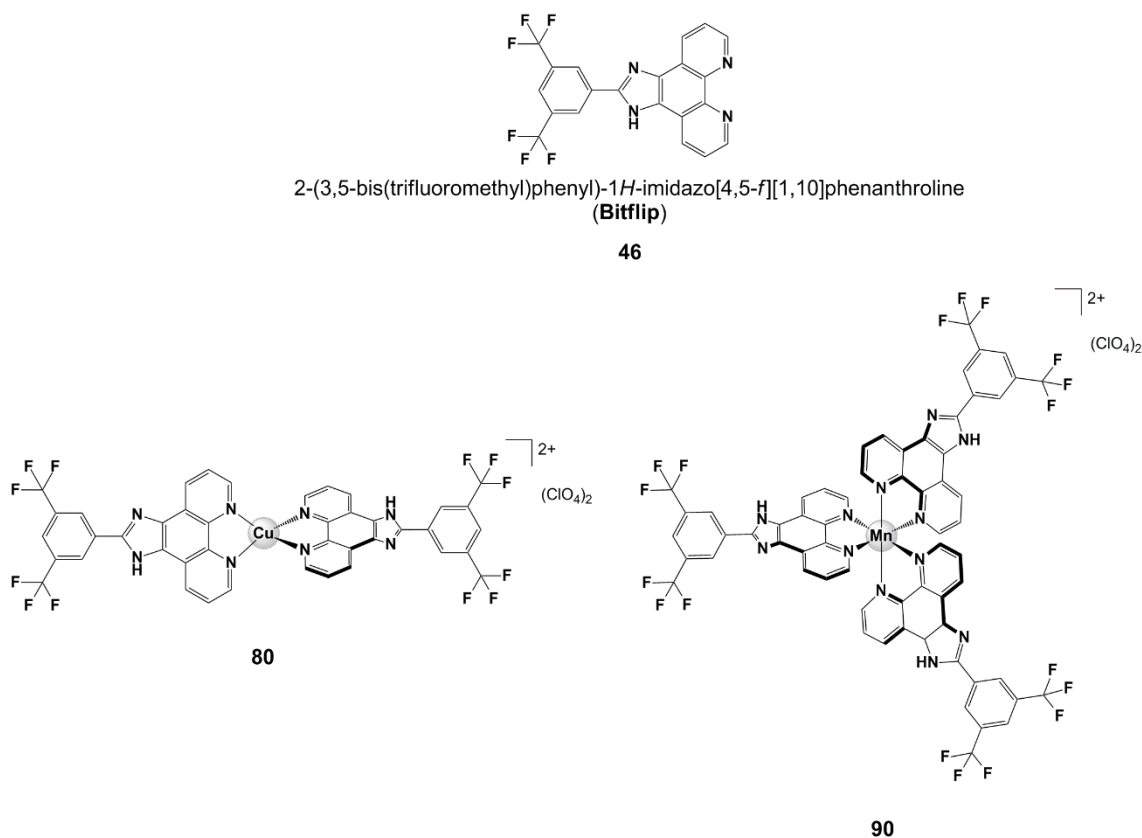


**Figure 5.8:** Structure of bitflip, **46**, and proposed structures of  $[\text{Cu}(\text{pyip})_2](\text{ClO}_4)_2$ , **80**,  $[\text{Mn}(\text{pyip})_3](\text{ClO}_4)_2$ , **90**.

All of the Im-phen ligands (both new and old) shown in Figure 5.7 were fully characterised by NMR ( $^1\text{H}$ ,  $^{13}\text{C}$ , DEPT 45, 90, 135, 135 Q and HSQC), by IR spectroscopy, elemental analysis (CHN) and mass spectrometry. Characterisation data matched those published in the literature for the previously known imidazo[4,5-*f*][1,10]-phenanthrolines. In addition to IR and elemental analysis, solid state magnetic susceptibility measurements were obtained for the Cu(II) and Mn(II) complexes and the magnetic moments were as expected. On the basis of this data the proposed general

formulae for the complexes is  $[\text{Cu}(\text{Im-phen})_2](\text{ClO}_4)_2$  and  $[\text{Mn}(\text{Im-phen})_3](\text{ClO}_4)_2$ . All spectroscopic and analytical data are given in the experimental section.

As a representative example, the  $^1\text{H}$ NMR spectrum of the novel Im-phen ligand 2-(9*H*-fluoren-3-yl)-1*H*-imidazo[4,5-*f*][1,10]phenanthroline (flip, **44**) is shown in Figure 5.9.

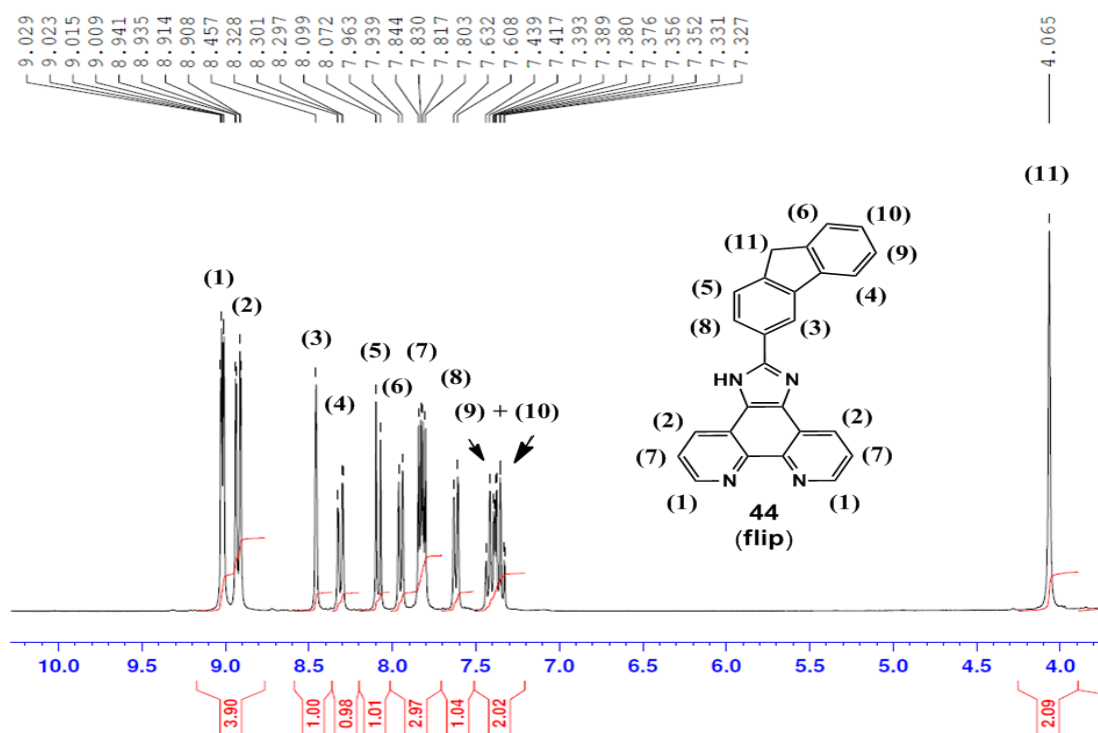


**Figure 5.9:**  $^1\text{H}$  NMR spectrum of the Im-phen ligand **44** (flip) in  $\text{DMSO-d}_6$ .

All  $^1\text{H}$  peaks positions and integrations were accounted for and correlated accurately with the expected structure of 2-(9*H*-fluoren-3-yl)-1*H*-imidazo[4,5-*f*][1,10]phenanthroline (flip, **44**) (Figure 5.9). Furthermore all other NMR spectra (DEPT 45, 90, 135, 135 Q,  $^{13}\text{C}$  and HSQC) matched the expected structure accurately and unambiguously.

In the DEPT 45 and DEPT 90 spectra 9 CH signals and one  $\text{CH}_2$  signal were observed for flip (**44**), although 13 CH signals were expected only 9 CH signals were observed due to the close proximity of certain  $^{13}\text{C}$  chemical shifts resulting in signal overlap for carbons 1, 2, 5, 6 and 8 (Figure 5.10, 5.11).

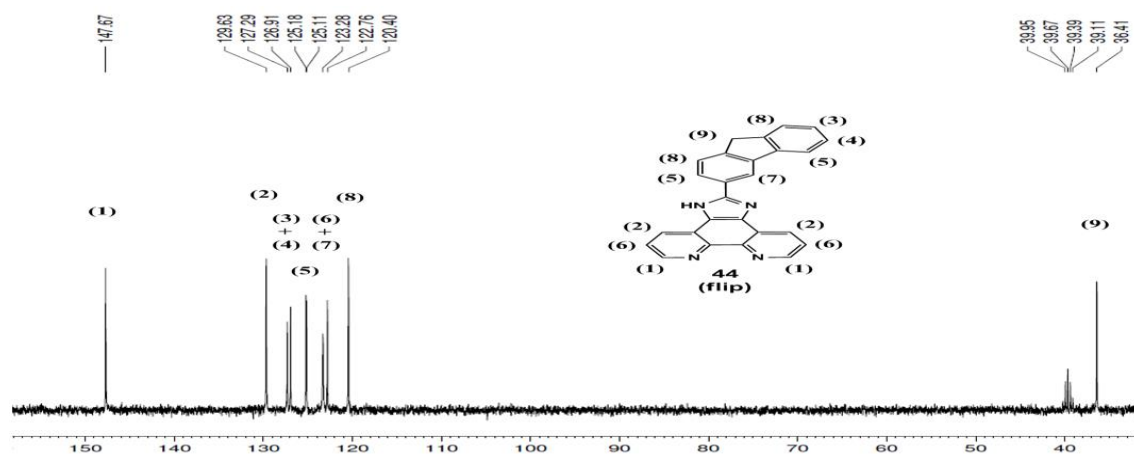


Figure 5.10: DEPT 45 NMR spectrum of the Im-phen ligand 44 (flip) in DMSO-d<sub>6</sub>.

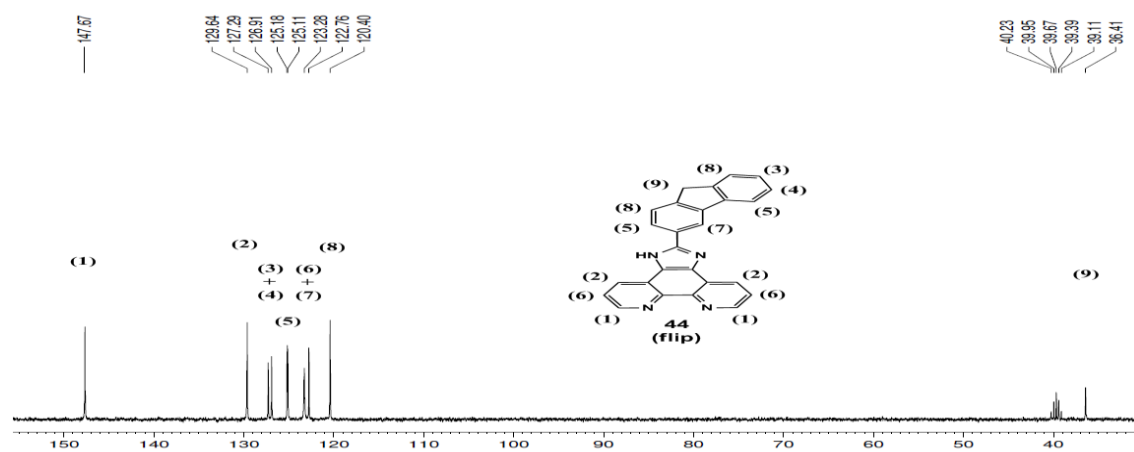


Figure 5.11: DEPT 90 NMR spectrum of the Im-phen ligand 44 (flip) in DMSO-d<sub>6</sub>.

The DEPT 135 NMR spectrum confirmed the presence of the CH<sub>2</sub> carbon at  $\delta = 36.41$  (Figure 5.12).

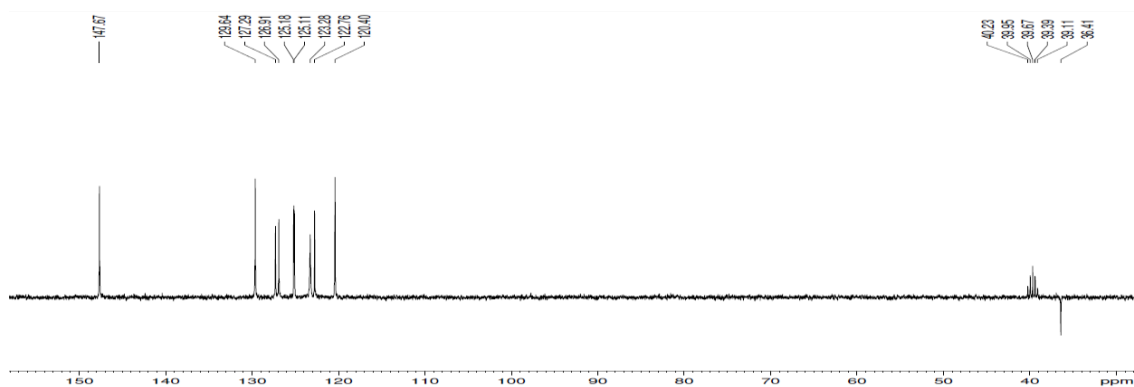


Figure 5.12: DEPT 135 NMR spectrum of the Im-phen ligand 44 (flip) in DMSO-d<sub>6</sub>.

The DEPT Q NMR spectrum displayed 6 quaternary  $^{13}\text{C}$  signals (missing one  $^{13}\text{C}$  quaternary signal, 7 expected), 8 CH signals and one  $\text{CH}_2$  signal (Figure 5.13).

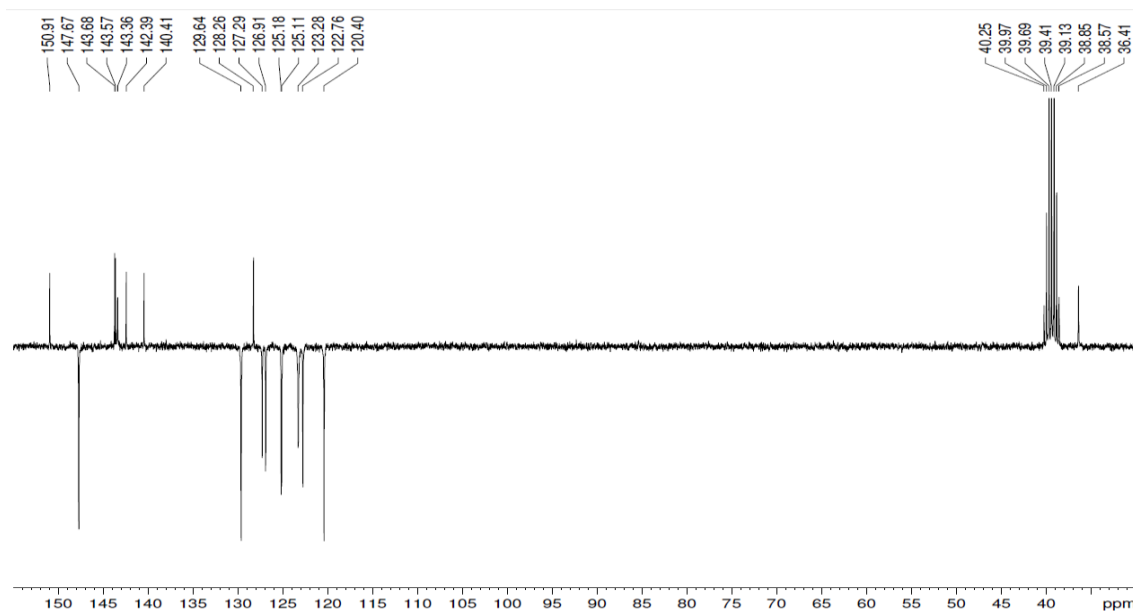


Figure 5.13: DEPT Q NMR spectrum of the Im-phen ligand **44** (flip) in DMSO- $d_6$ .

The  $^{13}\text{C}$  NMR spectrum displayed 9 CH signals (matching that of the DEPT 45 and 90), 7 quaternary  $^{13}\text{C}$  signals and one  $\text{CH}_2$  signal which was in agreement with the previous DEPT 45, 90 135 and Q spectra and matched the expected number of quaternary  $^{13}\text{C}$  signals expected (Figure 5.14).

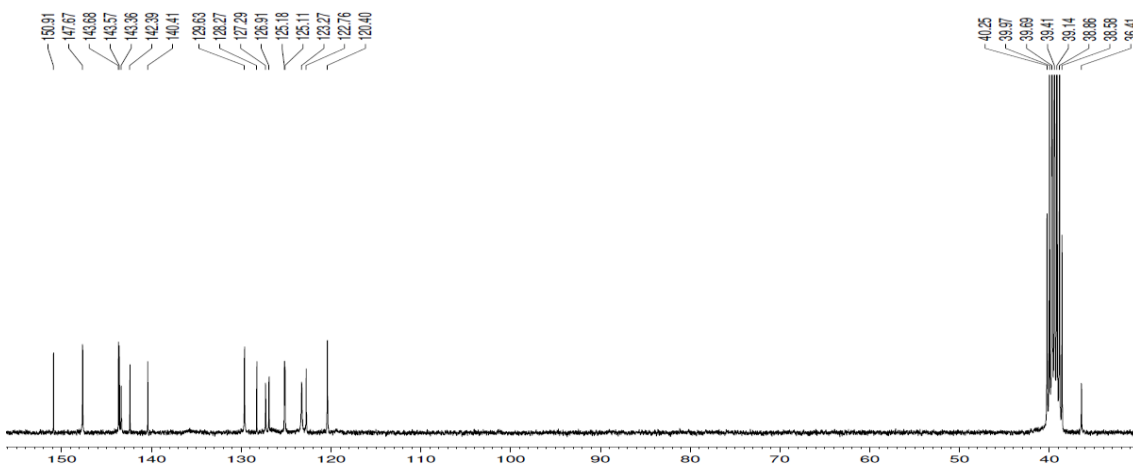
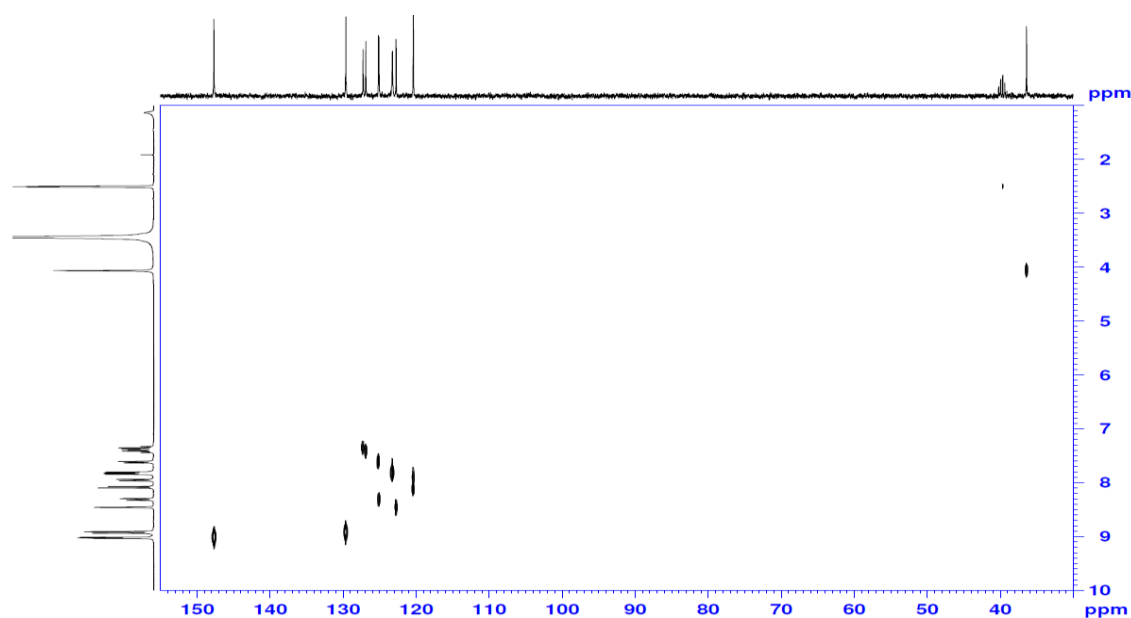


Figure 5.14:  $^{13}\text{C}$  NMR spectrum of the Im-phen ligand **44** (flip) in DMSO- $d_6$ .

Lastly the 2D HSQC  $^1\text{H} - ^{13}\text{C}$  NMR spectrum coupled the  $^1\text{H}$  spectrum with the DEPT 45 spectrum of the Im-phen ligand, flip (**44**) and the signals correlated as expected (Figure 5.15).



**Figure 5.15:** 2D HSQC  $^1\text{H} - ^{13}\text{C}$  NMR spectrum of the Im-phen ligand **44** (flip) in DMSO-d<sub>6</sub>.

### 5.6 DNA interaction studies/Nuclease mimetic activity

A group of seven Im-phen ligands were selected from the library of 30 Im-phens (Figure 5.7) and their Cu(II) bis-(Im-phen) perchlorate complexes (proposed structures shown in Figure 5.16) were tested for their relative cleavage efficiency of commercially available, supercoiled, superhelical pBR322 plasmid DNA. Our aim was to investigate how the systemic extension and adaption of the ligated Im-phen ligand with various planar aromatic, heteroaromatic, metallocene and various other substituents would influence the DNA oxidative degradation capabilities of these complexes. These data would ultimately supply structure-activity related information for the design of enhanced artificial metallonucleases with the potential to act as cytotoxic agents. The ability of the Cu(II) complexes, **54-60**, to cleave DNA was studied using agarose gel electrophoresis with supercoiled pBR322 plasmid DNA (Form I) (Figure 5.17).

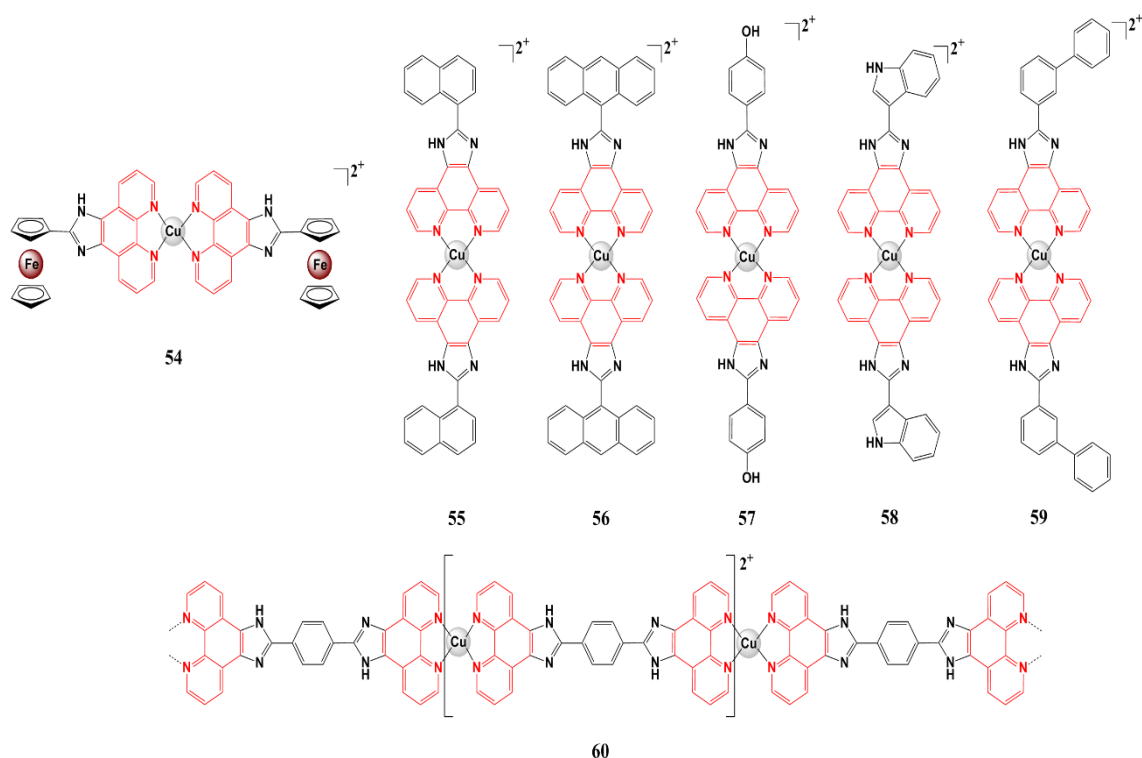


**Figure 5.16:** Proposed molecular structures of Cu(II) and Mn(II) complexes used for nuclease testing.

Relaxation of supercoiled (SC) pBR322 plasmid DNA (Form I) into open circular (OC, Form II) and linear (LC, Form III) conformations was used as a qualitative measure of the relative cleavage efficiency of the complexes (Figure 5.17 (A)). The DNA cleavage reactions were carried out at 37 °C using Cu(II) Im-phen complexes, and with  $[\text{Cu}_2(\text{OAc})_4(\text{H}_2\text{O})_2]$  as Control 1 and  $[\text{Cu}(\text{1,10-phen})_2](\text{ClO}_4)_2$  acting as positive Control 2. Results were then visualised using agarose gel electrophoresis. Form I is untouched, supercoiled DNA, form II is open circular DNA resulting from single strand scission, and form III is linear DNA arising from double strand scission of the DNA.

All of the Cu(II) complexes (Table 5.3, Figure 5.16) were screened at a concentration of 5  $\mu\text{M}$  (having previously been Shown to be inactive at a concentration of 1  $\mu\text{M}$  in the absence/presence of oxidant or reductant. The complexes were also pre-screened at 5  $\mu\text{M}$  in the absence of oxidant or reductant and were found to be essentially inactive. SC DNA was exposed to the Cu(II) complexes at a concentration of 5  $\mu\text{M}$  with 1 mM of added sodium-L-ascorbate reductant and incubated at 37 °C for 30 mins (Figure 5.17 (B)). All of the complexes displayed activity at this concentration, with the observed trend in nuclease activity being: Control 2  $[\text{Cu}(\text{phen})_2](\text{ClO}_4)_2 = \mathbf{54} = \mathbf{55} > \mathbf{56} > \mathbf{58} > \mathbf{57} \gg \mathbf{60} > \mathbf{59}$ . Complexes **54**, **55** and  $[\text{Cu}(\text{phen})_2]^{2+}$  at 5  $\mu\text{M}$  and 1 mM Na-L-ascorbate of added

reductant resulted in complete depletion of the parent SC band combined with an almost complete absence of any detectable form of DNA. Complexes **56** and **58** were also quite active. Complex **57** displayed a band of form III open circular DNA, indicating the presence of double strand scission. Complexes **59**, **60** and Control 1 were essentially inactive.

Under similar conditions, the complexes (5  $\mu$ M) were incubated with SC DNA with added H<sub>2</sub>O<sub>2</sub> oxidant (1 mM). This resulted in a markedly different activity trend (Figure **5.17** (C)). Once again, the most active complex was **54**, which caused complete depletion of the SC DNA parent band (form I). Although all of the complexes showed some nuclease activity under these conditions, upon comparison to the Cu(II) phen-free complex (Control 1, Lane 2) and the known chemical nuclease Control 2 (Lane 3) only **55** and **59** (Lanes 5, 9) exhibited superior nuclease activity. Complex **55** induced complete depletion of the SC parent DNA band (form I  $\rightarrow$  II) whilst **59** promoted an almost complete absence of any DNA.

It was then decided to investigate the effect of adding a large excess of the known metal chelator, EDTA. EDTA is known to have a high binding affinity for Cu(II) and should, theoretically, dampen the redox cycling of Cu(II) to Cu(I). It should be noted that a small amount of EDTA is present in commercially sourced pBR322 DNA in order to prevent Fenton type chemistry occurring during storage. The EDTA concentration used (80  $\mu$ M) (Figure **5.17** (D) and (E)) is a 60-times the concentration that is normally present in commercial pBR322 DNA.

The effect of the added EDTA was quite profound under the added reductant conditions (Figure **5.17** (D)). The activity of all of the test complexes was dramatically reduced, with **59** and **60** displaying no discernible nuclease activity. Complexes **55** and **56** have essentially equal activity with trend now being  $55 \approx 56 > 54 > 58 > 57$  (Figure **5.18**).

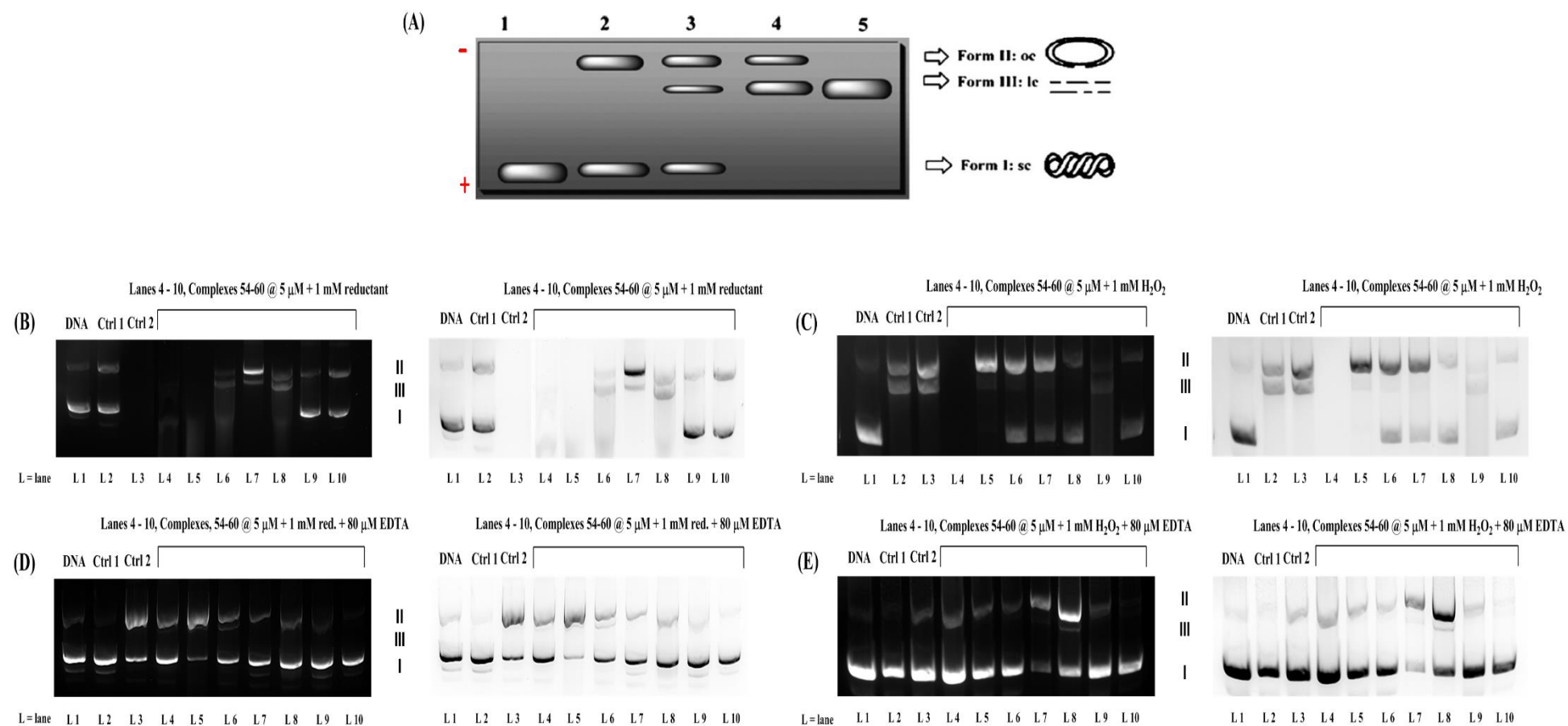


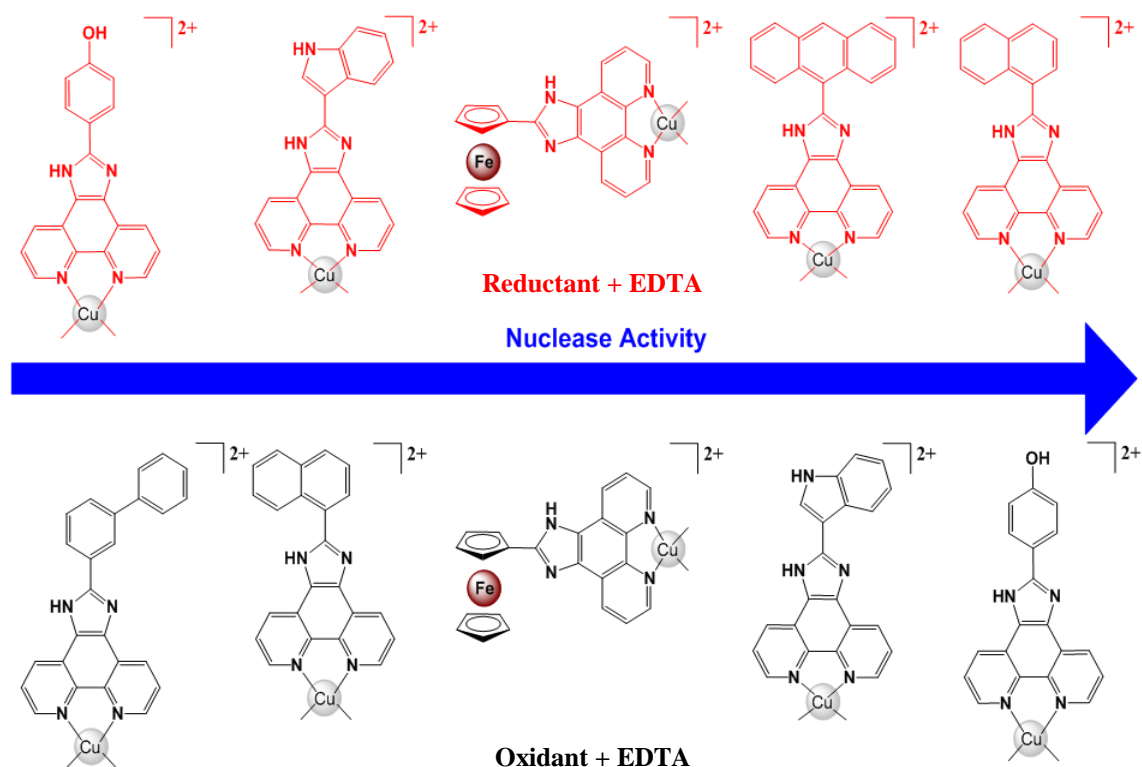
**Fig. 5.17:** (A) Schematic presentation of the different forms of the DNA: form I SC DNA; form II OC DNA; form III LC DNA. Direction of migration of DNA fragments from negative to positive via applied potential difference. (B) L1-3 DNA, Control 1, 2 and L4-10 contains **54-60** at 5  $\mu$ M with 1mM added Na-L-ascorbate reductant. (C) L1-3 DNA, Control 1, 2 and L4-10 contains **54-60** at 5  $\mu$ M with 1mM added H<sub>2</sub>O<sub>2</sub> oxidant. (D) L1-3 DNA, Control 1, 2 and L4-10 contains **54-60** at 5  $\mu$ M with 1mM added Na-L-ascorbate + 80  $\mu$ M EDTA. (E) L1-3 DNA, Control 1, 2 and L4-10 contains **54-60** at 5  $\mu$ M with 1mM added H<sub>2</sub>O<sub>2</sub> + 80  $\mu$ M EDTA.



**Table 5.3:** Formula and molecular weights of all the nuclease test complexes **54-60** and the two control agents.

Compound		Molecular Mass (g/mol)
Ctrl 1	$[\text{Cu}_2(\text{OAc})_4(\text{H}_2\text{O})_2]$	622.87
Ctrl 2	$[\text{Cu}(1,10\text{-phen})_2(\text{ClO}_4)_2]$	399.30
<b>54</b>	$[\text{Cu}(\text{ferrip})_2](\text{ClO}_4)_2 \cdot 2\text{H}_2\text{O}$	1070.954
<b>55</b>	$[\text{Cu}(\text{nip})_2](\text{ClO}_4)_2 \cdot 7.5\text{H}_2\text{O}$	1090.33
<b>56</b>	$[\text{Cu}(\text{aip})_2](\text{ClO}_4)_2 \cdot 7.5\text{H}_2\text{O}$	1190.45
<b>57</b>	$[\text{Cu}(4\text{phip})_2](\text{ClO}_4)_2 \cdot \text{MeOH} \cdot 5\text{H}_2\text{O}$	1009.22
<b>58</b>	$[\text{Cu}(\text{H}_2\text{IIP})_2](\text{ClO}_4)_2 \cdot \text{MeOH} \cdot 2\text{H}_2\text{O}$	1001.24
<b>59</b>	$[\text{Cu}(\text{biphip})_2](\text{ClO}_4)_2 \cdot \text{MeOH}$	1007.29
<b>60</b>	$\{[\text{Cu}(\text{bpibH}_2)](\text{ClO}_4)_2\}_n$	1039.44

With the addition of 1 mM  $\text{H}_2\text{O}_2$  and 80  $\mu\text{M}$  EDTA, the excess EDTA has a strongly deactivating effect on all complexes (Figure 5.17 (E)). Complex **56**, which was previously the most active complex in a reducing environment, is now essentially inactive under these conditions. Indeed, the activity trend is almost the reverse of that observed under the conditions with added Na-L-ascorbate reductant and excess EDTA (Figure 5.18).

**Fig. 5.18:** Nuclease activity trends for complexes **54-60** with an excess of added EDTA together with either 1 mM of Na-L-ascorbate (reductant) or 1 mM of  $\text{H}_2\text{O}_2$  (oxidant).

It would appear that it is the generation of ROS species by the Cu(II) complexes that is responsible for the observed nuclease activity in light of the highly deactivating effects caused by the addition of a large excess of EDTA. It is likely that the EDTA is sequestering the Cu(II) from the complexes and trapping it in a coordination environment that prevents it being reduced to Cu(I). It is noteworthy that complex **54** was nuclease active in both an oxidising and reducing environment, and that it retained some of this nuclease activity in the presence of a large excess of EDTA. This suggests that the ferrocene moiety may have a large role to play in this hetero-bimetallic complex. It is known that there is an innate overproduction of hydrogen peroxide in cancer cells.<sup>48</sup> Ferrocene has the redox capability ( $\text{Fe}^{2+}/\text{Fe}^{3+}$ ) to split hydrogen peroxide into hydroxide anions and highly reactive and damaging hydroxyl radicals.<sup>49</sup> As previously discussed, hydroxyl radicals are the most reactive and damaging species under the umbrella term of ROS. The hydroxyl radical ( $\text{OH}\cdot$ ), is much more reactive than both superoxide ( $\text{O}_2\cdot^-$ ) or nitric oxide ( $\cdot\text{NO}$ ). The latter two radicals can react directly with only a few molecules in the human body, whereas  $\text{OH}\cdot$  can react with almost anything, including DNA purine base pairs (forming further DNA base radicals/mutations and DNA scission), to abstract  $\text{H}\cdot$  and leave behind another radical.<sup>50</sup> The resulting free radical chain reaction can cause a cascade of damaging biological consequences, including DNA strand scission.<sup>51</sup> This effect could explain the sustained nuclease ability of **54**, as it is likely that the ferrocene moiety and the Cu(II) centre are both generating ROS. In addition, the possible ability of these nuclease mimetic complexes to interact with, and cleave, mitochondrial DNA (mtDNA) should also be taken into consideration. Mitochondrial DNA is highly susceptible to ROS-induced damage/scission due to the inherent increased production of reactive oxygen species (ROS) as a consequence of metabolism and in addition, a less robust DNA repair mechanism than that of nuclear DNA. The interaction of mtDNA with form the basis of a future study beyond the present work.

### 5.7 Targeted cytotoxic chemotherapy

The paragon of chemotherapy is the “targeting” or site-specific recognition of cancerous tissue by a therapeutic agent. The ability of a drug to discern and bind to a unique aspect of cancerous tissue and then preferentially deliver a precise cytotoxic effect, is highly desirable. Unlike older forms of treatment, targeted chemotherapy for cancer and other diseases is expected to be more effective. With this new approach, the vast majority of

the administered drug would reach its intended target (the tumour) and hence be less harmful to normal cells, and eliminating, or at least lessening, any adverse side effects. To achieve this, an anticancer agent must be able to recognise (or be recognised by) and bind to a unique aspect of a cancer cell that is not present on normal healthy cells. There are a few examples in the literature of the effective use of this strategy. For example, in the case of certain types of breast cancer the first instances of such a targeted treatment was trastuzumab emtansine (T-DM1).<sup>52</sup> T-DMI is a novel antibody-drug conjugate consisting of a potent cytotoxic drug (mertansine (DM1)) connected, via a stable linker, to the anti-HER2 antibody, trastuzumab. HER2 is a protein receptor that is overexpressed in certain types of cancer, such as breast cancer.<sup>53</sup> Trastuzumab can target and bind to this receptor, stopping the growth of the cancer cells whilst also delivering the mertansine drug to the cell, where it enters the cancer cells and destroys them by binding to tubulin.<sup>52</sup>

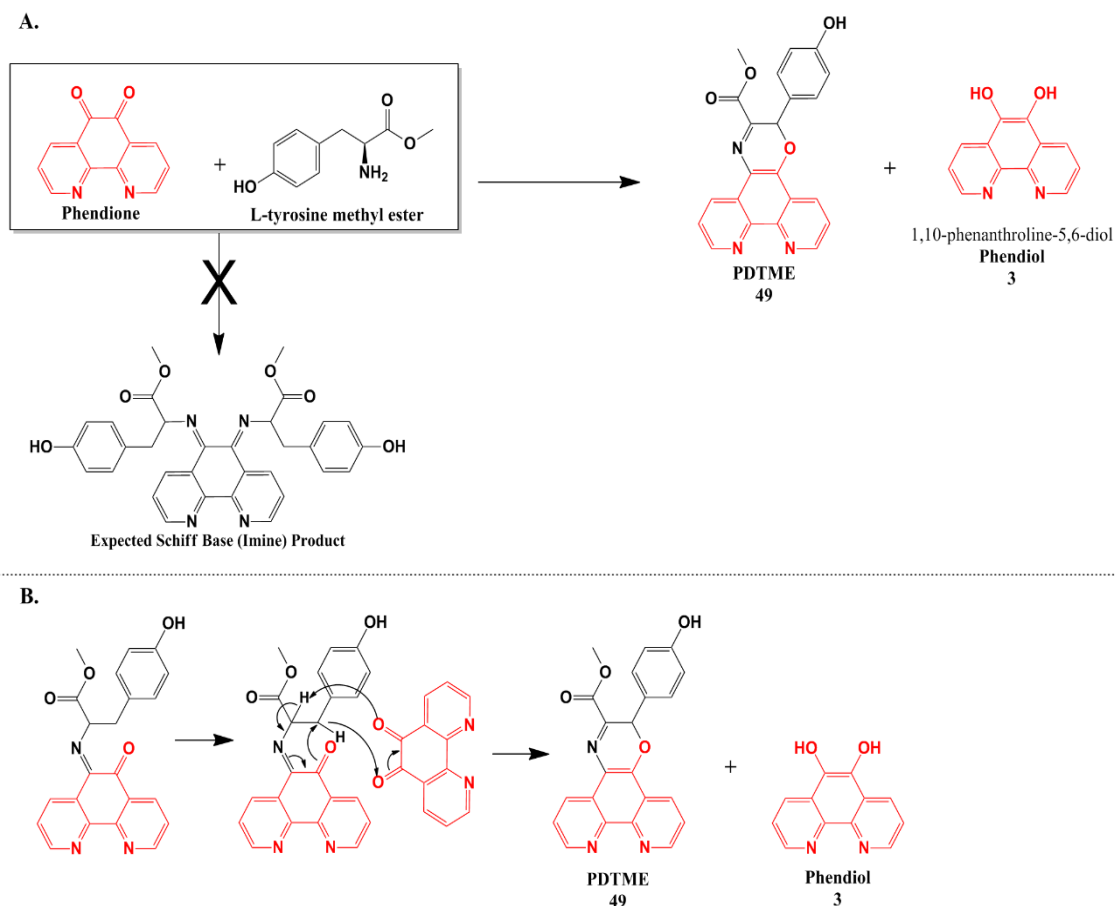
54

### 5.7.1 Nutrient targeted chemotherapeutics

Cancer progression is inherently linked to the ability of a cancerous cell to regulate its metabolism.<sup>55</sup> It is also known that the high cellular proliferation expressed by cancer cells is tightly regulated by the availability of nutrients. Therefore, oncogenes, that often promote proliferation, may also be responsible for metabolic changes. Cancer cells are known to require/metabolise vast quantities of glucose, far in excess of that of normal healthy cells. Furthermore, it was recently discovered that neoplastic cells also require and metabolise the amino acids, serine and glycine.<sup>56</sup> This promoted us to explore the possibility of covalently bonding an amino acid nutrient, such as glycine, to 1,10-phenanthroline with the goal of preferentially targeting cancer cells. To this end, a strategy was devised to form a double Schiff base/imine condensation product by reacting 1,10-phenanthroline-5,6-dione (phendione **2**) with two equivalents of L-tyrosine methyl ester (Scheme 5.4).<sup>57</sup>

The expected diimine product from this reaction was not obtained. Instead, the reaction produced a large quantity of the reduced phendione product, phendiol, **3**, and a small amount of an unexpected tetracycline oxazine or phenoxazine product, PDTME, **49** (Scheme 5.4).<sup>57</sup> PDTME has a new stereogenic centre on the C13 atom, whereas in the

starting material L-tyrosine methyl ester, it was on the C20 atom. An x-ray crystal structure was obtained for PDTME, **49** and this is shown in Figure 5.19.



**Scheme 5.4:** (A) Unexpected formation of the tetracycline oxazine or phenoxazine PDTME, **50**, as a minor product and the major product 1,10-phenanthroline-5,6-diol (phendiol, **3**). (B) Proposed reaction mechanism for the formation of the phenoxazine PDTME, **49**, from the reaction of phendione and L-tyrosine methyl ester.<sup>57</sup>

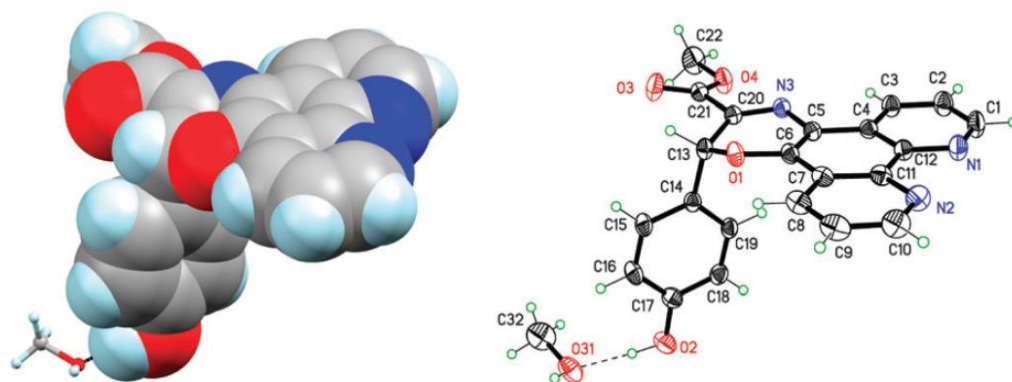


**Fig. 5.19:** Space-fill view of PDTME on the left and on the right, a view of PDTME with 50% ADPs.<sup>57</sup>

Initial attempts of this reaction only produced the phenoxazine product in very low yields. Scheme 5.4 (B) shows the proposed reaction mechanism, whereby the first most likely step is the formation of an imine condensation product. This is followed by a concerted ring formation in which a second phendione molecule acts as a deprotonating agent.<sup>57</sup> It was decided to further explore this reaction to see if (a) the reaction conditions could be further optimised to give a higher yield of the phenoxazine product and (b) if the reaction could be utilised to form a family of new phenoxazine products using structurally related amino acids. The yield of PDTME was found to double when the reactant ratio of phendione to L-tyrosine methyl ester was changed from 1:2 to 1:1. This was a somewhat unexpected result and counter intuitive, as based on the proposed reaction mechanism phendione has a dual role of both reactant and deprotonating agent.

In methanol as solvent, and using conventional oil bath heating, the optimum reaction time was found to be 24 hours (20.45 % yield). The use of microwave heating was then investigated in an effort to improve the yield and shorten the reaction time. The microwave reaction was conducted at 70 °C for 4 h, and using a 1:1 ratio. Disappointingly, PDTME was recovered in a reduced yield (4.09 %) perhaps suggesting that the unknown rate limiting step in this reaction cannot be hastened via more efficient microwave heating.

In order to see what effect the length of the alkyl chain of the amino acid ester had on the reaction, L-tyrosine ethyl ester hydrochloride was synthesized and used in the phenoxazine forming reaction with phendione.

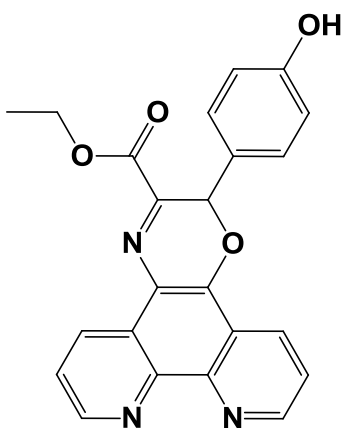


Fig. 5.20: Proposed structure of novel phenoxazine, PDTEE, 50.

The reaction was once again conducted using a 1;1 reactant ratio of L-tyrosine ethyl ester hydrochloride to phendione, in refluxing ethanol for 24 hours. The reaction proved successful, yielding the highly insoluble phendiol and the novel impure phenoxazine product, PDTEE, **50**, in a much lower yield of 12.14% (impure) (Figure 5.20). This new phenoxazine proved difficult to fully purify but characterization was attempted using standard spectroscopic methods and by elemental microanalysis.

It should also be noted that phenoxazine formation only occurs with the use of the ester of the amino acid. Reaction of phendione with the free carboxylate from L-tyrosine and numerous other amino acids was attempted (glycine, alanine, phenylalanine, asparagine) and results in the formation of phendiol and undetermined by-products.

In order to probe the scope of the phenoxazine formation reaction further, L-dopa methyl ester hydrochloride, which is structurally similar to L-tyrosine methyl ester (with the inclusion of a 2<sup>nd</sup> hydroxyl group on the phenyl ring) was reacted with phendione. This reaction was successful, and it proceeded in a similar fashion to that of its predecessor. The reaction was once again conducted using a 1;1 reactant ratio of L-dopa methyl ester HCL to phendione, in refluxing methanol for 24 hours. Phendiol formed as a by-product and a novel phenoxazine, PDDME, **51**, was obtained in 24.88 % yield (Figure 5.21).

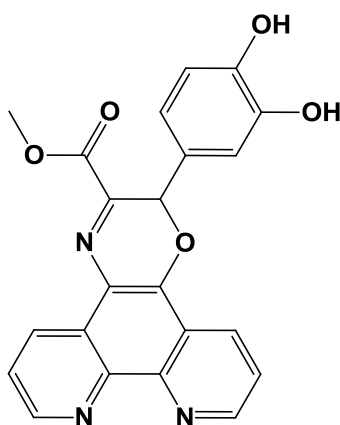


Fig. 5.21: Structure of novel phenoxazine, PDDME, **51**.

The product was characterized using routine methods and its <sup>1</sup>H NMR spectrum complete with chemical shift peak assignments, initial peak integrations and molecule structure are given in Figure 5.22.

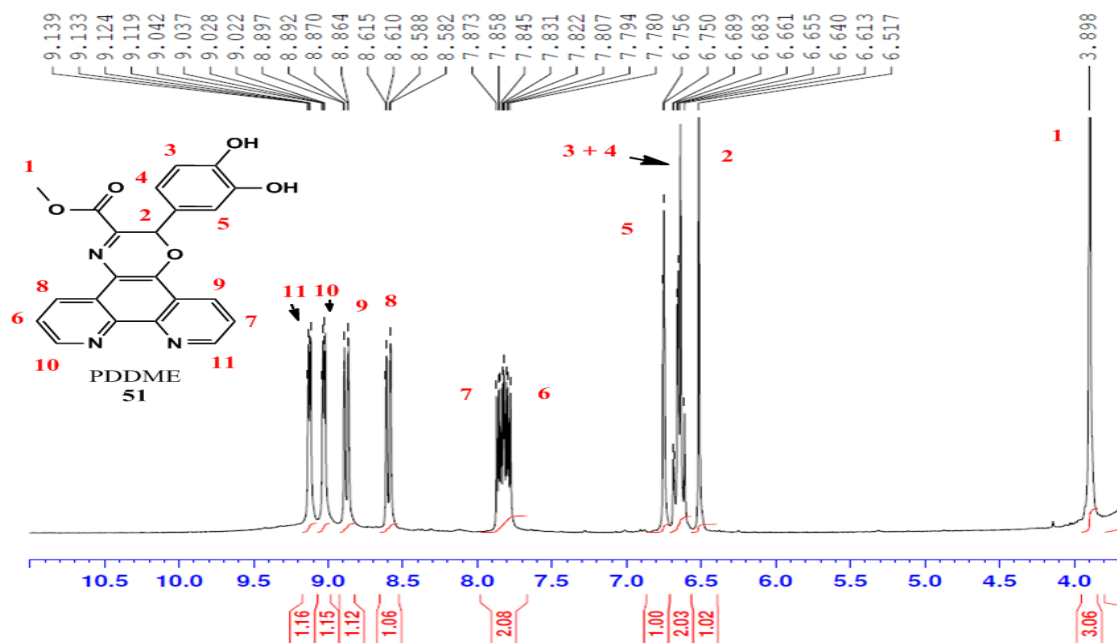


Fig. 5.22: <sup>1</sup>H NMR (300 MHz DMSO-d<sub>6</sub>) of PDDME, **51**, with peak assignments.

The <sup>13</sup>C NMR spectrum of PDDME, **51**, contained 22 individual <sup>13</sup>C signals, matching the expected number of signals for the proposed structure (Figure 5.23).

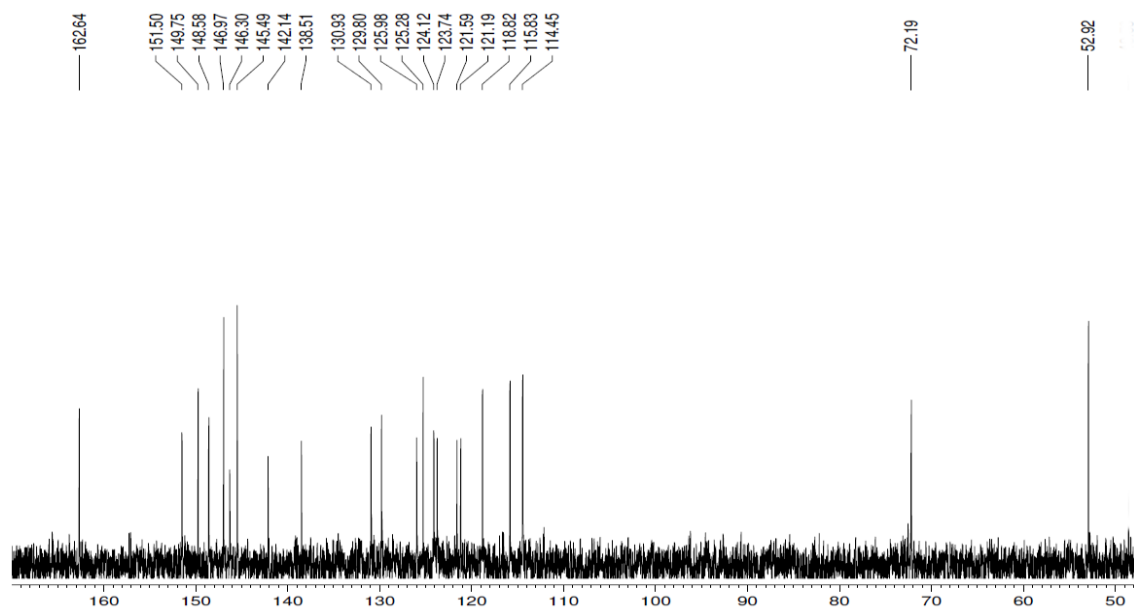


Fig. 5.23: <sup>13</sup>C NMR (DMSO-d<sub>6</sub>) of PDDME, **51**.

Once again, in order to see what effect the length of the alkyl chain of the ester had on the reaction, L-Dopa ethyl ester hydrochloride was synthesized and the phenoxazine forming reaction with phendione was repeated. Insoluble phendiol was again recovered and the novel phenoxazine product, PDDEE, **52**, was subsequently isolated in an almost identical yield of 24.03% (Figure 5.24).

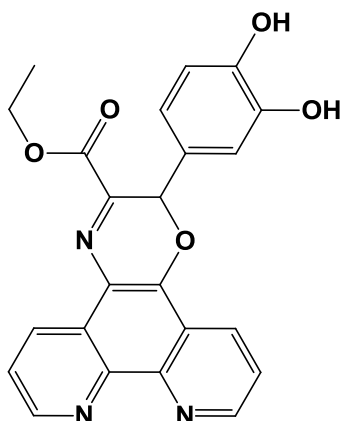


Fig. 5.24: Structure of novel phenoxazine, PDDEE, **52**.

Finally, to see if the electron-donating hydroxyl groups on the phenyl ring of the amino acids were having an effect on the phenoxazine formation, the structurally similar L-phenylalanine methyl ester hydrochloride was synthesised (Figure 5.25 (A)).

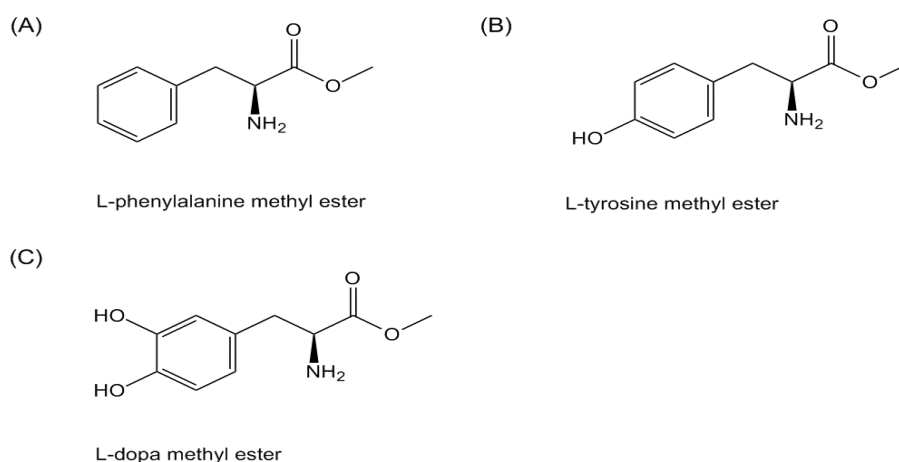


Fig. 5.25: Structure of amino acid methyl esters used in successful phenoxazine forming reactions.



This was then reacted with phendione (1:1 mole ratio) using the same reaction protocol utilized for PDDME (**51**) in an effort to synthesise a new phenoxazine, PDPME, **53** (Figure 5.26). Based on the NMR spectral data, a small amount of impure phenoxazine product, PDPME, **53**, was recovered. Although the compound proved very difficult to purify.

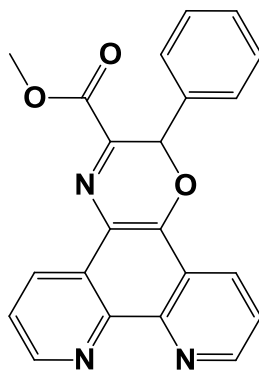


Fig. 5.26: Structure of phenoxazine, PDPME (**53**).

The Ag(I) and Cu(II) bis-PDTME complexes,  $[\text{Cu}(\text{PDTME})_2](\text{ClO}_4)_2$  and  $[\text{Ag}(\text{PDTME})_2](\text{ClO}_4)_2 \cdot 2\text{MeOH}$ , had been synthesised previously and tested for their ability to bind to and cleave high-purity calf thymus (CT) DNA and supercoiled pBR322 DNA.<sup>57</sup> The two complexes were found to have almost identical binding affinities for calf thymus (CT) DNA. The complex-DNA binding interactions were considered stronger than the known groove-binding drugs, pentamidine and netropsin, suggesting an alternate binding mode compared with their bis-phen intercalating analogues.<sup>57</sup> In addition,  $[\text{Cu}(\text{PDTME})_2](\text{ClO}_4)_2$  displayed negligible nuclease activity when incubated with supercoiled pBR322 in the presence of added reductant or oxidant. This result was very surprising given the known DNA nuclease abilities of the analogous  $[\text{Cu}(\text{phen})_2]^{2+}$ . Time restraints prevented the investigations of the interactions of the newly formed Cu(II) and Mn(II) complexes of PDME (**51**) and PDDEE (**52**). This will be the subject of a future study.

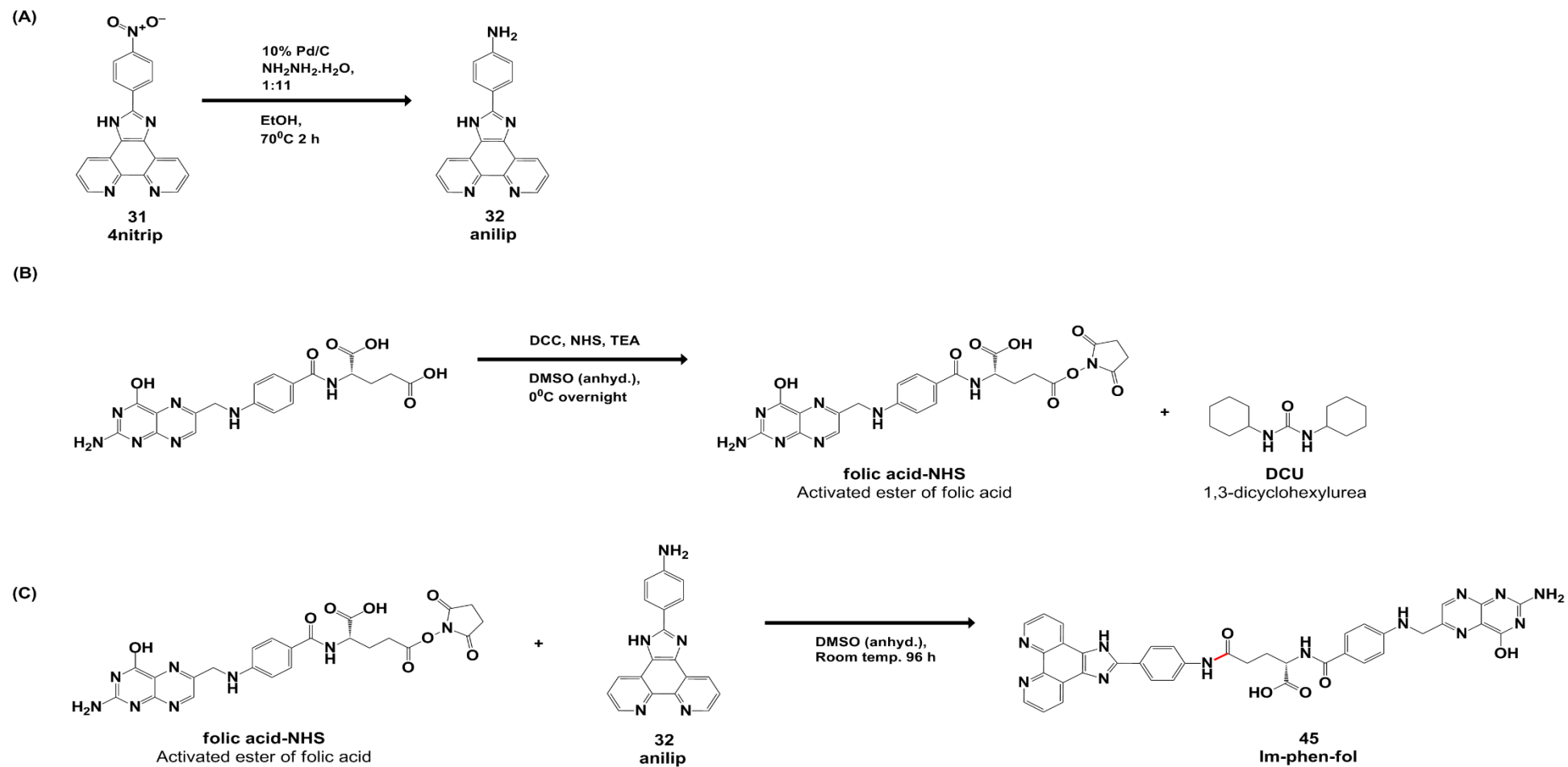
### 5.7.2 Folic acid mediated targeting

Our strategy here was to leverage the high binding affinity that the folate receptor (FR) has for the nutrient, folic acid (FA).<sup>58</sup> The folate receptor (FR) is a cell surface, membrane

bound glycoprotein that captures folic acid and internalises it. Whereas FR expression is largely absent from healthy mammalian tissues, numerous cancerous cell types (lung, epithelial, ovarian, cervical, breast, kidney, colorectal and brain tumours) display highly elevated FR expression.<sup>59</sup> Furthermore, activated macrophages, also exhibit highly elevated FR expression; this may also provide a means of preferentially targeting activated macrophages such as *Mycobacterium*-infected macrophages.<sup>60</sup> The recently published crystal structure of the FR with a bound folic acid molecule confirmed the assumed availability of the dicarboxylic acid moiety for modification without loss of binding capacity.<sup>61</sup>

In an effort to build upon our encouraging TB results (Chapter 4) we have developed manganese(II) imidazo-phen-folate-appended complexes which we envisage will specifically target TB-infected macrophages via the over expression of folate receptors and subsequently eradicate the replicating bacteria within them. In addition, building upon our encouraging anticancer results (Table 5.2) we have also developed Cu(II) imidazo-phen-folate-appended complexes with the view to selectively targeting FR expressing cancer cell types.

The novel ligand Im-phen-fol, **45**, was synthesised as per reaction scheme 5.5. The Im-phen ligand 4nitrip, **31**, was reduced using 10% Pd/C and hydrazine monohydrate to yield the aromatic amine bearing Im-phen ligand anilip, **32**.<sup>62</sup> The folic acid was then activated via ester formation using the base triethylamine (TEA), *N*-hydroxysuccinimide (NHS) and the coupling reagent dicyclohexylcarbodiimide (DCC) in anhydrous DMSO at 0 °C. The product Im-phen-fol, **45**, was formed via amide formation using the folic acid-NHS activated ester and the aromatic amine of **32**.<sup>63</sup> This new Im-phen-fol ligand, **45**, was characterized using standard spectroscopic methods and by elemental microanalysis. In addition to IR and elemental analysis, solid state magnetic susceptibility measurements were obtained for the Cu(II) and Mn(II) Im-phen-fol complexes and the magnetic moments were as expected. On the basis of this data the proposed general formulae for the complexes is [Cu(Im-phen-fol)<sub>2</sub>](ClO<sub>4</sub>)<sub>2</sub> (**73**) and [Mn(Im-phen-fol)<sub>3</sub>](ClO<sub>4</sub>)<sub>2</sub> (**91**) (Figure 5.27).



**Scheme 5.5:** (A) Synthesis of anilip (**32**) ligand via Pd-catalyzed reduction of aromatic nitro group to aromatic amine. (B) Folic acid-N-hydroxysuccinimide (folic acid-NHS) activated ester synthesis. (C) Amide coupling of activated ester, folic acid-NHS and the aromatic amine of anilip **32** in anhydrous DMSO over 96 h resulted in the formation of novel ligand Im-phen-fol, **45**.

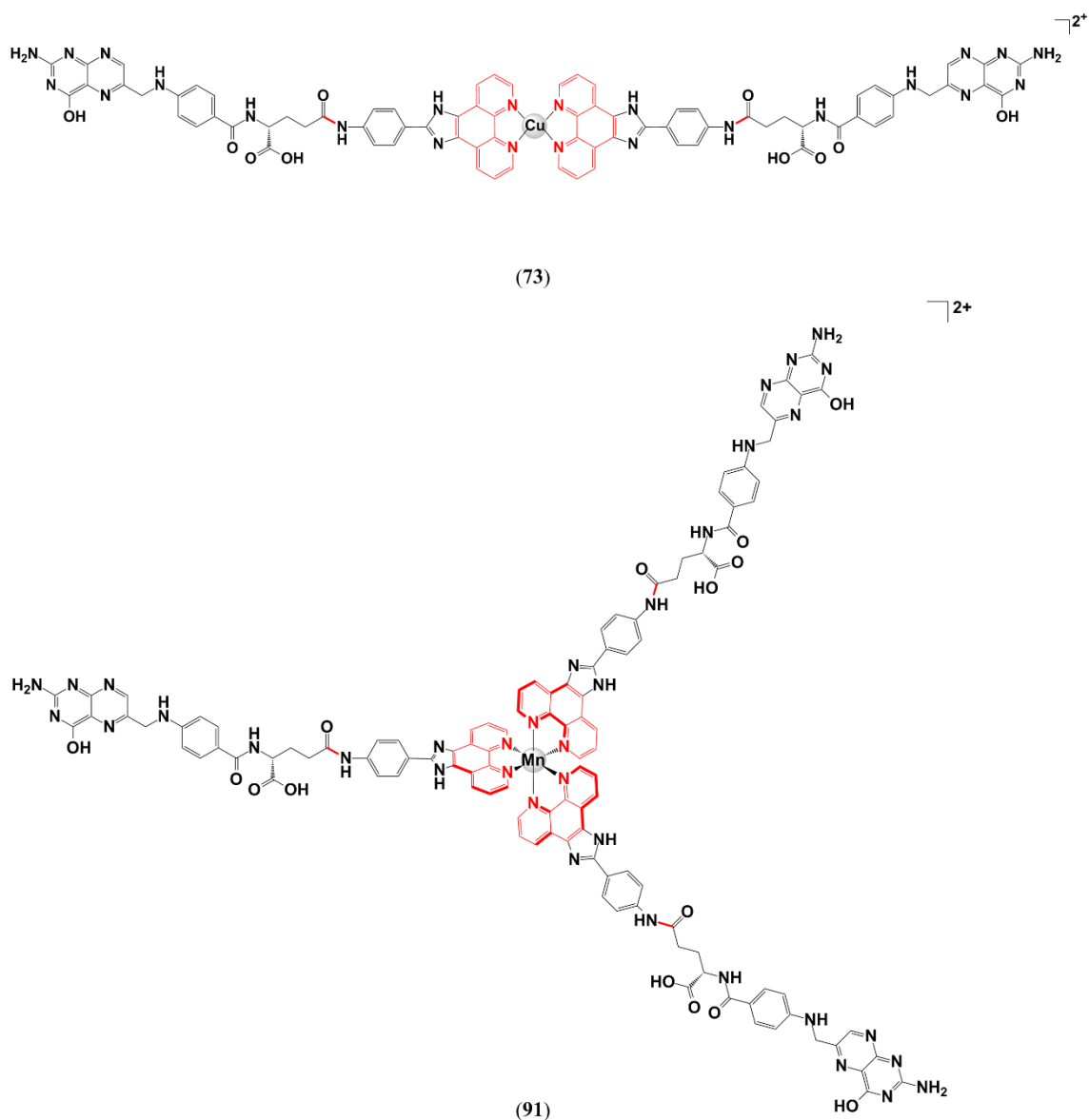


**Fig. 5.27:** Proposed structures of the complexes  $[Cu(Im-phen-fol)_2](ClO_4)_2$  (**73**) and  $[Mn(Im-phen-fol)_3](ClO_4)_2$  (**91**)

Finally, shown in Figure 5.28 the postulated folate receptor (FR) mediated cellular recognition and potocytosis of FA-appended Im-phen metal complexes.

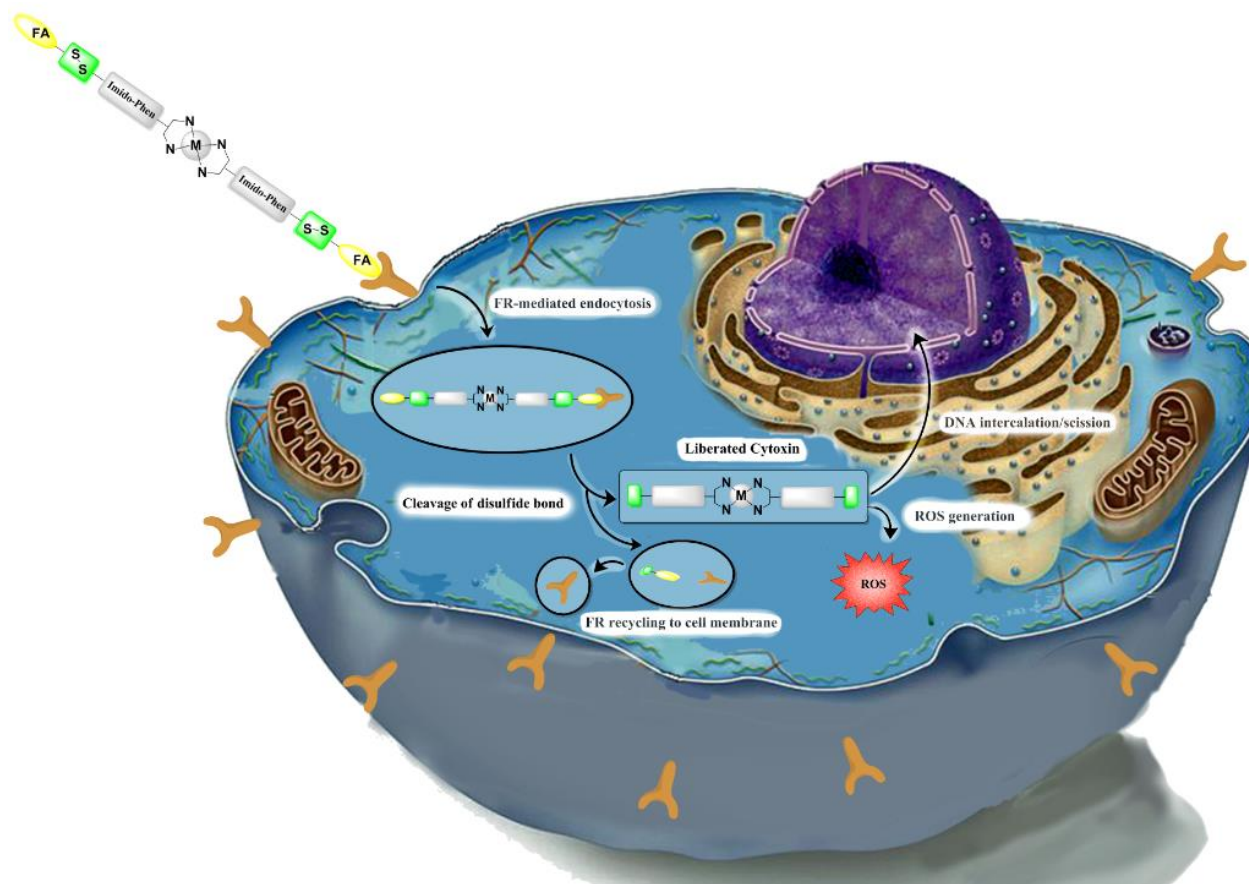


**Fig. 5.28:** Proposed folate receptor (FR) mediated cellular recognition and potocytosis of FA-appended Im-phen metal complex. Lowered pH release of metal complex cytotoxin. ROS production resulting in mitochondrial damage and incorporation of metal complex into the nucleus resulting in intercalation with nuclear DNA and double DNA strand scission mediated by ROS.

### 5.8 *In vivo* systemic toxicity/cytotoxicity studies using *Galleria mellonella*

As discussed previously the innate defences of insects are akin to that of vertebrate mammals. *G.mellonella* larvae possess an immune system which is analogous to the human innate immune system and hence are a convenient, inexpensive and less ethically sensitive *in vivo* screening model for ascertaining the systemic toxicity profile of novel anticancer agents, the results of which are comparable to murine models. All of the Im-phen ligands and phenoxazine ligands, **18-53** and their corresponding Cu(II) and Mn(II) complexes, **54-95** were found to be non-toxic to *G.mellonella* larvae (100% survival rate) up to a concentration of 500  $\mu\text{g}/\text{cm}^3$  (33.33 mg/kg or 10 10  $\mu\text{g}$  per larvae). Cisplatin was considerably more toxic to the larvae at this dosage (500  $\mu\text{g}/\text{cm}^3$ , 33.33 mg/kg or 10 10  $\mu\text{g}$  per larvae mg/kg) resulting in a low survival value (40%).

### 5.9 Conclusions

In summary, the favourable anticancer results of the 1,10-phen/dicarboxylate complexes and the impressive nuclease mimetic results of the Im-phen complexes represent auspicious compounds in the area of DNA-targeted chemotherapeutics. The novel phenoxazine complexes based on the initial DNA interaction results of  $[\text{Cu}(\text{PDTME})_2](\text{ClO}_4)_2$  and  $[\text{Ag}(\text{PDTME})_2](\text{ClO}_4)_2 \cdot 2\text{MeOH}$  which displayed very high DNA binding values may also find utility as minor groove binders and the Cu(II) and Mn(II) complexes of PDME (**51**) and PDDEE (**52**) will be the subject of a future study to access their cytotoxicity to cancer cells. Encouragingly, *in vivo* toxicity studies conducted using the insect larvae, *Galleria mellonella*, showed that all of the new compounds/complexes are extremely well tolerated.

Lastly, the cancer cell (FR positive) and activated macrophage targeting capability of the complexes has potentially been significantly enhanced via the development of the Im-phen-fol ligand. The  $[\text{Cu}(\text{Im-phen-fol})_2](\text{ClO}_4)_2$  (**73**) and  $[\text{Mn}(\text{Im-phen-fol})_3](\text{ClO}_4)_2$  (**91**) are anticipated to have superior efficacy, site-specific targeting (mediated by folate receptor cellular recognition) and vastly diminished systemic toxicity in comparison to the clinically administered anticancer and antitubercular drugs.

## 5.10 References

1. (a) <http://www.who.int/cancer/en/> Accessed on the 01/10/2014. ; (b) <http://www.cancer.gov/cancertopics/cancerlibrary/what-is-cancer> Accessed on the 01/10/2014. ; (c) <http://www.who.int/mediacentre/factsheets/fs297/en/> Accessed on the 01/10/2014.
2. Knowles, M.; Selby, P., *Introduction to the Cellular and Molecular Biology of Cancer*. OUP Oxford: 2005.
3. (a) King, R. J. B.; Robins, M. W., *Cancer Biology*. Pearson/Prentice Hall: 2006. ; (b) <http://www.cancer.org/cancer/cancerbasics/thehistoryofcancer/index> Accessed on the 01/10/2014.
4. Binder, M.; Roberts, C.; Spencer, N.; Antoine, D.; Cartwright, C., On the Antiquity of Cancer: Evidence for Metastatic Carcinoma in a Young Man from Ancient Nubia (c. 1200BC). *Plos One* 2014, 9 (3). 10.1371/journal.pone.0090924
5. Yarbro, C. H.; Goodman, M.; Frogge, M. H., *Cancer Nursing: Principles and Practice*. Jones and Bartlett Publishers: 2005.
6. Franks, L. M.; Teich, N. M., *Introduction to the Cellular and Molecular Biology of Cancer*. Oxford University Press: 1986.
7. <http://apps.who.int/classifications/icd10/browse/2010/en#/II> Accessed on the 15/10/2014.
8. Stedman, T. L., *Stedman's Medical Dictionary*. Lippincott Williams & Wilkins: 2006.
9. Mehlen, P.; Puisieux, A., Metastasis: a question of life or death. *Nature Reviews Cancer* 2006, 6 (6), 449-458. 10.1038/nrc1886
10. Chu, E.; DeVita, V. T., *Physicians' Cancer Chemotherapy Drug Manual 2013*. Jones & Bartlett Learning: 2012.
11. <http://www.who.int/mediacentre/factsheets/fs310/en/> Accessed on the 24/10/2014.
12. [http://www.iarc.fr/en/media-centre/pr/2014/pdfs/pr224\\_E.pdf](http://www.iarc.fr/en/media-centre/pr/2014/pdfs/pr224_E.pdf) Accessed on the 01/10/2014.
13. Reece, J. B., *Campbell Biology*. Benjamin Cummings / Pearson: 2011.
14. Blow, J. J.; Tanaka, T. U., The chromosome cycle: coordinating replication and segregation - Second in the Cycles Review Series. *Embo Reports* 2005, 6 (11), 1028-1034. 10.1038/sj.embor.7400557

15. [http://en.wikipedia.org/wiki/File:Cell\\_Cycle\\_2-2.svg](http://en.wikipedia.org/wiki/File:Cell_Cycle_2-2.svg) Accessed on the 12/10/2014.
16. Elledge, S. J., Cell cycle checkpoints: Preventing an identity crisis. *Science* 1996, 274 (5293), 1664-1672. 10.1126/science.274.5293.1664
17. Cho, Y. J.; Gorina, S.; Jeffrey, P. D.; Pavletich, N. P., Crystal-structure of a p53 tumor-suppressor dna complex - understanding tumorigenic mutations. *Science* 1994, 265 (5170), 346-355. 10.1126/science.8023157
18. Ventura, A.; Kirsch, D. G.; McLaughlin, M. E.; Tuveson, D. A.; Grimm, J.; Lintault, L.; Newman, J.; Reczek, E. E.; Weissleder, R.; Jacks, T., Restoration of p53 function leads to tumour regression in vivo. *Nature* 2007, 445 (7128), 661-665. 10.1038/nature05541
19. Champeris Tsaniras, S.; Kanellakis, N.; Symeonidou, I. E.; Nikolopoulou, P.; Lygerou, Z.; Taraviras, S., Licensing of DNA replication, cancer, pluripotency and differentiation: an interlinked world? *Seminars in cell & developmental biology* 2014, 30, 174-180. 10.1016/j.semcdb.2014.03.013
20. Poot, M.; Kavanagh, T. J.; Kang, H. C.; Haugland, R. P.; Rabinovitch, P. S., Flow cytometric analysis of cell cycle-dependent changes in cell thiol level by combining a new laser dye with Hoechst 33342. *Cytometry* 1991, 12 (2), 184-187. 10.1002/cyto.990120214
21. (a) Bencini, A.; Lippolis, V., 1,10-Phenanthroline: A versatile building block for the construction of ligands for various purposes. *Coordination Chemistry Reviews* 2010, 254 (17-18), 2096-2180. 10.1016/j.ccr.2010.04.008; (b) Kellett, A.; Howe, O.; O'Connor, M.; McCann, M.; Creaven, B. S.; McClean, S.; Kia, A. F. A.; Casey, A.; Devereux, M., Radical-induced DNA damage by cytotoxic square-planar copper(II) complexes incorporating o-phthalate and 1,10-phenanthroline or 2,2'-dipyridyl. *Free Radical Biology and Medicine* 2012, 53 (3), 564-576. 10.1016/j.freeradbiomed.2012.05.034; (c) Kellett, A.; O'Connor, M.; McCann, M.; Howe, O.; Casey, A.; McCarron, P.; Kavanagh, K.; McNamara, M.; Kennedy, S.; May, D. D.; Skell, P. S.; O'Shea, D.; Devereux, M., Water-soluble bis(1,10-phenanthroline) octanedioate Cu<sup>2+</sup> and Mn<sup>2+</sup> complexes with unprecedented nano and picomolar in vitro cytotoxicity: promising leads for chemotherapeutic drug development. *MedChemComm* 2011, 2 (7), 579. 10.1039/c0md00266f
22. Kelland, L., The resurgence of platinum-based cancer chemotherapy. *Nat Rev Cancer* 2007, 7 (8), 573-584. 10.1038/nrc2167



23. Lehninger, A. L.; Nelson, D. L.; Cox, M. M., *Lehninger Principles of Biochemistry*. W. H. Freeman: 2005.
24. (a) Chen, J. Y.; Stubbe, J., Bleomycins: Towards better therapeutics. *Nature Reviews Cancer* 2005, 5 (2), 102-112. 10.1038/nrc1547; (b) Goodwin, K. D.; Lewis, M. A.; Long, E. C.; Georgiadis, M. M., Crystal structure of DNA-bound Co(III)-bleomycin B-2: Insights on intercalation and minor groove binding. *Proceedings of the National Academy of Sciences of the United States of America* 2008, 105 (13), 5052-5056. 10.1073/pnas.0708143105
25. (a) Mancin, F.; Scrimin, P.; Tecilla, P.; Tonellato, U., Artificial metallonucleases. *Chem Commun (Camb)* 2005, (20), 2540-2548. 10.1039/b418164f; (b) Pitie, M.; Pratviel, G., Activation of DNA Carbon-Hydrogen Bonds by Metal Complexes. *Chemical Reviews* 2010, 110 (2), 1018-1059. 10.1021/cr900247m
26. Zeglis, B. M.; Pierre, V. C.; Barton, J. K., Metallo-intercalators and metallo-insertors. *Chem Commun (Camb)* 2007, (44), 4565-4579. 10.1039/b710949k
27. Gewirtz, D. A., A critical evaluation of the mechanisms of action proposed for the antitumor effects of the anthracycline antibiotics Adriamycin and daunorubicin. *Biochemical Pharmacology* 1999, 57 (7), 727-741. 10.1016/s0006-2952(98)00307-4
28. (a) Sigman, D. S., Chemical Nucleases. *Biochemistry* 1990, 29 (39), 9097-9105. 10.1021/bi00491a001; (b) Sigman, D. S.; Graham, D. R.; Daurora, V.; Stern, A. M., Oxygen-dependent cleavage of DNA by the 1,10-phenanthroline cuprous complex - inhibition of escherichia-coli DNA-polymerase-I. *Journal of Biological Chemistry* 1979, 254 (24), 2269-2272.
29. Valko, M.; Rhodes, C. J.; Moncol, J.; Izakovic, M.; Mazur, M., Free radicals, metals and antioxidants in oxidative stress-induced cancer. *Chemico-Biological Interactions* 2006, 160 (1), 1-40. 10.1016/j.cbi.2005.12.009
30. (a) Devereux, M.; McCann, M.; Leon, V.; Geraghty, M.; McKee, V.; Wikaira, J., Synthesis and biological activity of manganese (II) complexes of phthalic and isophthalic acid: X-ray crystal structures of  $[\text{Mn}(\text{ph})(\text{phen})_2(\text{H}_2\text{O})] \cdot 4\text{H}_2\text{O}$ ,  $[\text{Mn}(\text{phen})_2(\text{H}_2\text{O})_2]_2(\text{Isoph})_2(\text{phen}) \cdot 12\text{H}_2\text{O}$  and  $\{[\text{Mn}(\text{isoph})(\text{bipy})]_4 \cdot 2.75\text{bipy}\}_n$  (phH<sub>2</sub> = phthalic acid; isoph = isophthalic acid; phen = 1,10-phenanthroline; bipy = 2,2-bipyridine). *Metal-Based Drugs* 2000, 7 (5), 275-288. 10.1155/mbd.2000.275; (b) Kellett, A.; O'Connor, M.; McCann, M.; McNamara, M.; Lynch, P.; Rosair, G.; McKee, V.; Creaven, B.; Walsh, M.; McClean, S.;

- Foltyn, A.; O'Shea, D.; Howe, O.; Devereux, M., Bis-phenanthroline copper(II) phthalate complexes are potent in vitro antitumour agents with 'self-activating' metallo-nuclease and DNA binding properties. *Dalton Trans* 2011, 40 (5), 1024-1027. 10.1039/c0dt01607a; (c) McCann, M.; Kellett, A.; Kavanagh, K.; Devereux, M.; Santos, A. L. S., Deciphering the Antimicrobial Activity of Phenanthroline Chelators. *Current Medicinal Chemistry* 2012, 19 (17), 2703-2714. ; (d) McCann, M.; Santos, A. L. S.; da Silva, B. A.; Romanos, M. T. V.; Pyrrho, A. S.; Devereux, M.; Kavanagh, K.; Fichtner, I.; Kellett, A., In vitro and in vivo studies into the biological activities of 1,10-phenanthroline, 1,10-phenanthroline-5,6-dione and its copper(ii) and silver(i) complexes. *Toxicology Research* 2012, 1 (1), 47. 10.1039/c2tx00010e; (e) Molphy, Z.; Prisecaru, A.; Slator, C.; Barron, N.; McCann, M.; Colleran, J.; Chandran, D.; Gathergood, N.; Kellett, A., Copper Phenanthrene Oxidative Chemical Nucleases. *Inorganic Chemistry* 2014, 53 (10), 5392-5404. 10.1021/ic500914j; (f) Prisecaru, A.; Devereux, M.; Barron, N.; McCann, M.; Colleran, J.; Casey, A.; McKee, V.; Kellett, A., Potent oxidative DNA cleavage by the di-copper cytotoxin:  $[\text{Cu}_2(\mu\text{-terephthalate})(1,10\text{-phen})_4]^{2+}$ . *Chem Commun (Camb)* 2012, 48 (55), 6906-6908. 10.1039/c2cc31023f; (g) Prisecaru, A.; McKee, V.; Howe, O.; Rochford, G.; McCann, M.; Colleran, J.; Pour, M.; Barron, N.; Gathergood, N.; Kellett, A., Regulating bioactivity of  $\text{Cu}^{2+}$  bis-1,10-phenanthroline artificial metallonucleases with sterically functionalized pendant carboxylates. *J Med Chem* 2013, 56 (21), 8599-8615. 10.1021/jm401465m
31. (a) McCann, M.; Coyle, B.; McKay, S.; McCormack, P.; Kavanagh, K.; Devereux, M.; McKee, V.; Kinsella, P.; O'Connor, R.; Clynes, M., Synthesis and X-ray crystal structure of  $[\text{Ag}(\text{phendio})_2]\text{ClO}_4$  (phendio=1,10-phenanthroline-5,6-dione) and its effects on fungal and mammalian cells. *Biometals* 2004, 17 (6), 635-645. 10.1007/s10534-004-1229-5; (b) Zheng, R. H.; Guo, H. C.; Jiang, H. J.; Xu, K. H.; Liu, B. B.; Sun, W. L.; Shen, Z. Q., A new and convenient synthesis of phendiones oxidated by  $\text{KBrO}_3/\text{H}_2\text{SO}_4$  at room temperature. *Chinese Chemical Letters* 2010, 21 (11), 1270-1272. 10.1016/j.ccllet.2010.05.030; (c) Casey, M. T.; McCann, M.; Devereux, M.; Curran, M.; Cardin, C.; Convery, M.; Quillet, V.; Harding, C., Synthesis and structure of the  $\text{Mn}^{\text{II,III}}$  complex salt  $[\text{Mn}_2(\eta^1\eta^1\mu_2\text{-oda})(\text{phen})_4(\text{H}_2\text{O})_2][\text{Mn}_2(\eta^1\eta^1\mu_2\text{-oda})(\text{phen})_4(\eta^1\text{-oda})_2]\cdot 4\text{H}_2\text{O}$  (odaH<sub>2</sub> = octanedioic acid); a Catalyst for H<sub>2</sub>O<sub>2</sub> Disproportionation *Journal of the*

- Chemical Society-Chemical Communications* 1994, (22), 2643-2645. 10.1039/c39940002643; (d) Devereux, M.; McCann, M.; Cronin, J. F.; Ferguson, G.; McKee, V., Binuclear and polymeric copper(II) dicarboxylate complexes: syntheses and crystal structures of  $[\text{Cu}_2(\text{pda})(\text{Phen})_4](\text{ClO}_4)_2 \cdot 5\text{H}_2\text{O} \cdot \text{C}_2\text{H}_5\text{OH}$ ,  $[\text{Cu}_2(\text{oda})(\text{Phen})_4](\text{ClO}_4)_2 \cdot 2.67\text{H}_2\text{O} \cdot \text{C}_2\text{H}_5\text{OH}$  and  $\{[\text{Cu}_2(\text{pda})_2(\text{NH}_3)_4(\text{H}_2\text{O})_2] \cdot 4\text{H}_2\text{O}\}_n$  (odaH<sub>2</sub>=octanedioic acid; pdaH<sub>2</sub>=pentanedioic acid; Phen=1,10-phenanthroline). *Polyhedron* 1999, 18 (16), 2141-2148. 10.1016/s0277-5387(99)00100-x; (e) McCann, S.; McCann, M.; Casey, M. T.; Devereux, M.; McKee, V.; McMichael, P.; McCrea, J. G., Manganese(II) complexes of 3,6,9-trioxaundecanedioic acid (3,6,9-tddaH(2)): X-ray crystal structures of  $[\text{Mn}(3,6,9\text{-tdda})(\text{H}_2\text{O})_2] \cdot 2\text{H}_2\text{O}$  and  $\{[\text{Mn}(3,6,9\text{-tdda})(\text{phen})_2 \cdot 3\text{H}_2\text{O}] \cdot \text{EtOH}\}_n$ . *Polyhedron* 1997, 16 (24), 4247-4252. 10.1016/s0277-5387(97)00233-7
32. Pulukuri, S. M.; Gondi, C. S.; Lakka, S. S.; Jutla, A.; Estes, N.; Gujrati, M.; Rao, J. S., RNA interference-directed knockdown of urokinase plasminogen activator and urokinase plasminogen activator receptor inhibits prostate cancer cell invasion, survival, and tumorigenicity in vivo. *Journal of Biological Chemistry* 2005, 280 (43), 36529-36540. 10.1074/jbc.M503111200
33. (a) Chhipa, R. R.; Kumari, R.; Upadhyay, A. K.; Bhat, M. K., Abrogation of p53 by its antisense in MCF-7 breast carcinoma cells increases cyclin D1 via activation of Akt and promotion of cell proliferation. *Experimental Cell Research* 2007, 313 (19), 3945-3958. 10.1016/j.yexcr.2007.08.022; (b) Pratesi, G.; Perego, P.; Polizzi, D.; Righetti, S. C.; Supino, R.; Caserini, C.; Manzotti, C.; Giuliani, F. C.; Pezzoni, G.; Tognella, S.; Spinelli, S.; Farrell, N.; Zunino, F., A novel charges trinuclear platinum complex effective against cisplatin-resistant tumours: hypersensitivity of p53-mutant human tumour xenografts. *British Journal of Cancer* 1999, 80 (12), 1912-1919. 10.1038/sj.bjc.6690620; (c) Rodrigues, N. R.; Rowan, A.; Smith, M. E.; Kerr, I. B.; Bodmer, W. F.; Gannon, J. V.; Lane, D. P., p53 mutations in colorectal cancer. *Proc Natl Acad Sci U S A* 1990, 87 (19), 7555-7559.
34. (a) [http://www.ncri.ie/sites/ncri/files/factsheets/FACTSHEET\\_colorectal.pdf](http://www.ncri.ie/sites/ncri/files/factsheets/FACTSHEET_colorectal.pdf) Accessed on the 02/10/2014. ; (b) [http://www.ncri.ie/sites/ncri/files/factsheets/FACTSHEET\\_female%20breast.pdf](http://www.ncri.ie/sites/ncri/files/factsheets/FACTSHEET_female%20breast.pdf) Accessed on the 05/10/2014. ; (c) [http://www.ncri.ie/sites/ncri/files/factsheets/FACTSHEET\\_lung.pdf](http://www.ncri.ie/sites/ncri/files/factsheets/FACTSHEET_lung.pdf) Accessed on

- the 11/10/2014. ; (d)  
[http://www.ncri.ie/sites/ncri/files/factsheets/FACTSHEET\\_prostate.pdf](http://www.ncri.ie/sites/ncri/files/factsheets/FACTSHEET_prostate.pdf)  
Accessed on the 14/10/2014.
35. Dasari, S.; Tchounwou, P. B., Cisplatin in cancer therapy: Molecular mechanisms of action. *European Journal of Pharmacology* 2014, 740, 364-378. 10.1016/j.ejphar.2014.07.025
36. Park, G. Y.; Wilson, J. J.; Song, Y.; Lippard, S. J., Phenanthriplatin, a monofunctional DNA-binding platinum anticancer drug candidate with unusual potency and cellular activity profile. *Proceedings of the National Academy of Sciences of the United States of America* 2012, 109 (30), 11987-11992. 10.1073/pnas.1207670109
37. (a) Hudson, B. P.; Dupureur, C. M.; Barton, J. K., H-1-NMR STRUCTURAL EVIDENCE FOR THE SEQUENCE-SPECIFIC DESIGN OF AN INTERCALATOR - DELTA-ALPHA- RH (R,R)-ME(2)TRIEN PHI (3+) BOUND TO D(GAGTGCCTC)(2). *Journal of the American Chemical Society* 1995, 117 (36), 9379-9380. 10.1021/ja00141a041; (b) Krotz, A. H.; Kuo, L. Y.; Shields, T. P.; Barton, J. K., DNA RECOGNITION BY RHODIUM(III) POLYAMINE INTERCALATORS - CONSIDERATIONS OF HYDROGEN-BONDING AND VANDERWAALS INTERACTIONS. *Journal of the American Chemical Society* 1993, 115 (10), 3877-3882. 10.1021/ja00063a004; (c) Sitlani, A.; Dupureur, C. M.; Barton, J. K., ENANTIOSPECIFIC PALINDROMIC RECOGNITION OF 5'-D(CTCTAGAG)-3' BY A NOVEL RHODIUM INTERCALATOR - ANALOGIES TO A DNA-BINDING PROTEIN. *Journal of the American Chemical Society* 1993, 115 (26), 12589-12590. 10.1021/ja00079a050; (d) Terbrueggen, R. H.; Barton, J. K., SEQUENCE-SPECIFIC DNA-BINDING BY A RHODIUM COMPLEX - RECOGNITION BASED ON SEQUENCE-DEPENDENT TWISTABILITY. *Biochemistry* 1995, 34 (26), 8227-8234. 10.1021/bi00026a003
38. (a) Erkkila, K. E.; Odom, D. T.; Barton, J. K., Recognition and reaction of metallointercalators with DNA. *Chemical Reviews* 1999, 99 (9), 2777-2795. 10.1021/cr9804341; (b) Thuong, N. T.; Helene, C., SEQUENCE-SPECIFIC RECOGNITION AND MODIFICATION OF DOUBLE-HELICAL DNA BY OLIGONUCLEOTIDES. *Angewandte Chemie-International Edition* 1993, 32 (5), 666-690. 10.1002/anie.199306661; (c) Urathamakul, T.; Beck, J. L.; Sheil,

- M. M.; Aldrich-Wright, J. R.; Ralph, S. F., A mass spectrometric investigation of non-covalent interactions between ruthenium complexes and DNA. *Dalton Trans* 2004, (17), 2683-2690. 10.1039/b406889k
39. (a) Schafer, B.; Goerls, H.; Presselt, M.; Schmitt, M.; Popp, J.; Henry, W.; Vos, J. G.; Rau, S., Derivatives of dipyrido 3,2-a : 2',3'-c phenazine and its ruthenium complexes, influence of aryl substitution on photophysical properties. *Dalton Trans* 2006, (18), 2225-2231. 10.1039/b512773d; (b) Barton, J. K., Tris (phenanthroline) metal complexes: probes for DNA helicity. *J Biomol Struct Dyn* 1983, 1 (3), 621-632. 10.1080/07391102.1983.10507469
40. (a) Jamieson, E. R.; Lippard, S. J., Structure, recognition, and processing of cisplatin-DNA adducts. *Chemical Reviews* 1999, 99 (9), 2467-2498. 10.1021/cr980421n; (b) Lippard, S. J.; Bond, P. J.; Wu, K. C.; Bauer, W. R., STEREOCHEMICAL REQUIREMENTS FOR INTERCALATION OF PLATINUM COMPLEXES INTO DOUBLE-STRANDED DNAs. *Science* 1976, 194 (4266), 726-728. 10.1126/science.982037
41. Hiort, C.; Lincoln, P.; Norden, B., DNA-BINDING OF DELTA-RU(PHEN)2DPPZ 2+ AND LAMBDA-RU(PHEN)2DPPZ 2+. *Journal of the American Chemical Society* 1993, 115 (9), 3448-3454. 10.1021/ja00062a007
42. (a) Chang, L. L.; Sidler, K. L.; Cascieri, M. A.; de Laszlo, S.; Koch, G.; Li, B.; MacCoss, M.; Mantlo, N.; O'Keefe, S.; Pang, M.; Rolando, A.; Hagmann, W. K., Substituted imidazoles as glucagon receptor antagonists. *Bioorg Med Chem Lett* 2001, 11 (18), 2549-2553. ; (b) Verma, A.; Joshi, S.; Singh, D., Imidazole: Having Versatile Biological Activities. *Journal of Chemistry* 2013. 10.1155/2013/329412
43. (a) Sun, B.; Wang, Y. C.; Qian, C.; Chu, J.; Liang, S. M.; Chao, H.; Ji, L. N., Synthesis, characterization and DNA-binding studies of chiral ruthenium(II) complexes with 2-(5-nitrofuranyl)-1H-imidazo 4,5-f 1,10 phenanthroline. *Journal of Molecular Structure* 2010, 963 (2-3), 153-159. 10.1016/j.molstruc.2009.10.028; (b) Sun, D. D.; Wang, W. Z.; Mao, J. W.; Mei, W. J.; Liu, J., Imidazo 4,5f 1,10 phenanthroline derivatives as inhibitor of c-myc gene expression in A549 cells via NF-kappa B pathway. *Bioorg Med Chem Lett* 2012, 22 (1), 102-105. 10.1016/j.bmcl.2011.11.063; (c) Xu, H.; Zheng, K. C.; Deng, H.; Lin, L. J.; Zhang, Q. L.; Ji, L. N., Effects of the ancillary ligands of polypyridyl ruthenium(II) complexes on the DNA-binding behaviors. *New Journal of Chemistry* 2003, 27 (8), 1255-1263. 10.1039/b212826h; (d) Zhang, P.;

- Chen, J.; Liang, Y., DNA binding, cytotoxicity, and apoptotic-inducing activity of ruthenium(II) polypyridyl complex. *Acta Biochimica Et Biophysica Sinica* 2010, 42 (7), 440-449. 10.1093/abbs/gmq040
44. Wang, Z., Radziszewski Reaction. In *Comprehensive Organic Name Reactions and Reagents*, John Wiley & Sons, Inc.: 2010. 10.1002/9780470638859.conrr518
45. [http://www.rjpbcs.com/pdf/2010\\_1%284%29/%5B100%5D.pdf](http://www.rjpbcs.com/pdf/2010_1%284%29/%5B100%5D.pdf) Accessed on the 21/10/2014.
46. Kappe, C. O., Controlled microwave heating in modern organic synthesis. *Angewandte Chemie-International Edition* 2004, 43 (46), 6250-6284. 10.1002/anie.200400655
47. Eseola, A. O.; Li, W.; Sun, W. H.; Zhang, M.; Xiao, L. W.; Woods, J. A. O., Luminescent properties of some imidazole and oxazole based heterocycles Synthesis, structure and substituent effects. *Dyes and Pigments* 2011, 88 (3), 262-273. 10.1016/j.dyepig.2010.07.005
48. (a) Aykin-Burns, N.; Ahmad, I. M.; Zhu, Y.; Oberley, L. W.; Spitz, D. R., Increased levels of superoxide and H<sub>2</sub>O<sub>2</sub> mediate the differential susceptibility of cancer cells versus normal cells to glucose deprivation. *Biochemical Journal* 2009, 418, 29-37. 10.1042/bj20081258; (b) Lopez-Lazaro, M., Dual role of hydrogen peroxide in cancer: Possible relevance to cancer chemoprevention and therapy. *Cancer Letters* 2007, 252 (1), 1-8. 10.1016/j.canlet.2006.10.029
49. Fomin, F. M.; Zaitseva, K. S., Mechanism of the oxidation of ferrocene and its derivatives with hydrogen peroxide: A new effect. *Russian Journal of Physical Chemistry A* 2014, 88 (3), 466-470. 10.1134/s0036024414020101
50. Cooke, M. S.; Evans, M. D.; Dizdaroglu, M.; Lunec, J., Oxidative DNA damage: mechanisms, mutation, and disease. *Faseb Journal* 2003, 17 (10), 1195-1214. 10.1096/fj.02-0752rev
51. (a) Halliwell, B., Free Radicals and Other Reactive Species in Disease. In *eLS*, John Wiley & Sons, Ltd: 2001. 10.1038/npg.els.0003913; (b) Trumbore, C. N.; Ehrlich, R. S.; Myers, Y. N., Changes in DNA conformation induced by gamma irradiation in the presence of copper. *Radiation Research* 2001, 155 (3), 453-465. 10.1667/0033-7587(2001)155[0453:cidcib]2.0.co;2
52. Peddi, P. F.; Hurvitz, S. A., Trastuzumab emtansine: the first targeted chemotherapy for treatment of breast cancer. *Future Oncol* 2013, 9 (3), 319-326. 10.2217/fon.13.7



53. Mitri, Z.; Constantine, T.; O'Regan, R., The HER2 Receptor in Breast Cancer: Pathophysiology, Clinical Use, and New Advances in Therapy. *Chemotherapy research and practice* 2012, 2012, 743193. 10.1155/2012/743193
54. Teicher, B. A.; Doroshow, J. H., The Promise of Antibody-Drug Conjugates. *New England Journal of Medicine* 2012, 367 (19), 1847-1848. 10.1056/NEJMe1211736
55. (a) Jain, M.; Nilsson, R.; Sharma, S.; Madhusudhan, N.; Kitami, T.; Souza, A. L.; Kafri, R.; Kirschner, M. W.; Clish, C. B.; Mootha, V. K., Metabolite Profiling Identifies a Key Role for Glycine in Rapid Cancer Cell Proliferation. *Science* 2012, 336 (6084), 1040-1044. 10.1126/science.1218595; (b) Munoz-Pinedo, C.; El Mjiyad, N.; Ricci, J. E., Cancer metabolism: current perspectives and future directions. *Cell Death & Disease* 2012, 3. 10.1038/cddis.2011.123
56. Amelio, I.; Cutruzzola, F.; Antonov, A.; Agostini, M.; Melino, G., Serine and glycine metabolism in cancer. *Trends in Biochemical Sciences* 2014, 39 (4), 191-198. 10.1016/j.tibs.2014.02.004
57. McCann, M.; McGinley, J.; Ni, K.; O'Connor, M.; Kavanagh, K.; McKee, V.; Colleran, J.; Devereux, M.; Gathergood, N.; Barron, N.; Prisecaru, A.; Kellett, A., A new phenanthroline-oxazine ligand: synthesis, coordination chemistry and atypical DNA binding interaction. *Chem Commun (Camb)* 2013, 49 (23), 2341-2343. 10.1039/c3cc38710k
58. Vlahov, I. R.; Leamon, C. P., Engineering folate-drug conjugates to target cancer: from chemistry to clinic. *Bioconjug Chem* 2012, 23 (7), 1357-1369. 10.1021/bc2005522
59. Zwicke, G. L.; Mansoori, G. A.; Jeffery, C. J., Utilizing the folate receptor for active targeting of cancer nanotherapeutics. *Nano Rev* 2012, 3. 10.3402/nano.v3i0.18496
60. (a) Leemans, J. C.; Thepen, T.; Weijer, S.; Florquin, S.; van Rooijen, N.; van de Winkel, J. G.; van der Poll, T., Macrophages play a dual role during pulmonary tuberculosis in mice. *Journal of Infectious Diseases* 2005, 191 (1), 65-74. 10.1086/426395; (b) Xia, W.; Hilgenbrink, A. R.; Matteson, E. L.; Lockwood, M. B.; Cheng, J. X.; Low, P. S., A functional folate receptor is induced during macrophage activation and can be used to target drugs to activated macrophages. *Blood* 2009, 113 (2), 438-446. 10.1182/blood-2008-04-150789

61. Chen, C.; Ke, J. Y.; Zhou, X. E.; Yi, W.; Brunzelle, J. S.; Li, J.; Yong, E. L.; Xu, H. E.; Melcher, K., Structural basis for molecular recognition of folic acid by folate receptors. *Nature* 2013, 500 (7463), 486-+. 10.1038/nature12327
62. Dewar, M. J. S.; Mole, T., Palladised charcoal as a catalyst for the reduction of aromatic nitro-compounds by Hydrazine Hydrate. *Journal of the Chemical Society* 1956, (JUL), 2556-2557.
63. Atkinson, S. F.; Bettinger, T.; Seymour, L. W.; Behr, J. P.; Ward, C. M., Conjugation of folate via gelonin carbohydrate residues retains ribosomal-inactivating properties of the toxin and permits targeting to folate receptor positive cells. *Journal of Biological Chemistry* 2001, 276 (30), 27930-27935. 10.1074/jbc.M102825200